LATE QUATERNARY VOLCANIC STRATIGRAPHY OF THE SOUTHEASTERN SECTOR OF THE MOUNT RUAPEHU RING PLAIN NEW ZEALAND

A thesis presented as partial fulfilment of the requirements
for the degree of

Doctor of Philosophy in Soil Science

by

Susan Leigh Donoghue

MASSEY UNIVERSITY
PALMERSTON NORTH
NEW ZEALAND

June
1991

Mt Ruapehu viewed from the east, overlooking Whangaehu River and Rangipo Desert

'In the shadow of these cones, we face mystery and cataclysm where nature is met on its own terms'

Bill Hackett

ACKNOWLEDGEMENTS

I extend my sincere thanks and appreciation to my supervisors, Dr V.E. Neall, Dr A.S. Palmer, and Dr R.B. Stewart (Massey University) for the opportunity to embark on a particularly interesting area of study, and for their help and encouragement throughout.

I wish to thank the following people for their assistance and hospitality during the term of my field work:

- Captain G. Pullen, and staff of Operations Branch Headquarters, Army Training Group, Waiouru
- Sergeant W. Richards (Q Store HQ Coy.), Warrant Officer K. Haami, Corporal T. Kanara, Lance Corporal D. Baker, and Mrs M. Gunn (Barrack Section HQ Coy), Army Training Group, Waiouru
- Lyell Irwin, Teresa Chapman, and staff of Tongariro National Park Headquarters, Ohakune
- Mr D. Brown (Superintendent), Timberlands, Karioi Forest
- Constable Greg Whyte and Constable Keith O'Donnell, Waiouru Police Station

I would also like to thank the following people for their valuable contributions to this thesis:

- Dr J. Gamble, Victoria University of Wellington (XRF data, and discussion)
- Dr P. Froggatt, Victoria University of Wellington (EMP data, and discussion)
- Dr M. M^{c}Glone, Botany Division, DSIR, Christchurch (Palynological data)
- Mr D. Hopcroft (SEM micrographs)
- Dr D. Lowe, Waikato University (Olivine data)
- Dr C. Wallace, Massey University (Valuable discussion)
- Dr M. Ames (Levin) for his generous provision of printing facilities
- Paul Vautier for his technical assistance in the reproduction of the charts

Permission to reproduce the topographical maps was provided by the Department of Survey and Land Information.

Funding for this study was provided in part by a Helen E. Akers Scholarship, and the Ministry of Civil Defence.

Special thanks are also extended to Dr J. Kirkman, Cleland Wallace, Beth Palmer, Anne Rouse, Malcolm Boag, and Alan and Julie Palmer.

Finally, a very special thanks to Scott Bell and my family for their unfailing support, encouragement and understanding in all aspects of this project. I particularly thank Scott and my parents for their invaluable assistance with the presentation – thanks for the long hours and late nights endured in helping to produce this thesis!

ABSTRACT

Mt Ruapehu is an active composite strato-volcano situated within the Tongariro Volcanic Centre, North Island, New Zealand. It is surrounded by an extensive ring plain built principally from laharic deposits, capped by late Pleistocene and Holocene-aged tephras.

Stratigraphic studies and geologic mapping on the southeastern sector of the Mt Ruapehu ring plain have identified six andesitic tephra formations (Tufa Trig Formation, Ngauruhoe Formation, Mangatawai Tephra, Mangamate Tephra, Pahoka Tephra, Bullot Formation) erupted from Mt Ruapehu, Mt Tongariro and Mt Ngauruhoe during the past *c.* 22 500 years. A seventh formation, Papakai Formation, comprises both andesitic tephra and tephric loess.

Most of the tephras erupted from Mt Ruapehu are grouped into the Bullot and Tufa Trig formations which are of late Pleistocene to Holocene age. Other intermittent eruptions during the Holocene have contributed tephra to the Papakai Formation.

The Bullot Formation tephras represent a period of active and widespread tephra deposition from subplinian eruptions. Most of the tephras have been deposited to the east of the volcano under the influence of prevailing westerly winds, with an average eruption interval of approximately one event every 200 years. Tephras of Tufa Trig Formation are the products of small hydrovolcanic eruptions and, although erupted more frequently (one event approximately every 100 years), have contributed comparatively little tephra to the ring plain.

Tephras erupted from Mt Tongariro (Mangamate Tephra, Pahoka Tephra) comprise most of the Holocene tephra record on the Mt Ruapehu ring plain, being deposited during a period of quiescence at Mt Ruapehu. Their eruption is coincident with the introduction of mixed magmas beneath Mt Tongariro.

Fourteen rhyolitic tephra formations (Kaharoa Tephra, Mapara Tephra, Taupo Pumice, Waimihia Tephra, Hinemaiaia Tephra, Whakatane Tephra, Motutere Tephra, Poronui Tephra, Karapiti Tephra, Waiohau Tephra, ?Rotorua Tephra, Rerewhakaaitu Tephra, Okareka Tephra, Kawakawa Tephra Formation) erupted from the Okataina and Taupo volcanic centres of the central North Island have also been identified. They are important marker beds used to date andesitic tephras and laharic deposits preserved on the southeastern ring plain.

The stratigraphic relationships between these distal rhyolitic tephras, and their relationship to local andesitic tephras is discussed, and the stratigraphy of some rhyolitic tephras identified by Topping and Kohn (1973) revised. The tephras have been identified from their stratigraphic positions, ferromagnesian mineral assemblages and glass shard chemistries.

The mineralogy and chemistry of selected andesitic marker beds has been detailed for purposes of regional identification and correlation. A database for Tongariro Centre tephras is established using ferromagnesian mineral assemblages and major element chemistry of ferromagnesian phenocrysts, and glass determined by electron microprobe analysis. The potential for use of andesitic tephra mineralogy in stratigraphic studies is evaluated.

The ferromagnesian mineral assemblage of Tongariro Volcanic Centre tephras comprises orthopyroxene + clinopyroxene ± olivine ± hornblende. Orthopyroxene compositions project mostly as hypersthene, and clinopyroxenes as augite. Olivine and hornblende are valuable marker minerals to the identification of some tephras. The olivines are forsteritic, some of which show distinctive skeletal morphology. The hornblende phenocrysts are calcic amphiboles and project mostly as pargasitic hornblende. Groundmass glass compositions of some pumice lapilli range between andesite and rhyolite. Bulk rock compositions are andesite.

The deposits of debris flows and hyperconcentrated flood flows comprise much of the prehistoric stratigraphy of the southeastern Ruapehu ring plain, with minor fluvial lithologies, indicating lahars are common events at Mt Ruapehu. The deposits are grouped into five formations (Onetapu Formation, Manutahi Formation, Mangaio Formation, Tangatu Formation, Te Heuheu Formation) on the basis of lithology.

The stratigraphic relationships between these formations is discussed and their distributions mapped. These formations form the major constructional surfaces of the southeastern ring plain. They are envisaged as having been generated following large scale sector collapses of the southeastern flanks of Mt Ruapehu, and by snow and ice melt associated with eruption of hot pyroclastic ejecta, the ejection of Crater Lake waters, or by heavy rains inducing widespread flood events, capable of eroding flank and ring plain materials. Much of the erosion and aggradation that has occurred within the Rangipo Desert in the last *c.* 1800 years is attributable to lahars.

At least 35 laharic events are recorded on the southeastern ring plain within the last *c.* 22 500 years. The most active period of lahar generation is the present day, with an average incidence of one event every 11 years. Many of the recent lahars have been confined within Whangaehu Valley.

TABLE OF CONTENTS

VOLUME I

PREFACE

Frontispiece . . . . . *ii*
Acknowledgements . . . . . *iii*
Abstract . . . . . *iv*
Table of Contents . . . . . *vi*
List of Tables . . . . . *xii*
List of Figures . . . . . *xiii*
List of Plates . . . . . *xv*
List of Charts and Maps . . . . . *xviii*
List of Abbreviations . . . . . *xix*

CHAPTER ONE
INTRODUCTION

1.1 Regional Setting 1
Taupo Volcanic Zone 1
Tongariro Volcanic Centre 1
Mt Ruapehu Volcano and Ring Plain 4

1.2 Previous Work: Geology of Tongariro Volcanic Centre 5
Geology of Mt Ruapehu Volcano 6
Petrography of Tongariro Volcanic Centre Lavas 6
Geology of the Mt Ruapehu Ring Plain 7

1.3 Purpose and Scope of This Study 9

1.4 Location of the Study Area 11

CHAPTER TWO
IDENTIFICATION AND CORRELATION OF RHYOLITIC TEPHRAS, TONGARIRO VOLCANIC CENTRE

Introduction 14

2.1 Previous Work: Rhyolitic Tephrostratigraphy, Tongariro Volcanic Centre 14
Stratigraphy of the Taupo and Rotorua Subgroups 15
Stratigraphic Revision of Rhyolitic Tephra Formations 15
Taupo Pumice Formation 16
Hinemaiaia Ash 17
Whakatane Ash 18
Papanetu Tephra 19
Oruanui Formation 19

2.2 Previous work: Methods for Identifying Rhyolitic Tephras 21
Ferromagnesian Mineral Assemblages 21

continued ...

Taupo Volcanic Centre Tephras 21
Okataina Volcanic Centre Tephras 21
Tephra Chemistry 23
Bulk Chemical Methods 23
Discrete-Grain Methods 25
Other Methods 27
Summary of Methods 28

2.3 Methods for Identifying Rhyolitic Tephras on the Mt Ruapehu Ring Plain 29
Basis of Field Identification 29
Basis of Laboratory Identification 30
Tephra Sampling 31
Sample Preparation 32
Preparation of Samples for Mineralogical Analysis 34
Heavy Liquid Separation of Minerals 34
Preparation of Polished Thin Sections 36
Determining Ferromagnesian Mineral Assemblages 36
Electron Microprobe Analysis of Glass Shards 37

2.4 Results and Discussion 38
The Occurrence, Stratigraphy and Chronology of Rhyolitic Tephras in the Study Area 38
Identification of the Rhyolitic Tephras 39
Field Identification 39
Laboratory Identification 39
Ferromagnesian Mineral Assemblages 39
Electron Microprobe Analyses 43
Rhyolitic Tephrostratigraphy and Tephrochronology, Southeastern Mt Ruapehu Ring Plain 49
Kaharoa Tephra [Ka] 49
Taupo Pumice Formation [Tp] 51
Mapara Tephra [Mp] 54
Waimihia Tephra [Wm] 55
Hinemaiaia Tephra [Hm] 58
Whakatane Tephra [Wk] 60
Motutere Tephra [Mt] 63
Poronui Tephra [Po] 66
Karapiti Tephra [Kp] 67
Waiohau Tephra [Wh] 68
?Rotorua Tephra [Rr] 72
Rerewhakaaitu Tephra [Rk] 73
Okareka Tephra [Ok] 79
Kawakawa Tephra Formation [Kk] 80

continued ...

CHAPTER THREE
ANDESITIC TEPHROSTRATIGRAPHY AND TEPHROCHRONOLOGY, TONGARIRO VOLCANIC CENTRE

Introduction 84

3.1 Previous work: Andesitic Tephrostratigraphy and Tephrochronology, Tongariro Volcanic Centre 84
Stratigraphy of Tongariro Subgroup 85

3.2 Methods for Identifying Andesitic Tephras of Tongariro Volcanic Centre 86
Basis of Field Identification 86

3.3 Results and Discussion 87
General Stratigraphy of Andesitic Tephras 87
Definition of Subgroups 89
Tongariro Subgroup 89
Tukino Subgroup 91
Andesitic Tephrostratigraphy and Tephrochronology, Southeastern Mt Ruapehu Ring Plain 91
Ngauruhoe Formation [Ng] 91
Tufa Trig Formation [Tf] 93
Mangatawai Tephra [Mg] 107
Papakai Formation [Pp] 109
Mangamate Tephra [Mm] 115
Unnamed tephra [ut] 127
Pahoka Tephra [Pa] 127
Bullot Formation [Bt] 131
Correlation of Bullot Formation Tephras 147
Deposition and Erosion of Bullot Formation Tephras 150
Summary Stratigraphy and Chronology of Andesitic and Rhyolitic Tephras of the Southeastern Mt Ruapehu Ring Plain 151
Regional Marker Beds 152

CHAPTER FOUR
MINERALOGY AND CHEMISTRY OF TONGARIRO VOLCANIC CENTRE TEPHRAS

Introduction 154

4.1 Previous work: Mineralogy and Chemistry of Tongariro Volcanic Centre Tephras 155

4.2 Previous Work: Methods for Identifying Andesitic Tephras 155
Ferromagnesian Mineral Assemblage 155
Tephra Chemistry 156
Bulk Chemical Methods 156
Discrete Grain Methods 157
Other Methods 158

4.3 Methods for Fingerprinting Andesitic Tephras of Tongariro Volcanic Centre . . . 159
Basis of Laboratory identification 159
Tephra Sampling 160
Sample Preparation 160

continued ...

Preparation of Samples for Mineralogical Analysis 161
Determining Ferromagnesian Mineral Assemblages 162
Electron Microprobe Analysis of Ferromagnesian Minerals 162
Electron Microprobe Analysis of Glass 162
Scanning Electron Microscopy 163

4.4 Results and Discussion 163
Description of Hand Samples 163
Schist Xenoliths 164
Accretionary Lapilli 165
Ferromagnesian Mineral Assemblages of Tongariro Volcanic Centre Tephras 168
Major Element Chemistry of Ferromagnesian Minerals and Glass: Use in Tephra Fingerprinting 172
Clinopyroxene 172
Orthopyroxene 186

Morphology and Chemistry of Olivine Phenocrysts of Mangamate Tephra, Tongariro Volcanic Centre, New Zealand

Abstract 194
Introduction 195
Stratigraphy and Chronology 195
Sampling and Methods 195
Results 198
Ferromagnesian Mineral Assemblages 198
Morphology of Olivine 199
Chemistry of Olivine 202
Discussion 202
Melt Conditions for Mangamate Tephras 203
Implications for Correlation of Distal Mangamate Tephras 204
Conclusions 205
Acknowledgements 206

Olivine 207
Olivine Morphology and Major Element Chemistry of Other Tongariro Volcanic Centre Tephras 207
Hornblende 212
Hornblende Mineralogy and Chemistry of Te Rato Lapilli and Pahoka Tephra 216
Magma Mixing in Pahoka Tephra and Te Rato Lapilli 216
Fe-Ti Oxides 219
Glass 222
Tephra Fingerprinting – Summary and Conclusions 233
Changes in the Mineralogy and Chemistry of Tephras Over the Past c. 22 500 Years 236
Eruption Styles at Mt Ruapehu 238
Subplinian Eruptions 238
Ignimbrite Eruptions 239
Hydrovolcanic (Phreatomagmatic and Phreatic) Eruptions 239
Future Tephra Eruptions 242

continued ...

CHAPTER FIVE
STRATIGRAPHY AND CHRONOLOGY OF LAHARIC DEPOSITS ON THE SOUTHEASTERN MT RUAPEHU RING PLAIN

Introduction 243

5.1 Nomenclature 243
Types of Lahars 244
Debris Flow 244
Hyperconcentrated Flood Flow 245
Stream Flow 245
Flow Transitions 246
Erosivity of Lahars 246
Distinction Between Volcanic Debris Avalanche and Lahar Deposits 246

5.2 Lahar Stratigraphy of the Southeastern Mt Ruapehu Ring Plain 247
Onetapu Formation [On] 248
Mangaio Formation [Mn] 259
Manutahi Formation [Mi] 262
Tangatu Formation [Ta] 265
Te Heuheu Formation [Hh] 270

5.3 Discussion 276
Summary of Stratigraphy 276
Lahar Distribution 276
Mechanisms of Lahar Formation 278

5.4 Holocene Geology of the Upper Whangaehu River 283

5.5 Ring Plain Construction and Erosion 284
Susceptibility of Tephra and Lahar Deposits to Erosion 286
Summary of Events 288

CHAPTER SIX
VOLCANIC HAZARD

Introduction 290
Hazard Assessment 291
Previous Work 291

6.1 Products of Eruptions and Associated Hazard 291
Hazard from Tephra Eruptions 294
Hazard from Lahars 298
Hazard from Lavas 302
Hazard from Pyroclastic Flows 305

6.2 Discussion 305

continued ...

CHAPTER SEVEN
SUMMARY

7.1 Summary of Findings 307

7.2 Future Work 319

BIBLIOGRAPHY 321

VOLUME II

APPENDICES

APPENDIX I: METHODOLOGIES *A1*
APPENDIX II: STRATIGRAPHIC SECTION DESCRIPTIONS *A16*
APPENDIX III: EMP AND XRF DATA *A167*
APPENDIX IV: MISCELLANEOUS *A294*

LIST OF TABLES

Table 2.1 Stratigraphy of Taupo and Rotorua subgroup tephras 16
2.2 Stratigraphy of Hinemaiaia Tephra, Motutere Tephra (Taupo Subgroup) and Whakatane Tephra (Rotorua Subgroup) 18
2.3 Ferromagnesian mineral abundances, rhyolitic tephras, study area 41
2.4 Ferromagnesian mineral abundances, rhyolitic tephras, type areas 42
2.5 Electron microprobe analyses of glass, rhyolitic tephras, study area 44
2.6 Electron microprobe analyses of glass, rhyolitic tephras, type areas . . . 45
2.7 Similarity Coefficients and Coefficients of Variation, comparison with type data 48
2.8 Similarity Coefficients and Coefficients of Variation 49
2.9 Stratigraphy of Holocene and late Pleistocene rhyolitic tephras preserved in the study area, comparison with Topping and Kohn (1973) and Topping (1973). 61
2.10 Radiocarbon ages 61
3.1 Stratigraphy and chronology of rhyolitic and andesitic tephras, study area 90
3.2 Stratigraphy of Mangatawai Tephra and Papakai Formation, comparison with Topping (1973) and Topping and Kohn (1973). 107
4.1 Schist xenolith abundances in andesitic tephras 165
4.2 Ferromagnesian mineral abundances, andesitic tephras 169
4.3 Electron microprobe analyses of clinopyroxene, andesitic tephras 173
4.4 Electron microprobe analyses of orthopyroxene, andesitic tephras 187
4.5 Dominant ferromagnesian assemblages, Mangamate Tephra 199
4.6 Electron microprobe analyses of clinopyroxene, orthopyroxene, and hornblende, Mangamate Tephra 200
4.7 Dominant olivine morphology, Mangamate Tephra. 202
4.8 Electron microprobe analyses of olivine, Mangamate Tephra 203
4.9 Electron microprobe analyses of olivine, andesitic tephras 208
4.10 Electron microprobe analyses of hornblende, andesitic tephras 213
4.11 Electron microprobe analyses of titanomagnetite and ilmenite, andesitic tephras 221
4.12 Electron microprobe analyses of glass, andesitic tephras 225
5.1 Stratigraphy of laharic deposits 249
6.1 Estimates of tephra volume 295
7.1 Lahar formation lithology and age. 309

LIST OF FIGURES

Figure 1.1 Volcanic centres of Taupo Volcanic Zone 2
1.2 Andesitic massifs and cones of Tongariro Volcanic Centre 3
1.3 Lahar formations of the southeastern Mt Ruapehu ring plain, mapped by Grindley (1960) 9
1.4 Location of the study area 12
1.5 Geographic locations 13
2.1 Location of type and reference sections, rhyolitic tephras 33
2.2 Total alkali silica (TAS) diagram, rhyolitic tephra compositions 46
2.3 Plot of CaO *vs* FeO contents, rhyolitic tephras 47
2.4 Plots of isopach thickness *vs* distance from isopach centre for Puketarata, Rotorua, Rerewhakaaitu, Okareka and Waiohau tephras. . . 75
2.5 Plots of FeO and CaO contents, Rerewhakaaitu Tephra 78
2.6 Distribution of rhyolitic tephras in the study area 83
3.1 Flow diagram illustrating field and laboratory based fingerprinting procedures 88
3.2 Location of type and reference sections, andesitic tephras 94
3.3 Isopach map of Tufa Trig Formation member Tf8 100
3.4 Isopach map of Tufa Trig Formation member Tf6 102
3.5 Isopach map of Tufa Trig Formation member Tf5 104
3.6 Isopach map of Tufa Trig Formation member Tf4 105
3.7 Isopach map of Mangatawai Tephra 110
3.8 Isopach map of Poutu Lapilli Member, Mangamate Tephra 118
3.9 Isopach map of Wharepu Tephra Member, Mangamate Tephra 120
3.10 Isopach map of Ohinepango Tephra Member, Mangamate Tephra 122
3.11 Isopach map of Waihohonu Lapilli Member, Mangamate Tephra 123
3.12 Isopach map of Oturere Lapilli Member, Mangamate Tephra 125
3.13 Isopach map of Pahoka Tephra 130
3.14 Distribution of Ngamatea lapilli-1 member, Bullot Formation 136
3.15 Isopach map of Pourahu Member [tephra unit] 140
3.16 Isopach map of Shawcroft Tephra Member, Bullot Formation 143
4.1 Trend plots of major oxide contents *vs* Mg number in clinopyroxenes . . 175
4.2 Compositions of clinopyroxenes, orthopyroxenes and olivines in Tongariro Volcanic Centre tephras. 176
4.3 MGMT and NCMT scatter plots showing compositions of clinopyroxenes in tephras from Mt Ruapehu and Mt Tongariro 181
4.4 Mean oxide contents in clinopyroxenes 182
4.5 Plot of CaO *vs* Mg number in clinopyroxenes in tephras from Tongariro, Taupo, and Egmont volcanic centres 184
4.6 Trend plots of major oxide contents *vs* Mg number in orthopyroxenes . . 188
4.7 MGMT scatter plot showing compositions of orthopyroxenes in tephras from Mt Ruapehu and Mt Tongariro 189
4.8 Plot of MnO *vs* Mg number in orthopyroxenes in tephras from Tongariro, Taupo, and Egmont volcanic centres 190
4.9 Mean oxide contents in orthopyroxenes 191
4.10 Location of Tongariro Volcanic Centre 196
4.11 Andesitic massifs and cones of Tongariro Volcanic Centre 197
4.12 Stratigraphic columns of Mangatawai and Poutu reference sections . . . 198
4.13 Olivine compositions, Mangamate tephras 201
4.14 Compositions of type [I] non-skeletal and type [II] skeletal olivines, Waihohonu Lapilli Member, Mangamate Tephra 201
4.15 Trend plots of major oxide contents *vs* Forsterite % in olivines 208

continued ...

Figure 4.16 Mean compositions of olivine, and coexisting clinopyroxene and orthopyroxene 209
4.17 MNCA scatter plot showing compositions of olivines in Mt Ruapehu and Mt Tongariro tephras 210
4.18 Mean oxide contents in olivines 211
4.19 Olivine compositions, Tongariro Volcanic Centre tephras 212
4.20 Trend plots of major oxide contents *vs* Mg number in hornblendes 214
4.21 Compositions of calcic amphiboles in Tongariro Volcanic Centre tephras 215
4.22 Plot of K_2O *vs* Mg number in amphiboles in tephras of Tongariro, Taupo, and Egmont volcanic centres. 220
4.23 Plot of MnO *vs* Cr_2O_3 in titanomagnetites, Mt Ruapehu tephras 222
4.24 Mean oxide contents in titanomagnetites 223
4.25 Plots of MnO *vs* MgO and Al_2O_3 *vs* MgO, titanomagnetites 224
4.26 Glass compositions, Mt Ruapehu tephras 226
4.27 Plot of CaO *vs* FeO in glasses of Mt Ruapehu tephras 227
4.28 Mean oxide contents in glass 229
4.29 Plot of K_2O *vs* SiO_2 in glasses of Mt Ruapehu tephras 232
5.1 Location of type and reference sections, laharic formations 250
5.2 Sketch of type locality for Onetapu Formation 251
5.3 Distribution of Onetapu Formation laharic deposits 258
5.4 Distribution of Mangaio Formation laharic deposit 261
5.5 Distribution of Manutahi Formation laharic deposits 265
5.6 Distribution of Tangatu Formation laharic deposits 269
5.7 Distribution of Te Heuheu Formation laharic deposits 272
5.8 Stratigraphy of tephras on Te Heuheu Formation surfaces 273
5.9 Scenario sketches 277
5.10 Stratigraphy, upper Whangaehu River. 284
6.1 Major features at risk from future lahars and tephra eruptions 292
6.2 Tongariro Power Development 293
6.3 Tephra hazard zones 297
6.4 Lahar hazard zones 303
6.5 Transect profiles, Rangipo Desert 304
7.1 Summary stratigraphy and chronology of tephras and laharic deposits . 310

LIST OF PLATES

Plate 1.1 Crater Lake, Mt Ruapehu P1
1.2 Mt Ruapehu ring plain, northern view P2
1.3 Mt Ruapehu ring plain, southeastern view P2
2.1 Ohakune Mountain Road [S20/271074]; Kaharoa Tephra, Taupo Pumice P3
2.2 Ohakune Mountain Road [S20/271074]; Kaharoa Tephra P4
2.3 Tufa Trig S.2 [T20/375046]; Taupo Pumice, Mapara Tephra, Waimihia Tephra; Mangatawai Tephra, Papakai Formation P5
2.4 Desert Road S.11 [T20/464092]; Taupo Pumice, Waimihia Tephra; Mangatawai Tephra, Papakai Formation P5
2.5 Aqueduct S.1, Southern Rangipo Desert [T20/418982]; Taupo Pumice P6
2.6 Southern Rangipo Desert; tephra cover beds P6
2.7 Ngamatea Swamp [T21/413874]; Taupo Pumice P7
2.8 Ngamatea Swamp [T21/413874]; Taupo Pumice, Mapara Tephra, Wamihia Tephra, Hinemiaia Tephra P7
2.9 Tufa Trig S.2 [T20/375046]; Mapara Tephra, Mangatawai Tephra P8
2.10 Tufa Trig S.2 [T20/375046]; Mapara Tephra, Waimihia Tephra, Mangatawai Tephra, Papakai Formation P8
2.11 Tufa Trig S.2 [T20/375046]; Mapara Tephra, Waimihia Tephra, Mangatawai Tephra, Papakai Formation P9
2.12 Desert Road S.12 [T20/458119]; Hinemaiaia Tephra, Papakai Formation P9
2.13 Desert Road S.15 [T20/462135]; Wamihia Tephra, Hinemaiaia Tephra, Motutere Tephra, Mangatawai Tephra, Papakai Formation, Mangamate Tephra P10
2.14 Death Valley Type Locality; Hinemaiaia Tephra, Papakai Formation . . . P11
2.15 Death Valley S.5 [T20/409045]; Whakatane Tephra, Motutere Tephra P11
2.16 Desert Road S.17 [T19/482199]; Hinemaiaia Tephra, Motutere Tephra, Papakai Formation P12
2.17 Death Valley S.3 [T20/409042]; Motutere Tephra P12
2.18 Desert Road S.15 [T20/462135]; Poronui Tephra, Mangamate Tephra P13
2.19 Desert Road [T19/524283]; Poronui Tephra, Karapiti Tephra, Mangamate Tephra P13
2.20 Wahianoa Aqueduct S. [T20/435990]; Waiohau Tephra, Rerewhakaaitu Tephra, Shawcroft Tephra P14
2.21 Whangaehu River S.1 [T20/399954]; Waiohau Tephra, Rerewhakaaitu Tephra, Shawcroft Tephra P14
2.22 Whangaehu River S.1 [T20/399954]; Waiohau Tephra, Shawcroft Tephra P15
2.23 Bullot Track S.1 [T20/412108]; Okareka Tephra P15
2.24 Desert Road S.10 [T20/464091]; Kawakawa Tephra Formation P16
2.25 Desert Road S.10 [T20/464091]; Kawakawa Tephra Formation, Rerewhakaaitu Tephra P17
2.26 Waikato Stream S.2 [T20/469102]; pull-apart structure P18
2.27 Waikato Stream S.2 [T20/469102]; Kawakawa Tephra Formation infilling pull-apart structure P18
3.1 Tufa Trig S.1 [T20/378045]; Tufa Trig Formation P19
3.2 Tufa Trig S.2 [T20/375046]; Tufa Trig Formation (Tf8, Tf6, Tf5) P19

continued ...

LIST OF PLATES

Plate 3.3 Tufa Trig S.2 [T20/375046]; Tufa Trig Formation *P20*
3.4 Mangatoetoenui Quarry [T20/459153]; Mangatawai Tephra *P21*
3.5 Paradise Valley Road [T20/494046]; Papakai Formation, Poutu Lapilli . . *P21*
3.6 Desert Road Unnamed Section [T20/465099]; erosional unconformity above Poutu Lapilli *P22*
3.7 Desert Road S.12 [T20/458119]; Papakai Formation, Mangamate Tephra *P22*
3.8 Rock Road, Karioi Forest [T20/322941]; Papakai Formation *P23*
3.9 Death Valley Type Locality; Papakai Formation, Waimihia Tephra, Hinemaiaia Tephra *P23*
3.10 Poutu S. [T19/481325]; Mangamate Tephra, Rotoaira Lapilli *P24*
3.11 Mangatoetoenui Quarry [T20/459153]; Mangamate Tephra *P24*
3.12 Desert Road S.11 [T20/464092]; Mangamate Tephra, Pahoka Tephra, Poronui Tephra *P25*
3.13 Mangatoetoenui Quarry [T20/459153]; Pahoka Tephra *P25*
3.14 Bullot Track S.1 [T20/412108]; Bullot Formation type section *P26*
3.15 Waikato Stream S.1 [T20/467102]; Bullot Formation, Mangamate Tephra *P26*
3.16 [T20/463101]; Bullot Formation, Pahoka Tephra, Mangamate Tephra . . *P27*
3.17 Desert Road S.11 [T20/464092]; Bullot Formation, Mangamate Tephra *P27*
3.18 Wahianoa Road S.1 [T20/391986]; Bullot Formation, Waimihia Tephra *P28*
3.19 The Chute S.3 [T20/437045]; Pourahu Member *P28*
3.20 Mangatoetoenui Quarry [T20/459153]; Pourahu Member, Mangamate Tephra *P29*
3.21 The Chute Type Locality; pumice bomb *P29*
3.22 Whangaehu River S.1 [T20/399954]; Shawcroft Tephra *P30*
3.23 Helwan Quarry [T20/408921]; Shawcroft Tephra *P30*
3.24 Rangipo Desert; Bullot Formation surfaces *P31*
4.1 Accretionary lapilli *P32*
4.2 Non-skeletal type [I] and skeletal type [II] olivines *P33*
4.3 Skeletal olivines *P34*
4.4 Vitric pyroclasts: Tufa Trig Formation tephras *P35*
4.5 Colour-banded lapilli; Pourahu Member *P37*
4.6 Type-1 vitric pyroclast morphology *P38*
4.7 Type-1 vitric pyroclast morphology *P39*
4.8 Type-2 vitric pyroclast morphology *P39*
4.9 Vitric pyroclast morphology *P40*
4.10 Vitric pyroclasts *P41*
4.11 Pumice fragment *P42*
4.12 Type-4 vitric pyroclast morphology *P42*
4.13 Ferromagnesian crystal morphology *P43*
4.14 Concoidally fractured pyroxene crystals *P44*
4.15 Rhyolitic glass shards *P45*
5.1 Onetapu Formation Type Locality, Karioi Forest *P46*
5.2 Onetapu Formation Type Section [T20/319906] *P46*
5.3 Onetapu Formation Type Section [T20/319906] *P47*
5.4 Type Locality, S.2 [T20/320904]; Onetapu Formation *P47*
5.5 Type Locality, S.3 [T20/319904]; Onetapu Formation *P48*
5.6 Rangipo Desert; Onetapu Formation *P48*

continued ...

LIST OF PLATES

Plate 5.7 Whangaehu River; Onetapu Formation *P49*
5.8 Northwestern Rangipo Desert; Onetapu Formation *P49*
5.9 Southern Rangipo Desert; Onetapu Formation *P50*
5.10 Scorpion Gully Reference Locality; Onetapu Formation, Mangaio Formation *P50*
5.11 Scorpion Gully Reference Locality; Mangaio Formation, Onetapu Formation *P51*
5.12 Scorpion Gully Reference Locality; Mangaio Formation *P51*
5.13 Mangaio Formation Type Section [T20/408047]; Mangaio Formation . . *P52*
5.14 Manutahi Formation Type Section [T20/410035]; Manutahi Formation *P52*
5.15 Manutahi Formation Type Section [T20/410035]; Manutahi Formation *P53*
5.16 Death Valley S.5 [T20/409045]; Manutahi Formation, Whakatane Tephra, Motutere Tephra, Tangatu Formation *P53*
5.17 Bullot Track S.2 [T20/420110]; Manutahi Formation *P54*
5.18 Tangatu Formation Type Section [T20/409045]; Tangatu Formation . . *P54*
5.19 The Badlands, Rangipo Desert *P55*
5.20 Helwan S.2 [T20/407917]; Tangatu Formation, Bullot Formation *P55*
5.21 Helwan Quarry (north face) [T20/408921]; Tangatu Formation, Bullot Formation *P56*
5.22 Helwan Quarry (north face) [T20/408921]; Tangatu Formation *P56*
5.23 Helwan Quarry (south face) [T20/408921]; Tangatu Formation *P57*
5.24 Helwan Quarry (south face) [T20/408921]; Tangatu Formation, Ngamatea lapilli-1 . . . . . *P57*
5.25 Whangaehu Escarpment; Te Heuheu Formation *P58*
5.26 Southern Rangipo Desert; dune sands *P58*
5.27 Bullot Track; eroding Bullot Formation tephras *P59*
5.28 Passage of 1975 lahar across Whangaehu Fan *P60*

LIST OF CHARTS AND MAPS

Chart	1	Stratigraphy of tephras younger than Bullot Formation (< *c.* 10 000 years B.P.)	pocket
	2	Stratigraphy of Mangamate Tephra members (*c.* 9780 – 9700 years B.P.)	pocket
	3	Stratigraphy of Bullot Formation tephras (*c.* 22 500 – 10 000 years B.P.)	pocket
	4	Stratigraphy of laharic deposits (*c.* 22 500 – 0 years B.P.)	pocket
Map	1	Section locations	pocket
	2	Distribution of laharic deposits	pocket

LIST OF ABBREVIATIONS

TVZ	Taupo Volcanic Zone
RVC	Rotorua Volcanic Centre
OVC	Okataina Volcanic Centre
MVC	Maroa Volcanic Centre
TVC	Taupo Volcanic Centre
TgVC	Tongariro Volcanic Centre
T.L.	Type locality
T.S.	Type section
R.S.	Reference section
S.	Section
Opx.	Orthopyroxene
Cpx.	Clinopyroxene
Oliv.	Olivine
Hbe.	Hornblende
Bio.	Biotite
Cmgt.	Cummingtonite
Wo/Wo%	Wollastonite
En/En%	Enstatite
Fs/Fs%	Ferrosilite
Mg №	Magnesium number
MGMT	MgO *vs* $(MnO + TiO_2)$
NCMT	$Na_2O/(Na_2O + CaO)$ *vs* $(MnO + TiO_2)$
MNCA	MnO *vs* CaO
C.V.	Coefficient of variation
S.C.	Similarity coefficient
EMP	Electron microprobe
XRF	X-ray fluorescence
TAS	Total alkali silica
HFF	Hyperconcentrated flood flow
DF	Debris flow
SF	Stream flow

CHAPTER ONE
INTRODUCTION

1.1 Regional Setting

Taupo Volcanic Zone

Taupo Volcanic Zone [TVZ] (Figure 1.1, p. 2) is a volcanic arc and marginal basin of the Taupo – Hikurangi arc system, representing the southern continuation of the Tonga – Kermadec Island arc, and the oblique subduction of the Pacific plate beneath the Indian plate (Cole and Nairn 1975; Hackett 1985; Graham and Hackett 1987; Patterson and Graham 1988). TVZ extends 250 km northeast across the central portion of the North Island from Ohakune to White Island. It is a region of Pliocene to Recent tectonic activity and volcanism, and forms the eastern half of a much larger area of crustal extension and Quaternary volcanism termed the Central Volcanic Region (Stern 1986). It is described as a volcano-tectonic depression marked by grabens and calderas (Healy 1964b).

Rhyolitic volcanism has dominated at TVZ, with four late Quaternary rhyolitic volcanic centres (Rotorua [RVC], Okataina [OVC], Maroa [MVC], Taupo [TVC]) situated in the broad *c.* 50 km central portion of the region [1]. Voluminous siliceous deposits (pyroclastic flows, lavas, tephras) of Pleistocene and Holocene age erupted from these centres have infilled this central region to a depth of several kilometres (Ewart *et al.* 1975; Cole 1981, 1990; Graham and Hackett 1986) (Figure 1.1, p. 2).

Tongariro Volcanic Centre

Most of the andesites of TVZ occur within Tongariro Volcanic Centre [TgVC] located at the southwestern end of TVZ (Cole 1990) (Figure 1.1, p. 2; Figure 1.2, p. 3). Tongariro Volcanic Centre is part of a young (< 250 ka) andesitic – dacitic volcanic arc which extends along the eastern margin of TVZ, and which has no associated rhyolitic volcanism (Graham and Hackett 1987).

Tongariro Volcanic Centre comprises four major andesitic massifs (Kakaramea – Tihia, Pihanga, Tongariro and Ruapehu), two smaller eroded centres (Maungakatote, Hauhungatahi), and two satellite vents (Pukeonake scoria cone, Ohakune Craters) (Cole *et al.* 1986). The volcanoes of TgVC rest on non-volcanic marine sediments which are of Tertiary age, and which overlie basement Mesozoic greywacke (Fleming and Steiner 1949; Grindley 1960, 1965; Hackett 1985).

---

[1] Two additional rhyolitic volcanic centres (Kapenga, Mangakino) from which ignimbrites were erupted are recognised by Wilson *et al.* 1984. These structures are largely buried by younger TVZ ignimbrites.

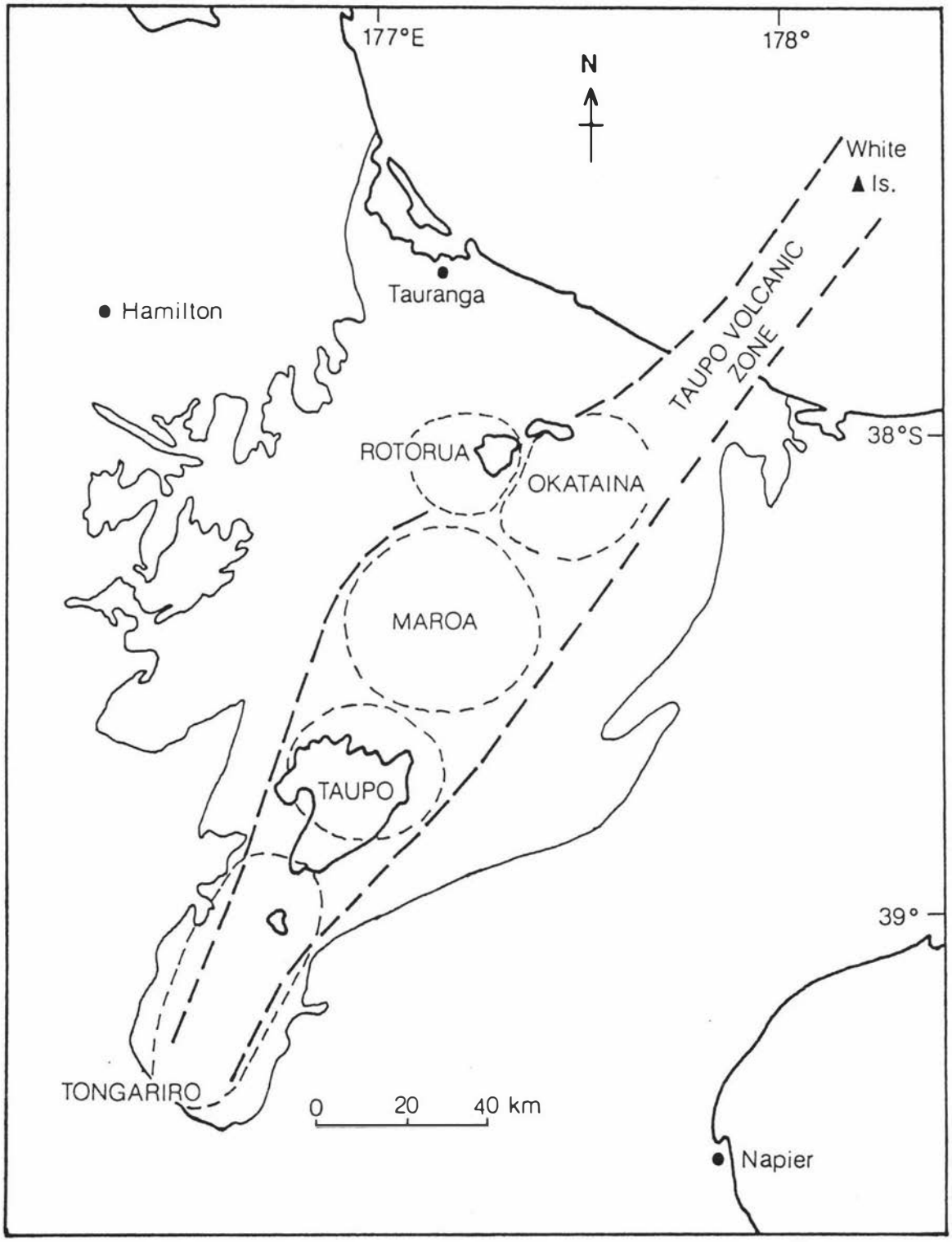

Figure 1.1 Volcanic centres of Taupo Volcanic Zone (Rotorua, Okataina, Maroa, Taupo, Tongariro), central North Island, New Zealand (after Cole and Nairn 1975).

Volcanism probably began at TgVC in the lower Pleistocene [2], *c.* 1.7 million years ago,

[2] Gregg (1960a) had earlier suggested that the onset of volcanism at TgVC occurred within the Quaternary, based on the age of andesitic pebbles (late Castlecliffian age) found within conglomerates in the Rangitikei Valley and Pliocene-aged (Opoitian) non-volcanic marine sediments which underlie TgVC volcanics.

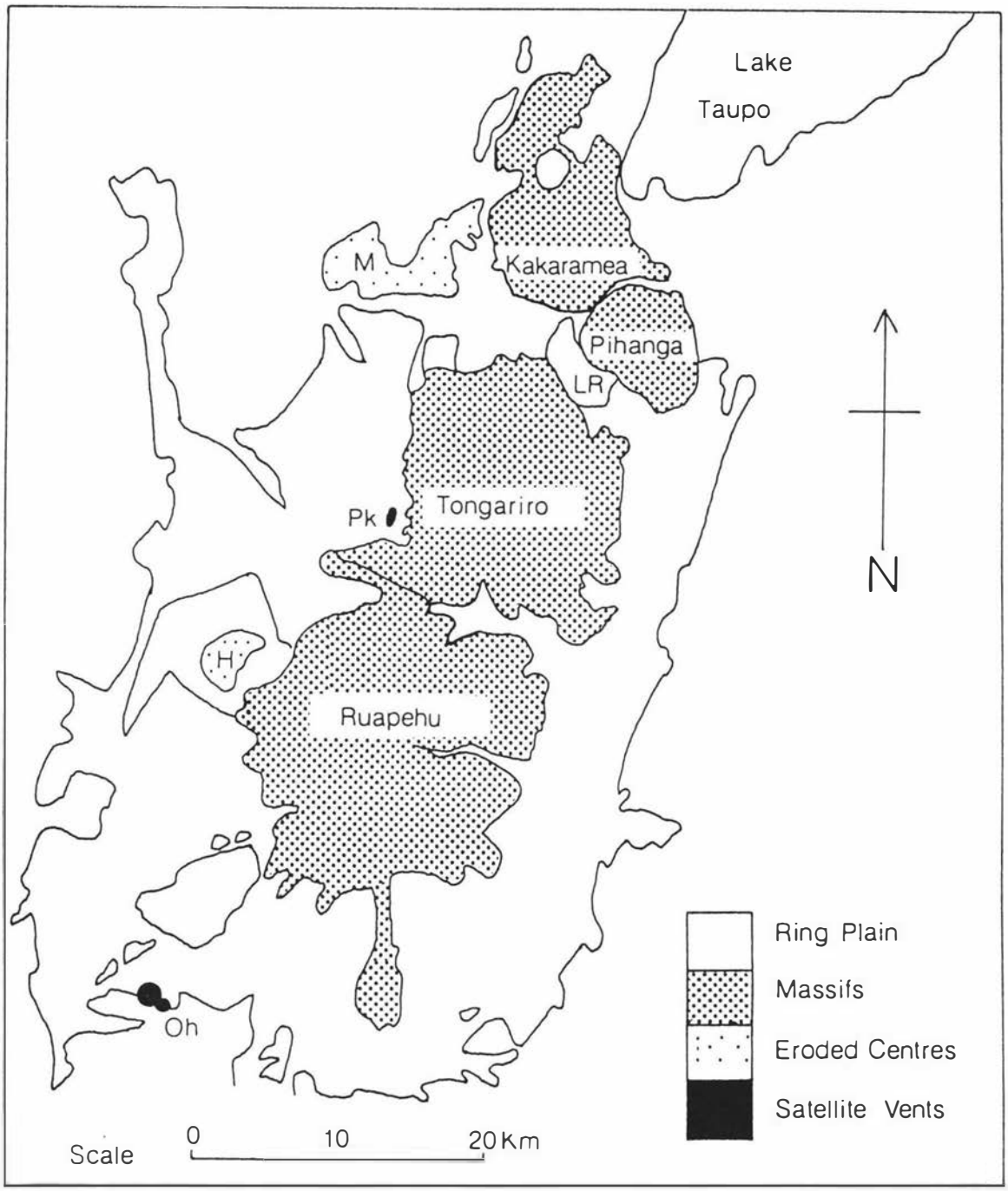

Figure 1.2 Andesite massifs and cones of Tongariro Volcanic Centre, and surrounding ring plains of Mt Ruapehu and Mt Tongariro (adapted from Cole *et al.* 1986).
(M = Maungakatote, Pk = Pukeonake, H = Hauhungatahi, Oh = Ohakune Craters, LR = Lake Rotoaira).

based on the age of andesite pebbles found near Wanganui (Williams 1986). The oldest exposed lavas at Mt Tongariro and Mt Ruapehu have been dated at 260 ka and 230 ka (K – Ar dates by Stipp 1968, *in* Cole 1982, and Patterson and Graham 1988 respectively).

Kakaramea – Tihia Massif is a multiple volcano situated in the northwestern part of TgVC. It is divided into two topographic units, Kakaramea and Tihia, separated by NNE – SSW trending normal faults. Mt Kakaramea (1300 m), which is an andesitic cone, forms the

summit of the massif. Mt Tihia, a lava dome, lies 3.5 km to the southeast. The oldest lava flows of Kakaramea Massif date between 190 – 222 ka. The youngest vents are located on the down-faulted Tihia block (Cole 1978; Williams 1986).

The younger and less dissected andesitic cone of Mt Pihanga (1325 m) lies southeast of Kakaramea – Tihia Massif. On the northwestern flanks of Pihanga are several young vents (including the Onepoto Craters and Lake Rotopounamu) associated with the Rotopounamu Graben which separates Mt Pihanga and Mt Tihia.

Mt Tongariro volcano comprises at least 12 composite cones. The summit, which reaches 1978 m, comprises seven craters (North Crater, West Crater, Upper Te Maari Crater, Lower Te Maari Crater, Red Crater, Blue Lake Crater, Oturere Crater). Depressions previously named South Crater and Central Crater are no longer considered craters, but are structural depressions bounded by the rims of craters and glacially eroded cones (Williams 1986). The presence of moraine bounded glaciated valleys (Matthews 1965; Topping 1974; Hackett and Houghton 1986) indicate erosion of the massif at some stage during the Last Glacial.

Mt Ngauruhoe (2291 m) is the youngest volcanic cone of Mt Tongariro, formed on the eroded southern flanks of an older remnant of Mt Tongariro. Eruptions at Mt Ngauruhoe began *c.* 2500 years B.P. (Nairn and Self 1978) resulting in the deposition of the widespread andesitic marker bed, Mangatawai Tephra.

Today Mt Tongariro is surrounded by the deeply dissected remnants of a lahar ring plain (Grindley 1960), and thick deposits of late Pleistocene to Holocene-aged tephras (Topping 1973).

Mt Ruapehu Volcano and Ring Plain

Mt Ruapehu is a composite andesitic strato-volcano comprising interbedded lava flows and thick pyroclastic deposits. It is the largest volcanic edifice of TgVC. The summit is 2797 m a.s.l. and is the highest point in the North Island.

The broad summit topography is thought to have formed as a result of multiple explosive vents and subsequent glacial erosion, rather than by caldera collapse (Cole and Nairn 1975; Hackett 1985). Five summit craters (East Crater, West Crater, North Crater, Girdlestone Crater, Dome Crater) are recognised (Williams 1986). The presently active summit vent situated within the western crater is occupied by Crater Lake – a warm, acidic (pH $\approx$ 1.2 – 1.8) lake, 0.2 x10^6 m^2 in area (Plate 1.1) (Giggenbach 1974; Cole and Nairn 1975).

Nine alpine glaciers occupy the present summit. The six major glaciers are Whangaehu and Mangatoetoenui (eastern side), Whakapapa and Mangaturuturu (western side), and

Mangaehuehu and Wahianoa (southeastern side). Other glaciers are Crater Basin Glacier, Tuwharetoa Glacier and Whakapapanui Glacier (Noble 1988).

Much of the volcano was eroded by glaciers during the Last (Otira) Glaciation (Hackett 1985). During this period the glaciers were considerably more extensive. Moraines on the massif, mapped by Hackett (1985) and M^{c}Arthur and Shepherd (1990) show the glaciers once extended down to approximately 1200 m a.s.l. Today they are all less than 1 km long, and occur above 2100 m a.s.l. Crater Basin Glacier is ablating at a rate of 3 – 5 m year^{-1} (Williams 1986). Wahianoa Valley on the southeastern flanks is a particularly prominent U-shaped glacial valley bounded by fluvially breached lateral and terminal moraines.

The river systems radiating from the summit of Mt Ruapehu are fed by these glaciers. Whangaehu River, which drains the southeastern slopes, is acidic due to contamination by highly acidic Crater Lake waters [3] which drain into its headwaters via a natural ice cave at the head of Whangaehu Glacier.

Below *c.* 1100 m, Mt Ruapehu is surrounded by an extensive ring plain constructed mainly from debris flow, hyperconcentrated flood flow, and tephra deposits (Plate 1.2; Plate 1.3). The ring plain is bounded to the north by lahar and tephra deposits of the Mt Tongariro ring plain, and to the south and west by block-faulted Tertiary marine sediments of the Wanganui Basin. In the east the volcanic deposits abut the Mesozoic greywacke of the Kaimanawa Range.

The location of vents within TgVC have been controlled by regional faulting (Gregg 1960a; Hackett 1985). These regional faults strike mostly NNE paralleling those of TVZ and show displacements of up to *c.* 15 m with downthrow toward the volcanic line (Gregg 1960a). At the southern end of TgVC, on the southeastern and southern flanks of Mt Ruapehu, these faults progressively change trend from NNE to E (Hackett 1985).

Small fissures or pull-apart structures identified in the Mt Tongariro and Mt Ruapehu regions probably formed during tectonism accompanying the ignimbrite-producing eruptions of the rhyolitic Kawakawa Tephra Formation and Taupo Pumice formations from TVC.

1.2 Previous Work: Geology of Tongariro Volcanic Centre

The geology of the four massifs (Ruapehu, Tongariro, Kakaramea, Pihanga), Pukeonake Scoria Cone, Pukekaikiore, and Hauhungatahi was first mapped by Grindley (1960) and Hay (1967) as twelve andesitic flows of Holocene and late Pleistocene age – Ruapehu Andesite (Ruapehu Massif); Tongariro, Red Crater, Te Maari, Pukekaikiore, North Crater, and

[3] Aspects of the chemistry of Crater Lake are discussed in Giggenbach (1974) and Wood (1977).

Ngauruhoe andesites (Tongariro Massif); and Kakaramea, Pihanga, Pukeonake, Pukekaikiore and Hauhungatahi andesites (named after the massifs and source vents). Many of these lavas were later dated and mapped by Topping (1974) using the cover bed tephrostratigraphy. Topping (1974) also mapped and dated lahar deposits of Kakaramea – Tihia (Hauhungaroa Lahars), Pihanga and Tongariro massifs.

Geology of Mt Ruapehu Volcano

Detailed study of the geology of Mt Ruapehu volcano was made by Hackett (1985), who defined four cone-building episodes at Mt Ruapehu, spanning the period *c.* 250 000 years B.P. to the present. These episodes are represented by the Te Herenga (> *c.* 130 000 years B.P.), Wahianoa (*c.* 120 000 – 60 000 years B.P.), Mangawhero (*c.* 60 000 – 15 000 years B.P.) and Whakapapa (*c.* 15 000 – 0 years B.P.) formations.

Te Herenga Formation deposits are exposed at Pinnacle Ridge, which is an eroded remnant of the former Te Herenga Cone. Deposits of Wahianoa Formation comprise the broad planeze surface between Wahianoa and Whangaehu river valleys on the southeastern flanks, and are particulary well exposed in both of these valleys. Mangawhero Formation deposits are exposed over most of Mt Ruapehu except in the southeast. These deposits comprise the main cone of Mt Ruapehu, and most of the present-day high peaks. Whakapapa Formation lavas are mostly restricted to the vent and flank areas.

The volcanic deposits of these formations have been grouped into four lithofacies associations – central and flank vent, proximal cone-building, distal ring plain, and satellite vent associations (Cole *et al.* 1986; Hackett and Houghton 1989). The first two associations include the deposits of the massif. The central and flank vent association occurs within *c.* 1.5 km of the vent regions. The principal lithofacies include small plug and dome-like intrusions, welded tephras and vent breccias. Deposits in the vent areas show pervasive hydrothermal alteration. The proximal cone-building association includes deposits of the slopes and outer flanks of the cone. The principal lithofacies are block lava flows and autobrecciated lavas.

Petrography of Tongariro Volcanic Centre Lavas

Early descriptions of lavas of TgVC were made by O'Shea (1959) who described the mineralogy of the Whakapapanui Gorge andesites of Mt Ruapehu. Following O'Shea, Clark (1960) classified the lavas of TgVC into five types (plagioclase andesite; plagioclase-pyroxene andesite; pyroxene andesite; olivine andesite; hornblende andesite) based on mineralogical differences. Following Clark (1960) the mineralogy of TgVC lavas has been extensively studied by many other workers (Ewart 1971; Topping 1974 [Tongariro]; Cole 1978; Kohn and Topping 1978 [Tongariro]; Cashman 1979; Hackett 1985 [Ruapehu]; Graham 1985; Graham

and Hackett 1986, 1987 [Ruapehu]; Patterson and Graham 1988 [Mangatepopo Valley, Upper Tama Lake]). Many of these studies have also detailed the bulk chemistry of TgVC lavas.

The compositions of lavas identified at TgVC range between basalts and dacites (52 – 67% SiO_2), but most of the lavas are porphyritic medium-K acid and basic andesites characterised by phenocrysts of calcic plagioclase, orthopyroxene, clinopyroxene, titanomagnetite, less commonly olivine, and rarely calcic hornblende.

Olivine andesites have been identified at the Te Maari and Red craters, Pukekaikiore, Pukeonake, Hauhungatahi, the Ohakune Craters, and in some lavas at Mt Ruapehu. Hornblende andesites show very restricted occurrences, at Tama Lakes and in flows of Maungakatote and Kakaramea. Basalts are restricted to Red Crater (Tongariro Massif) and a single flow on Mt Ruapehu, and dacites have so far been identified only on Mt Ruapehu. Hornblende dacite occurs within the lahar mounds of Murimotu Formation, dated [NZ1338] at 9500 ± 100 years B.P. by Topping (1974).

The petrography and bulk major and trace element chemistry of Mt Ruapehu lavas have been studied in detail by Hackett (1985). Lava compositions identified encompass the entire compositional range identified within TgVC, from basaltic (Ruapehu Basalt of Mangawhero Formation) to dacitic (also of Mangawhero Formation). The oldest lavas of Te Herenga Formation are dominantly olivine-free basic andesites, and acid andesites with SiO_2 contents between 53.8 and 58.8%. The younger Wahianoa lavas also include basic and acid andesites (54.3 – 61.2% SiO_2) but with greater compositional diversity. Mangawhero Formation lavas show the greatest compositional diversity, ranging from basalts to dacites (52.2 – 63.6% SiO_2), and including olivine-bearing basic and acid andesites. The youngest lavas of Whakapapa Formation include olivine-free acid andesites, one basic-andesite and two dacites (56.6 – 65.6% SiO_2) (Hackett 1985).

A new classification of TgVC lavas based on mineralogy, bulk rock and isotope chemistry (Graham 1985) is summarised in Cole *et al.* (1986), together with discussion of the petrogenesis of TgVC lavas.

Geology of the Mt Ruapehu Ring Plain

Descriptions prior to 1960, of ring plain deposits and their possible origins from lahars are reviewed in Gregg (1960b). Of significance is the work by Te Punga (1952). Andesitic boulders and fragmental andesitic materials recognised within the Hautapu and Rangitikei Valleys, south of TgVC, were defined and mapped as the Hautapu Valley Agglomerate by Te Punga (1952). Te Punga proposed that the source of the materials was Mt Ruapehu, and that they had been deposited by lahars of late Castlecliffian age that travelled south along Hautapu River. The deposit had previously been described as till by Park (1909, *in* Te Punga 1952).

The former course of Whangaehu River, and hence the passage of lahars, appears to have been down the Hautapu Valley. Later movement on the Whangaehu fault however, saw the capture of the headwaters of Hautapu River by the Whangaehu River (Topping 1974). Today the Hautapu and Whangaehu rivers drain quite separate catchments. Hautapu River now drains hill country east and south of Waiouru. Tributaries of Whangaehu River flow to the east of Mt Ruapehu, but upon meeting the Whangaehu fault escarpment become channelled into one main flow directed to the south.

Grindley (1960) was the first to distinguish and map lahar formations on the Mt Ruapehu ring plain. He defined five lahar formations: Murimotu, Hautapu, Waimarino, Rangipo, and the informally defined 'Lahars of Whangaehu River'. The Waimarino Lahars form a ring plain around Mt Ruapehu, with the younger Hautapu and Murimotu Lahars occurring at more restricted localities. Rangipo Lahars form the ring plain of Mt Tongariro (Grindley 1965; Cole and Nairn 1975).

Lahars mapped on the southeastern Mt Ruapehu ring plain are shown in Figure 1.3 (p. 9). The Murimotu, Hautapu and Waimarino lahars are mapped as late Pleistocene in age, and lahars of Whangaehu River as Holocene in age (Grindley 1960). Lahars on the western Mt Ruapehu ring plain were later mapped by Hay (1967) as the Waimarino and Murimotu formations.

Only an approximate lahar chronology was established by Grindley (1960) as none of the formations had been directly dated. Topping (1974) however identified Kawakawa Tephra Formation overlying Waimarino Lahars, and occurring beneath Murimotu Lahars, indicating that the Waimarino Lahars are older than, and the Murimotu Lahars younger than, *c.* 22 500 years B.P.

Based on the radiocarbon ages of Okupata Tephra (dated [NZ1189, NZ1374] between 12 450 ± 340 and 9790 ± 160 years B.P.[4]) found beneath a lahar unit of Murimotu Formation; wood from within the same unit (dated [NZ1338] at 9540 ± 100 years B.P.), and the age of Papakai Formation (dated by Topping [1973] between *c.* 9700 – 3400 years B.P.) found overlying these lahars, the Murimotu Formation lahars were dated by Topping (1974) at between *c.* 12 450 and 9540 years B.P.

Grindley (1960), Hay (1967), and Topping (1974) considered the deposits of Murimotu Formation to be from lahars. More recently, Palmer and Neall (1989) have shown the formation comprises the deposit of a single debris avalanche, and associated lahars. The surface topography of the avalanche deposit is characterised by numerous mounds or hummocks.

---

[4] Lowe (1988a) has dated Okupata Tephra between 13 000 and 10 000 years B.P. (see section 3.3).

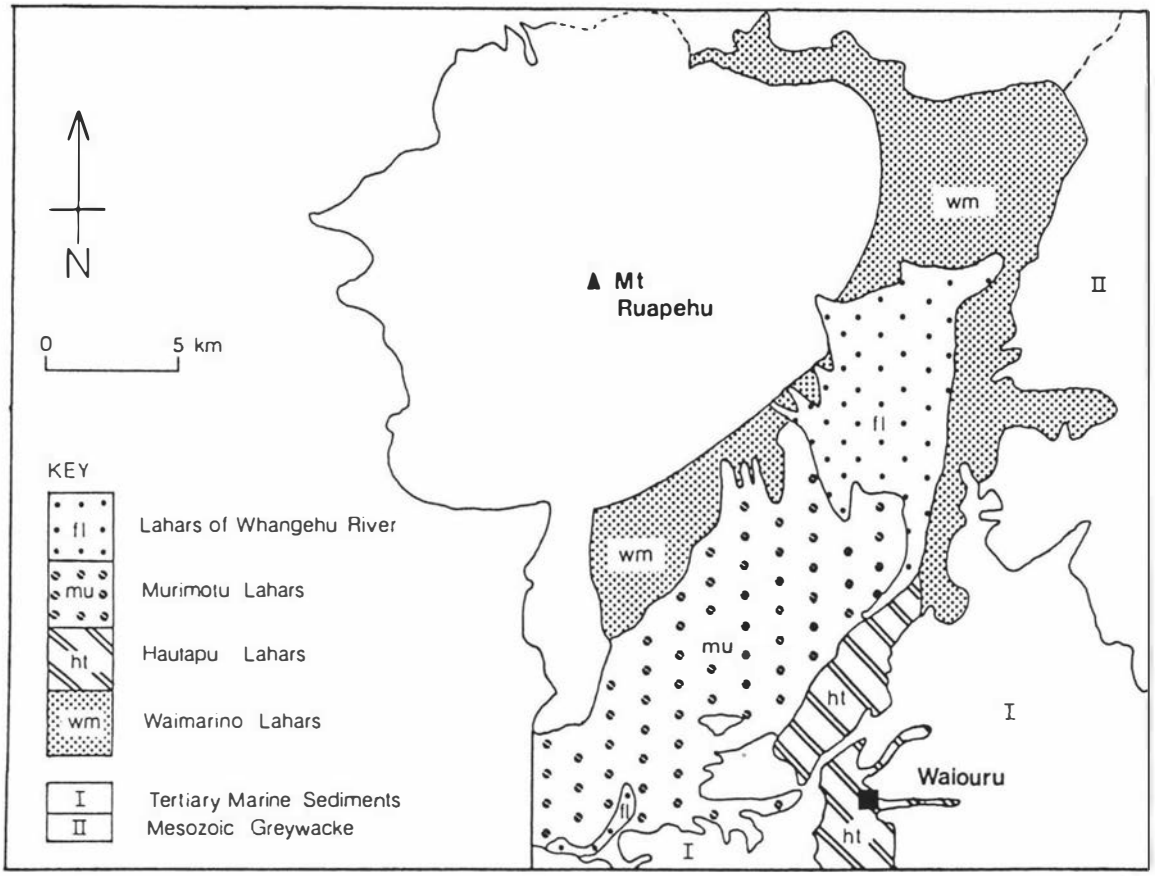

Figure 1.3 Lahar formations of the southeastern Mt Ruapehu ring plain, mapped by Grindley (1960). Figure adapted from Grindley's (1960) *Geological Map of New Zealand*, Sheet 8 Taupo 1:250 000.

Deposits of the ring plain have been only briefly discussed by Hackett (1985). These deposits comprise Hackett's (1985) distal ring plain association, which includes tephras, the deposits of lahars (debris flows and hyperconcentrated flood flows), stream flow, debris avalanches and valley-filling lava flows. Lavas comprise only a small proportion of the ring plain deposits – most lava flows do not extend beyond the base of the cone.

Prior to this study, tephras preserved on the Mt Ruapehu ring plain, with the exception of the *c.* 13 000 – 10 000 year old Okupata Tephra of Topping (1973), had not been studied in detail. Only a framework stratigraphy of these deposits existed, established from the isopach maps of tephras sourced from Mt Tongariro and mapped on the Mt Tongariro ring plain by Topping (1973).

1.3 Purpose and Scope of This Study

Previous studies conducted within TgVC have so far detailed the stratigraphy and chronology of pyroclastic deposits of the Mt Tongariro ring plain (Topping 1974) and Mt Ruapehu volcano (Hackett 1985). Other recent studies (Palmer and Neall 1989; Purves 1990) have detailed aspects of the Holocene stratigraphy on the Mt Ruapehu ring plain, but

as yet there has been no overall detailed study of the pre-historic [5] activity at Mt Ruapehu as determined from the types, stratigraphy and chronology of the ring plain deposits.

From a study of the historic record (Gregg 1960a; Cole and Nairn 1975; Houghton *et al.* 1987) it can be readily ascertained that Mt Ruapehu has been very active in recent time. The propensity of lahar generation at this volcano within the last 130 years is well recognised and documented.

To date, studies of the potential hazard to the Mt Ruapehu region from future eruptions at Mt Ruapehu volcano have been based only on these most recent events. Far greater appreciation of the potential hazard at this volcano can be obtained from the study of pre-historic deposits preserved on the ring plain.

The mineralogy and chemistry of TgVC lavas has been exhaustively researched and there now exists a large database for TgVC lavas. Prior to this study however, there were very few published accounts of the mineralogy and chemistry of tephra deposits within TgVC, and virtually no data existed on the tephras erupted from Mt Ruapehu.

Detailed study of the mineralogy and chemistry of TgVC tephras [6] would provide a database useful to the identification and correlation of these tephras and the subsequent dating of landforms within the region, and an understanding of eruption processes both at Mt Ruapehu and within TgVC.

The principal objectives of this study were therefore as follows:

1. To elucidate the stratigraphic record of tephras and lahars sourced from Mt Ruapehu within the last *c.* 22 500 years and directed to the east of the volcano.

2. To map the distribution of the tephra and lahar deposits identified on the southeastern Mt Ruapehu ring plain.

3. To investigate the mineralogy and chemistry of tephras erupted from Mt Ruapehu and Mt Tongariro.

---

[5] In this study 'historic' is used to refer to the period of written, documented accounts of volcanic activity (*i.e.* since 1861 A.D.), while 'pre-historic' refers to the period prior to such recording.

[6] Thorarinsson (1974) defines tephra *as a collective term for all airborne pyroclastics, including both air-fall and flow pyroclastic material.* In New Zealand, the term 'tephra' is generally equated with pyroclastic fall deposits, and the term 'ignimbrite' with pyroclastic flow deposits (welded or unwelded). This usage of 'tephra' and 'ignimbrite' is adopted in this study.

Descriptive size terms for tephra, as defined by Fisher (1961) and Schmid (1981) are: fine ash (<0.063 mm), coarse ash (0.063 – 2 mm), lapilli (2 – 64 mm), blocks or bombs (>64 mm). In this study, the lapilli fraction is subdivided into very fine lapilli (2 – 4 mm), fine lapilli (4 – 16 mm), medium lapilli (16 – 32 mm), and coarse lapilli (32 – 64 mm).

4. **To produce integrated lahar and tephra hazard maps based on the distribution and frequency of the late Quaternary and Holocene lahar and tephra deposits recognised and mapped in this study.**

1.4 Location of the Study Area

The study area is principally confined to the southeastern sector of the Mt Ruapehu ring plain as depicted in Figure 1.4 (p. 12). Boundaries are approximated by the Rangataua Lava Flow to the west, the Mt Tongariro ring plain to the north, the foothills of the Kaimanawa Range to the east, and State Highway 49 (S.H.49) to the south. The area enclosed is *c.* 200 km^2, encompassing the entire Karioi State Forest and Rangipo Desert (below 1200 m a.s.l.), and much of the length of the Desert Road. Areas within Rangipo Desert which fall outside of the National Park boundary are zoned for military use by the New Zealand Army. Access to this area by non-military personnel is restricted [7].

The southeastern sector of the Mt Ruapehu ring plain was selected for study because it is here that most of the tephras have been deposited under the influence of the prevailing northwesterly and westerly winds, and where the most complete tephra record is therefore preserved. It is also an area where the deposits of many Mt Ruapehu-sourced lahars have accumulated.

Geographic Names – Rangipo Desert

The absence of named features (vehicle and walking tracks, river tributaries, trig points) within Rangipo Desert has necessitated the naming of localities and topographic features to clarify location of type, reference and information sections defined within the study area (Map 1). The locality names used here (Figure 1.5, p. 13) are informal, and are not approved New Zealand Geographic Board names.

[7] Permission to enter this area must be obtained from the Operations Branch at Waiouru Military Camp.

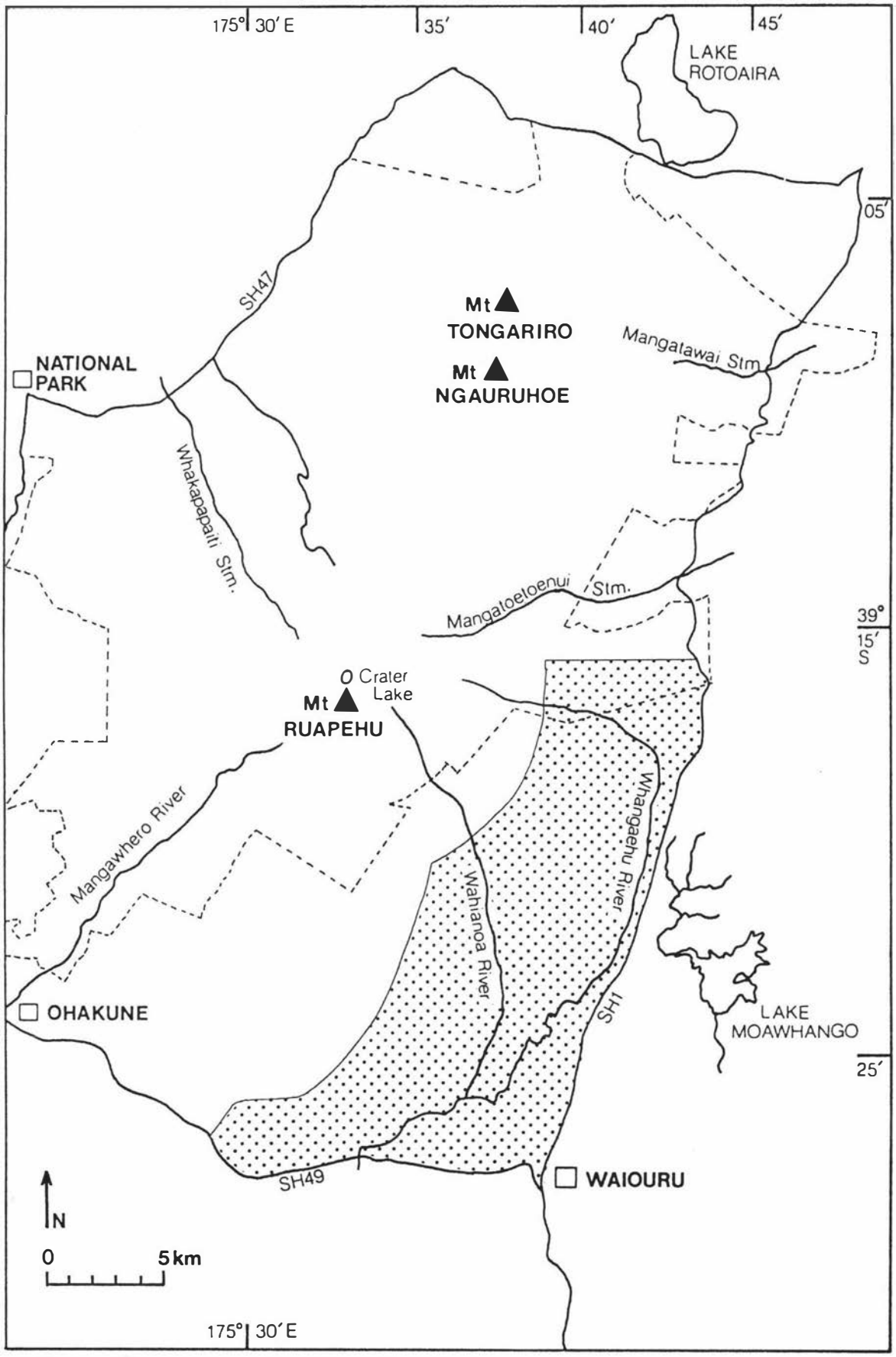

Figure 1.4 Location of the study area (shaded) on the southeastern Mt Ruapehu ring plain, Tongariro Volcanic Centre.

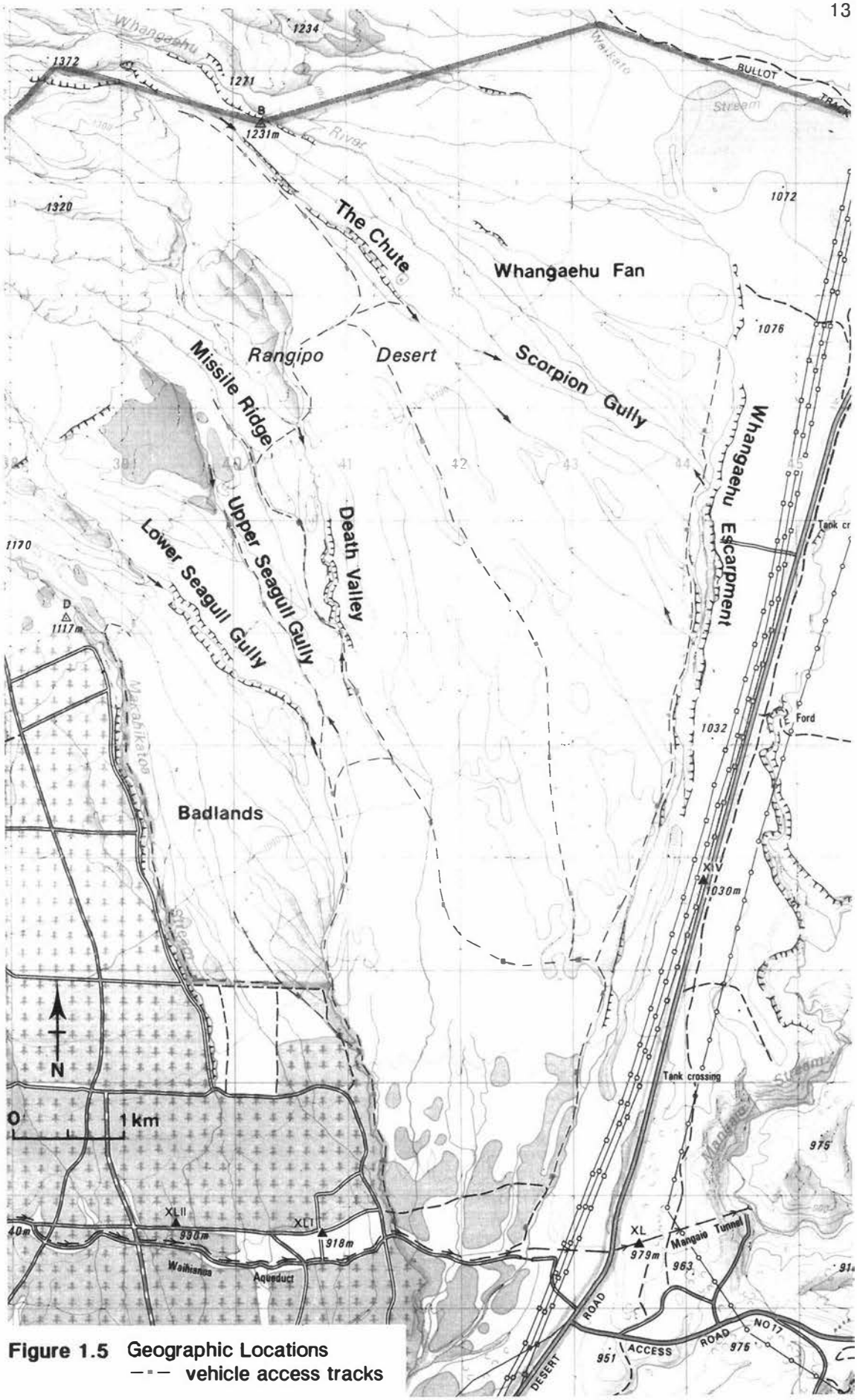

Figure 1.5 Geographic Locations
— · — vehicle access tracks

CHAPTER TWO
IDENTIFICATION AND CORRELATION OF RHYOLITIC TEPHRAS, TONGARIRO VOLCANIC CENTRE

Introduction

Tongariro Volcanic Centre [TgVC] is the most southern of the main tephra-producing volcanic centres of the Central North Island. To the north are Taupo Volcanic Centre [TVC], Maroa Volcanic Centre [MVC] and Okataina Volcanic Centre [OVC], from which tephras of rhyolitic composition were dispersed southwards to TgVC. Most of the late Pleistocene and Holocene rhyolitic tephras have been reliably dated.

Rhyolitic tephras identified within the TgVC are valuable time-planes for the dating of andesitic tephras and sediments with which they are interbedded. In this study the rhyolitic, and previously dated andesitic tephras (Topping 1973, 1974) are used to establish a new chronology of andesitic tephras and lahar deposits of the southeastern Mt Ruapehu ring plain.

The first part of this chapter reviews the existing stratigraphy and chronology of rhyolitic tephras identified and correlated within TgVC. The later sections detail the stratigraphy, mineralogy and distribution of the rhyolitic tephras identified in this study. Identification and correlation of these rhyolitic tephras has been determined from their stratigraphic positions, ferromagnesian assemblages and chemistry of glass shards. Fourteen rhyolitic tephras are identified. A nearly complete Holocene stratigraphy of TVC rhyolitic tephras is recorded in sequences throughout the Mt Ruapehu region. Three of the tephras (Kaharoa Tephra, Whakatane Tephra, Waiohau Tephra) have not previously been identified within TgVC. The known range for most of the other tephras is also now extended.

2.1 Previous Work: Rhyolitic Tephrostratigraphy, Tongariro Volcanic Centre

The stratigraphy of rhyolitic tephras erupted over the past *c.* 22 500 years and preserved in the northern part of TgVC has been detailed by Topping and Kohn (1973). Earlier studies at TgVC had identified only Taupo Pumice (Thomas 1889; Grange and Hurst 1929; Grange 1931; Baumgart 1954; Healy 1964a), and Oruanui Formation (Gorton 1966; Vucetich and Pullar 1969) within the tephra record at TgVC. Topping and Kohn (1973) identified thirteen rhyolitic tephras of late Pleistocene to Holocene age, erupted from TVC, OVC, and MVC, and belonging to the Taupo and Rotorua subgroups. The tephras were used to date and correlate andesitic tephras of the northern Mt Tongariro region.

The 13 rhyolitic tephras were identified by stratigraphic position, radiocarbon dating, heavy mineral assemblages, and titanomagnetite chemistry. Also identified was Puketarata

Tephra, erupted from MVC, which is not grouped into either the Taupo or Rotorua subgroups. A further six rhyolitic tephras were identified by Topping (1974), and include Okareka Tephra, dated at *c.* 17 000 years B.P. (Nairn 1981), Okaia Tephra dated at *c.* 22 000 years B.P. (Howorth *et al.* 1981), and Rotoehu Tephra, dated at *c.* 50 000 years B.P. (Froggatt and Lowe 1990).

Stratigraphy of the Taupo and Rotorua Subgroups

Taupo Subgroup

Taupo Subgroup comprises tephras of Holocene age (10 000 years B.P. to present) erupted from TVC. Healy (1964a) redescribed members of the Taupo Ash Sequence of Baumgart (1954), retaining the 26 members originally defined and renaming the sequence the Taupo Subgroup. A description of named members is given in Healy (1964a, 1965). The youngest member is Taupo Pumice Formation and the oldest, Karapiti Tephra (Howorth *et al.* 1981) (Table 2.1, p. 16). Tephras of late Pleistocene age (*c.* 40 000 – 22 500 years B.P.) erupted from TVC are grouped into the Okaia Subgroup (Howorth *et al.* 1981). Together, Taupo Subgroup tephras, Kawakawa Tephra Formation, and Okaia Subgroup tephras form the Lake Taupo Group (Howorth *et al.* 1981).

Rotorua Subgroup

Rotorua Subgroup (Howorth *et al.* 1981) is defined as all rhyolitic tephras erupted from OVC younger than Kawakawa Tephra Formation (dated *c.* 22 500 years B.P.). The youngest member is Tarawera Formation (1886 A.D.) and the oldest, Te Rere Tephra (*c.* 21 100 years B.P., Froggatt and Lowe 1990). Rotorua Subgroup had previously been defined by Vucetich and Pullar (1964) to comprise tephras from OVC, extending from Rerewhakaaitu Tephra (14 700 years B.P.) at the base, up to and including Rotomahana Mud Member of Tarawera Formation (Table 2.1, p. 16). Tephras of late Pleistocene age (*c.* 40 000 – 22 500 years B.P.) erupted from OVC comprise the Mangaone Subgroup (Howorth *et al.* 1981). The Rotorua and Mangaone subgroups together form the Okataina Group (Howorth *et al.* 1981).

Stratigraphic Revision of Rhyolitic Tephra Formations

Recent revision of the stratigraphy of the Central North Island rhyolitic tephras has led to redefinition of three tephra formations (Hinemaiaia Ash, Papanetu Tephra, Oruanui Formation) which were recognised by Topping and Kohn (1973) at TgVC. The stratigraphy of Taupo Pumice Formation, and the stratigraphic relationships of Whakatane Ash (Vucetich and Pullar 1964) and Hinemaiaia Ash (Vucetich and Pullar 1973), have also been revised.

Table 2.1 Stratigraphy of Taupo and Rotorua subgroup tephras (adapted from Howorth *et al.* 1981).

Taupo Subgroup Tephras	Rotorua Subgroup Tephras	Age * (years B.P.)	^{14}C No †	Reference to Age
	Tarawera Tephra	(1886 A.D.)		Pullar *et al.* (1973)
	Kaharoa Ash	665 ± 58	XP7,XP9	Lawlor (1980)
Taupo Pumice		1819 ± 17 ‡		Healy (1964a)
Mapara Tephra		*c.* 2100	NZ1068 NZ1069	Vucetich & Pullar (1973)
Whakaipo Tephra		*c.* 2700	NZ1070 NZ1071	Vucetich & Pullar (1973)
Waimihia Tephra		*c.* 3400	NZ179	Healy (1964a)
Hinemaiaia Tephra		4650 ± 80	NZ4574	Froggatt (1981b)
	Whakatane Tephra	4770 ± 170 ‡		Lowe (1986)
Motutere Tephra		5370 ± 90	NZ4846	Froggatt (1981b)
	Mamaku Tephra	7050 ± 77	NZ1152	Pullar *et al.* (1973)
	Rotoma Tephra	7330 ± 235	NZ1119	Pullar *et al.* (1973)
Opepe Tephra		8850 ± 1000	NZ185	Pullar *et al.* (1973)
Poronui Tephra		*c.* 9900 ‡	Wk351 Wk352 Wk491	Lowe & Hogg (1986)
Karapiti Tephra		9910 ± 130	NZ4847	Froggatt (1981a)
	Waiohau Tephra	11 250 ± 200	NZ568	Cole (1970a)
	Rotorua Tephra	13 450 ± 250	NZ1615	Nairn (1980)
Puketerata Tephra ◆		*c.* 14 000 §		Lowe (1988a)
	Rerewhakaaitu Tephra	14 700 ± 200	NZ716	Pullar *et al.* (1973)
	Okareka Tephra	*c.* 17 000 §		Nairn (1981)
	Te Rera Tephra	21 500 ± 450	NZ5171	Nairn (1981)
Kawakawa Tephra Fm.		22 590 ± 230 ‡		Wilson *et al.* (1988)

* All ^{14}C ages discussed are conventional ages in radiocarbon years B.P. based on the old (Libby) half life of 5568 years.
† NZ prefix: New Zealand Radiocarbon Dating Laboratory (Lower Hutt).
Wk prefix: University of Waikato Radiocarbon Dating Laboratory (Hamilton).
‡ Average or combined radiocarbon age.
§ Estimated age.

◆ Puketerata Tephra, erupted from Maroa Volcanic Centre and dated *c.* 14 000 years B.P. (Lowe 1988a) is not included in either the Taupo or Rotorua subgroups.

Taupo Pumice Formation

Taupo Pumice Formation was originally defined by Healy (1964a) to comprise the uppermost members 1 to 8 of the Taupo Subgroup, revising the stratigraphy of earlier workers (Baumgart 1954; Baumgart and Healy 1956). This stratigraphy and nomenclature was adopted by Vucetich and Pullar (1964, 1973) but was later revised by Froggatt (1981d) to

comprise four members of airfall and pyroclastic flow origin erupted from TVC *c.* 1819 years B.P. The four members are listed below with their equivalent Taupo Subgroup (TSG) member names in parentheses.

Taupo Ignimbrite	(TSG members 1 and 2)	– youngest
Taupo Lapilli	(TSG member 3)	
Rotongaio Ash	(TSG member 4)	
Hatepe Tephra	(TSG members 5, 6 and 7)	– oldest

A comparison of the stratigraphy and nomenclature of Taupo Pumice Formation with that of other workers is given in Froggatt (1981d) [1].

Topping and Kohn (1973) identified Rotongaio Ash (Baumgart 1954; Healy 1964a) and 'putty ash' (Vucetich and Pullar 1973) members of Taupo Pumice Formation (Healy 1964a) in the Mt Tongariro region. Using the stratigraphy and nomenclature of Froggatt (1981d), 'putty ash' member is stratigraphically equivalent to the 'ash unit' within Hatepe Tephra.

Many names have been used in both the mapping and description of Taupo Subgroup members 1 and 2. Froggatt (1981d) recommended use of only Taupo Ignimbrite and Taupo Pumice Formation for description of these units. However, Froggatt and Lowe (1990) have since proposed use of the name Taupo Tephra Formation.

Hinemaiaia Ash

Hinemaiaia Ash was defined by Vucetich and Pullar (1973) as the rhyolitic tephra lying conformably between Whakatane Ash and Rotoma Ash (Table 2.2, p. 18). Hinemaiaia Ash was redefined and renamed by Froggatt (1981b) to comprise two formations; Hinemaiaia Tephra and Motutere Tephra (Table 2.2, p. 18). Motutere Tephra (Froggatt 1981b) is a new formation belonging to the Taupo Subgroup. These formations are separated by a paleosol, representing about 750 years between the eruption of the basal lapilli (Motutere Tephra) and the upper ash layers (Hinemaiaia Tephra) (Froggatt 1981b).

In the Taupo region, Froggatt (1981b) defined Motutere Tephra as the rhyolitic tephra lying conformably between the paleosol on Opepe Formation, and the paleosol below Hinemaiaia Tephra Formation. He defined Hinemaiaia Tephra Formation as the rhyolitic tephra lying conformably between Waimihia Lapilli and the paleosol that caps Motutere Tephra (Froggatt 1981b). Hinemaiaia Tephra is dated [NZ4574] at 4650 ± 80 years B.P., and Motutere Tephra is dated [NZ4846] at 5370 ± 90 years B.P. (Froggatt 1981b) (Table 2.1, p. 16).

---

[1] See Figure 1 (p. 233) in Froggatt (1981d).

At the De Bretts type section for Hinemaiaia Ash (Vucetich and Pullar 1973), Motutere Tephra is absent, so that here Hinemaiaia Tephra occupies the stratigraphic position of Vucetich and Pullar's (1973) 'Hinemaiaia Ash'.

Topping and Kohn (1973) correlated a rhyolitic tephra interbedded with the andesitic Papakai Tephra Formation of Topping (1973) to Hinemaiaia Ash of Vucetich and Pullar (1973) (Table 2.2, p. 18). Motutere Tephra is interbedded with a bed of the andesitic Papakai Tephra east and south of Taupo (Froggatt 1981b), which suggests the ash identified as Hinemaiaia Ash by Topping and Kohn (1973) in the Mt Tongariro region is probably Motutere Tephra.

Table 2.2 Comparison of the stratigraphy of Hinemaiaia Tephra, Motutere Tephra (Taupo Subgroup) and Whakatane Tephra (Rotorua Subgroup) of Lowe (1986) with that of previous workers.

Vucetich & Pullar (1973)	Topping & Kohn (1973)	Kohn *et al.* (1981)	Howorth & Ross (1981)	Froggatt (1981b)	Lowe (1986)	Age * (years B.P.)
Waimihia Formation	Waimihia Lapilli	Waimihia Lapilli	Waimihia Lapilli	Waimihia Lapilli	Waimihia Lapilli	*c.* 3400
		unnamed ash			Hinemaiaia Tephra	*c.* 4650
Whakatane Ash		Whakatane Tephra	Whakatane Tephra	Whakatane Tephra	Whakatane Tephra	*c.* 4770
				Hinemaiaia Tephra		
Hinemaiaia Ash	Hinemaiaia Ash	Hinemaiaia Ash	Hinemaiaia Ash	Motutere Tephra	Motutere Tephra	*c.* 5370
			Mamaku Tephra			*c.* 7050
Rotoma Ash	Rotoma Ash					*c.* 7730
Opepe Tephra	Opepe Tephra			Opepe Tephra		*c.* 8850

* All ^{14}C ages discussed are conventional ages in radiocarbon years B.P. based on the old (Libby) half life of 5568 years.

Whakatane Ash

Recent revision of the tephra stratigraphy of Tiniroto and Poukawa sites in Hawke's Bay by Lowe (1986) has re-established the stratigraphic relationship of Waimihia Formation, Whakatane Ash and Hinemaiaia Ash. Hinemaiaia Ash identified beneath Whakatane Ash (Howorth *et al.* 1980; Howorth and Ross 1981; Kohn *et al.* 1981) is re-identified as Motutere Tephra based on radiocarbon age of the tephra determined from the enclosing peat (Froggatt 1981b), and stratigraphic position relative to Hinemaiaia Tephra (Lowe 1986) (Table 2.2, p. 18). An unnamed rhyolitic tephra identified between Waimihia Formation and Whakatane Ash by Kohn *et al.* (1981) is identified as Hinemaiaia Tephra (Lowe 1986) (Table 2.2, p. 18) based on stratigraphic position, radiocarbon age, ferromagnesian mineralogy and glass shard chemistry. Mineralogy and glass chemistry indicate a TVC source. Whakatane Ash is

therefore bracketed by TVC-sourced tephras which have now been identified as the Hinemaiaia Tephra and Motutere Tephra formations (Lowe 1986), revising the earlier stratigraphy of Vucetich and Pullar (1973), Howorth and Ross (1981), and Kohn *et al.* (1981), who placed Whakatane Ash above Hinemaiaia Ash (Table 2.2, p. 18).

Mean radiocarbon ages determined for Hinemaiaia Tephra and Whakatane Tephra are *c.* 4500 and *c.* 4800 years B.P. respectively (Lowe 1986), based on new dates obtained from Lakes Poukawa (Hawke's Bay), Rotomanuka (Hamilton), Okoroire (Tirau), Kaipo Lagoon (Waikaremoana), and existing dates from previous workers.

Papanetu Tephra

Papanetu Tephra (Topping and Kohn 1973) was a new formation name given to a rhyolitic tephra exposed in areas north of Mt Tongariro, within TgVC. Papanetu Tephra immediately underlies Te Rato Lapilli (Topping 1973) and occupies the same stratigraphic position as the rhyolitic Karapiti Tephra. The name Karapiti Tephra (Froggatt 1981a) replaces the previous Karapiti Lapilli of Vucetich and Pullar (1973).

Topping and Kohn (1973) proposed that the eruption of Papanetu Tephra immediately followed that of Karapiti Tephra, and assigned both tephras an age of 9785 years B.P., based on bracketing radiocarbon ages [NZ1372, NZ1373] of Papanetu Tephra. Karapiti Tephra has since been radiocarbon dated [NZ4847] at 9910 ± 130 years B.P. by Froggatt (1981a) (Table 2.1, p. 16). Froggatt and Solloway (1986) have since established the newly proposed Papanetu Tephra as the distal correlative of Karapiti Tephra, based on stratigraphy, chronology, ferromagnesian mineralogy, and glass and mineral chemistry.

Karapiti Tephra is used in preference to Papanetu Tephra (Froggatt and Solloway 1986) since the name Karapiti has been applied to the most extensive and stratigraphically useful part of the distribution. A revised isopach map for Karapiti Tephra is presented in Froggatt and Solloway (1986) [2].

Oruanui Formation

Vucetich and Pullar (1969) defined Oruanui Formation as rhyolitic tephra of airfall and pyroclastic flow origin which underlies Mokai Sand, and overlies Mangaone Formation. The upper contact with Mokai Sand is an erosional unconformity.

---

[2] See Figure 5 (p. 310) in Froggatt and Solloway (1986).

The stratigraphy and nomenclature of Oruanui Formation (Vucetich and Pullar 1969) has been revised many times (Nairn 1971; Howorth 1975). Vucetich and Howorth (1976a, 1976b) revised the stratigraphy and nomenclature of all earlier workers by redefining Oruanui Formation of Vucetich and Pullar (1969) to comprise three new tephra formations – Kawakawa Tephra Formation, Poihipi Tephra and Okaia Tephra. Kawakawa Tephra Formation represents the youngest tephra identified within Vucetich and Pullar's Oruanui Formation. It comprises three members – Oruanui Breccia, Scinde Island Ash Member and Aokautere Ash Member. Oruanui Breccia (Vucetich and Howorth 1976b) is stratigraphically equivalent to the Oruanui Breccia of Vucetich and Pullar (1969).

A comparison of the stratigraphy and nomenclature of Vucetich and Howorth (1976a, 1976b) with that of earlier workers (Vucetich and Pullar 1969; Nairn 1971; Howorth 1975) is given in Vucetich and Howorth (1976b) [3]. Recent discussion of the nomenclature for the *c.* 22 500 years B.P. (Wilson *et al.* 1988) event from Taupo has seen recommendation for replacement of the name Kawakawa Tephra Formation (Vucetich and Howorth 1976a, 1976b) with Wairakei Breccia (Self and Healy 1987) and Oruanui Formation (Wilson 1988), and for the retention of Kawakawa Tephra Formation (Froggatt *et al.* 1988; Froggatt and Lowe 1990). The formation name 'Kawakawa Tephra' is recommended for use by Vucetich and Howorth (1976a) in preference to Aokautere Ash where two or more members of Kawakawa Tephra Formation are identified. Aokautere Ash, identified in the Manawatu by Cowie (1964), is able to be correlated with Kawakawa Tephra Formation (Kohn 1973, 1979; Mew *et al.* 1986). More recently, Froggatt and Lowe (1990) have proposed redefinition of Kawakawa Tephra Formation to include only two formations – Oruanui Ignimbrite (previously Oruanui Breccia of Vucetich and Pullar 1976a) and Aokautere Ash. The authors propose that the name Aokautere Ash be used for all the airfall ash within Kawakawa Tephra Formation, previously described as two formations – Scinde Island Ash and Aokautere Ash (Vucetich and Howorth 1976a). The nomenclature of Froggatt and Lowe (1990) is adopted in this study.

In the Mt Tongariro region, Topping and Kohn (1973) identified Oruanui Breccia and Oruanui Ash at Poutu S. [T19/481325]. Using the nomenclature and stratigraphy of Froggatt and Lowe (1990), Oruanui Breccia and the chalazoidite-studded Oruanui Ash of Topping and Kohn (1973) correlate with the Oruanui Ignimbrite and Aokautere Ash members of Kawakawa Tephra Formation, respectively.

[3] See Figure 1 (p. 52) in Vucetich and Howorth (1976a).

2.2 Previous work: Methods for Identifying Rhyolitic Tephras

Ferromagnesian Mineral Assemblages

As a first approach, in both New Zealand and overseas studies, the identification of rhyolitic tephras has relied upon the determination of ferromagnesian mineral assemblages, and the recognition of diagnostic ferromagnesian minerals within the phenocryst assemblage.

The ferromagnesian mineralogy of Central North Island rhyolitic tephras has been determined by many workers, especially Ewart (1963, 1966, 1967b, 1971), Cole (1970a), Kohn (1973), Kohn and Glasby (1978), and Froggatt (1982a). A summary of the ferromagnesian mineral assemblages characteristic of eruptives from the Central North Island rhyolitic centres (Taupo, Okataina, Maroa) determined by these and other authors is presented in Lowe (1980) and given below. Three dominant ferromagnesian mineral assemblages are identified:

(1) Hypersthene ± augite
(2) Hypersthene + calcic hornblende ± cummingtonite
(3) Biotite + calcic hornblende ± hypersthene

Taupo Volcanic Centre Tephras

Tephras erupted from TVC comprise assemblage (1), and may in addition contain rare biotite, amphibole and olivine (Ewart 1963; Ewart *et al.* 1975). All TVC tephras are hypersthene-dominant with minor amounts of augite (< 20%) (Froggatt 1981c), hornblende and biotite (Froggatt 1981c, 1982a).

Within the Lake Taupo Group two distinct mafic mineralogies are identified. Tephras of the Taupo Subgroup (10 000 – 0 years B.P.) are distinctly more orthopyroxene- and less hornblende-rich than the older Okaia Subgroup tephras (*c.* 45 000 – 20 000 years B.P.). The distinction is reflected in contrasting glass and Fe-Ti oxide chemistries (Froggatt 1982a). Late Pleistocene tephras from TVC contain hornblende and cannot be distinguished from OVC tephras on this basis (Lowe 1980).

Okataina Volcanic Centre Tephras

Tephras erupted from OVC comprise assemblages (2) and (3), with the exception of three OVC tephras which are hornblende-poor and which exhibit assemblage (1) mineralogy (Lowe 1980). Howorth (1976) and Lowe (1987, 1988a, 1989) define OVC tephra assemblages as comprising hornblende + hypersthene + augite ± cummingtonite ± biotite. Biotite, hornblende and hypersthene are the most useful minerals in tephra identification (Kohn 1973). Biotite and cummingtonite are diagnostic minerals of eruptives from OVC and

MVC (Ewart 1966, 1968, 1971; Cole 1970a, 1970c; Ewart *et al.* 1971; Kohn 1973; Nairn and Kohn 1973; Howorth 1976; Kohn and Glasby 1978).

Biotite is a useful marker mineral for tephra identification when present in amounts greater than 15%, as in Kaharoa Tephra (>15%), Rotorua Tephra (15 – 20%), Puketarata Tephra (35 – 80%), Rerewhakaaitu Tephra (35 – 80%), and Okareka Tephra (15 – 20%) (Kohn and Glasby 1978).

Cummingtonite has only been identified in tephras erupted from Haroharo Complex, located to the north of OVC (Ewart 1966, 1968, 1971; Ewart *et al.* 1971; Kohn 1973), and occurs as the dominant ferromagnesian mineral in Whakatane Tephra, Rotoma Tephra (Ewart 1966), and Rotoehu Tephra (Kohn 1973; Howorth 1976; Lowe 1980) (dated *c.* 50 000 years B.P.). Cummingtonite occurs in minor amounts (<5%) in other OVC tephras (Kaharoa Tephra, Waiohau Tephra, Rerewhakaaitu Tephra, Te Rere Tephra, Mangaone Formation) (Kohn 1973).

Ferromagnesian mineralogy distinguishes Taupo Subgroup tephras and older TVC (Okaia Subgroup), OVC and MVC tephras. The uniform mineralogy exhibited by tephras of the Taupo Subgroup, however, prevents distinction between formations on mineralogy alone (Froggatt 1981c).

OVC tephras (Kaharoa Tephra, Rotorua Tephra, Rerewhakaaitu Tephra) and the only MVC eruptive presently identified (Puketarata Tephra), can be distinguished by the relative abundance of biotite in the ferromagnesian mineral assemblage and stratigraphic position (Kohn and Glasby 1978). Absolute abundances are dependent upon effects of sedimentary fractionation and winnowing of minerals during transport (Westgate and Gorton 1981; Froggatt 1982a), and post-depositional effects of contamination through reworking and mixing with local tephra. They are therefore not necessarily diagnostic of individual tephras (Smith and Westgate 1969; Westgate and Fulton 1975).

Studies by Cole (1970a), Pullar *et al.* (1977), Kohn and Glasby (1978), Howorth *et al.* (1980, 1981), Lowe *et al.* (1980), Froggatt (1981a, 1981b), Kohn *et al.* (1981), Hogg and McGraw (1983), and Lowe and Hogg (1986) have seen tephras identified from relative stratigraphic position, radiocarbon age and ferromagnesian mineralogy without the assistance of glass and mineral chemistry.

Tephra Chemistry

(I) Bulk Chemical Methods

Fe-Ti Oxides

During the late 1960s and early 1970s bulk sample techniques were used in an attempt to distinguish and correlate individual late Pleistocene and Holocene tephras of the Taupo and Rotorua subgroups, based on their chemical composition. Such techniques involved analysis of bulk titanomagnetite separates for both trace and major element chemistry by optical emission spectroscopy and X-ray fluorescence.

Preliminary investigation of titanomagnetite chemistry of Taupo Subgroup tephras was carried out by Ewart (1967a) and is reviewed in Kohn (1973). More recent studies have focused on the use of titanomagnetite chemistry for identification and correlation of tephras.

Kohn (1970) introduced the use of titanomagnetite chemistry as a rapid means of tephra identification, by determining the titanomagnetite chemistry of 15 Central North Island Quaternary tephras younger than 50 000 years B.P., and demonstrating that all could be distinguished by their titanomagnetite compositions. The ratios of Ti:V, V:Mn, and Co:Mn used in combination, and elemental abundances of V and Cr served to distinguish each of the tephras. Additional separation was facilitated using titanomagnetite chemistry in conjunction with ferromagnesian assemblage and to a lesser extent, bulk pumice chemistry (Kohn 1970).

Kohn (1973) and Kohn and Topping (1978) identified two compositional groupings within Taupo Subgroup tephras based on titanomagnetite compositions. Tephras older than Hinemaiaia Tephra (*c.* 4650 years B.P.) can be distinguished from the younger tephras (Hinemaiaia Tephra – Taupo Pumice) by their higher V, Cr and Ni contents.

Other studies have demonstrated the use of titanomagnetite chemistry in the identification and correlation of distal rhyolitic tephras (Kohn 1973; Lewis and Kohn 1973; Milne 1973; Nairn and Kohn 1973; Topping and Kohn 1973; Pullar *et al.* 1977; Kohn and Glasby 1978), and ignimbrites (Kohn 1973; Nairn and Kohn 1973; Kohn 1979), and in the support of correlations of distal rhyolitic tephras made on the basis of stratigraphy and ferromagnesian mineralogy. Titanomagnetite chemistry supported correlation of seven Holocene to late Pleistocene tephras (Waimihia Tephra, Hinemaiaia Ash, Poronui Tephra, Karapiti Tephra, Puketarata Tephra, Rerewhakaaitu Tephra, Kawakawa Tephra Formation) (Topping and Kohn 1973). Lewis and Kohn (1973) and Kohn and Glasby (1978) later used titanomagnetite chemistry to identify and correlate rhyolitic tephras preserved offshore in deep-sea cores. Taupo Pumice Formation, Waimihia Formation (Lewis and Kohn 1973), Rerewhakaaitu Tephra and Kawakawa Tephra Formation (Kohn and Glasby 1978) were each identified by titanomagnetite chemistry in conjunction with ferromagnesian mineral assemblage.

Bulk Tephra Composition

There are few studies in which the bulk compositions of pumice or ash have been determined for purposes of tephra identification and distinction (Kohn 1973; Pullar *et al.* 1977; Nairn 1980; Froggatt 1981c, 1982a). Earlier work by Ewart (1966, 1969) and others [4] used bulk tephra chemistry principally as a means of compositionally characterising and classifying rhyolitic pyroclastic deposits of the Central North Island.

Kohn (1973) established that bulk tephra analysis was a quick method for identifying major chemical differences between tephras. Compared to bulk titanomagnetite analyses, bulk tephra compositions were shown to be a less useful means of separating OVC and TVC tephras, with most tephras already adequately distinguished by titanomagnetite chemistry and ferromagnesian assemblage (Kohn 1973). Similarly, bulk compositions of Holocene tephras from TVC were determined by Froggatt (1981c, 1982a). The Holocene tephras collectively show higher CaO, MgO, Al_2O_3, and FeO, and lower SiO_2 abundances. Although individual eruptives within the Taupo Subgroup vary little in both major and trace element chemistry, three broad compositional groups may be discerned: Taupo Pumice – Mapara Tephra, Whakaipo Tephra – Motutere Tephra, and Opepe Tephra – Karapiti Tephra.

Other studies have applied bulk chemistry of glass separates to problems of tephra identification and distinction (Ewart 1963; Howorth and Rankin 1975; Howorth 1976; Froggatt 1982a). Kohn (1973) reviews the earliest studies using bulk glass chemistry for purposes of distinguishing Central North Island Taupo and Rotorua subgroup rhyolitic tephras. The glass analyses enabled identification of some chemical differences between TVC, OVC and MVC tephras.

Limitations inherent in bulk analysis methods have led to a decline in this approach to tephra correlation studies in preference for discrete-grain methods such as electron microprobe analysis. Discrete-grain methods are a preferred analysis option, especially in tephra studies which involve the correlation of thin, often poorly preserved distal tephras where contamination of bulk samples is unavoidable. Bulk tephra analysis has not been widely applied to tephra correlation studies because of the effect on composition of detrital contaminants, weathering products, variations in the kind and amount of primary minerals within a single tephra, and the presence of inclusions and microlites (Wilcox 1965; Smith and Westgate 1969; Kohn 1973; Cole 1978; Westgate and Gorton 1981; Froggatt 1983). Discrete differences in composition and effects of zoning are obscured in bulk analysis (Ewart 1971).

[4] See p. 22, in Kohn (1973).

(II) Discrete-Grain Methods

Electron Microprobe Analysis of Fe-Ti Oxides

Toward the end of the 1970s and especially within the last decade, electron microprobe (EMP) analysis of tephric components (ferromagnesian minerals, plagioclase, glass) has become a standard procedure in the discrimination of rhyolitic tephras based on their chemical composition.

Early work by Ewart *et al.* (1971) determined coexisting titanomagnetite and ilmenite compositions of some Taupo Subgroup tephras, and OVC domes and tephras. Their work is reviewed in Kohn (1973). Abundance of Ti, Al, V and Fe in titanomagnetites, and Ti and Mn abundances in ilmenites, served to distinguish eruptives of TVC from those of OVC (Kohn 1973).

Kohn (1973, 1979) used EMP analysis of titanomagnetites to avoid problems of contamination in the correlation of distal Kawakawa Tephra Formation (Tirimoana Ash), and to support and revise earlier identifications and correlations of Central North Island ignimbrite deposits older than 44 000 years B.P. Titanomagnetite chemistry, used in conjunction with ferromagnesian assemblage, served to distinguish most TVZ ignimbrites. Froggatt (1982a), however, found Fe-Ti oxide chemistry of no use in distinguishing older ignimbrite deposits.

Fe-Ti oxide compositions have been used by Froggatt and Solloway (1986) in the identification and correlation of the distal Papanetu Tephra with Karapiti Tephra, and by Froggatt (1982a) in an attempt to distinguish between Taupo Subgroup tephras. Only Taupo Pumice Formation and Mapara Tephra can be distinguished using the FeO, MgO and TiO_2 content of their titanomagnetites. Hogg and M^{c}Graw (1983) used Fe-Ti ratios in titanomagnetites to identify individual tephras and their source, especially Rotoehu Tephra, in mixed tephra sequences at Coromandel.

Ti, V, and Cr abundances are the most useful elements for identification (Kohn 1973). Bulk titanomagnetite and EMP analyses are comparable in all elements except Si, Al, and Mg which are affected by orthopyroxene and glass impurities in bulk analysis.

Electron Microprobe Analysis of Volcanic Glass

Recent tephra studies in New Zealand have emphasised use of glass shard chemistry determined by electron microprobe as a means of identifying and correlating Central North Island rhyolitic tephras. The method was introduced into New Zealand tephra studies by Froggatt (1982a, 1983), following the work of Smith and Westgate (1969) in the United States. Smith and Westgate (1969) developed the technique as an accurate and rapid means of determining the chemical composition of tephras. Froggatt (1982a) used glass chemistry

to compositionally distinguish Central North Island Quaternary rhyolitic tephras and ignimbrites.

Froggatt (1982a) concluded that the major element chemistry of glass shards could be used to distinguish Holocene (Taupo Subgroup) and late Pleistocene (Okaia Subgroup) tephras erupted from TVC, and Taupo Subgroup tephras from Kawakawa Tephra Formation, Puketarata Tephra (MVC), and OVC (Rotorua Subgroup tephras). The distinction was made using abundances of the oxides FeO, CaO, Al_2O_3, TiO_2, MgO and K_2O. Lowe (1986, 1989) used FeO and CaO contents of glass shards to distinguish between Taupo and Rotorua Subgroup tephras, with the latter showing lower FeO, CaO, Al_2O_3, TiO_2 and MgO, and higher K_2O content. Stokes and Lowe (1988) identified FeO, MgO, K_2O, TiO_2 and Na_2O as the most discriminatory elements.

Tephras within Taupo Subgroup vary little in chemistry and generally cannot be distinguished on glass chemistry, with the exception of Taupo Pumice Formation and Mapara Tephra which show more mafic chemistry (higher MgO, FeO, TiO_2) (Froggatt 1982a), and Whakaipo Tephra which is distinguished by its lower FeO and CaO contents (Lowe 1988a, 1988b). Similarly, tephras within Rotorua Subgroup are difficult to distinguish. Rotorua Tephra, however, can be distinguished from the others by its higher FeO and CaO contents (Lowe 1988a, 1988b) (Figure 2.3, p. 47). Puketarata Tephra (erupted from MVC) is also distinguished by its distinctly lower Ti and Mg contents (Lowe 1988b).

Glass chemistry has been used in many other studies to support the identification and correlation of distal rhyolitic tephras where provisional correlation had been made on the basis of field stratigraphy and ferromagnesian assemblage – for example; Kohn (1979) [correlation of Tirimoana Ash to Kawakawa Tephra Formation], Green and Lowe (1985) [correlation with Waiohau Tephra], Froggatt and Solloway (1986) [correlation of Papanetu Tephra with Karapiti Tephra], Lowe (1986) [correlation of an unnamed ash (Kohn *et al.* 1981) with Hinemaiaia Tephra], Mew *et al.* (1986) [correlation with Kawakawa Tephra Formation], Lowe (1987, 1988a, 1988b), Wallace (1987), Pillans (1988), and Froggatt and Rodgers (1990) [identification of TVC and OVC tephras]. Overseas studies (Westgate and Fulton 1975, 1981; Smith and Okazaki 1977; Westgate and Gorton 1981) have shown preference toward using glass shard chemistry in the identification and correlation of tephras.

Microprobe Analysis in Tephra Studies

EMP analysis is a discrete-grain method highly suited to studies involving the identification and correlation of distal tephras by their chemical compositions. Contaminant detrital materials, weathering products, bubbles, inclusions and microlites within phenocryst phases or glass shards can be avoided during analysis (Kohn 1973; Westgate and Fulton 1975). Furthermore, mixed populations in samples, resulting from reworking and mixing with local tephras, can be identified (Kohn 1973; Froggatt 1982a, 1983).

The ability to avoid contaminants is a major advantage of the microprobe, as is the ability to analyse very small tephra samples. Only a few individual grains are required to adequately characterise a tephra (Froggatt 1982a) thus allowing tephras of only a few millimetres in thickness, or microscopically represented tephras, to be readily identified. Glass is generally abundant, easily concentrated, and shows a narrow compositional range within individual tephras (Westgate and Gorton 1981). One disadvantage of EMP analysis, however, is the limited capability for measuring trace elements (Westgate and Gorton 1981). Concentrations of Ni, Co, Cr, Zr and Cu have been shown to be useful in tephra correlation (Kohn 1970, 1973) but are most often present in concentrations below the detection limits of the microprobe.

EMP analysis of volcanic glass has proved an effective and popular method for determining the chemical compositions of pyroclastic deposits, and is perhaps the single most useful method for determining tephra source.

Other Methods

Studies both overseas and in New Zealand have attempted differentiation of tephras using refractive index measurements of glass and ferromagnesian minerals (Powers and Wilcox 1964; Wilcox 1965; Randle *et al.* 1971; Kittleman 1973; Mullineaux 1974; Hodder and Wilson 1976; Steen-M^{ac}Intyre 1977). Refractive index measurement as a method of tephra identification is limiting because of the generally narrow refractive index range exhibited by rhyolitic tephras (Ewart 1963; Ninkovich 1968; Smith and Westgate 1969; Kohn 1970; Mullineaux 1974) and the effect of weathering and hydration on refractive index measurements (Froggatt 1982a; Fisher and Schmincke 1984).

The refractive index of glass has not been found useful in New Zealand tephra studies (Kohn 1973) but has been found useful in overseas studies (Powers and Wilcox 1964; Wilcox 1965) for distinguishing some major tephra marker beds (Mazama and Glacier Peak tephras). Refractive index determination is a time-consuming method and this has discouraged its use (Westgate and Gorton 1981).

The major and trace element chemistry of ferromagnesian phenocryst separates (augite, amphibole [including cummingtonite], and biotite) from some TVZ rhyolitic pyroclastics (tephras and domes) has been determined by Ewart (1967a, 1971) and Ewart and Taylor (1969) using X-ray fluorescence and emission spectrographic analysis. Phenocryst chemistries were determined as part of geochemical and petrographic studies of TVZ rhyolites, rather than for purposes of tephra identification and correlation.

Froggatt (1982a) analysed phenocryst orthopyroxene and hornblende in TVC rhyolitic tephras by EMP to evaluate their use in chemically fingerprinting tephras. He concluded that ferromagnesian mineral chemistry was of little use in tephra separation and that analysis of

orthopyroxenes as a means of chemically discriminating between TVC rhyolitic tephras is inconclusive. However, Froggatt and Solloway (1986) have since used major element pyroxene chemistry (determined by EMP) to assist the correlation of Papanetu Tephra (Topping and Kohn 1973) with Karapiti Tephra.

Major element (EMP) analyses of ferromagnesian minerals (pyroxene, biotite, amphibole [including cummingtonite] in OVC tephras (*esp*. Rotorua Tephra, Rerewhakaaitu Tephra, Whakatane Tephra and Rotoehu Ash) are given in Howorth (1976), Lowe (1987), Howorth and Ross (1981), but these have not been used specifically for purposes of tephra correlation. Overseas studies by Dudas *et al.* (1973) used the chemistry of phenocryst ferromagnesian mineral separates to successfully distinguish and correlate Quaternary rhyolitic tephras in the western United States.

Summary of Methods

Determination of the chemistry of Central North Island rhyolitic tephras by X-ray fluorescence analysis, emission spectrographic analysis, and more recently EMP analysis, has generated a wealth of chemical information used in the 'fingerprinting' of these tephras. For many years now, attempts have been made to discriminate tephras on their mineralogy (ferromagnesian mineral assemblages), chemical compositions (bulk and microprobe analysis of Fe-Ti oxide, glass, and to a lesser extent, ferromagnesian mineral chemistry), refractive indices of glass, and by statistical analysis of chemical data (Howorth and Rankin 1975; Stokes and Lowe 1988).

Ferromagnesian assemblages, glass and titanomagnetite chemistries all serve to distinguish source – however, the chemical similarity of tephras within each centre limits the ability of any one method for distinguishing tephras at member level. Present-day identification of distal tephras most often employs, as a 'first approach', determination of the ferromagnesian assemblage together with EMP analysis of major element glass shard chemistry. Both glass chemistry and ferromagnesian assemblages are valuable identifiers of tephra source.

Most late Pleistocene and Holocene rhyolitic tephras (younger than 20 000 years B.P.) have been adequately fingerprinted through a combination of stratigraphic information, mineralogical assemblages and glass shard chemistry, facilitating their identification and correlation in distal areas.

Recognised inaccuracies and limitations of bulk analysis methods in determining chemical compositions of tephras, critical to correlation, has seen progressive replacement of these methods by EMP analysis. However bulk methods are necessary for determination of trace element compositions which have been found useful in distinguishing tephras (Kohn 1973; Westgate and Gorton 1981).

Recent tephra studies in New Zealand have employed neither refractive index measurement nor chemistry of phenocryst ferromagnesian minerals as a means of distinguishing rhyolitic tephras.

Future tephra studies will undoubtedly involve the identification of tephras at ever-increasing distances from source. Identification will best be achieved using grain discrete methods suited to the analysis of small samples which may be contaminated with local deposits.

2.3 Methods for Identifying Rhyolitic Tephras on the Mt Ruapehu Ring Plain

The various methods used to characterise, distinguish and correlate rhyolitic tephras have been discussed in the previous section. Based on previous findings, the methods described below have been selected as the most suitable for the identification and correlation of rhyolitic tephras recognised in the study area.

Basis of Field Identification

1. Recognition of Rhyolitic Tephras

(a) Tephra colour and composition

Rhyolitic tephras are characteristically light coloured due to the dominance of glass shards, and may be recognised from their strong colour contrast with the enclosing andesitic tephras. The latter are typically iron-stained producing strong brown, yellowish brown and orange colours. The abundance of glass shards in rhyolitic tephras imparts a quite different field character to that of the andesitic ash and lapilli beds. Tephras from TVC and OVC are relatively distal, and therefore are more likely to be preserved as fine ash layers rather than lapilli layers.

(b) Expected occurrence

Using the isopach information of Central North Island rhyolitic tephras (Lloyd 1972; Pullar and Birrell 1973) and other work (Topping and Kohn 1973), we can expect Holocene and late Pleistocene tephras from TVC and OVC to be found within TgVC. The stratigraphic positions of these tephras within the local andesitic tephra sequence can be established once the andesitic tephra stratigraphy and chronology is determined.

2. Provisional Correlation with Tephra Source and Named Tephra Formations

(a) Numerical-age dating of tephras

Numerical age dating (Colman *et al.* 1987) of tephras (*e.g.* by radiocarbon dating of interbedded wood, twigs, charcoal, or enclosing peats) will provide a quantitative

estimate of age, and improve the likelihood of correct correlation. Most of the rhyolitic tephras younger than *c.* 22 500 years B.P. are already reliably dated.

(b) Correlated-age dating

Correlated-age dating (Colman *et al.* 1987) provides an age for a tephra where it can be demonstrably correlated with an independently dated tephra (*e.g.* by equivalence of stratigraphic position and field characteristics).

(c) Relative-age dating

Relative-age dating (Colman *et al.* 1987) will provide an approximate chronology (a 'ball-park' age) for the rhyolitic tephras, established from their relative stratigraphic positions to known and dated andesitic tephra formations, thus narrowing the field of possible correlatives.

(d) Field appearances

Rhyolitic tephras within the Mt Ruapehu region are preserved most commonly as thin pocketing or 'cream cake' fine ash and lapilli layers interbedded with locally derived andesitic tephras, medial, and sedimentary deposits. Bedding characteristics and appearances may be used to provisionally distinguish some tephra members (*e.g.* Waimihia Lapilli, Aokautere Ash Member of Kawakawa Tephra Formation). Ignimbrites are readily distinguished from airfall tephras on field appearances. Distinctive characteristics may be used for correlation with known ignimbrite deposits of the central North Island.

Basis of Laboratory Identification

As discussed in section 2.2, confident identification and correlation of distal rhyolitic tephras with known tephra formations nearly always requires support from laboratory-based fingerprinting methods. Fingerprinting methods used in this study, and the reasons for their selection are outlined below.

1. Identification of Tephra Source

(a) Ferromagnesian mineral assemblages

Ferromagnesian assemblages and diagnostic ferromagnesian minerals characteristic of the Central North Island tephras are used to identify tephra source. The presence, and less so the absence, of diagnostic ferromagnesian minerals is a reliable indicator of tephra source.

(b) Glass shard chemistry

Compositional differences in major element chemistry of glass shards can be used to identify the source of distal tephras. The chemistry of glass shards is used in

preference to the analysis of Fe-Ti oxides and ferromagnesian minerals for the following reasons:

(i) Glass shards constitute the greater volume of the tephras and are easily separated.

(ii) The distinct morphology of rhyolitic and andesitic glass shards allows contaminant andesitic tephra to be avoided during analysis. Recognition of contaminant ferromagnesian minerals and Fe-Ti oxides is undoubtedly more difficult, especially where abundances are minor and concentration of the minerals is required.

(iii) The most recent tephra studies in New Zealand have applied EMP analysis of glass shards to tephra identification and correlation. Although many analyses are not yet published, there is a sufficient database available from which comparisons to known tephra sources and formations can be made.

*2. **Identification of Tephra Formations***

(a) Ferromagnesian assemblage
Comparison of relative abundances of diagnostic ferromagnesian minerals (*e.g.* biotite) may distinguish tephra members from the same eruptive centre when used in conjunction with field stratigraphy or other identifying criteria.

(b) Glass chemistry
Glass chemistry generally is unable to distinguish between tephra formations because of the similarity of the mineralogy within each volcanic centre – however, some individual tephras have been distinguished using major element chemistry of glass shards.

Stratigraphic position, ferromagnesian assemblage and glass chemistry together distinguish most tephra formations younger than *c.* 22 500 years B.P.

Tephra Sampling

Most of the rhyolitic tephras are preserved as thin lenses or pocketing layers of fine ash, interbedded within andesitic tephras, medial units and sedimentary deposits. The tephras are visibly mixed with andesitic materials, with some containing fine andesitic lithic and pumice lapilli in the base of the ash. Impurities of andesitic ash occur within most 'cream cakes' and may reflect bioturbation. Tephras sampled therefore undoubtedly contain a proportion of contaminant andesitic ash. To minimise contamination during sampling, the surface of an outcrop was first cleaned off, then many very small samples were taken from

the cleanest and least visibly contaminated portions, avoiding where possible sampling close to the tephra contacts.

Tephras were sampled at reference sections (R.S.), which best show the stratigraphic relationship of a rhyolitic tephra to known andesitic tephra beds, or at sites where the tephra is particularly well preserved. The locations of the reference sections are shown in Figure 2.1 (p. 33).

Sample Preparation

Cleaning Tephra Samples

All rhyolitic tephras were cleaned to remove amorphous oxides (principally derived from the andesitic contaminants), ensuring pristine shards for mounting, sectioning and polishing.

The acid oxalate extraction method (Blakemore *et al.* 1987), adapted by Alloway (1989) for use in cleaning rhyolitic tephras, was used in preference to the dithionite – citrate method of Blakemore *et al.* (1987).

Method

Approximately 25 grams of ash was weighed into each of several 250 ml centrifuge bottles, and the bottles filled with 0.2 M acid oxalate reagent[5]. A tephra:reagent ratio of 1:10(by weight) is sufficient for thorough cleaning of both ferromagnesian minerals and glass shards. Samples were shaken overnight in an end-over-end shaker (shaker method), then washed into a 0.063 – 0.125 micron sieve and thoroughly rinsed with distilled water. Distilled water was used in the preparation of reagents and the washing of all tephra samples to prevent the formation of insoluble calcium tungstate which may form if free calcium ions are introduced into sodium polytungstate heavy liquid (Sometu, written comm. 1986; Gregory and Johnston 1987).

The 0.063 – 0.125 mm fractions were transferred to filter paper and dried. Since the samples were not required for dating, the tephras were oven-dried at approximately 60°C to speed operations.

Sieving

Tephra samples were dry-sieved through a nest of sieves (0.063 – 1.0 mm). Much of the contaminant andesitic tephra was held in the coarser sieves. Fractions <0.063 mm were not retained as a rule because the very fine size of the tephras is unsuited to quantitative

[5] For reagent preparation see Blakemore *et al.* (1987).

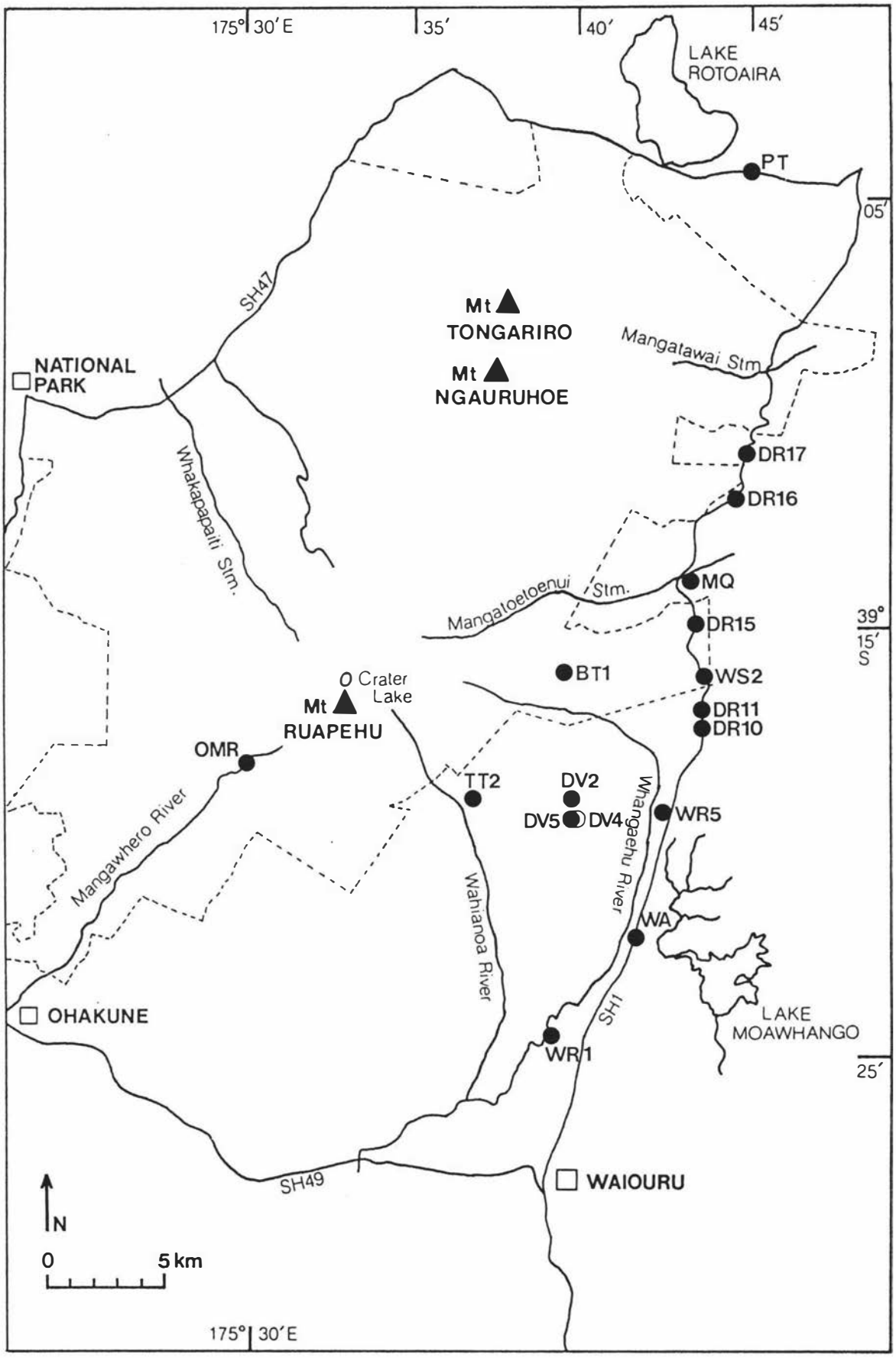

Figure 2.1 Location of type and reference sections designated for rhyolitic tephras identified in the study area *(see text for section codes).*

optical mineralogy and chemical analysis by EMP (Froggatt and Gosson 1982). Sieve fractions were stored in plastic vials for later heavy liquid separation. Sieves were cleaned by washing with a soft paint brush and undiluted detergent, followed by thorough rinsing. Other cleaning methods (*e.g.* dry brushing and sonic probe) were found to be less effective.

Preparation of Samples for Mineralogical Analysis

Heavy Liquid Separation of Minerals

Heavy liquid separation techniques were used to separate the heavy mineral fraction and glass shards.

Heavy liquid separation was chosen in preference to Frantz isodynamic electromagnetic separation as many of the tephra volumes were small, and all contained low concentrations of heavy minerals which may best be concentrated using heavy liquids. Heavy liquid methods minimise opportunity for contamination and loss in small samples, although the method is notably more time-consuming. The low abundance of ferromagnesian minerals in these tephras (often only trace amounts) necessitated processing of many subsamples in order to concentrate sufficient grains for point counting. The volume of ash able to be separated at one time was small due to the volume limitations of the apparatus and properties of the heavy liquid.

Rankin *et al.* (1975) considered Frantz isodynamic separation of minerals superior to heavy liquid methods where bulk glass separates are required. Weathered grains and grains coated with clay can be successfully separated and removed from the sample so that effects of contamination by trace elements within the heavy liquids is avoided. The argument does not necessarily hold, however, where the chemistry of a tephra is to be determined by discrete-grain methods. In this case it is more a matter of personal preference.

Heavy Liquid Materials

Sodium polytungstate ($3Na_2WO_4.9WO_3.H_2O$) heavy liquid is a new product available for use in liquid density separation of mineral grains. The advantages of sodium polytungstate over other previously used liquids (*e.g.* bromoform [tribromomethane], $CHBr_3$) are that it is non-toxic and easy to recover.

Preparation

Aqueous sodium polytungstate is prepared by mixing the salt with distilled water. It is best prepared using a mechanical stirrer, as the salt tends to form sticky clumps when added

to water. A ratio of 1:5 water to salt [6] (by weight) gives a density of about 2.90 g cm^{-3}. The density is adjustable from 1.0 to 3.1 g cm^{-3} and was checked using density beads, and adjusted by adding water or salt accordingly.

Densities

The 0.063 – 0.250 mm (4 – 2 ϕ) fractions of each tephra were split into heavy and light mineral fractions using a liquid density set between 2.87 and 2.95 g cm^{-3}. The light fraction, comprising glass shards and feldspar was then further split using a density between 2.38 and 2.45 g cm^{-3} to separate the glass shards. The purity of the splits at these set densities was optically checked using a binocular microscope. Both density settings facilitated almost pure splits.

Separation

Separation was achieved by density separation of samples within stop-cocked separation tubes. Tubes were filled with heavy liquid to within 10 – 20 mm of the top. Tephra samples were added and stirred into the liquid [7].

Heavy minerals were allowed to free-settle for a few minutes, and then samples were centrifuged at 1000 – 2000 rpm for 5 minutes, stirred, and recentrifuged. This step was repeated until all heavy minerals were freed from the light mineral fraction and the tube constriction where grains tend to collect and stick.

After centrifuging, the light and heavy mineral fractions were separately poured off into filter paper lined funnels, and the heavy liquid collected. Residual heavy liquid held within the filter papers and on grains was recovered by vigorous rinsing with distilled water. Glassware and filter papers retain a significant heavy liquid film due to the viscosity of the liquid. They need to be thoroughly rinsed to prevent both the sticking of filter papers to the funnels, and the adhesion of grains when the residue dries [8]. Samples were oven-dried on the filter papers. Removal of the sample from the filter paper after drying is easiest if Whatman Nº 41 paper is used. Softer papers are more textured and fibres tend to trap a small number of grains, especially biotite.

---

[6] Sometu (written comm. 1986) recommends a ratio of 1:4 water to salt (by weight) to get a density of ≈ 2.90 g cm^{-3}, but a ratio of 1:5 (by weight) was found to more closely approximate this density. [Sometu, Falkenried 4, D-1000 Berlin 33, Germany].

[7] A long tipped glass pipette heat-sealed at the end is an ideal stirring instrument. The bulkier glass or stainless steel stirring rods retain thick heavy-liquid films, trapping many grains.

[8] Filtration is impeded by the high viscosity of the heavy liquid. Callahan (1987) recommends use of coffee filters instead of laboratory grade filters.

Simple gravity separation by free-standing without centrifugation is a time-consuming method which produces impure mineral separates. Impure separates arise from the caking of the light mineral fraction (*i.e.* formation of an aggregated crust) resulting from partial drying of the liquid via evaporation at the grain-liquid interface. This causes heavy minerals to be trapped within the light mineral fraction. Some caking results from the high viscosity and sticky nature of this heavy liquid at densities >2.8 g cm^{-3}, but is not generally a problem with thinner liquids (*e.g.* bromoform). The effect is minimised if the separation apparatus is covered with parafilm. This problem of crystallisation through evaporation is also reported by Gregory and Johnston (1987) using simple gravity filtration, and similar remedies have been suggested. Incomplete mineral separation also arises if samples are not frequently stirred, in which case heavy mineral grains tend to collect and stick at the neck (or constriction) of the separation tube and thus are retained with the light fraction. In order to effect pure mineral separations samples must be frequently stirred (to prevent caking and withholding of heavy minerals) and centrifuged (Callahan 1987; Eden and Whitton 1988).

Recovery of Heavy Liquid

Recovery simply requires evaporation of excess water until the required density is achieved. The most controlled method is to place washings in a glass beaker and evaporate under a fume hood. This method is ideal if immediate recovery is not required – alternatively, the washings can be gently heated (at temperatures $<60°C$, Gregory and Johnston 1987) to speed the operation. Care should be taken to avoid overheating and subsequent evaporation to dryness. If the aqueous solution is heated to dryness, a rock-hard salt with slight bluish tinge forms. This salt can be redissolved in distilled water by stirring continuously for about 30 minutes, but the solution will need repeated filtering to remove very fine undissolved material and bring back clarity.

Preparation of Polished Thin Sections

All thin sections were made following the preparation guidelines of Wallace *et al.* (1985). Sections were sanded to approximately 0.1 mm using carborundum paper, working progressively through 240, 400, 600 and 1000 grit papers. Sections were polished following the procedure outlined in Appendix Ia. Surface polish was checked at each polishing stage using a reflected light attachment on a polarising microscope.

Determining Ferromagnesian Mineral Assemblages

Thin sections were made of the 0.125 – 0.250 mm fractions and, where possible, permanent grain mounts were made for the coarser 0.250 – 0.500 mm and finer 0.063 – 0.125 mm fractions. Proportions of ferromagnesian minerals in the 0.125 – 0.250 mm fraction were determined by point counts (line or ribbon method, Galehouse 1969; Froggatt and Gosson 1982) using a polarising microscope, in which all

mineral grains intersecting the cross-hairs are counted as the slide is manually moved in a mechanical stage along traverses which sample the entire area of the slide. Where possible 400 grains were counted per sample. The error associated with point count estimates is shown graphically in Plas and Tobi (1965) [9]. For point counts of 400 grains the actual frequency is within ± 2 to 5% of the estimated frequency. Minerals were identified by their optical properties. Grain mounts and thin sections of each tephra were optically checked for uniformity of mineral types between fractions.

Electron Microprobe Analysis of Glass Shards

Rhyolitic glass shards were mounted and prepared as polished thin sections (see section 2.3) for analysis by electron microprobe. The chemistry of rhyolitic glass shards was determined using the fully automated JEOL JXA733 superprobe housed in the analytical facility, Research School of Earth Sciences, Victoria University of Wellington. Analysis methodology follows that of Froggatt (1982a, 1983) and Froggatt and Gosson (1982).

Instrument Settings

Instrument settings used in the analysis of glass standards and samples are shown below. All settings were adopted from Froggatt (1982a, 1983) except the count time. Froggatt (1982a) recommends use of 3 x 10 s peak counts and 1 x 10 s background count on each side of the peak. Analysis of the glass standards KN-18 (comenditic glass) and VG-A99 (basaltic glass) using these count times, however, gave consistently poor reproduction of standard analyses and so count times were reduced to 1 x 10 s peak count and 1 x 10 s background count. These count times gave good reproduction of standards and so were adopted for all glass analyses in this study.

Beam diameter	10 μm
Probe current	8 na (nanoamps) at 15 kV
Count Time	1 x 10 s peak count; 1 x 10 s background count

Glass standards were analysed with a 20 μm beam. Beam diameter was reduced to 10 μm for analysis of glass shards to suit the small available surface area of most shards.

Major Element Analysis

Oxides measured were SiO_2, TiO_2, Al_2O_3, FeO, MgO, CaO, Na_2O, K_2O, and Cl. MnO, although determined for some tephras, occurs in very minor amounts (mostly below the detection limits of the probe) and has not been found useful in rhyolitic tephra identification

[9] See chart on p. 88, in Plas and Tobi (1965).

studies (Froggatt 1982a, 1983). Fe in the divalent and trivalent states cannot be distinguished by microprobe analysis and therefore all iron is recorded as FeO.

Inherent variability associated with analysis of the alkalis Na_2O and K_2O (Nielsen and Sigurdsson 1981), due to volatilisation and physical damage to the glass (Froggatt 1983), is a problem with EMP analysis of volcanic glass. To minimise loss these elements were always measured first. The probe conditions (beam current, beam diameter and count time) suggested by Froggatt (1982a, 1983) are aimed at minimising the alkali loss upon exposure to the electron beam.

To check for possible differences due to operator technique and microprobe error, Okareka Tephra sampled from Okareka Loop Road [U16/018316] and Kawakawa Tephra Formation (Oruanui Ignimbrite Member) from Desert Road S.10 (study area) were analysed. The analyses provide a reference for comparison with TVC and OVC glass chemistries, and a check on the consistency of analyses with those of other authors. Where possible at least ten individual and randomly selected shards were analysed, following recommendations of Froggatt (1982a). Frequent peak search analysis of glass standards (obsidian, comenditic KN-18 glass, and basaltic glass, VG-A99) provided a check on probe performance and stability.

2.4 Results and Discussion

The Occurrence, Stratigraphy and Chronology of Rhyolitic Tephras in the Study Area

Rhyolitic tephras are recognised in nearly all tephra sections of the southeastern Mt Ruapehu ring plain. They are found interbedded with andesitic tephras erupted principally from Mt Ruapehu, and Mt Tongariro and Mt Ngauruhoe. Fourteen rhyolitic tephras of both airfall and pyroclastic flow origin are recognised within the 22 500 – 0 years B.P. record. Most tephra sections contain at least two rhyolitic tephras. Up to six are exposed in any one section in more northern areas where the late Pleistocene stratigraphy is more frequently exposed. Few rhyolitic tephras are recognised in the southern part of the study area.

All rhyolitic tephras have been recognised by their distinct glassy composition, and their colour (white to pale brown), which contrasts strongly with the yellowish brown colours of enclosing andesitic tephras. Most rhyolitic tephras are preserved as thin discontinuous (pocketing) well sorted fine or coarse ash layers which invariably show mixing with andesitic tephras. The fine grain size is indicative of a distal source. Tephras from OVC are characteristically finer grained than those from TVC. The rhyolitic tephras mantle the topography and are therefore regarded as representing primary airfall tephras.

The tephras are generally too thin for bedding characteristics to be discerned and used in identification. Airfall tephras are readily distinguished from the ignimbrite units on field characteristics – the latter being ungraded and poorly sorted, and comprising coarse ash and pumice lapilli.

The stratigraphy and chronology of the rhyolitic tephras in the Mt Ruapehu region has been determined from their relative stratigraphic positions and relationships to dated andesitic tephra marker beds (relative-age dating), and by stratigraphic equivalence with rhyolitic tephras identified in the Mt Tongariro region by Topping and Kohn (1973) (correlative-age dating). Most of the rhyolitic tephras are of Holocene age and are readily correlated throughout the study area from field appearance and stratigraphic position. Two new radiocarbon dates [NZ7532, NZ7729] obtained from interbedded Holocene-aged peat and wood provide some additional chronological control.

Detailed mapping of local andesitic tephras is required to identify occurrences of the more obscure and thin late Pleistocene rhyolitic tephras. Few late Pleistocene andesitic tephras within TgVC have been dated (Topping 1973, 1974) by numerical-age (^{14}C) dating, and no dateable material has been found interbedded with these tephras in the Mt Ruapehu region. The chronology of rhyolitic tephras older than *c.* 10 000 years B.P. is therefore less clearly defined.

Identification of the Rhyolitic Tephras

Field Identification

Six of the fourteen recognised rhyolitic formations have been identified from their stratigraphic positions and field appearances. Field identification of the remaining eight tephras is provisional since the record of Holocene and late Pleistocene rhyolitic tephras is incomplete in the study area. Their correlation with known TVC and OVC tephras requires investigation of their mineralogy and chemistry.

Laboratory Identification

Binocular examination of the tephras shows that all comprise vitric shards and pumice fragments, feldspar, and minor amounts of ferromagnesian minerals. Fe-Ti oxide contents are negligible in most of the tephras.

Ferromagnesian Mineral Assemblages

Ferromagnesian mineral assemblages of some of the Holocene and late Pleistocene rhyolitic tephras recognised are presented in Table 2.3 (p. 41), and may be compared with previously published analyses (Table 2.4, p. 42). Assemblages have not been determined for

those tephras which are readily identified from stratigraphic position. Most tephras show assemblages dominated by orthopyroxene and clinopyroxene. Tephras erupted from TVC and OVC may contain clinopyroxene (augite), although generally in only minor amounts (Lowe 1980, 1988a; Froggatt 1982a). High augite abundance (>40%) is indicative of an andesitic source (Lowe 1980; Wallace 1987). Therefore, the high clinopyroxene contents exhibited by many of the rhyolitic tephras (Table 2.3, p. 41) probably reflect contamination from local andesitic tephras. Partial mixing with andesitic tephras was observed in most of the rhyolites sampled.

The ferromagnesian minerals present in the tephras have been identified from the following optical properties:

Orthopyroxene is typically brown to pale brown in thin section, and dark brown in grain mounts. Grains are distinctly pleochroic (commonly from brown to green), and show low birefringence colours. Orthopyroxene has distinct basal cleavage. Grains may show simple parallel twinning.

Clinopyroxene is typically pale green in thin section and dark green in grain mounts. Grains are non-pleochroic although slight pleochroism may be seen in thicker sections. High-angle (40–60°) inclined extinction and high order birefringence colours distinguish clinopyroxene from orthopyroxene. Clinopyroxene shows distinct basal cleavage. Grains commonly show simple parallel twinning.

Hornblende is typically dark greenish brown in thin section, and strongly pleochroic. Birefringence colours are masked by the strong mineral colour. Grains typically show straight extinction, but may also exhibit low-angle (5–15°) inclined extinction. Hornblende is readily identified in thin section from its distinctive cleavage. Pleochroism, extinction, and birefringence distinguish hornblende from both orthopyroxene and clinopyroxene.

Biotite is typically dark brown to yellowish brown in thin section and strongly pleochroic from brown to dark blackish brown. In grain mounts biotite shows distinctive hexagonal morphology. Grains are slender and often appear bent in cross section. Extinction is straight and undulose, and distinguishes biotite from hornblende and clinopyroxene.

Cummingtonite is typically pale green in thin section and green brown in grain mounts. Grains are moderately pleochroic from pale to dark green, and show high order birefringence colours. Cummingtonite shows low angle, and commonly incomplete, extinction. Grains characteristically show multiple simple twinning. Twins show uniform extinction. Multiple twinning, birefringence, and pleochroism

distinguish cummingtonite from other amphiboles. Extinction angle, twinning, and birefringence distinguishes cummingtonite from orthopyroxene and clinopyroxene.

Grain mounts of the 0.250 – 0.500 mm and 0.063 – 0.125 mm fractions show tephras are dominated by orthopyroxene and clinopyroxene in the coarser fractions. Biotite and hornblende are found concentrated in the finer fraction reflecting the dominance of the fine grain sizes of these tephras at these distal sites. Abundances of biotite and hornblende within the 0.125 – 0.250 mm fraction might best be considered a minimum in view of the concentration in the finer fractions and possible dilution through contamination by andesitic pyroxene.

Hypersthene-dominant assemblages and presence of both biotite and cummingtonite indicate that tephras from TVC, OVC, and possibly MVC, are present. Relative abundances of these diagnostic ferromagnesian minerals may be used in conjunction with glass chemistry to distinguish OVC eruptives.

Table 2.3 Representative ferromagnesian mineral abundances in the 0.125 – 0.250 mm (3 – 2 ϕ) fraction in Holocene and late Pleistocene rhyolitic tephras identified in the study area.*

Formation		Opx.† %	Cpx.† %	Hbe.† %	Bio.† %	Cmgt.† %	Grain Count	Indicated Source§
Kaharoa Tephra	[R1][a]	12	39	32	17	-	400	OVC
	[R2][b]	30	32	26	12	-	400	OVC
Mapara Tephra	[R3][c]	75	25	tr.‡	-	-	400	TVC
Waimihia Tephra	[R5][d]	73	23	4	-	-	250	TVC
Whakatane Tephra	[R8][e]	61	36	2	tr.‡	tr.‡	400	OVC
Motutere Tephra	[R9][f]	54	43	3	-	-	400	TVC
	[R10][g]	57	38	5	-	-	400	TVC
Waiohau Tephra	[R11][h]	60	36	tr.‡	4	-	400	OVC
	[R13][c]	53	37	2	8	-	400	OVC
Rerewhakaaitu Tephra	[R14][i]	51	25	2	22	-	400	OVC
	[R15][i]	42	32	4	22	-	400	OVC
	[R16][k]	25	25	4	46	-	400	OVC
	[R17][c]	41	24	5	30	-	400	OVC
Okareka Tephra	[R18][i]	38	31	4	27	-	500	OVC

* All abundances are expressed as percentages of the ferromagnesian mineral assemblage.
† Opx. = orthopyroxene; Cpx. = clinopyroxene; Hbe. = hornblende; Bio. = biotite; Cmgt. = cummingtonite.
‡ tr. (trace) is <1.0%.
§ TVC = Taupo Volcanic Centre; OVC = Okataina Volcanic Centre.

[a] Ohakune Mountain Road.
[b] Rangipo Desert.
[c] Tufa Trig S.2
[d] Wahianoa Road S.1.
[e] Death Valley R.L.
[f] Death Valley S.4.
[g] Whangehu Ford.
[h] Wahianoa Aqueduct.
[i] Bullot Track S.1.
[j] Whangehu River S.5.
[k] Desert Road S.10.

Table 2.4 Ferromagnesian mineral abundances in Holocene and late Pleistocene rhyolitic tephras from Taupo and Okataina volcanic centres.*

Formation		Opx.† %	Cpx.† %	Hbe.† %	Bio.† %	Cmgt.† %	Indicated Source§
Kaharoa Tephra	f	37	5	12	46	-	OVC
Mapara Tephra	f	97	2	1	-	-	TVC
	d	95	4	2	-	-	
	g	91	7	2	-	-	
Whakaipo Tephra	d	94–96	0–3	1–4	-	-	TVC
	g	70–92	6–23	1–7	tr.‡	-	
Waimihia Lapilli	f	94	6	-	-	-	TVC
	d	92–99	1–4	0–4	-	-	
	c	86	13	-	-	-	
Hinemaiaia Tephra	g	92	3	3	-	2	TVC
	d	98–99	0–2	0–1	-	-	
	f	95	5	-	-	-	
	a	84	11	-	-	-	
Whakatane Tephra	f	30	1	4	-	65	OVC
	g	8–21	1–13	5–12	tr.‡	56–84	
	a	53	13	23	-	11	
	b	2	-	7	-	90	
Motutere Tephra	d	98–99	0–2	0–1	-	-	TVC
Waiohau Tephra	e	74	-	26	1	tr.‡	OVC
	g	34–73	2–36	5–38	0–3	0–tr.‡	
Rotorua Tephra	g	19–59	4–38	30–34	3–12	0–tr.‡	OVC
Rerewhakaaitu Tephra	g	2–13	1–34	18–21	32–79	-	OVC
Okareka Tephra	g	23–43	4–22	16–32	15–40	1–5	OVC
	a	19	9	20	49	-	
	b	16	1	61	-	19	

* Abundances are expressed as percentages of the ferromagnesian mineral assemblage.
† Opx. = orthopyroxene; Cpx. = clinopyroxene; Hbe. = hornblende; Bio. = biotite; Cmgt. = cummingtonite.
‡ tr. (trace) is <1.0%.
§ TVC = Taupo Volcanic Centre; OVC = Okataina Volcanic Centre.

[a] Howorth *et al.* (1980), Lake Poukawa, Hawkes Bay.
[b] Howorth *et al.* (1980), Gavin Road.
[c] Howorth *et al.* (1980), De Bretts.
[d] Froggatt (1982a), type areas.
[e] Froggatt and Solloway (1986). Gavin Road.
[f] Lowe and Hogg (1986), Kaipo Lagoon, Urewera National Park.
[g] Lowe (1988a), Waikato Lakes.

Glass Morphology and Chemistry

The morphology of silicic glass fragments has been classified (Ross 1928; Ewart 1963; Wilcox 1965; Heiken 1972) and three habits defined. Fragmentation of vesicle or bubble walls produces (a) platy and (b) cuspate shards which are commonly tri-pointed or Y-shaped

and poorly to non-vesicular. The third type comprises (c) vesicular pumice fragments. All three morphologies are recognised in each of the tephras, thus identifying a rhyolitic origin. Glass fragments typical of rhyolitic tephras derived from Taupo Pumice are shown in Plate 4.15a,b.

Electron Microprobe Analyses

The major element chemistry of glass shards from ten rhyolitic tephras has been determined by EMP analysis. Sampling sites are shown in Figure 2.1 (p. 33) and stratigraphic positions are shown in Charts 1 – 3. Analysis totals are generally greater than 95%, but seldom total 100%. Low analysis totals are typical of volcanic glass and are considered the result of hydration (Smith and Westgate 1969; Froggatt 1982a). The water content of the glass is therefore calculated as the difference between the total and 100. To allow for variable hydration all analyses are normalised to 100% anhydrous before comparison (Froggatt 1982a). Original and normalised analyses are given in Appendix IIIa. Mean analyses of each tephra are presented in Table 2.5 (p. 44) and are in general agreement with analyses from other workers of TVC and OVC tephras (Table 2.6, p. 45). Mean SiO_2 and ($Na_2O + K_2O$) contents vary between 76 – 79% and 6.4 – 7.7% respectively, and identify all tephras as rhyolitic in composition, according to the total alkali silica diagram (TAS) classification of Le Maitre (1984) (Figure 2.2, p. 46). Using the classification of Kohn (1973) all are rhyolitic on the basis of SiO_2 content.

Two discrete compositional groupings within the tephras are apparent by comparing FeO and CaO contents of the glasses (Figure 2.3, p. 47). Analyses of Okareka Tephra collected from the type section [U16/018316], and Kawakawa Tephra Formation (Oruanui Ignimbrite Member) from Desert Road S.10 [T20/464091], are used to define approximate compositional fields for TVC and OVC tephras. The groupings agree with those defined using TVC and OVC data from Froggatt (1982a, pers. comm. 1990), Froggatt and Solloway (1986), and Lowe (1986, 1988b) (Table 2.7, p. 48; Figure 2.3, p. 47).

The atypical chemistry of Whakaipo Tephra and Kawakawa Tephra Formation, and Rotorua Tephra compared with that of other TVC and OVC tephras, respectively, is apparent in Figure 2.3 (p. 47).

Distinguishing Tephra Source and Formations Using Similarity Coefficients

To demonstrate the similarity in chemical composition of tephras for correlation, Froggatt (1982a, 1983) compared the chemistry of tephras at type sections and their correlatives at distal localities. This was done by calculating the Coefficients of Variation (C.V.) (Appendix Ia) between glass analyses (after Borchardt *et al.* 1971) – a method which compares all analysed variables for a pair of samples. The coefficient is zero for identical analyses. A value less than 12 indicates chemical similarity between tephras and is used to identify correlative tephras, although tephras showing higher C.V. values (> 15) have also been correlated where stratigraphic position or unique chemistry are consistent with their

Table 2.5 Electron microprobe analyses (meaned) of glass in Taupo and Okataina volcanic centre tephras identified in the study area, Tongariro Volcanic Centre.*

Formation	Waimihia Tephra [R4] [a]		Hinemaiaia Tephra [R7] [b]		Hinemaiaia Tephra [R6] [c]		Whakatane Tephra [R8] [d]		Motutere Tephra [R9] [e]		Waiohau Tephra [R11] [f]		Waiohau Tephra [R12] [g]	
SiO_2	76.82	(0.24)	76.62	(0.19)	76.61	(0.28)	78.54	(0.49)	76.51	(0.35)	78.68	(0.44)	78.60	(0.28)
Al_2O_3	12.79	(0.08)	12.84	(0.07)	12.89	(0.11)	12.26	(0.15)	12.85	(0.13)	12.10	(0.16)	12.15	(0.12)
TiO_2	0.18	(0.04)	0.21	(0.03)	0.20	(0.09)	0.14'	(0.02)'	0.20'	(0.05)'	0.15'	(0.04)'	0.14'	(0.04)'
FeO	1.72	(0.12)	1.67	(0.08)	1.60	(0.11)	0.78	(0.18)	1.70	(0.15)	0.86	(0.13)	0.94	(0.07)
MnO	-.-	-.-	-.-	-.-	-.-	-.-	-.-	-.-	-.-	-.-	-.-	-.-	-.-	-.-
MgO	0.17'	(0.04)'	0.18	(0.04)	0.19	(0.03)	0.10'	(0.02)'	0.16	(0.03)	0.12'	(0.02)'	0.12	(0.02)
CaO	1.27	(0.09)	1.23	(0.12)	1.29	(0.07)	0.73	(0.05)	1.49	(0.08)	0.88	(0.07)	0.92	(0.14)
Na_2O	3.96	(0.24)	4.14	(0.14)	4.12	(0.22)	3.80	(0.18)	3.87	(0.16)	3.74	(0.33)	3.87	(0.15)
K_2O	2.99	(0.11)	3.00	(0.13)	2.98	(0.07)	3.63	(0.22)	3.10	(0.20)	3.36	(0.15)	3.20	(0.21)
Cl	0.11	(0.02)	0.14'	(0.02)'	0.15'	(0.03)'	0.15'	(0.03)'	0.13	(0.02)	0.14	(0.02)	0.13'	(0.03)'
Water ‡	0.88	(0.66)	1.33	(1.32)	2.16	(1.24)	0.63	(0.67)	1.24	(1.03)	2.10	(1.43)	1.86	(1.36)
n §	$n=11$		$n=14$		$n=19$		$n=8$		$n=12$		$n=21$		$n=11$	

Formation	Rerewhakaaitu Tephra [R14] [h]		Rerewhakaaitu Tephra [R15] [i]		Rerewhakaaitu Tephra [R16] [j]		Okareka Tephra [R18] [h]		Kawakawa Tephra Fm. [R19] [j]	
SiO_2	77.82	(0.39)	77.68	(0.52)	77.65	(0.33)	78.25	(0.26)	78.79	(0.38)
Al_2O_3	12.55	(0.34)	12.64	(0.21)	12.39	(0.28)	12.15	(0.09)	12.17	(0.11)
TiO_2	0.13	(0.05)	0.16'	(0.07)'	0.15'	(0.05)'	0.14'	(0.04)'	0.14'	(0.06)'
FeO	0.96	(0.24)	0.97	(0.29)	1.03	(0.19)	0.95	(0.09)	1.09	(0.13)
MnO	-.-	-.-	-.-	-.-	-.-	-.-	-.-	-.-	-.-	-.-
MgO	0.13'	(0.08)'	0.14'	(0.07)'	0.17'	(0.09)'	0.12'	(0.03)'	0.13'	(0.03)'
CaO	0.83	(0.32)	0.92	(0.37)	0.94	(0.37)	0.85	(0.08)	1.05	(0.07)
Na_2O	3.66	(0.16)	3.78	(0.20)	3.63	(0.13)	3.70	(0.17)	3.36	(0.20)
K_2O	3.83	(0.55)	3.65	(0.64)	3.98	(0.70)	3.76	(0.44)	3.11	(0.18)
Cl	0.14	(0.03)	0.14	(0.03)	0.13	(0.04)	0.15'	(0.02)'	0.21'	(0.07)'
Water ‡	2.16	(0.97)	2.52	(0.97)	1.24	(0.90)	2.23	(1.26)	3.53	(0.64)
n §	$n=17$		$n=14$		$n=9$		$n=23$		$n=21$	

* All analyses are normalised to 100% loss free; values in parentheses are standard deviations; mean and standard deviations are for values above detection limit only.
† Indicates at least one analysis gave a result below detection limit (not included in these statistics).
‡ Water value is assumed to be the difference between original analytical total and 100.
§ n = number of analyses; nd = not detected; -.- = not determined.

[a] Tufa Trig S.2.
[b] Death Valley T.L.
[c] Desert Road S.11.
[d] Death Valley T.L.
[e] Death Valley S.4.
[f] Wahianoa Aqueduct S.
[g] Missile Ridge.
[h] Bullot Track S.1
[i] Whangehu River S.5.
[j] Desert Road S.10.

correlation (Froggatt 1982a). In a recent study by Lowe (1986) coefficients of variation on glass analyses were used to indicate correlative tephras.

More recently the Similarity Coefficient (S.C.) (Appendix Ia) has been adopted as a method for comparing the similarity in chemistry of tephras (Froggatt and Solloway 1986; P.C. Froggatt, written comm. 1990; Riehle *et al.* 1990). S.C. values approaching 1.0 indicate increasing similarity, with values of ≥0.94 indicating that the tephras are chemically indistinguishable (P.C. Froggatt, pers. comm. 1990).

Similarity Coefficients and Coefficients of Variation calculated between rhyolitic tephras recognised in the Mt Ruapehu region and tephras from the type areas (TVC, OVC, MVC) are presented in Table 2.7 (p. 48). S.C. values calculated for comparison of known Kawakawa

Table 2.6 Electron microprobe analyses (meaned) of glass in near source Taupo and Okataina volcanic centre tephras.*

Formation	Whakaipo Tephra [a]		Whakaipo Tephra [e]		Waimihia Lapilli [a]		Hinemaiaia Tephra [f]		Whakatane Tephra [f]		Motutere Tephra [b]		Waiohau Tephra [d]	
SiO_2	77.30	(0.48)	77.91	(0.26)	76.43	(0.41)	77.30	(0.59)	78.41	(0.24)	77.01	(0.22)	78.10	(0.41)
Al_2O_3	12.37	(0.34)	12.48	(0.07)	13.06	(0.13)	12.80	(0.36)	12.41	(0.15)	13.18	(0.11)	12.33	(0.27)
TiO_2	0.15	(0.04)	0.16	(0.05)	0.20	(0.03)	0.19	(0.08)	0.12	(0.03)	0.16	(0.01)	0.14	(0.03)
FeO	1.47	(0.18)	1.52	(0.08)	1.73	(0.11)	1.71	(0.16)	0.78	(0.11)	1.62	(0.08)	0.98	(0.07)
MnO	0.07	(0.04)	-.-	-.-	0.10	(0.03)	-.-	-.-	-.-	-.-	0.08	(0.04)	-.-	-.-
MgO	0.11	(0.04)	0.13	(0.01)	0.18	(0.04)	0.17	(0.03)	0.10	(0.01)	0.19	(0.03)	0.14	(0.02)
CaO	0.99	(0.04)	0.98	(0.03)	1.34	(0.10)	1.30	(0.17)	0.67	(0.05)	1.30	(0.04)	0.87	(0.06)
Na_2O	4.40	(0.27)	3.62	(0.11)	4.13	(0.22)	3.56	(0.46)	3.77	(0.08)	3.59	(0.08)	3.95	(0.31)
K_2O	3.13	(0.14)	3.09	(0.10)	2.84	(0.05)	2.92	(0.26)	3.62	(0.09)	2.88	(0.08)	3.31	(0.18)
Cl	-.-	-.-	0.12	(0.02)	-.-	-.-	0.09	(0.09)	0.14	(0.02)	-.-	-.-	-.-	-.-
Water‡	2.13	(0.29)	1.55	(0.79)	3.27	(1.00)	1.95	(1.77)	2.51	(1.45)	1.79	(1.66)	3.57	(2.76)
n§	n=11		n=11		n=10						n=9		n=58	

Formation	Waiohau Tephra [e]		Rotorua Tephra [f]		Rotorua Tephra [e]		Puketarata Tephra [f]		Puketarata Tephra [e]		Rerewhakaaitu Tephra [f]		Rerewhakaaitu Tephra [e]	
SiO_2	78.81	(0.30)	77.66	(0.43)	77.57	(0.58)	78.85	(0.29)	78.49	(0.45)	77.97	(0.42)	78.34	(0.41)
Al_2O_3	12.35	(0.13)	12.72	(0.23)	12.68	(0.32)	12.05	(0.22)	12.28	(0.10)	12.39	(0.18)	12.41	(0.18)
TiO_2	0.13	(0.03)	0.19	(0.06)	0.21	(0.05)	0.07	(0.03)	0.08	(0.02)	0.11	(0.04)	0.14	(0.04)
FeO	0.92	(0.08)	1.15	(0.20)	1.26	(0.09)	0.80	(0.22)	0.90	(0.10)	0.95	(0.09)	1.00	(0.13)
MnO	-.-	-.-	-.-	-.-	-.-	-.-	-.-	-.-	-.-	-.-	-.-	-.-	-.-	-.-
MgO	0.14	(0.01)	0.19	(0.07)	0.20	(0.08)	0.06	(0.03)	0.07	(0.03)	0.10	(0.03)	0.13	(0.03)
CaO	0.89	(0.04)	1.12	(0.26)	1.20	(0.33)	0.68	(0.09)	0.64	(0.04)	0.82	(0.08)	0.88	(0.07)
Na_2O	3.60	(0.28)	3.82	(0.19)	3.55	(0.29)	3.62	(0.13)	3.23	(0.38)	3.70	(0.22)	3.42	(0.34)
K_2O	3.26	(0.10)	3.07	(0.47)	3.19	(0.44)	3.88	(0.20)	4.17	(0.48)	3.78	(0.43)	3.56	(0.34)
Cl	0.10	(0.03)	0.13	(0.03)	0.14	(0.03)	-.-	-.-	0.15	(0.03)	0.15	(0.02)	0.12	(0.03)
Water‡	4.99	(3.00)	2.86	(1.74)	7.07	(1.71)	0.10	(0.15)	5.07	(1.09)	3.63	(1.74)	3.38	(2.12)
n§	n=10				n=10				n=12				n=12	

Formation	Okareka Tephra [f]		Okareka Tephra [e]		Okareka Tephra [g]		Kawakawa Tephra Fm. [c]	
SiO_2	78.42	(0.19)	78.53	(0.47)	78.33	(0.30)	79.04	(0.31)
Al_2O_3	12.43	(0.19)	12.34	(0.08)	12.12	(0.15)	12.49	(0.18)
TiO_2	0.11	(0.05)	0.11	(0.04)	0.14'	(0.06)'	0.11	(0.02)
FeO	0.87	(0.06)	0.87	(0.06)	0.84	(0.11)	1.16	(0.09)
MnO	-.-	-.-	-.-	-.-	-.	-.-	0.06	(0.05)
MgO	0.10	(0.04)	0.11	(0.03)	0.10'	(0.02)'	0.12	(0.04)
CaO	0.73	(0.04)	0.82	(0.06)	0.81	(0.06)	1.03	(0.07)
Na_2O	3.57	(0.14)	3.37	(0.26)	3.51	(0.12)	2.99	(0.18)
K_2O	3.71	(0.24)	3.71	(0.32)	4.06	(0.15)	3.01	(0.11)
Cl	-.-	-.-	0.14	(0.02)	0.13'	(0.02)'	-.-	-.-
Water‡	1.58	(1.37)	5.79	(1.66)	2.07	(0.92)	6.72	(0.93)
n§			n=9		n=21		n=14	

* All analyses are normalised to 100% loss free; values in parentheses are standard deviations.
† Mean and standard deviation for values above detection limit only; at least one analysis gave a result below detection limit (not included in these statistics).
‡ Water value is assumed to be the difference between original analytical total and 100.
§ *n* = number of analyses; nd = not detected; -.- = not determined.

[a] Froggatt (1982a), De Bretts.
[b] Froggatt (1982a), Opawa Road.
[c] Froggatt (1982a), Gavin Road.
[d] Froggatt and Solloway (1986), Gavin Road.
[e] Lowe (1988a), Lake Rotomanuka, Waikato Lakes.
[f] P.C. Froggatt, pers. comm. (1990), type sections.
[g] this thesis, Okareka Loop Road.

Tephra Formation sampled from the study area with Kawakawa Tephra Formation sampled

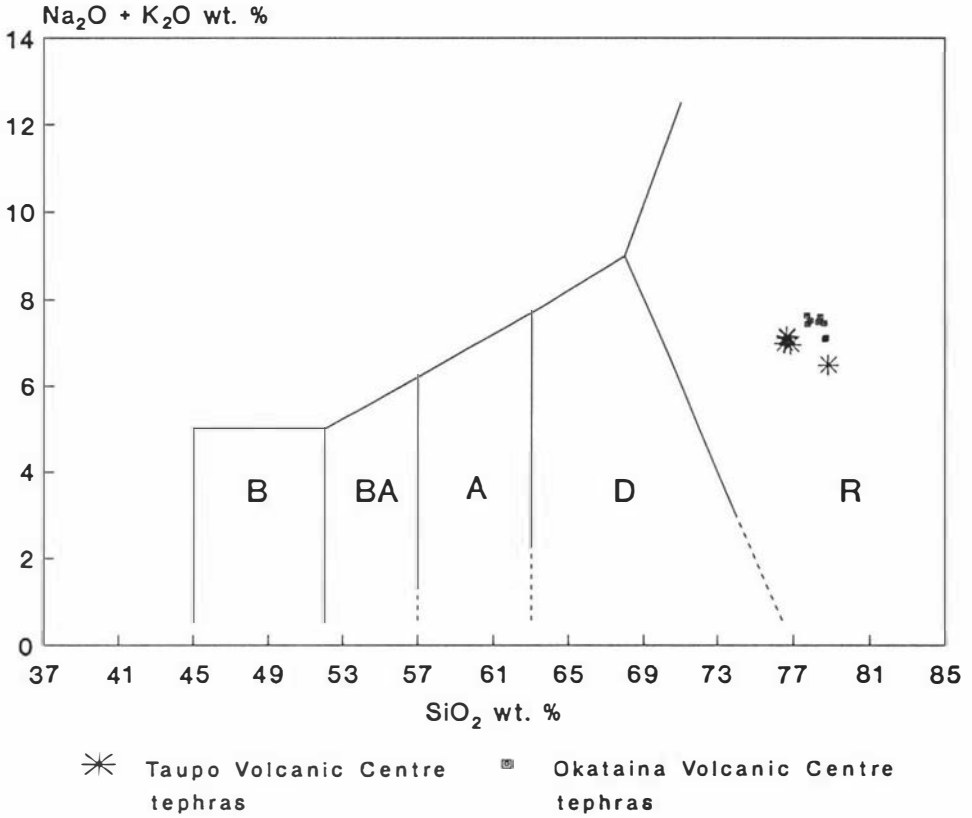

Figure 2.2 Total alkali silica (TAS) diagram, showing basalt (B), basaltic andesite (BA), andesite (A), dacite (D), and rhyolite compositional fields (after Le Maitre 1984). Tephras from the Taupo and Okataina volcanic centres (mean analyses) are of rhyolitic composition.

from the type section (representative mean analysis from Froggatt 1982a), and Okareka Tephra sampled from Okareka Loop Road, with Froggatt's Okareka Tephra (mean analysis from P.C. Froggatt, written comm. 1990) are 0.94 and 0.95 respectively. These values demonstrate general agreement in the analyses between authors, and support the use of S.C. values as a valid means for comparing and correlating tephras in this study.

Comparison of tephras considered correlatives on the basis of stratigraphic position and ferromagnesian mineralogy with tephras from type sections (Table 2.7, p. 48) produces S.C. values of 0.90 or greater. Comparison of non-correlative Holocene TVC tephras also produces high S.C. values (mostly >0.92), demonstrating that TVC tephras have very similar glass chemistries. Comparison to either Whakaipo Tephra or Kawakawa Tephra Formation, however, gives lower S.C. values ($0.80-0.91$), indicating greater chemical dissimilarity between these two tephras and other Holocene TVC tephras. This is consistent with the observation of Lowe (1988a) that Kawakawa Tephra and Whakaipo Tephra have distinctive and distinguishable glass chemistries. Comparison of tephras from different volcanic centres (TVC *vs* OVC) also gives lower S.C. values, typically <0.80. These values show the general dissimilarity in glass chemistry between TVC and OVC tephras. Exceptions to this are Whakaipo Tephra and Kawakawa Tephra which give higher S.C. values when compared to OVC tephras. These have a chemistry intermediate between that of the other TVC tephras and OVC tephras, as shown in Figure 2.3 (p. 47).

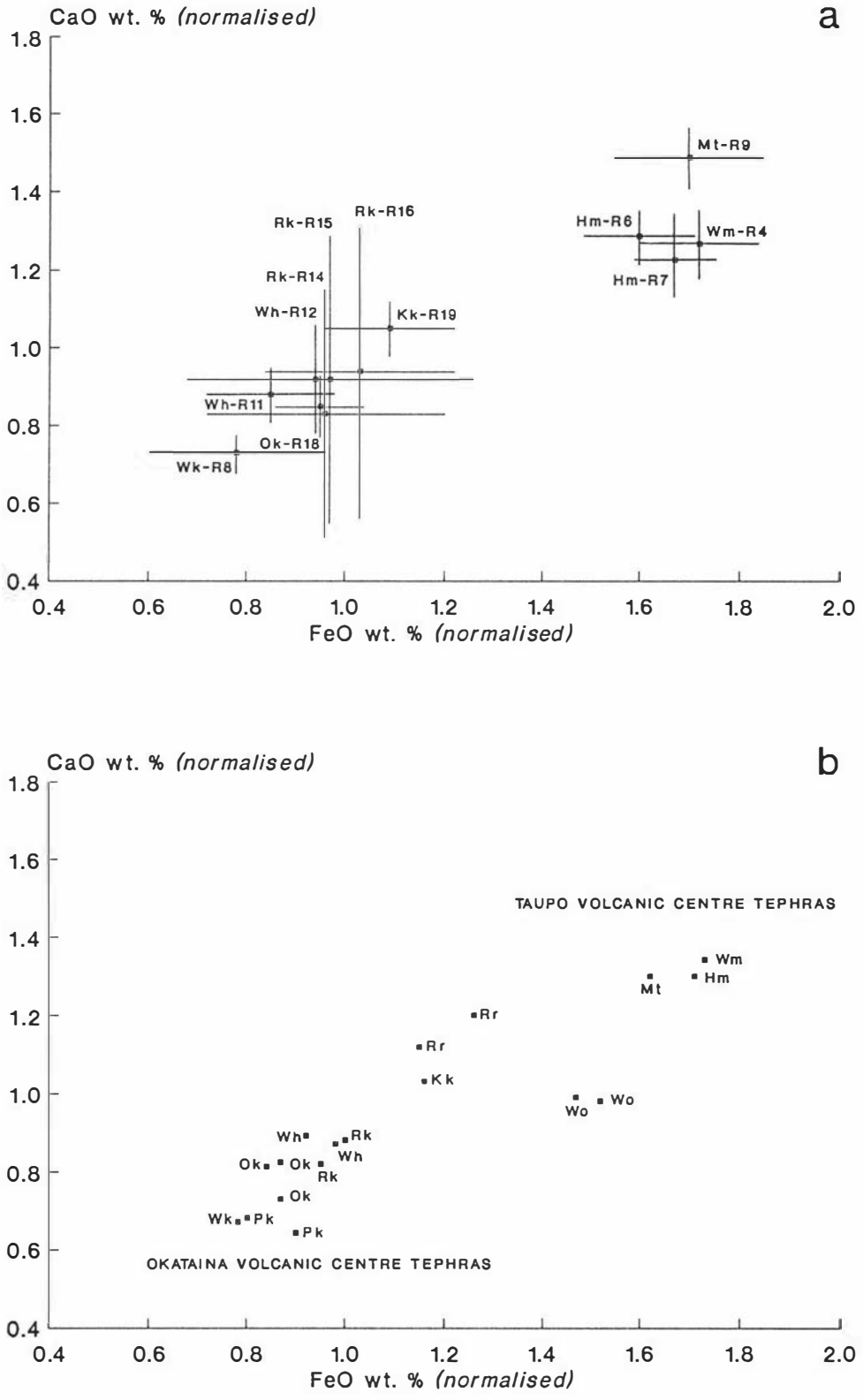

Figure 2.3 Plot of CaO *vs* FeO (total) contents in glass of late Pleistocene and Holocene-aged tephras from Taupo and Okataina volcanic centres, identified in the study area (Fig. 2.3a). *(see text for tephra codes).* Tephra codes are suffixed with sample numbers, bars show standard deviation from mean. The lower plot (Fig. 2.3b) is produced using mean glass data for Taupo, Okataina and Maroa volcanic centre tephras from Froggatt (1982a, pers. comm 1990) and Lowe (1988a). Whakaipo Tephra, Rotorua Tephra, Kawakawa Tephra Formation show atypical chemistries *(see text for discussion).*

Similarity Coefficients calculated for comparison of the glass chemistry of each rhyolitic tephra identified in the study area to all others are given in Table 2.8 (p. 49). Similar trends are evident. Tephras considered correlatives on the basis of stratigraphic position and field appearances give S.C. values of >0.92. However, similar values are obtained for comparisons between tephras not considered correlatives, but which are sourced from the same volcanic centre, thus demonstrating the similarity in chemistry of eruptives from the same source. S.C. values cannot, therefore, be used to correlate TVC, or OVC tephras between sites in the study area. Tephra sourced from TVC and OVC are however distinguished using S.C. values.

The coefficients have been calculated using eight oxides (SiO_2, Al_2O_3, TiO_2, FeO, MgO, CaO, Na_2O, K_2O). Manganese (MnO) and Cl are too low in concentration and are not used in the calculations.

Table 2.7 Similarity Coefficients and Coefficients of Variation derived from comparison of rhyolitic tephras identified in study area with analyses from Taupo and Okataina centres.*,†

Formation	R4	R6	R7	R8	R9	R11	R12	R14	R15	R16	R18	R19
Whakaipo Tephra	0.86	0.96	0.96	0.96	0.95	0.99	0.91	0.96	0.97	0.98	0.97	0.90
Waimihia Tephra	0.96	0.97	0.97	0.74	0.95	0.78	0.79	0.77	0.81	0.82	0.76	0.81
Hinemaiaia Tephra	0.98	0.95	0.95	0.76	0.95	0.91	0.91	0.79	0.94	0.95	0.79	0.84
Whakatane Tephra	0.74	0.73	0.73	0.96	0.74	0.90	0.99	0.90	0.96	0.94	0.90	0.94
Motutere Tephra	0.94	0.95	0.93	0.77	0.91	0.91	0.92	0.90	0.94	0.96	0.90	0.95
Waiohau Tephra[a]	0.82	0.90	0.90	0.90	0.91	0.95	0.95	0.95	0.94	0.91	0.94	0.92
Waiohau Tephra[b]	0.84	0.92	0.92	0.90	0.92	0.96	0.95	0.95	0.95	0.92	0.95	0.92
Rotorua Tephra	0.92	0.92	0.91	0.90	0.90	0.95	0.96	0.94	0.99	0.99	0.94	0.99
Puketarata Tephra	0.67	0.66	0.66	0.86	0.66	0.81	0.79	0.82	0.78	0.78	0.82	0.76
Rerewakaaitu Tephra	0.76	0.74	0.74	0.92	0.75	0.90	0.91	0.94	0.89	0.88	0.94	0.86
Okareka Tephra	0.74	0.73	0.73	0.94	0.73	0.90	0.99	0.92	0.97	0.95	0.91	0.95
Kawakawa Tephra Fm.	0.81	0.80	0.80	0.83	0.79	0.87	0.88	0.87	0.85	0.85	0.87	0.93
Whakaipo Tephra	10.66	13.01	12.58	14.40	12.58	12.66	10.94	9.96	10.42	13.39	10.14	9.61
Waimihia Tephra	2.63	2.63	2.93	17.05	3.95	14.38	14.27	13.99	12.92	13.02	13.40	11.02
Hinemaiaia Tephra	3.20	4.57	4.61	17.26	4.19	14.93	13.92	14.91	13.36	14.14	14.11	11.64
Whakatane Tephra	18.44	18.10	18.16	5.29	19.96	9.06	8.79	8.16	12.96	13.62	8.30	11.27
Motutere Tephra	4.47	6.95	7.49	17.76	6.48	15.53	14.16	14.45	13.47	12.98	14.12	11.25
Waiohau Tephra[a]	14.19	13.53	14.26	8.32	16.31	5.08	5.50	4.67	6.27	7.35	4.79	5.62
Waiohau Tephra[b]	14.19	13.35	13.82	9.44	15.94	4.82	5.20	4.31	4.69	6.42	4.91	6.05
Rotorua Tephra	10.45	8.80	8.33	15.33	11.62	11.49	12.54	11.97	8.66	7.92	11.50	11.17
Puketarata Tephra	21.41	21.36	21.48	18.44	22.39	19.94	17.74	19.21	20.91	22.42	19.28	18.30
Rerewakaaitu Tephra	16.01	16.09	16.32	7.84	17.43	8.90	7.93	8.42	12.77	13.98	8.32	8.23
Okareka Tephra	16.78	16.75	16.91	7.16	18.24	9.29	7.78	7.62	12.36	13.87	7.76	10.06
Kawakawa Tephra Fm.	13.81	14.69	15.48	10.55	14.40	10.03	8.81	8.15	9.56	10.43	8.39	7.06

* Shaded cells indicate correlative tephra identified in study area.
† Analyses from Froggatt (1982), P.C. Froggatt, pers. comm. (1990) except where otherwise noted.

[a] Waiohau Tephra data from Lowe (1988a), Lake Rotomanuka, Waikato Lakes.
[b] Waiohau Tephra data from Froggatt and Solloway (1986), Gavin Road.

Table 2.8 Similarity Coefficient (shaded) and Coefficient of Variation (unshaded) values derived by comparing rhyolitic tephras identified in study area.*

Formation		R4	R6	R7	R9	R19	R8	R11	R12	R14	R15	R16	R18
Waimihia Tephra	R4		3.58	4.07	4.96	11.03	17.47	14.86	14.60	13.96	13.40	12.99	13.43
Hinemaiaia Tephra	R6	0.96		2.39	4.92	11.22	16.88	14.04	14.22	13.49	11.92	11.38	12.94
Hinemaiaia Tephra	R7	0.96	0.97		5.68	12.04	16.82	14.25	14.51	13.76	12.17	12.50	13.16
Motutere Tephra	R9	0.96	0.95	0.95		12.49	16.65	16.20	16.21	15.63	14.79	14.01	14.96
Kawakawa Tephra Fm.	R19	0.84	0.82	0.82	0.83		11.23	7.40	6.83	7.54	4.53	8.85	7.15
Whakatane Tephra	R8	0.77	0.75	0.75	0.76	0.87		6.13	7.75	6.76	10.38	12.86	7.04
Waiohau Tephra	R11	0.81	0.79	0.79	0.80	0.92	0.93		3.10	4.54	4.88	9.49	4.45
Waiohau Tephra	R12	0.82	0.80	0.81	0.81	0.94	0.92	0.96		4.93	6.75	10.52	4.81
Rerewhakaaitu Tephra	R14	0.80	0.78	0.78	0.78	0.91	0.92	0.94	0.93		6.29	8.38	1.26
Rerewhakaaitu Tephra	R15	0.85	0.83	0.83	0.83	0.90	0.89	0.93	0.93	0.94		4.90	5.79
Rerewhakaaitu Tephra	R16	0.85	0.83	0.83	0.82	0.90	0.87	0.91	0.90	0.92	0.94		8.73
Okareka Tephra	R18	0.80	0.78	0.78	0.78	0.92	0.93	0.95	0.95	0.98	0.94	0.92	

Rhyolitic Tephrostratigraphy and Tephrochronology, Southeastern Mt Ruapehu Ring Plain

Fourteen rhyolitic tephras have been identified in the southeastern Mt Ruapehu region and correlated with tephras erupted from TVC and OVC by means of their stratigraphic position, field appearances, ferromagnesian mineral assemblages, and glass chemistries. All tephras are preserved as macroscopic layers. The stratigraphic relationships of these rhyolitic tephras to locally derived TgVC andesitic tephras are shown in Charts 1 – 3.

Kaharoa Tephra [Ka]

Definition and Age

Kaharoa Shower (Grange 1929), renamed Kaharoa Ash by Vucetich and Pullar (1964) and later revised to Kaharoa Tephra (Cole 1970a), was erupted from the Tarawera Volcanic Complex, located in the southern part of OVC (Cole and Nairn 1975). Kaharoa Tephra is radiocarbon dated at 665 ± 58 years B.P., based on two bracketing radiocarbon ages [XP7; XP9] (Lawlor 1980) (Table 2.1, p. 16), revising earlier ages of *c.* 900 years B.P. (Vucetich and Pullar 1964; Pullar *et al.* 1973; Pullar and Birrell 1973; Nairn 1981). In the Central North Island, Cole (1970a) describes Kaharoa Tephra as rhyolitic tephra overlying Taupo Pumice Formation, and underlying Tarawera Formation. Kaharoa Tephra has not previously been described from TgVC.

Description and Identification

A reference section is here designated at S20/271074, a cutting at the northern end of Ohakune Mountain Road [OMR] (Plate 2.1; Figure 2.1, p. 33; Chart 1) [10].

Here, Kaharoa Tephra is preserved as thin (10 mm) pocketing, fine white ash with irregular but sharp contacts (Plate 2.2). It overlies 90 mm of interbedded and reworked Tufa Trig Formation tephras and leaf-bearing Makahikatoa Sands (defined by Purves 1990) above a prominent, uncorrelated member of Tufa Trig Formation, and occurs 1.3 m above Taupo Pumice. It is overlain by 0.21 m of sandy loam textured paleosols containing leaves, and Tufa Trig Formation tephras. Due to the absence of identifying characteristics, Tufa Trig Formation tephras have not been correlated with members at the type section, and the exact stratigraphic position of Kaharoa Tephra relative to members of Tufa Trig Formation is therefore not established at this site.

Two radiocarbon dates [Wk1488, Wk1489] obtained on peat immediately above and below Tufa Trig Formation member Tf5 at Ngamatea Swamp S.1 [T21/413874] returned ages of 650 ± 50 years B.P. and 830 ± 60 years B.P. respectively. Peats are not generally affected by old carbon but may be contaminated by modern carbon from the living vegetation cover (Zoltai 1989). The peat samples were taken at shallow depths (*c.* 0.29 m) from the swamp surface, and therefore both dates may be affected by modern carbon (giving younger radiocarbon ages). The ages obtained should probably be regarded as minimum ages. The approximate stratigraphic position of Kaharoa Tephra, dated *c.* 650 years B.P. (Table 2.1, p. 16) therefore probably occurs closer to member Tf8 than Tf6. At Tufa Trig T.S., a reasonably well developed paleosol overlies member Tf5, and a thinner paleosol separates members Tf6 and Tf7 from member Tf8 (Plate 3.1). Collectively these paleosols may represent *c.* 200 – 300 years of soil development. Given a maximum age of 830 ± 60 years B.P. for member Tf5, and the time represented by the paleosols, member Tf8 would date *c.* 600 years B.P., a little younger than the Kaharoa Tephra. A stratigraphic position for Kaharoa Tephra close to member Tf8 is therefore indicated.

At Tufa Trig S.1 (type section for Tufa Trig Formation tephras), it is probable that Kaharoa Tephra is preserved microscopically within an intervening paleosol, and therefore sampling of these paleosols for glass shards may identify its position. Additionally, dating of fossil beech leaves contained in many of the Tufa Trig Formation tephras may further help identify its stratigraphic position.

Kaharoa Tephra has been identified at few other sites. At T20/403072 in the Rangipo Desert, a thin white ash found interbedded with fluvially reworked Tufa Trig Formation tephras and Makahikatoa Sands above Taupo Pumice (Purves 1990) is here identified as

---

[10] Stratigraphic descriptions of all reference sections defined for rhyolitic tephras in the study area are given in Appendix II. Correlations made between these sections are shown in Charts 1 – 4.

Kaharoa Tephra. At this site Kaharoa Tephra is contaminated with fine Taupo Pumice lapilli and ash.

Kaharoa Tephra, sampled from the reference section [sample R1] and at T20/403072 [sample R2], has a ferromagnesian mineral assemblage comprising clinopyroxene, hornblende, biotite and orthopyroxene (Table 2.3, p. 41). Presence of biotite identifies an OVC source. Grain mounts show biotite is concentrated in the 0.063–0.125 mm and <0.063 mm fraction. Coarser fractions (>0.250 mm) contain minor to trace amounts of biotite. Some, but not all biotite grains show glassy selvedges, indicating that the biotite in this tephra is not detrital (Wilcox 1965; Kohn 1973; Wilcox and Izett 1973). Stratigraphic position and ferromagnesian mineralogy identify this tephra as Kaharoa Tephra. Previous workers (Lewis and Kohn 1973; Pullar *et al.* 1977; Kohn and Glasby 1978; Lowe and Hogg 1986) identified Kaharoa Tephra on the basis of radiocarbon age and presence of abundant biotite (>15%) in the ferromagnesian assemblage.

Distribution

Kaharoa Tephra was not identified by Topping and Kohn (1973) in the Mt Tongariro region. Macroscopic preservation of this tephra may be restricted to areas where recent dune development and tephra accumulation has occurred sufficiently rapidly to enable its burial and preservation.

Kaharoa Tephra is identified at few sites in the study area (Figure 2.6, p. 83) and therefore isopachs are not shown for the southeastern Mt Ruapehu region. An isopach map of Kaharoa Tephra is presented in Healy (1964a).

Significance

Kaharoa Tephra is the only post-Taupo Pumice aged rhyolitic tephra identified from OVC, and it is therefore a valuable marker bed within the andesitic tephra sequences at Mt Ruapehu. Kaharoa Tephra is a potentially important time-plane in the establishment of the chronology of post-Taupo Pumice aged tephras, laharic deposits and the paleo-environment of the southeastern Mt Ruapehu ring plain.

Taupo Pumice Formation [Tp]

Definition and Age

Taupo Pumice Formation (Froggatt 1981d) comprises tephra and pyroclastic flow deposits erupted from TVC. It is dated at 1819 ± 17 years B.P. by Healy (1964a), from an average of many radiocarbon dates (Table 2.1, p. 16). Froggatt (1981d) calculates an age of 1820 ± 80 years B.P., little different to that of Healy.

Froggatt describes four members within the formation: Taupo Ignimbrite, Taupo Lapilli, Rotongaio Ash and Hatepe Tephra. Early descriptions of the deposits included within this formation were made by Baumgart (1954), Baumgart and Healy (1956), Healy (1964a), and Vucetich and Pullar (1964, 1973).

In the Central North Island, north of TgVC, Vucetich and Pullar (1973) described Taupo Pumice Formation as rhyolitic tephra and pyroclastic flow deposits which are overlain by Kaharoa Tephra, separated from the latter by a paleosol developed in Taupo Pumice Formation, and which overlie a paleosol developed on Mapara Tephra. In the Mt Tongariro region, Topping (1973, 1974) and Topping and Kohn (1973) described Taupo Pumice Formation as rhyolitic tephra and pyroclastic flow deposits underlying Ngauruhoe Formation (previously Ngauruhoe Tephra Formation, see section 3.3), and overlying a weak paleosol developed in Mangatawai Tephra.

Description and Identification

On the southeastern Mt Ruapehu ring plain, Taupo Pumice Formation is represented by Taupo Ignimbrite Member. Reference sections are at Tufa Trig S.2 [T20/375046] and Desert Road S.11 [T20/464092] (Chart 1).

At Tufa Trig R.S. [TT2] (Figure 2.1, p. 33; Plate 2.3), Taupo Ignimbrite Member is 0.28 m thick. It overlies a 0.26 m thick dark brown greasy sandy loam textured paleosol above Mapara Tephra, and is overlain by 1.5 m of aeolian Makahikatoa Sands below Tufa Trig Formation.

At Desert Road S.11 [DR11] (Figure 2.1, p. 33; Plate 2.4) where Mapara Tephra is absent, Taupo Ignimbrite is 0.72 m thick. Here it overlies a 0.31 m dark brown greasy sandy clay loam textured paleosol developed in Mangatawai Tephra. It is overlain by Tufa Trig Formation and interbedded Makahikatoa Sands. At this site Taupo Ignimbrite occurs as strong pink and grey coloured poorly sorted ash and lapilli, with a sharp smooth basal contact on Mangatawai Tephra.

At uneroded sites a prominent greasy dark brown paleosol is developed in Taupo Ignimbrite, and is conformably overlain by either Tufa Trig Formation tephras and interbedded sands of the Makahikatoa Formation, or debris and hyperconcentrated flow deposits of Onetapu Formation. Contacts are generally sharp and wavy. At other sites an erosional unconformity (noted also by Topping 1974) commonly occurs above Taupo Pumice Formation. The eroded upper surface of Taupo Ignimbrite is often sharp and smooth and is unconformably overlain by Onetapu Formation deposits. This is particularly evident in exposures of Taupo Ignimbrite proximal to the Whangaehu River (Whangaehu River S.6 [T20/438033] and Scorpion Gully S.1 [T20/442054]).

At Desert Road S.10 [T20/464091] and more northern sections, and exposures along S.H.49, Taupo Ignimbrite commonly shows a pink coloration (Plate 2.4). At most other sites it is characteristically white or pale grey. Charcoalised wood is a ubiquitous feature in exposures of the ignimbrite, and is especially prominent at a section just south of the road bridge over Waihohonu Stream, on the Desert Road [T20/463172]. Here large charcoalised logs are embedded in poorly sorted pumiceous ash, lapilli and blocks.

Sections, at for example T20/399954 [WR1] and T20/438033 [WR6] along the Whangaehu River, and at Bullot Track S.2 [T20/420110] in Rangipo Desert, show Taupo Ignimbrite immediately underlain by a coarse crystal-rich deposit. This deposit is correlated with the 'ground layer' (Walker *et al.* 1981), also termed 'layer 1' by Sparks *et al.* (1973) of Taupo Ignimbrite, and is interpreted as a deposit of a pyroclastic surge (ground surge) which preceded the main pyroclastic flow (Sparks *et al.* 1973).

The thickness of Taupo Ignimbrite varies markedly throughout the field area, from a minimum *c.* 40 mm to a maximum exposed thickness of 3 m at Aqueduct S.1 [T20/418982], in a small tributary river channel in the southern end of Rangipo Desert (Plate 2.5).

Taupo Ignimbrite is a distinctive charcoal-bearing pyroclastic flow deposit and is readily distinguished from the much older Oruanui Ignimbrite Member of Kawakawa Tephra Formation also identified in the Mt Ruapehu region, by field characteristics (characteristic white or grey colour, presence of charcoalised logs and a crystal- and lithic-rich ground layer, and absence of bedding features) and stratigraphic position.

Distribution

Taupo Ignimbrite Member is preserved over most of the study area, but forms an incomplete cover within Rangipo Desert where wind and stream erosion have removed much of the tephra cover younger than Papakai Formation (Plate 2.6). Fine ash, lapilli and charcoal fragments from Taupo Ignimbrite have been reworked and incorporated into recent and presently accumulating sand dunes of post-Taupo Pumice age (Makahikatoa Sands). Lenses of reworked Taupo Ignimbrite are also found within fluvial deposits of Onetapu Formation (see section 5.2). At Tufa Trig T.S., a 300 mm thick deposit of reworked Taupo Ignimbrite is interbedded with Makahikatoa Sands.

The southernmost occurrence of Taupo Pumice Formation recorded in this study is at Ngamatea Swamp S.1 [T21/413874]. Here, Taupo Ignimbrite Member is 0.28 m thick and is found interbedded within peat (Plate 2.7; Plate 2.8). The westernmost recorded occurrence is on Ohakune Mountain Road, [S20/271074], where the formation is present only as a thin line of fine pumice lapilli within andesitic ash.

Figure 2.6 (p. 83) shows the distribution of Taupo Pumice Formation in the study area. Local erosion, and topographic overthickening of the formation does not allow depiction of meaningful isopachs.

Significance

Taupo Pumice Formation is a readily identifiable marker bed throughout TgVC and is an especially valuable time-plane for establishing the chronology of the most recent tephras and laharic deposits of the Mt Ruapehu ring plain.

Mapara Tephra [Mp]

Definition and Age

Mapara Tephra was erupted from TVC and is dated at *c.* 2100 years B.P. based on the bracketing radiocarbon ages of NZ1068 and NZ1069 (Vucetich and Pullar 1973; Table 2.1, p. 16). In the Taupo area, Vucetich and Pullar (1973) describe Mapara Tephra as rhyolitic tephra which overlies a paleosol developed in Whakaipo Tephra and which is unconformably overlain by Hatepe Tephra Member of Taupo Pumice Formation.

Description and Identification

The reference section for Mapara Tephra, on the southeastern Mt Ruapehu ring plain, is at Tufa Trig S.2 [TT2] [T20/375046] (Figure 2.1, p. 33; Chart 1). At this site, Mapara Tephra is 60 mm thick. It is preserved as conspicuous white to pale brown discontinuous fine ash 'cream cakes' up to 60 mm depth and shows partial mixing with the enclosing andesitic ash. Contacts are sharp and irregular. It conformably overlies a greasy sandy loam textured paleosol (0.13 m thick) developed in Mangatawai Tephra. It is conformably overlain by a thick (0.26 m) greasy sandy loam textured paleosol beneath Taupo Pumice, with a thin (10 mm) interbedded pocketing black ash (Plate 2.9; Plate 2.10; Plate 2.11).

At Ngamatea Swamp [T21/413874] Mapara Tephra is exposed along the length of a drainage ditch, and occurs as a thin (10 mm) pale brown to white pocketing ash layer interbedded with peat (Plate 2.8).

The ferromagnesian mineral assemblage of Mapara Tephra sampled at Tufa Trig S.2 [sample R3] comprises orthopyroxene, clinopyroxene and traces of hornblende (Table 2.3, p. 41). This is consistent with the ferromagnesian mineralogy of TVC tephras (Ewart 1963; Lowe 1980; Froggatt 1982a). The finer fractions (<0.125 mm) comprise only pyroxene. The high clinopyroxene content in this tephra compared with the low augite abundances recognised in Mapara Tephra at other localities (Table 2.4, p. 42) is attributed to local andesitic contamination of the rhyolitic ash. Stratigraphic position, and ferromagnesian mineralogy identify the tephra as Mapara Tephra.

Distribution

Mapara Tephra is identified in sections proximal to Tufa Trig S.2 at the northern end of Karioi Forest. Mapara Tephra has not been identified in sections along the Desert Road and was not recognised by Topping and Kohn (1973) in the Mt Tongariro region. Kohn (1973) makes reference to the occurrence of Mapara Tephra in TgVC, but does not give localities where it could be recognised.

In southern areas Mapara Tephra is preserved at sites where there has been local dune development, such as those developed at the northern end of Karioi Forest. Apparent absence of Mapara Tephra as a macroscopic tephra in areas north of Mt Ruapehu suggests its preservation in southern areas may have been afforded through the stabilisation of tephra deposits by native beech stands, presently colonising dunes in the area.

The distribution of Mapara Tephra in the southeastern Mt Ruapehu region is shown in Figure 2.6 (p. 83), extending the known distribution shown by Vucetich and Pullar (1973). Isopachs of Mapara Tephra are not shown for the Mt Ruapehu region because of the limited number of sites at which it has been identified. The southernmost occurrence of Mapara Tephra recorded in this study is at Ngamatea Swamp.

Significance

Mapara Tephra provides a time-plane useful to the dating of andesitic tephras in the study area, although application in this area is limited due to the few recognised occurrences of this tephra. Mapara Tephra however does provide an important time-plane for use in paleo-environmental studies of the southeastern Mt Ruapehu ring plain where it is found interbedded with peat deposits.

Waimihia Tephra [Wm]

Definition and Age

Waimihia Tephra [11], previously Waimihia Formation (Baumgart 1954; Healy 1964a; Vucetich and Pullar 1973) was erupted from TVC and is radiocarbon dated at *c.* 3400 years B.P. (Baumgart 1954; Healy 1964a) (Table 2.1, p. 16). Recent radiocarbon ages obtained by Alloway (1989) date Waimihia Lapilli Member at *c.* 4000 years B.P. [Wk1032, Wk1259], considerably older than the conventionally accepted *c.* 3400 years B.P.

In the Taupo area Vucetich and Pullar (1973) describe Waimihia Tephra as rhyolitic tephra (Waimihia Lapilli Member) and pyroclastic flow deposits (Waimihia Ignimbrite Member) which conformably underlie Whakaipo Tephra, being separated from it by a paleosol

[11] Waimihia Tephra is the formal stratigraphic name proposed by Froggatt and Lowe (1990). Members of Waimihia Tephra are Waimihia Ignimbrite and Waimihia Lapilli.

developed in the top of Waimihia Formation. Waimihia Formation conformably underlies Whakaipo Tephra and overlies Hinemaiaia Tephra (Lowe 1986).

Early descriptions of Waimihia Tephra at Taupo were made by Baumgart (1954) and Healy (1964a). Healy (1964a) defined Waimihia Formation to comprise Taupo Subgroup members 14 and 15.

Description and Identification

Reference sections for Waimihia Tephra on the southeastern Mt Ruapehu ring plain are here designated at Poutu S. [PT] [T19/481325], Desert Road S.16 [DR16] [T20/481186], Tufa Trig S.2 [TT2] [T20/375046], and Death Valley S.2 [DV2] [T20/408047], Rangipo Desert (Figure 2.1, p. 33; Chart 1).

In the Mt Ruapehu and Mt Tongariro regions, Waimihia Tephra is found interbedded with Papakai Formation (previously Papakai Tephra Formation, see section 3.3).

At Poutu R.S., Waimihia Tephra occurs as a coarse white ash interspersed within Papakai Formation. Detailed mapping of Waimihia Tephra to the south shows the tephra progressively grading from a coarse to fine ash.

At Desert Road R.S.16, Waimihia Tephra is preserved as both a dispersed coarse ash and scattered 5 – 10 mm thick fine ash 'cream cakes' interbedded within dark yellowish brown Papakai Formation. Waimihia Tephra is interbedded 90 mm below the upper contact of Papakai Formation with Mangatawai Tephra and 0.18 m above Hinemaiaia Tephra.

At more southern sections Waimihia Tephra occurs only as fine ash 'cream cakes'. At Tufa Trig S.2, the tephra, which is 50 mm thick, is preserved as very pale brown conspicuous 'cream cakes'. It is interbedded within Papakai Formation, 0.18 m below the upper contact of Papakai Formation with Mangatawai Tephra and occurs 20 mm above Papakai Formation member black ash-2, and 0.24 m above Hinemaiaia Tephra (Plate 2.10; Plate 2.11).

At Death Valley S.2, Waimihia Tephra, which is 20 mm thick, is preserved as discrete 'cream cakes' of pale brown to white fine ash with distinct contacts. It is interbedded within Papakai Formation and occurs 0.16 m below the upper contact of Papakai Formation with Mangatawai Tephra and 20 mm above Papakai Formation member black ash-2 (Chart 1). Waimihia Tephra is particularly well exposed in sections at Death Valley. The stratigraphic relationship of Waimihia Tephra to the younger Mangatawai Tephra and Papakai Formation members black ash-1 and black ash-2 is shown in Plate 2.11 and Plate 3.9.

At all sections where Waimihia Tephra is recognised it is clearly distinguished from the older Hinemaiaia and Motutere tephras (which are also found interbedded within Papakai Formation) by its finer grain size, pale brown colour and distinctive 'cream cake' appearance.

The ferromagnesian mineral assemblage of Waimihia Tephra (Table 2.3, p. 41) is based on a sample from Wahianoa Road S.1, Karioi Forest [T20/391986], [sample R5]. Here it is 30 mm thick and occurs 0.19 m below Taupo Pumice Formation and 0.19 m above Hinemaiaia Tephra. The assemblage comprises orthopyroxene, clinopyroxene and minor hornblende, consistent with the mineralogy of TVC tephras, and more particularly Waimihia Tephra near source (Table 2.4, p. 42). Finer fractions (<0.125 mm) show only traces of hornblende.

Electron microprobe analyses of glass shards from a correlative tephra (correlated from stratigraphic position) sampled from Tufa Trig S.2 [sample R4], are presented in Appendix IIIa. The mean analysis is given in Table 2.5 (p. 44) and may be compared with (mean) analyses of Waimihia Tephra from the type area (Froggatt 1982a; Lowe 1988a) in Table 2.6 (p. 45). Glass chemistry shows the tephra has major element concentrations typical of Holocene tephras from TVC (Figure 2.3, p. 47).

The Similarity Coefficient calculated for the comparison of this tephra [sample R4] to Waimihia Tephra (Froggatt 1982a) is 0.96 (Table 2.7, p. 48) and indicates the two tephras are chemically indistinguishable, supporting correlation with Waimihia Tephra.

On the basis of both stratigraphic position and ferromagnesian mineral assemblage, the tephra could equally be Whakaipo Tephra – however, the Similarity Coefficient of 0.86 obtained from comparison of this tephra with Whakaipo Tephra from the type area shows the glass chemistries of these two tephras are dissimilar and are therefore unlikely to be correlatives (Table 2.7, p. 48). The dissimilarity in glass composition of Whakaipo and Waimihia tephras is shown in Figure 2.3 (p. 47).

Stratigraphic position distinguishes this tephra from the older Hinemaiaia and Motutere tephras which are indistinguishable from Waimihia Tephra on glass chemistry.

In the Mt Tongariro region Topping and Kohn (1973) identified two rhyolitic tephras occurring below Mangatawai Tephra and interbedded within Papakai Formation. The upper rhyolitic tephra (Whakaipo Tephra, Topping and Kohn 1973) has been carefully mapped into the study area and found to occupy the same stratigraphic position as the tephra here identified as Waimihia Tephra. It is therefore here re-identified as Waimihia Tephra (Table 2.9, p. 61).

Distribution

Waimihia Tephra is identified in most tephra sections in the study area, and is especially prominent in sections within Rangipo Desert and along the Desert Road, north of Wahianoa Aqueduct S. [T20/435990]. The southernmost occurrence of Waimihia Tephra identified in this study is at Ngamatea Swamp [T21/413874] where it is 30 mm thick and is found interbedded with peat. Waimihia Tephra is absent in sections west of Waiouru along S.H.49.

The stratigraphic position of Waimihia Tephra in relation to local andesitic and other rhyolitic tephras in the study area is shown in Chart 1. The distribution of Waimihia Tephra in the southern Mt Ruapehu region is shown in Figure 2.6 (p. 83), extending the distribution depicted by Topping and Kohn (1973) and Vucetich and Pullar (1973).

Significance

Waimihia Tephra is a readily identifiable marker bed providing a useful time-plane for establishing the chronology of andesitic tephras and debris flow deposits preserved on the southeastern Mt Ruapehu ring plain. Preservation within peat at Ngamatea Swamp provides an important time-plane for paleo-environmental studies of the southern Mt Ruapehu region.

Hinemaiaia Tephra [Hm]

Definition and Age

Hinemaiaia Tephra (Froggatt 1981b) was erupted from TVC and is assigned a mean age of 4490 ± 140 years B.P. (Lowe 1986) (Table 2.1, p. 16).

In the Hawke's Bay region at Tiniroto and Poukawa, and at three other North Island localities (Kaipo Lagoon, Lake Rotomanuka near Hamilton, Lake Okoroire at Tirau), Lowe (1986) describes Hinemaiaia Tephra as rhyolitic tephra which underlies Waimihia Lapilli and overlies Whakatane Tephra (Table 2.2, p. 18).

Earlier descriptions of the stratigraphy at Tiniroto and Poukawa are found in Howorth and Ross (1981) and Kohn *et al.* (1981) and are summarised in Table 2.2 (p. 18).

Hinemaiaia Tephra has not previously been identified within TgVC.

Description and Identification

Reference sections for Hinemaiaia Tephra are here defined at Desert Road S.11 [DR11] [T20/464092], Desert Road S.15 [DR15] [T20/462135] and Death Valley S.2 [DV2] [T20/408047] (Figure 2.1, p. 33; Chart 1).

At Desert Road R.S.11, Hinemaiaia Tephra is 70 mm thick. It occurs as an olive yellow and white coarse pumiceous ash with diffuse upper and lower boundaries (Plate 2.12) interbedded within Papakai Formation. At the southern end of the section it occurs 0.56 m below Waimihia Tephra. At the northern end of the section however, where fluvial deposits overlying Papakai Formation pinch out, Hinemaiaia Tephra occurs 0.21 m below Waimihia Tephra.

At Desert Road R.S.15, Hinemaiaia Tephra, which is 90 mm thick, occurs as a distinctive olive yellow and white coarse ash with diffuse upper and lower contacts,

interbedded within Papakai Formation. It occurs 0.27 m below Waimihia Tephra, 0.41 m above Motutere Tephra, and 0.70 m above the basal contact of Papakai Formation with Poutu Lapilli Member of Mangamate Tephra (Plate 2.13). Hinemaiaia Tephra is distinguished from the overlying Waimihia Tephra and underlying Motutere Tephra by its coarser grain size and distinctive yellow colour.

At Death Valley T.L., Hinemaiaia Tephra is preserved as pocketing lenses of coarse yellow and white ash, with indistinct boundaries (Plate 2.14). It is found interbedded within Papakai Formation, below black ash-2 member. Ba-2 member is not recognised at Desert Road R.S.11 and R.S.15.

At Death Valley R.S.2, Hinemaiaia Tephra is 30 mm thick. Here it overlies 3.89 m of interbedded tephras and diamictons above Whakatane Tephra. It is overlain by 30 mm thick Papakai Formation and black ash-2 member. A peat layer (30 mm thick) occurs 0.15 m above Hinemaiaia Tephra and directly underlies a 2.03 m thick debris flow deposit (Mangaio Formation). This peat is radiocarbon dated [NZ7532] at 4850 ± 90 years B.P., and wood within the overlying debris flow is also dated [NZ7729] at 4600 ± 110 years B.P., giving an age of >*c.* 4850 years B.P. for Hinemaiaia Tephra (Table 2.10, p. 61). Where Mangaio Formation is not preserved, Hinemaiaia Tephra underlies Waimihia Tephra, being separated from it by Papakai Formation and member black ash-2.

Hinemaiaia Tephra is identified in most sections within Rangipo Desert, and also along the Desert Road south of Poutu S. [T19/481325]. At all localities where it is identified, the tephra is very similar in field appearance to Waimihia Lapilli, described as 'sago-like' by Vucetich and Pullar (1964), and cannot be distinguished from Waimihia Lapilli on field appearance, stratigraphy or glass chemistry.

Electron microprobe analyses of pumiceous fragments and glass shards from Hinemaiaia Tephra, sampled from Desert Road R.S.11 [sample R6] and Death Valley T.L. [sample R7], are presented in Appendix IIIa. Mean analyses are given in Table 2.5 (p. 44) and may be compared with the mean analysis of Hinemaiaia Tephra from the type area (P.C. Froggatt, written comm. 1990) (Table 2.6, p. 45). Glass chemistry shows the tephras have major element concentrations typical of Holocene tephras from TVC (Figure 2.3, p. 47).

Similarity Coefficients calculated for the comparison of samples R6 and R7 to Hinemaiaia Tephra (S.C. values of 0.95) and Waimihia Lapilli (mean analyses; P.C. Froggatt, written comm. 1990) (S.C. values of 0.97) show samples R6 and R7 could be correlatives of either Waimihia Tephra or Hinemaiaia Tephras. Distinction cannot be made from S.C. values.

At Death Valley S.2, a radiocarbon date obtained from peat found overlying Hinemaiaia Tephra [sample R7] provides a minimum age of *c.* 4800 years B.P. for this tephra – a little

older than the age currently assigned to Hinemaiaia Tephra by Lowe (1986) (Table 2.1, p. 16). On the basis of radiocarbon age this tephra is not a correlative of Waimihia Tephra. Radiocarbon age, stratigraphic position, ferromagnesian mineralogy, and glass chemistry all support correlation with Hinemaiaia Tephra. Stratigraphic position and field appearances distinguish it from the older Motutere Tephra (dated at *c.* 5370 years B.P.).

At Poutu S. [T19/481325], Topping and Kohn (1973) recognised two rhyolitic tephras within Papakai Formation, occurring below Mangatawai Tephra and above Hinemaiaia Ash (now re-identified as Motutere Tephra). The lower tephra has been mapped in detail south into the Mt Ruapehu region and is shown to have the same field characteristics and stratigraphic position as the tephra here identified as Hinemaiaia Tephra. It is therefore here re-identified as Hinemaiaia Tephra (Table 2.9, p. 61).

Distribution

Hinemaiaia Tephra is recognised in many sections in the study area, and is best identified in sections along the Desert Road between Waihohonu Stream and Tukino Road. The southernmost occurrence identified in this study is at Ngamatea Swamp [T21/413874] where it is approximately 0.11 m thick and is found interbedded with peat. Hinemaiaia Tephra has not been identified in sections west of Waiouru along S.H.49.

The stratigraphic position of Hinemaiaia Tephra in relation to local andesitic and other rhyolitic tephras in the Mt Ruapehu region is shown in Chart 1. Isopachs of Hinemaiaia Tephra are given in Lowe (1986). The distribution of Hinemaiaia Tephra in the southeastern Mt Ruapehu region is shown in Figure 2.6 (p. 83).

Significance

Hinemaiaia Tephra provides a time-plane for the dating of andesitic tephras and debris flow deposits preserved within the study area, and is an important marker bed for paleo-environmental studies. Hinemaiaia Tephra dates a major period of erosion in the Mt Ruapehu region (see section 5.2) and where found interbedded with peat (*e.g.* at Ngamatea Swamp) provides a time-plane for palynology studies of Holocene vegetation change in the southeastern Mt Ruapehu region.

Whakatane Tephra [Wk]

Definition and Age

Whakatane Tephra was erupted from the Haroharo Complex of OVC. It is dated at 4770 ± 170 years B.P. by Lowe (1986) (Table 2.1, p. 16), from an average of many radiocarbon dates obtained by Lowe (1986) and earlier workers [12]. In this study the revised

[12] Samples dated were from both near and distal to source and are listed in Lowe (1986).

Table 2.9 Comparison of the stratigraphy of Holocene and late Pleistocene rhyolitic tephras preserved in the study area with that of Topping and Kohn (1973) and Topping (1973).

Topping (1973) Topping & Kohn (1973)	This Thesis	Age (years B.P.)
Taupo Pumice	Taupo Pumice	*c.* 1819
Whakaipo Tephra	Waimihia Tephra	*c.* 3400
Waimihia Lapilli	Hinemaiaia Tephra	*c.* 4650
Hinemaiaia Ash	Motutere Tephra	*c.* 5370
Rotoma Ash	-	*c.* 7330
Opepe Tephra	-	*c.* 8850
Poronui Tephra	Poronui Tephra	*c.* 9900
Karapiti Tephra	Karapiti Tephra	*c.* 9910
?Rotorua Ash	?Waiohau Tephra	*c.* 11 250
?Puketarata Ash	?Rotorua Tephra	*c.* 13 450
Rerewhakaaitu Ash	Rerewhakaaitu Tephra	*c.* 14 700
Oruanui Formation	Kawakawa Tephra Formation	*c.* 22 500

Table 2.10 Radiocarbon ages determined in this study.

^{14}C Nº	^{14}C Age * (years B.P.)	Events Aged	Sample Description and Stratigraphic Position	Locality †
NZ7728	282 ± 35	Provides a maximum age for the youngest hyperconcentrated flood flow deposit of Onetapu Formation preserved at Tangiwai Swamp (member Ong), and a minimum age for the second-youngest hyperconcentrated flood flow deposit (member Onf) of Onetapu Formation at this site.	Peat which overlies Onetapu Formation member Onf, and which occurs 2.73 m above the base of Onetapu Formation member Ond. Immediately west of this exposure, the base of member Ond occurs 1.78 m above the base of Taupo Ignimbrite.	Tangiwai Swamp Type Section for Onetapu Formation Karioi State Forest [T20/319906]
NZ7388	390 ± 55	Provides a maximum age for the second-youngest hyperconcentrated flood flow deposit of Onetapu Formation at Tangiwai Swamp (member Onf) and minimum age for member Ond.	Peat which overlies member Ond, 2.02 m above its base.	Tangiwai Swamp Type Section for Onetapu Formation Karioi State Forest [T20/319908]
NZ7465	450 ± 55	Provides an age for the debris flow member Ond of Onetapu Formation at Tangiwai S.2, and a minimum age for older lahar events at this site. At an adjacent section, the base of this member occurs 1.7 m above Taupo Ignimbrite.	Small branches within debris flow - Onetapu Formation member Ond.	Tangiwai S.2 Karioi State Forest [T20/320904]
Wk1488	650 ± 50	Provides a minimum age for Tufa Trig Formation member Tf5, and a maximum age for Tufa Trig Formation member Tf6.	Peat 0.19 m above Taupo Ignimbrite, and immediately above Tufa Trig Formation member Tf5.	Ngamatea Swamp Waiouru [T21/413874]
Wk1489	830 ± 60	Provides a maximum age for Tufa Trig Formation member Tf5 and a minimum age for older members of Tufa Trig Formation.	Peat 0.15 m above Taupo Ignimbrite, and immediately below Tufa Trig Formation member Tf5.	Ngamatea Swamp Waiouru [T21/413874]
NZ7729	4600 ± 110	Provides an age for the Mangaio Formation debris flow deposit, and a minimum age for Hinemaiaia Tephra.	Small branches within debris flow; 0.88 m below base of Taupo Ignimbrite, 0.15 m above Hinemaiaia Tephra.	Death Valley S.2 Rangipo Desert [T20/408047]
NZ7532	4850 ± 90	Provides a maximum age for the Mangaio Formation debris flow deposit, and a minimum age for Hinemaiaia Tephra.	Peat from a 30 mm horizon immediately beneath Mangaio Formation debris flow, and 0.12 m above Hinemaiaia Tephra.	Death Valley S.2 Rangipo Desert [T20/408047]

* All ^{14}C ages discussed are conventional ages in radiocarbon years B.P. based on the old (Libby) half life of 5568 years.

† All grid references based on NZMS 260 topographical maps.

---

stratigraphy of Whakatane Tephra, after Lowe (1986), is adopted and therefore Lowe's

revised radiocarbon age for Whakatane Tephra is used.

In the Hawke's Bay region, Lowe (1986) describes Whakatane Tephra as rhyolitic tephra which overlies Motutere Tephra and underlies Hinemaiaia Tephra. In the Taupo region, Central North Island, Vucetich and Pullar (1973) and Froggatt (1981b) had previously described Whakatane Tephra as rhyolitic tephra underlying Waimihia Lapilli (Table 2.2, p. 18).

Description and Identification

A reference section for Whakatane Tephra on the southeastern Mt Ruapehu ring plain is here designated at Death Valley S.5 [DV5] [T20/409045] (Figure 2.1, p. 33; Plate 5.16; Chart 1). At this site, Whakatane Tephra, which is 5 mm thick, is interbedded within dark yellowish brown greasy silty clay loam which in turn is interbedded with diamictons of Manutahi Formation. It occurs *c.* 1.49 m below Hinemaiaia Tephra and *c.* 1.08 m above Motutere Tephra. The tephra is preserved as discrete white fine ash cream cakes with distinct, irregular contacts.

A section [T20/408045] immediately opposite the reference section also contains Whakatane Tephra. Here Whakatane Tephra forms a more continuous layer of white fine ash (Plate 2.15). The strong white colour of Whakatane Tephra is distinctive in these sections.

Whakatane Tephra is recognised at only one other site (Death Valley S.2), where it is 25 mm thick and has a distinct grey fine ash base. It is interbedded within fluvial deposits of Manutahi Formation and occurs 3.89 m below Hinemaiaia Tephra.

The ferromagnesian mineral assemblage of Whakatane Tephra at T20/408045 [sample R8] comprises orthopyroxene, clinopyroxene, minor hornblende and traces of cummingtonite. The finer (0.063–0.125 mm) fraction contains only minor cummingtonite and traces of hornblende (visual estimates only). Compared to previously published analyses of the ferromagnesian mineral contents in Whakatane Tephra (Table 2.4, p. 42), this tephra is cummingtonite-poor. Presence of this mineral however identifies an OVC source. Cummingtonite has been identified in five Holocene-age tephras from OVC: Kaharoa Tephra, Whakatane Tephra, Rotoma Tephra (Lowe 1980; Green and Lowe 1985), Waiohau Tephra (Kohn 1973) and Rerewhakaaitu Tephra (Kohn 1973; Lowe 1980).

At all sites where this tephra is identified it occurs above Motutere Tephra. Stratigraphic position and ferromagnesian mineral assemblage identifies this tephra as Whakatane Tephra. It is distinguished by stratigraphic position from the older cummingtonite-bearing Rotoma Tephra (dated at 7330 ± 235 years B.P., Table 2.1, p. 16). Both Whakatane Tephra and Rotoma Tephra were erupted from OVC during the deposition interval of Papakai Formation at TgVC. Rotoma Tephra has been identified at only one site in TgVC, where it was found interbedded with peat (Topping and Kohn 1973).

EMP analyses of glass shards from sample R8 are presented in Appendix IIIa. The mean analysis is given in Table 2.5 (p. 44) and may be compared with the mean analysis of Whakatane Tephra from its type section (data from P.C. Froggatt, written comm. 1990) (Table 2.6, p. 45). Glass chemistry shows the tephra has major element concentrations typical of OVC tephras (Figure 2.3, p. 47). Glass chemistry and ferromagnesian mineralogy therefore prevent correlation to the similarly aged Hinemaiaia Tephra (4650 ± 80 years B.P. [NZ4574]) erupted from TVC.

The Similarity Coefficient obtained for the comparison of this tephra with Whakatane Tephra (mean analysis, P.C. Froggatt, written comm. 1990) (Table 2.7, p. 48) is 0.96 and supports the correlation.

Distribution

Whakatane Tephra has not previously been identified within TgVC. Kohn (1973) states that Whakatane Tephra undoubtedly reached TgVC, but because it was incorporated into the developing Papakai Formation it is no longer preserved as a discrete layer. At sites where Whakatane Tephra is identified it is found interbedded with local fluvial deposits and tephras sourced from Mt Ruapehu, which occupy an equivalent stratigraphic interval to that of Papakai Formation. The nature of the enclosing sediments perhaps explains its preservation at these sites.

The stratigraphic position of Whakatane Tephra in relation to local andesitic and other rhyolitic tephras in the Mt Ruapehu region is shown in Chart 1. Sites where Whakatane Tephra is identified in the study area are shown in Figure 2.6 (p. 83), extending the known distribution of Whakatane Tephra identified by Pullar (1973). Isopachs of Whakatane Tephra are not presented for the Mt Ruapehu region because of the small number of sites at which it has been identified.

Significance

Whakatane Tephra provides a valuable time-plane for the dating of andesitic tephras, fluvial, and lahar deposits preserved within the study area on the southeastern Mt Ruapehu ring plain.

Motutere Tephra [Mt]

Definition and Age

Motutere Tephra was erupted from TVC, and is radiocarbon dated [NZ4846] at 5370 ± 90 years B.P. (Froggatt 1981b) (Table 2.1, p. 16).

Lowe (1986) defined Motutere Tephra as rhyolitic tephra which underlies Whakatane Tephra and overlies Opepe Tephra (Table 2.2, p. 18). In the Taupo region Froggatt (1981b)

describes Motutere Tephra as rhyolitic tephra which overlies in turn the andesitic Papakai Formation and rhyolitic Opepe Tephra.

Description and Identification

Reference sections for Motutere Tephra on the southeastern Mt Ruapehu ring plain are here designated at Desert Road S.17 [DR17] [T19/482199], Desert Road S.15 [DR15] [T20/462135], and Death Valley S.4 [DV4] [T20/410041] (Figure 2.1, p. 33; Chart 1).

Within TgVC Motutere Tephra is found interbedded within Papakai Formation.

At Desert Road R.S.17, adjacent to an unnamed tributary of Pangarara Stream, Motutere Tephra is found interbedded near the base of Papakai Formation, 0.12 m above the lower contact of Papakai Formation with Poutu Lapilli Member of Mangamate Formation, and 0.32 m below Hinemaiaia Tephra (Plate 2.16). The tephra is 60 mm thick and is preserved as a distinctive, nearly continuous layer of pinkish brown fine ash, and common fine scattered pumice fragments. It is distinguished from all other rhyolitic tephras in the section by its stratigraphic position and colour.

To the south, at Desert Road R.S.15, Motutere Tephra is 25 mm thick, and is found interbedded within Papakai Formation, 0.27 m above the basal contact of Papakai Formation with the underlying Poutu Lapilli, and 0.41 m below Hinemaiaia Tephra. Here, Motutere Tephra occurs as discrete, firm 'cream cakes' of pale grey, fine and coarse pumiceous ash, and scattered very fine pumice fragments (Plate 2.13).

At these sites, Motutere Tephra is the lowermost of the rhyolitic tephras found interbedded within Papakai Formation, and typically occurs within 0.30 m of the base of the formation.

At Death Valley S.4, Motutere Tephra, which is 30 mm thick, occurs as a pale pinkish brown layer of fine and coarse ash, with sharp contacts. It overlies 0.42 m of Tangatu Formation diamictons above an andesitic marker bed, Ngamatea lapilli-1 of Bullot Formation. Here Motutere Tephra is overlain by 3.25 m of Manutahi Formation diamictons below Hinemaiaia Tephra. At an adjacent section, Death Valley S.3, a discontinuous bed of reworked Motutere Tephra is found interbedded with Manutahi Formation sands, 0.21 m above primary Motutere Tephra (Plate 2.17).

At Whangaehu Ford [T20/425984], Motutere Tephra is 20 mm thick and occurs as discrete 'cream cakes' interbedded within greasy fine sandy clay loam. Here it is distinctly bedded, showing a central lamina of coarse pumiceous ash and very fine pumice lapilli enclosed within fine ash. The coarse ash-pumice lapilli component is characteristic of Motutere Tephra at all localities where it has been identified and is diagnostic of the Tephra in the study area.

At many sites, Motutere Tephra is indistinct, and difficult to recognise, especially where tephra sections have dried out producing poor colour contrast between dry andesitic and pale rhyolitic tephra.

In the Mt Ruapehu region, Motutere Tephra (Plate 2.16) occupies the same stratigraphic position as a rhyolitic tephra identified by Topping and Kohn (1973) in sections along the Desert Road south to Mangatoetoenui Stream and correlated with Hinemaiaia Ash. Hinemaiaia Ash in the Mt Tongariro region is most probably the correlative of Motutere Tephra, following the stratigraphic revision of Hinemaiaia Ash by Froggatt (1981b) (Table 2.2, p. 18).

The ferromagnesian assemblage of Motutere Tephra, sampled at Death Valley R.S.4 [sample R9] (Table 2.3, p. 41) and Whangaehu Ford R.S. [sample R10] comprises orthopyroxene, clinopyroxene and minor hornblende, consistent with the ferromagnesian mineralogy of TVC tephras, although the clinopyroxene abundance is considerably greater than recognised by Froggatt (1982a) in the source area (Table 2.4, p. 42). EMP analyses of glass shards from sample R9 are presented in Appendix IIIa. The mean analysis is given in Table 2.5 (p. 44) and may be compared with the mean analysis of Motutere Tephra from the type section (data from P.C. Froggatt, written comm. 1990) (Table 2.6, p. 45). Glass chemistry shows the tephra has major element concentrations typical of TVC tephras (Figure 2.3, p. 47). The Similarity Coefficient calculated for this tephra [sample R9] compared to Froggatt's Motutere Tephra is 0.91 and can be used, in conjunction with stratigraphic position and ferromagnesian mineralogy, to support correlation with Motutere Tephra.

According to ferromagnesian mineralogy and glass chemistry this tephra could equally be correlated with the older Opepe Tephra, dated *c.* 8850 years B.P. (Table 2.1, p. 16). Both Motutere and Opepe tephras were erupted during deposition of Papakai Formation. Motutere Tephra is here correlated with Hinemaiaia Ash of Topping and Kohn (1973) in the Mt Tongariro region. Opepe Tephra has been identified at only one site within TgVC, where it is found interbedded with peat (Topping and Kohn 1973).

Distribution

Motutere Tephra is identified in many sections in the southeastern Mt Ruapehu region, especially within Rangipo Desert and along the Desert Road, north of Wahianoa Aqueduct S. [T20/435990]. Motutere Tephra has not been identified in sections south or west of Waiouru. It is best preserved in sections along the Desert Road where its preservation was afforded by enclosure within the actively accumulating Papakai Formation at the time of its eruption.

The stratigraphic position of Motutere Tephra in relation to local andesitic and other rhyolitic tephras in the Mt Ruapehu region is shown in Chart 1. The distribution of Motutere Tephra in the study area is shown in Figure 2.6 (p. 83), extending the recognised distribution of Motutere Tephra (mapped previously as Hinemaiaia Ash by Topping and Kohn 1973) within TgVC.

Significance

Motutere Tephra is an important marker bed useful for dating debris flow deposits on the southeastern Mt Ruapehu ring plain.

Poronui Tephra [Po]

Definition and Age

Poronui Tephra was erupted from TVC, and is dated at *c.* 9900 years B.P., based on three radiocarbon dates [Wk351, Wk352, Wk491] (Lowe and Hogg 1986; Table 2.1, p. 16). Previously Poronui Tephra had been given an extrapolated age of *c.* 9740 years B.P. (Topping and Kohn 1973).

In the Taupo area of the Central North Island, Vucetich and Pullar (1973) describe Poronui Tephra as rhyolitic tephra which paraconformably underlies Opepe Tephra and conformably overlies Te Rato Lapilli. Froggatt (1981a) identifies Poronui Tephra incorporated within a weak paleosol beneath Opepe Tephra.

In the Mt Tongariro region, Topping and Kohn (1973) describe Poronui Tephra as fine yellow rhyolitic tephra which overlies Karapiti Tephra (previously Papanetu Tephra) and underlies Opepe Tephra. It is interbedded with members of Mangamate Tephra.

Description and Identification

Poronui Tephra is best preserved in sections north of Mt Ruapehu on the Mt Tongariro ring plain, at reference sections defined by Topping and Kohn (1973). It has been identified in the study area by detailed mapping of the enclosing andesitic Wharepu Tephra and Ohinepango Tephra members of Mangamate Tephra.

Reference sections for Poronui Tephra on the southeastern Mt Ruapehu ring plain are here defined at Desert Road S.15 [DR15] [T20/462135] and Desert Road S.11 [DR11] [T20/464092] (Figure 2.1, p. 33; Chart 1).

At Desert Road R.S.15, Poronui Tephra is preserved as a 15 mm thick distinctive white to yellow fine ash, forming a near continuous horizon, 1.38 m below Motutere Tephra (Plate 2.18). It directly overlies distinctive orange and black colour-banded Ohinepango Tephra (0.39 m), and is overlain by dark grey Wharepu Tephra (0.71 m).

In sections further to the south, Poronui Tephra is less distinct, occurring as a thin discontinuous pocketing fine ash. At these sites the stratigraphic position of Poronui Tephra is readily identified from the position of Ohinepango Tephra, which is a prominent andesitic marker bed throughout most of the Mt Ruapehu region.

At Desert R.S.11, Poronui Tephra is preserved as a 3 mm thick discontinuous fine white ash. It overlies black Ohinepango Tephra (20 mm thick) and is conformably overlain by Wharepu Tephra (0.54 m thick).

At sections where Poronui Tephra is not recognised as a macroscopic tephra layer, it may be identified from the presence of glass shards. Rhyolitic glass shards were recognised within the base of Wharepu Tephra at a section on the Desert Road [T19/492213], just south of Oturere Trig. The tephra is correlated with Poronui Tephra from its stratigraphic position. Topping and Kohn (1973) identified Poronui Tephra from stratigraphic position, ferromagnesian assemblage (hypersthene + augite), and titanomagnetite chemistry.

Distribution

Poronui Tephra is recognised in exposures north of Desert Road R.S.11, but in few sections south of here. The southernmost occurrence identified in this study is at Whangaehu River S.5 [T20/443045]. Sites at which Poronui Tephra is identified in the study area are shown in Figure 2.6 (p. 83), extending the previously recognised distribution of Topping and Kohn (1973) and Vucetich and Pullar (1973). The stratigraphic position of Poronui Tephra in relation to local andesitic and other rhyolitic tephras in the study area is shown in Charts 1 and 2.

Significance

Poronui Tephra is a valuable marker bed for identifying the stratigraphic position of Mangamate Tephra, and especially Wharepu Tephra Member at more distal sites on the southeastern Mt Ruapehu ring plain.

Karapiti Tephra [Kp]

Definition and Age

Karapiti Tephra is the oldest of the Holocene rhyolitic tephras erupted from TVC (Howorth *et al.* 1981). Karapiti Tephra was erupted after *c.* 10 000 years of quiescence at TVC following the *c.* 22 500 years B.P. Kawakawa Tephra Formation eruption. It is radiocarbon dated [NZ4847] at 9910 ± 130 years B.P. (Froggatt 1981a) (Table 2.1, p. 16). Previously Karapiti Tephra had been dated at *c.* 9785 years B.P. based on bracketing radiocarbon ages [NZ1372, NZ1373, NZ1374] (Topping and Kohn 1973), and had been assigned an extrapolated age of *c.* 10 000 years B.P. by Lowe and Hogg (1986).

In the northern Tongariro – Taupo region, Froggatt and Solloway (1986) describe Karapiti Tephra as rhyolitic tephra lying between the rhyolitic Poronui and Rotorua tephras erupted from TVC and OVC respectively. More specifically Topping and Kohn (1973) described Karapiti Tephra in the Mt Tongariro region, as rhyolitic tephra which directly underlies Te Rato

Lapilli Member of Mangamate Tephra and overlies Okupata Tephra, separated from it by unnamed andesitic tephras.

Description and Identification

In the study area, Karapiti Tephra has been identified only at Mangatoetoenui Quarry [MQ] [T20/459153] (Figure 2.1, p. 33). At this site it is preserved as a 5 mm thick discontinuous pocketing white to pale grey fine ash. It is interbedded within grey sandy clay textured ash, 15 mm below Oturere Lapilli Member and 0.12 m above Pahoka Tephra.

Karapiti Tephra is identified on the basis of its stratigraphic position. It should however be noted that the older Waiohau Tephra (*c.* 11 250 years B.P.) occupies a similar stratigraphic position, occurring beneath Te Rato Lapilli and above Rotorua Tephra (dated *c.* 13 450 years B.P.).

Karapiti Tephra was identified by Topping and Kohn (1973) and its identification in the Mt Tongariro region was confirmed by the ferromagnesian mineralogy and glass chemistry determined by Froggatt and Solloway (1986).

Plate 2.19 shows the stratigraphic relationship of the Karapiti Tephra to Mangamate Tephra Formation and the older Pahoka Tephra at a cutting on the Desert Road at [T19/524283].

Distribution

An isopach map of Karapiti Tephra (previously Papanetu Tephra) presented by Topping and Kohn (1973) places the limit of distribution just south of Mangatawai S., where it is present as trace light yellowish brown fine ash. Preservation of this tephra at Mangatoetoenui Quarry, however, indicates deposition occurred at least 10 km further to the south.

Significance

Because Karapiti Tephra has been identified at only one site in the study area, its use in establishing a chronology of local andesitic tephras is severely limited. However, presence of this tephra does confirm the identification of the overlying tephra at Mangatoetoenui Quarry as Mangamate Tephra.

Waiohau Tephra [Wh]

Definition and Age

Waiohau Tephra was erupted from OVC, and is dated [NZ568] at 11 250 ± 250 years B.P. (Cole 1970a) (Table 2.1, p. 16).

In the Central North Island, Vucetich and Pullar (1964, 1973) describe Waiohau Tephra as rhyolitic tephra which overlies Rotorua Tephra, and underlies Karapiti Tephra. Waiohau Tephra has not previously been described from TgVC.

Description and Identification

Reference sections for Waiohau Tephra on the southeastern Mt Ruapehu ring plain are here designated at Wahianoa Aqueduct S. [WA] [T20/435990] and Whangaehu River S.1 [WR1] [T20/399954] (Figure 2.1, p. 33; Chart 3).

At Wahianoa Aqueduct R.S., Waiohau Tephra is preserved as an almost continuous, distinctive white very fine ash. With the exception of Kawakawa Tephra Formation, Waiohau Tephra is the most distinctive of all the rhyolitic tephras recognised in the study area. At this site it is 30 mm thick. It overlies *c.* 2.1 m of andesitic lapilli and ash beds of Bullot Formation, above Rerewhakaaitu Tephra (Plate 2.20) and underlies Shawcroft Tephra Member of Bullot Formation, being separated from it by an 80 mm thick greasy sandy loam textured medial unit. A distinctive dark purplish black andesitic tephra of coarse ash to lapilli grade occurs 20 mm below Waiohau Tephra, separated from it by coarse sandy loam textured ash.

Waiohau Tephra is identified in many sections south of Wahianoa Aqueduct R.S. At Whangaehu River S.1, located on the Whangaehu escarpment, Waiohau Tephra overlies 0.90 m of uncorrelated Bullot Formation tephras, above Rerewhakaaitu Tephra (Plate 2.21) and is overlain by Shawcroft Tephra Member of Bullot Formation (Plate 2.22), being separated from it by 30 mm of sandy loam textured ash. Waiohau Tephra occurs as 30 mm thick pocketing white fine ash.

Within the study area, Waiohau Tephra is always of fine ash grade. At all localities the tephra overlies a distinctive purplish black andesitic tephra, and is found interbedded with coarse pumiceous lapilli units of Bullot Formation. Waiohau Tephra has been identified in these sections by detailed correlation of enclosing andesitic tephras, and the presence of a distinctive underlying purplish black marker tephra.

In sections north of Wahianoa Aqueduct R.S., Shawcroft Tephra Member has not been recognised and therefore this tephra cannot be used to identify the stratigraphic position of Waiohau Tephra at these sites. Based, however, on correlations with Bullot Formation tephras at other sites (Chart 3), the position of Waiohau Tephra is provisionally placed at the base of Bullot Formation member L16.

The ferromagnesian mineral assemblage of Waiohau Tephra, sampled at Wahianoa Aqueduct R.S. [sample R11], Whangaehu River S.5 [T20/443045], Missile Ridge [T20/398063], and Tufa Trig S.2 [T20/375046] [sample R13] comprises orthopyroxene, clinopyroxene, minor biotite and trace amounts of hornblende. This is consistent with the mineralogy of OVC tephras near source (Table 2.4, p. 42). Presence of biotite in these

tephras is indicative of an Okataina source. Dominance of orthopyroxene and clinopyroxene may reflect partial contamination from local andesitic tephras. Both biotite and hornblende are concentrated in the finer 0.063 – 0.125 mm fraction. Biotite occurs in minor amounts in the 0.125 – 0.250 mm fractions of samples R11 (4%) and R13 (8%) (Table 2.3, p. 41).

Biotite is identified in four late Pleistocene tephras from OVC (Waiohau, Rotorua, Rerewhakaaitu and Okareka tephras) and in Puketarata Tephra, erupted from MVC. Waiohau Tephra contains only minor (<4%) biotite (Stewart 1982; Green and Lowe 1985; Lowe 1988a). Cole (1970a), however, did not recognise biotite in the ferromagnesian assemblage of Waiohau Tephra at the type section at Rerewhakaaitu. The older Rotorua and Okareka tephras generally contain up to 20% biotite (Kohn 1973; Kohn and Glasby 1978; Lowe 1980), although abundances of only 3 – 12% in Rotorua Tephra, and 15 – 40% in Okareka Tephra are reported by Lowe (1988a). Both Puketarata and Rerewhakaaitu tephras are distinctly more biotite-rich and contain between 35% and 80% biotite (Kohn and Glasby 1978; Lowe 1988a). Biotite content cannot be used in this instance to provide unequivocal correlation with Waiohau Tephra, and according to stratigraphic position and ferromagnesian mineralogy the tephra could equally be correlated with the older Rotorua Tephra (*c.* 13 450 years B.P.), previously identified in TgVC by Froggatt and Solloway (1986).

EMP analyses of glass shards from sample R11 [Wahianoa Aqueduct R.S.], and R12 [Missile Ridge] are presented in Appendix IIIa. Mean analyses are given in Table 2.5 (p. 44), and may be compared with mean analyses of Waiohau Tephra from the type area (data from Froggatt and Solloway 1986; Lowe 1988a) and Rotorua Tephra from the type section (data from P.C. Froggatt, written comm. 1990) (Table 2.6, p. 45). Glass chemistry shows the tephras have major element concentrations typical of OVC tephras (Figure 2.3, p. 47). Concentrations of both FeO and CaO are, however, quite variable between individual shards. The Similarity Coefficient calculated for comparison of Rotorua Tephra (data from P.C. Froggatt, written comm. 1990) and Waiohau Tephra (data from Froggatt and Solloway 1986) is 0.87. A value of 0.84 is obtained using Waiohau Tephra data from Lowe (1988a). Both values indicate chemical dissimilarity between these two tephras. Waiohau Tephra has lower TiO_2, FeO, MgO and CaO contents than Rotorua Tephra (Green and Lowe 1985). Similarity Coefficients derived from the comparison of tephras sampled at Wahianoa Aqueduct R.S. and Missile Ridge S. [T20/398063] in Rangipo Desert to Froggatt and Solloway's Waiohau Tephra are both 0.95. The same comparison made to Lowe's Waiohau Tephra also gives S.C. values of 0.95. Comparison with Rotorua Tephra from the type area gives S.C. values of 0.85 and 0.86 respectively (Table 2.8, p. 49). Still lower values (<0.80) are obtained by comparison to Rotorua Tephra using data from Lowe (1988a) and show the two tephras are chemically different. This difference in chemistry is also apparent in Figure 2.3 (p. 47). Similarity Coefficient values indicate stronger chemical similarity of the tephra to Waiohau Tephra (as do elemental abundances of TiO_2, FeO, MgO and CaO).

The tephra is therefore correlated with Waiohau Tephra from stratigraphic position, ferromagnesian mineralogy and glass chemistry.

A yellow fine rhyolitic tephra, occurring stratigraphically below Mangamate Tephra and Karapiti Tephra, and above Rotoaira Lapilli at Poutu and Access 10 reference sections was correlated with Rotorua Tephra (Topping and Kohn 1973). The tephra is correlative-age dated from two radiocarbon ages [NZ1187, NZ1186] at *c.* 12 500 years B.P. At these sites, a black pocketing coarse ash is found underlying the tephra. In the study area, the association of Waiohau Tephra to the underlying distinctive purplish black marker tephra is a unique stratigraphic characteristic, and on this basis, the tephra identified by Topping and Kohn as ?Rotorua Tephra is provisionally re-identified as Waiohau Tephra. The radiocarbon age is however significantly older than that of Waiohau Tephra, and younger than the accepted age for Rotorua Tephra.

At a more southern section [T19/488213, Oturere Trig S.1, a rhyolitic tephra identified 1.43 m below Pahoka Tephra occurs in a similar stratigraphic position. It overlies a strong purplish black coarse ash and is shown by detailed mapping of both andesitic and rhyolitic tephras, south of Mangatawai Stream, to occupy the same stratigraphic position as ?Rotorua Tephra at Mangatawai R.S. (Topping and Kohn 1973). On this basis the ?Rotorua Tephra of Topping and Kohn (1973) is here provisionally correlated with Waiohau Tephra.

Correlation with either Waiohau Tephra or Rotorua Tephra might best be established by analysis of glass shards of Topping and Kohn's (1973) ?Rotorua Tephra from the reference section.

There are few sections which expose the older than *c.* 10 000 years B.P. stratigraphy between Oturere Trig S. to the north, and Wahianoa Aqueduct R.S. to the south. This prevents detailed correlation of late Pleistocene rhyolitic and andesitic tephras identified in the Mt Tongariro region by Topping and Kohn (1973) with tephras in the southern study area on the Mt Ruapehu ring plain. Correlations in the Mt Ruapehu region are therefore principally established from comparison of relative stratigraphic positions, ferromagnesian mineralogy and glass chemistry of the tephras.

Distribution

Waiohau Tephra has not previously been identified in the TgVC, nor in areas southeast of Lake Taupo (Vucetich and Pullar 1973; Froggatt and Solloway 1986). Isopachs for Waiohau Tephra are given in Pullar and Birrell (1973). A plot of isopach thickness against distance (Figure 2.4, p. 75), however, shows that it is not unexpected to find Waiohau Tephra deposited in TgVC.

Waiohau Tephra is identified in many sections in the southern part of the study area, in sections along the Desert Road and immediately west in sections along the Whangaehu

escarpment, and within Rangipo Desert. The southernmost occurrence identified in this study is at Ngamatea Swamp [T21/413874]. The stratigraphic position of Waiohau Tephra in relation to local andesitic and other rhyolitic tephras in the Mt Ruapehu region is shown in Chart 3. Localities at which Waiohau Tephra has been identified in the southeastern Mt Ruapehu region are shown in Figure 2.6, p. 83.

Significance

Waiohau Tephra is a prominent rhyolitic marker bed in the study area, useful for the dating of andesitic tephras of Bullot Formation and local ring plain-forming debris flow deposits.

?Rotorua Tephra [Rr]

Definition and Age

Rotorua Tephra [13] was erupted from OVC and is dated [NZ1615] at 13 450 ± 250 years B.P. (Nairn 1980) (Table 2.1, p. 16).

Rotorua Tephra, originally defined by Grange (1931) was redefined as two formations, Waiohau Tephra and Rotorua Tephra, by Vucetich and Pullar (1964). In the Central North Island, Vucetich and Pullar (1964) defined Rotorua Tephra as the rhyolitic tephra and overlying paleosol which stratigraphically overlies Puketarata Tephra (dated at *c.* 14 000 years B.P., Lowe 1988a, Table 2.1, p. 16) and underlies Waiohau Tephra, dated at 11 250 ± 250 years B.P.

Description

?Rotorua Tephra has been identified only at Oturere Trig S.1 [T19/488213]. Here it is preserved as a 10 mm thick pocketing white fine ash. It is interbedded with greasy sandy clay loam textured medial deposits *c.* 2.25 m below Pahoka Tephra and 0.75 m below a rhyolitic tephra, here provisionally re-identified as Waiohau Tephra.

Detailed mapping of rhyolitic and andesitic tephras from Mangatawai S. [T19/489238] south to this site establishes that the tephra occupies the same stratigraphic position as ?Puketarata Tephra at Mangatawai S. Here, ?Puketarata Tephra is identified below ?Rotorua Tephra (provisionally re-identified as Waiohau Tephra, this thesis) and above Rotoaira Lapilli (Topping 1973). The tephra contains minor biotite (5 – 9%) in the ferromagnesian mineral assemblage (Topping and Kohn 1973; Topping 1974). A suggested age of *c.* 14 000 years B.P. is given for Puketarata Tephra (Lowe 1988a) based on its stratigraphic position between Rotorua and Rerewhakaaitu tephras. Rotoaira Lapilli is radiocarbon dated [NZ1559] at

[13] Rotorua Tephra is the formal stratigraphic name proposed by Froggatt and Lowe (1990). The name Rotorua Ash appears in earlier literature *e.g.* Grange (1931a) and Vucetich and Pullar (1973).

c. 13 800 years B.P. (Topping 1973). Thus the relative stratigraphic position of Puketarata Tephra to Rotoaira Lapilli is not known given that the age of Puketarata Tephra is an estimated-age. The rhyolite identified as ?Puketarata Tephra by Topping and Kohn (1973) could then be either Rotorua Tephra or Puketarata Tephra.

Isopachs for Puketarata Tephra (Lloyd 1972) and the thickness–distance plot (Figure 2.4, p. 75) indicate that this tephra would not have been deposited in southern TgVC. Furthermore, Puketarata Tephra contains between 35% and 80% biotite (Kohn 1973; Kohn and Glasby 1978; Lowe 1980, 1988a). The biotite content in ?Puketarata Tephra (Topping and Kohn 1973) is more consistent with that recognised in Rotorua Tephra (< 20%) (Kohn and Glasby 1978). Both Puketarata and Rerewhakaaitu tephras are biotite-rich, with much lower biotite levels observed in Waiohau and Rotorua tephras. Stratigraphic position (above Rotoaira Lapilli), isopach thickness, ferromagnesian mineralogy and biotite content suggest the tephra identified as ?Puketarata Tephra is more likely to be Rotorua Tephra.

Rerewhakaaitu Tephra [Rk]

Definition and Age

Rerewhakaaitu Tephra [14] was erupted from Tarawera Volcanic Complex, located within OVC, and is dated [NZ716] at 14 700 ± 200 years B.P. (Pullar *et al.* 1973) (Table 2.1, p. 16).

In the Okataina region, Vucetich and Pullar (1964) describe Rerewhakaaitu Tephra at the type section as rhyolitic tephra underlying Rotorua Tephra. In the Mt Tongariro region Topping and Kohn (1973) describe Rerewhakaaitu Tephra as rhyolitic tephra occurring between Rotoaira Lapilli and Kawakawa Tephra Formation.

Description and Identification

Reference sections for Rerewhakaaitu Tephra in the study area are here designated at Bullot Track S.1 [BT1] [T20/412108], Whangaehu River S.5 [WR5] [T20/443045] and Desert Road S.10 [DR10] [T20/464091] (Figure 2.1, p. 33; Chart 3).

At Bullot Track, Rerewhakaaitu Tephra is preserved as a discontinuous thin (10 mm) white glassy fine ash within pale brown andesitic ash of Bullot Formation. It overlies Bullot Formation member L7, being separated from it by 0.61 m of unnamed ash and lapilli beds, and occurs 6.32 m above Kawakawa Tephra Formation. It underlies Bullot Formation member L8, being separated from it by 0.56 m of unnamed Bullot Formation ash and lapilli beds.

---

[14] Rerewhakaaitu Tephra is the proposed formal stratigraphic name used by Froggatt and Lowe (1990). The name Rerewhakaaitu Ash appears in earlier literature *e.g.* Vucetich and Pullar (1964), Topping and Kohn (1973).

The ferromagnesian mineral assemblage of Rerewhakaaitu Tephra sampled at Bullot Track T.S. [sample R14] comprises orthopyroxene, clinopyroxene, biotite and minor hornblende (Table 2.3, p. 41), and is consistent with the ferromagnesian mineralogy identified for OVC tephras (Table 2.4, p. 42). Biotite occurs in significant amounts (22%) in the 0.125 – 0.250 mm fraction, and together with hornblende is found concentrated in the finer 0.063 – 0.125 mm fraction. The presence of biotite indicates the tephra has an Okataina source. Biotite abundance cannot be used in this instance to provide unequivocal correlation with Rerewhakaaitu Tephra because it is more consistent with levels identified in the Rotorua or Okareka tephras. According to ferromagnesian mineralogy the tephra could equally be correlated with the younger Waiohau, Rotorua or Puketarata tephras. Figure 2.4 (p. 75) shows the isopach thicknesses of the Waiohau, Rotorua, Puketarata, Rerewhakaaitu, and Okareka tephras plotted against distance from source [15]. Isopachs (Lloyd 1972) and thickness – distance plots indicate that Puketarata Tephra is unlikely to have been deposited in TgVC. The other tephras, especially Waiohau Tephra, are however, very likely preserved.

The correlation of Bullot Formation tephras with members at Bullot Track S.1 (Chart 3) indicates that the stratigraphic position of Waiohau Tephra probably occurs just below Bullot Formation member L16. On the basis of stratigraphic position, the rhyolitic tephra identified below member L8 at Bullot Track S.1 is therefore not a correlative of Waiohau Tephra. Furthermore the field characteristics of the rhyolitic tephra and the enclosing andesitic tephras are inconsistent with those observed for Waiohau Tephra and associated andesites at Wahianoa Aqueduct R.S. and other sites.

EMP analyses of glass shards from sample R14 [Bullot Track S.1] are presented in Appendix IIIa. The mean analysis is given in Table 2.5 (p. 44) and may be compared with mean analyses of Waiohau, Rotorua, Puketarata and Rerewhakaaitu tephras from their type areas (Table 2.8, p. 49). Glass chemistry shows the tephra has major element concentrations typical of OVC tephras.

The Similarity Coefficient values obtained from comparison of the glass chemistry of sample R14 to Rotorua and Puketarata tephras are 0.84 and 0.82 respectively, clearly indicating dissimilarity in the glass compositions of these tephras. Puketarata Tephra shows distinctive glass chemistry, with much lower concentrations of MgO and TiO_2 than are present in OVC tephras. Both the S.C. values and major element chemistry show the tephra [sample R14] is not a correlative of either Puketarata Tephra or Rotorua Tephra.

---

[15] A discussion of the relationship between tephra thickness and distance from source is found in Fisher and Schmincke (1984) pp. 137 – 139. Lines on plots assume that tephra thickness (T) is an exponential function of distance (x) from the source ($T = ae^{-kx}$; straight line on a semi-log plot; after Thorarinsson (1954) *in* Fisher and Schmincke (1984)). Note that Waiohau, Rotorua and Rerewhakaaitu tephras exhibit relatively poor fit against a single slope line and may be better described by incorporating a slope change (see Williams and Goles (1968) *in* Fisher and Schmincke (1984)).

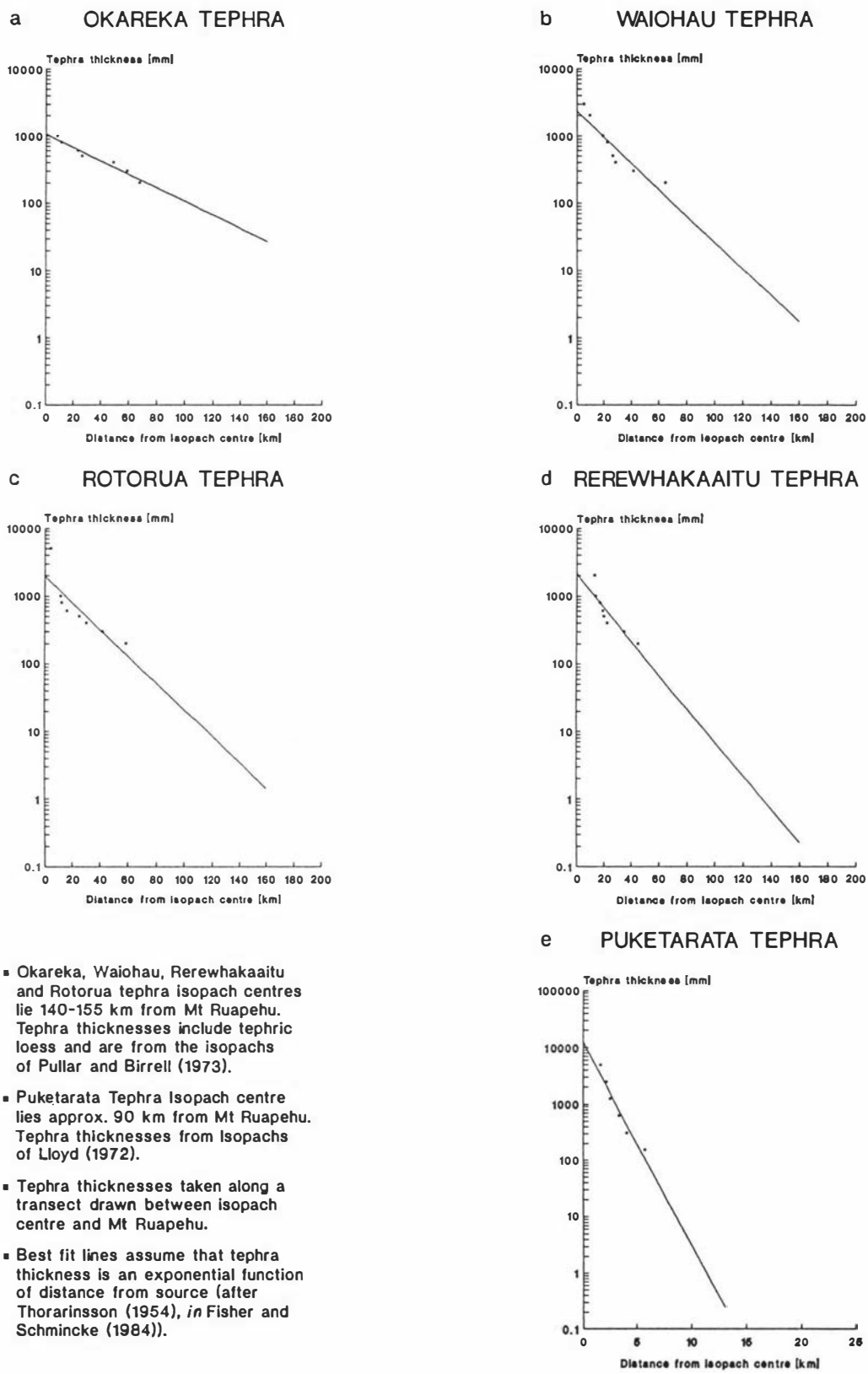

- Okareka, Waiohau, Rerewhakaaitu and Rotorua tephra isopach centres lie 140-155 km from Mt Ruapehu. Tephra thicknesses include tephric loess and are from the isopachs of Pullar and Birrell (1973).
- Puketarata Tephra Isopach centre lies approx. 90 km from Mt Ruapehu. Tephra thicknesses from Isopachs of Lloyd (1972).
- Tephra thicknesses taken along a transect drawn between isopach centre and Mt Ruapehu.
- Best fit lines assume that tephra thickness is an exponential function of distance from source (after Thorarinsson (1954), *in* Fisher and Schmincke (1984)).

Figure 2.4 Plots of isopach thickness *vs* distance from isopach centre for Puketarata, Rotorua, Rerewhakaaitu, Okareka and Waiohau tephras.

Comparison to Rerewhakaaitu Tephra (using data from P.C. Froggatt, written comm. 1990) gives an S.C. value of 0.94, and shows the tephras are indistinguishable on glass

chemistry. Stratigraphic position, ferromagnesian mineral assemblage and glass chemistry suggest correlation with Rerewhakaaitu Tephra.

A white fine rhyolitic ash identified at Whangaehu River S.5 [sample R15] is also correlated with Rerewhakaaitu Tephra. Here, the tephra is preserved as a discontinuous, 40 mm thick, white fine glassy ash interbedded with coarse ash and lapilli of Bullot Formation. It overlies 0.52 m of Bullot Formation tephras above coarse diamictons of Te Heuheu Formation, and underlies 1.03 m of Bullot Formation tephras below Waiohau Tephra. No older rhyolitic tephras are recognised at this site.

The ferromagnesian mineral assemblage of sample R15 comprises orthopyroxene, clinopyroxene, biotite and minor hornblende. Biotite comprises 22% of the total ferromagnesian mineral assemblage (Table 2.3, p. 41). The presence of biotite indicates an OVC source – however, the abundance cannot be used in this instance to provide unequivocal correlation with Rerewhakaaitu Tephra. Dominance of orthopyroxene and clinopyroxene may reflect contamination from enclosing andesitic tephras.

EMP analyses of glass shards from this tephra are presented in Appendix IIIa. The mean analysis is given in Table 2.5 (p. 44), and may be compared with mean analyses of Rotorua, Rerewhakaaitu and Okareka tephras from type areas (data from Froggatt and Solloway 1986; Lowe 1988a; P.C. Froggatt, written comm. 1990) (Table 2.6, p. 45). Glass chemistry shows the tephra has major element concentrations typical of OVC tephras (Figure 2.3, p. 47).

The Similarity Coefficient derived from comparison of the glass chemistry of this rhyolitic tephra [sample R15] with Rerewhakaaitu Tephra is 0.89, indicating the tephras have dissimilar glass chemistries. A similar value (0.87) is obtained by comparison with Okareka Tephra. Comparison with the younger Rotorua, Waiohau and Puketarata tephras gives S.C. values of 0.89, 0.94 and 0.78 respectively. S.C. and C.V. values would favour correlation with Waiohau Tephra. However, based on stratigraphic position at this site (Whangaehu River S.5), and the stratigraphy at other sites (Chart 3) correlation with Rerewhakaaitu Tephra is preferred.

At Desert Road R.S.10, Rerewhakaaitu Tephra [sample R16] is preserved as a thin (20 mm) discontinuous pale grey to white fine ash. It occurs 0.74 m above Kawakawa Tephra Formation and is correlated with Rerewhakaaitu Tephra (Plate 2.25). On the basis of stratigraphic position (Chart 3), ferromagnesian mineral assemblage and glass chemistry, the tephra could equally be a correlative of the older Okareka Tephra. The ferromagnesian mineralogy of this tephra [sample R16] comprises dominant biotite, orthopyroxene, clinopyroxene and minor hornblende. Biotite comprises 46% of the ferromagnesian mineral assemblage and indicates an Okataina source. The biotite abundance is higher than that previously observed in Okareka Tephra (Kohn and Glasby 1978; Lowe 1988a) and more closely approximates that observed for the younger Rerewhakaaitu Tephra. Electron

microprobe analyses of glass shards from this tephra are presented in Appendix IIIa. The mean analysis is given in Table 2.5 (p. 44) and may be compared with the mean analysis of Okareka and Rerewhakaaitu tephras from the type areas (Table 2.6, p. 45). Glass chemistry shows the tephra has major element concentrations typical of OVC tephras (Figure 2.3, p. 47). Similarity Coefficients derived from comparison of the glass chemistry of this tephra [sample R16] to Okareka and Rerewhakaaitu tephras are 0.88 and 0.85 respectively, and indicate dissimilar glass chemistries. No preferred correlation with any of the late Pleistocene OVC tephras (Waiohau Tephra, Rotorua Tephra, Rerewhakaaitu Tephra, Okareka Tephra) is indicated from the S.C. values.

At this site, the tephra is interbedded with andesitic lapilli and ash beds. An erosion break is identified *c.* 0.45 m below the rhyolitic tephra, and above primary Kawakawa Tephra Formation. It is marked by reworked Kawakawa Tephra, sands and gravels (diamictons), and the absence at this site of Bullot Formation member L1. Here, and at other sites (Chart 3), the fluvial and debris flow deposits found above Kawakawa Tephra Formation identify a regional unconformity. A period of climatically induced widespread erosion occurred throughout the Central North Island between *c.* 22 500 and *c.* 14 000 years B.P. and mostly prior to the deposition of Rerewhakaaitu Tephra. Tephras older than Rerewhakaaitu Tephra (Okareka Tephra, Kawakawa Tephra Formation) were consequently eroded at many sites. Topping and Kohn (1973) and Topping (1974) identified Rerewhakaaitu Tephra as the first conformable rhyolitic tephra found mantling moraine deposits on the western Mt Ruapehu ring plain and aggradational gravels of Hinuera Formation in the northern Mt Tongariro region. On this basis, correlation with Rerewhakaaitu Tephra is preferred.

At other sites (*e.g.* Wahianoa Aqueduct R.S. [T20/435990], Tufa Trig S.2 [T20/375046], Whangaehu River S.1 [T20/399954] Plate 2.21) the return of stability to the landscape following the period of erosion is quite possibly indicated by the change from a diamicton dominated stratigraphy to one dominated by primary tephra deposits. The close stratigraphic association of the rhyolitic tephra to the diamicton deposits, and the absence of any older rhyolitic tephras (Kawakawa Tephra Formation) in these sections further suggests correlation with Rerewhakaaitu Tephra.

The FeO and CaO concentrations of individual glass shards in Rerewhakaaitu Tephra [samples R14, R15 and R16], analysed from the three reference sections vary considerably, as reflected in the higher than usual standard deviations of these elements (Table 2.5, p. 44; Figure 2.3, p. 47). The FeO and CaO contents of glass shards from each of these tephras is compared in Figure 2.5 (p. 78). Each of the tephras shows bimodal glass chemistries, indicating that Rerewhakaaitu Tephra was erupted from magma of mixed composition.

At the three reference sections, the basal rhyolitic tephra is correlated with Rerewhakaaitu Tephra on the basis of stratigraphic position, ferromagnesian mineralogy, and to a lesser degree, glass chemistry. At all other sites (Chart 3), the first rhyolitic tephra

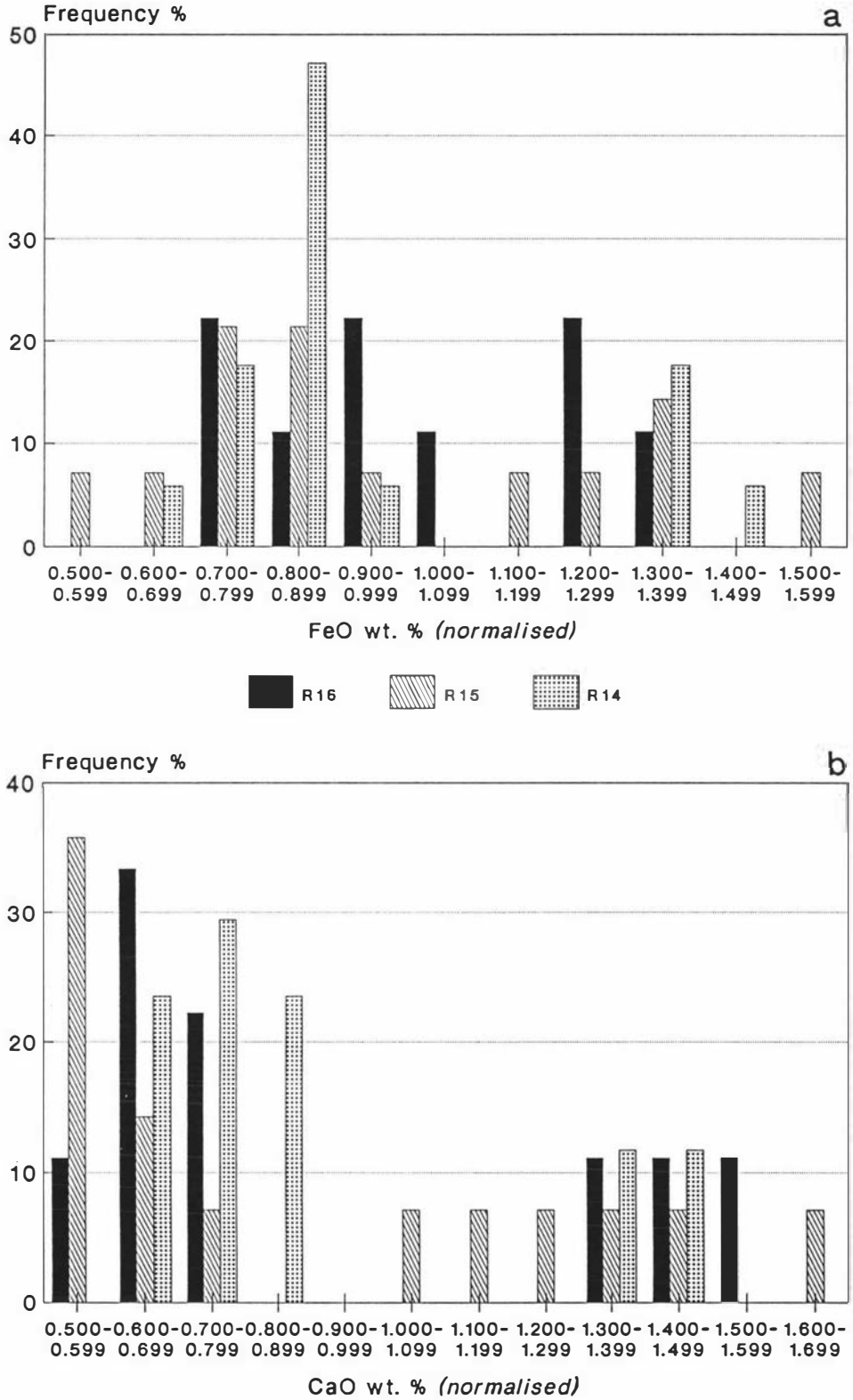

Figure 2.5 Plots of FeO (total) and CaO contents in glass of distal rhyolitic tephras identified in the study area [samples R14, R15, R16] and correlated with Rerewhakaaitu Tephra. The bimodal distributions of FeO (Fig. 2.5a) and CaO (Fig. 2.5b) in the glasses suggests Rerewhakaaitu Tephra was erupted from a melt of mixed composition.

identified beneath Waiohau Tephra is correlated with Rerewhakaaitu Tephra on the basis of stratigraphy and the presence of biotite.

Distribution

Rerewhakaaitu Tephra is identified in numerous sections in the study area (Figure 2.6, p. 83). The most southern occurrence identified is at Wahianoa Aqueduct R.S. The stratigraphic relationship of this tephra to other rhyolitic and local andesitic tephras in the study area is shown in Chart 3.

Significance

In the Mt Ruapehu region, where Kawakawa Tephra Formation or Okareka Tephra have either not been deposited, or preserved, Rerewhakaaitu Tephra is the basal rhyolitic tephra found overlying ring plain diamictons. This tephra therefore provides a minimum age for these deposits which form the major constructional surfaces of the southeastern Mt Ruapehu ring plain. The tephra is also useful to the dating of andesitic tephra members of Bullot Formation.

Okareka Tephra [Ok]

Definition and Age [16]

Okareka Tephra was erupted from OVC and has an estimated age of *c.* 17 000 years B.P. (Table 2.1, p. 16), based on extrapolated radiocarbon ages obtained for the overlying Rerewhakaaitu Tephra and underlying Te Rere Tephra and Kawakawa Tephra Formation (Nairn 1981).

In the Central North Island, Vucetich and Pullar (1969) describe Okareka Tephra as rhyolitic tephra conformably underlying Rerewhakaaitu Tephra, dated [NZ716] at *c.* 14 700 years B.P., and overlying Te Rere Tephra, dated [NZ5171] at *c.* 21 500 years B.P. (Table 2.1, p. 16).

In TgVC, Topping (1974) describes Okareka Tephra as rhyolitic Tephra occurring beneath the andesitic Rotoaira Lapilli and above reworked Kawakawa Tephra Formation.

Description and Identification

A reference section for Okareka Tephra on the southeastern Mt Ruapehu ring plain is here designated at Bullot Track S.1 [BT1] [T20/412108] (Figure 2.1, p. 33; Chart 3).

At Bullot R.S., Okareka Tephra is preserved as a thin (10 mm) white fine ash, interbedded with brown and black andesitic ash. It occurs 90 mm above Bullot Formation member L3 (Plate 2.23), and 2.28 m above Kawakawa Tephra Formation. It is overlain by Rerewhakaaitu Tephra, separated from it by 4.03 m of andesitic ash and lapilli beds of Bullot Formation. Contacts are sharp and distinct.

---

[16] In keeping with the nomenclature of Vucetich and Pullar (1969), tephras older than Rerewhakaaitu Tephra (*c.* 14 700 years B.P.) are referred to as late Pleistocene tephras.

The ferromagnesian mineral assemblage of this tephra [sample R18] comprises orthopyroxene, clinopyroxene, biotite and minor hornblende. Biotite comprises 27% of the assemblage, and indicates an Okataina source. The biotite content cannot be used to show unequivocal correlation with Okareka Tephra.

EMP analyses of glass shards from sample R18 are presented in Appendix IIIa. The mean analysis is given in Table 2.5 (p. 44) and may be compared with a mean analysis of Okareka Tephra from the type section (data from P.C. Froggatt, pers. comm. 1990) and type area (Table 2.6, p. 45). Glass chemistry shows the tephra has major element concentrations typical of OVC tephras (Figure 2.3, p. 47).

The Similarity Coefficient derived from comparison of the glass chemistry of sample R18 to Okareka Tephra from the type section (Table 2.8, p. 49) is 0.91, indicating that the glass chemistries of these tephras are very similar. The tephra is therefore correlated with Okareka Tephra on the basis of stratigraphic position, ferromagnesian mineralogy and glass chemistry.

Distribution

The stratigraphic relationship of this tephra to other rhyolitic and local andesitic tephras is shown in Chart 3. Isopachs are not shown for the Mt Ruapehu region because in the study area, Okareka Tephra has been identified at only one site.

Significance

Okareka Tephra is useful to the dating of Bullot Formation tephra members at Bullot Track S.1, type section for the Bullot Formation.

Kawakawa Tephra Formation [Kk]

Definition and Age

Kawakawa Tephra Formation [17] was erupted from TVC and is dated at 22 590 ± 230 years B.P. (Wilson *et al.* 1988) (Table 2.1, p. 16), revising earlier dates of *c.* 20 000 years B.P. (Vucetich and Pullar 1969 [NZ12]; Nairn 1971 [NZ1056]).

Kawakawa Tephra Formation comprises two members – Oruanui Ignimbrite (formerly Oruanui Breccia of Vucetich and Howorth 1976a), and Aokautere Ash (which comprises all the airfall ash within Kawakawa Tephra Formation) (Froggatt and Lowe 1990).

[17] Kawakawa Taphra Formation is the formal stratigraphic nama proposad by Froggatt and Lowa (1990). Tha nama Oruanui Formation appaars in aarliar literatura, *e.g.* Vucatich and Pullar (1969), Topping and Kohn (1973).

In the Taupo area, Central North Island, Vucetich and Howorth (1976a) describe Kawakawa Tephra Formation as rhyolitic tephra (airfall and pyroclastic origin) which underlies tephric loess or Mokai Sand and overlies an erosion surface on Okaia Tephra.

In the Mt Tongariro region, Topping and Kohn (1973) describe Kawakawa Tephra Formation as rhyolitic tephra (airfall and pyroclastic flow origin) which underlies Hinuera Formation, and overlies alluvium and tuff deposits.

Description and Identification

On the southeastern Mt Ruapehu ring plain, Kawakawa Tephra Formation is represented by Oruanui Ignimbrite and Aokautere Ash members. Reference sections are at Desert Road R.S.10 [DR10] [T20/464091] and Waikato Stream R.S.2 [WS2] [T20/469102] (Figure 2.1, p. 33; Chart 3).

At Desert Road R.S.10, Kawakawa Tephra Formation is 0.47 m thick (Plate 2.24). It overlies sands and andesitic diamictons of Te Heuheu Formation, and is overlain by 0.15 m of reworked Kawakawa Tephra Formation and Te Heuheu Formation sands and gravels. It is found 0.74 m beneath Rerewhakaaitu Tephra (Plate 2.25). The upper contact of the formation is erosive and sharp identifying an erosional unconformity immediately above Oruanui Ignimbrite. The lower contact is sharp and smooth. The erosional unconformity is also noted by Topping and Kohn (1973) in the Mt Tongariro region, and by Kohn (1973) in sections at the type locality at Taupo.

At this site, the overlying 0.15 m of sands and reworked Kawakawa Tephra Formation can be correlated with Hinuera Formation deposits, noted by Topping as occurring above Kawakawa Tephra Formation in all exposures in the Mt Tongariro region, and comprising current-bedded rhyolitic pumiceous and ignimbrite sands derived from Oruanui Ignimbrite, and local volcanic and sedimentary deposits. The upper 0.34 m of Kawakawa Tephra Formation is correlated with Oruanui Ignimbrite Member. It comprises massive fine pale pink ash with dispersed fine pumice lapilli and occasional chalazoidites, less than 10 mm in diameter. The lower contact is sharp and smooth. Oruanui Ignimbrite Member overlies 0.13 m of pink, grey and white fine ash beds studded with chalazoidites in the upper 50 mm, and correlated with Aokautere Ash Member. The lower 87 mm is chalazoidite-free.

At Waikato Stream R.S.2, Kawakawa Tephra Formation occurs as a vein of ash, occupying a vertical distance of *c.* 4 m, averaging 0.15 m width and dipping at a maximum of 63°. The vein cross cuts older horizontally bedded andesitic diamictons and tephra deposits from Mt Ruapehu. The ash vein flattens towards the former ground surface and pinches out downslope (Plate 2.26). Lobes of ash are preserved within the vein (Plate 2.27) and show original stratification of a fine white ash base overlain by a thicker massive unit. This vein is interpreted as representing a pull-apart structure created by tectonic faulting possibly associated with the eruption of Kawakawa Tephra Formation from Lake Taupo,

40 km north of Mt Ruapehu. Infilling with Kawakawa Tephra Formation implies that the structure could not have existed for a long period before or after the eruption or it would have become filled with local andesitic materials.

Pull-apart features have also been recognised by Topping (1974), in the Lake Rotoaira area, north of Mt Tongariro. These structures are found infilled with Kawakawa Tephra Formation, and younger ones with Taupo Pumice.

At Bullot Track S.1 [T20/412108] Kawakawa Tephra Formation is 40 mm thick. It overlies unnamed ash and diamictons of Te Heuheu Formation. It is overlain by Okareka Tephra, being separated from it by 2.23 m of Bullot Formation tephras. Here Kawakawa Tephra Formation is preserved as an isolated lens, comprising 30 mm of pink fine ash with pumice lapilli (Oruanui Breccia Member) over 10 mm of fine white ash (?Aokautere Ash Member).

Kawakawa Tephra Formation is also identified in sections south of Waiouru, along S.H.1 at, for example, T21/404818, T21/407811 and T21/421783 within loess. At these sites Kawakawa Tephra Formation is represented only by Aokautere Ash Member, which occurs as a coarse pumiceous ash overlying a fine ash base.

Distribution

Within the study area, Kawakawa Tephra Formation is preserved at sites both south and north of Waiouru. To the south it is represented by Aokautere Ash Member, and to the north by both Oruanui Ignimbrite and Aokautere Ash members. The southernmost occurrence of Oruanui Ignimbrite recognised in this study is at Bullot Track S.1. Sites at which Kawakawa Tephra Formation is identified in the study area are shown in Figure 2.6 (p. 83), revising the distribution recognised by Topping and Kohn (1973) to the north of Mt Tongariro, and Topping (1974) who considered Kawakawa Tephra Formation absent in sections along the Desert Road.

Kawakawa Tephra Formation has also been identified at Ohakune (Gorton 1966; Topping 1974; Houghton and Hackett 1984) where it closely overlies a tephra layer (Ohakune Tephra Formation) found within loess. Ohakune Tephra was erupted from the nearby Ohakune craters (Froggatt and Lowe 1990).

Significance

Kawakawa Tephra Formation is a readily identifiable *c.* 22 500 years B.P. marker bed, valuable to the dating of the oldest exposed tephras and debris flow deposits on the Mt Ruapehu ring plain.

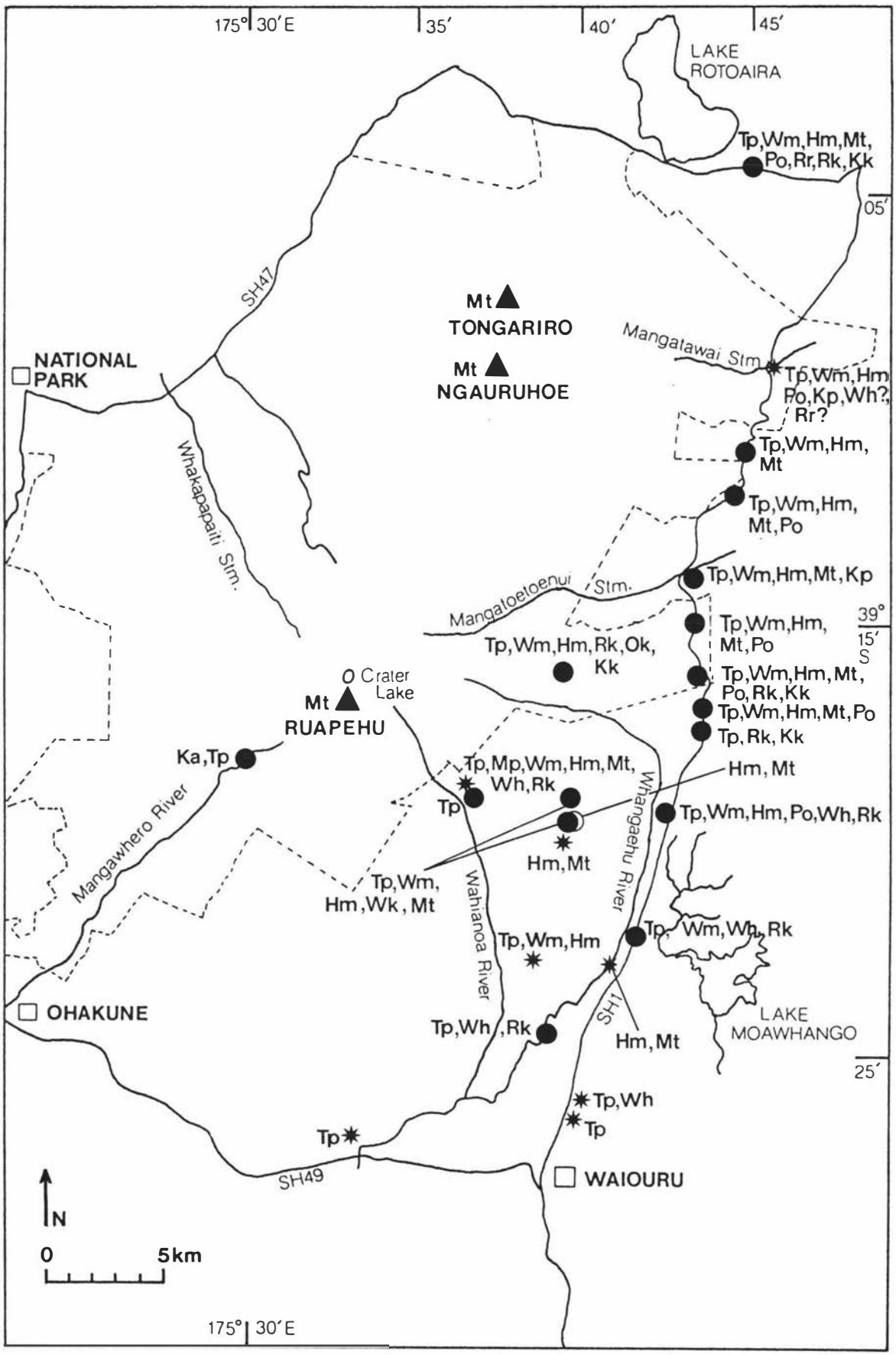

Figure 2.6 Distribution of rhyolitic tephras (from Taupo and Okataina volcanic centres) identified in the study area at type and reference sections for tephras (●) and laharic deposits (✱) *(see text for tephra codes).*

CHAPTER THREE
ANDESITIC TEPHROSTRATIGRAPHY AND TEPHROCHRONOLOGY, TONGARIRO VOLCANIC CENTRE

Introduction

The stratigraphy and chronology of tephras erupted from Mt Ruapehu is best constructed from the tephra record preserved on the eastern sector of the ring plain where tephras erupted from the TgVC volcanoes have accumulated in thick sequences under the influence of the prevailing westerly winds. Tephras are found interbedded with local ring plain forming debris flow and stream flow deposits, and distal rhyolitic tephras from TVC and OVC in the Central North Island.

The stratigraphy and chronology of andesitic tephras from Mt Ruapehu is here established using stratigraphic relationships to previously dated prominent andesitic and rhyolitic tephra marker beds identified in TgVC. Andesitic tephras recognised and identified on the northern Mt Tongariro ring plain (Topping 1973) have been correlated into the study area, and are used as stratigraphic markers and time planes within the tephra record preserved on the southeastern Mt Ruapehu ring plain. The tephrochronology established in the study area dates from the present to *c.* 22 500 years B.P., with base of this time frame readily identified by the prominent rhyolitic tephra marker, Kawakawa Tephra Formation. In later sections the tephrostratigraphy and tephrochronology of andesitic tephras is used to establish a stratigraphy and chronology of local ring plain forming lahar and stream flow deposits.

The first part of this chapter reviews the existing stratigraphy and chronology of andesitic tephras identified and correlated within TgVC. The second section details revisions made to the existing stratigraphy of Topping (1973, 1974) and the stratigraphy and distribution of andesitic tephra formations identified in the study area.

3.1 Previous work: Andesitic Tephrostratigraphy and Tephrochronology, Tongariro Volcanic Centre

The stratigraphy of andesitic tephras erupted over the past *c.* 22 500 years, and preserved in the north of TgVC has been determined by Topping (1973, 1974). The earliest descriptions of andesitic tephras of TgVC date back to Thomas (1889), Grange and Hurst (1929), and Grange (1931) who mapped and made observations on the soil forming ash showers of the Rotorua, Taupo, and Tongariro districts. These first descriptions defined three tephras: Ngauruhoe Ash, Mangatawai Ash, and Tongariro Ash. Ngauruhoe Ash was defined by Grange and Hurst (1929), and later named Ngauruhoe Ash by Grange and Taylor (1931).

It was given formation status by Topping (1973) and renamed Ngauruhoe Tephra Formation. Mangatawai Ash was described by Grange and Hurst (1929), and was formally named Mangatawai Ash by Gregg (1960a). Mangatawai Ash was given formation status by Topping (1973) and renamed Mangatawai Tephra Formation.

Tephras older than Mangatawai Tephra Formation were first described by Thomas (1889), and collectively referred to as Tongariro Ash (Grange and Hurst 1929; Grange and Williamson 1930) and Tongariro Shower (Grange 1931). No stratigraphic criteria were established by which to define the base of Tongariro Ash. The name 'Tongariro Ash' remained in use until studies undertaken by Topping (1973) north of Mt Tongariro required more precise definition of the tephra. He redefined Tongariro Ash to comprise four tephra formations: Papakai Tephra Formation (erupted between *c.* 9700 and 3400 years B.P.), Mangamate Tephra Formation (dated [NZ1372] between *c.* 9780 ± 170 and 9700 years B.P.), Okupata Tephra Formation (dated [NZ1374] 9790 ± 160 years B.P.), and Rotoaira Lapilli (dated [NZ1559] 13 800 ± 300 years B.P.).

Detailed description, dating, and mapping of andesitic and rhyolitic tephras within TgVC (Topping 1973, 1974; Topping and Kohn 1973) led to the first detailed tephra stratigraphy and chronology for Holocene and late Pleistocene andesitic tephras on the northern Mt Tongariro ring plain. The stratigraphy of Topping (1973, 1974) and Topping and Kohn (1973) spans the period from *c.* 22 500 years B.P. to the present, with a detailed chronology of andesitic tephras extending back to *c.* 13 800 years B.P. A chronology of the andesitic tephras was established using interbedded rhyolitic tephras and radiocarbon dates obtained from other interbedded deposits.

Until now, Topping's stratigraphy has not been expanded or revised. His studies of andesitic tephras within TgVC have concentrated on tephras erupted from Mt Tongariro. Tephras erupted from Mt Ruapehu received little study and were only identified as comprising in part the collective Ngauruhoe Tephra and Papakai Tephra Formation, and Okupata Tephra (Topping 1973).

Stratigraphy of Tongariro Subgroup

All tephras of Aranuian Age (<14 ka) erupted from TgVC were originally defined by Grindley (1960) to comprise the Tongariro Subgroup. The Tongariro Subgroup thus comprised the previously defined Ngauruhoe, Mangatawai and Tongariro ashes. With the renaming of both Ngauruhoe Ash and Mangatawai Ash, and replacement of 'Tongariro Ash' with four named tephra formations, Topping (1973, 1974) redefined Tongariro Subgroup to include Ngauruhoe Tephra Formation, Mangatawai Tephra Formation, Papakai Tephra Formation, Mangamate Tephra Formation, Pahoka lapilli, Okupata Tephra Formation, and interbedded unnamed tephras younger than Rotoaira lapilli Formation. Rotoaira Lapilli, dated 13 800 years B.P. [NZ1559] defines the base of the subgroup. Andesitic tephras older than Rotoaira

Lapilli were recognised but not mapped or named by Topping (1973, 1974), so were not grouped into formations or subgroups.

3.2 Methods for Identifying Andesitic Tephras of Tongariro Volcanic Centre

Field procedures undertaken to fingerprint andesitic tephras are summarised in Figure 3.1 (p. 88). Methods for recognising and correlating andesitic tephras from field characteristics are discussed below.

Basis of Field Identification

1. Recognising Andesitic Tephra Formations and Members

(a) Tephra colour and composition

Andesitic tephras are typically iron-stained, producing strong brown and yellow colours, contrasting with the white to pale grey colours characteristic of rhyolitic tephras. At source, andesitic tephras may be of ash, lapilli, and block grade, and comprise both pumice and lithics. Variation in the type and abundance of each lapilli type between units may distinguish some tephras. Diagnostic features such as presence of accessory lithics, pumiceous bombs, or colour-banded pumices may permit field correlation. Grain size and composition distinguishes these tephras from the interbedded rhyolitic tephras which occur as fine to coarse pumiceous ashes. Andesitic ash is commonly greasy due to weathering of glass to allophane.

(b) Expected occurrence

Using the isopach information of Topping (1973, 1974) most of the andesitic tephras identified on the northern Mt Tongariro ring plain can be expected to be preserved on the southeastern Mt Ruapehu ring plain.

2. Correlation with Formations and Members

(a) Boundary criteria and field appearance

Formation boundaries are most commonly designated at the contact with paleosols. Paleosols, contact features (*e.g.* iron pans, peat horizons) and erosion breaks may be used as diagnostic stratigraphic markers for identifying formations and members. Colour, thickness, bedding characteristics, grain size, and composition may be useful in field correlation.

(b) Numerical-age dating (see section 2.3)
Numerical-age dating (*e.g.* radiocarbon dating) provides a quantitative estimate of tephra age. Correlative tephras may be identified by equivalence of age and stratigraphic position.

(c) Correlated-age dating (see section 2.3)
Tephras on the Mt Ruapehu ring plain may be dated and correlated by demonstrating equivalence of stratigraphic position (by detailed mapping) with dated andesitic and rhyolitic tephras on the Mt Tongariro ring plain.

(d) Relative-age dating (see section 2.3)
The age of andesitic tephras may be estimated from their stratigraphic relationships to numerically dated andesitic or rhyolitic tephras. Estimated ages may be used to narrow the field of possible correlatives.

3.3 Results and Discussion

General Stratigraphy of Andesitic Tephras

Holocene-aged andesitic tephra formations, previously defined by Topping (1973, 1974) on the northern Mt Tongariro ring plain, have been identified and correlated within the study area by the above methods. In the study area, tephras erupted from Mt Tongariro and Mt Ngauruhoe contrast lithologically with most eruptives from Mt Ruapehu, and are readily distinguished by field characteristics.

Tephras erupted from Mt Ruapehu comprise the greater part of the 22 500 – 0 years B.P. tephra record on the southeastern Mt Ruapehu ring plain. These tephras are grouped into two new formations, Tufa Trig Formation (dated *c.* 1800 years B.P. to present) and Bullot Formation (dated *c.* 22 500 – 10 000 years B.P.). Marker beds within each formation, and within Papakai Formation are designated as both formal and informal members.

Six andesitic formations (Ngauruhoe Formation, Tufa Trig Formation, Mangatawai Tephra, Papakai Formation, Mangamate Tephra and Bullot Formation) have been correlated throughout the study area using field appearances and stratigraphic positions. Attempts at correlating tephra members have, however, met with varied success, especially within Bullot Formation. Relatively few andesitic tephras within the 22 500 – 0 years B.P. record and erupted from Mt Ruapehu, possess sufficiently diagnostic field characteristics to enable local and regional correlation. As a result, many of the tephra members are only provisionally correlated.

FINGERPRINTING PROCEDURES FOR ANDESITIC TEPHRAS

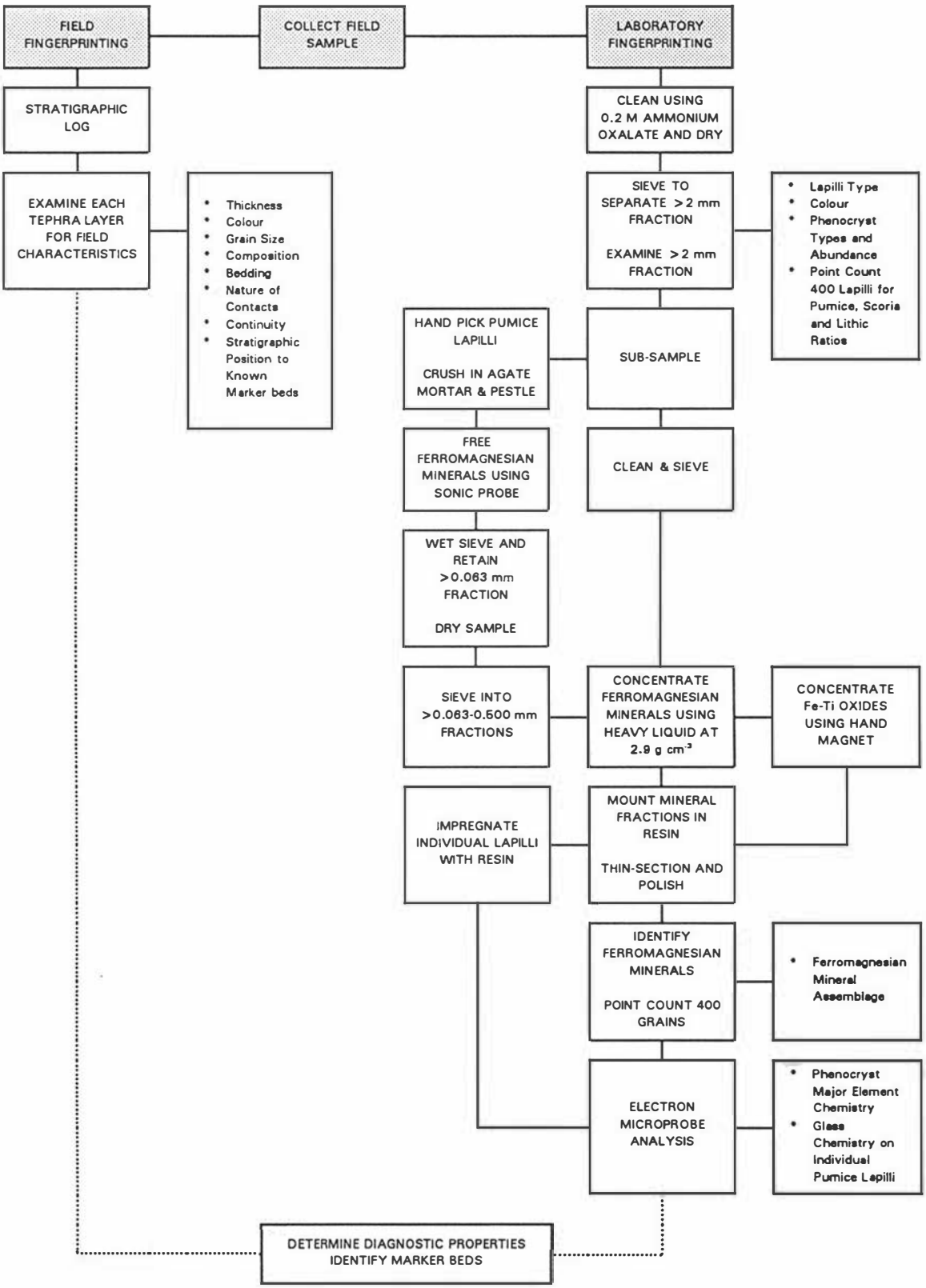

Figure 3.1 Flow diagram illustrating field and laboratory-based fingerprinting procedures for Tongariro Volcanic Centre andesitic tephras.

Close to source the majority of the tephras erupted from Mt Ruapehu are of lapilli grade, dominated by pumice with subordinate amounts of lithics and ash. The lapilli mantle the physiography and are therefore regarded to be primary airfall tephras. Many of the older eruptives are of plinian origin and form thick sequences of horizontally bedded lapilli and ash layers over much of the southeastern ring plain. Most lapilli units are strongly iron-stained showing yellowish brown, yellowish red, and strong brown colours. Ash grade tephras are predominantly dark grey to black and are found interbedded with the lapilli units.

Medial Units

At distal sites (off the dispersal axis), fewer tephras are preserved, with many occurring as thin, discontinuous lapilli units. They are separated by ash grade tephras, and fine grained medial units representing intermittent accumulation of volcaniclastic materials. The medial units show prominent relief in section, and varying degrees of soil development. They have sandy loam to sandy clay loam textures, and commonly contain scattered fine andesitic lapilli. Rhyolitic tephras are most commonly found interbedded within these medial deposits and less frequently with mantling lapilli or ash grade tephras.

A stratigraphy and chronology of tephras preserved on the southeastern Mt Ruapehu ring plain has been established using relative stratigraphic positions to previously dated andesitic and rhyolitic tephra marker beds. The stratigraphy is detailed in Table 3.1 (p. 90). Most tephras have been relative-age or correlated-age dated. Few opportunities exist for direct, or numerical-age dating of andesitic tephras in the study area due to the virtual absence of interbedded dateable material. Most of the radiocarbon ages obtained for andesitic tephras on the northern Mt Tongariro ring plain were from samples obtained within peat swamps. Little dateable material was found interbedded with the tephras in road sections (Topping 1973, 1974).

Definition of Subgroups

Tongariro Subgroup

Tongariro Subgroup was originally defined by Topping (1973) to comprise tephras erupted from TgVC, and dated *c.* 13 800 years B.P. to the present. The initial criterion for which the base of Tongariro Subgroup was defined by Topping was the oldest andesitic tephra (Rotoaira Lapilli) accordant with the present-day (non-glacial environment) physiography.

It is here proposed that the lower boundary of this subgroup be redefined to the base of Pahoka Tephra, dated *c.* 10 000 years B.P. Unlike Rotoaira Lapilli, Pahoka Tephra is a readily identifiable marker bed on both the Mt Tongariro and Mt Ruapehu ring plains, and therefore redefinition as the base of Pahoka Tephra would allow the base of the subgroup to

Table 3.1 Stratigraphy and chronology of rhyolitic (italicised) and andesitic tephras on the southeastern sector of the Mt Ruapehu ring plain.

Formation	Member		Source [§]	Age [*] (years B.P.)	^{14}C N°	Reference to Age
Tufa Trig Formation & Ngauruhoe Formation	Tf18 – Tf8 [a]	Tf Ng	Mt Ruapehu TgVC	*c.* 1800 to present		Defined this study Redefined this study
Kaharoa Tephra		*Ka*	*OVC*	*666 ± 58*		
Tufa Trig Formation & Ngauruhoe Formation	Tf7 – Tf1	Tf Ng	Mt Ruapehu TgVC			Defined this study Redefined this study
Taupo Pumice	*Taupo Ignimbrite*	*Tp*	*TVC*	*c. 1819 ± 17* [†]		
Mangatawai Tephra		Mg	Mt Ngauruhoe			Redefined this study
Mapara Tephra		*Mp*	*TVC*	*c. 2100*		
Mangatawai Tephra		Mg	Mt Ngauruhoe	2500 ± 200	NZ186	Fergusson & Rafter (1959)
Papakai Formation		Pp	TgVC			
Waimihia Tephra		*Wm*	*TVC*	*c. 3400*		
Papakai Formation	black ash-2	ba-2	Mt Ruapehu			
Hinemaiaia Tephra		*Hm*	*TVC*	*4660 ± 80*		
Papakai Formation	black ash-1 orange lapilli-2 orange lapilli-1	ba-1 or-2 or-1	Mt Ruapehu Mt Ruapehu Mt Ruapehu			
Whakatane Tephra		*Wk*	*OVC*	*4770 ± 170* [†]		
Papakai Formation		Pp	TgVC			
Motutere Tephra		*Mt*	*TVC*	*5370 ± 90*		
Papakai Formation		Pp	TgVC			
Mangamate Formation		Mm	Mt Tongariro			
	Poutu Lapilli	Pt	Mt Tongariro	*c.* 9700		Topping (1973)
	Wharepu Tephra	Wp	Mt Tongariro			
Poronui Tephra		*Po*	*TVC*	*c. 9900* [†]		
Mangamate Formation	Ohinepango Tephra	Oh	Mt Tongariro			
	Waihohonu Lapilli	Wa	Mt Tongariro			
	unnamed tephra	ut'	-			
	Otutere Lapilli	Ot	Mt Tongariro			
	Te Rato Lapilli	Tt	Mt Tongariro	9780 ± 170	NZ1372	Topping (1973)
unnamed	unnamed tephra		-			
Karapiti Tephra		*Kp*	*TVC*	*9910 ± 130*		
unnamed tephra			-			
Pahoka Tephra		Pa	Mt Tongariro	*c.* 10 000 – 9800		Topping (1974)
Bullot Formation (upper)		Bt	Mt Ruapehu	*c.* 10 000		
	Ngamatea lapilli-2	Nt-2	Mt Ruapehu			
	Ngamatea lapilli-1	Nt-1	Mt Ruapehu			
	Pourahu Member	Ph	Mt Ruapehu			Defined this study
	L18 – L17		Mt Ruapehu			
	Shawcroft Tephra	Sh	Mt Ruapehu			
	L16		Mt Ruapehu			
Waiohau Tephra		*Wh*	*OVC*	*11 260 ± 200*		
Bullot Formation (upper)	L15 – L8	Bt	Mt Ruapehu			
?Rotorua Tephra [b]		*Rr*	*OVC*	*13 460 ± 260*		
Bullot Formation (upper)		Bt	Mt Ruapehu			
Rotoaira Lapilli [b]		Rt	Mt Tongariro	13 800 ± 200	NZ1559	Topping (1973)
Bullot Formation (upper)	L15 – L8	Bt	Mt Ruapehu			
Rerewhakaaitu Tephra		*Rk*	*OVC*	*14 700 ± 200*		
Bullot Formation (middle)	L7b – L4	Bt	Mt Ruapehu			
Okareka Tephra		*Ok*	*OVC*	*c. 17 000* [‡]		
Bullot Formation (lower)	L3 – L1	Bt	Mt Ruapehu			
Kawakawa Tephra Fm.		*Kk*	*TVC*	*22 690 ± 230* [†]		

[*] All ^{14}C ages discussed are conventional ages in radiocarbon years B.P. based on the old (Libby) half life of 5568 years. Radiocarbon numbers and reference to age for rhyolitic tephras are presented in Table 2.1, p. 16.

[†] Average or combined radiocarbon age.

[‡] Estimated age.

[§] TVC = Taupo Volcanic Centre; OVC = Okataina Volcanic Centre; TgVC = Tongariro Volcanic Centre.

[a] Exact stratigraphic position of Kaharoa Tephra relative to Tufa Trig Formation members is unknown.

[b] Exact stratigraphic position of these tephras relative to Bullot Formation members is unknown.

be recognised throughout much of Mt Tongariro and Mt Ruapehu regions. Rotoaira Lapilli was not recognised in the Mt Ruapehu region by Topping (1974) and has not been identified on the Mt Ruapehu ring plain in this study. A boundary placed at the base of Pahoka Tephra is better suited to widespread recognition of both Mt Tongariro and Mt Ruapehu tephras, and would allow newly defined tephra formations sourced from Mt Ruapehu to belong to a single subgroup. The boundary placed at the base of Pahoka Tephra also serves to group the Pahoka and Mangamate Tephra formations which are of similar lithology into the one subgroup, thus distinguishing them from the lithologically dissimilar Bullot Formation tephras.

Tukino Subgroup

Tukino Subgroup is a new subgroup, defined to comprise all tephras older than Pahoka Tephra (dated *c.* 10 000 years B.P.) and younger than Kawakawa Tephra Formation (dated *c.* 22 500 years B.P.) erupted from TgVC. Future work in TgVC may lead to revision of the base of this subgroup.

Andesitic Tephrostratigraphy and Tephrochronology, Southeastern Mt Ruapehu Ring Plain

Tongariro Subgroup Tephras

Ngauruhoe Formation [Ng]

Revised Stratigraphy

Ngauruhoe Tephra Formation was defined by Topping (1973, 1974) as comprising all andesitic tephras erupted from the TgVC volcanoes (Mt Ruapehu, Mt Ngauruhoe, Mt Tongariro) which are younger than the rhyolitic Taupo Pumice.

The type section, defined by Topping (1973) is at Mangatawai S. [MS] [T19/489238], (Figure 3.2, p. 94). Here, Topping describes Ngauruhoe Tephra Formation as very dark grey to dark brown fine and medium ash. Within Ngauruhoe Tephra Formation, in exposures closer to Mt Ngauruhoe and Mt Ruapehu, discrete lapilli units were recognised. Topping (1973) proposed that these tephras could be named as members of Ngauruhoe Tephra Formation.

On the southeastern Mt Ruapehu ring plain, the post-Taupo Pumice stratigraphy comprises numerous discrete tephras and interbedded aeolian sands (defined as the Makahikatoa Sands by Purves 1990). Isopachs of the tephras suggest a Mt Ruapehu source. In this study, these tephras have been grouped into a new formation, Tufa Trig Formation (dated *c.* 1800 years B.P. to present), rather than being defined as members of Ngauruhoe Tephra Formation. The reasons for defining a new formation are as follows: Ngauruhoe Tephra Formation is a miscellany of tephras of multiple origin. Isopachs of Ngauruhoe Tephra Formation (Gregg 1960a, as Ngauruhoe Ash; Topping 1973) show that most of the tephra is sourced from Mt Ruapehu, and therefore the name Ngauruhoe is inappropriate and even

misleading for tephras from this source. On the Mt Ruapehu ring plain, tephras of Tufa Trig Formation are prominent marker beds, crucial to the future establishment of a post-Taupo Pumice debris flow stratigraphy and chronology. Their use in these studies warrants the grouping of these tephras into a separate formation.

Similarly, an assessment of the frequency of eruptions at Mt Ruapehu requires that tephras sourced from Mt Ruapehu be distinguished from those derived from other TgVC volcanoes. Ngauruhoe Tephra Formation is therefore redefined to comprise only tephras erupted from Mt Tongariro and Mt Ngauruhoe, thus excluding tephras here identified as members of Tufa Trig Formation. Ngauruhoe Tephra Formation is renamed Ngauruhoe Formation because Ngauruhoe Tephra Formation comprises aeolian materials in addition to tephra. Loess derived from Aranuian-aged tephras and alluvium, and aeolian reworked Taupo Tephra is currently being incorporated into Ngauruhoe Tephra (Topping 1974).

Ngauruhoe Formation is retained for tephras erupted from both Mt Tongariro and Mt Ngauruhoe, for which there are no currently named tephra members. On the Mt Ruapehu ring plain where the volcaniclastics have been resorted by aeolian processes the term Makahikatoa Sands is used. Where soil development has masked the origin, so that a deposit might comprise tephras from Mt Ngauruhoe and Mt Tongariro, Makahikatoa Sands, and distal tephras from Mt Ruapehu, use of Ngauruhoe Formation is permissible.

In future studies, discrete tephra beds may be recognised in addition to those here defined as members of Tufa Trig Formation. These may be defined either as additional members of the Tufa Trig Formation where a Mt Ruapehu source is indicated, or as members of Ngauruhoe Formation.

Definition and Age

Ngauruhoe Formation comprises all andesitic tephras, including currently accumulating tephras, erupted from Mt Ngauruhoe and Mt Tongariro, dated between *c.* 1800 years B.P. and the present, which overlie the rhyolitic Taupo Pumice. The upper contact of the formation is the present soil surface.

Description and Identification

The type section [1] for Ngauruhoe Formation is at Mangatawai S. [MS] [T19/489238], (Figure 3.2, p. 94) on the Desert Road, on the south side of Mangatawai Stream (Topping 1974). Here Ngauruhoe Formation is 0.44 m thick, and comprises very dark grey to dark brown fine and medium ash (Topping 1973). Tephras of Tufa Trig Formation are found interbedded with Ngauruhoe Formation in sections up to 2 km north of the type section.

---

[1] Stratigraphic descriptions of the type and reference sections defined for andesitic tephras in the study area are given in Appendix II. Descriptions for some of the other (information) sections mentioned in the text are also given. Correlations made between sections are shown in Charts 1–4.

To the south, where tephras of the Mt Tongariro and Mt Ruapehu ring plains interfinger, Ngauruhoe Formation and Tufa Trig Formation are found interbedded. Tufa Trig Formation tephras characteristically comprise black coarse ash, and are readily distinguished from the typically brown coloured Ngauruhoe Formation. Further south, on the Mt Ruapehu ring plain, Tufa Trig Formation tephras are found interbedded with locally derived grey aeolian Makahikatoa Sands.

At sites along the Desert Road north of Mangatawai S., Ngauruhoe Formation comprises massive dark brown greasy sandy loam textured ash.

Distribution

The isopach map of Ngauruhoe Tephra (Topping 1973) shows the total thickness of post-Taupo tephras in TgVC. As a result of the redefinition of Ngauruhoe Tephra Formation To Ngauruhoe Formation, isopach measurements obtained in the Mt Ruapehu region are no longer considered representative of the thickness of Ngauruhoe Formation, and instead reflect the combined thicknesses of Tufa Trig Formation, Makahikatoa Sands, and Ngauruhoe Formation.

Significance

Ngauruhoe Formation is of limited stratigraphic value in both the Mt Tongariro and Mt Ruapehu regions as there are no currently recognised members within the formation. Possible future identification of members may be useful to the establishment of a post-Taupo tephra stratigraphy and chronology in the Mt Tongariro region.

Tufa Trig Formation [Tf]

Definition and Age

Tufa Trig Formation (Table 3.1, p. 90) constitutes a new formation name within Tongariro Subgroup, and comprises a sequence of 18 andesitic tephras erupted from Mt Ruapehu. Tufa Trig Formation dates between *c.* 1800 years B.P. and the present. The age of the underlying Taupo Pumice, dated at *c.* 1819 years B.P. (Healy 1964a), provides a maximum age for the formation. A paleosol developed in the top of Taupo Pumice suggests the oldest Tufa Trig Formation member is much younger than *c.* 1800 years B.P. One of the basal tephra members (Tf5) has been radiocarbon dated from peat sampled immediately above and below the tephra, returning radiocarbon ages of 650 ± 50 years B.P. [Wk1488] and 830 ± 60 years B.P. [Wk1489] respectively. These ages indicate that the greater part of the formation has been deposited post-900 years B.P.

Description and Identification

Tufa Trig Formation is characterised by multiple, black to dark grey, coarse ash to lapilli grade tephras. Near source, locally derived aeolian Makahikatoa Sands are found interbedded with Tufa Trig Formation tephras, while in exposures along the northern Desert Road, Tufa

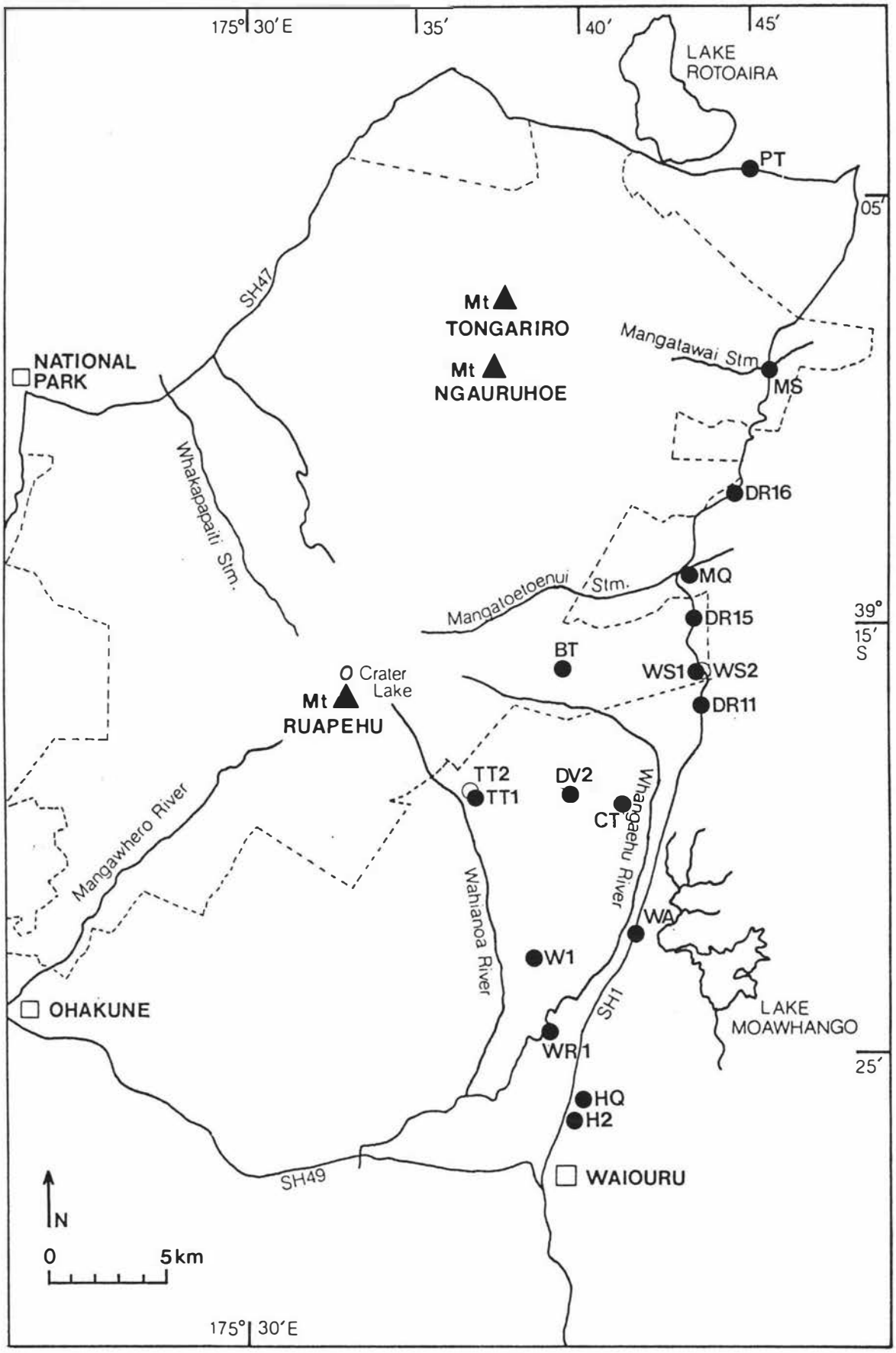

Figure 3.2 Location of type and reference sections designated for andesitic tephras in the study area *(see text for section codes).*

Trig Formation tephras are interbedded with Ngauruhoe Formation. Tufa Trig Formation overlies the rhyolitic Taupo Ignimbrite. Stratigraphic position prevents the misidentification of Tufa Trig Formation tephras as beds of Mangatawai Tephra, which are similar in appearance. Both formations contain prominent interbedded fossil leaves, dominantly of *Nothofagus*.

The type locality for the formation is near Tufa Trig at the top end of Main Road, Karioi Forest. The type section is here designated at Tufa Trig S.1 [TT1] [T20/378045] (Figure 3.2, p. 94; Plate 3.1; Chart 1). A reference section is designated at Tufa Trig S.2 [TT2] [T20/375046] (Plate 2.3). All members of Tufa Trig Formation are given informal status and are designated by the symbol [Tf] in stratigraphic sections.

At the type section, 17 members (Tf2 – Tf18) are defined (Chart 1). The upper 16 comprise coarse black sandy ash and lapilli beds. The basal member comprises greyish brown scoriaceous lapilli and overlies a prominent olive brown sandy loam to sandy clay loam textured paleosol developed in Taupo Ignimbrite. Recently accumulated aeolian Makahikatoa Sands are found interbedded with Tufa Trig Formation tephras. Many of the older interbeds show soil development, indicated by their darker colour, greasy sandy loam to sandy clay loam texture, structure and presence of root channels. The younger interbeds are typically grey loamy sands and sandy loams, and contain distinct reworked fine Taupo Pumice lapilli. The degree of soil development within these sands varies throughout the Mt Ruapehu region, being more pronounced in distal sections to the east along the Desert Road and less so within recent and currently accumulating sand dunes of the Rangipo Desert.

The reference section is in the face of a large sand dune near Tufa Trig S.1. here, Tufa Trig Formation tephras mantle older andesitic and rhyolitic tephras. At this site the basal contact of the formation, with a paleosol developed in Taupo Pumice, is indistinct. All members identified at the type section (Tf2 – Tf18) are recognised here, and are interbedded with grey Makahikatoa Sands containing obvious reworked Taupo Pumice.

Tufa Trig Formation tephras are well exposed in the face of an isolated and prominent dune, at Missile Ridge [T20/398062] within Rangipo Desert. Here, a near complete stratigraphy is identified (Chart 1). Tephras are correlated with members Tf1 – Tf6, and Tf8 and Tf14. Other tephras recognised are provisionally correlated with members Tf10, Tf11 and Tf13 from relative stratigraphic position.

At Missile Ridge Dune, a section on Main Road [T20/371021] (south of the type section), exposures within Death Valley (Rangipo Desert) and some sections on the Desert Road, an additional member (Tf1) is identified. At these sites, two lapilli layers are recognised above Taupo Pumice, whereas only one is recognised at the type section. Based on the field appearances of the lapilli at the Death Valley exposure, the upper lapilli is correlated with the

lowest lapilli member recognised at the type section (designated member Tf2). The lower lapilli seen at Death Valley is designated member Tf1.

Best Localities

Tufa Trig Formation is best preserved in sand dunes at the northern margin of Karioi Forest, where native beech stands have assisted preservation of these and older rhyolitic and andesitic tephras. Also within Karioi Forest, Tufa Trig Formation tephras are identified in shallow tephra sections north of Aqueduct Road. In the southern Karioi Forest, earthworks associated with the planting and milling of pines have removed and obscured much of the post-Taupo Pumice stratigraphy.

Tufa Trig Formation members are not recognised at Tangiwai Swamp [T20/319906] (southern Karioi Forest). At this site, Taupo Ignimbrite is overlain by debris flow and hyperconcentrated flood flow deposits of Onetapu Formation (see section 5.2). Tufa Trig Formation tephras were either not deposited this far south or were eroded by younger Onetapu Formation deposits.

Tufa Trig Formation tephras are prominent within Rangipo Desert, and in sections southeast of Mt Ruapehu along the Whangaehu escarpment (at Whangaehu Junction [T20/445069] and Whangaehu River S.5 [T20/443045]) where they are found interbedded with Makahikatoa Sands. They are also preserved in sections along the Desert Road, south of Mangatawai R.S.

Within Rangipo Desert, the apparent stratigraphy of Tufa Trig Formation varies, and is dependent upon dune age and stability. Rarely is the full stratigraphy seen within any one dune. Best localities within Rangipo Desert are at Missile Ridge Dune [T20/398062] (Plate 3.24; Chart 1), and exposures in Death Valley. Tufa Trig Formation is also identified within small remnant dunes (pedestals) in the area east of the junction of Tukino Road (Bullot Track) and the Desert Road [T20/464084]. Here tussock clad dunes containing Tufa Trig Formation tephras are scattered across a low flat plain formed by Taupo Ignimbrite.

Distribution

Tufa Trig Formation is identified throughout the study area, and in the southern Mt Tongariro region. The westernmost occurrence identified in this study is at a section near the top of Ohakune Mountain Road [S20/271074]. At this site Kaharoa Tephra is found interbedded with Tufa Trig Formation and Makahikatoa Sands. In a recent study by Steel (1989) tephras identified in peat swamps in the Lake Surprise area, west of Mt Ruapehu, are here considered correlatives of Tufa Trig Formation.

Tufa Trig Formation tephras are not recognised in sections along the Desert Road, north of T19/496253, (*c.* 1.5 km north of Mangatawai Stream). The southernmost occurrence is

at Ngamatea Swamp [T21/413874], where only two of the eighteen members are recognised.

Source

Isopachs of Tufa Trig Formation members Tf4, Tf5, Tf6 and Tf8 indicate a Mt Ruapehu source and dispersal axis principally to the southeast of Mt Ruapehu.

Members

Seventeen informal members are defined from the type section (members Tf18 – Tf2). An eighteenth member (Tf1) is identified in a section at the top end of Death Valley at T20/406056. Many of the members are characterised by the presence of a thin pale grey fine ash at their base, which although distinctive, is not always present and thus cannot be relied upon as a tool for member identification and correlation. Only the thicker tephra members are consistently seen at the type and reference sections as laterally continuous units. The basal two tephras are of lapilli grade and comprise medium and fine scoriaceous and pumiceous lapilli with minor lithics (Plate 3.1). The most distinctive members, which are used as marker beds, are members Tf1, Tf2, Tf4, Tf5, Tf6, Tf8, and Tf14 (Plate 3.1). The other members are of limited stratigraphic value because they are thin units which lack diagnostic characteristics, and are rarely correlated into more distal sections. Where the full stratigraphy is preserved these members may be identified from their relative stratigraphic position. Descriptions of the members and section measurements described below are taken from Tufa Trig S.1.

Members Tf18, Tf17, Tf16, and Tf15

Members Tf18, Tf17 and Tf16 occur within 0.48 m of the soil surface. They occur as thin (20 mm) discontinuous very dark grey coarse ash beds, containing many *Nothofagus* leaves, separated by dark greyish brown Makahikatoa Sands of sandy loam texture and with soil development.

These members show a limited dispersal, having been identified in only a few sections in the study area where they occur as thin pocketing tephras. Isopachs are therefore not presented.

Member Tf14

Member Tf14 which is 45 mm thick, occurs 0.79 m below the soil surface (Plate 3.1), and underlies a 280 mm thick, prominent dark brown sandy loam textured paleosol developed in Makahikatoa Sands. The tephra comprises bedded black coarse ash, and occurs as a continuous unit, with distinct contacts. It is distinguished from other Tufa Trig Formation members by its darker colour, comparative thickness and stratigraphic association to the distinctive overlying paleosol. Colour of interbedded paleosols may be used to a limited extent

in correlation. The most distinctive paleosols in the sequence are those which lie below members Tf14 and Tf6. They are distinguished by their stronger colour. Used in conjunction, these characteristics identify member Tf14 in distal sections where the full stratigraphy is not preserved.

Member Tf14 is a prominent tephra, identified in sections throughout Rangipo Desert, and in sections within Karioi Forest. Although member Tf14 is not dated, it is a potentially important marker bed for establishing a chronology of local debris flow deposits (post-1800 years B.P.) on the southeastern Mt Ruapehu ring plain.

Members Tf13, Tf12, and Tf11

Members Tf13, Tf12 and Tf11 occur between 0.89 and 0.97 m below the soil surface. They occur as thin, discontinuous black coarse ash units separated by dark greyish brown fine sandy loam textured paleosols developed in Makahikatoa Sands. While members Tf13 and Tf12 show a fine ash base, and member Tf11 a fine ash top, the presence of fine ash is not unique to these members. Correlations to sections with an incomplete stratigraphy are provisional due to a lack of identifying member characteristics, but where a full stratigraphy exists these members can be identified from their relative stratigraphic positions.
Members Tf13, Tf12 and Tf11 are identified within Karioi Forest and Rangipo Desert.

Members Tf10 and Tf9

Member Tf10, which is 20 mm thick, occurs 30 mm below member Tf11, being separated from it by a dark greyish brown sandy loam textured paleosol. The tephra comprises a discontinuous bedded dark greyish brown and black coarse ash with distinct contacts. At the type section, member Tf10 is one of the more prominent tephras in the formation, but due to a lack of diagnostic field characteristics it has been identified at only a few sites from relative stratigraphic position.

Member Tf9, which is 25 mm thick, comprises a discontinuous black coarse ash with a fine ash top and base, and is separated from member Tf10 by a 40 mm thick dark greyish brown sandy loam textured paleosol. This tephra occurs as small pockets of ash with indistinct contacts, and like members Tf18, Tf17 and Tf16, field characteristics suggest the tephra was dispersed only a short distance from source.

Members Tf9 and Tf10 are identified within Karioi Forest and Rangipo Desert.

Member Tf8

Member Tf8 which is 60 mm thick, occurs at *c.* 1.15 m below the soil surface and 10 mm below member Tf9 (Plate 3.1; Plate 3.2). It comprises bedded coarse ash and lapilli,

with a discrete pumice-rich bed at the base, and contains many yellow beech leaves. The basal pumice bed is a diagnostic feature of this member and serves to distinguish it from all other members of Tufa Trig Formation.

An age close to *c.* 600 years B.P. is suggested from its relative stratigraphic position to the older radiocarbon dated members Tf5 and Tf6.

Member Tf8 is more widespread than most younger Tufa Trig Formation members. It occurs as a continuous unit within most sections, and is identified east of Mt Ruapehu, in sections within Rangipo Desert and along the Desert Road. A partial isopach map of member Tf8 shows a southeasterly dispersal axis (Figure 3.3, p. 100). The volume of this member is about 51 x 10^6 m^3 (Table 6.1, p. 295)

Member Tf8 is a potentially valuable marker bed for establishing a chronology of local debris flow deposits (post-1800 years B.P.) on the southeastern Mt Ruapehu ring plain.

Member Tf7

Member Tf7 is an indistinct, discontinuous unit, comprising black bedded coarse ash. Members Tf7 and Tf8 are separated by a thin dark brown paleosol. Where this paleosol thins, the contact between these members is indistinct and difficult to define. The lower contact with member Tf6 is indistinct. Member Tf7 shows a very localised distribution, being identified in only a few sections close to source. Isopachs are therefore not shown for this member.

Member Tf7 is provisionally dated between *c.* 650 – 600 years B.P., based on the maximum age of member Tf6 (650 ± 50 years B.P. [Wk1488]), which it directly overlies and the probable stratigraphic position of Kaharoa Tephra.

Member Tf6

Member Tf6, which is 70 mm thick, occurs immediately below member Tf7, 1.21 m below the soil surface, and 60 mm above member Tf5, separated from it by a well developed greasy fine sandy loam textured paleosol (Plate 3.1; Plate 3.2; Plate 3.3). Member Tf6 comprises bedded black coarse ash with a thin (10 mm) fine ash top, and contains abundant yellow beech leaves. The paleosol underlying this member is more strongly coloured than most, and is prominent in exposures along the Desert Road.

At some sections member Tf6 separates into two distinct black ash beds, for example at Whangaehu River S.6 [T20/438033]. Here it is found interbedded with debris flow deposits of Onetapu Formation (see section 5.2), and is identified from its field appearance and stratigraphic position relative to member Tf5. Member Tf6 is the second most prominent

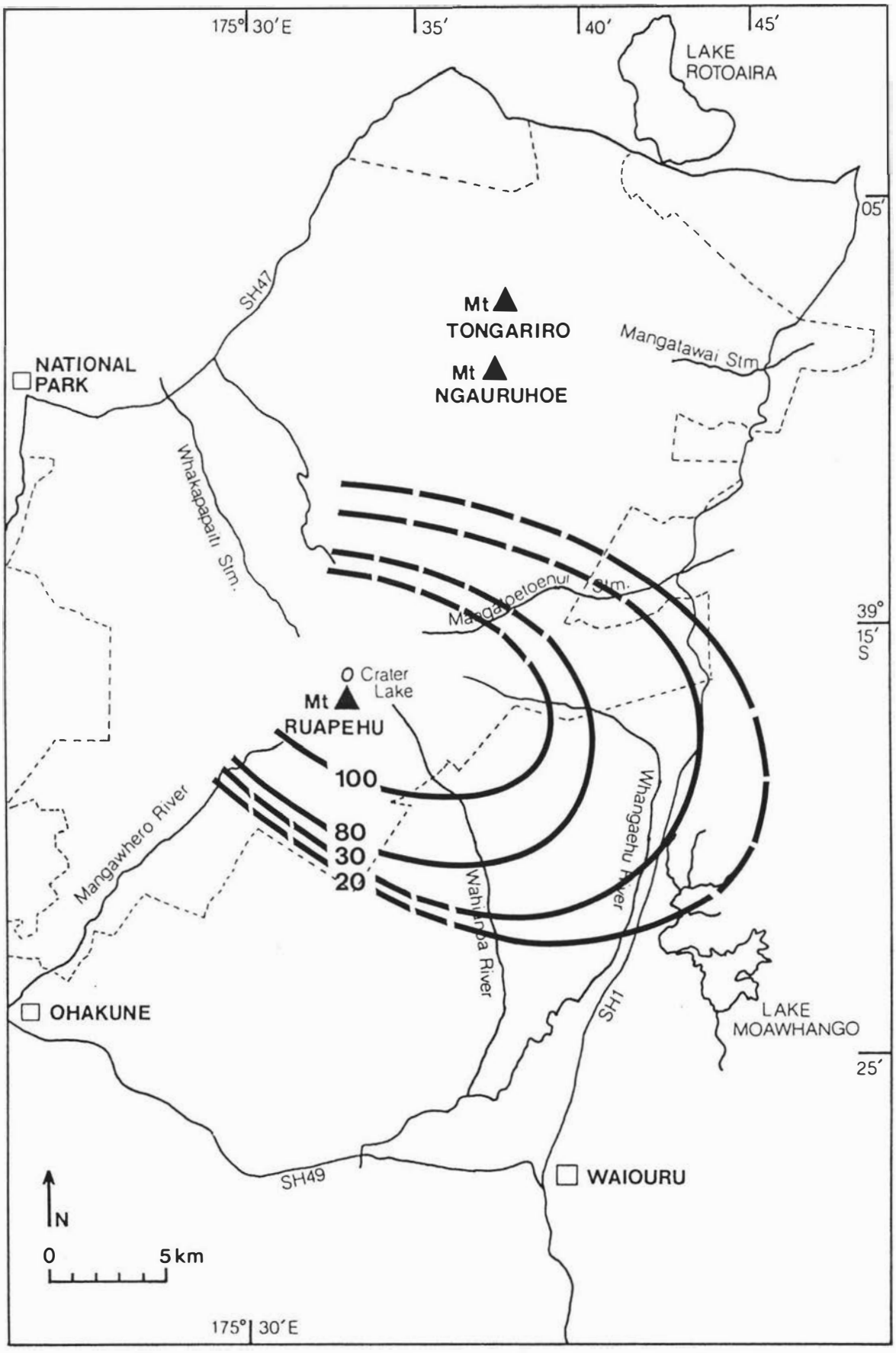

Figure 3.3 Isopach map of Tufa Trig Formation member Tf8 (all thicknesses are in millimetres).

tephra in Tufa Trig Formation and is recognised in all sections within Rangipo Desert, in sections within Karioi Forest and east of Mt Ruapehu along the Whangaehu escarpment and the Desert Road. It is a valuable marker bed for establishing both the stratigraphy and an approximate chronology of local post-Taupo Pumice debris flow deposits.

Isopachs of member Tf6 are shown in Figure 3.4 (p. 102), and indicate a dispersal axis to the southeast of Mt Ruapehu. The southernmost occurrence of member Tf6 is at Ngamatea Swamp, where it occurs as indistinct pockets of coarse ash (10 mm depth), interbedded with peat. At this site, peat sampled immediately above member Tf5 is radiocarbon dated [Wk1488] at 650 ± 50 years B.P., providing a maximum age for member Tf6. The volume of member Tf6 is about 33 x 10^6 m^3 (Table 6.1, p. 295).

Member Tf5

Member Tf5 which is 75 mm thick, occurs 60 mm below member Tf6, 100 mm above member Tf4 and 1.34 m below the soil surface. This tephra comprises black, olive and dark greyish brown coarse ash and fine lithic lapilli, with minor amounts of dark greyish brown fine pumice lapilli, and contains many yellow beech leaves. Close to source, member Tf5 shows a fine ash base, but at some localities further east of the type section this fine ash is not present.

Member Tf5 is the most prominent member of Tufa Trig Formation (Plate 3.1; Plate 3.2; Plate 3.3) and is a valuable marker bed. It is readily distinguished from all other members by its consistently greater thickness, coarser grain size, lateral continuity, and at some sites, reverse grading, *e.g.* at Death Valley S.5 [T20/409045].

At Ngamatea Swamp [T21/413874] member Tf5 is 30 mm thick and is found interbedded with peat, 150 mm above Taupo Pumice. Peat sampled immediately below member Tf5 is radiocarbon dated [Wk1489] at 830 ± 60 years B.P., providing a maximum age for this tephra.

At Whangaehu River S.6 [T20/438033], and at Aqueduct S.1 [T20/418982] in the southern Rangipo Desert (Chart 1; Chart 4), member Tf5 is found interbedded with debris flow deposits of Onetapu Formation, thereby dating the enclosing deposits. Member Tf5 is a valuable marker bed to the establishment of a post-Taupo Pumice debris flow stratigraphy in the study area. It is the only member presently numerically dated.

Member Tf5 is the most widespread member of Tufa Trig Formation, and is identified in exposures within Karioi State Forest, Rangipo Desert, sections along the Whangaehu escarpment (*e.g.* Whangaehu Junction [T20/445069] and Whangaehu River S.5 [T20/443045]), and on the Desert Road. In Desert Road sections, member Tf5 is commonly 90 mm thick and shows reverse grading. It is a prominent and readily identified unit in all

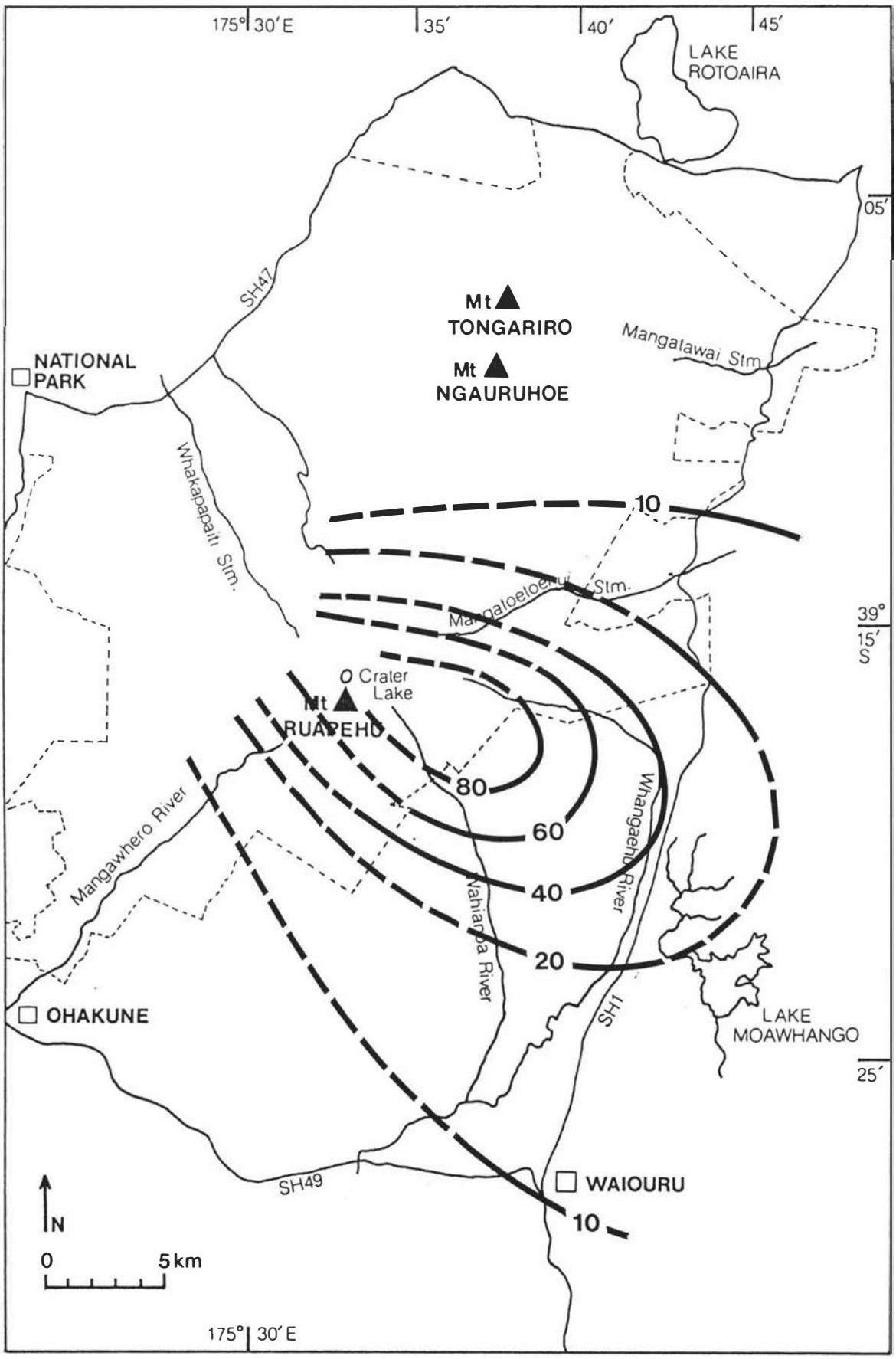

Figure 3.4 Isopach map of Tufa Trig Formation member Tf6 (all measurements are in millimetres).

these sections. It has been identified to within 2 km north of Mangatawai Stream [T19/489238]. The southernmost occurrence identified in this study is at Ngamatea Swamp, south of Waiouru.

Isopachs of this member (Figure 3.5, p. 104) show a dispersal axis to the east of Mt Ruapehu. The volume of Member Tf5 is about 88 x 10^6 m^3 (Table 6.1, p. 295).

Members Tf4 and Tf3

Members Tf4 and Tf3, although thin, are distinct tephras, comprising dark greyish brown to black coarse ash, separated by a thick (0.19 m) sandy loam to sandy clay loam textured paleosol developed in Makahikatoa Sands (Plate 3.1; Plate 3.3). They occur between 1.51 and 1.73 m below the soil surface, and 0.59 m and 0.39 m above Taupo Pumice respectively.

Member Tf4 is identified in sections within Karioi Forest, Rangipo Desert and sections along the southern Desert Road, south of Mt Tongariro. Isopachs for member Tf4 are shown in Figure 3.6 (p. 105) and indicate a dispersal axis to the southeast of Mt Ruapehu. The volume of this member is about 19 x 10^6 m^3 (Table 6.1, 295).

Members Tf2 and Tf1

At the type section, member Tf2 occurs 0.22 m above Taupo Pumice and *c.* 1.90 m below the soil surface (Plate 3.1). It comprises dark greyish brown medium and coarse vesicular scoriaceous lapilli and fewer grey lithic lapilli, and overlies a fine sandy loam to sandy clay loam textured paleosol developed in Taupo Ignimbrite. Within Death Valley, at T20/406056, member Tf1 directly overlies Taupo Pumice, and is overlain by member Tf2. It comprises white iron-stained dominantly medium pumice lapilli and few lithic lapilli. Both members are readily distinguished from all other Tufa Trig Formation members by their colour, composition and grain size.

Significance

On the southeastern Mt Ruapehu ring plain, tephras of Tufa Trig Formation are found interbedded with post-Taupo Pumice debris flow deposits. Potentially, these tephras offer the best opportunity for establishing both a stratigraphy and chronology of these deposits which form the most recent surfaces of the Mt Ruapehu ring plain. Where dated these tephras also provide time planes useful in paleo-environmental interpretation in the study area, in assessing erosion and sedimentation rates and changes in surface vegetation over time. Where these tephras are found interbedded with peats they similarly provide time planes for palynological studies of the last *c.* 1800 years B.P.

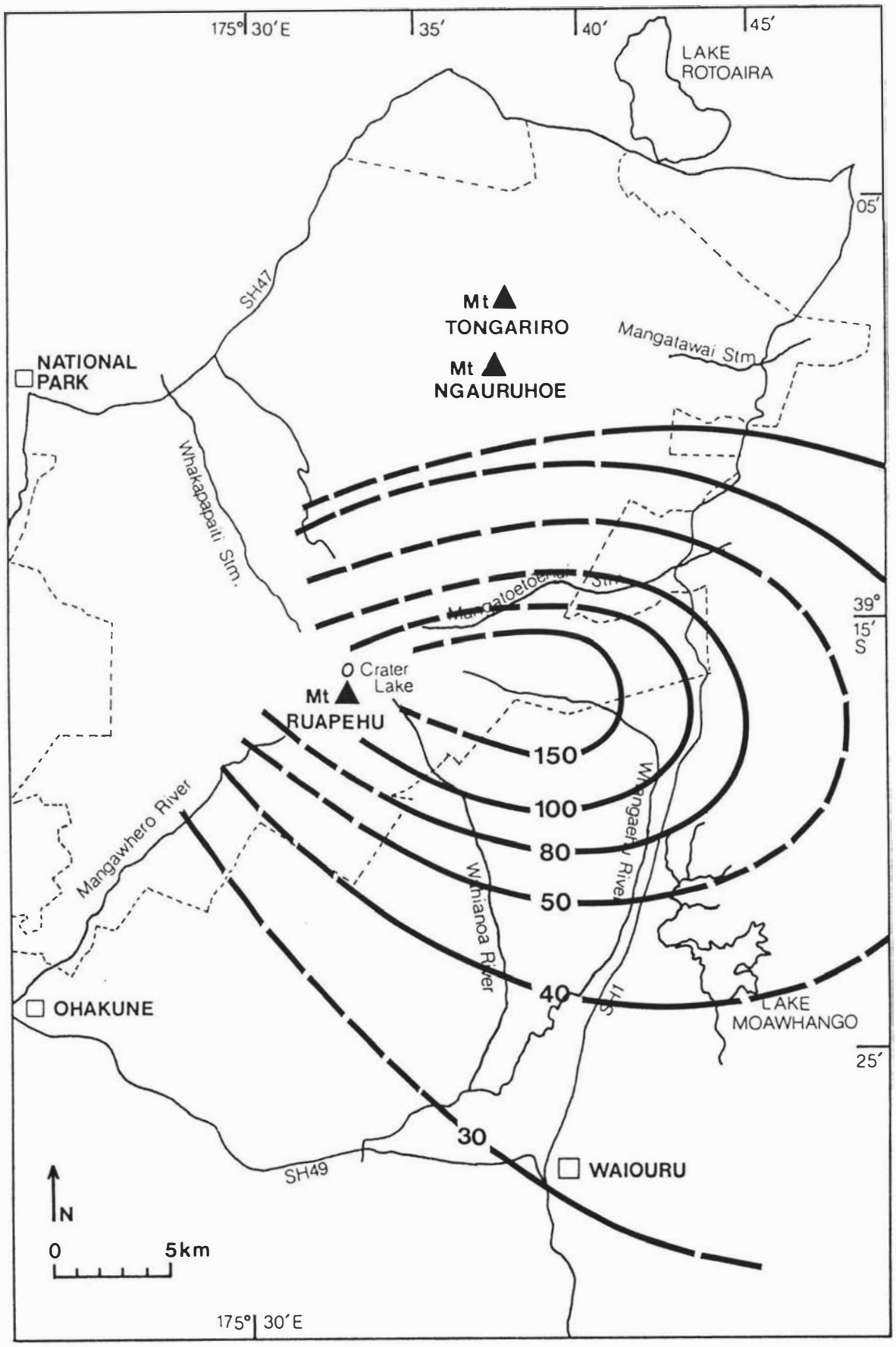

Figure 3.5 Isopach map of Tufa Trig Formation member Tf5 (all measurements are in millimetres).

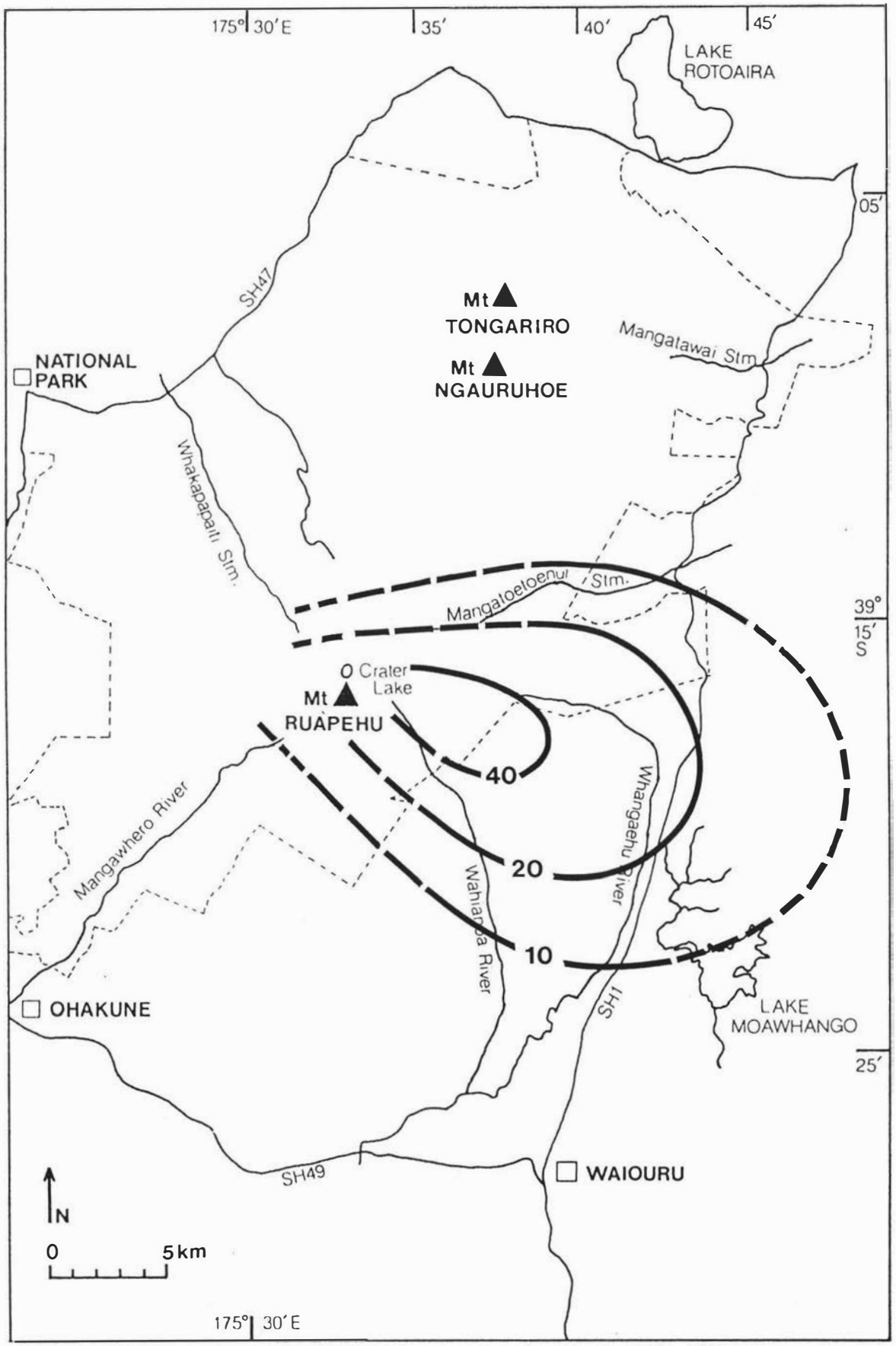

Figure 3.6 Isopach map of Tufa Trig Formation member Tf4 (all measurements are in millimetres).

Coring of local peat swamps located east or northeast of Mt Ruapehu may provide opportunity for further dating of members of Tufa Trig Formation. Reconnaissance coring of shallow swamp land east of Main Road within Karioi Forest [T20/349937] identified Tufa Trig Formation tephras, but provided no additional stratigraphic control.

Tufa Trig Formation tephras constitute excellent local marker beds, but their restricted dispersal elsewhere within TgVC limits their use as regional marker beds.

Correlation

Few sites contain a complete stratigraphy and at many sites contacts between members are indistinct, making member identification difficult. Where the full sequence is not preserved, the field characteristics of interbedded paleosols, and the relative stratigraphic positions of the members are used to support member correlations. Most members cannot be distinguished from colour or grain size, and only members Tf5, Tf6 and Tf8 can be confidently correlated at distal sections from field appearances.

The rhyolitic Kaharoa Tephra is a potentially valuable marker bed to both the dating and correlation of Tufa Trig Formation members. It has however, been identified at only two sites in the study area, and at both sites Tufa Trig Formation members have not been confidently identified to member level. Kaharoa Tephra therefore is not used as a marker bed in Tufa Trig Formation member correlations.

Future opportunities for correlation of Tufa Trig Formation members is greatest where members can be numerically dated from organic material found interbedded within intervening paleosols, or within the tephras themselves. Some of the younger members may be too young to be dated by the radiocarbon method.

The stratigraphic relationship of Tufa Trig Formation to other andesitic and rhyolitic formations at the type and reference sections on the southeastern Mt Ruapehu ring plain is shown in Chart 1.

Other Tephras Associated with the Formation

Associated with Tufa Trig Formation are two unnamed, white, strongly pocketing fine ashes, occurring between members Tf3 and Tf4 and above member Tf8 at Tufa Trig S.2 (Plate 3.3). These tephras dominantly comprise white poorly vesicular pumice fragments together with free pyroxene crystals, black and brown vitric pyroclasts, and some cuspate-shaped rhyolitic shards. The rhyolitic shards are probably derived from reworked Taupo Ignimbrite. These tephras have been identified in few sections within both Karioi Forest and Rangipo Desert. Their restricted dispersal probably indicates a Mt Ruapehu source.

Mangatawai Tephra [Mg]

Revised Stratigraphy

Mangatawai Tephra Formation was defined by Topping (1973), as andesitic ash which underlies Taupo Pumice and overlies unnamed andesitic ash above Whakaipo Tephra (Table 3.2, p. 107). Topping and Kohn (1973), however, describe Mangatawai Tephra Formation as andesitic tephra overlying Waimihia Lapilli. In the definition of Whakaipo Tephra (p. 381, Topping and Kohn 1973) the authors refer to the andesitic ash separating the rhyolitic Whakaipo Tephra and Waimihia Lapilli as Mangatawai Tephra Formation (Table 3.2, p. 107), and not as unnamed andesitic ash as in Topping (1973). Furthermore, the description on p. 381 contradicts the stratigraphy of Mangatawai Tephra as shown in Table 1, p. 377 of the same article. This contradiction in the definition of Mangatawai Tephra Formation between Topping (1973) and Topping and Kohn (1973) and within Topping and Kohn (1973), requires that Mangatawai Tephra Formation be clearly defined on the basis of stratigraphic information obtained in this study.

Table 3.2 Comparison of the stratigraphy of Mangatawai Tephra and Papakai Formation (as defined this thesis) with that of Topping (1973) and Topping and Kohn (1973).

Topping (1973)	Topping & Kohn (1973)	This Study (1990)	Age Used This Study (years B.P.)
Taupo Pumice	Taupo Pumice	Taupo Pumice	*c.* 1819
Mangatawai Tephra Formation	Mangatawai Tephra Formation	Mangatawai Tephra	*c.* 2500
andesitic tephra		Papakai Formation	*c.* 2500†
Whakaipo Tephra*	Whakaipo Tephra	Waimihia Tephra	*c.* 3400
andesitic tephra	Mangatawai Tephra Formation	Papakai Formation	
Waimihia Lapilli*	Waimihia Lapilli	Hinemaiaia Tephra	*c.* 4650
Papakai Tephra Formation	Papakai Tephra Formation	Papakai Formation	
Hinemaiaia Ash	Hinemaiaia Ash	Motutere Tephra	*c.* 5370
Papakai Tephra Formation	Papakai Tephra Formation	Papakai Formation	
Mangamate Tephra Formation	Mangamate Tephra Formation	Mangamate Tephra	*c.* 9780–9700†

* Interbedded within unnamed andesitic tephra.
† Inferred stratigraphic age – not ^{14}C dated.

Definition and Age

Mangatawai Tephra Formation, here renamed Mangatawai Tephra, was erupted from TgVC, and principally from Mt Ngauruhoe, and is dated between *c.* 1819 and 2500 years B.P. The base of Mangatawai Tephra is radiocarbon dated [NZ186] from beech leaves found interbedded in the tephra, at 2500 ± 200 years B.P. (Fergusson and Rafter 1959). Mangatawai Tephra accumulated over a period of *c.* 680 years (Topping 1974).

Description and Identification

In TgVC, Mangatawai Tephra is here defined as andesitic tephra which conformably underlies Taupo Pumice and overlies Papakai Formation (Table 3.2, p. 107). The upper contact is with Taupo Pumice, and the basal contact is defined by the lower limit of the black ash beds (Plate 3.4), consistent with the original descriptions of 'Mangatawai Tephra Formation' found in Topping (1973).

The type section for Mangatawai Tephra, defined by Topping (1973), is at Mangatawai S. [MS] [T19/489238] [2]. Reference sections are here designated at Desert Road S.16 [DR16] [T20/481186], Mangatoetoenui Quarry [MQ] [T20/459153], Desert Road S.15 [DR15] [T20/462135] (Plate 2.13) and Tufa Trig S.2 [TT2] [T20/375046] (Figure 3.2, p. 94; Plate 2.10; Chart 1).

At the type section, Mangatawai Tephra is 0.79 m thick, comprising 0.29 m of dark brown fine ash, over 0.50 m of dark grey and very dark grey medium ash containing beech leaves (Topping 1973).

At the reference sections Mangatawai Tephra comprises an upper well developed dark greyish brown, greasy, sandy loam to sandy clay loam textured paleosol over multiple-bedded black and dark purplish grey coarse ash beds containing beech leaves, and dark yellowish brown greasy sandy loam textured ash. At Tufa Trig R.S.2 the rhyolitic Mapara Tephra is found interbedded with Mangatawai Tephra (Plate 2.10; Chart 1). At the reference sections, Mangatawai Tephra conformably overlies yellowish brown Papakai Formation with interbedded rhyolitic Waimihia, Hinemaiaia and Motutere tephras, and is conformably overlain by Taupo Pumice (Taupo Ignimbrite Member). Upper and lower formation contacts are sharp and distinct.

At Desert Road R.S.15, Mangatoetoenui Quarry R.S, and more northern sites, black ash beds are also found interbedded within the upper paleosol of Mangatawai Tephra. At sections south of Wahianoa Aqueduct R.S. [T20/435990] discrete ash beds of Mangatawai Tephra and the underlying rhyolitic Waimihia and Hinemaiaia tephras are no longer identified.

Mangatawai Tephra is identified from its stratigraphic position and distinctive field characteristics.

Distribution

Mangatawai Tephra is identified in all exposures along the Desert Road between Poutu R.S. (Topping 1973) and Wahianoa Aqueduct R.S., and within Rangipo Desert. Isopachs of Mangatawai Ash of Gregg (1960a) show that most of the tephra was erupted

[2] The grid reference used here is the metric equivalent of that defined for Mengatawai [N112/250806], in Topping (1973).

from Mt Ngauruhoe. Revised isopach thicknesses of Mangatawai Tephra determined in this study for the southeastern Mt Ruapehu region are shown in Figure 3.7 (p. 110) and are in good agreement with those shown in Gregg (1960a).

Significance

Mangatawai Tephra is a prominent and distinctive tephra, and is one of few andesitic tephras within TgVC that has been numerically dated. This, together with its widespread distribution makes it an excellent regional marker bed. In the study area Mangatawai Tephra is useful to the establishment of a stratigraphy and chronology of local andesitic tephra and lahar deposits, and distal rhyolitic tephras from TVC.

Papakai Formation [Pp]

Revised Stratigraphy

Papakai Tephra Formation was originally defined by Topping (1973, 1974) to comprise andesitic tephras erupted from TgVC between *c.* 9700 and 3400 years B.P., which underlie the rhyolitic Waimihia Lapilli and overlie Poutu Lapilli Member of Mangamate Tephra. For reasons that follow, Papakai Tephra Formation is here redefined and renamed Papakai Formation.

Topping (1973) defined the top of Papakai Tephra Formation by *"the first appearance of Waimihia Lapilli*[3]*, or where Waimihia Lapilli is absent, on the upper limit of both cracking and interspersed lapilli"*, thus excluding from the formation the unnamed tephra between it and Mangatawai Tephra (Table 3.2, p. 107). Therefore, following the stratigraphy of Topping, in the Mt Tongariro and Mt Ruapehu regions, Papakai Formation overlies Mangamate Tephra, and is overlain by unnamed andesitic tephra in which the rhyolitic Whakaipo Tephra[4] is found interbedded.

At most sections along the Desert Road north of S.15 [T20/462135], the contact between the overlying unnamed tephra and Papakai Tephra Formation (Topping 1973, 1974) is distinct. At Desert Road S.15, the contact is marked by Hinemaiaia Tephra and more pronounced paleosol development within Papakai Tephra Formation (Plate 2.13). Both the unnamed tephra and Papakai Tephra Formation show paleosol development, indicated by colour, structure, surface cracking and presence of numerous root channels.

In most sections within Rangipo Desert, Karioi Forest, and along S.H.49, the contact between the unnamed tephra and Papakai Tephra Formation is indistinct, with no recognised

---

[3] Waimihia Lapilli identified by Topping and Kohn in the Mt Tongariro region is re-identified as Hinemaiaia Tephra in this study.

[4] Whakaipo Tephra identified by Topping and Kohn in the Mt Tongariro region is re-identified as Waimihia Tephra in this study.

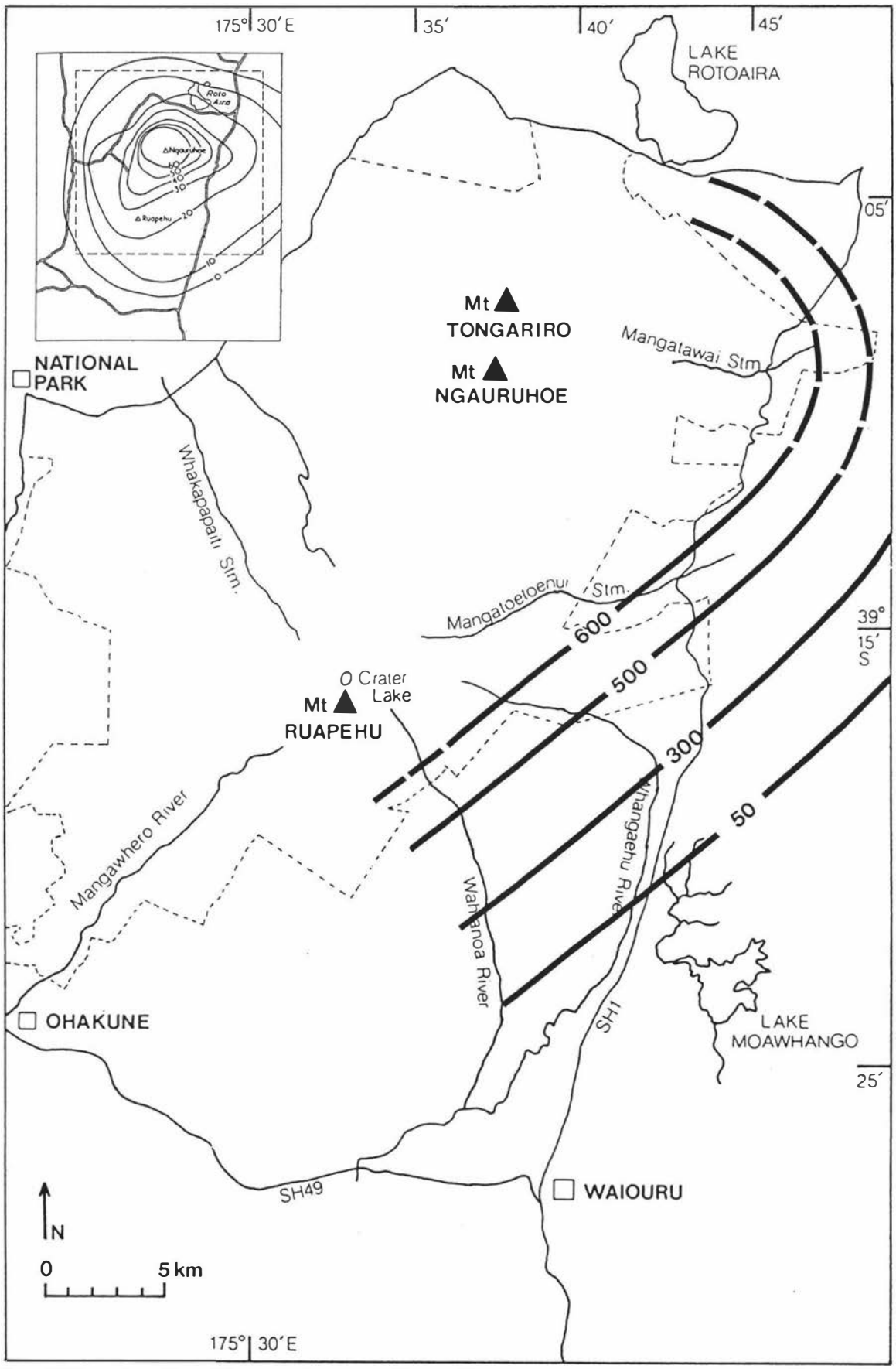

Figure 3.7 Partial isopach map of Mangatawai Tephra (all measurements in millimetres). Insert shows isopachs of Mangatawai Tephra from Gregg (1960a).

difference in field appearance between these units (Plate 3.8; Plate 3.9). The two diagnostic criteria of Papakai Tephra Formation are absent – these being prominent surface cracking and the presence of interspersed Poutu Lapilli at the base. Only the presence of Hinemaiaia Tephra serves to indicate a boundary.

Although in most sections along the Desert Road a distinction can be made between the overlying unnamed tephra and Papakai Tephra Formation on field appearances, there is no demonstrable stratigraphic value to be gained by defining these two units as separate formations. Therefore, both the unnamed tephra and Papakai Tephra Formation have been grouped into a newly defined Papakai Formation, with discrete tephras recognised within the formation defined as members.

Furthermore, in the Mt Ruapehu region, some materials within Papakai Formation are probably tephric loess. Therefore use of the word 'tephra' in the formation name is misleading since not all deposits in the formation are necessarily primary tephra.

Redefinition and Age

Papakai Formation comprises andesitic tephra erupted from TgVC, and possibly tephric loess, dated between *c.* 9700 and 2500 years B.P. Papakai Formation overlies Mangamate Tephra and underlies the andesitic Mangatawai Tephra. The lower contact with Mangamate Tephra is commonly unconformable.

Papakai Formation is informally divided into upper Papakai Formation (ash occurring above Hinemaiaia Tephra) and lower Papakai Formation (ash occurring below Hinemaiaia Tephra, incorporating also Motutere Tephra).

Description and Identification

At most sites the lower contact of Papakai Formation is unconformable with Poutu Lapilli Member of Mangamate Tephra, and the base contains abundant fine bluish grey and strong brown iron-stained lapilli derived from this member (Plate 3.5). This erosional unconformity was identified by Topping (1974) in the Mt Tongariro region, and is commonly seen in sections within the study area. The deposition of Mangamate Tephra resulted in the destruction of the forest cover over much (1000 km^2) of the Mt Tongariro region. This may have accentuated erosion of Poutu Lapilli until the vegetation regenerated (Topping 1974).

The type section for Papakai Formation on the southeastern Mt Ruapehu ring plain is here designated at Desert Road S.15 [DR15] [T20/462135]. Reference sections are designated at Waikato Stream S.1 [WS1] [T20/467102] and Desert Road S.11 [DR11] [T20/464092] (Figure 3.2, p. 94; Chart 1).

At the type section (Plate 2.13; Chart 1), Papakai Formation is 1.26 m thick. It overlies Poutu Lapilli Member of Mangamate Tephra, and is overlain by Mangatawai Tephra. Both the upper and lower contacts with Mangatawai Formation and Poutu Lapilli are sharp and distinct.

The upper 0.47 m (upper Papakai Formation) comprises dark yellowish brown greasy sandy loam textured ash grading down to sandy clay loam textured ash, with some surface cracking, and distinct dark coated root channels. The lower 0.70 m (lower Papakai Formation) comprises dark yellowish brown and dark brown very greasy sandy clay loam textured ash with prominent surface cracking, medium nut structure and dark coated root channels denoting paleosol development. Many bluish grey fine lithic lapilli are interspersed within the base of the formation. These lapilli are poorly vesicular with field characteristics typical of Mangamate Tephra and are probably derived by reworking from Poutu Lapilli. The stronger colour and greater degree of paleosol development seen in the lower 0.70 m is characteristic of Papakai Formation in most Desert Road exposures.

Three rhyolitic tephras, Waimihia Tephra, Hinemaiaia Tephra and Motutere Tephra are found interbedded within Papakai Formation. Waimihia Tephra occurs 0.18 m below the contact with Mangatawai Tephra and occurs as distinct white fine ash 'cream cakes' (Plate 2.13). Hinemaiaia Tephra is found 0.27 m below Waimihia Tephra, occurring as a reasonably discrete horizon of yellow coarse ash. Motutere Tephra occurs 0.41 m below Hinemaiaia Tephra, and 0.27 m above the basal contact of Papakai Formation with Poutu Lapilli.

At Waikato Stream R.S.1, Papakai Formation is 0.89 m thick. Here, upper Papakai Formation which is 0.38 m comprises reddish brown and dark yellowish brown greasy sandy clay loam textured ash with iron-stained root channels. Lower Papakai Formation which is 0.37 m thick comprises gleyed greyish brown sandy clay loam textured ash, with distinct surface cracking and iron-stained root channels. Motutere Tephra is found interbedded in the lower 0.18 m, and occurs as scattered fine white pumice fragments. Much of the character of Papakai Formation is masked by post-depositional iron-staining and gleying. Contacts with Mangatawai Tephra Formation and Poutu Lapilli Member are distinct.

At Desert Road R.S.11 (Plate 3.17), Papakai Formation is 0.97 m thick. It overlies 1.64 m of bedded fluvial sands and pumice and lithic pebbles, and is overlain by Mangatawai Tephra. It comprises 0.20 m of dark yellowish brown greasy fine sandy loam over 0.38 m of interbedded grey sands, white and pale grey clay beds, and reworked Hinemaiaia Tephra in brown andesitic ash. Lower Papakai Formation which is 0.17 m thick shows typical Papakai Formation characteristics, and comprises dark yellowish brown greasy sandy clay textured ash, with prominent cracking and abundant dark coated root channels, denoting paleosol development. Motutere Tephra is interbedded within this unit and occurs as scattered white fine pumice fragments. The base of the formation is strongly iron-stained. Upper and lower contacts are distinct and sharp.

At T20/465099 (Plate 3.6), immediately south of Waikato Stream R.S.1, the erosional unconformity between Poutu Lapilli and Papakai Formation is particularly evident. Here, a discontinuous bed comprising reworked Poutu Lapilli, and Papakai Formation unconformably overlie tephras and fluvial sediments older than Poutu Lapilli Member.

Papakai Formation is characterised by its strong yellowish brown colour, greasy consistency, and surface cracking, denoting paleosol development.

At the type section, the relative depths of the interbedded rhyolitic Waimihia, Hinemaiaia and Motutere tephras indicate that the basal part of Papakai Formation (up to Motutere Tephra) accumulated more slowly than the remainder of the formation. In the initial *c.* 4300 years of deposition only 0.27 m was deposited – this is compared to 0.86 m over the next *c.* 2900 years, approximately five times the former accumulation rate. The much stronger paleosol development observed in this lower 0.27 m (Plate 2.13) (and also in exposures of Papakai Formation in the Mt Tongariro region by Topping 1973, 1974), may be attributed to greater weathering as a consequence of the slower rate of deposition.

At some sites Papakai Formation is strongly gleyed to an atypical pale grey. Gleying is particularly evident at Desert Road S.12 [T20/458119] (Plate 3.7). In more southern exposures within Rangipo Desert (at Death Valley T.L.), Karioi Forest (*e.g.* Rock Road [T20/322941]) and sections along S.H.49, Papakai Formation is distinctly sandier in texture than to the north, occurring commonly as yellowish brown massive sandy loam textured ash, without distinctive surface cracking (Plate 3.8; Plate 3.9).

Members

Four informal members are defined within Papakai Formation. Reference sections for these members are at Tufa Trig S.2 [TT2] [T20/375046], and Death Valley S.2 [DV2], Rangipo Desert [T20/408047] (Figure 3.2, p. 94; Chart 1).

Black Ash-2 [ba-2]

At Tufa Trig R.S.2, black ash-2 is 10 mm thick. It is interbedded within yellowish brown to olive brown ash, 0.25 m below the upper contact of Papakai Formation with Mangatawai Tephra, and 0.02 m below Waimihia Tephra. It occurs as a prominent black pocketing coarse ash (Plate 2.10; Plate 2.11) within upper Papakai Formation . It is dated at *c.* 3500 years B.P. based on the age of the overlying Waimihia Tephra.

At Death Valley R.S.2, black ash-2 member occurs 0.20 m below the upper contact of Papakai Formation with Mangatawai Tephra, and 0.02 m below the interbedded Waimihia Tephra. At this site upper Papakai Formation and black ash-2 member overlie a prominent andesitic diamicton of the Mangaio Formation.

Black ash-2 member sampled from Death Valley type locality dominantly comprises free ferromagnesian minerals, together with feldspar, black and brown vesiculated vitric pyroclasts with subconchoidal and conchoidal facial fracture, highly vesicular andesitic pumice fragments and some rhyolitic glass shards. Lithic lapilli are absent. Ferromagnesian minerals show thick glassy coatings and blocky morphology with some showing sub-conchoidal and conchoidal facial fracture. Rhyolitic glass shards are assumed to be derived from aeolian reworking of rhyolitic tephra and incorporated into the tephra during its accumulation. Compositionally, this tephra is very similar to members of Tufa Trig Formation.

Black Ash-1 [ba-1]

At Tufa Trig R.S.2, black ash-1 is 10 mm thick. It is interbedded within yellowish brown ash, 0.44 m below Mangatawai Tephra and 0.02 m above the rhyolitic Hinemaiaia Tephra. It occurs as a distinct and prominent black pocketing coarse ash within upper Papakai Formation (Plate 2.11). The tephra is slightly younger than the rhyolitic Hinemaiaia Tephra and is therefore dated at *c.* 4500 years B.P.

At Death Valley S.2, it is found below Mangaio Formation, separated from it by a 0.10 m sandy clay textured paleosol and a 30 mm peat deposit. Here it occurs as a distinct, prominent, pocketing black coarse ash overlying the rhyolitic Hinemaiaia Tephra.

The stratigraphic relationships of black ash-2 and black ash-1 members to the interbedded rhyolitic Waimihia and Hinemaiaia tephras are shown in Plate 3.9 in an exposure within Death Valley. At this site the Mangaio Formation diamicton is absent so that both members are separated only by intervening ash of Papakai Formation. The stratigraphic relationship of black ash-1 to the underlying Hinemaiaia Tephra and overlying Mangaio Formation is shown in Plate 2.14.

Black ash-2 and black ash-1 members are very similar in appearance to the members of Tufa Trig Formation and ash beds of Mangatawai Tephra. They are however distinguished from both of these formations by stratigraphic position. Both members are recognised in many exposures within Rangipo Desert, and especially in sections in Death Valley. The thickness – distribution of these tephras and the absence of them in sections where tephras from Mt Ngauruhoe and Mt Tongariro are at their thickest, suggests source at Mt Ruapehu. Black ash-2 and black ash-1 have been used within the study area to assist in the field correlation of Waimihia and Hinemaiaia tephras, and the Mangaio Formation diamicton (see section 5.2).

Orange Lapilli-2 [or-2] and Orange Lapilli-1 [or-1]

The reference section for these two members is at Tufa Trig S.2 [TT2] (Figure 3.2, p. 94; Chart 1). Both members are found within lower Papakai Formation. At this site, orange

lapilli-2 is 0.08 m thick. It occurs 0.10 m above orange lapilli-1 member, and is overlain by Hinemaiaia Tephra. It comprises dominantly strong brown pumiceous fine and medium lapilli. Orange lapilli-1, which is 0.30 m thick, occurs 0.50 m above the interbedded rhyolitic Motutere Tephra and comprises strong brown fine and medium pumice lapilli. Although this member is much thicker, it is very similar in appearance to orange lapilli-2. Both tephras are strongly coloured and thus are distinctive.

Two lapilli layers identified below Hinemaiaia Tephra at Wahianoa Road S.1, Karioi Forest [T20/391986], are provisionally correlated with orange lapilli-1 and orange lapilli-2 members from stratigraphic position. Here, orange lapilli-2 is indistinct, occurring as scattered orange fine pumice lapilli in brown andesitic ash. Orange lapilli-1 is more distinct, and comprises brownish yellow fine and medium pumice lapilli and a few grey lithic lapilli scattered through a *c.* 60 mm zone within brown ash of Papakai Formation.

Both members are identified at too few sections to permit isopachs to be shown, but their presently recognised distribution suggests a reasonably confined southeasterly dispersal axis. These lapilli are useful marker beds in sections within Death Valley and The Chute (Chart 1).

Distribution

Papakai Formation is identified throughout TgVC, but is especially well exposed in sections along the Desert Road, north of S.11 [T20/464092].

Isopachs of Papakai Formation (Topping 1973, as Papakai Tephra Formation) show it was principally derived from the Tama Lakes – Mt Ngauruhoe region and from Mt Tongariro, with a lesser component from Mt Ruapehu (Topping 1973).

Significance

Papakai Formation constitutes a regional marker bed within TgVC. It was deposited over a period of *c.* 7200 years, with the upper and lower contacts of the formation identifying *c.* 2500 and 9700 years B.P. time planes, respectively. In the study area, Papakai Formation is useful to the establishment of a stratigraphy and chronology (relative-age dating) of locally distributed andesitic tephras, and distal rhyolitic tephras sourced from TVC.

Mangamate Tephra [Mm]

Definition and Age

Mangamate Tephra Formation (Topping 1973), here renamed Mangamate Tephra, is a formation comprising a closely spaced sequence of tephras, erupted from Mt Tongariro between *c.* 9780 and 9700 years B.P. (Topping 1973). The basal member of the formation, Te Rato Lapilli, is radiocarbon dated [NZ1372] at 9780 ± 170 years B.P. The youngest

member, Poutu Lapilli is dated at *c.* 9700 years B.P. based on peat accumulation rates (Topping 1973).

Six named members within Mangamate Tephra were defined by Topping (1973). These are: Te Rato Lapilli, Oturere Lapilli, Waihohonu Lapilli, Ohinepango Tephra, Wharepu Tephra and Poutu Lapilli (in stratigraphic order from oldest to youngest). In the Mt Tongariro region, Mangamate Tephra overlies the rhyolitic Karapiti Tephra, and is overlain by Papakai Formation.

Description and Identification

Mangamate Tephra is best exposed in sections along the Desert Road, east of Mt Ruapehu. On the southeastern Mt Ruapehu ring plain reference sections are here designated at: Desert Road S.16 [DR16] [T20/481186], Mangatoetoenui Quarry [MQ] [T20/549153], and Desert Road S.15 [DR15] [T20/462135] (Figure 3.2, p. 94; Chart 1; Chart 2).

Type sections for Mangamate Tephra members are here designated at: Poutu S. [PT] [T19/481325] [5] (Poutu Lapilli Member), Desert Road S.15 [DR15] [T20/462135] (Wharepu Tephra Member, Ohinepango Tephra Member), Desert Road S.16 [DR16] (Waihohonu Lapilli Member), Mangatoetoenui Quarry [MQ] [T20/459153] (Oturere Lapilli Member) (Figure 3.2, p. 94), (Chart 2). A reference section for Te Rato Lapilli Member is at T19/377351.

At Desert Road R.S.16 and R.S.15 (Plate 2.13; Plate 2.18), Mangamate Tephra (which is 2.64 m and 2.42 m thick, respectively) overlies unnamed tephra above Pahoka Tephra, and is overlain by Papakai Formation. The rhyolitic Karapiti Tephra has not been identified below Mangamate Tephra at either of these sites. Five of the six named members of Mangamate Tephra are identified. They are Poutu Lapilli, Wharepu Tephra, Ohinepango Tephra, Waihohonu Lapilli and Oturere Lapilli. Poutu Lapilli, Wharepu Tephra and Ohinepango Tephra are particularly well exposed.

At Mangatoetoenui Quarry, Mangamate Tephra is 2.25 m thick. It overlies 0.14 m of unnamed tephra (with the interbedded Karapiti Tephra) above Pahoka Tephra, and is separated from Papakai Formation by an overlying unit comprising reworked Mangamate Tephra. Here four members (Poutu Lapilli, Wharepu Tephra, Waihohonu Lapilli, Oturere Lapilli) are identified and are particularly well exposed.

---

[5] Topping (1973) designated Poutu S. [N112/239901] and a section at N112/124928 on S.H.47 as reference sections for Poutu Lapilli and Te Rato Lapilli members. The grid references used here are the metric equivalents – T19/481325 and T19/377351, respectively.

Poutu Lapilli Member [Pt]

At the type section (Plate 3.10), Poutu Lapilli is 0.9 m thick. It overlies Wharepu Tephra Member, and is overlain by Papakai Formation. Here it comprises bedded brownish yellow iron-stained pumice lapilli, grey lithic lapilli, and coarse ash (Topping 1973). At the reference sections, it comprises strong brown, dark greyish brown and olive grey dominantly fine, angular lithic lapilli, and strong brown iron-stained finely vesicular pumice lapilli, weakly cemented by iron oxide. The unit shows weak normal grading from a fine and medium lapilli base to a fine and very fine lapilli and coarse ash top. A distinctive dark grey to black coarse ash occurs immediately below Poutu Lapilli (Plate 3.11; Plate 2.13).

At many sites within the study area an erosional unconformity occurs above Poutu Lapilli. This unconformity is most commonly marked by a sharp straight contact between Poutu Lapilli and the overlying Papakai Formation. At Mangatoetoenui Quarry (Plate 3.11) and other localities (*e.g.* Desert Road S.12 [T20/458119], Waikato Stream S.1 [T20/467102], Bullot Track S.1 [T20/412108] and Whangaehu River S.5 [T20/443045]), a fine grained unit separates Poutu Lapilli and Papakai Formation. This unit comprises weakly bedded fine angular and platy, dominantly lithic lapilli fragments, and is assumed to represent reworked Poutu Lapilli deposited after the erosion event which followed the deposition of Poutu Lapilli. The lower contact of this unit with Poutu Lapilli is erosional, sharp and distinct, and is marked by a sharp change in grain size between units.

At Desert Road R.S.17, the unconformity is marked by a discrete line of coarse pebbles occurring along the contact of Poutu Lapilli with the base of Papakai Formation (Plate 2.16).

At all sites the lower contact of Poutu Lapilli with Wharepu Tephra is distinct and sharp. Poutu Lapilli can be identified by its stratigraphic position, strong colour, exterior cementing of lapilli, the presence of an underlying grey to black loamy ash, and the sharp change in grain size between it and the underlying finer grained Wharepu Tephra Member.

Topping identified a tri-lobed distribution for Poutu Lapilli, with deposition NW, NE and SE of Mt Tongariro, and source at Blue Lake. A partial isopach map of Poutu Lapilli (Figure 3.8, p. 118), based on measurements taken along the Desert Road, is in agreement with that shown in Topping (1973) and supports existence of a southeasterly lobe. Using the isopachs shown in Figure 3.8, Poutu Lapilli has a volume of about 1070 $x10^6$ m^3. A similar volume (900 $x10^6$ m^3) was determined by Topping (1973).

Wharepu Tephra Member [Wp]

At the type section Wharepu Tephra (Plate 2.13; Plate 2.18) is 0.77 m thick. Here, and at Desert Road R.S.16, Wharepu Tephra conformably overlies the rhyolitic Poronui Tephra and is conformably overlain by Poutu Lapilli Member. The lower contact with Poronui Tephra is

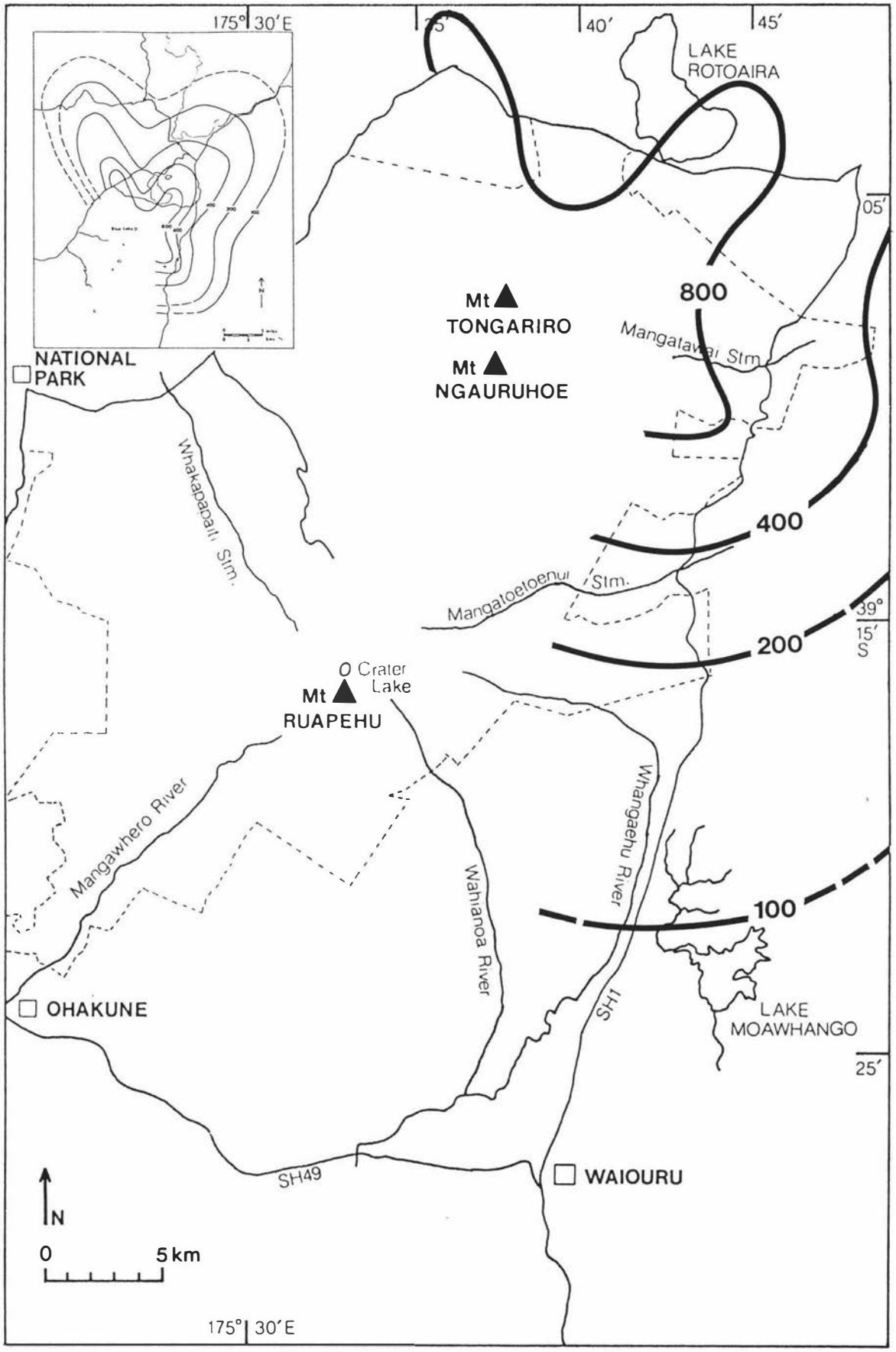

Figure 3.8 Partial isopach map of Poutu Lapilli Member of Mangamate Tephra (all measurements in millimetres). The 800 mm isopach is from the Poutu Lapilli isopach map of Topping (1973) (insert).

sharp and distinct (Plate 2.18). Wharepu Tephra comprises bedded lapilli and coarse ash, with three beds identified. The upper two beds comprise loose, grey and strong brown angular fine and very fine lithic lapilli and a few strong brown iron-stained pumice lapilli. The thinner (0.11 m) and finer grained basal bed dominantly comprises strong brown iron-stained lapilli and coarse ash, and is distinguished from the overlying beds by its colour. Contacts between the beds are distinct. Wharepu Tephra is the thickest of all the Mangamate Tephra members at this site. The upper contact of Wharepu Tephra Member with Poutu Lapilli Member is distinct and sharp, and marked by a distinct change in grainsize and colour. At this site a 30 mm thick brown, greasy, silt textured ash with prominent relief underlies Wharepu Tephra.

In the Mt Tongariro region, Topping (1974) recognised an erosional unconformity below Wharepu Tephra Member. This unconformity was identified by partial erosion of Ohinepango Tephra Member and the absence of Poronui Tephra (Topping 1974). At Mangatoetoenui Quarry (Plate 3.11) both Poronui Tephra and Ohinepango Tephra Member are absent, although they are recognised in sections both north and south of this site. Here, Wharepu Tephra (0.71 m) unconformably overlies Waihohonu Lapilli. The absence of Poronui Tephra and Ohinepango Tephra at this site is attributed to localised erosion, and possibly identifies the unconformity identified by Topping (1974).

Wharepu Tephra everywhere comprises bedded black and dark grey lapilli over a basal strong brown lapilli and ash bed. Beds are distinguished by their colour and grain size. The basal lapilli bed is particularly distinctive in all exposures, and is commonly underlain by a brown fine ash. Wharepu Tephra is distinguished from the underlying Ohinepango Tephra by its coarser grain size, and its stratigraphic position to the rhyolitic Poronui Tephra.

A new partial isopach map of Wharepu Tephra Member (Figure 3.9, p. 120) shows a dispersal axis to the south east of Mt Tongariro. A source in the Tama Lakes – Mt Ngauruhoe area is suggested by Topping (1973). Based on the isopachs shown in Figure 3.9, Wharepu Tephra has a volume of $\sim 360 \times 10^6$ m^3 (Figure 6.3, p. 295).

Ohinepango Tephra Member [Oh]

At the type section Ohinepango Tephra (Plate 2.13; Plate 2.18) is 0.39 m thick. It conformably overlies Waihohonu Lapilli, and underlies Poronui Tephra, which is prominent in this section. It comprises alternating 30 mm beds of strong brown and black coarse ash and very fine lapilli. Strong brown beds are pumice dominant, and black beds lithic dominant. Contacts between beds are sharp and distinct. Here, and at Desert Road R.S.16, Ohinepango Tephra is a particularly distinctive tephra, and is readily distinguished from all other Mangamate Tephra members by its colour-banding and dominant ash grade. Ohinepango Tephra is not identified at Mangatoetoenui Quarry.

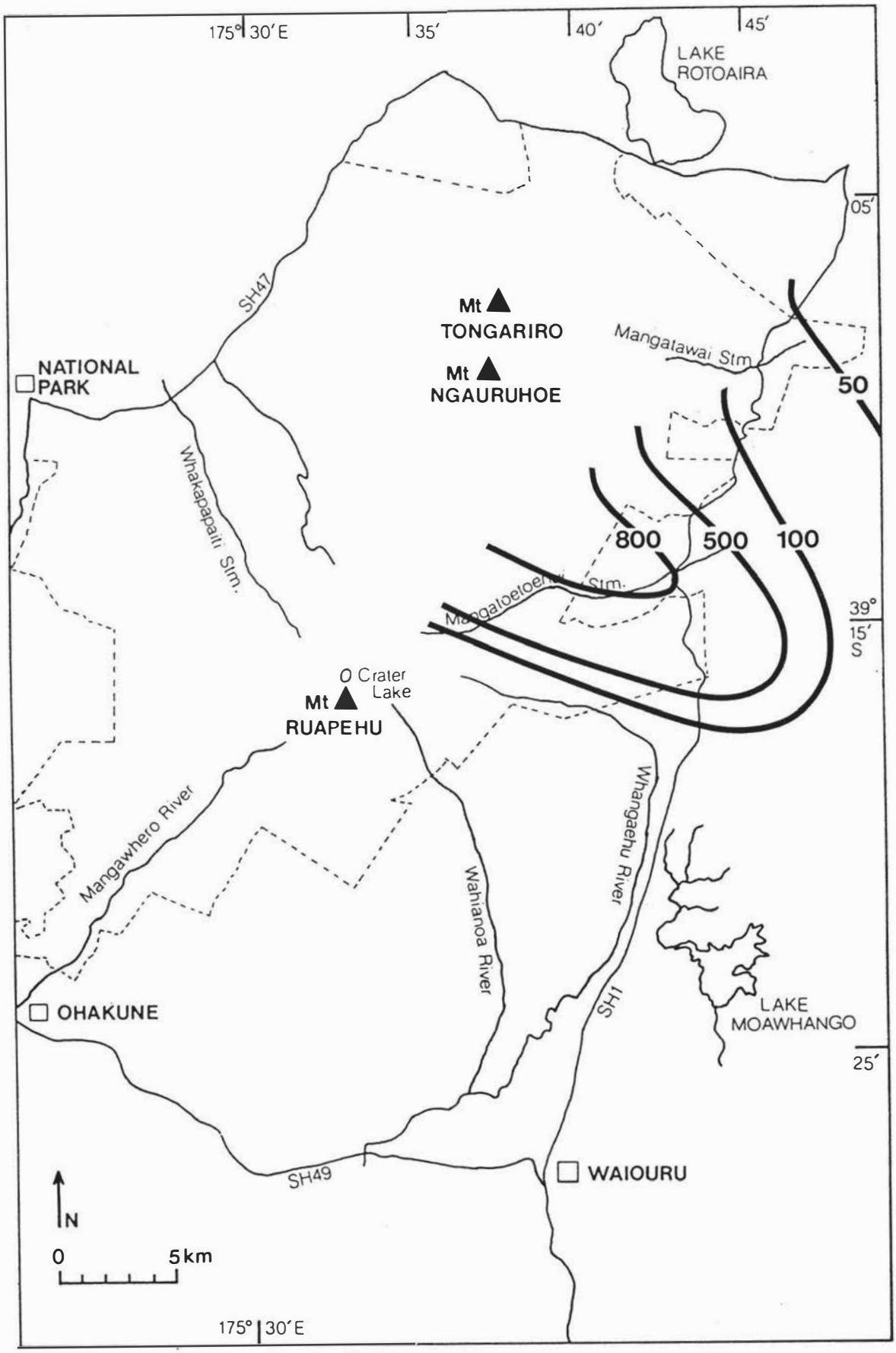

Figure 3.9 Partial isopach map of Wharepu Tephra Member of Mangamate Tephra (all measurements are in millimetres).

Topping (1973) noted that Ohinepango Tephra and Wharepu Tephra are very similar in field appearance and the presence of Poronui Tephra is needed to tell them apart. At all but one section (Desert Road S.11 [T20/464092]) on the southeastern Mt Ruapehu ring plain, Ohinepango Tephra is readily distinguished by its prominent and distinctive black and strong brown colour-banding and consistently finer grain size. Poronui Tephra need not be recognised in order to distinguish these two tephras near source.

A new partial isopach map of Ohinepango Tephra (Figure 3.10, p. 122) shows a dispersal axis to the southeast of Mt Tongariro, and possibly a second axis (bi-lobed distribution) to the east. A source in the Tama Lakes – Mt Ngauruhoe area is suggested by Topping (1973).

Waihohonu Lapilli Member [Wa]

At the type section Waihohonu Lapilli is 1.18 m thick, and is the thickest of all the Mangamate Tephra members at this site. Here, and at Desert Road R.S.15, Waihohonu Lapilli conformably overlies unnamed tephra above Oturere Lapilli, and underlies Ohinepango Tephra Member. Contacts are distinct and sharp, although the lower contact is partially obscured by scree. Waihohonu Lapilli comprises loose, weakly bedded dominantly fine yellowish brown iron-stained, and very dark grey and black lithic lapilli, with fewer iron-stained finely vesicular pumice lapilli. Interbedded at 0.35 m from the top of the unit is a prominent thin dark brown fine ash bed, useful to the identification of this member – Topping (1973) identified a similar brown ash bed within Waihohonu Lapilli Member in exposures on the Mt Tongariro ring plain.

At Mangatoetoenui Quarry, and Desert Road R.S.15, two thin yellowish brown pumice-rich beds are found near the base of Waihohonu Lapilli Member. The lowermost of these is particularly distinctive (Plate 3.11). The presence of these two beds distinguishes Waihohonu Lapilli from Oturere Lapilli, which is otherwise very similar in appearance. They are identified in all exposures within the Mt Ruapehu region, and are diagnostic of Waihohonu Lapilli Member.

Waihohonu Lapilli is characterised by the presence of strongly coloured yellowish brown pumice dominant beds near the base of the unit, and especially by the brown ash interbed.

A new partial isopach map of Waihohonu Lapilli (Figure 3.11, p. 123) shows a dispersal axis to the southeast of Mt Tongariro. A source in the Tama Lakes – Mt Ngauruhoe area is suggested in Topping (1973). Based on the isopachs shown in Figure 3.11, Waihohonu Lapilli has a volume of $\sim 490 \times 10^6$ m^3 (Table 6.1, p. 295).

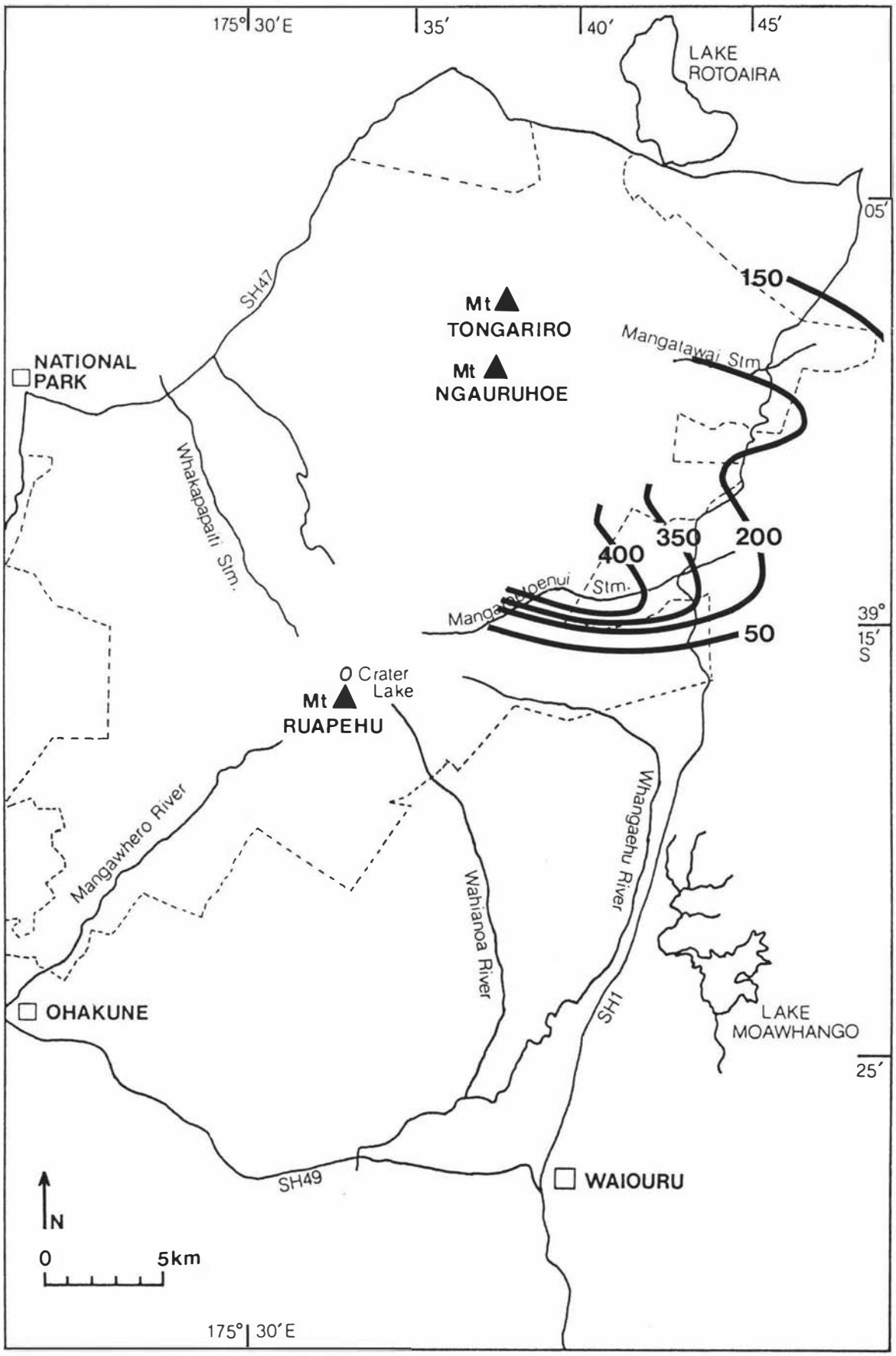

Figure 3.10 Partial Isopach map of Ohinepango Tephra Member of Mangamate Tephra (all measurements are in millimetres).

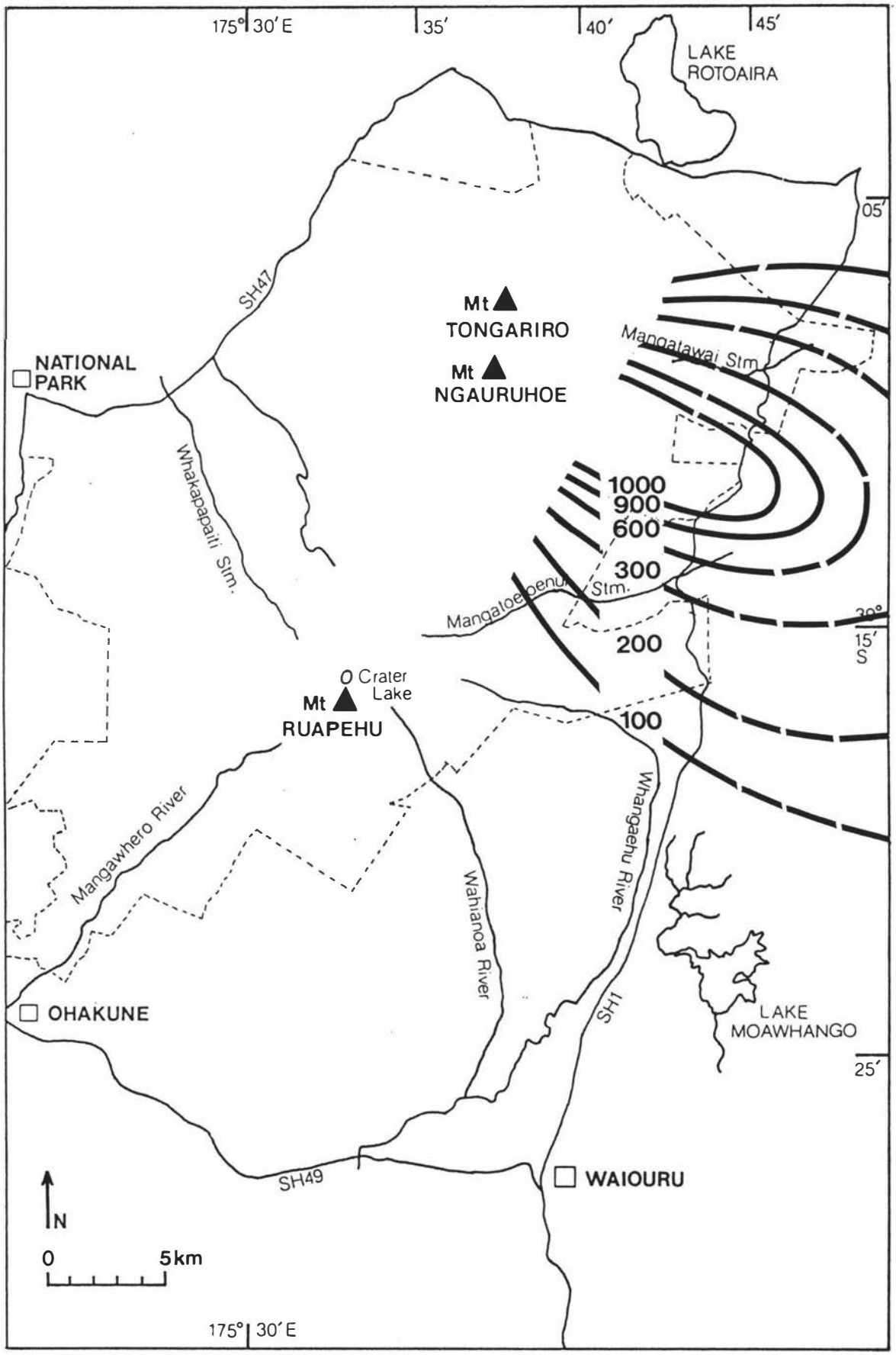

Figure 3.11 Partial isopach map of Waihohonu Lapilli Member of Mangamate Tephra (all measurements are in millimetres).

Unnamed tephra [ut']

At all localities within the Mt Ruapehu region, this unnamed tephra (Plate 2.18; Plate 3.11), conformably overlies Oturere Lapilli Member and underlies Waihohonu Lapilli Member (Chart 2). It comprises bedded ash and lapilli of finer grade and paler colour than the enclosing Mangamate Tephra members, and is distinctive because of its prominent relief. The upper and lower contacts are distinct, with some lapilli from the enclosing lapilli layers incorporated at the contacts.

Oturere Lapilli Member [Ot]

At the type section Oturere Lapilli is 0.48 m thick. It overlies unnamed andesitic tephra (with interbedded Karapiti Tephra) above Pahoka Tephra, and underlies Waihohonu Lapilli Member. In the Mt Tongariro region, Oturere Lapilli conformably overlies Te Rato Lapilli Member (Topping 1973). Te Rato Lapilli is, however, not identified at this site.

At the type section (Plate 3.11), Oturere Lapilli comprises loose, very dark grey and dark greyish brown angular lithic lapilli, with fewer yellowish brown iron-stained lithic, and finely vesicular pumice lapilli. The unit is weakly bedded and shows weak overall normal grading. The very basal lapilli are bluish grey in colour, resembling the lithic lapilli of the Te Rato Lapilli Member. The upper and lower contacts are distinct.

Although Oturere Lapilli lacks diagnostic field characteristics by which it can be correlated (at both the type and reference sections) it is readily identified by its stratigraphic position.

A new partial isopach map of Oturere Lapilli (Figure 3.12, p. 125) shows a dispersal axis east of Mt Tongariro. A source in the Tama Lakes – Mt Ngauruhoe area is suggested in Topping (1973). Based on the isopachs shown in Figure 3.12, this member has a volume of $\sim 370 \times 10^6$ m^3 (Table 6.1, p. 295).

Te Rato Lapilli Member [Tt]

At the type section Te Rato Lapilli is 0.41 m thick. It comprises very dark grey, dominantly fine lithic lapilli, and light yellowish brown finely vesicular pumice lapilli (Topping 1973). Here it conformably overlies the rhyolitic Karapiti Tephra and underlies Oturere Lapilli. Te Rato Lapilli is distinguished from the other members of Mangamate Tephra by its distinctive dark grey colour, and stratigraphic position. It is not identified on the Mt Ruapehu ring plain.

Isopachs of Te Rato Lapilli (Topping 1973) show a dispersal axis to the NNE of Mt Tongariro, with source at North Crater. Te Rato Lapilli has a volume of about 100×10^6 m^3 (Topping 1973) (Table 6.1, p. 295).

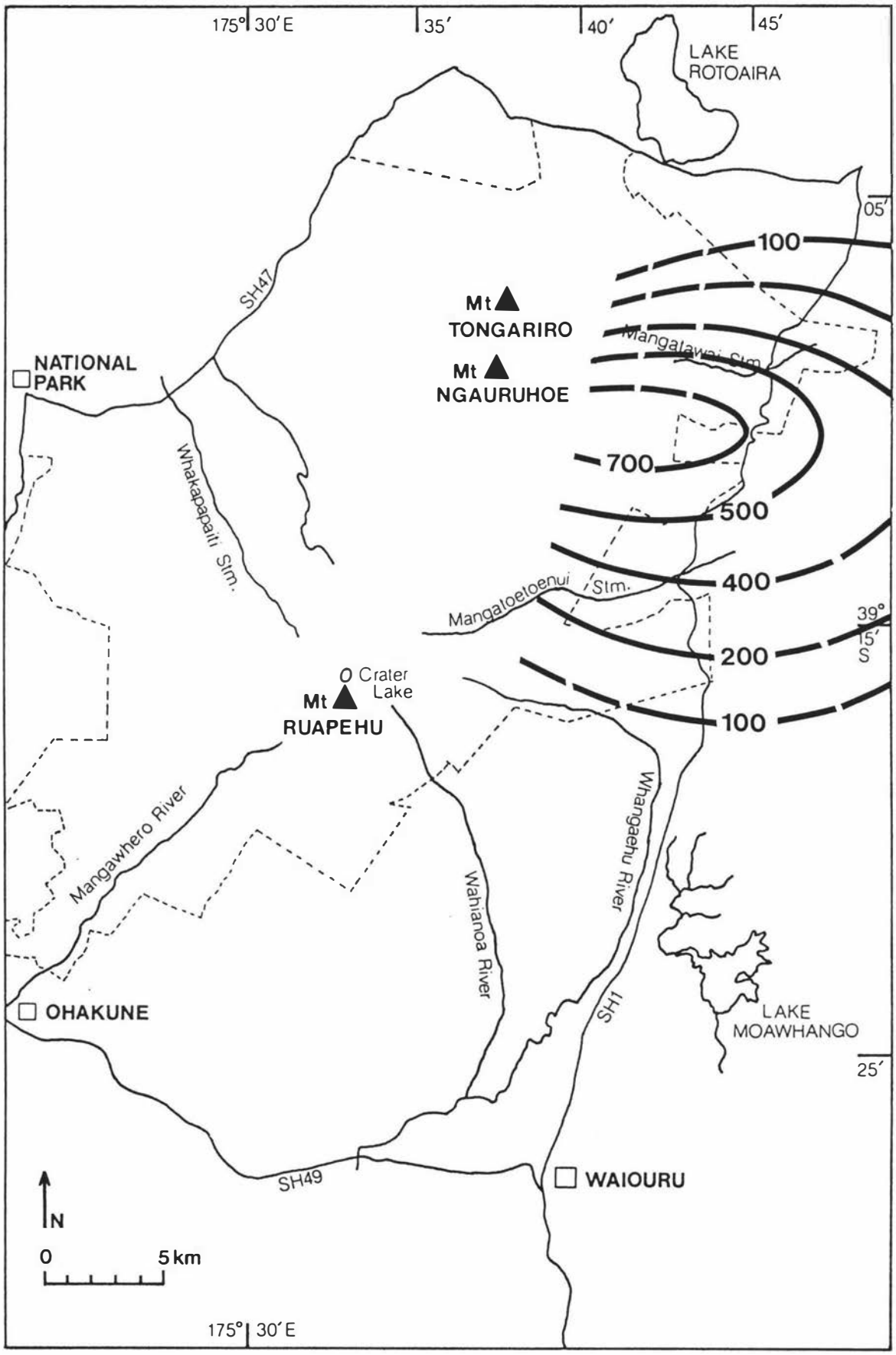

Figure 3.12 Partial isopach map of Oturere Lapilli Member of Mangamate Tephra (all measurements are in millimetres).

Best Localities for Mangamate Tephra

At T20/463101 (Plate 3.16), the tephra cover above Mangamate Tephra has been almost entirely stripped, so that only pedestals of Papakai Formation remain. At this section, Poutu Lapilli and Wharepu Tephra are particularly prominent. Here Mangamate Tephra overlies older Pahoka Tephra and Bullot Formation tephras.

At Desert Road S.11 [T20/464092], located well south of Mt Tongariro (Figure 3.2, p. 94), Mangamate Tephra thins to *c.* 1.20 m. Here it is separated from the overlying Papakai Formation by a dark grey fluvial deposit, possibly comprising reworked Mangamate Tephra. The contact is therefore difficult to define, and is provisionally placed at 1.87 m below the base of Papakai Formation. Here, identification of Poutu Lapilli Member is provisional. However, Wharepu Tephra, Ohinepango Tephra, Waihohonu Lapilli and Oturere Lapilli are all identified (Plate 3.12). The strong brown basal bed of Wharepu Tephra is particularly distinctive, and overlies in turn, Poronui Tephra (20 mm) and Ohinepango Tephra. The presence of the Poronui Tephra confirms the identification of the overlying tephra as Wharepu Tephra. Waihohonu Lapilli has thinned to 0.21 m, and Oturere Tephra to 0.18 m. South of this locality, Poutu Lapilli, Wharepu Tephra, and Ohinepango Tephra are identified, but in few sections.

At all sites within the study area, members of Mangamate Tephra are identified from diagnostic field characteristics, and stratigraphic positions. Diagnostic field characteristics of these tephras have been identified from exposures within the northern Mt Ruapehu region where most of the members are at their thickest, bedding characteristics are accentuated, and contact features useful to their correlation are identified. Mangamate tephras are lithologically distinct from other TgVC eruptives, and are typically grey in colour and comprise angular fine grey lithic lapilli and brown finely-vesicular pumice lapilli.

Distribution of Mangamate Tephra

Mangamate Tephra is identified in nearly all sections along the Desert Road to just north of Waiouru Township at Helwan R.S.2, where only Poutu Lapilli Member can be individually identified. Poutu Lapilli, Wharepu Tephra, and Ohinepango Tephra have been identified in sections along the Whangaehu escarpment, and sites east of the Desert Road, but at few sections in Rangipo Desert.

With the exception of Te Rato Lapilli, which has not been identified in the Mt Ruapehu region, members of Mangamate Tephra thicken appreciably to the south, toward Mt Ruapehu. This is especially marked in Wharepu Tephra, Ohinepango Tephra and Waihohonu Lapilli Members. Plate 2.19 and Plate 3.10 show Mangamate Tephra members at localities east [T19/524283] and north (Poutu R.S. [T19/481325]) of Mt Tongariro. The marked thickening of these units, and the development of bedding features in more southern sections may be

seen by comparing Plate 2.19 with Plate 3.11 (Mangatoetoenui Quarry R.S.) and Plate 2.13 (Desert Road S.15). Thickening trends along the Desert Road are shown in Chart 2.

Source

Four of the members (Wharepu Tephra, Ohinepango Tephra, Waihohonu Lapilli, Oturere Lapilli) are thought to have been erupted from the Tama Lakes – Mt Ngauruhoe area. Poutu Lapilli is thought to have been erupted from Blue Lake, Mt Tongariro and Te Rato Lapilli was most likely erupted from North Crater, Mt Tongariro (Topping 1973, 1974).

Significance

Mangamate Tephra comprises a particularly distinctive sequence of tephras, with each member constituting a regional marker bed within TgVC, and identifying a *c.* 10 000 years B.P. time plane. Within the study area, members of Mangamate Tephra are particularly important marker beds to the establishment of a stratigraphy and chronology of locally distributed tephra deposits.

Unnamed tephra [ut]

Unnamed tephra is an informal unit comprising several thinly bedded andesitic tephras erupted from TgVC, and is dated between *c.* 10 000 and *c.* 9780 years B.P., based on the ages of bracketing andesitic tephras.

At all localities in the Mt Ruapehu and Mt Tongariro regions, this unit underlies Mangamate Tephra and overlies Pahoka Tephra. In the study area where Te Rato Lapilli is absent, the unnamed tephra directly underlies Oturere Lapilli. The rhyolitic Karapiti Tephra, dated [NZ4847] at 9910 ± 130 years B.P. is interbedded in the top of this unnamed tephra.

Unnamed tephra is presently identified and mapped only in sections along the Desert Road between Poutu R.S. (Topping 1973) and Desert Road S.11, where the base of Mangamate Tephra, and Pahoka Tephra are clearly identified (Chart 1; Chart 2).

Pahoka Tephra [Pa]

Topping (1974) identified a lapilli unit beneath Mangamate Tephra, and informally referred to this as Pahoka lapilli. It is here formalised to Pahoka Tephra because of its usefulness as a marker bed within TgVC.

Definition and Age

Pahoka Tephra is thought to have erupted from Mt Tongariro (Topping 1974) and is dated between 10 000 and 9800 years B.P. Pahoka Tephra is slightly older than the rhyolitic Karapiti Tephra (9910 ± 130 years B.P. [NZ4847]), which overlies it.

Description and Identification

The type section for Pahoka Tephra is here defined at Desert Road S.16 [DR16] [T20/481186]. A reference section for Pahoka Tephra is designated at Mangatoetoenui Quarry [MQ] [T20/459153] (Figure 3.2, p. 94; Chart 1; Chart 2). At the type section, Pahoka Tephra is 0.34 m thick. It overlies andesitic tephras of Bullot Formation and is overlain in turn by 0.33 m of unnamed tephra and Oturere Lapilli Member of Mangamate Tephra. At this site, Pahoka Tephra comprises bedded fine to medium pumice lapilli and a few lithic lapilli. Strongly weathered, extremely soft lapilli form a greasy matrix. Pumiceous lapilli vary from very dark grey to olive grey, with many colour-banded (pale yellow and grey) lapilli. Three beds are recognised. The upper and middle beds are dominated by colour-banded lapilli, and the lower by pale olive non-banded pumiceous lapilli. Both the upper and lower contacts of this formation are distinct. Pahoka Tephra is distinguished from all other tephras in this section by its paler grey colour and the presence of distinctive colour-banded pumiceous lapilli.

At Mangatoetoenui Quarry, Pahoka Tephra is 0.24 m thick. It directly overlies a 0.34 m thick andesitic diamicton of Tangatu Formation-age (Plate 3.13) and is overlain by 0.16 m of unnamed tephra (below Oturere Lapilli) in which the rhyolitic Karapiti Tephra is interbedded (Plate 3.11).

Pahoka Tephra comprises grey and light olive grey colour-banded lapilli, light grey non-banded lapilli, and some black to very dark grey lithic lapilli. The basal 20 mm comprises coarse pumiceous and lithic ash. The formation is poorly sorted and shows weak normal grading. Stratigraphic position and the presence of diagnostic colour-banded pumiceous lapilli distinguish this tephra from all others in the section.

Pahoka Tephra thins in sections south of Mangatoetoenui Quarry. At Desert Road S.12 [T20/458119] (Plate 3.7) it has thinned to 95 mm. Here, Pahoka Tephra comprises grey fine and very soft pumiceous lapilli and platy angular pumiceous and lithic fragments. It is identified by its distinctive colour and stratigraphic position. Still further south, at Desert Road S.11 [T20/464092] (Plate 3.12), Pahoka Tephra has thinned to a pocketing 5 mm. The contacts with the overlying unnamed tephra and underlying Bullot Formation are discontinuous but distinct.

At other sections north of Mt Ruapehu (*e.g.* Mangatawai S., Access 10, Poutu S.; Chart 2), Pahoka Tephra overlies probable correlatives of Bullot Formation and the interbedded Rotoaira Lapilli, and is overlain in turn by unnamed tephra and Te Rato Lapilli Member of Mangamate Tephra.

Topping (1973), identified a prominent andesitic lapilli unit, Okupata Tephra, in sections north of Mt Ruapehu and identified a Mt Ruapehu source for this tephra. Okupata Tephra is radiocarbon dated (from wood within peat immediately above it [NZ1374], and charcoal within it [NZ1189]) between 12 450 ± 340 and 9790 ± 160 years B.P. (Topping 1973). The exact stratigraphic relationship of Pahoka Tephra to Okupata Tephra is however not known. To date, these two tephras have not been identified together in any one section. Okupata Tephra is not recognised in sections east of Mt Ruapehu.

Lowe and Hogg (1986) identified Okupata Tephra in Kaipo Lagoon bog, Urewera National Park. Based on peat accumulation rates the authors dated Okupata Tephra at 10 600 ± 90 years B.P. More recently, Lowe (1988a) correlated a tephra identified within the Waikato lakes region with the basal lapilli bed of Okupata Tephra. The tephra is radiocarbon dated [Wk514] at 12 700 ± 200 years B.P.) (Lowe 1988a). Based on ages obtained for the tephra both near source and at distal sites, Lowe (1988a) concludes that Okupata Tephra is time transgressive with units erupted between *c.* 13 000 and 10 000 years B.P. Okupata Tephra is therefore most probably older than Pahoka Tephra which has an estimated age of between 10 000 and 9800 years B.P. (Topping 1974).

Distribution

Pahoka Tephra has been identified in all sections along the Desert Road between Desert Road S.11 and Poutu R.S., and in a few sections west of the Desert Road in the vicinity of Bullot Track, in the northern Rangipo Desert. Changes in the thickness of this formation along the Desert Road are shown in Charts 1 and 2. A new partial isopach map (Figure 3.13, p. 130) shows a dispersal axis to the southeast of Mt Tongariro. A source at North Crater is suggested in Topping (1974). Based on the isopachs shown in Figure 3.13, the volume of Pahoka Tephra is ~250 $x10^6$ m^3 (Table 6.1, p. 295).

Significance

The base of Pahoka Tephra defines the contact between the Tongariro and Tukino subgroups. Pahoka Tephra is a particularly distinctive tephra. This, together with its widespread distribution within TgVC makes it an excellent regional marker bed.

In the Mt Ruapehu region it is useful to the establishment of a stratigraphy and chronology of locally preserved eruptives from Mt Ruapehu.

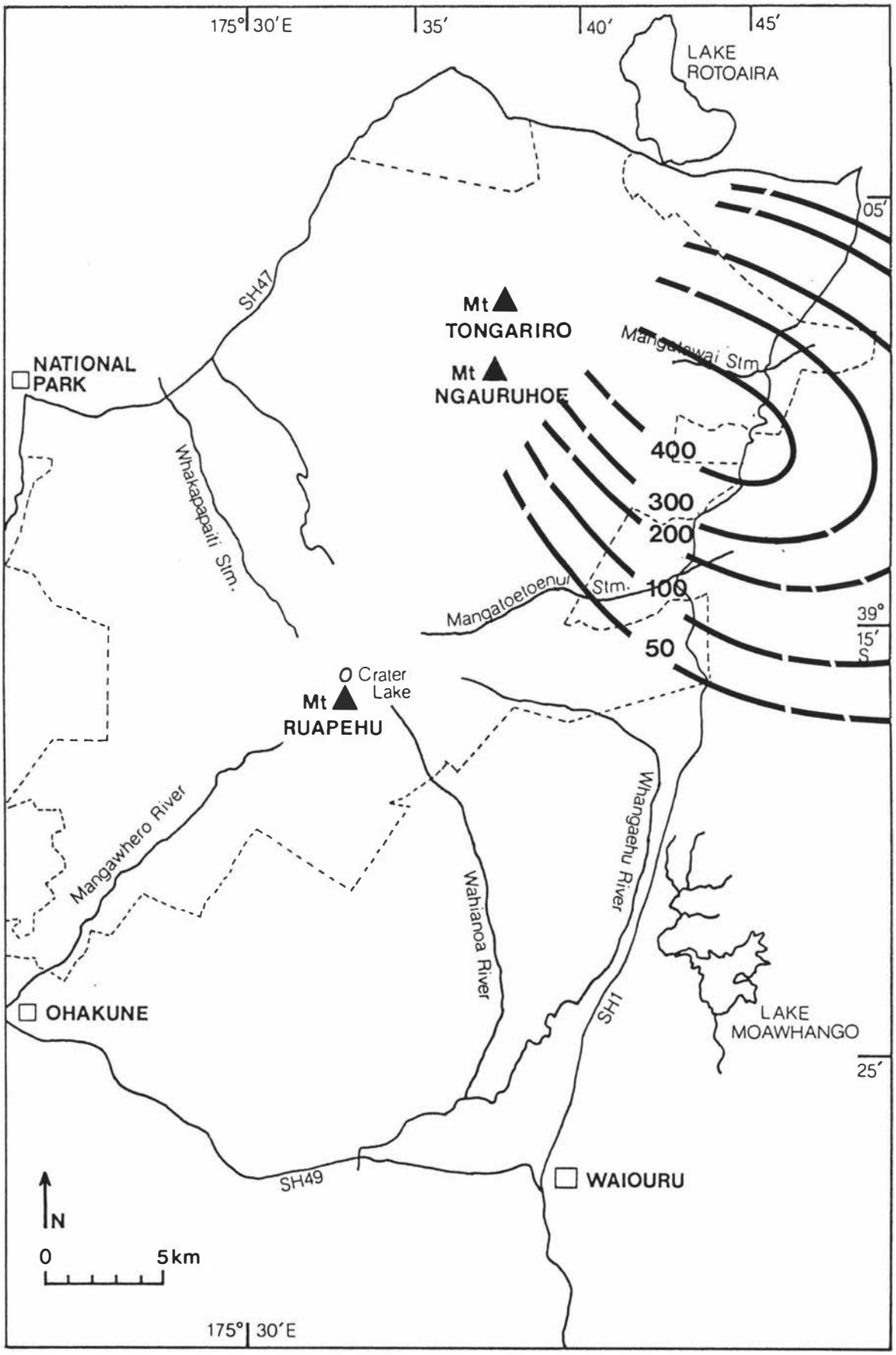

Figure 3.13 Partial isopach map of Pahoka Tephra (all measurements are in millimetres).

Tukino Subgroup Tephras

Bullot Formation [Bt]

Definition and Age

Bullot Formation (Table 3.1, p. 90) is a new formation name for a sequence of airfall tephras erupted from Mt Ruapehu, dating between *c.* 22 500 and 10 000 years B.P. and belonging to Tukino Subgroup. The upper contact of Bullot Formation is with the base of Pahoka Tephra. The base of the formation is defined by the contact with the rhyolitic Kawakawa Tephra Formation.

At sites in the southeastern Mt Ruapehu region where Pahoka Tephra and Kawakawa Tephra Formation are absent, the upper contact of Bullot Formation is with the base of Mangamate Tephra, or, where this is absent, the base of Papakai Formation. Here the base of the formation is defined by the contact with underlying andesitic diamictons which are older than either Rerewhakaaitu Tephra or Okareka Tephra.

The Bullot Formation is subdivided into three informal units – upper, middle, and lower units. Bullot Formation tephras younger than Rerewhakaaitu Tephra comprise the upper unit. Tephras older than Rerewhakaaitu Tephra and younger than Okareka Tephra comprise the middle unit, and tephras older than Okareka Tephra and younger than Kawakawa Tephra Formation comprise the lower unit.

Twenty three members are defined from the type and reference sections. Nineteen of these are defined from the type section (Bullot Track S.1) (Plate 3.14). Four members are given formal status.

Description and Identification

The type section on the southeastern Mt Ruapehu ring plain is here designated at Bullot Track S.1 [BT1] [T20/412108], an exposure within a gully proximal to Bullot Track (also known as Tukino Skifield Road) from where the formation takes its name. Reference sections are designated at Desert Road S.11 [DR11] [T20/464092], Waikato Stream S.1 [WS1] [T20/467102], Waikato Stream S.2 [WS2] [T20/469102] and Wahianoa Aqueduct [WA] [T20/435990] (Figure 3.2, p. 94; Chart 3).

At its type section (Chart 3) Bullot Formation is *c.* 10.5 m thick and comprises numerous horizontally bedded lapilli and ash units (Plate 3.14). It overlies 0.04 m of Kawakawa Tephra Formation and underlies the 0.06 m thick Pahoka Tephra. Here, Kawakawa Tephra Formation is poorly preserved and occurs as a thin discontinuous lens of coarse and fine ash. Two rhyolitic tephras, which are correlated with Okareka Tephra (*c.* 17 000 years B.P.) and Rerewhakaaitu Tephra (radiocarbon dated at 14 700 ± 200 years B.P. [NZ716]), are found interbedded with the formation.

Major units within Bullot Formation which can be correlated at other localities are formally designated members. The other units which have shown a limited ability for correlation are given informal member status.

At Waikato Stream R.S.1 (Plate 3.15) Bullot Formation is *c.* 2.70 m thick, and comprises numerous horizontally bedded lapilli and ash layers. The formation overlies fluvial sands and andesitic diamictons above Kawakawa Tephra Formation, and is overlain by Pahoka Tephra. Rerewhakaaitu Tephra is interbedded 1.62 m above the basal contact of Bullot Formation with Kawakawa Tephra Formation.

Slightly older Bullot Formation tephras, not preserved at Waikato Stream S.1 are identified at Waikato Stream S.2 (Figure 3.2, p. 94) located just north of and opposite S.1, above cliffs adjacent to Waikato Stream. At this site, Bullot Formation tephras overlie andesitic diamictons above *c.* 0.15 m Kawakawa Tephra Formation (Plate 2.26).

In sections immediately west of Waikato Stream S.1, Bullot Formation tephras are well exposed in narrow meandering channels where they are capped by Pahoka Tephra, Mangamate Tephra, and eroded Papakai Formation (Plate 3.16).

The base of Bullot Formation is exposed in a section to the south at Desert Road S.10 [T20/464091]. At this site, Bullot Formation tephras overlie 0.47 m of Kawakawa Tephra Formation (Oruanui Ignimbrite and Aokautere Ash members). Rerewhakaaitu Tephra is interbedded within the formation 0.74 m above Kawakawa Tephra Formation (Plate 2.25). At the adjacent Desert Road R.S.11 (Plate 3.17) only upper Bullot Formation tephras are exposed. Here the formation shows a maximum exposed thickness of 2.5 m.

At Wahianoa Aqueduct R.S. (Plate 2.20), located approximately 20 km to the south of the type section (Bullot Track S.1), Bullot Formation thins to 3.97 m. Here it overlies the rhyolitic Rerewhakaaitu Tephra, which in turn overlies andesitic diamictons of Te Heuheu Formation, and underlies Mangamate Tephra (Poutu Lapilli and ?Wharepu Tephra members). Pahoka Tephra is not identified at this site. The basal contact of the formation with Rerewhakaaitu Tephra is irregular and indistinct. Waiohau Tephra is found interbedded within Bullot Formation, 2.32 m below the upper contact of Bullot Formation with Mangamate Tephra, and 2.12 m above the basal contact with Rerewhakaaitu Tephra. At this site and all sections south of here, only tephra of the upper Bullot Formation are preserved, and these occur as wavy discontinuous lapilli and ash beds, separated by medial units with prominent relief and weak paleosol development, and andesitic ash.

In sections north of Mt Ruapehu (*e.g.* Mangatawai S., Access 10, Poutu S., Okupata S.), previously unnamed andesitic lapilli layers occurring below Pahoka Tephra are here provisionally correlated with Bullot Formation. At Poutu S. (the northernmost section), these lapilli layers are thin and indistinct. They are found interbedded within medial units both above

and below Rotoaira Lapilli which was erupted from Mt Tongariro *c.* 13 800 ± 300 years B.P. (Topping 1973). At this site, tephras erupted from Mt Tongariro (excluding Pahoka Tephra) are considerably thicker than the unnamed lapilli layers correlated with Bullot Formation. This, together with the observation that these lapilli thicken to the south (*e.g.* at Access 10, Mangatawai S.), suggests correlation with Bullot Formation.

Marker Ash Sequences

Marker ash sequences are here defined as two or more adjacent beds, which collectively are distinguished from adjacent lapilli beds by their colour and grain size. Individual beds within the sequence are not necessarily distinctive. Three marker ash sequences are recognised within Bullot Formation at the type section and are here designated as M_1, M_2 and M_3. These are shown in Chart 3 and are described from the type section at Bullot Track. The most distinctive of the marker ash sequences is M_1, which is 0.04 m thick and overlies Bullot Formation member L18. It comprises 0.02 m of grey firm, prominent ash with interbedded scattered strong yellow fine lapilli, over 0.02 m of yellow firm and prominent ash. M_1 is identified in sections within Rangipo Desert and north of the type section in cuttings along the Desert Road (Plate 3.16; Plate 3.17; Chart 3). M_2 is 0.13 m thick and overlies member L16. It comprises bedded brown, black and olive ash, and lapilli. M_3 is 70 mm thick and overlies member L15. It comprises bedded grey, yellow and dark grey loamy ash. Where identified, these marker ash sequences are useful in the identification and correlation of Bullot Formation members.

Tephra Parcels

A tephra parcel is here defined as a set of two or more beds which occur in close succession, and in which the beds themselves are able to be distinguished from adjacent beds by field characteristics. Tephra parcels comprise a characteristic stratigraphic association (ordering) of distinctive tephra beds. At Bullot Track T.S., tephra parcels comprise two or more distinctive black to purplish black dominantly coarse ash beds. The stratigraphic position of these tephra parcels is shown in Chart 3. Three parcels are identified at the type section, occurring between members L11 – L12, L12 – L14, and L17 – L18. Other distinctive black ash beds identified in the section are also shaded. Where recognised, tephra parcels may be used to provide 'ball-park' correlations of members.

Upper Bullot Formation Members

Ngamatea lapilli-2 [Nt-2] and lapilli-1 [Nt-1]

Reference sections for Ngamatea lapilli-2 and -1 are at Wahianoa Road S.1 [W1] [T20/391986], Karioi Forest, Helwan S.2 [H2] [T20/407917], and Helwan Quarry [HQ] [T20/408921] (Figure 3.2, p. 94; Chart 3).

At Wahianoa Road R.S. (Plate 3.18; Chart 3), Ngamatea lapilli-2 is 0.06 m thick. It overlies 0.10 m of unnamed Bullot Formation andesitic ash above Ngamatea lapilli-1, and is overlain in turn by 0.13 m of unnamed Bullot Formation ash and lapilli, and Poutu Lapilli Member of the Mangamate Tephra. Ngamatea lapilli-2 comprises brownish yellow and yellow, ungraded, fine pumice lapilli, with fewer grey lithic lapilli. Contacts are gradational. Ngamatea lapilli-1 is 0.06 m thick and overlies unnamed lapilli and ash beds of Bullot Formation (Chart 3). Ngamatea lapilli-1 comprises loose, strong brown and light yellowish brown, fine pumice lapilli and shows slight reverse grading.

Ngamatea lapilli-2 and -1 lack diagnostic field characteristics by which they may be individually correlated. At Wahianoa Road R.S. they occur as a distinct lapilli couplet (Plate 3.18) separated by andesitic ash with strong relief. At sections where this coupling is a prominent feature, the lapilli are correlated with Ngamatea lapilli-2 and -1 on the basis of stratigraphic position, grain size, and thickness of the units. At sites where this coupling is not evident, and more than two lapilli are preserved, correlation with the Ngamatea lapilli members is tentative. Detailed mapping shows that at some sites (*e.g.* sections on Rock Road [T20/322941] (Plate 3.8), Swamp Road [T20/345965], and Duncan Road [T20/333983]) only Ngamatea lapilli-1 is present, and is found overlying ?lapilli ul_1 and older unnamed Bullot Formation tephras.

Strong brown coloured lapilli identified in some sections along S.H.49 are provisionally correlated with Ngamatea lapilli-1 and -2. Near Waiouru [T20/386898] these lapilli overlie Bullot Formation tephras and medial deposits on Tertiary fossiliferous marine sands. In sections opposite Karioi pulp mill they overlie andesitic ash and diamictons.

At Helwan R.S.2, a prominent lapilli couplet is recognised below Poutu Lapilli (Mangamate Tephra) and the overlying Papakai Formation. The upper lapilli unit, which is 0.07 m thick, comprises strong brown and brownish yellow, fine and medium poorly vesicular pumice lapilli, and light grey fine lithic lapilli. It is separated from the lower lapilli by a prominent light olive grey fine ash. The lower lapilli is 0.10 m thick and comprises dominantly fine and medium dark brown and strong brown pumice lapilli, with fewer dark grey lithic lapilli. These lapilli are correlated with Ngamatea lapilli-2 and -1 respectively from field appearances and stratigraphic positions. Here they overlie pebbly sands of Tangatu Formation.

At Helwan Quarry (Chart 3) Ngamatea lapilli-2 is 0.07 m thick. It overlies 0.03 m of greyish brown sandy loam textured ash above Ngamatea lapilli-1 and underlies 0.13 m of andesitic ash below Poutu Lapilli. Ngamatea lapilli-2 comprises dark brown iron-stained medium to fine pumice lapilli with minor sandy loam textured ash matrix. Ngamatea lapilli-1 is 0.11 m thick, and overlies a 0.49 m thick unit comprising andesitic lapilli and interbedded medial units above Shawcroft Tephra. It comprises loose dark brown dominantly fine pumice lapilli.

The stratigraphy at the reference sections establishes the Ngamatea lapilli members as being younger than Shawcroft Tephra and the underlying rhyolitic Waiohau Tephra (dated [NZ568] at *c.* 11 250 years B.P.). The exact stratigraphic positions of these members within the Bullot Formation tephra sequence cannot be established from these sites, however, because neither member, nor Shawcroft Tephra, are recognised at the type section. Within exposures at the southern end of The Chute, however, a lapilli layer found overlying Pourahu Member [ignimbrite unit] is correlated with Ngamatea lapilli-1 from field characteristics and stratigraphic position (Chart 3). Ngamatea lapilli-1 and -2 are therefore younger than Pourahu Member, the latter being the uppermost Bullot Formation tephra in more northern sections.

Ngamatea lapilli-1 and -2 are identified in sections throughout the southern part of the study area where they are found overlying older Bullot Formation tephras. The southernmost occurrence of these lapilli recognised in this study is at Ngamatea Swamp, where they overlie uncorrelated tephras of the upper Bullot Formation, which in turn overlie Waiohau Tephra. The distribution and thickness of these lapilli, at sites on the southern Mt Ruapehu ring plain, is shown in Figure 3.14, p. 136.

Pourahu Member [Ph]

Pourahu Member comprises two units – a pumiceous ignimbrite and an airfall tephra, hereafter referred to as 'Pourahu Member [ignimbrite unit]' and 'Pourahu Member [tephra unit]', respectively.

Pourahu Member [ignimbrite unit] [Ph-Ig]

The type locality for Pourahu Member [ignimbrite unit] is at the southern end of The Chute [CT], Rangipo Desert (Figure 1.2, p. 3) [T20/437045], where three sections are described (The Chute S.1 – 3, Appendix II).

Pourahu Member [ignimbrite unit] is older than Bullot Formation member Ngamatea lapilli-1 which overlies it, and is younger than the rhyolitic Waiohau Tephra (dated [NZ568] at 11 250 years B.P.) which is found interbedded with older Bullot Formation tephras. Pourahu Member [tephra unit] and Pourahu Member [ignimbrite unit] are relative-age dated between *c.* 11 250 – 10 000 years B.P.

At the type locality Pourahu Member [ignimbrite unit] shows a maximum exposed thickness of 1.1 m (Plate 3.19). It comprises weakly bedded pumice lapilli, blocks and bombs, and lithic lapilli in a poorly sorted crystal-rich ash matrix. Most of the pumice lapilli within the ignimbrite are white and pinkish white in colour, and are phenocryst-rich. A much smaller proportion comprises colour-banded (white and dark grey) pumiceous, and more dense black scoriaceous clasts. The pumiceous blocks are both matrix- and clast-supported and are distinctly subrounded to rounded. The pumiceous bombs show distinctive prismatic jointing.

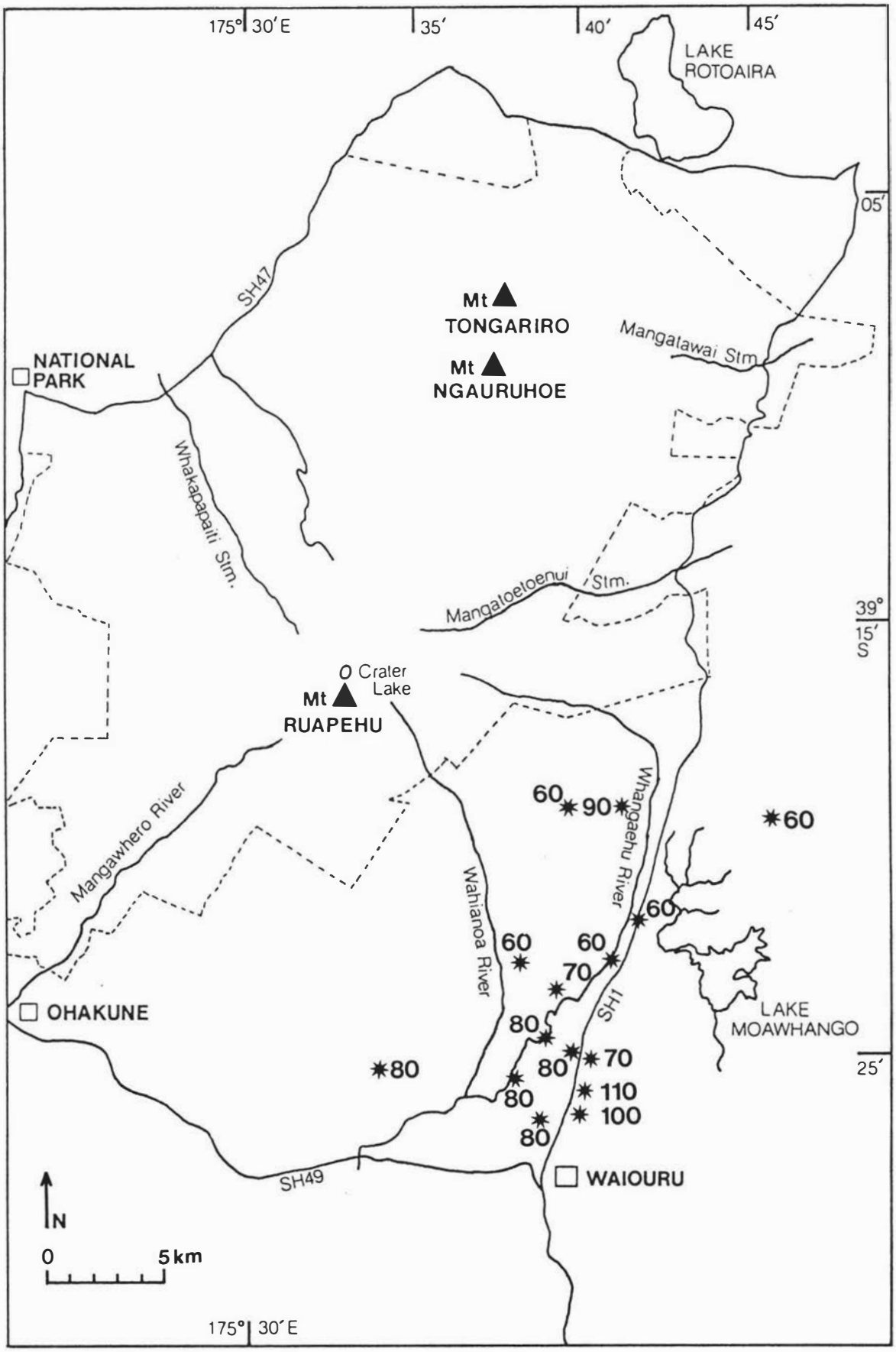

Figure 3.14 Distribution of Ngamatea lapilli-1 member of Bullot Formation (all measurements are in millimetres).

At The Chute S.3, three beds are recognised within the unit. The lowermost of these has a distinct pinkish brown sandy clay loam textured ash matrix, which contrasts with the crystal- and pumice-rich ash matrix of the overlying two units. Interbedded within the unit, and at the bed contacts, are thin sandy lenses. At all exposures, weakly bedded pebbly sand units of Tangatu Formation are interbedded with the deposit. Contacts with these units are sharp and irregular.

The deposits of pyroclastic flows (ignimbrites) are characterised by poor sorting and lack of internal stratification. Clasts within these deposits are typically rounded and monolithologic, and may show evidence of heat (*e.g.* breadcrust textures and welding of clasts) (Peterson 1970; Sparks *et al.* 1978; Smith and Roobol 1982; Rowley *et al.* 1985). The deposits of pyroclastic surges (ground surge and ash flow surge) are much finer and are enriched in crystals and vitrics (Smith and Roobol 1982).

A pumiceous pyroclastic flow, or 'pumice flow', is a dry mixture of hot pumice lapilli and ash, which may also contain breadcrusted pumice bombs and subordinate lithic fragments, crystals and gases (Crandell and Mullineaux 1973; Crandell, Booth *et al.* 1984), in which pumice lapilli comprise more than 50 volume percent of the deposit (Fisher and Schmincke 1984). Ignimbrite is synonymous with the deposits of pumiceous pyroclastic flows (Rowley *et al.* 1985). At the type locality Pourahu Member is interpreted as the deposit of a pumiceous pyroclastic flow, or 'pumice flow', based on the overall poor sorting of clasts, the very high proportion of pumice lapilli, blocks and ash compared to lithic clasts, and near monolithologic composition of the deposit. Pourahu Member [ignimbrite unit] is not welded, but the pink coloration of some pumice lapilli, and prismatic or jigsaw jointing of pumice bombs are indicative of a high temperature origin. Charcoal has not been identified within the deposit and the thermoremnant magnetisation of clasts has not been determined.

A pumice-rich deposit described at Mangatoetoenui Quarry [T20/459153] is also correlated with Pourahu Member [ignimbrite unit] based on stratigraphic position and field appearance. Here it is 0.49 m thick, and overlies 6^{+} m of andesitic diamictons (Plate 3.20). It underlies 0.76 m of andesitic diamictons and interbedded coarse ash deposits below Pahoka Tephra. Pourahu Member comprises bedded fine pumice lapilli and blocks, with overall reverse grading. Three beds are recognised. The lowermost bed comprises rounded and angular pale yellow and pinkish yellow dominantly fine pumice lapilli in a coarse ash matrix. The middle bed comprises similar coloured dominantly medium pumice lapilli, with common coarse lapilli and blocks. The uppermost bed comprises poorly sorted and ungraded pale yellow and pinkish brown dominantly medium pumice lapilli and blocks in a fine to coarse ash matrix. In places, the uppermost bed is separated from the middle bed by a thin and discontinuous pale grey sandy unit. At this site Pourahu Member is distinguished by its distinctive colouring and stratigraphic position.

Implications

Perfectly preserved pumice bombs with jigsaw jointing derived from Pourahu Member [ignimbrite unit] are found embedded within debris flow deposits of Tangatu Formation (Plate 3.21) in exposures in The Chute. Their presence within these deposits suggests the deposition of the sands was directly associated with the eruption of the pyroclastic flow deposit. Pumiceous pyroclastic flows generally originate from the rapid eruption of large volumes of pumiceous ash, lapilli, and blocks (Hyde 1975; Rowley *et al.* 1985), and are commonly of silicic composition (Fisher and Schmincke 1984). The interfingering of the pumice flow and sand deposits suggests deposition from a series of small events or pulses of activity. Pourahu Member [ignimbrite unit] probably comprises several flow units (Fisher and Schmincke 1984), closely spaced in time. Banded pumice and the presence of scoriaceous lapilli are evidence for a magma mixing event having occurred prior to the eruption of the Pourahu Member [ignimbrite unit]. The black scoria probably represent juvenile material associated with the eruption. The mineralogy and chemistry of Pourahu Member [tephra unit] and Pourahu Member [ignimbrite unit] are discussed in Chapter 4.

Pourahu Member [ignimbrite unit] is only exposed within the southern end of The Chute and at Mangatoetoenui Quarry (Figure 3.15, p. 140). Absence of sections exposing this member elsewhere within Rangipo Desert precludes detailed mapping of this deposit, identification of a probable source area, and an estimation of volume.

Although Pourahu Member [ignimbrite unit] is presently the only recognised ignimbrite deposit of the southeastern Mt Ruapehu ring plain, other small pyroclastic flows are associated with the Rangataua and Iwikau members of Whakapapa Formation (Hackett 1985). The pyroclastic flows are of small volume and are not a common feature in the pre-historic record.

Pourahu Member [tephra unit] [Ph-T]

The type section for Pourahu Member [tephra unit] is Desert Road S.16 [DR16] [T20/481186]. Reference sections are at Waikato Stream S.1 [WS1] [T20/467102], Desert Road S.11 [DR11] [T20/464092] and Bullot Track S.1 [BT1] [T20/412108] (Figure 3.2, p. 94; Chart 3).

At the type section, Pourahu Member [tephra unit] is 0.22 m thick. It overlies 1.21^{+} m of andesitic diamictons and interbedded Bullot Formation tephras, and is overlain in turn by 0.24 m of unnamed Bullot Formation tephras and Pahoka Tephra. Here it comprises light yellowish brown dominantly medium, subangular, soft pumice lapilli, and coarse ash. Pourahu Member [tephra unit] is readily distinguished by its colour, and stratigraphic position to Pahoka Tephra.

In sections south of the type section (Desert Road S.12, Waikato Stream R.S.1, Desert Road R.S.11 (Plate 3.12), Bullot Track R.S.), Pourahu Member [tephra unit] is found

interbedded with other Bullot Formation tephras, and does not directly overly andesitic diamictons as at the type section. At the reference sections it comprises white to pale yellow (with some pink colouring) medium to coarse, very vesicular pumice lapilli, with a coarse ash base and matrix. Contacts are distinct. It is distinguished from all other Bullot Formation tephras by its pale colour, coarser grain size, and stratigraphic position to the overlying Pahoka Tephra (Chart 3).

Pourahu Member [tephra unit] is recognised in sections along the Desert Road, between Wahianoa Aqueduct S. [T20/435990] and Oturere Trig S. [T19/488213]. The thickness distribution of Pourahu Member [tephra unit] in sections along the Desert Road is shown in Chart 3. It is a prominent andesitic marker bed within the Mt Ruapehu region. In more northern sections where Ngamatea lapilli-1 and -2 are absent, Pourahu Member [tephra unit] identifies the upper contact of Bullot Formation and the Tukino Subgroup.

Pourahu Member is of similar age and stratigraphic position to Okupata Tephra, erupted from Mt Ruapehu between *c.* 13 000 and 10 000 years B.P. (Topping 1973; Lowe 1988a). On the Mt Tongariro ring plain, Okupata Tephra overlies andesitic tephras provisionally correlated with Bullot Formation, and underlies, in turn, Karapiti Tephra and Mangamate Tephra. Isopachs of the basal lapilli of Okupata Tephra (Topping 1973) indicate that this tephra was probably not deposited on the southeastern Mt Ruapehu ring plain. The similarity in age and stratigraphic position of the units may, however, suggest correlation of Pourahu Member with Okupata Tephra, with the ignimbrite unit of Pourahu Member in particular representing a more southerly directed, and previously unrecognised, product of the Okupata eruption. Further detailed mapping of Pourahu Member in the Mt Ruapehu region is required to support such correlation.

A partial isopach map of Pourahu Member [tephra unit] (Figure 3.15, p. 140) shows a dispersal axis to the northeast of Mt Ruapehu. Based on these isopachs, this member has a volume of ~90 $x10^6$ m^3. The volume of Okupata tephra is ~200 $x10^6$ m^3 (Topping 1973) (Table 6.1, p. 295).

Members L18 and L17

At the type section, member L18, which is 0.09 m thick, and member L17 which is 0.25 m thick, are similar in appearance. They both comprise ungraded dominantly dark brown pumice lapilli and black lithic lapilli, and are separated by 0.13 m of unnamed ash and lapilli. Member L18 underlies a prominent marker ash sequence (M_1) comprising bedded grey over yellow ash. Similarly, member L17 overlies a marker ash sequence (M_2), separating it from member L16. Member L18 has not been correlated into other sections. Member 17, however, is correlated at Desert Road S.11, Waikato Stream S.1 and S.2, Tufa Trig S.2 and Seagull Gully S.1, and is provisionally correlated at two other sites (Chart 3) from field appearances and stratigraphic position.

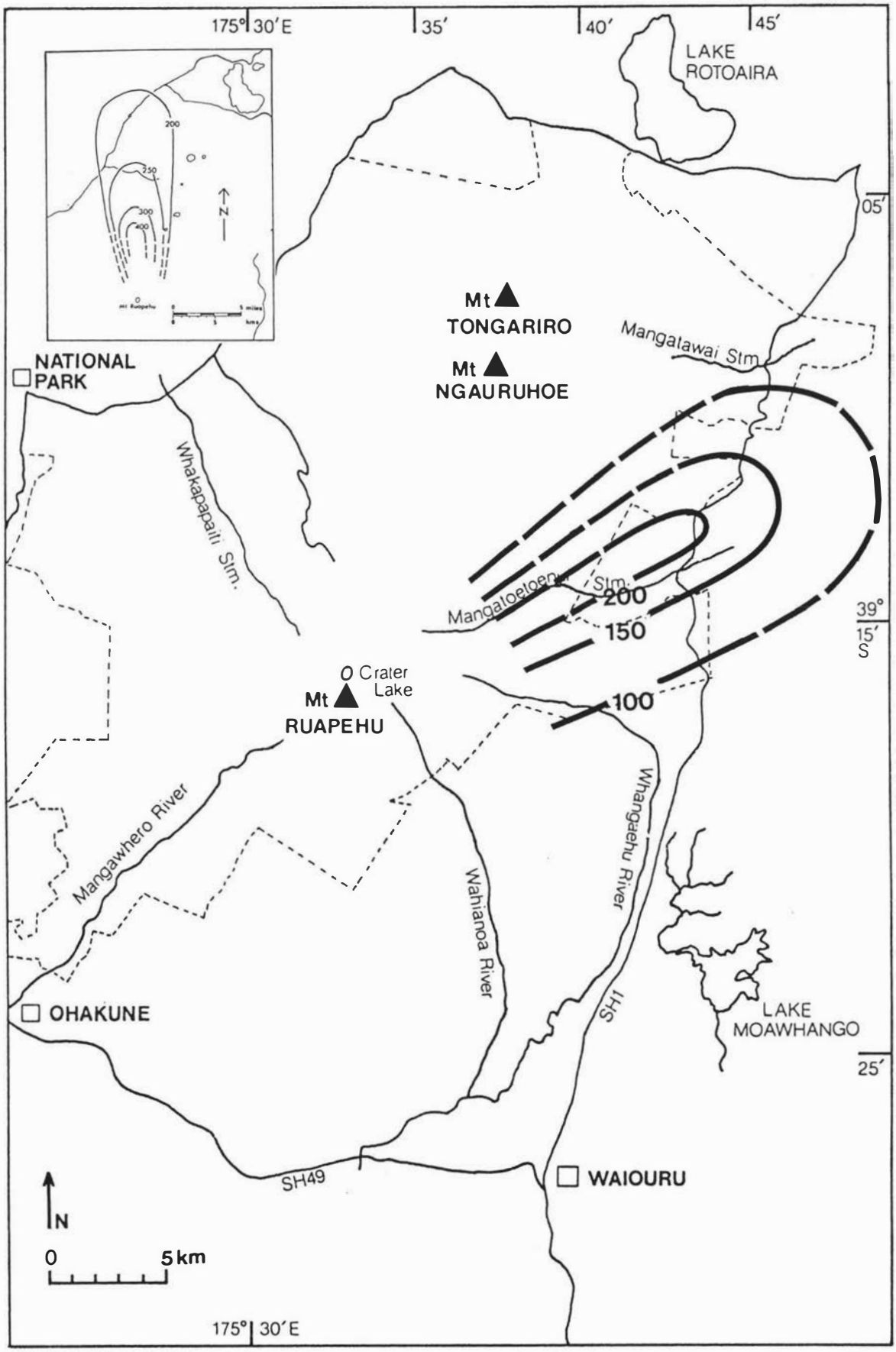

Figure 3.15 Partial isopach map of Pourahu Member [tephra unit] (all measurements are in millimetres). Insert shows isopachs of Okupata Tephra (from Topping 1973).

Members L16 and L15

Bullot Formation members L16 and L15 are very similar in appearance, comprising dominantly strong brown vesicular angular pumice lapilli and distinctive dark grey and some red lithic lapilli. The two tephras are separated by a 0.07 m marker ash sequence (M_3) comprising bedded grey and yellow coarse ash. Member L16 underlies a second marker ash sequence (M_2), comprising bedded brown, black and yellow coarse ash and lapilli. Both tephras are distinctive because of their strong colours. They are correlated from their stratigraphic positions relative to the overlying and interbedded marker ash sequences. Both tephras are correlated at Desert Road S.10 and S.11, and Waikato Stream S.1. Member L16 is correlated at several other sections (Chart 3) where it is found overlying Waiohau Tephra.

From stratigraphic position, member L16 is presumed to be of equivalent age to Shawcroft Tephra member.

Shawcroft Tephra [Sh]

Description and Identification

The type section for Shawcroft Tephra Member is at Wahianoa Aqueduct S. [WA] [T20/435990]. Reference sections are designated at Whangaehu River S.1 [WR1] [T20/399954] and Helwan Quarry [HQ] [T20/408921] (Figure 3.2, p. 94; Chart 3).

At Wahianoa Aqueduct T.S. (Plate 2.20), Shawcroft Tephra is 0.14 m thick. It overlies a 0.08 m thick greasy sandy loam textured paleosol above Waiohau Tephra and is overlain by other Bullot Formation lapilli and ash beds. Here, Shawcroft Tephra comprises dominantly very dark grey fine lithic lapilli, and strong brown and brownish yellow fine pumice lapilli, with a distinctive 30 mm basal bed comprising strong brown fine and very fine pumice lapilli. The upper and lower contacts of this member are sharp and smooth.

At the reference sections (Plate 3.22; Plate 3.23) Shawcroft Tephra is readily identified by its field characteristics and stratigraphic position to Waiohau Tephra. It is distinguished from all other Bullot Formation tephras by its distinctive colouring and strong brown pumice-rich base. At all sites it is of lapilli grade. It is also well exposed at Waiouru tip, and a section on Shawcroft Road [T20/385937], from where the tephra takes its name.

The Bullot Formation lapilli and ash beds enclosing Shawcroft Tephra at its type section (Wahianoa Aqueduct S.) have not been correlated with recognised members at Bullot Track S.1 (type section for Bullot Formation) due to the absence of sections occurring between these sites. Neither Shawcroft Tephra nor the underlying Waiohau Tephra are recognised at the type section of Bullot Formation. The stratigraphic position of Waiohau Tephra has, however, been provisionally placed at the base of Bullot Formation member L16 by correlation

of Bullot Formation tephras at sites within Rangipo Desert (where Waiohau Tephra is identified) with members at the type section. Shawcroft Tephra is therefore assumed to be of approximately equivalent age to member L16 (Chart 3), and is relative-age dated at *c.* 11 000 years B.P.

Distribution

Shawcroft Tephra is recognised only in more southern sections within the Mt Ruapehu region, along the Desert Road and within Karioi State Forest. It has not been identified in any section north of Wahianoa Aqueduct T.S. Partial isopachs (Figure 3.16, p. 143) indicate a dispersal axis to the southeast.

Significance

Shawcroft Tephra is an excellent andesitic marker bed within the study area. It is readily identified by its field appearance, and its stratigraphic position to Waiohau Tephra. Shawcroft Tephra provides a *c.* 11 000 years B.P. time plane useful to the dating of other andesitic tephra members of Bullot Formation and Tangatu Formation hyperconcentrated flood flow and debris flow deposits preserved in the study area. Its restricted dispersal, however, limits its use as a regional marker bed.

Members L14 and L13

At the type section, member L14, which is 0.09 m thick, and member L13, which is 0.19 m thick, comprise ungraded strong brown pumice, and black lithic lapilli. They are separated by 0.10 m of yellowish brown and purplish black coarse ash and lapilli. Member L13 overlies a thin 0.05 m purplish black ash above member L12. These two tephras do not show diagnostic field characteristics useful for correlation, but the purplish black ash beds have potential for future correlation. Presently, member L14 is correlated only to the proximal sites at Desert Road S.10 and S.11, and Waikato Stream S.1 (Chart 3). Few Bullot Formation tephras older than member L16 are exposed in sections throughout the Mt Ruapehu region.

Members L12 and L11

At Bullot Track type section, member L11 is 0.11 m thick. It overlies 0.12 m of unnamed lapilli and ash above member L10, and is overlain by 0.71 m of unnamed lapilli and ash beds below member L12. This tephra comprises dark greyish brown fine and medium pumice lapilli and black lithic lapilli. It is provisionally correlated as far as Desert Road S.11 based on stratigraphic position.

Member L12 also comprises dark greyish brown fine pumice lapilli with black lithic lapilli and is very similar in appearance to member L11. These two tephras are distinguished from enclosing lapilli by their colour, but otherwise do not show diagnostic field characteristics useful for correlation.

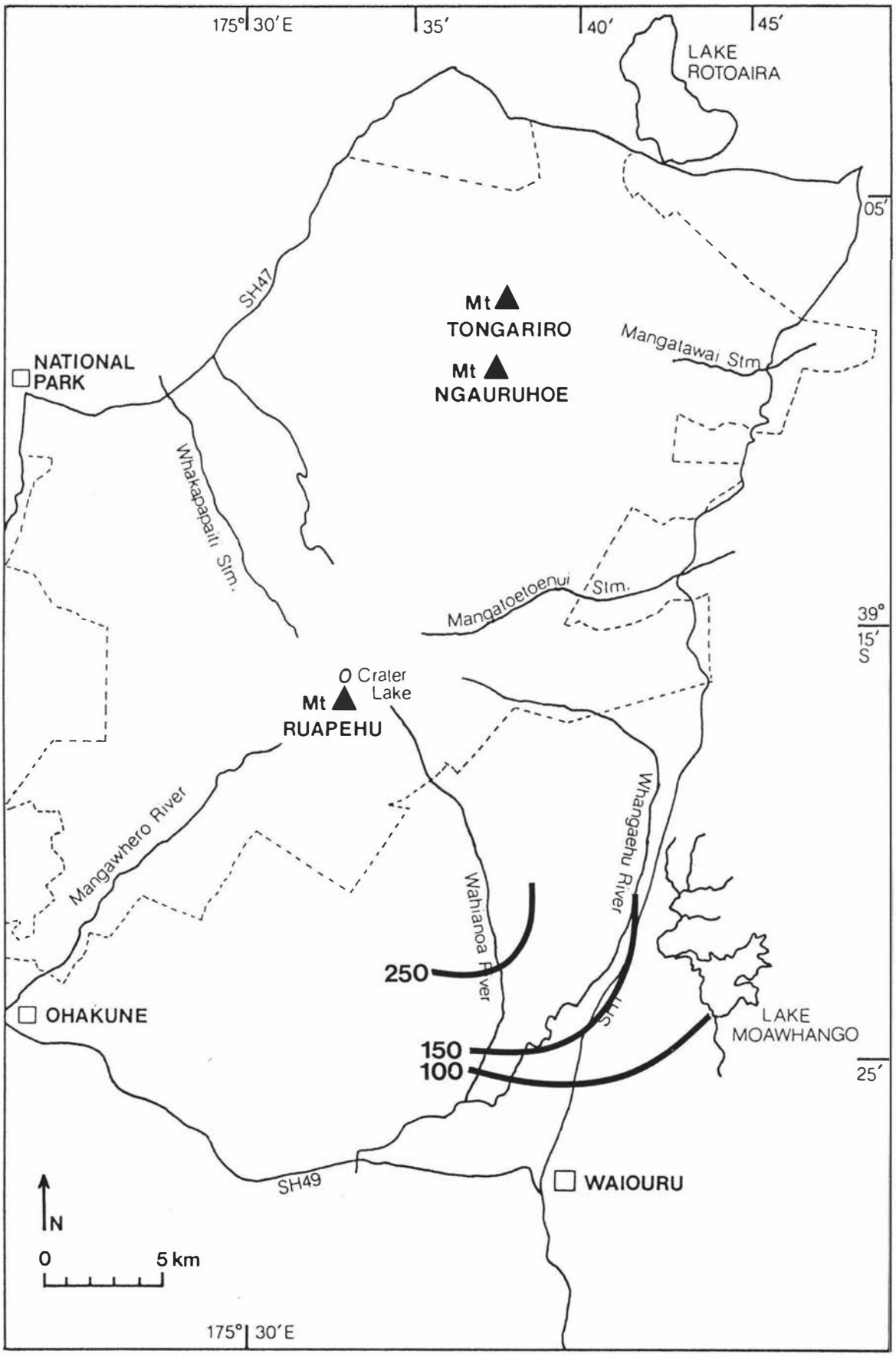

Figure 3.16 Partial isopach map of Shawcroft Tephra member of Bullot Formation (all measurements are in millimetres).

Members L10, L9 and L8

Members L10, L9 and L8 are all very similar in appearance and colour, and may represent separate beds within one eruptive unit. They are, however, described and sampled as three separate units. Together they occupy a thickness of 0.48 m. Member L10 occurs 0.12 m below member L11, and member L8 occurs *c.* 0.60 m above Rerewhakaaitu Tephra. Each member comprises light olive brown vesicular pumice lapilli and black lithic lapilli. Pumice in the lowermost unit, member L8, is more weathered and very soft. Its bulk rock composition (determined for pumice lapilli only) is andesite (54.3% SiO_2, Appendix IIIh). These three units are distinguished from all other tephras in the section by their pale colour (Plate 3.14), and are provisionally correlated as far south as Tufa Trig S.2 (Chart 3).

Middle Bullot Formation Tephras

Member L7

At the type section member L7, which is 0.18 m thick, overlies 10 mm of black coarse ash above member L6 (pink lapilli), and underlies 0.61 m of unnamed lapilli and ash beds below the rhyolitic Rerewhakaaitu Tephra (dated at *c.* 14 700 years B.P.). Here, member L7 comprises black angular lithic and yellowish brown fine and very fine pumiceous lapilli. It is distinguished from enclosing tephras by its distinctly lithic dominant composition. This member is provisionally correlated as far as Desert Road S.10 and Whangaehu Junction. Few sites within the Mt Ruapehu region expose Bullot Formation tephras which are older than Rerewhakaaitu Tephra (middle and lower Bullot Formation tephras) thus restricting local and regional correlation of member L7 and older tephras (members L6–L1) in the formation.

Member L6 (Pink Lapilli)

At the type section, member L6 (pink lapilli) is 0.14 m thick. It overlies 0.67 m of unnamed lapilli and ash beds above member L5, and is overlain by member L7, being separated from it by 10 mm of black coarse ash. The tephra occurs 0.80 m below Rerewhakaaitu Tephra.

Member L6 comprises pinkish grey to pale brown and pale yellow very vesicular, firm angular fine and very fine pumice lapilli and coarse ash, and few black lithic lapilli. It is distinguished from all other Bullot Formation tephras by its distinctive pink coloration.

Member L5

At the type section, member L5 is 0.10 m thick. It overlies 0.13 m of lapilli and ash above member L4, and underlies 0.35 m of unnamed lapilli and ash beds below member L6

(pink lapilli). This tephra comprises brown to dark brown fine pumice lapilli and minor black scoria, in a coarse ash matrix. It is distinguished from other members in the section by its colour, and is provisionally correlated at Whangaehu River S.5 from stratigraphic position. This tephra has not been correlated into any other sections in which middle Bullot Formation tephras are exposed.

Member L4

At Bullot Track T.S., member L4 is 0.29 m thick. It overlies 0.38 m of unnamed ash and lapilli beds above a 1.80 m thick fluvial deposit over Okareka Tephra (dated at *c.* 17 000 years B.P.), and underlies 0.13 m of unnamed ash and lapilli below member L5. Member L4 comprises pale brown and light yellowish brown fine to coarse pumice lapilli and bombs, with black and grey very fine lithic lapilli. The unit shows weak normal grading, with sharp and distinct contacts. Here member L4 is distinguished from other members of Bullot Formation in the section by its comparative thickness, coarser grain size, colour and relative stratigraphic position to the underlying Okareka Tephra. At the southern end of the exposure where the 1.80 m fluvial sands pinch out, member L4 closely overlies Okareka Tephra (Plate 2.23). Although this member is distinct at the type section, it has not been correlated at other sections. An age close to *c.* 17 000 years B.P. is indicated for this member, based on the age of Okareka Tephra.

Lower Bullot Formation

Member L3 (Hokey Pokey Lapilli)

At the type section, member L3 (hokey pokey lapilli) is 0.23 m thick. It overlies 0.99 m of fluvial sands and pumice beds above member L2 (Plate 3.14), and underlies Okareka Tephra (Plate 2.23), being separated from it by 0.09 m of coarse sandy ash. Member L3 comprises ungraded yellowish brown, yellowish red and very dark greyish brown pumice lapilli and blocks, with some black scoria lapilli and occasional white hydrothermally altered lithic lapilli. Contacts are distinct and sharp. It is the most prominent tephra in the formation, and is distinguished from all other members in the section by its strong brown colour and coarse grain size (Plate 3.14).

Member L3 is identified in sections in the northern Rangipo Desert (in the vicinity of Bullot Track) where the base of the formation is exposed. It is, however, not identified in proximal sections (Desert Road S.10 and S.11, Waikato Stream S.1 and S.2) from where it has most probably been eroded.

Member L2

Member L2, which is 0.27 m thick overlies member L1 (green ash) and underlies fluvial deposits below member L3. Member L2 comprises light olive brown and brown fine to coarse pumice lapilli with a distinctive black coarse ash matrix. Although this lapilli is a prominent unit at the type section, it has not been identified in reference sections on the Desert Road (Desert Road S.10, Waikato Stream S.2) where the base of the formation is exposed.

Member L1 (Green Ash)

At the type section, member L1 (green ash) is 0.22 mm thick. It overlies 0.48 m of unnamed andesitic lapilli and ash beds above Kawakawa Tephra Formation, and underlies member L2. It comprises pale greenish grey and yellow bedded coarse ash and very fine lapilli. Colour and bedding distinguish it from other Bullot Formation tephras and it is therefore a useful marker bed within the formation.

Member L1 is also recognised at Waikato Stream S.2 [T20/469102], where it is 0.15 m thick and occurs 0.60 m above Kawakawa Tephra Formation (Chart 3).

Distribution

Bullot Formation tephras are thickest and most numerous in sections east of Mt Ruapehu, indicating principal distribution to the east. They form the greater part of the tephra cover throughout the Mt Ruapehu region and are best exposed in the more northern sections of Rangipo Desert, and along the Whangaehu escarpment where they mantle late Pleistocene deposits of Te Heuheu Formation.

In the southern part of the study area, only tephras of the youngest 'upper unit' are preserved. At Wahianoa Aqueduct R.S. [T20/435990], these tephras overlie Rerewhakaaitu Tephra and andesitic diamictons of Te Heuheu Formation (dated *c.* > 22 500 – 14 700 years B.P.). A strong southeasterly dispersal axis is indicated for Shawcroft Tephra and the Ngamatea lapilli members which are identified only in sections south of the type section.

Few sections north of the type section expose tephras older than Mangamate Tephra, and therefore interpretation of the thickness – distribution of Bullot Formation tephras at more distal sites is difficult. The total thickness of Bullot Formation thins rapidly to the north (Chart 3), and it is therefore unlikely that many of these tephras would occur as distinct units north of the Mt Tongariro ring plain. Bullot Formation tephras have not been identified in lakes within the Waikato region where other TgVC tephras (Okupata Tephra, Rotoaira Lapilli, Mangamate Tephra) have been identified by Lowe (1988a). It is probable that many of the Bullot Formation tephras older than Rotoaira Lapilli (*c.* 13 800 years B.P.), are missing in sections on the Mt Tongariro ring plain as a result of the erosion prevalent during Ohakean time. Here, Ohakean erosion is marked by Hinuera Formation deposits overlying Kawakawa

Tephra Formation and below Rotoaira Lapilli (dated [NZ1559] at 13 800 ± 300 years B.P.) (Topping 1973). In fact, Rotoaira Lapilli is the first tephra within the Mt Tongariro region identified as conformable with the present-day post-erosion surface (Topping 1973). In the Mt Ruapehu region, occurrence of fluvial deposits above Kawakawa Tephra Formation, and the marked change at *c.* 14 700 years B.P. from a stratigraphy dominated by andesitic diamictons to one dominated by primary tephras, probably reflects this change.

Significance

Bullot Formation tephras constitute the greater part of the andesitic tephra record on the Mt Ruapehu ring plain. This formation defines the base of the Tukino Subgroup. Together with the interbedded rhyolitic tephras, Bullot Formation tephras are used to date locally exposed debris flow and fluvial deposits preserved on the southeastern Mt Ruapehu ring plain, and their respective geomorphic surfaces. Additional age constraints are also provided for the Rangataua Lava Flow (see section 6.1). Bullot Formation tephras are potentially important marker beds for the dating of tephra and lahar deposits in northern and western areas of Mt Ruapehu ring plain.

Correlation of Bullot Formation Tephras

The field identification and correlation of tephras relies upon the recognition of diagnostic characteristics of each individual tephra, or of the enclosing deposits. The colour, thickness, grain size and bedding characteristics of tephras when used in conjunction with their relative stratigraphic positions to known marker beds may be sufficiently distinct to allow their correlation.

Attempts at correlating andesitic tephras within Bullot Formation have met with varied success because few tephras possess sufficiently diagnostic characteristics to permit either their correlation by field properties alone, or to serve as stratigraphic markers within the 22 500 – 10 000 years B.P. tephra sequence.

Use of field colour as a means of correlation is limited because of the similarity in colour of most tephras, and is further complicated by observed changes in lapilli colour as a function of site hydrology. Pumice lapilli within the andesitic tephras are typically iron-stained to strong brown and yellowish brown colours. Tephra colours are more intense in Desert Road sections where many of the exposures are shaded and do not dry out over the summer. Gelatinous iron oxide deposits are common on the exposed tephra surfaces at these sites. Strong iron-staining and other weathering products can also mask the physical attributes of the pumice and lithic lapilli (*e.g.* colour-banding in Mangamate tephras) which would otherwise be useful to their field identification and correlation. Contacts between units are mostly gradational and difficult to define, and are not necessarily indicated by changes in grain size. Use of grain size to distinguish between units representing single eruptive events and therefore to identify member boundaries is difficult. There is little marked variation in grain size between lapilli

units, and thus the use of grain size for correlation is also limited. Most units comprise fine and medium lapilli and only those tephras which show exceptional relative grain size (*e.g.* those which contain blocks or bombs) can be reliably correlated on grain size alone. Similarly, there is little marked variation in the thickness of individual Bullot Formation tephras, with only a few members clearly separable on thickness basis alone. At sites east of the type section, however, the relative thickness of tephras can be used to support correlation between the major units. Other characteristics, such as bedding and grading within individual lapilli units, may support correlation. Most lapilli layers within the formation are, however, ungraded and show no distinctive bedding features. Only those members described above, are distinguished from other tephras at the type or reference sections, by their combined field characteristics of colour, thickness, and grain size. These 23 members constitute local marker beds within the *c.* 22 500 – 10 000 years B.P. sequence. Their correlation is dependent upon recognition of field characteristics and stratigraphic positions with respect to regional rhyolitic tephra marker beds sourced from TVC and OVC.

At the type section for the Bullot Formation, only two rhyolitic tephras, Okareka Tephra and Rerewhakaaitu Tephra, are found interbedded, providing *c.* 17 000 and 14 700 years B.P. time planes. The younger Waiohau Tephra (*c.* 11 250 years B.P. [NZ568]) is identified in sections to the south but is not found at the type section. The stratigraphic position of Waiohau Tephra is provisionally placed at the base of member L16 based on andesitic tephra correlations.

Where present, paleosols, peats, sedimentary deposits and erosion breaks are also valuable marker beds or marker horizons. At the type section, the only recognised erosion break in Bullot Formation occurs near the base of the formation and is marked by a 1.8 m thick fluvial unit (Plate 3.14). There are no interbedded paleosols by which the formation can be subdivided into members, and no recognised dateable material by which members can be dated. Commonly tephra formations and members are defined at the contact with paleosols (Vucetich and Pullar 1969; Kohn and Neall 1973; Vucetich and Pullar 1973). Paleosols, however, are more useful in rhyolitic terrains where eruptions are less frequent and there is sufficient time between eruptions for paleosols to form.

Rotoaira Lapilli, erupted from Mt Tongariro, and dated [NZ1559] at 13 800 ± 300 years B.P. is a prominent marker bed in the Mt Tongariro region and has been correlated as far south as Mangatawai S. [T19/489238] by Topping (1973). In this study, attempts were made to correlate Rotoaira Lapilli further south to the Bullot Formation type section, so that it could be used as a marker bed within the Bullot Formation tephra sequence. There are, however, no sections between Mangatawai S. and the type section which are deep enough to expose Rotoaira Lapilli and older tephras. Therefore Rotoaira Lapilli has not been correlated into tephra sequences on the Mt Ruapehu ring plain. It is also not identified within the Bullot Formation tephra sequence on mineralogical criteria (see section 4.4).

The ability to correlate individual Bullot Formation tephras near to source by detailed mapping is limited by the multiplicity of units, the small number of sections exposing a near complete stratigraphy, and the limited consistent exposure of the tephras between sites. The principle of correlating groups of tephra rather than individual units, where field characteristics of individual tephras are not distinctive, was used by Crandell and Mullineaux (1973), Mullineaux *et al.* (1975), and Mullineaux (1986) at Mt St Helens, where tephras were grouped into tephra sets based on field relations, phenocryst assemblages and radiocarbon age; with each set comprising a number of individual tephra layers. Few of the layers are individually distinctive enough to be correlated between sites on field characteristics, however most were identifiable as a part of a set (Mullineaux *et al.* 1975), with tephra sets identified in the field by colour, composition, grain size and stratigraphic position (Mullineaux 1986).

Using a similar principle, the field appearances and properties of tephra parcels and marker ash sequences within Bullot Formation, rather than just those of individual units and their boundary criteria, have proven useful to the correlation of some members within the formation.

At present none of the Bullot Formation tephras have been radiocarbon dated due to the absence of interbedded organic materials. Opportunity for the dating of these tephras and subsequent correlation by age is greater at sites distal to the type section *e.g.* Wahianoa Aqueduct [T20/435990] where the full stratigraphy is not preserved and lapilli units are separated by ash and medial units with some degree of paleosol development. Correlations between members of Bullot Formation and interbedded rhyolitic tephras provide the most ready means of age determination (Chart 1; Chart 3). Most correlations are between members of the upper Bullot Formation, which date between *c.* 14 700 and *c.* 10 000 years B.P. No single section records the complete Bullot Formation stratigraphy.

In sections north of the type section (Desert Road S.10, Waikato Stream S.1 and S.2 to Bullot Track T.S.), four Bullot Formation members (L17–L14), are correlated from field appearance and stratigraphic position. Marker ash sequence M_1 and tephra parcels comprising multiple black coarse ash beds provide additional stratigraphic control on member correlations. At these sites, Pourahu Member [tephra unit] is the uppermost Bullot Formation member present and identifies the top of the formation. The basal contact of the formation with the rhyolitic Kawakawa Tephra Formation is seen only at these sites. In sections south of the type section (Wahianoa Aqueduct S. to Helwan S.2), a number of lapilli units are recognised above Pourahu Member [tephra unit] that are not seen in the more northern sections. The uppermost of these tephras (Ngamatea lapilli-2 and -1, and Shawcroft Tephra) are correlated between sites only in the southern areas of the Mt Ruapehu ring plain.

Several correlations are established between sites located on the Whangaehu escarpment and sections within Rangipo Desert (*e.g.* Whangaehu Junction, The Chute S.3). At most of these sites only tephras of the upper Bullot Formation are present because

surfaces on which the sections rest are younger than 15 000 years B.P. Many of the members described from the type section are not recognised at these southern sites, with principal tephras being separated by medial units showing weak soil development.

Marker ash sequences M_1 and M_2, Shawcroft Tephra, members L16, L17, Ngamatea lapilli-1 and Pourahu Member, and the rhyolitic Waiohau and Rerewhakaaitu tephras are key marker beds to the establishment of a stratigraphy and chronology of Bullot Formation tephras, and to their correlation across the Mt Ruapehu ring plain.

Deposition and Erosion of Bullot Formation Tephras

Deposition

Tephras of the Bullot Formation were deposited over a *c.* 12 500 year period. The formation comprises a distinctive sequence of horizontally bedded airfall lapilli and ash beds, which form a major constructional surface on the southeastern Mt Ruapehu ring plain between *c.* 1100 m and 1200 m a.s.l. This surface is a prominent feature within the western and northern areas of Rangipo Desert (Plate 3.24), particularly in the vicinity of Bullot Track.

Most of the tephras were deposited between *c.* 14 700 and *c.* 10 000 years B.P.. These tephras comprise the upper Bullot Formation, and are the most widely preserved tephras of the formation. The deposition of the middle and lower Bullot Formation tephras (between *c.* 17 000 – 14 000 years B.P., and *c.* 22 500 – 17 000 years B.P., respectively) however, coincided with the maximum cold phase of the Last Glacial (*c.* 20 000 – 14 000 years B.P.). During this period tephra surfaces on the lower ring plain were most probably poorly vegetated (as implied by the absence of interbedded paleosols within the formation) and subject to erosion. The physical characteristics of the lapilli, the frequency of their eruption, and the cold climate would have inhibited the colonisation of Bullot Formation surfaces by plants. Even today the Bullot Formation surfaces are sparsely vegetated, with most of the present-day vegetation restricted to surfaces where the cover bed stratigraphy (Papakai Formation, Mangatawai Tephra, Tufa Trig Formation tephras and aeolian Makahikatoa Sands) has not been completely eroded.

Erosion

At Desert Road S.10 there is an erosion break just above Kawakawa Tephra Formation. It is identified by the presence of reworked Kawakawa Tephra Formation and thin fluvial deposits on primary Oruanui Ignimbrite. This erosion break identifies a regional erosion episode which occurred within TgVC between *c.* 22 500 and *c.* 14 700 years B.P. The unconformity is identified in a number of sections in the Mt Ruapehu region. In the north of the study area it is identified by the presence of interbedded sands, andesitic diamictons and reworked Kawakawa Tephra Formation above Primary Kawakawa Tephra. At more southern

sites (where Kawakawa Tephra Formation is not preserved) the unconformity occurs below Rerewhakaaitu Tephra. At these sites, Rerewhakaaitu Tephra is the first conformable rhyolitic tephra found overlying andesitic diamictons. The deposition of the diamictons identifies a major and prolonged period of instability on the Mt Ruapehu ring plain, and is coincident with the deposition of Hinuera Formation sediments in the Mt Tongariro and Waikato regions.

There are no other regional erosion episodes recorded within Bullot Formation time (*c.* 22 500 – 10 000 years B.P.). Other unconformities within the late Pleistocene stratigraphy, marked either by the absence of lower Bullot Formation marker beds at some sites, or fluvial and debris flow deposits found interbedded with lower and middle Bullot Formation tephras, record only localised erosion events on the Mt Ruapehu ring plain.

Summary Stratigraphy and Chronology of Andesitic and Rhyolitic Tephras of the Southeastern Mt Ruapehu Ring Plain

The stratigraphy and chronology of andesitic and rhyolitic tephras preserved on the southeastern Mt Ruapehu ring plain is shown in Table 3.1 (p. 90).

Fourteen rhyolitic tephras from TVC and OVC (Kaharoa Tephra, Taupo Pumice, Mapara Tephra, Waimihia Tephra, Hinemaiaia Tephra, Whakatane Tephra, Motutere Tephra, Poronui Tephra, Karapiti Tephra, Waiohau Tephra, ?Rotorua Tephra, Rerewhakaaitu Tephra, Okareka Tephra and Kawakawa Tephra Formation) are found interbedded with seven andesitic formations (Ngauruhoe Formation, Tufa Trig Formation, Mangatawai Tephra, Papakai Formation, Mangamate Tephra, Pahoka Tephra, Bullot Formation), sourced from Mt Ruapehu, Mt Tongariro and Mt Ngauruhoe.

The chronology of the andesitic tephras is determined principally from the radiocarbon ages of the interbedded rhyolitic tephras. Radiocarbon ages obtained on the andesitic Mangatawai Tephra [NZ186] (Fergusson and Rafter 1959), Te Rato Lapilli [NZ1372] and Rotoaira Lapilli [NZ1559] (Topping 1973), and new dates obtained on Tufa Trig Formation member Tf5 [Wk1488, Wk1489] provide additional control.

There are three distinct periods of tephra deposition from Mt Ruapehu. The most recent period is represented by the eruption of the Holocene-aged Tufa Trig Formation (dated *c.* 1800 years B.P. to the present), which followed a *c.* 8000 year period dominated by activity from Mt Ngauruhoe and Mt Tongariro. Tufa Trig Formation tephras are the products of frequent, low magnitude, small volume eruptions. At the type locality the total thickness of the individual members is only 0.52 m. Tufa Trig Formation tephras contrast lithologically with tephras of the earliest eruptive period, represented by the late Pleistocene to Holocene-aged Bullot Formation (dated *c.* 22 500 – 10 000 years B.P.). Mt Ruapehu was most active during this period. Numerous lapilli and ash beds were deposited, which today form a > *c.* 11 m thick sequence on the southeastern ring plain.

A less significant period of eruptive activity occurred between *c.* 9700 – 2500 years B.P., during which time Papakai Formation, derived principally from eruptions at Mt Tongariro, was deposited. This activity followed an earlier (*c.* 10 000 – 9700 years B.P.) period of intense volcanism at Mt Tongariro, during which time the Pahoka and Mangamate tephras were deposited. Mt Ruapehu was relatively inactive during this period. Between *c.* 2500 and 1800 years B.P., most activity was from Mt Ngauruhoe which deposited the Mangatawai Tephra. Later intermittent activity from both Mt Tongariro and Mt Ngauruhoe is recorded in the Ngauruhoe Formation.

The relationship of the eruptive periods at Mt Ruapehu to other depositional and erosional events on the Mt Ruapehu ring plain is discussed in Chapter 5.

Regional Marker Beds

Rhyolitic Tephras

Within TgVC, tephras sourced from TVC tend to be more widespread, and are generally coarser grained than those sourced from the more distal OVC. The Holocene-aged Taupo Pumice, Waimihia Tephra, Hinemaiaia Tephra and Motutere Tephra, and the late Pleistocene-aged Waiohau Tephra, Rerewhakaaitu Tephra and Kawakawa Tephra Formation are the most widespread rhyolitic tephras identified within the study area. Rhyolitic tephras are identified in most sections to the southeast of Mt Ruapehu, but occur less frequently in the more southern of these sections. Taupo Pumice, Mapara Tephra, Waimihia Tephra, Hinemaiaia Tephra, Waiohau Tephra and Kawakawa Tephra Formation are identified south of Waiouru township, and are likely to be useful marker beds within the southern Mt Ruapehu region. The other rhyolitic tephras (Poronui Tephra, Karapiti Tephra, [TVC], Kaharoa Tephra, Rerewhakaaitu Tephra and Okareka Ash [OVC]) show very restricted occurrence in the study area, and might be expected to occur only as microscopic tephras in areas to the south.

To the north of Mt Ruapehu, few sections expose tephras older than *c.* 10 000 years B.P. and therefore late Pleistocene rhyolitic tephras from TVC and OVC are not often recognised. The younger Holocene tephras (Waimihia Tephra, Hinemaiaia Tephra, Motutere Tephra and Poronui Tephra) are, however, recognised in nearly all sections.

In western and northern areas of the Mt Ruapehu ring plain, both andesitic and rhyolitic tephras are poorly represented. The deposition of these tephras is strongly controlled by the prevailing westerly winds and therefore the most complete stratigraphy is recorded east of the volcanoes. Only Kawakawa Tephra Formation, Waiohau Tephra (previously ?Rotorua Ash, Topping and Kohn 1973), and Taupo Pumice have been identified on the western ring plain by Topping and Kohn (1973).

Andesitic Tephras

Within TgVC, Mangatawai Tephra, Papakai Formation, and Mangamate Tephra are the most widespread andesitic formations. On the Mt Ruapehu ring plain, Tufa Trig Formation, Papakai Formation, Mangamate Tephra and Bullot Formation are the dominant formations.

Few tephras erupted from either Mt Ruapehu or Mt Tongariro have been directed to the south. It is therefore unlikely that many of these tephras will occur macroscopically or be useful as marker beds within the tephra and loess cover beds south of the study area. Only Papakai Formation and Bullot Formation members Shawcroft Tephra and Ngamatea lapilli-1 and -2 (which show a more southerly dispersal) are likely to be useful as marker beds.

Mangamate Tephra members are particularly useful marker beds east and north of Mt Ruapehu, but based on their thickness distribution they are unlikely to be preserved as macroscopic tephra further south than presently recognised. Poutu Lapilli Member is presently identified to within a few kilometres north of Waiouru Township. Mangamate Formation is recognised in sections west of Mt Tongariro by Topping (1973), but individual members are not identified.

The lack of diagnostic field characteristics of most Bullot Formation tephras presents problems in their correlation to areas further north, south and west of the study area. The identification of members, especially at more distal sites will rely on both field and laboratory based fingerprinting methods and the identification of distal interbedded rhyolitic tephras.

Distal andesitic tephras erupted from Mt Ruapehu have been recognised in peat swamps of the Kaimanawa Range, east of Mt Ruapehu (Froggatt and Rodgers 1990), in the Waikato lakes region (Lowe 1988a) and in the southern Mt Ruapehu region at Lake Surprise (Steel 1989).

On the southern Mt Ruapehu ring plain, peat swamps offer perhaps the best opportunity for establishing the stratigraphy and chronology of distal Holocene and late Pleistocene rhyolitic tephras, and andesitic tephras of TgVC. The rhyolitic Mapara Tephra, Waimihia Tephra, Hinemaiaia Tephra and Waiohau Tephra, and members of the andesitic Tufa Trig Formation, which are not recognised in exposures south of Wahianoa Aqueduct, are preserved within peat at Ngamatea Swamp, just south of Waiouru (Chart 1, Chart 3).

CHAPTER FOUR
MINERALOGY AND CHEMISTRY OF TONGARIRO CENTRE TEPHRAS

Introduction

Andesitic tephras identified within the 22 500 – 0 years B.P. tephra sequence on the southeastern Mt Ruapehu ring plain are potentially important marker beds useful to the establishment of a local debris flow stratigraphy and chronology, and hence, an assessment of the types, frequency and magnitude of eruptions from Mt Ruapehu.

The identification of tephras has traditionally been achieved by recognition of field characteristics and stratigraphic position. Whilst this approach has been broadly successful, particularly with rhyolitic eruptives (Vucetich and Pullar 1969), more detailed examination of rhyolitic tephra sequences has shown that many tephras have very similar field appearances, and without stratigraphic control cannot be differentiated. As a consequence, increasingly more refined laboratory-based techniques were used (*e.g.* determination of ferromagnesian mineral assemblages, Fe-Ti oxide and glass chemistries) to fingerprint the tephras.

The identification of andesitic tephras similarly requires application of laboratory-based fingerprinting techniques to overcome the problems of their restricted distribution and their uniformity in field appearance. The identification and correlation of many of the andesitic tephras recognised within the *c.* 22 500 years B.P. stratigraphic record on the southeastern Mt Ruapehu ring plain is equivocal when based only on field characteristics and stratigraphic position. The mineralogical and chemical properties of the tephras were therefore examined in order to determine diagnostic features which could be employed as tools in identification and correlation. The laboratory-based studies included determination of ferromagnesian mineral assemblages, ferromagnesian mineral major element chemistry, and glass chemistry.

Analyses obtained from 23 andesitic tephras, dating between *c.* 22 500 years B.P. and the present form the first detailed mineralogical data base for near source andesitic tephras of TgVC, and provides in part, a basis for petrogenetic study of eruptive mechanisms at TgVC.

The first part of this chapter reviews earlier work relating to the mineralogy and chemistry of TgVC andesitic tephras, and methods used by earlier workers to identify andesitic tephras. The second section details aspects of the mineralogy and chemistry of andesitic marker beds erupted from Mt Ruapehu and Mt Tongariro, determined for purposes of correlating tephras within the study area, and regionally within TgVC.

Later sections discuss changes in the mineralogy and chemistry of TgVC eruptives with time.

4.1 Previous work: Mineralogy and Chemistry of Tongariro Volcanic Centre Tephras

Little definitive work has been done on the ferromagnesian mineralogy of near source TgVC andesitic tephras. Most published results relate to analyses of TgVC lavas.

Lavas of TgVC are typically porphyritic andesites characterised by phenocrysts of plagioclase, orthopyroxene, clinopyroxene, and less commonly, olivine. Hornblende is rare (Cole *et al.* 1986; Graham and Hackett 1987).

Most of the current tephra data has been derived from the study of distal TgVC andesitic tephras by Lowe *et al.* (1980) [Mangamate Tephra], Green and Lowe (1985) [Mangamate Tephra], Lowe and Hogg (1986) [Okupata Tephra], Lowe (1988a, 1988b) [Okupata Tephra, Mangamate Tephra, Rotoaira Lapilli], and Froggatt and Rodgers (1990) [uncorrelated tephra]. From this work, the ferromagnesian assemblage of TgVC tephras has been defined as comprising orthopyroxene + clinopyroxene ± olivine ± hornblende. Olivine is present in small amounts (Lowe *et al.* 1980; Lowe 1988b) and is characteristic of some TgVC tephras. Few tephras contain hornblende (Lowe 1988b; Wallace 1987). Topping (1974) noted occurrence of trace amounts of green brown hornblende in the lithic and pumice lapilli of Te Rato Lapilli Member of Mangamate Tephra.

Andesitic tephras from TgVC are high (15 – 25%) in heavy minerals and relatively low in Fe-Ti oxides (10%), Lowe (1988b, 1989). Augite abundance is commonly twice that of most rhyolitic tephras (Lowe and Hogg 1986). Fe-Ti oxides comprise mostly titanomagnetite with rare magnetite and ilmenite (Lowe 1988a).

4.2 Previous Work: Methods for Identifying Andesitic Tephras

Ferromagnesian Mineral Assemblage

Studies of andesitic tephras in New Zealand have shown that although ferromagnesian mineral assemblages can be used to distinguish tephras sourced from different volcanic centres (*e.g.* TgVC and EVC tephras), the similarity in andesite mineralogy exhibited by tephras derived from the same centre precludes the distinction of most tephras, and limits its use as a means of identifying and correlating individual tephras within a particular centre (Kohn and Neall 1973; Lowe 1987, 1988a; Wallace 1987).

In overseas studies, andesitic and dacitic tephras have been identified and correlated on the basis of distinctive ferromagnesian mineral assemblages (Mullineaux *et al.* 1972; Crandell and Mullineaux 1973; Mullineaux 1974; Smith and Leeman 1982; Riehle *et al.* 1990). Crandell and Mullineaux (1973), Mullineaux *et al.* (1975), Westgate (1977), and Mullineaux

(1986) were able to characterise and distinguish between tephra sets sourced from Mt St Helens Volcano (*e.g.* sets S, J, Y and W), and some tephra layers within these sets by differences in their ferromagnesian mineral assemblages. In a similar study, Mullineaux (1974) used ferromagnesian mineral assemblages and proportions of component minerals, especially hornblende and olivine, to distinguish tephra layers sourced from Mt Rainier, and to distinguish these from other distal tephra layers sourced from Mt St Helens. Smith and Leeman (1982) concluded that the most effective technique for distinguishing Mt St Helens tephras is the identification of ferromagnesian mineral assemblages. Riehle *et al.* (1990) used the proportion of amphibole to pyroxene, together with glass chemistry, to identify and correlate tephras of the Hayes Tephra Set, sourced from Hayes Volcano, Alaska.

Tephra Chemistry

(I) Bulk Chemical Methods

Bulk Tephra Composition

Early studies utilized bulk analysis methods as a means of chemically characterising andesitic tephras. The only presently published bulk chemical analyses of TgVC tephras are those of Topping (1974), and Kohn and Topping (1978). They determined the major and minor element compositions of pumice lapilli of three TgVC tephras (Rotoaira Lapilli, Pahoka Tephra [previously Pahoka lapilli of Topping 1974], Te Rato Lapilli) by X-ray fluorescence. Pumice lapilli within Te Rato Lapilli and Pahoka Tephra are dacitic in composition (63.47% and 63.10% SiO_2 respectively), while lithic lapilli in these tephras are andesitic (57.16% and 59.50% SiO_2 respectively) using the classification of Le Maitre (1984). Rotoaira Lapilli is of andesitic composition (58.99% SiO_2).

Fe-Ti Oxide Chemistry

Kohn (1970) introduced use of Fe-Ti oxide chemistry as a rapid means of identifying rhyolitic tephras. Later studies by Kohn (1973) and Kohn and Neall (1973) used titanomagnetite chemistry of andesitic tephras (determined by optical emission spectrography) to distinguish EVC and TgVC (Poutu Lapilli, Te Rato Lapilli, Rotoaira Lapilli) tephras. Vanadium, Mn, Ni and especially Cr were found to be diagnostic elements. TgVC tephras were found to contain lower Mn contents but higher V, Ni, and distinctly higher Cr contents than the EVC tephras.

Topping (1974) and Kohn and Topping (1978) also used major element titanomagnetite chemistry to distinguish older (>10 000 years B.P.) and younger (<10 000 years B.P.) TgVC tephras and lavas, the latter having distinctly lower V, Cr, Ni, and Co abundances.

(II) Discrete Grain Methods

Electron Microprobe Analysis of Fe-Ti Oxides

Lowe (1987, 1988a) used the major element chemistry of titanomagnetites and ilmenites, determined by EMP analysis, to distinguish distal TgVC and EVC tephras. Lowe concluded that Cr and Mn abundances in titanomagnetites can be used as a reliable indicator of tephra source. However, no attempt has yet been made to distinguish individual eruptives. Lowe's findings support the earlier work of Kohn and Neall (1973) and Wallace (1987), and show TgVC tephras contain distinctly higher Cr and lower Mn contents, with Cr contents of EVC tephras mostly below detection limits.

Electron Microprobe Analysis of Ferromagnesian Minerals

The chemistry of ferromagnesian minerals (orthopyroxene, clinopyroxene, hornblende) from some distal TgVC and EVC tephras were determined by Lowe (1988a) in an attempt to distinguish tephra source. Lowe (1988a, 1988b) concluded that some tephras from these two volcanic centres were able to be distinguished by comparison of the calcium content of clinopyroxenes and magnesium content of orthopyroxenes. For most tephras however, pyroxene chemistries give inconclusive identification of source.

Wallace (1987) showed that it is possible to distinguish EVC tephras from those of the TVZ using Cr abundance in clinopyroxenes. TgVC and TVC tephras however cannot be distinguished on clinopyroxene chemistry.

Smith and Leeman (1982) investigated the potential for using the major element chemistry of ferromagnesian minerals extracted from pumice lapilli, to distinguish tephras from the same source (Mt St Helens) and different sources (Mt St Helens, Glacier Peak, Mt Mazama). The chemistry of hornblende phenocrysts and Fe-Ti oxides could be used to distinguish tephra sets W and Y, and tephra source. Individual layers within these sets were, however, not distinguished.

In New Zealand studies, the chemistry of ferromagnesian minerals has been used primarily to identify the source volcanic centre of distal tephras, and less so as a means of fingerprinting and correlating individual tephras from the same centre.

Electron Microprobe Analysis of Glass

Although EMP analysis of glass has proved useful in identifying rhyolitic tephra formations and their source centres (Froggatt 1982a, 1983; Wallace 1987; Lowe 1988a; Pillans 1988) little detailed work on the glass chemistry of andesitic tephras has been done. The use of glass chemistry as a means of distinguishing tephras sourced from the same

centre but different volcanoes (*e.g.* Mt Ruapehu *vs* Mt Tongariro) is yet to be evaluated for andesitic tephras. Recent overseas studies by Sarna-Wojcicki *et al.* (1981) showed that tephra layers erupted during the 1980 Mt St Helens eruption could be successfully distinguished from one another, and older Mt St Helens tephras, by both the major and minor element chemistry of their glasses. Riehle *et al.* (1990) used major element chemistry of glass to attempt correlation of distal and proximal tephra of the Hayes Tephra Set. Not all deposits however could be uniquely identified from glass chemistry.

Glass chemistry data previously available for TgVC tephras has been derived from the study of distal tephras, analysed for purposes of identifying tephra source (Lowe 1987, 1988a, 1988b, 1989; Stokes and Lowe 1988; Froggatt and Rodgers 1990). Glass of andesitic (56 – 63% SiO_2, Lowe 1988a) and rhyolitic composition has been identified. Glasses from TgVC tephras contain up to ten times as much FeO, CaO, TiO_2 and MgO as rhyolitic tephras, typical of a more basic affinity (Lowe 1988b).

Wallace (1987) showed that tephras from TVC and EVC can be clearly distinguished on the SiO_2 and alkali (Na_2O and K_2O) contents of their glasses. Similarly, Stokes and Lowe (1988) showed that the major element chemistry of glass shards from five late Quaternary volcanoes (Egmont, Mayor Island, Okataina, Taupo, Tongariro) are distinct, and therefore that the major element chemistry of the glasses could be used to distinguish between these sources.

Lowe (1988a) analysed glasses of distal tephras sourced from EVC and TgVC, and found EVC tephras more silicic with high K_2O contents, and rhyolitic – dacitic compositions. Lowe concluded that the TiO_2, FeO (total), MgO and CaO contents of glass shards could be used to distinguish tephras from each of the North Island volcanic centres.

Other Methods

Mullineaux (1974) used the refractive indexes of iron-magnesium minerals (olivines and hypersthenes), in preference to using both the refractive index of glass and whole rock analyses, to distinguish four tephra layers with similar ferromagnesian mineral assemblages, sourced from Mt Rainier.

Hodder and Wilson (1986) used refractive index in conjunction with mineral assemblages and glass chemistry, to successfully establish the stratigraphic relationships and provenance of the Tirau Ash and Mairoa Ash deposits of the Waikato and King Country districts.

Bogaard and Schmincke (1985) used the petrographic composition (glass:lithic:crystal ratios) of tephras, in conjunction with their major element glass chemistry to correlate distal Laacher See ash to source deposits derived from various eruptive phases.

4.3 Methods for Fingerprinting Andesitic Tephras of Tongariro Volcanic Centre

Most laboratory-based tephra studies within New Zealand have concentrated on the analysis of Central North Island (TVZ) rhyolitic tephras, with very few studies providing detailed mineralogical information on TVZ andesitic tephras. Most studies within the andesite centres have focused on the petrography and chemistry of near source lavas rather than tephras. Consequently, the suitability of the methods employed in the identification and correlation of TVZ rhyolitic tephras as means of distinguishing andesitic tephras is relatively unknown.

The methods selected to fingerprint andesitic tephras in this study (detailed below) are based on methods used in previous work, and involve detailed examination of the tephras both in the field and the laboratory, aiming where possible to identify tephras by the least complicated methods.

Basis of Laboratory identification

(I) Correlation with Formations and Members

(a) Physical Properties of Tephras

Physical attributes of tephras are frequently masked in the field situation by weathering products. Careful examination of the physical characteristics of the tephras in the laboratory, however, may identify features useful to the identification and correlation of the tephras when used in conjunction with field stratigraphic position.

(b) Tephra Composition

Distinct differences in lithology, reflected in the pumice and lithic contents of the tephras, provide additional criteria by which individual tephras may be identified and correlated.

(c) Ferromagnesian Mineral Assemblages

Differences in the type and abundance of ferromagnesian minerals in tephras may be sufficient to characterise and identify some tephras, when used in conjunction with field stratigraphy or other identifying criterion. Given that the tephras are andesites however, the mineralogy of most of the tephras is expected to be similar.

(d) Ferromagnesian Mineral Chemistry

Previous work suggests that tephras derived from different volcanic centres exhibit some differences in the chemical composition of pyroxenes, and more distinct differences in olivine and amphibole chemistries. Differences in the major element chemistry of these minerals may distinguish some tephras. In this study EMP analysis is selected as a means of determining the chemistry of ferromagnesian phenocrysts.

(e) Fe-Ti Oxide Chemistry

Determination of the major and minor element chemistry of Fe-Ti oxides is a popular fingerprinting method adopted in studies of both rhyolitic and andesitic tephras because Fe-Ti oxides occur in virtually all tephras (although generally in low concentrations in andesites), and have been shown to be stable during weathering (Aomine and Wada 1962; Ruxton 1968, *in* Kohn 1970). Subtle differences and changes in the composition of parent melts are reflected in the chemistry of Fe-Ti oxides (Kohn 1973). These differences may be used to fingerprint tephras. In this study EMP analysis is selected as a means of determining the chemistry of titanomagnetite phenocrysts.

(f) Glass Chemistry

The chemistry of groundmass glass in pumice lapilli may offer an opportunity for identifying chemical differences between andesitic tephras, in a similar manner to methods proven for rhyolitic tephras. However, rapid weathering, and the vesicularity and microlite content of most andesitic glasses, however, may restrict the use of this method in tephra fingerprinting.

Laboratory procedures used to fingerprint andesitic tephras are summarised in Figure 3.1 (p. 88)

Tephra Sampling

The surface of an outcrop was first cleaned off, then many small samples were taken along the exposure, sampling most of the depth of the deposit, but avoiding sampling at the very contacts of the deposits. Tephras were sampled at type and reference sections which best show the stratigraphic relationships of the tephra to other andesitic and rhyolitic tephras.

Most of the tephras erupted from Mt Ruapehu and Mt Tongariro are of fine lapilli and ash grade. Contacts between many of these tephra layers are indistinct. This, together with the virtual absence of interbedded paleosols in the thickest of tephra sequences makes definition of contacts difficult. In these instances, lapilli layers have been sampled from their central portions where characteristics such as colour and grain size appear most uniform (showing lateral and vertical continuity) and representative of the character of the tephra in the outcrop. This avoids the possibility of sampling across a contact, from layers of potentially different composition.

Sample Preparation

Cleaning Tephras

All tephras were cleaned to remove amorphous and crystalline oxides, ensuring pristine ferromagnesian minerals and glass for mounting, sectioning and polishing.

Tephras were cleaned using the acid oxalate extraction method of Tamm 1922, *in* Blakemore *et al.* (1987) in preference to the dithionite – citrate method of Blakemore *et al.* (1987). Cleaning with dithionite – citrate was found to cause significant etching of the soft pumice materials.

Methodology follows that outlined in section 2.3. Tephra samples were cleaned by washing in 0.2 M acid oxalate reagent (using a similar tephra:reagent ratio to that used in the cleaning rhyolitic tephras), and gently agitated in a reciprocal shaker overnight. An end-over-end shaker was not used as this caused severe attrition and disintegration of most pumice lapilli. Samples were thoroughly rinsed in distilled water and oven-dried in preparation for later mineralogical analysis.

Description of Tephras

Tephra samples were first examined in their field state for colour, lapilli types and dominance, angularity, and range in grain size. Cleaned pumice lapilli were optically examined and compared for colour, phenocryst types and abundance, vesicularity and strength. The proportions of component lapilli (pumice, scoria, lithics) and xenoliths in cleaned samples were quantitatively determined by counting a randomly selected population of at least 400 lapilli.

Ferromagnesian Mineral Extraction

Dry pumice lapilli were hand picked from cleaned subsamples and gently crushed using an agate mortar and pestle. Crushings were placed in a beaker of distilled water and agitated using a sonic probe to free phenocryst minerals. Samples were then washed into filter papers and dried prior to sieving. Samples were sieved following the procedure outlined in section 2.3.

Preparation of Samples for Mineralogical Analysis

Heavy Liquid Separation

The 0.063 – 0.250 mm (4 – 2 ϕ) fractions of each tephra were separated into heavy and light mineral fractions using sodium polytungstate heavy liquid, following the procedure outlined in section 2.3.

Following separation, the Fe-Ti oxides were concentrated by removal from the heavy mineral fraction. This was achieved by repeatedly passing a hand magnet over the tephra sample. By repeating the procedure a reasonably pure Fe-Ti oxide concentrate was obtained.

Preparation of Polished Thin Sections

Ferromagnesian minerals were mounted and sectioned following the procedure outlined in section 2.3. Samples of the relatively unweathered cores of pumice lapilli required for glass analysis were impregnated with resin and sectioned before mounting.

Determining Ferromagnesian Mineral Assemblages

Methodology follows that outlined in section 2.3.

Electron Microprobe Analysis of Ferromagnesian Minerals

The chemistry of these minerals was determined using the fully automated JEOL JXA733 superprobe housed in the Analytical Facility, Research School of Earth Sciences, Victoria University. Analysis methodology follows that of Froggatt (1982a, 1983) and Froggatt and Gosson (1982).

Oxides measured were SiO_2, TiO_2, Al_2O_3, FeO, MnO, MgO, CaO, Na_2O, K_2O, NiO, and Cr_2O_3. Analysis of phenocryst cores and rims, and use of back-scatter electron imagery were undertaken to detect any compositional zoning not always apparent in the optical examination of phenocrysts.

Values below the detection limit are tagged with an asterisk in tabled results (Appendix III), and are not included in the calculation of the means and standard deviations.

Instrument Settings

Instrument settings used in the analysis of mineral standards and samples (shown below) differed from those used for analysis of rhyolitic glass. Peak search analysis of standards (Springwater olivine and Engels amphibole) provided a check on probe performance.

Beam diameter	3 μm
Probe current	12 na (nanoamps at 15kV)
Count Time	3 x 10 second peak count; 1 x 10 second background count

Electron Microprobe Analysis of Glass

Pumice lapilli, and glass fragments (vitric pyroclasts and shards) were mounted and prepared as polished thin sections for analysis by electron microprobe. The analysis procedure and instrument settings follows that used for rhyolitic glass shards, and is outlined in section 2.3.

Presence of numerous vesicles and microlites within andesitic glasses makes analysis difficult. Samples were therefore viewed in transmitted light so that optically pure areas of glass, relatively free of microlites and inclusions could be analysed. Glassy selvedges on plagioclase and ferromagnesian minerals were also analysed in some tephras.

Elements measured were SiO_2, TiO_2, Al_2O_3, FeO, MnO, MgO, CaO, Na_2O, K_2O and Cl. MnO generally occurs in very minor amounts in rhyolitic tephras and is therefore not usually analysed. Andesitic tephras however contain greater amounts of Mn, warranting the inclusion of MnO in the analyses.

Scanning Electron Microscopy

Cleaned samples were inspected with a binocular microscope to distinguish glass, crystals and lithics. Individual grains from the 0.250 and 0.500 mm fractions were oriented and mounted on metal stubs for viewing under the scanning electron microscope [1].

4.4 Results and Discussion

Description of Hand Samples

Kohn and Neall (1973) attempted identification of EVC tephras by physical and optical methods but met with little success, and concluded that distinctive properties of glasses or phenocrysts were required to facilitate identification. Results of this study indicate that this is also true of most TgVC tephras. It is found, however, that the identification and subsequent correlation of some TgVC tephras can be achieved simply through the examination of hand samples.

Several characteristics observed in cleaned hand samples serve to distinguish tephras erupted from Mt Tongariro (excluding Rotoaira Lapilli) and those from Mt Ruapehu. The Mt Tongariro eruptives which comprise dark grey strongly angular lithic and scoriaceous lapilli, and only minor amounts of pale, poorly vesicular pumiceous lapilli, are distinguished by their darker colour, scoriaceous-dominant compositions, and comparatively finer grain size. Additional characteristics include colour-banded (grey and pale yellow) scoriaceous and pumiceous lapilli, not seen in airfall tephra samples from Mt Ruapehu.

Some tephras from Mt Ruapehu are distinguished by the colour of their pumice lapilli, but for the majority of tephras pumice colour is not a diagnostic criterion because non-compositional factors such as site hydrology and grain size are principal factors affecting the weathering and colour (exterior and interior) of lapilli.

---

[1] SEM analysis was performed by Mr D. Hopcroft, Electron Microscopy Laboratory, DSIR, Palmerston North.

The compositions of tephras erupted from Mt Tongariro and Mt Ruapehu have been compared using the component proportions (quantified) of pumiceous, lithic and scoriaceous lapilli in each of the tephras. Results are presented in Appendix IVa, and are inconclusive in distinguishing between formations, members and source, although high pumice, and scoriaceous contents tend to reflect sources at Mt Ruapehu and Mt Tongariro, respectively. The examination of hand samples is shown to be a more useful method of distinguishing source.

Optical examination of cleaned pumice and lithic lapilli using a binocular microscope was undertaken in an attempt to identify further distinguishing characteristics of the pyroclasts which may have been masked in the field situation by iron-staining or exterior coatings of ash.

The majority of pumice lapilli in TgVC tephras show uneven fracture surfaces and contain between 2% and 10% phenocrysts of pyroxene, feldspar, olivine and hornblende, and minor amounts of Fe-Ti oxides, which occur more commonly as microphenocrysts. Phenocryst content was estimated using the percentage estimate charts of Shvetsov (1954), reproduced in Terry and Chilingar (1955). Lithic types are variable, with most probably accessory, and of little apparent use in correlation. Within some tephras however, the presence of white, and colour-banded pumices, poorly vesicular pumice, accretionary lapilli, schist xenoliths, and phenocrysts of hornblende and olivine are diagnostic of the tephras in which they occur (Table 7.1, p. 314). The identification of such features attests the value of hand description in tephra identification studies.

Schist Xenoliths

Schist xenoliths have been identified within both the lithic fraction of Te Rato Lapilli and Poutu Lapilli members of Mangamate Tephra, and within the slightly older Pahoka Tephra, all of which were erupted from Mt Tongariro. The abundance of these xenoliths (expressed as a proportion of the lithic fraction) within the greater than 2 mm lapilli fraction of Te Rato Lapilli and Pahoka Tephra is shown in Table 4.1 (p. 165), and ranges between 19% and 44%. The schist xenoliths occur in only trace amounts in Poutu Lapilli.

These xenoliths are very fine grained, with distinct foliation. Some contain prominent cross-cutting quartz veins. They are distinct from the other predominantly andesitic lithics within the tephras.

The lithic xenoliths are upper crustal rocks, presumably related to Kaimanawa Schist. Occurrence of schist xenoliths within tephra deposits of TgVC therefore suggests an origin by entrainment of basement Kaimanawa Schist during magma ascension. The Kaimanawa Range lies directly east of Mt Ruapehu. The basement geology of the Kaimanawa Mountains has been mapped and described by Grindley (1960, 1965) as comprising two formations of

Table 4.1 Schist xenolith abundances in andesitic tephras, Tongariro Volcanic Centre, for >2 mm fraction.*

Tephra	Schist %	Lapilli Count	Section Location	Grid Reference †
Te Rato Lapilli	19	400	Poutu	[T19/481325]
Te Rato Lapilli	24	400	-	[T19/377351]
Pahoka Tephra	24	400	Access 10	[T19/536270]
Pahoka Tephra	23	400	Mangatawai	[T19/489328]
Pahoka Tephra bed (a)	19	324	Desert Road S.16	[T20/481186]
Pahoka Tephra bed (b)	27	400	Desert Road S.16	[T20/481186]
Pahoka Tephra bed (c)	44	500	Desert Road S.16	[T20/481186]
Pahoka Tephra	19	354	Oturere Trig S.1	[T19/488213]
Pahoka Tephra	35	400	Mangatoetoenui Quarry	[T20/459153]
Pahoka Tephra	32	400	Desert Road S.15	[T20/462135]

* Schist xenolith abundances expressed as percentages of the total lithic fraction.
† Grid references based on NZMS 260 topographical maps.

Mesozoic age – the Kaimanawa Greywacke and Kaimanawa Schist, also termed Mesozoic metagreywacke by Hackett (1985). Tertiary-aged marine sediments overlie this basement greywacke and are seen outcropping near Waiouru (Fleming and Steiner 1951). The greywacke basement occurs at a depth of approximately 3 km beneath Mt Ruapehu (Latter 1981a; Houghton *et al.* 1987).

Metamorphic xenoliths, derived from the subvolcanic basement (metaquartzites, hornfelses, biotite-plagioclase-spinel schists and gneiss, low-grade metagreywackes), are described as a common component in TgVC lavas (Hackett 1985; Graham 1987; Graham and Hackett 1987). The lithic xenoliths identified in Te Rato Lapilli and Pahoka Tephra are most probably equivalents of the low-grade metagreywacke xenoliths of Hackett (1985).

Significance

Metamorphic xenoliths have been identified only in tephras erupted from Mt Tongariro (Mangamate Tephra, Pahoka Tephra), and are therefore diagnostic of source. Their presence has been used to support correlation of Pahoka Tephra at more northern sections, and Mangamate Tephra at more southern sections in the study area (*e.g.* at Wahianoa Aqueduct R.S. [T20/435990] and a section on Paradise Valley Road [T20/494046].

Accretionary Lapilli

Accretionary lapilli, also termed pisolites or chalazoidites, are concentric ash aggregates which typically form by accretion of moist ash in concentric layers about a nucleus, and less commonly, by the rolling of lapilli nuclei over fresh ash surfaces or by the action of rain and

wind on newly fallen ash. They may be spherical, slightly roller shaped or flattened (Moore and Peck 1961; Fisher and Schmincke 1984; R. Schumacher, written comm. 1989).

Occurrence

Accretionary lapilli are found associated with tephra from highly explosive plinian and phreatomagmatic eruption clouds (in which large volumes of ash are injected into the atmosphere), and elutriation clouds associated with pyroclastic flow and surge deposits.They are also commonly associated with proximal fine grained ignimbrite (ash flow) and surge deposits, formed during transport and deposition (Swanson and Christiansen 1973; Schumacher and Schmincke, written comm. 1989).

Types of Lapilli

Accretionary lapilli differ in field relationships, internal structures, and grain-size characteristics depending upon their origin (Schumacher and Schmincke, written comm. 1989). The types of accretionary lapilli identified within tephra deposits and ignimbrites have been studied and classified by Schumacher, and Schumacher and Schmincke (written comm. 1989) Two morphologically different types are defined: rim-type and core-type. A third category, armoured lapilli, is defined by Waters and Fisher (1971).

Rim-type (R-type)

Rim-type lapilli comprise a coarse ash core surrounded by a densely packed fine grained rim. They are found associated with proximal fallout from elutriation clouds, ignimbrite and surge deposits. The fine grained rim may be internally graded, or made up of discontinuous alternating fine and very fine ash layers without a well defined core (multiple-rim lapilli) (Schumacher and Schmincke, written comm. 1989).

Core-type (C-type)

Core-type lapilli comprise a coarse ash core without a finer grade rim. They are mostly found associated with distal fallout (from eruption clouds), ignimbrite, tuff and surge deposits. Only C-type lapilli have been described from phreatomagmatic eruption clouds (R. Schumacher, written comm. 1989).

Armoured lapilli

Armoured lapilli are accretionary lapilli which contain a crystal, rock, or pumice fragment core, rather than ash, which is coated by rinds of fine to coarse ash (Waters and Fisher 1971). They are found associated with phreatomagmatic deposits (Lorenz 1974; Fisher and Schmincke 1984).

Lapilli in Mt Ruapehu Tephras

Accretionary lapilli have been identified within two tephra members of Bullot Formation (members L16 and L17). They occur in minor amounts and were identified within the ashy matrix of these lapilli units. They occur as fine pale brown spherical, and flattened balls, up to 5 mm in diameter. Flattened lapilli, composed entirely of ash, form upon the impact of the wet sticky balls of ash (Fisher and Schmincke 1984).

Some of these lapilli were mounted in epoxy resin and sectioned. Four different lapilli types were identified (Plate 4.1).

Type (a) Lapilli with a lithic or pumice fragment core, surrounded by ungraded accreted ash.

Type (b) Lapilli comprising concentric layers of coarse and fine ash.

Type (c) Lapilli with a coarse ash core grading to fine ash rim.

Type (d) Lapilli comprising poorly sorted ash without a distinct core. They also occur as flattened lapilli.

Using the classification of Schumacher, Schumacher and Schmincke, and Waters and Fisher (1971), type (a) can be classified as armoured lapilli, types (b) and (c) as R-type lapilli, and type (d) as C-type lapilli. Each lapilli type has been identified within both tephras, although types (a) and (d) are clearly dominant.

Both tephras are coarse pumiceous eruptives and are probably the products of plinian eruptions. The occurrence of both R- and C-type lapilli within these tephras is not diagnostic, *per se*, of an origin in a plinian eruption column, as both types, and armoured lapilli, are also recognised in base surge deposits of phreatomagmatic (hydrovolcanic) eruptions. Other field characteristics of these tephras, however, are inconsistent with a phreatomagmatic origin. The tephras mantle older tephra deposits and do not show antidune or cross-bedding sedimentary structures characteristic of ground or ash-cloud surge deposits (Crowe and Fisher 1973; Wright *et al.* 1980; Fisher and Schmincke 1984). The origin of the accretionary lapilli is therefore not known, but is most probably within a plinian eruption column. Dominance of rim-type lapilli would indicate proximal fallout, within only a few kilometres of the vent.

The significance of accretionary lapilli in these andesitic tephras is not presently understood as accretionary lapilli have previously only been reported within rhyolitic plinian deposits in New Zealand tephra studies (*e.g.* Kawakawa Tephra Formation, Self and Sparks 1978). If the lapilli in these andesitic tephras are products of a hydrovolcanic eruption phase, then their presence might suggest former existence of a crater lake *c.* 14 000 – 12 000 years B.P.

Accretionary lapilli have so far been identified only in these two Bullot Formation tephras. This has allowed correlation of one of them (member L16) from Bullot Track T.S. to Desert Road S.10, based on the presence of the accretionary lapilli and stratigraphic position.

Ferromagnesian Mineral Assemblages of Tongariro Volcanic Centre Tephras

The ferromagnesian mineral assemblages of 23 andesitic tephras sourced from both Mt Ruapehu and Mt Tongariro are presented in Table 4.2, p. 169. The error associated with these counts is discussed in section 2.3.

Ferromagnesian minerals have been identified by their optical properties and identification confirmed by electron microprobe analysis. For all tephras of lapilli grade, ferromagnesian minerals were extracted from pumice lapilli. The assemblages are therefore representative of the erupting magma and do not reflect post-depositional contamination as is often the case with determination of assemblages for ash grade tephras.

Mineral Assemblages

An assemblage representative of all TgVC tephras may be given as orthopyroxene + clinopyroxene ± olivine ± hornblende, and supports that defined by Lowe (1988a, 1989) and based on the mineralogy of distal tephras.

Results (Table 4.2, p. 169) show all tephras contain two pyroxenes. The variation in ferromagnesian mineral assemblages amongst TgVC tephras is defined by four assemblages.

(1) Orthopyroxene > Clinopyroxene
(2) Orthopyroxene > Clinopyroxene > ± Olivine ± Hornblende
(3) Olivine > Clinopyroxene >> Orthopyroxene ± Hornblende
(4) Hornblende >> Orthopyroxene > Clinopyroxene ± Olivine

Where present, olivine and hornblende phenocrysts are found concentrated in the <0.125 mm fraction, due to their overall smaller size and acicular habit. The larger pyroxene phenocrysts dominate the coarser fractions in which olivine and hornblende are generally found in only minor to trace amounts. The effect of this concentration of olivine and hornblende in the finer fractions is to produce lower apparent abundances of these minerals in the 2–3 ϕ fractions of the tephras. For example, 15% olivine is recorded in the 0.125–0.250 mm fraction of Poutu Lapilli (Table 4.2, p. 169). However, a grain mount of the 0.063–0.125 m fraction is almost pure olivine. Similarly in Bullot Formation member L3, olivine occurs in only trace amounts in the 0.125–0.250 mm fraction but comprises up to 24% of the 0.063–0.125 mm fraction. Therefore the presence of these minerals might not be detected if only selected fractions are examined.

Table 4.2 Ferromagnesian mineral abundances in the 0.125 – 0.250 mm (3 – 2 ϕ) fraction in andesitic tephras, Tongariro Volcanic Centre.*

Formation	Member		Opx %	Cpx %	Hbe %	Oliv %	Grain Count	Source Volcano
Tufa Trig Formation	Member Tf14	a	63	37	-	-	400	Ruapehu
	Member Tf8	a	67	33	-	-	400	Ruapehu
	Member Tf5	a	58	42	-	-	350	Ruapehu
	Member Tf1	b	80	20	-	-	400	Ruapehu
Mangamate Tephra	Poutu Lapilli	c	44	41	tr.†	15 ‡	200	Tongariro
	Waihohonu Lapilli	d	16	36	-	48	400	Tongariro
	Oturere Lapilli	d	50	28	1	21	400	Tongariro
	Te Rato Lapilli	c	11	6	83 ‡	-	400	Tongariro
Okupata Tephra		f	85	15	tr.†	tr.†	400	Ruapehu
Pahoka Tephra		e	21	22	57 ‡	tr.†	400	Tongariro
Bullot Formation	Pourahu Member [tephra unit]	g	72	28	-	-	400	Ruapehu
	"	h	67	31	2	tr.†	400	Ruapehu
	"	i	86	13	1	-	400	Ruapehu
	"	j	84	16	-	-	400	Ruapehu
	Pourahu Member [ignimbrite unit]	k	67	33	-	-	400	Ruapehu
	"	f	80	20	tr.†	-	400	Ruapehu
	Ngamatea lapilli-1	l	63	36	1	-	400	Ruapehu
	Member L17	g	78	22	tr.†	-	400	Ruapehu
	Shawcroft Tephra	m	66	20	-	14	400	Ruapehu
	Member L16	g	85	15	-	-	400	Ruapehu
	Helwan lapilli	n	80	20	-	-	400	Ruapehu
Rotoaira Lapilli		c	73	27	-	tr.†	400	Tongariro
Bullot Formation *(continued)*	Member L8	g	93	7	-	-	400	Ruapehu
	Member L7b	j	77	23	-	-	400	Ruapehu
	Member L6	g	79	20	1	-	400	Ruapehu
	Member L4	g	76	24	-	-	400	Ruapehu
	Member L3	g	74	26	tr.†	tr.†	400	Ruapehu
	Member L1	o	77	23	tr.†	-	400	Ruapehu

* Abundances are expressed as percentages of the total ferromagnesian mineral assemblage.
† tr. (trace) is <1.0%.
‡ Mineral type abundant in <0.125 mm fraction.

[a] Tufa Trig S.1.
[b] Death Valley.
[c] Poutu S. (defined in Topping 1973).
[d] Mangatawai S. (defined in Topping 1973).
[e] Mangatoetoenui Quarry.
[f] Okupata S. (defined in Topping 1973).
[g] Bullot Track S.1.
[h] Oturere Trig S.1.
[i] Desert Road S.16.
[j] Waikato Stream S.1.
[k] The Chute.
[l] Wahianoa Road S.1.
[m] Wahianoa Aqueduct T.S.
[n] Helwan Quarry.
[o] Waikato Stream S.2.

This contrast in the grain size of phenocryst minerals has earlier been observed in

Egmont tephras by Kohn and Neall (1973), who identified small acicular hypersthene phenocrysts of much finer grain size than the predominant augite phenocrysts.

Clinopyroxene

Clinopyroxene is present as phenocrysts in all TgVC tephras, and most commonly occurs as pale to dark green euhedral elongated crystals. Crystals may appear slightly pleochroic in thicker sections. Most tephras contain clinopyroxenes which show resorbtion features, *i.e.* rounded crystal faces and embayed edges (Donaldson and Henderson 1988). Embayments are filled with brown andesitic glass. Crystals are infrequently zoned (both normal and reverse zoning), and are commonly twinned. Most crystals contain numerous inclusions of brown glass and occasional Fe-Ti oxide grains.

Crystal aggregates, also termed glomerocrysts or crystal clots (Garcia and Jacobson 1979; Kuo and Kirkpatrick 1982; Scarfe and Fujii 1987) of clinopyroxene and orthopyroxene are common in some tephras, and comprise only those mineral types present in the ferromagnesian phenocryst assemblage. Crystals within these commonly show resorbed edges. The various origins of crystal clots are discussed in Kuo and Kirkpatrick (1982) and Scarfe and Fujii (1987).

Orthopyroxene

Orthopyroxene is the dominant mineral in most of the tephras and occurs as dark brown euhedral, elongated crystals; rarely it may exhibit a skeletal habit. Crystals show strong pleochroism from brown to green. In some tephras orthopyroxenes show distinctive resorbed outlines. Some phenocrysts show normal zoning from bronzite cores to hypersthene rims, or reverse zoning from hypersthene cores to bronzite rims. Glomerocrysts comprising orthopyroxene and clinopyroxene are common in some tephras. Phenocrysts are infrequently zoned or twinned. Inclusions of brown glass are ubiquitous, and Fe-Ti oxide inclusions are also present. Glass selvedges on grains commonly contain numerous microlites of pyroxene and feldspar.

Olivine

Olivine is present in tephras from both Mt Ruapehu and Mt Tongariro, and occurs as colourless, euhedral, equant grains and also as much smaller sized skeletal crystals (see p. 194). Skeletal crystals usually contain inclusions of brown glass of basaltic andesite – andesite composition. In some tephras olivine occurs in quantities >10%, together with clinopyroxene and orthopyroxene.

Hornblende

Hornblende is present in tephras erupted from both Mt Ruapehu and Mt Tongariro. Hornblende occurs as subhedral, acicular crystals which are green brown in colour and are strongly pleochroic. They are distinguished from orthopyroxene by their much stronger pleochroism, low extinction angle and distinctive cleavage. Few crystals are larger than 0.25 mm. Some crystals are reversely zoned.

Fe-Ti Oxides

Fe-Ti oxides occur most commonly as euhedral microphenocrysts and are also present as inclusions in pyroxene. Both titanomagnetite, and less commonly ilmenite, are present in these tephras.

Source

The occurrence of olivine and hornblende as dominant ferromagnesian minerals in tephras from TgVC has not previously been recognised.

Olivine has been reported as occurring in only minor to trace amounts in distal TgVC tephras (Lowe *et al.* 1980; Lowe 1988b), but would here appear to be more abundant than previously suggested. Olivine with non-skeletal and skeletal habits occurs in tephras sourced from both Mt Tongariro and Mt Ruapehu. Therefore the presence and morphology of olivine does not distinguish these sources.

At present, significant levels of hornblende have been identified only within tephras erupted from Mt Tongariro. Therefore, hornblende abundance can be used as a provisional indicator of a Mt Tongariro source.

Previously, tephras found to contain significant levels of hornblende have been attributed an EVC source. The presence of hornblende in TgVC tephras now precludes distinction between these sources on this basis. TgVC tephras may, however, be distinguished from EVC eruptives by their two-pyroxene assemblage and, in most tephras, dominance of orthopyroxene. Eruptives from EVC characteristically contain clinopyroxene, and rarely orthopyroxene (Kohn and Neall 1973; Neall *et al.* 1986; Wallace 1987).

Members

The ferromagnesian mineral assemblages of most TgVC tephras is shown to be very similar (Table 4.2, p. 169). Only seven tephras can be clearly distinguished on the basis of ferromagnesian mineral assemblages, together with the relative proportions of olivine and hornblende. The proportions of orthopyroxene and clinopyroxene are not diagnostic of any

tephra. Five tephras sourced Mt Tongariro (Pahoka Tephra, Poutu Lapilli, Waihohonu Lapilli, Oturere Lapilli, Te Rato Lapilli) and two key stratigraphic markers in the Bullot Formation, sourced from Mt Ruapehu (Shawcroft Tephra, member L3) (Table 3.1, p. 90) are distinguished by their olivine content.

Pahoka Tephra and the slightly younger Te Rato Lapilli are distinguished from all other TgVC tephras by their hornblende dominant assemblages, and are distinguished from each other by the proportion of hornblende in the assemblage (Table 4.2, p. 169). Poutu Lapilli, Waihohonu Lapilli and Oturere Lapilli are distinguished from all other TgVC tephras (except the Mt Ruapehu-sourced Bullot Formation members Shawcroft Tephra and L3) by the presence of olivine. They are distinguished from each other by the proportion of olivine in the assemblage, and the relative proportions of skeletal and non-skeletal olivines. Shawcroft Tephra and member L3 can similarly be distinguished on olivine abundance and morphology.

Okupata Tephra and Pahoka Tephra occupy very similar stratigraphic positions. In the Mt Tongariro region both tephra are overlain by the rhyolitic Karapiti Tephra. They have not yet been identified together in sections within the Mt Ruapehu and Mt Tongariro regions, and are not therefore distinguished by stratigraphic position. It is possible, however, to distinguish these tephras on ferromagnesian mineral assemblages; hornblende is identified in only trace amounts in the ferromagnesian assemblage of Okupata Tephra, but is abundant in Pahoka Tephra (Table 4.2, p. 169).

Major Element Chemistry of Ferromagnesian Minerals and Glass: Use in Tephra Fingerprinting

Twenty three tephras erupted from Mt Ruapehu and Mt Tongariro have been chemically fingerprinted to evaluate the use of tephra chemistry in identifying and correlating tephras of TgVC. The major element chemistry of individual ferromagnesian mineral phenocrysts (orthopyroxene, clinopyroxene, olivine, hornblende and Fe-Ti oxides) has been determined by electron microprobe analysis. Results are presented in Appendix III.

Clinopyroxene

Major element analyses of clinopyroxenes in TgVC tephras are presented in Appendix IIIb. Mean compositions are given in Table 4.3, p. 173.

Optical examination, back-scatter electron imagery, and comparison of core and rim analyses (Appendix IIIb) shows that most clinopyroxenes are compositionally homogenous. Some phenocrysts show normal zoning, indicated by higher FeO and lower MgO contents in rims compared with cores. Occasional grains show reverse zoning with more Fe-rich cores and a slight Mg enrichment in the rims (*e.g.* from core En39 to rim En45).

Table 4.3 Electron microprobe analyses (meaned) of clinopyroxene in andesitic tephras of Tongariro Volcanic Centre.*

Formation	Tf14		Tf8		Tf5		Tf1		Pt		Wa		Ot	
SiO_2	50.99	(0.53)	51.22	(0.81)	50.67	(0.45)	51.79	(0.91)	52.38	(0.84)	52.24	(0.80)	50.87	(1.28)
Al_2O_3	2.49	(0.43)	2.41	(0.64)	2.28	(0.55)	2.63	(1.05)	2.23	(0.84)	1.67	(0.65)	3.65	(1.45)
TiO_2	0.40	(0.11)	0.40	(0.16)	0.51	(0.11)	0.44	(0.17)	0.24'	(0.05)'	0.22'	(0.16)'	0.44	(0.18)
FeO	8.20	(1.90)	7.78	(2.02)	9.68	(2.11)	8.18	(2.66)	6.91	(0.80)	6.17	(2.03)	7.55	(0.83)
MnO	0.24'	(0.06)'	0.21'	(0.08)'	0.25'	(0.05)'	0.24	(0.06)	0.20'	(0.02)'	0.19'	(0.04)'	0.21'	(0.04)'
MgO	15.42	(1.08)	15.80	(1.27)	14.64	(1.01)	16.34	(1.83)	18.95	(0.59)	17.19	(1.05)	15.88	(1.08)
CaO	20.89	(0.49)	21.01	(0.86)	20.49	(0.87)	19.78	(0.90)	21.33	(0.84)	21.76	(1.02)	21.20	(0.78)
Na_2O	0.32	(0.03)	0.29	(0.05)	0.32	(0.07)	0.28	(0.08)	0.22'	(0.03)'	0.23'	(0.06)'	0.28'	(0.05)'
NiO	nd	nd	nd	nd	nd	nd	nd	nd	nd	nd	nd	nd	nd	nd
Cr_2O_3	0.29'	(0.10)'	0.29'	(0.09)'	0.19'	(0.02)'	0.38'	(0.27)'	0.39'	(0.15)'	0.82'	(0.28)'	0.19'	(0.02)'
Total	99.08	(0.38)	98.98	(0.32)	98.88	(0.47)	99.88	(0.49)	99.55	(0.52)	99.04	(0.43)	99.82	(0.48)
n	*n* = 11		*n* = 10		*n* = 15		*n* = 10		*n* = 28		*n* = 19		*n* = 14	
Formation	Tt		Pa		Ph-T [BT1]		Ph-T [WS1]		Ph-T [DR16]		Ph-T [OT]		Ph-Ig [CT]	
SiO_2	51.53	(0.46)	50.30	(1.30)	50.81	(0.72)	51.37	(0.32)	51.54	(0.68)	51.13	(0.42)	51.70	(0.52)
Al_2O_3	2.24	(0.53)	3.99	(1.41)	2.36	(0.94)	1.85	(0.38)	2.23	(1.24)	3.02	(0.98)	1.85	(0.48)
TiO_2	0.48	(0.11)	0.48'	(0.15)'	0.58	(0.14)	0.44	(0.12)	0.43	(0.11)	0.45	(0.07)	0.41	(0.12)
FeO	8.84	(1.65)	8.17	(1.80)	10.51	(0.65)	10.37	(0.47)	9.34	(1.42)	8.77	(1.86)	10.48	(0.51)
MnO	0.28'	(0.05)'	0.22'	(0.01)'	0.31	(0.07)	0.31	(0.02)	0.26	(0.07)	0.25	(0.08)	0.28	(0.03)
MgO	15.13	(0.76)	15.07	(1.16)	14.39	(0.28)	14.11	(0.42)	14.72	(0.49)	14.88	(0.69)	14.74	(0.31)
CaO	20.83	(0.26)	20.64	(1.06)	20.08	(0.51)	20.81	(0.39)	20.80	(0.46)	20.70	(0.67)	20.36	(0.55)
Na_2O	0.25'	(0.00)'	0.31'	(0.04)'	0.20	(0.06)	0.25	(0.07)	0.30	(0.04)	0.31	(0.04)	0.28	(0.07)
NiO	nd	nd	nd	nd	nd	nd	0.11'	(0.00)'	0.12'	(0.00)'	nd	nd	nd	nd
Cr_2O_3	0.89'	(0.48)'	0.37'	(0.21)'	0.15'	(0.02)'	nd	nd	0.21'	(0.11)'	0.24'	(0.10)'	nd	nd
Total	99.45	(0.62)	99.06	(0.53)	99.30	(0.39)	99.13	(0.22)	99.70	(0.29)	99.61	(0.85)	99.88	(0.35)
n	*n* = 9		*n* = 5		*n* = 6		*n* = 5		*n* = 12		*n* = 8		*n* = 7	
Formation	Ph-Ig [MQ]		Ok		Nt-1		HI		L17		L16		Sh	
SiO_2	51.45	(0.39)	50.52	(0.50)	51.39	(0.81)	50.72	(0.31)	50.09	(0.71)	51.12	(0.38)	50.80	(0.50)
Al_2O_3	1.71	(0.32)	2.08	(0.37)	2.07	(0.62)	2.25	(0.50)	2.68	(1.07)	2.25	(0.56)	2.88	(0.73)
TiO_2	0.45	(0.05)	0.49'	(0.11)'	0.50	(0.08)	0.57	(0.07)	0.52	(0.07)	0.51	(0.05)	0.38'	(0.13)'
FeO	10.42	(0.77)	9.98	(1.44)	9.92	(0.43)	10.87	(0.48)	9.48	(1.73)	9.89	(0.75)	9.57	(1.86)
MnO	0.34	(0.05)	0.29'	(0.08)'	0.30	(0.05)	0.27	(0.08)	0.28'	(0.05)'	0.26'	(0.03)'	0.24'	(0.08)'
MgO	14.33	(0.34)	14.55	(0.96)	14.77	(0.32)	14.28	(0.41)	14.22	(0.75)	14.55	(0.53)	14.65	(1.05)
CaO	20.34	(0.45)	20.48	(0.43)	20.37	(0.36)	20.49	(0.34)	20.98	(0.58)	20.67	(0.33)	20.12	(0.81)
Na_2O	0.29	(0.05)	0.36	(0.06)	0.28	(0.05)	0.38	(0.06)	0.32	(0.05)	0.29	(0.05)	0.35	(0.07)
NiO	nd	nd	nd	nd	nd	nd	nd	nd	nd	nd	nd	nd	nd	nd
Cr_2O_3	0.14'	(0.05)'	0.24'	(0.05)'	0.17'	(0.00)'	0.61'	(0.00)'	0.35'	(0.00)'	0.20'	(0.00)'	0.29'	(0.14)'
Total	99.38	(0.24)	98.77	(0.20)	99.61	(0.51)	99.88	(0.34)	98.56	(0.41)	99.48	(0.59)	98.87	(0.36)
n	*n* = 5		*n* = 10		*n* = 9		*n* = 15		*n* = 9		*n* = 5		*n* = 12	
Formation	Rt		L8		L7b		L6		L4		L3		L1	
SiO_2	51.31	(0.81)	51.38	(0.44)	51.46	(0.36)	51.30	(0.35)	51.15	(0.80)	51.91	(0.84)	51.99	(1.11)
Al_2O_3	1.85	(0.37)	1.92	(0.29)	2.23	(0.53)	1.99	(0.40)	2.13	(0.75)	2.98	(0.92)	2.49	(0.84)
TiO_2	0.37'	(0.04)'	0.52	(0.04)	0.44	(0.11)	0.47	(0.11)	0.48	(0.13)	0.38	(0.12)	0.48	(0.18)
FeO	9.55	(2.57)	10.26	(0.81)	8.77	(1.52)	10.70	(1.17)	9.42	(1.17)	6.83	(1.82)	7.72	(1.95)
MnO	0.31	(0.07)	0.27	(0.03)	0.24	(0.06)	0.29	(0.07)	0.30	(0.05)	0.23'	(0.07)'	0.22	(0.07)
MgO	15.24	(1.86)	14.44	(0.67)	15.19	(0.70)	14.12	(0.64)	14.98	(1.02)	16.60	(1.35)	15.95	(1.55)
CaO	20.07	(0.31)	20.75	(0.53)	20.88	(0.47)	20.75	(0.72)	20.83	(0.83)	20.49	(1.00)	20.82	(0.41)
Na_2O	0.28	(0.04)	0.28	(0.03)	0.29	(0.03)	0.37	(0.07)	0.28	(0.03)	0.31	(0.05)	0.29	(0.05)
NiO	nd	nd	0.22'	(0.00)'	nd	nd	nd	nd	nd	nd	nd	nd	nd	nd
Cr_2O_3	0.70'	(0.08)'	nd	nd	0.43'	(0.31)'	0.29'	(0.00)'	0.29'	(0.12)'	0.55'	(0.23)'	0.30'	(0.11)'
Total	99.11	(0.48)	99.83	(0.41)	99.46	(0.25)	100.05	(0.18)	99.82	(0.37)	99.97	(0.30)	99.96	(0.30)
n	*n* = 8		*n* = 7		*n* = 11		*n* = 9		*n* = 12		*n* = 11		*n* = 4	

* All statistics are for core values above detection limit only; values in parentheses are standard deviations. Tephra codes are given in text with tephra descriptions. nd = no values above detection limit.

† At least one analysis gave a result below detection limit (not included in these statistics).

Within each tephra there is marked variation in FeO and MgO contents of clinopyroxene cores [2], and less variation in the Al_2O_3 contents between individual grains. This variation is reflected in the higher than usual standard deviations on these elements (Appendix IIIb). Cr_2O_3 occurs in minor amounts in the more Mg-rich clinopyroxenes of some tephras. Plots of mean oxide contents *vs* mean Mg number (Mg Nº) of clinopyroxenes (cores only) for all tephras (Figure 4.1, p. 175) shows that TiO_2, MnO and Na_2O contents increase with decreasing Mg Nº. CaO, Al_2O_3 and Cr_2O_3 contents show no trend, although in some analyses there is a slight Ca (Wo%) enrichment in the rims. A decline in TiO_2 content could be expected if, in these tephras, the crystallisation of titanomagnetite was contemporaneous with that of the clinopyroxene.

Clinopyroxene core and rim compositions collectively fall within the augite-salite and endiopside-diopside fields (Figure 4.2, p. 176). Most analyses project as augite (Appendix IIIb). Clinopyroxenes core compositions range between Wo49 – 36, En54 – 37, and Fs21 – 5, with Mg Nº between 94 – 61.

Clinopyroxenes within the Mt Ruapehu tephras show similar compositions to those within Mt Ruapehu lavas, which, with the exception of Waimarino Basalt, are all classified as augite (Hackett 1985) (Figure 4.2, p. 176).

Tephras sourced from Mt Ruapehu and Mt Tongariro are compared using x-y scatter plots of MgO *vs* $MnO + TiO_2$ (MGMT scatter plot) and $Na_2O/(Na_2O + CaO)$ *vs* $MnO + TiO_2$ (NCMT scatter plot), mean oxide contents (Al_2O_3, TiO_2, FeO, MnO, CaO), mean Mg Nº and mean Wollastonite (Wo%), Enstatite (En%), and Ferrosilite (Fs%) contents. The oxides selected for comparison are those that recognised major element substitutions in clinopyroxenes (Deer *et al.* 1966) suggest are likely to identify compositional differences.

Source

Tephras sourced from Mt Ruapehu (Tufa Trig Formation, Okupata Tephra, Bullot Formation) and Mt Tongariro (Mangamate Tephra Formation, Pahoka Tephra, Rotoaira Lapilli) cannot be distinguished from comparison of the major element chemistries of their clinopyroxenes. Using MGMT and NCMT scatter plots (Figure 4.3, p. 181) and comparisons of mean oxide contents and Mg Nº's (Figure 4.4, p. 182), tephras from Mt Tongariro and Mt Ruapehu do not group into discrete fields, and therefore no separation can be made according to source.

---

[2] A wide range of ionic substitutions is present in the monoclinic pyroxenes; there is complete replacement of Mg by Fe^{+2} and of Fe^{+2} by Mn. The general formula of the pyroxene group may be expressed $X_{1-p}Y_{1+p}Z_2O_6$ where X = Ca,Na; Y = Mg,Fe^{+2},Mn,Li,Ni,Al,Fe^{+3},Cr,Ti; Z = Si,Al (Deer *et al.* 1966).

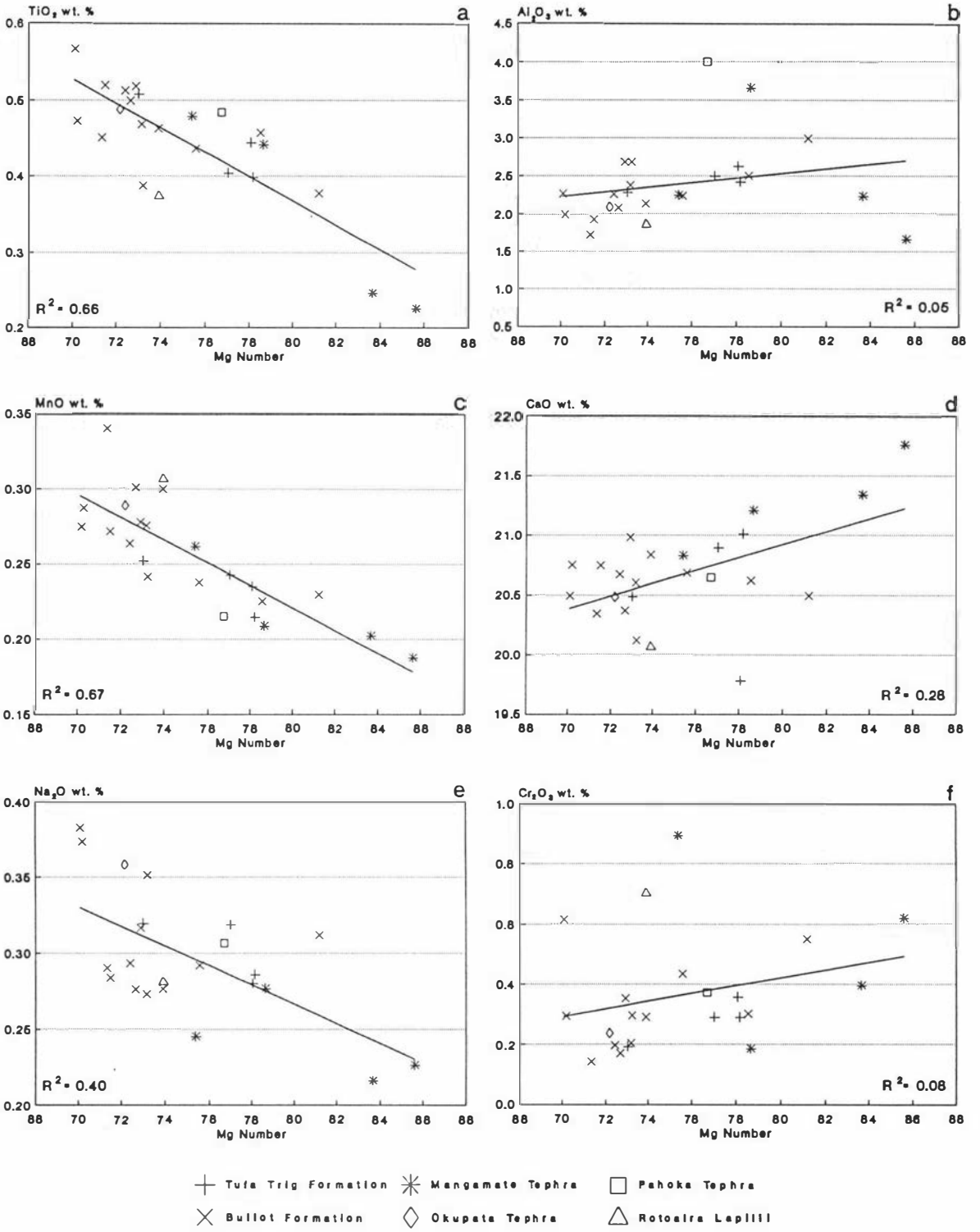

Figure 4.1 Plots of major oxide contents (mean wt.%) *vs* Mg number in clinopyroxene phenocrysts of Tongariro Volcanic Centre tephras.

Tephras from TgVC and EVC are also not distinguished by comparison of the major element chemistry (CaO contents and Mg Nº's) of clinopyroxene phenocrysts (Figure 4.5, p. 184). Furthermore, tephras of TgVC and TVC (both of TVZ) are also not distinguished by clinopyroxene phenocryst chemistry, supporting the finding of Wallace (1987). Clinopyroxene chemistry does not therefore distinguish these sources.

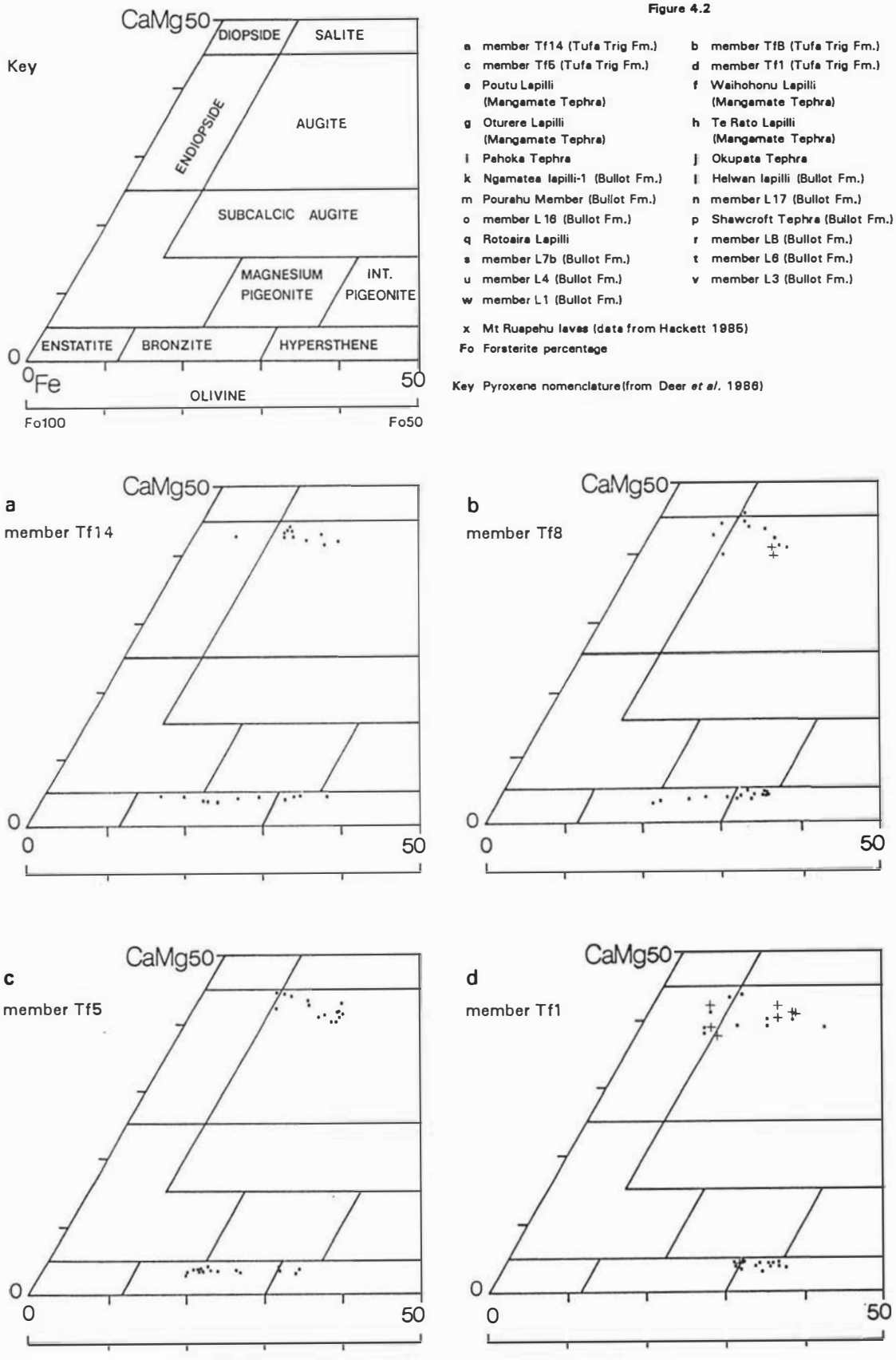

Figure 4.2

a member Tf14 (Tufa Trig Fm.)
b member Tf8 (Tufa Trig Fm.)
c member Tf5 (Tufa Trig Fm.)
d member Tf1 (Tufa Trig Fm.)
e Poutu Lapilli (Mangamate Tephra)
f Waihohonu Lapilli (Mangamate Tephra)
g Oturere Lapilli (Mangamate Tephra)
h Te Rato Lapilli (Mangamate Tephra)
i Pahoka Tephra
j Okupata Tephra
k Ngamatea lapilli-1 (Bullot Fm.)
l Helwan lapilli (Bullot Fm.)
m Pourahu Member (Bullot Fm.)
n member L17 (Bullot Fm.)
o member L16 (Bullot Fm.)
p Shawcroft Tephra (Bullot Fm.)
q Rotoaira Lapilli
r member L8 (Bullot Fm.)
s member L7b (Bullot Fm.)
t member L6 (Bullot Fm.)
u member L4 (Bullot Fm.)
v member L3 (Bullot Fm.)
w member L1 (Bullot Fm.)

x Mt Ruapehu lavas (data from Hackett 1985)
Fo Forsterite percentage

Key Pyroxene nomenclature (from Deer *et al.* 1966)

Figure 4.2 Compositions of clinopyroxenes, orthopyroxenes and olivines in Tongariro Volcanic Centre tephras. Nomenclature of pyroxenes is from Deer *et al.* (1966). *(continued ...)*

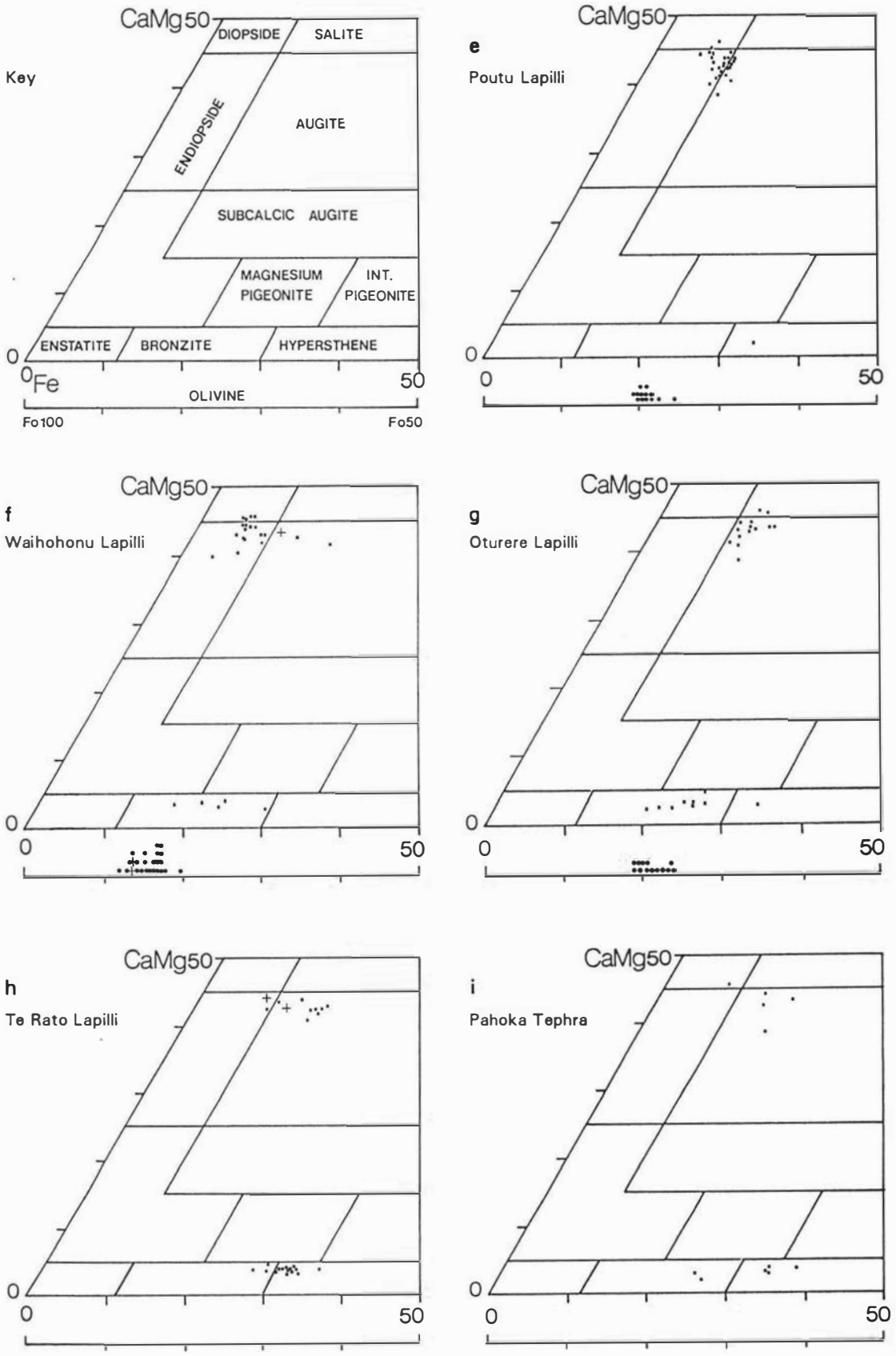

Figure 4.2 Compositions of clinopyroxenes, orthopyroxenes and olivines in Tongariro Volcanic Centre tephras. Nomenclature of pyroxenes is from Deer *et al.* (1966). *(... continued ...)*

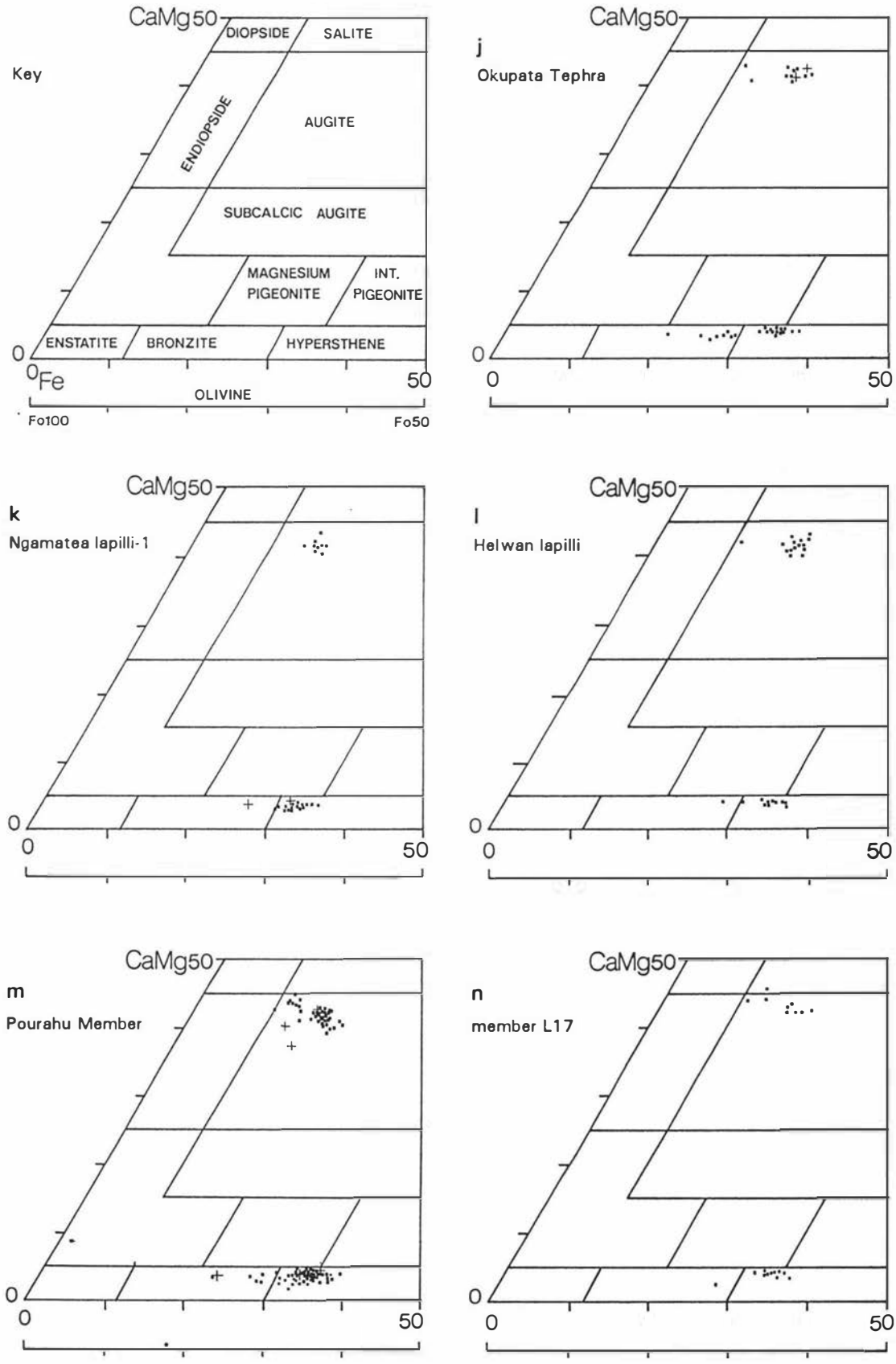

Figure 4.2 Compositions of clinopyroxenes, orthopyroxenes and olivines in Tongariro Volcanic Centre tephras. Nomenclature of pyroxenes is from Deer *et al.* (1966). *(... continued ...)*

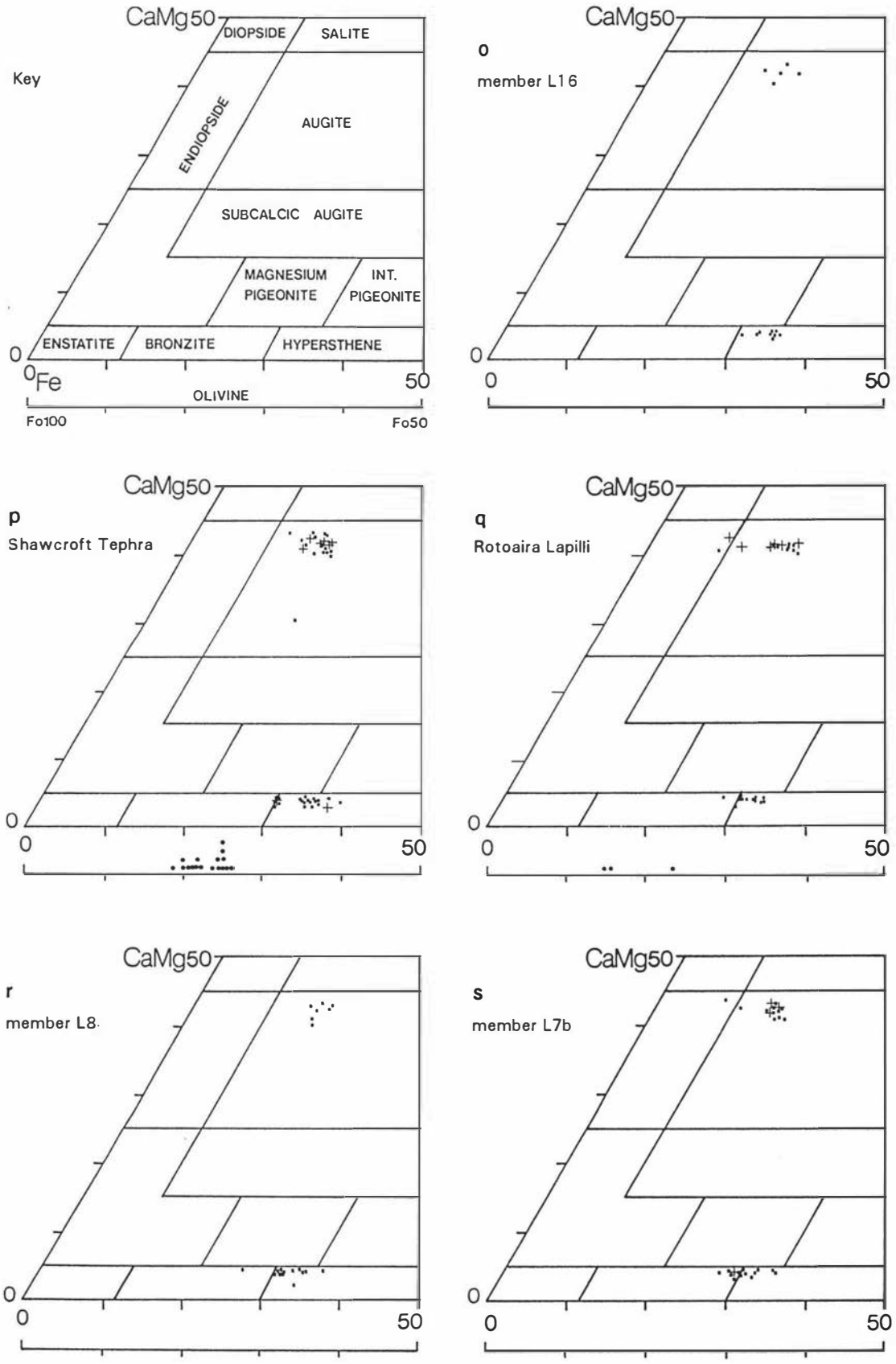

Figure 4.2 Compositions of clinopyroxenes, orthopyroxenes and olivines in Tongariro Volcanic Centre tephras. Nomenclature of pyroxenes is from Deer *et al.* (1966). *(... continued ...)*

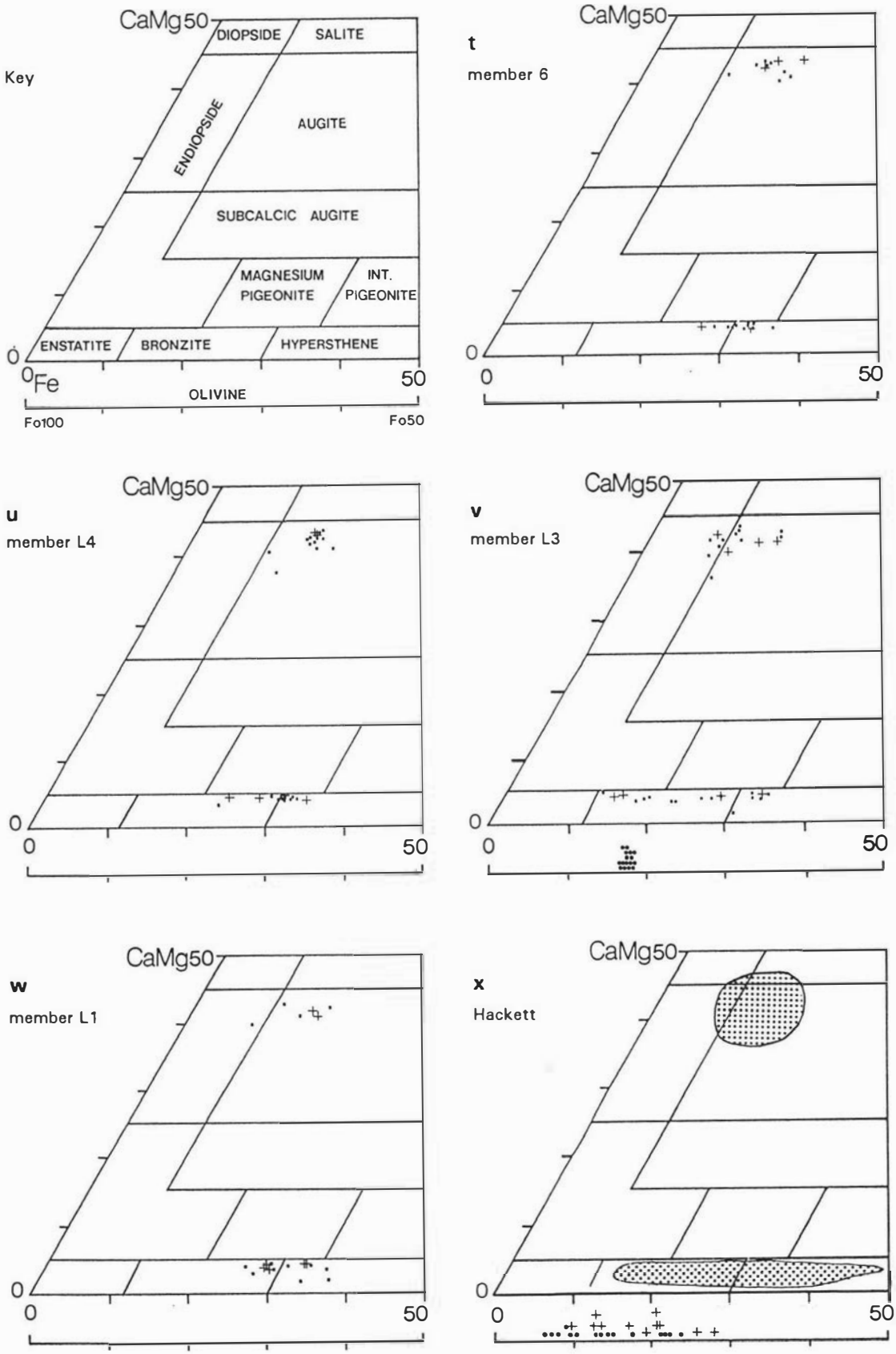

Figure 4.2 Compositions of clinopyroxenes, orthopyroxenes and olivines in Tongariro Volcanic Centre tephras. Nomenclature of pyroxenes is from Deer *et al.* (1966). *(... continued)*

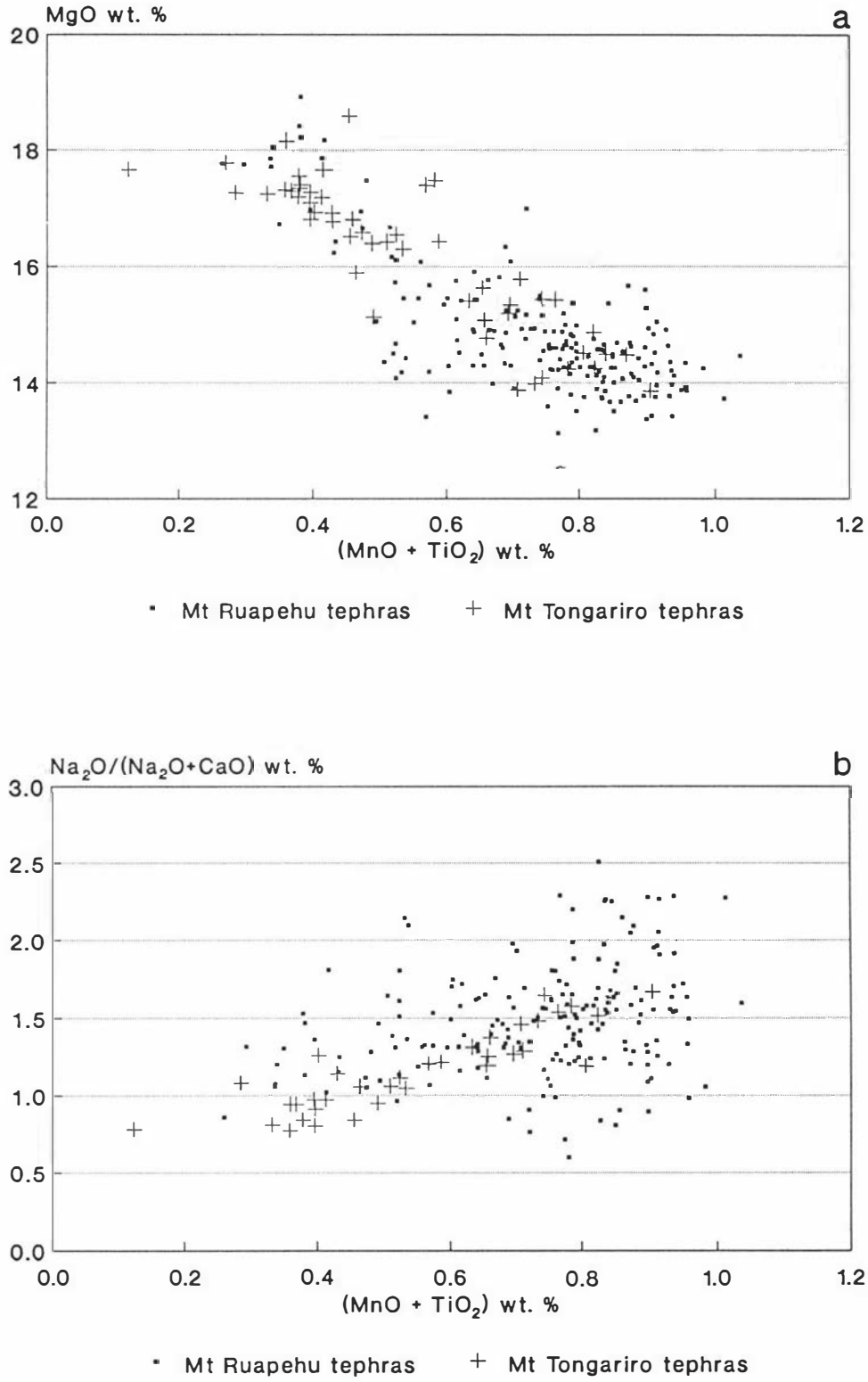

Figure 4.3 MGMT (Fig. 4.3a) and NCMT (Fig. 4.3b) scatter plots showing compositions of clinopyroxene phenocrysts in tephras from Mt Ruapehu and Mt Tongariro, Tongariro Volcanic Centre.

Clinopyroxene compositions in EVC eruptives are diopside–diopsidic augite (Gow 1966; Neall *et al.* 1986).

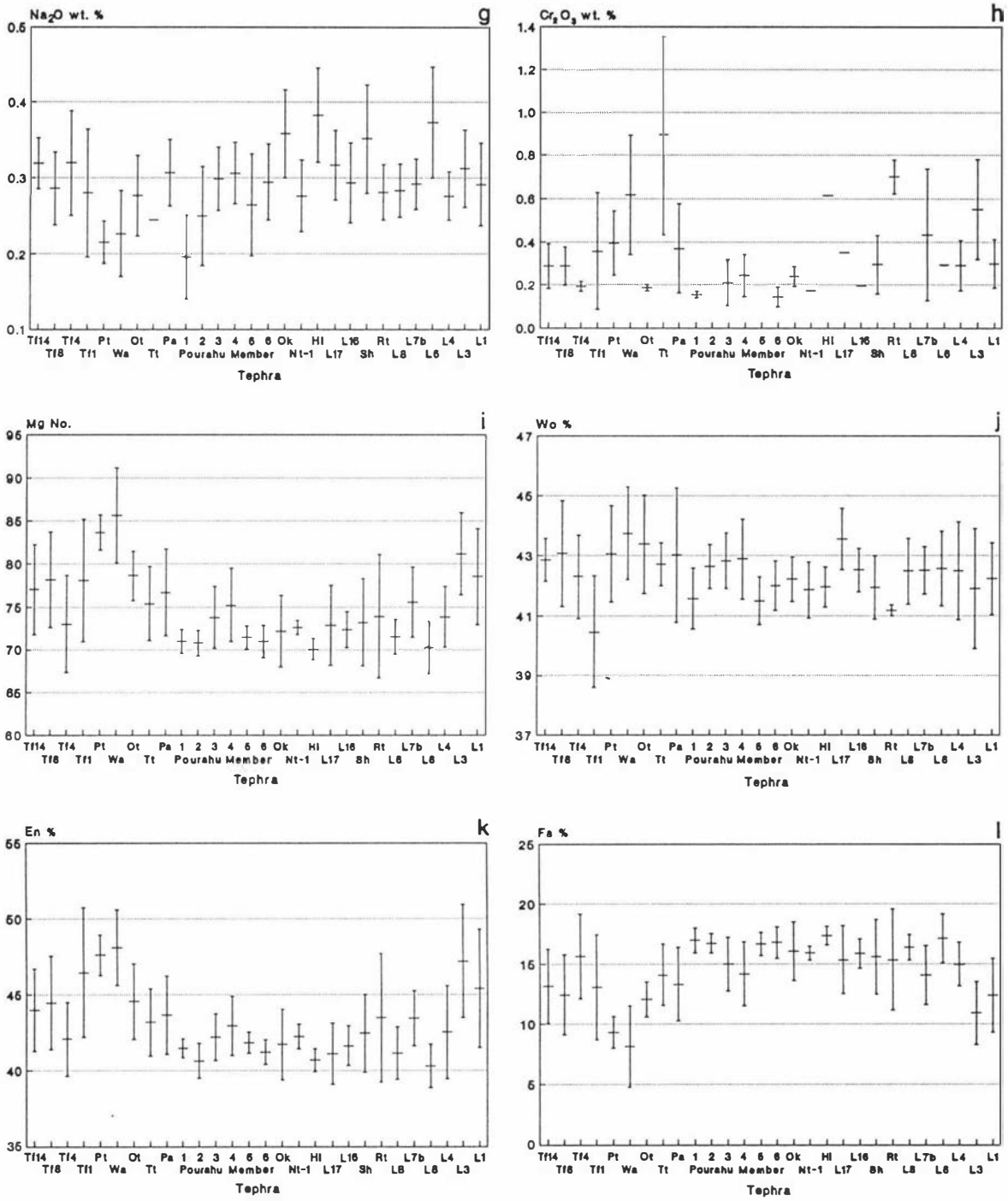

Figure 4.4 Mean oxide contents, Mg numbers (Mg Nº), Wo% (Wollastonite), En% (Enstatite) and Fs% (Ferrosilite) contents in clinopyroxene phenocrysts of Tongariro Volcanic Centre tephras. Bars show standard deviation from mean *(see text for tephra codes; continued ...)*.

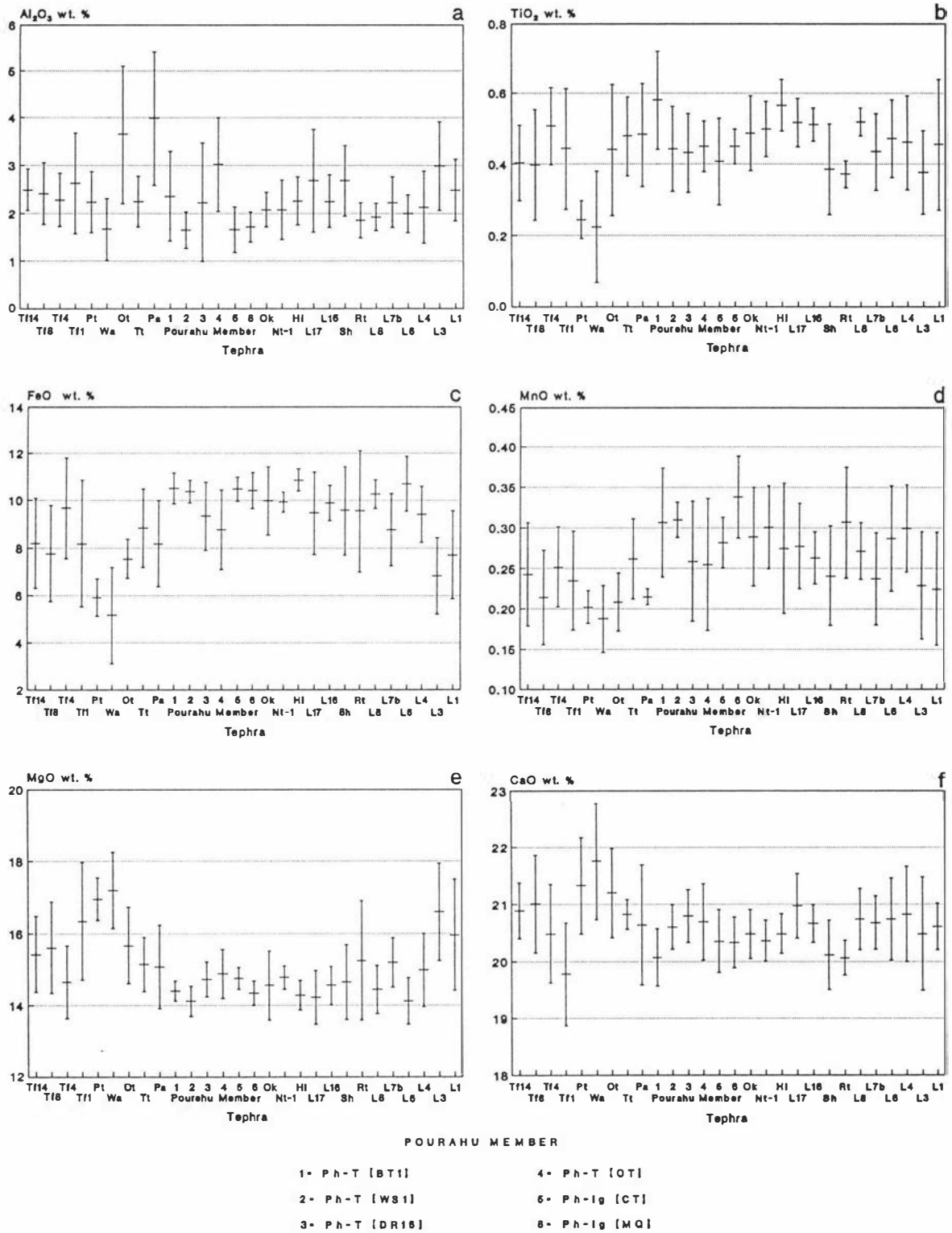

Figure 4.4 Mean oxide contents, Mg numbers (Mg Nº), Wo% (Wollastonite), En% (Enstatite) and Fs% (Ferrosilite) contents in clinopyroxene phenocrysts of Tongariro Volcanic Centre tephras. Bars show standard deviation from mean *(see text for tephra codes; ... continued).*

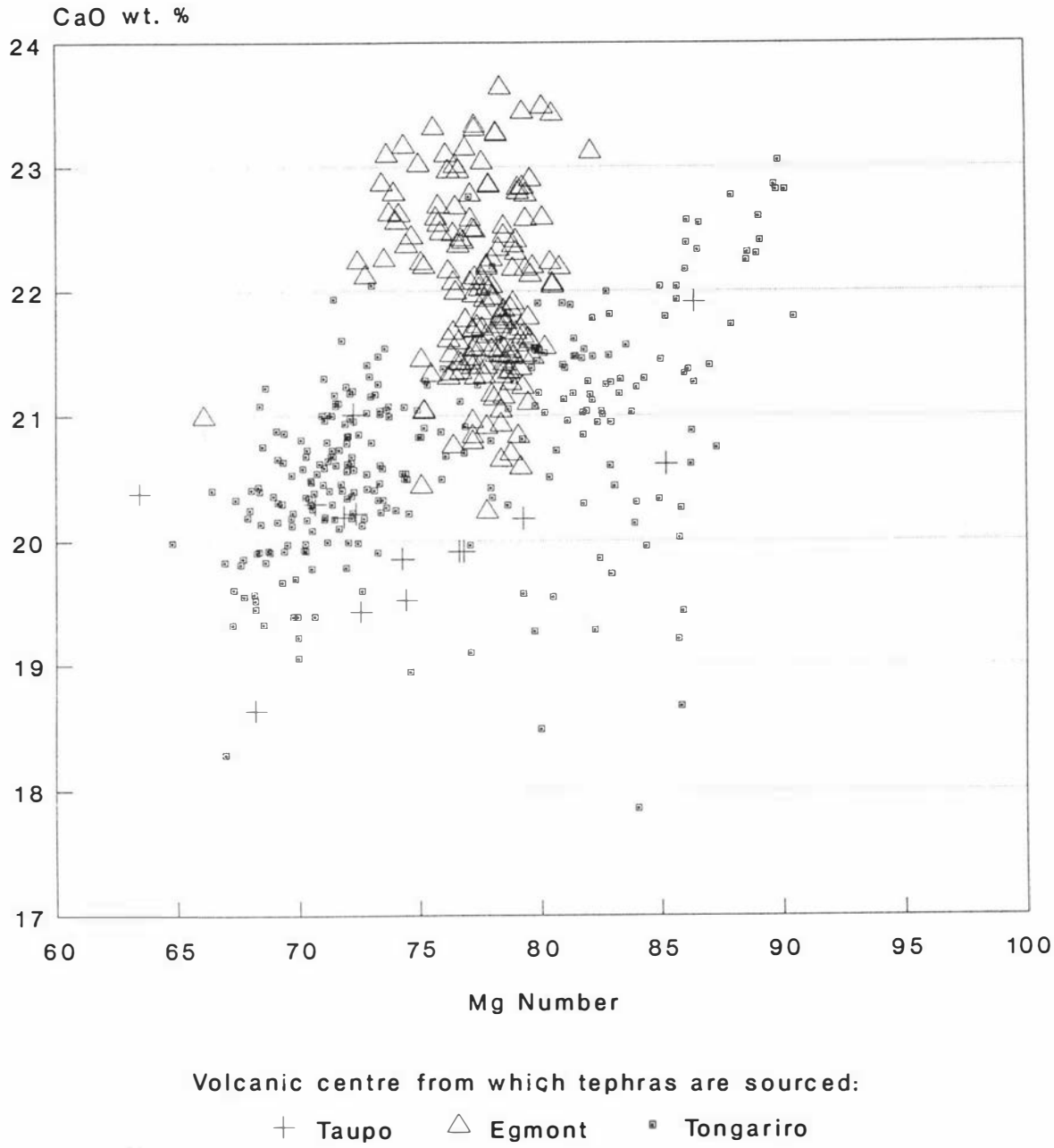

Figure 4.5 Plot of CaO content (wt.%) *vs* Mg number of clinopyroxene phenocrysts in tephras from Tongariro, Taupo, and Egmont volcanic centres. Taupo and Egmont volcanic centre data from Howorth (1976) and Wallace (1987).

Comparison of Formation and Member Cpx-chemistries

Tufa Trig Formation, Mangamate Tephra, Pahoka Tephra, Okupata Tephra, Bullot Formation and Rotoaira Lapilli show similar clinopyroxene chemistries and cannot be distinguished by comparison of their major element cpx-chemistries. The similarity in the cpx-chemistry of members, both within and between these formations, also precludes the distinction of most members (Figure 4.4, p. 182).

Members within Tufa Trig Formation are not distinguished on cpx-chemistry (Figure 4.4, 182). Within Mangamate Tephra, Poutu Lapilli Member is distinguished from Oturere Lapilli and Te Rato Lapilli members on mean Mg Nº (Figure 4.4i, p. 182) but is not distinguished from Waihohonu Lapilli Member. Both Poutu Lapilli and Waihohonu Lapilli show ferromagnesian mineral assemblages dominated by forsteritic olivine. The dominant occurrence of Mg-rich endiopside in these two tephras is consistent with their more magnesian chemistry, exhibited by the high olivine contents.

Both Te Rato Lapilli Member of Mangamate Tephra and Pahoka Tephra show ferromagnesian mineral assemblages dominated by hornblende. They are not distinguished on cpx-chemistry, and similarly, are not distinguished from most other non-hornblende-bearing tephras. This indicates that the occurrence of hornblende in these tephras is not reflected in the chemistry of the clinopyroxenes, and it is therefore probable that either the hornblendes, or the clinopyroxenes, or both, are xenocrystic.

Two olivine-bearing members of Bullot Formation, Shawcroft Tephra and L3, are not clearly distinguished on cpx-chemistry (Figure 4.4, p. 182). The presence of olivine in the ferromagnesian mineral assemblages of both tephras is reflected in the more Mg-rich chemistry of clinopyroxenes in member L3, but not in Shawcroft Tephra. Clinopyroxenes in Shawcroft Tephra have compositions similar to those in the other, non-olivine-bearing Bullot Formation tephras.

The clinopyroxene chemistry of tephras considered to be correlatives of Pourahu Member [tephra unit] (Ph-T) and Pourahu Member [ignimbrite unit] (Ph-Ig) on the basis of stratigraphic position, field characteristics and ferromagnesian mineral assemblages, are compared in Figure 4.4, p. 182.

Samples Ph-T [BT1], Ph-T [WS1] and Ph-T [OT] are correlated with Ph-T sampled from the type section at Desert Road S.16 (Ph-T [DR16]). Sample Ph-Ig [MQ] is correlated with Ph-Ig sampled from The Chute T.L. (Ph-Ig [CT]). Tephras correlated with Ph-T [DR16], and samples Ph-Ig [MQ] and Ph-Ig [CT] are indistinguishable on cpx-chemistry. There are some differences in mean Na_2O contents between samples Ph-T [BT1], and Ph-T [DR16] and Ph-T [Ot], and in mean Al_2O_3 contents between samples Ph-T [WS1] and Ph-T [Ot], but each is not consistently distinguished (Figure 4.4, p. 182). Due to the similarity in cpx-chemistry of the Pourahu Member correlatives, and their similarity to other TgVC tephras, cpx-chemistry cannot be used to prove or disprove correlation with Pourahu Member tephra or ignimbrite units.

The mean clinopyroxene composition of Rotoaira Lapilli projects as augite. Some phenocrysts project as the more Mg-rich endiopside (Figure 4.2, p. 176) and probably reflect the presence of olivine in the ferromagnesian mineral assemblage. Rotoaira Lapilli can be distinguished from the olivine-bearing Poutu Lapilli Member of Mangamate Tephra on its lower

mean Mg Nº, and from all Mangamate Tephra members on its lower CaO (and Wo%) content (Figure 4.4f,j, p. 182). It is distinguished from Pahoka Tephra on Al_2O_3 content, and Bullot Formation members younger than it (excluding the olivine-bearing Shawcroft Tephra) on TiO_2 content (Figure 4.4a,b, p. 182). The similarity in the cpx-chemistry of Rotoaira Lapilli and members of the Bullot Formation (with which it is interbedded in time) as exhibited by all other major element contents suggests this tephra is unlikely to be correlated using cpx-chemistry. Rotoaira Lapilli is an important marker bed in the northern Mt Tongariro region, and if it were able to be correlated into the study area, using diagnostic phenocryst chemistry, it would be a valuable marker bed within the Bullot Formation tephra sequence.

Orthopyroxene

Major element analyses of orthopyroxenes from all TgVC tephras are presented in Appendix IIIc. Mean compositions are given in Table 4.4, p. 187. Orthopyroxenes within Mt Ruapehu lavas are mostly bronzite and hypersthene, with few ferrohypersthenes and enstatites (Hackett 1985) (Figure 4.2, p. 176).

Optical examination, back-scatter electron imagery, and comparison of core and rim analyses shows that most orthopyroxenes are compositionally homogenous. Some phenocrysts show normal zoning indicated by more Mg-rich (bronzite) cores and more Fe-rich (hypersthene) rims, and rarely show reverse zoning from hypersthene cores to more Mg-rich bronzite rims (*e.g.* from core En64 to rim En70). Within most of the tephras there is a marked variation in the FeO and MgO contents of orthopyroxene cores. This variation is reflected in the higher than usual standard deviations (for mean compositions) on these elements. For some tephras, large standard deviations are due both to the variability in chemistry of phenocrysts and the small number of analyses (less than ten) obtained. Plots of mean oxide contents *vs* mean Mg Nº (cores only) for all tephras (Figure 4.6, p. 188) shows that MnO contents increase, and Al_2O_3 contents decrease with decreasing Mg Nº[3]. TiO_2 and CaO show no trend.

Compositions of orthopyroxene (cores and rims) in TgVC tephras range between hypersthene and bronzite (Figure 4.2, p. 176) with En83 – 59, Fs38 – 14, Wo5 – 1, and Mg Nº's between 88 – 61. The Mg Nº's are lower than those in the coexisting clinopyroxenes of most tephras. Two orthopyroxene analyses from Bullot Formation member L3 show En% values between En83 – 80. These analyses are from the more Mg-rich rims of reversely zoned orthopyroxenes. Most analyses project as hypersthene.

---

[3] A wide range of ionic substitutions is present in the monoclinic pyroxenes. In other pyroxenes, substitutions are limited. Ions other than Mg and Fe^{+2} are invariably present in the orthopyroxenes and these commonly include Ca, Mn, Ni, Fe^{+3}, Cr, Al and Ti. Cr and Ni occur mainly in the magnesium-rich orthopyroxenes of igneous rocks. High contents of Mn are found in the iron-rich orthopyroxenes of igneous rocks. The CaO content is generally not greater than 1.5 wt% (Deer *et al.* 1966).

Table 4.4 Electron microprobe analyses (meaned) of orthopyroxene in andesitic tephras of Tongariro Volcanic Centre.*

Formation	Tf14		Tf8		Tf5		Tf1		Pt		We		Ot	
SiO_2	52.77	(0.98)	52.28	(0.63)	53.10	(0.70)	52.62	(0.52)	52.72	(0.00)	53.10	(0.60)	52.59	(0.70)
Al_2O_3	1.44	(0.35)	1.34	(0.39)	1.45	(0.44)	1.11	(0.38)	0.84	(0.00)	2.01	(0.26)	2.59	(0.78)
TiO_2	0.22	(0.10)	0.27	(0.08)	0.17'	(0.05)'	0.29	(0.05)	nd	nd	0.18	(0.03)	0.23	(0.05)
FeO	16.24	(3.83)	18.61	(2.78)	15.16	(3.06)	20.59	(1.22)	20.79	(0.00)	14.48	(2.23)	15.85	(2.40)
MnO	0.35	(0.10)	0.39	(0.09)	0.33	(0.06)	0.46	(0.05)	0.71	(0.00)	0.32	(0.07)	0.35	(0.09)
MgO	25.55	(2.83)	23.76	(2.07)	26.53	(2.25)	23.07	(0.83)	22.98	(0.00)	26.98	(1.56)	25.81	(1.59)
CaO	1.82	(0.19)	1.71	(0.15)	1.60	(0.14)	1.67	(0.14)	1.13	(0.00)	1.54	(0.16)	1.67	(0.16)
Na_2O	nd	nd	nd	nd	nd	nd	0.14'	(0.07)'	nd	nd	nd	nd	nd	nd
NiO	nd	nd	nd	nd	nd	nd	nd	nd	nd	nd	nd	nd	nd	nd
Cr_2O_3	0.28'	(0.01)'	0.21'	(0.04)'	0.39'	(0.10)'	nd	nd	nd	nd	nd	nd	0.16'	(0.00)'
Total	98.45	(0.26)	98.38	(0.25)	98.38	(0.31)	99.82	(0.27)	99.18	(0.00)	98.61	(0.32)	99.11	(0.61)
n	*n = 11*		*n = 15*		*n = 15*		*n = 13*		*n = 1*		*n = 5*		*n = 9*	
Formation	Tt		Pa		Ph-T (BT1)		Ph-T (WS1)		Ph-T (DR18)		Ph-T (OT)		Ph-lg (CT)	
SiO_2	52.91	(0.39)	52.47	(0.46)	52.23	(0.35)	52.15	(0.39)	52.34	(0.41)	52.56	(0.49)	52.22	(0.53)
Al_2O_3	1.06	(0.24)	1.84	(1.15)	1.42	(0.52)	1.21	(0.27)	1.04	(0.22)	1.52	(0.94)	1.18	(0.19)
TiO_2	0.27	(0.06)	0.24	(0.03)	0.26	(0.07)	0.28	(0.02)	0.29	(0.03)	0.26	(0.04)	0.27'	(0.04)'
FeO	19.49	(1.12)	19.47	(2.74)	20.64	(1.19)	21.13	(0.51)	21.73	(0.61)	20.10	(3.03)	21.21	(1.00)
MnO	0.44	(0.04)	0.45	(0.10)	0.49	(0.08)	0.50	(0.05)	0.51	(0.05)	0.54	(0.09)	0.49	(0.07)
MgO	23.68	(0.95)	23.35	(1.79)	23.48	(0.93)	22.42	(0.29)	22.31	(0.51)	23.51	(2.04)	22.97	(0.93)
CaO	1.61	(0.11)	1.38	(0.15)	1.47	(0.14)	1.55	(0.10)	1.54	(0.14)	1.49	(0.11)	1.53	(0.07)
Na_2O	nd	nd	nd	nd	nd	nd	nd	nd	nd	nd	nd	nd	0.07'	(0.00)'
NiO	nd	nd	nd	nd	nd	nd	nd	nd	nd	nd	0.13'	(0.00)'	nd	nd
Cr_2O_3	nd	nd	nd	nd	0.28'	(0.00)'	nd	nd	nd	nd	0.09'	(0.00)'	0.33'	(0.00)'
Total	99.47	(0.44)	99.20	(0.46)	100.02	(0.40)	99.24	(0.52)	99.75	(0.56)	100.03	(0.28)	99.87	(0.45)
n	*n = 15*		*n = 6*		*n = 18*		*n = 9*		*n = 13*		*n = 5*		*n = 16*	
Formation	Ph-lg (MQ)		Ok		Nt-1		HI		L17		L16		Sh	
SiO_2	52.26	(0.54)	51.60	(0.54)	52.20	(0.39)	51.53	(0.63)	51.64	(0.44)	52.18	(0.34)	51.88	(0.28)
Al_2O_3	1.25	(0.38)	1.54	(0.49)	1.22	(0.20)	1.50	(0.55)	1.40	(0.50)	1.29	(0.30)	1.38	(0.36)
TiO_2	0.25	(0.04)	0.27	(0.05)	0.25	(0.05)	0.27'	(0.04)'	0.28	(0.06)	0.27	(0.05)	0.22	(0.04)
FeO	21.55	(1.60)	20.05	(1.98)	20.65	(0.77)	20.96	(1.28)	20.92	(1.39)	21.08	(0.69)	20.75	(1.30)
MnO	0.49	(0.06)	0.45	(0.09)	0.49	(0.05)	0.47	(0.08)	0.48	(0.05)	0.49'	(0.03)'	0.47	(0.07)
MgO	22.32	(1.11)	23.34	(1.51)	23.31	(0.77)	23.06	(1.13)	22.29	(1.03)	22.46	(0.56)	22.73	(0.84)
CaO	1.50	(0.18)	1.50	(0.14)	1.46	(0.10)	1.53	(0.11)	1.61	(0.12)	1.62	(0.09)	1.51	(0.12)
Na_2O	0.06'	(0.00)'	nd	nd	nd	nd	nd	nd	nd	nd	nd	nd	nd	nd
NiO	0.12'	(0.00)'	nd	nd	nd	nd	nd	nd	nd	nd	nd	nd	nd	nd
Cr_2O_3	nd	nd	nd	nd	nd	nd	0.15'	(0.01)'	nd	nd	nd	nd	nd	nd
Total	99.64	(0.63)	98.76	(0.42)	99.57	(0.59)	99.32	(0.63)	98.62	(0.43)	99.34	(0.59)	98.94	(0.63)
n	*n = 9*		*n = 22*		*n = 16*		*n = 11*		*n = 11*		*n = 9*		*n = 18*	
Formation	Rt		L8		L7b		L6		L4		L3		L1	
SiO_2	52.53	(0.26)	52.56	(0.47)	52.70	(0.55)	52.50	(0.52)	52.29	(0.60)	53.10	(1.02)	52.69	(0.59)
Al_2O_3	1.00	(0.10)	0.95	(0.14)	0.99	(0.21)	1.23	(0.35)	1.58	(0.70)	1.72	(0.72)	1.19	(0.25)
TiO_2	0.19'	(0.03)'	0.25'	(0.06)'	0.25	(0.03)	0.28	(0.07)	0.29'	(0.06)'	0.23'	(0.09)'	0.23	(0.08)
FeO	19.45	(0.86)	20.07	(1.38)	19.45	(1.01)	19.59	(1.12)	18.82	(1.29)	16.36	(4.13)	19.76	(2.03)
MnO	0.48'	(0.06)'	0.56	(0.08)	0.47	(0.05)	0.46	(0.06)	0.45'	(0.07)'	0.35	(0.09)	0.41	(0.06)
MgO	23.75	(0.66)	23.09	(0.83)	23.99	(0.90)	23.68	(1.00)	23.93	(1.05)	25.69	(2.90)	23.85	(1.49)
CaO	1.71	(0.07)	1.60	(0.28)	1.52	(0.13)	1.60	(0.12)	1.53	(0.14)	1.65	(0.37)	1.34	(0.36)
Na_2O	nd	nd	0.27'	(0.00)'	nd	nd	nd	nd	nd	nd	nd	nd	nd	nd
NiO	nd	nd	nd	nd	nd	nd	nd	nd	nd	nd	nd	nd	0.13'	(0.00)'
Cr_2O_3	nd	nd	0.24'	(0.00)'	nd	nd	nd	nd	nd	nd	0.36'	(0.20)'	0.11'	(0.03)'
Total	99.04	(0.38)	99.09	(0.50)	99.37	(0.55)	99.34	(0.39)	98.81	(0.49)	99.27	(0.61)	99.52	(0.34)
n	*n = 11*		*n = 14*		*n = 13*		*n = 11*		*n = 11*		*n = 14*		*n = 10*	

* All statistics are for core values above detection limit only; values in parentheses are standard deviations. Tephra codes given in text with tephra descriptions. nd = no values above detection limit.

† At least one analysis gave a result below detection limit (not included in these statistics).

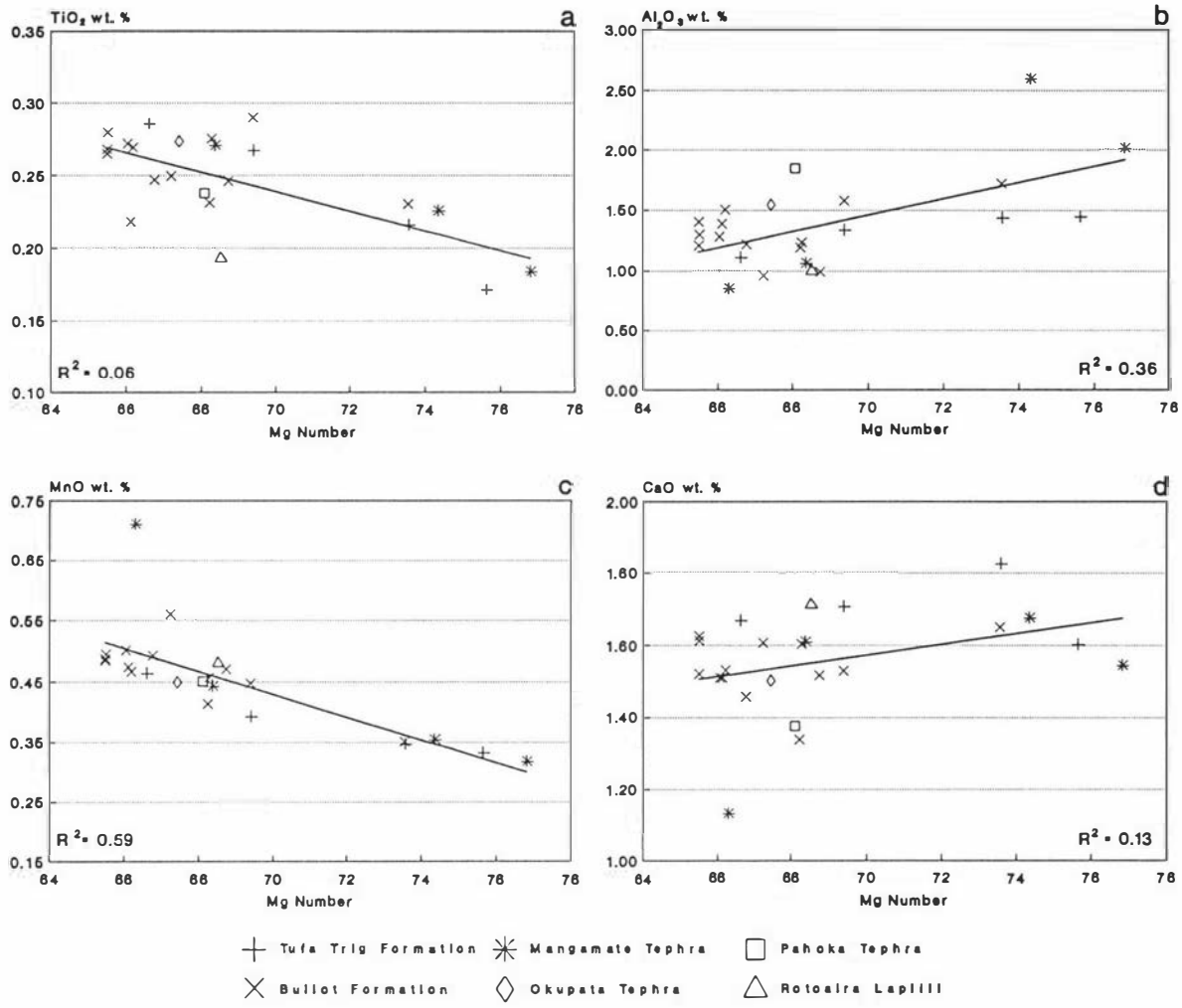

Figure 4.6 Plots of major oxide contents (mean wt.%) *vs* Mg number in orthopyroxene phenocrysts of Tongariro Volcanic Centre tephras.

Tephras sourced from Mt Ruapehu and Mt Tongariro are compared using an x-y scatter plot of MgO *vs* MnO + TiO2 (MGMT scatter plot), mean oxide contents (Al_2O_3, TiO_2, FeO, MnO, MgO, CaO), mean Mg Nº's and mean En%, Fs% and Wo% contents. The oxides selected for comparison are those that recognised major element substitutions in orthopyroxenes suggest are likely to identify compositional differences.

Source

Orthopyroxene compositions in tephras sourced from Mt Ruapehu (Tufa Trig Formation, Okupata Tephra, Bullot Formation) are similar to the Mt Tongariro-sourced tephras (Mangamate Tephra, Pahoka Tephra, Rotoaira Lapilli). No separation of Mt Tongariro and Mt Ruapehu tephras is obtained using an MGMT scatter plot (Figure 4.7, p. 189).

Major element chemistry (Mg Nºand MnO contents) of orthopyroxene phenocrysts does, however, distinguish tephras sourced from TVC and EVC (Figure 4.8, p. 190), in agreement with the findings of Wallace (1987). The similarity in chemistry of some orthopyroxenes from TgVC and TVC tephras, however, prevents clear distinction between these two sources.

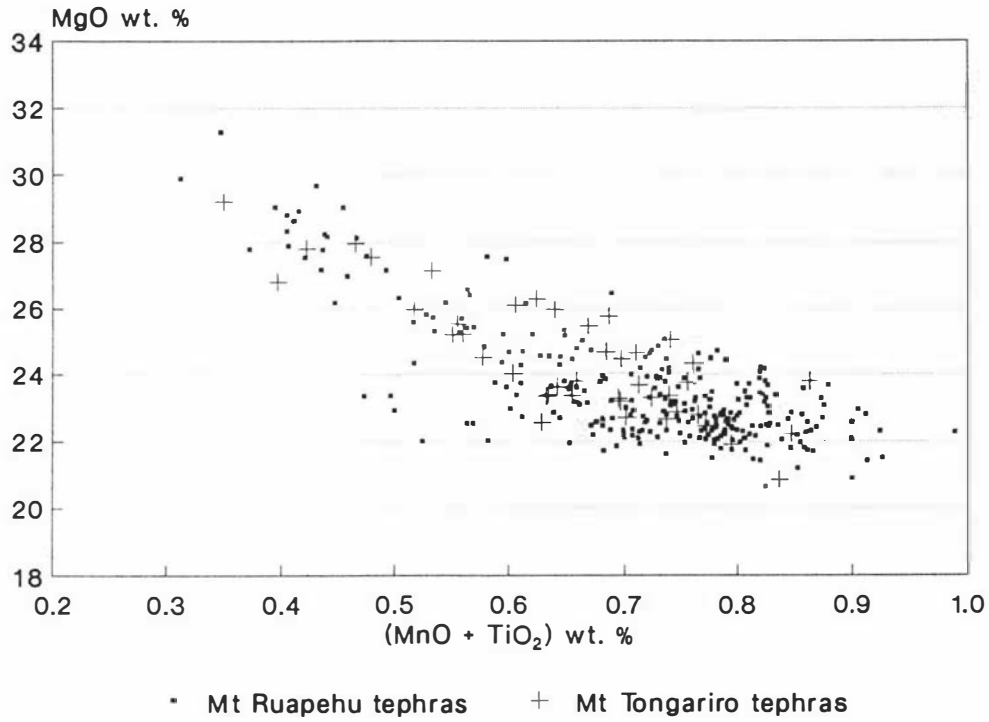

Figure 4.7 MGMT scatter plot showing compositions of orthopyroxene phenocrysts in tephras from Mt Ruapehu and Mt Tongariro, Tongariro Volcanic Centre.

Comparison of Formation and Member Opx-chemistries

Each of the formations, Tufa Trig Formation, Mangamate Tephra, Pahoka Tephra, Okupata Tephra, Bullot Formation and Rotoaira Lapilli, cannot be distinguished by comparing their opx-chemistries. The similarity in the opx-chemistry of the members both within and between these formations also precludes distinction of most members (Figure 4.9, p. 191).

Within Tufa Trig Formation, only members Tf1 and Tf4 are distinguished from one another. In member Tf1, mean MnO and TiO_2 contents are higher, and mean enstatite content (En%) and Mg Nº lower than in member Tf4. In both members, the mean enstatite content and Mg Nº's of their orthopyroxenes are higher than almost all other tephras sourced from Mt Ruapehu.

Within Mangamate Tephra, Waihohonu Lapilli Member is distinguished from the hornblende-dominant Te Rato Lapilli Member by the lower mean MnO and TiO_2 contents, higher mean Al_2O_3 content, and higher mean En% and Mg Nº of its orthopyroxenes. Oturere Lapilli is similarly distinguished from Te Rato Lapilli by the higher mean Al_2O_3 contents and mean Mg Nº of its orthopyroxenes. Only a single analysis was obtained for Poutu Lapilli Member and therefore valid comparisons between the opx-chemistries of this and the other members cannot be made.

While Waihohonu Lapilli and Oturere Lapilli members cannot be distinguished on opx-chemistry, they are distinguished from many other TgVC tephras by the comparatively higher

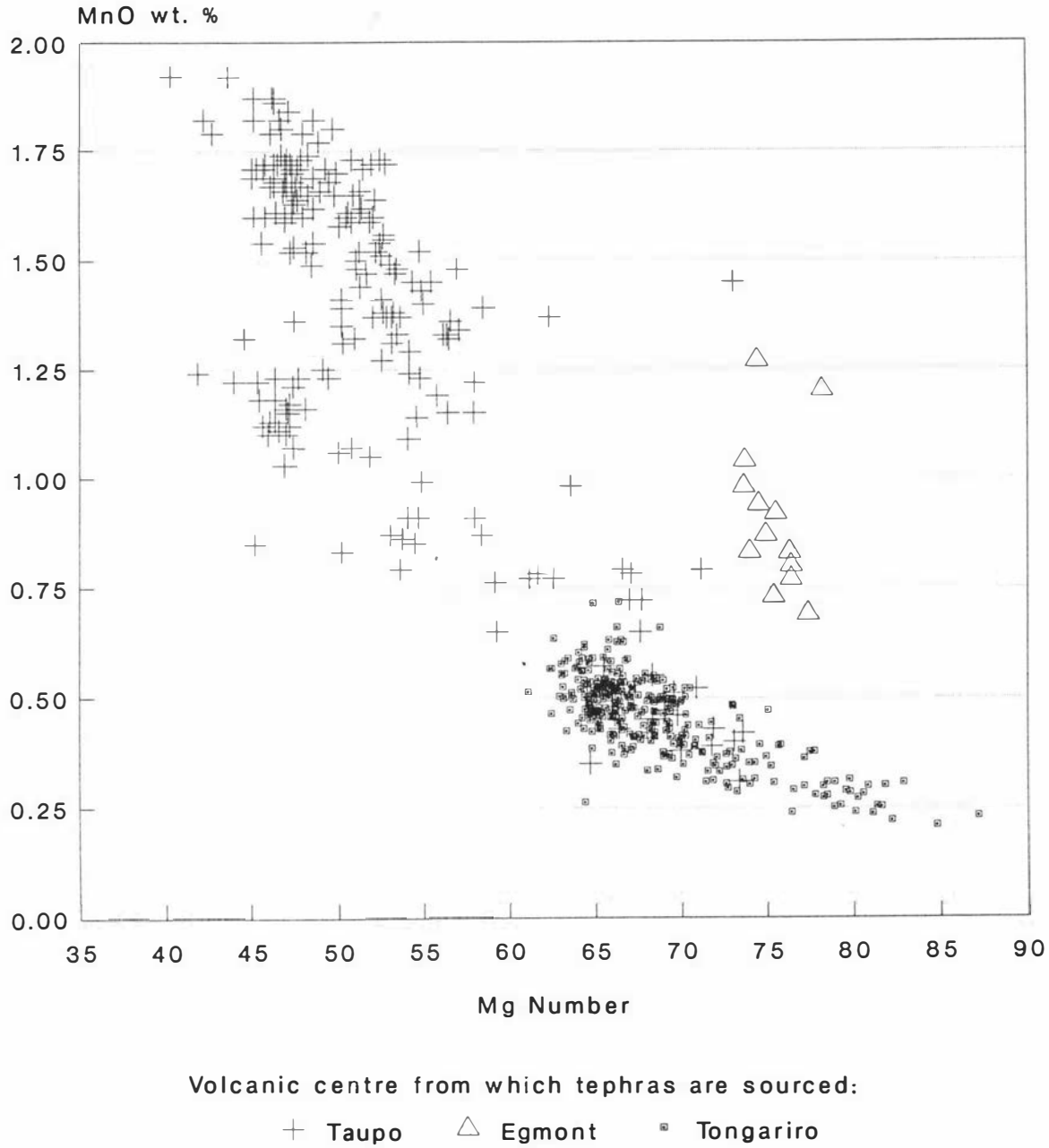

Figure 4.8 Plot of MnO content (wt.%) *vs* Mg number of orthopyroxenes in tephras from Tongariro, Taupo and Egmont volcanic centres. Taupo and Egmont data from Howorth (1976) and Wallace (1987).

mean En% (and Mg Nº's) of their orthopyroxenes (Figure 4.9$_{h,g}$, p. 191). Mean orthopyroxene compositions in both these tephras project as bronzite and probably therefore reflect the presence of dominant forsterite olivine in the ferromagnesian mineral assemblages.

The hornblende-bearing tephras, Te Rato Lapilli and Pahoka Tephra are not distinguished from one another on the opx-chemistry of their orthopyroxenes (Figure 4.9, p. 191). The presence of hornblende in these tephras appears not to be reflected in the chemistry of the orthopyroxene phenocrysts, as these tephras are not distinguished from most other non-hornblende-bearing TgVC tephras on opx-chemistry.

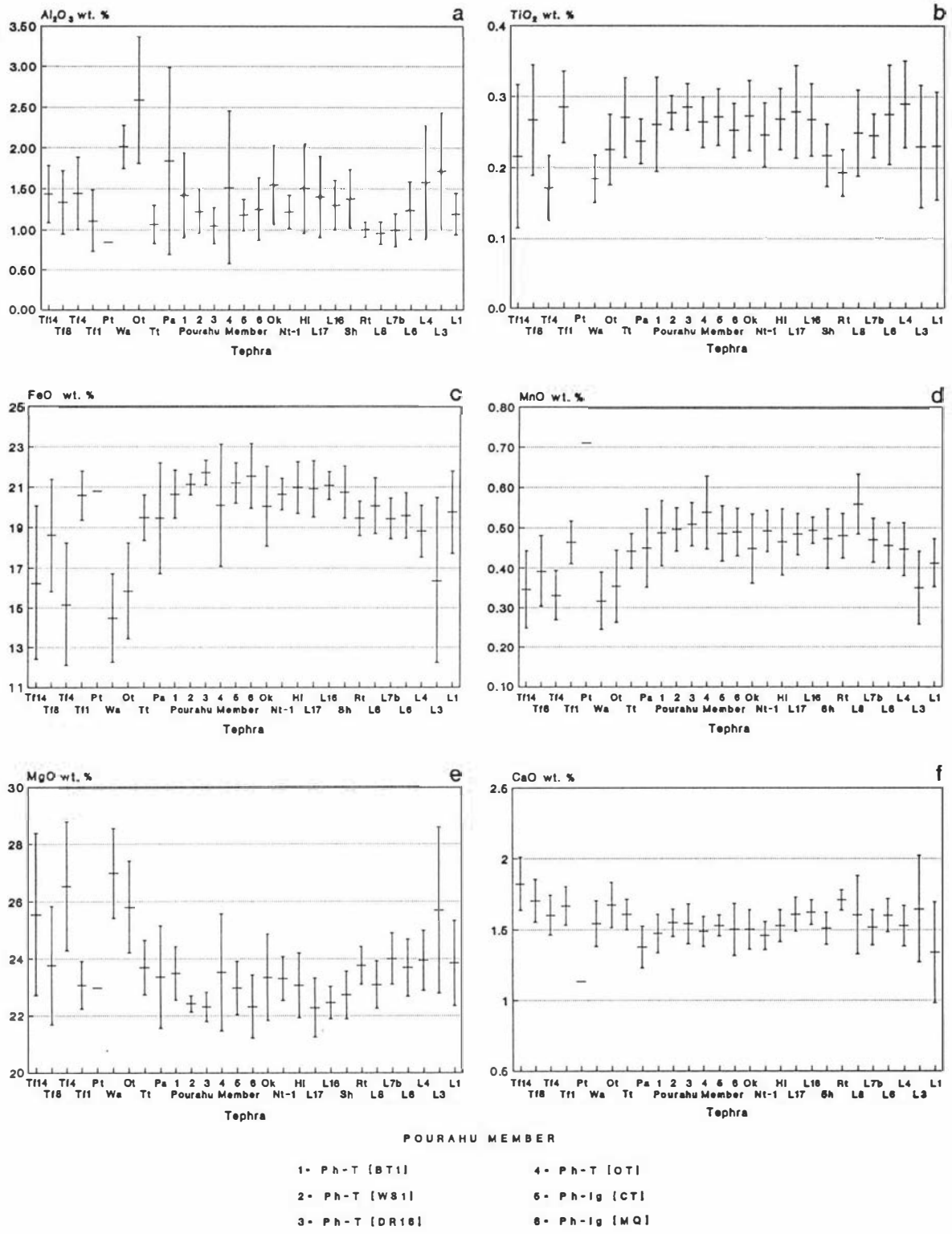

Figure 4.9 Mean oxide contents, Mg numbers (Mg Nº), En% (Enstatite), Fs% (Ferrosilite) and Wo% (Wollastonite) contents in orthopyroxene phenocrysts of Tongariro Volcanic Centre tephras. Bars show standard deviation from mean *(see text for tephra codes; continued ...)*.

Okupata Tephra shows similar orthopyroxene chemistry to most other TgVC tephras (Figure 4.9, p. 191), including Pourahu Member of Bullot Formation which may be a correlative. It is therefore not distinguished on its opx-chemistry.

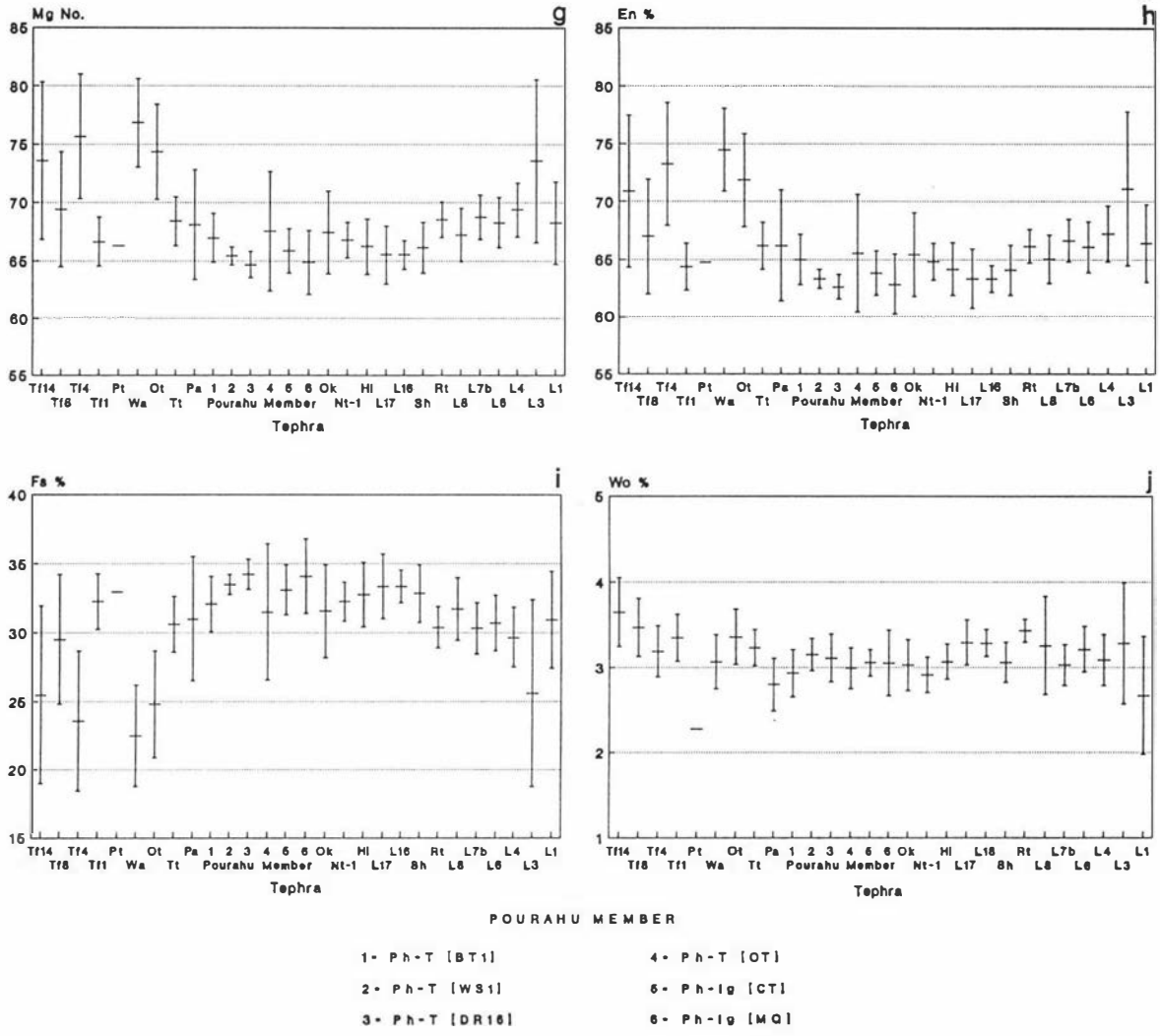

Figure 4.9 Mean oxide contents, Mg numbers (Mg Nº), En% (Enstatite), Fs% (Ferrosilite) and Wo% (Wollastonite) contents in orthopyroxene phenocrysts of Tongariro Volcanic Centre tephras. Bars show standard deviation from mean *(see text for tephra codes; ... continued).*

The opx-chemistry of Rotoaira Lapilli is also not distinctive, and cannot be used to correlate this formation. Rotoaira Lapilli cannot be distinguished from any of the other formations on opx-chemistry (Figure 4.9, p. 191), but is distinguished from the younger Bullot Formation members Ngamatea lapilli-1 and Shawcroft Tephra, and the older Bullot Formation member L7b, on the higher mean CaO content (and Wo%) (Figure 4.9f,j, p. 191) of its orthopyroxenes.

Morphology and Chemistry of Olivine Phenocrysts of Mangamate Tephra, Tongariro Volcanic Centre, New Zealand.

S. L. Donoghue, R. B. Stewart, and A. S. Palmer [4]

Manuscript submitted to *Journal of the Royal Society of New Zealand*

[4] Department of Soil Science, Massey University, Private Bag, Palmerston North, New Zealand.

Abstract

Four members of Mangamate Tephra, erupted *c.* 10 000 years B.P. from Mt Tongariro, are identifiable in tephra sequences of both the Mt Tongariro and Mt Ruapehu ring plains and are morphologically and mineralogically distinct from underlying andesitic tephras derived from Mt Ruapehu. Mangamate Tephra comprises dominantly grey angular lithic lapilli units, contrasting strongly with older and younger, distinctly pumiceous lapilli units from Mt Ruapehu. Three members of Mangamate Tephra contain forsteritic olivine (Fo75–88). Two olivine habits are identified. Type [I] non-skeletal (granular or polyhedral) olivines are subhedral equant to tabular crystals in thin section and occur only in Waihohonu Lapilli Member. Type [II] skeletal olivines are euhedral elongate, incomplete crystals with hollow interiors and hopper and H-shaped chain morphologies. They are found in Poutu Lapilli, Waihohonu Lapilli and Oturere Lapilli members. Type [II] skeletal olivines, not previously reported in Central North Island tephras, provide a useful marker mineral for discriminating Mt Tongariro-sourced from Mt Ruapehu-sourced tephras erupted over this time period.

Ferromagnesian assemblages identified for four members of Mangamate Tephra are:

Opx > Cpx ≫ Ol ± Hb	[Poutu Lapilli]
Ol > Cpx ≫ Opx ± Hb	[Waihohonu Lapilli]
Opx ≫ Cpx > Ol ± Hb	[Oturere Lapilli]
Hb ≫ Opx > Cpx ± Ol	[Te Rato Lapilli]

Olivine morphology and ferromagnesian assemblage are useful for correlation of distal andesitic tephras to member level where field criteria are equivocal. A correlative of Mangamate Tephra known from the Waikato region, previously of uncertain member status, is provisionally identified as Waihohonu Lapilli Member.

Skeletal fo-rich olivine indicates melt supercooling and rapid changes in melt conditions just prior to the eruption of Mangamate Tephra. Comparison of ferromagnesian mineral assemblages in Mangamate Tephra and older tephras of Tongariro Volcanic Centre indicate introduction of new magma into Tongariro Volcanic Centre *c.* 10 000 years B.P.

Keywords: *Andesitic, Tongariro Volcanic Centre, ring plain, olivine, forsteritic, morphology, skeletal, Mangamate Tephra, Poutu Lapilli, Waihohonu Lapilli, Oturere Lapilli, Te Rato Lapilli, correlation, supercooling.*

Introduction

Field studies within TgVC (Figure 4.10, p. 196) have been conducted to establish the tephrostratigraphy and chronology of andesitic and rhyolitic tephra cover beds and laharic deposits of the Mt Ruapehu ring plain, North Island, New Zealand (Figure 4.11, p. 197). The andesitic Mangamate Tephra erupted from Mt Tongariro *c.* 10 000 years B.P., and mapped and described by Topping (1973, 1974), has been correlated with tephra sequences of the Mt Ruapehu ring plain that overlie tephra deposits erupted from Mt Ruapehu. At two reference sections defined by Topping (1973) (Figure 4.10, p. 196), the six named members of Mangamate Tephra are readily identified by their field characteristics, and comprise dominantly grey, angular, andesitic lithic lapilli with minor amounts of poorly vesicular andesitic pumice lapilli. In contrast, older andesitic tephras, principally from Mt Ruapehu, comprise highly vesicular, pumice-dominant lapilli and coarse ash. All the members of Mangamate Tephra have a similar appearance at the two reference sites (Figure 4.10, p. 196). Colour, grain size and thickness relationships, however, vary from site to site especially to the south, and thus are unreliable for the correlation of members at more distant sections. The ferromagnesian mineral assemblages and olivine compositions of four members of Mangamate Tephra (Poutu Lapilli, Waihohonu Lapilli, Oturere Lapilli, Te Rato Lapilli) were determined to assist with correlation of members at these more distant locations. Three of these members contain olivines with forsteritic compositions Fo75 – 88, and distinctive morphologies. Together with other mineralogical and compositional aspects, the morphological characteristics of the olivines, not previously described in tephra deposits from TgVC, provide a means for correlating the members of Mangamate Tephra.

Stratigraphy and Chronology

Mangamate Tephra (previously Mangamate Tephra Formation, Topping 1973) comprises six named tephra members that form a closely spaced sequence of eruptives from Mt Tongariro. In order from youngest to oldest these are Poutu Lapilli, Wharepu Tephra, Ohinepango Tephra, Waihohonu Lapilli, Oturere Lapilli, and Te Rato Lapilli. In the Ruapehu region, Mangamate Tephra underlies Papakai Formation and overlies Karapiti Tephra (dated [NZ4847] at 9910 ± 130 years B.P. [5], Froggatt 1981a) (Figure 4.12, p. 198). Poutu Lapilli has a minimum radiocarbon age of 9560 ± 100 years B.P. [NZ1335] (Topping 1973). Te Rato Lapilli has a maximum age of 9780 ± 170 years B.P. [NZ1372] (Topping 1973).

Sampling and Methods

Four members of Mangamate Tephra (Figure 4.12, p. 198) were sampled from type and reference sections (Figure 4.10, p. 196). The surface of an outcrop was first cleaned off,

[5] All ^{14}C ages discussed in the text are conventional ages in radiocarbon years B.P. based on the old (Libby) half life of 5568 years.

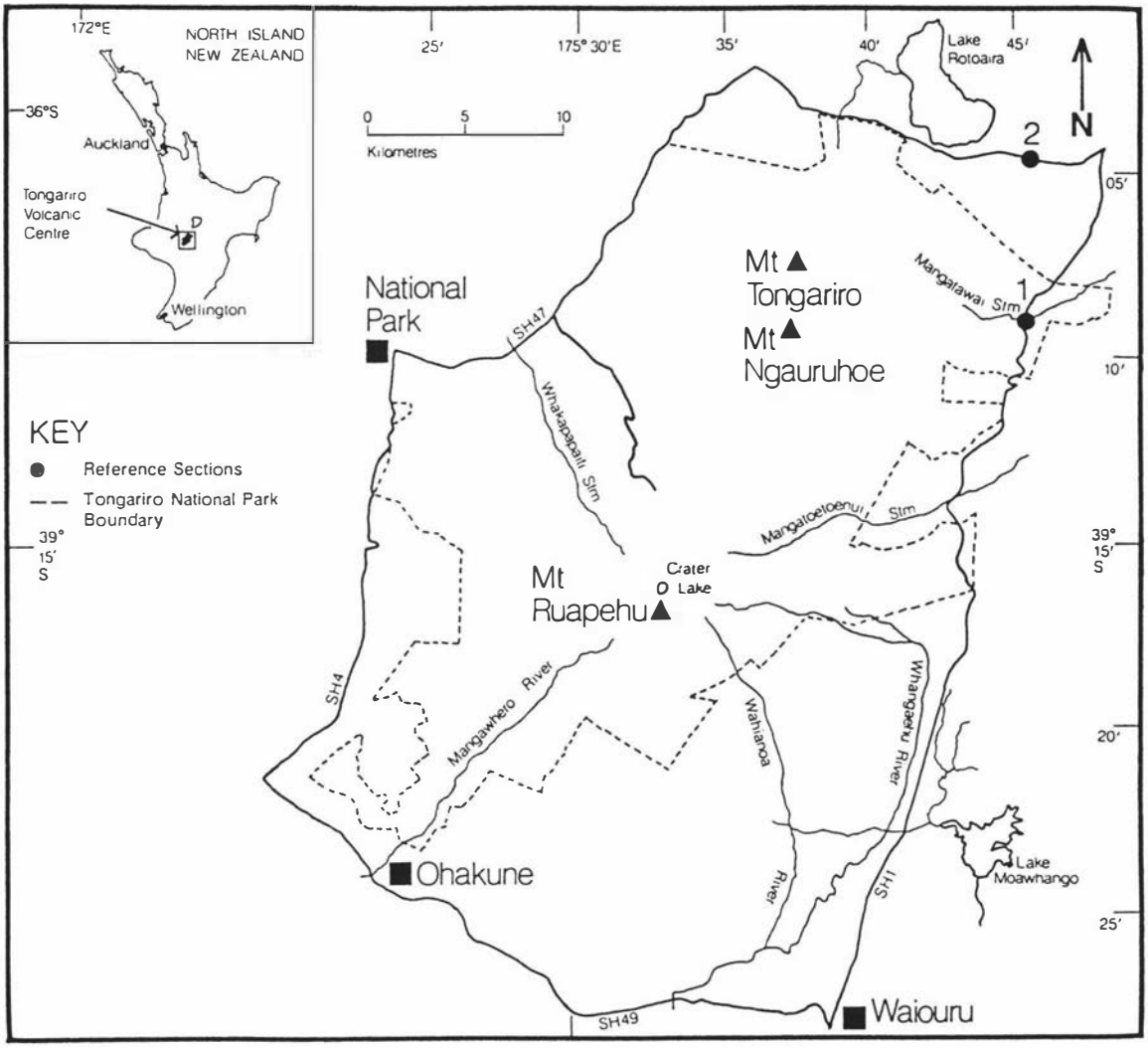

Figure 4.10 Location of Tongariro Volcanic Centre. Numbers denote reference sections (after Topping 1973). (1 = Mangatawai S.; 2 = Poutu S.).

then many small samples were taken along the exposure, avoiding sampling close to the contacts. Samples were cleaned by treatment with acid-oxalate, following the reagent preparation of Blakemore *et al.* (1987). The acid oxalate method was found to give superior cleansing of tephric materials to that of the citrate-dithionite method of Blakemore *et al.* (1987) (B.V. Alloway, pers. comm., 1989), by removing both amorphous and crystalline iron and aluminium. After cleaning, samples were washed thoroughly with water and oven-dried at *c.* 40°C. Pumice lapilli were crushed using an agate mortar and pestle, to free ferromagnesian minerals. Samples were sieved into 0.063 – 0.250 mm fractions. Ferromagnesian minerals were separated using sodium polytungstate [6] with density set at 2.9 g cm^{-3}.

Ferromagnesian minerals were mounted in epoxy resin, thin sectioned, and polished. The ferromagnesian minerals (clinopyroxene, orthopyroxene, olivine, and hornblende) were

[6] Reviews on the use and versatility of this product are found in Callahan (1987), Gregory and Johnston (1987), and Eden and Whitton (1988).

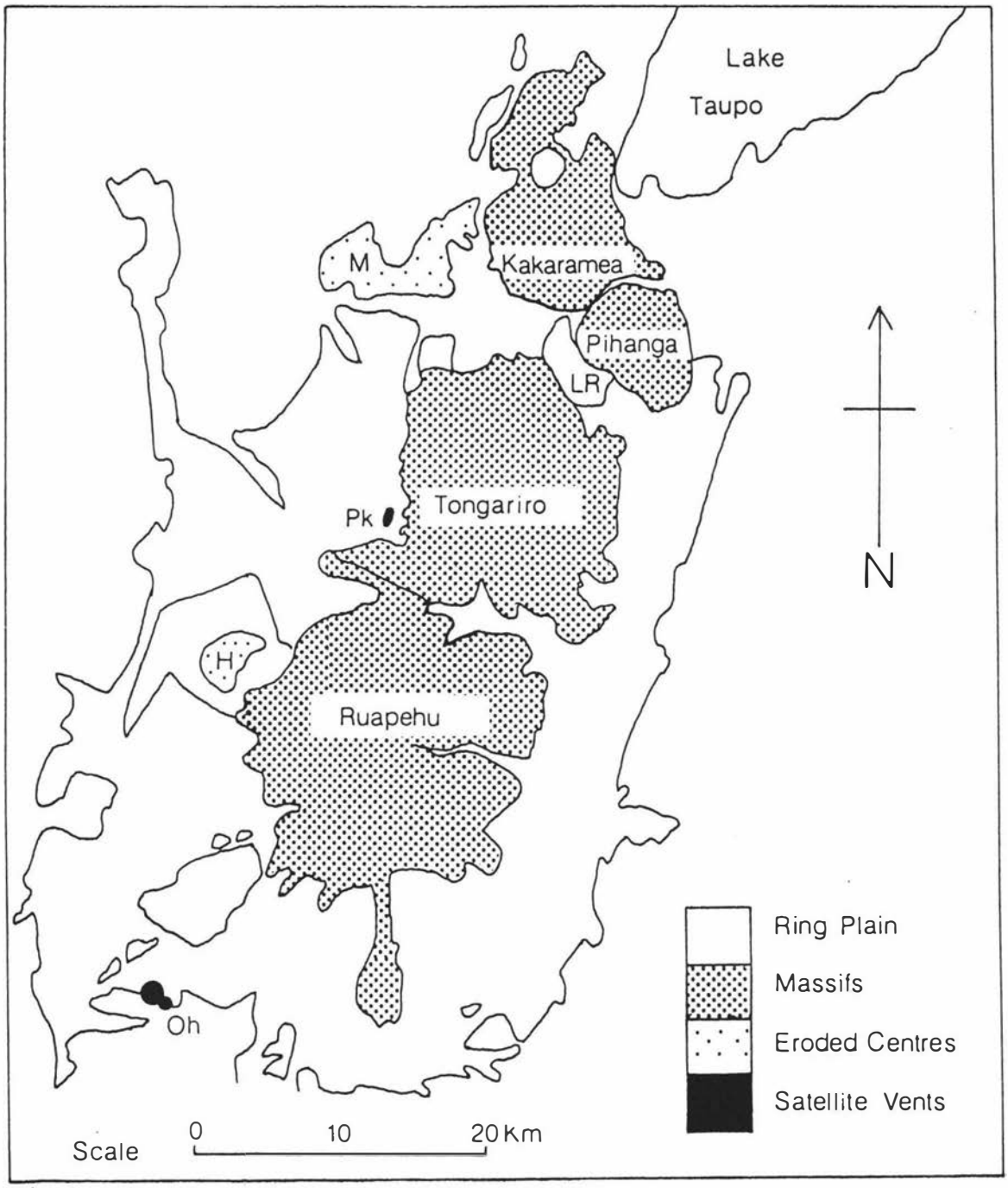

Figure 4.11 Andesite massifs and cones of Tongariro Volcanic Centre, and surrounding ring plains of Mt Ruapehu and Mt Tongariro (adapted from Cole *et al.* 1986).
(M = Maungakatote, Pk = Pukeonake, H = Hauhungatahi, Oh = Ohakune Craters, LR = Lake Rotoaira)

analysed using the JEOL 733 Superprobe at Victoria University of Wellington. Instrument analysing conditions used were a 12 nA beam current at 15 kV and 3 μm beam, and three ten-second peak counts (meaned). Where possible, at least ten analyses were obtained for each of the ferromagnesian minerals in Mangmate tephras, following the recommendations of Froggatt and Gosson (1982).

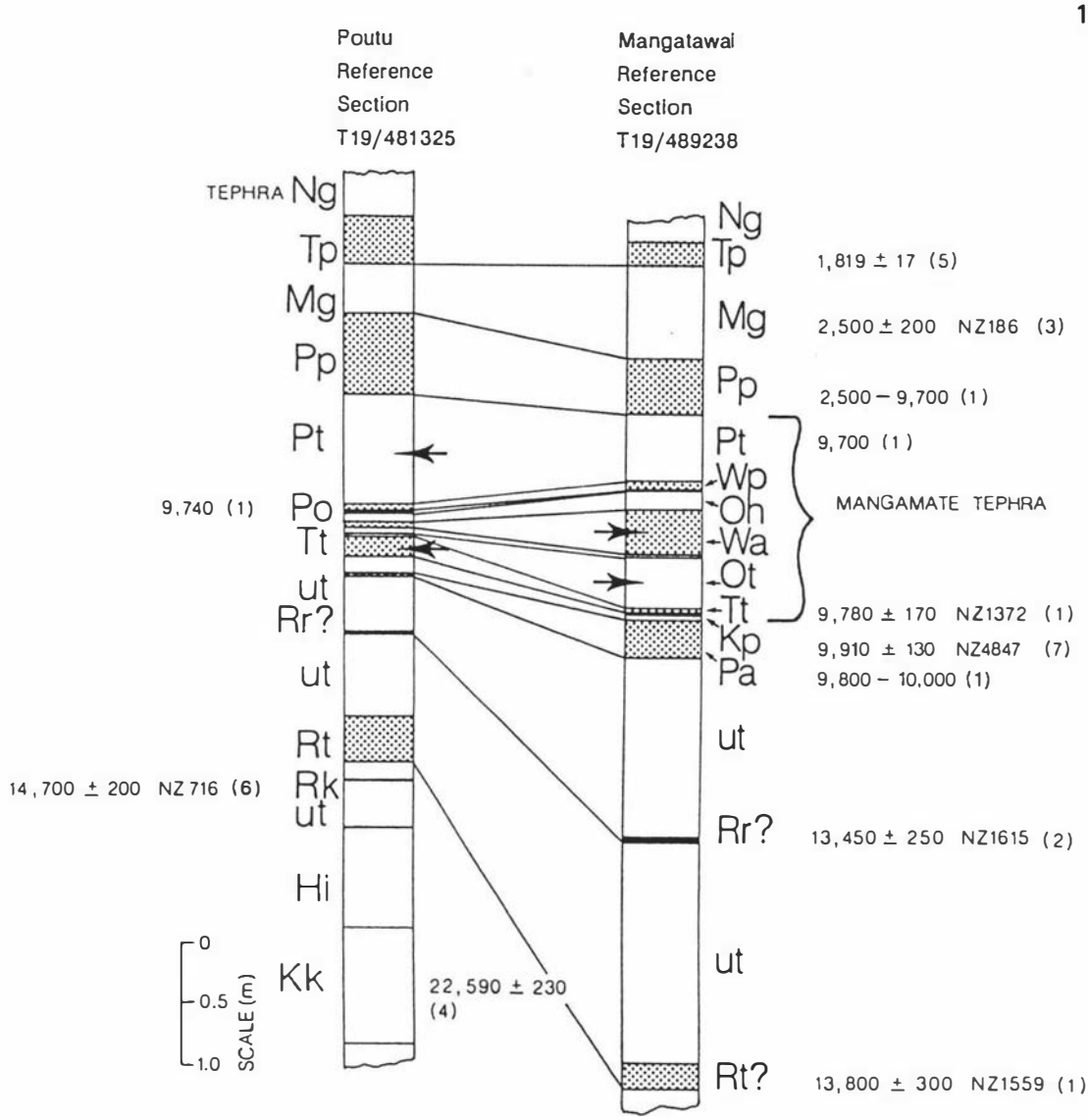

Figure 4.12 Stratigraphic columns of Mangatawai and Poutu reference sections (adapted from Topping 1973, 1974). Grid references based on 1:50 000 NZMS 260 topographic maps, sheets T19 and T20. Arrows indicate units sampled. Tephra ages after:
(1) Topping 1973, 1974 (2) Nairn 1980
(3) Fergusson and Rafter 1959 (4) Wilson *et al.* 1988
(5) Healy 1964 (6) Pullar *et al.* 1973
(7) Froggatt 1981.
Andesitic tephras: Ngauruhoe Tephra [Ng]; Mangatawai Tephra [Mg]; Papakai Formation [Pp]; Mangamate Tephra (members are: Poutu Lapilli [Pt], Wharepu Tephra [Wp], Ohinepango Tephra [Oh], Waihohonu Lapilli [Wa], Oturere Lapilli [Ot], Te Rato Lapilli [Tt]); Pahoka Tephra [Pa]; unnamed tephras [ut]; Rotoaira Lapilli [Rt].
Rhyolitic tephras: Taupo Pumice [Tp]; Poronui Tephra [Po]; Karapiti Tephra [Kp]; Rotorua Tephra [Rr]; Rerewhakaaitu Tephra [Rk]; Kawakawa Formation [Kk].
Hinuera Formation [Hi].

Results

Ferromagnesian Mineral Assemblages

The dominant minerals identified in the four members of Mangamate Tephra are given in Table 4.5 (p. 199). Te Rato Lapilli is readily distinguished from the other members because

it is hornblende dominant (Table 4.5, p. 199) and has only traces of olivine. The other three tephra members (Poutu Lapilli, Waihohonu Lapilli, Oturere Lapilli) contain ≥ 15% olivine with only traces of hornblende (Table 4.5, p. 199). Waihohonu Lapilli can be distinguished from Poutu Lapilli and Oturere Lapilli on the distinctly higher olivine and lower orthopyroxene content.

Table 4.5 Dominant ferromagnesian assemblages of four members of Mangamate Tephra determined by point count of the 0.125–0.250 mm fraction.

Member	Opx.* %	Cpx.* %	Oliv.* %	Hbe.* %	Total Count
Poutu Lapilli	44	41	15	tr.†	200
Waihohonu Lapilli	16	36	48	-	400
Oturere Lapilli	50	28	21	1	400
Te Rato Lapilli	11	6	-	83	400
Uncorrelated ‡	43–44	22–30	26–34	0–1	365

* Opx. = orthopyroxene; Cpx. = clinopyroxene; Oliv. = olivine; Hbe. = hornblende.
† tr (trace) is <1.0%.

‡ Range of modal analysis of three samples of an uncorrelated member of Mangamate Tephra in Waikato lake cores (Lowe 1988, p. 141). Member is provisionally correlated with Waihohonu Lapilli (see text).

Clinopyroxenes within the Mangamate Tephra members fall within the augite, endiopside, diopside and salite fields, and the orthopyroxenes fall within the bronzite and hypersthene fields. Hornblende compositions are dominantly pargasitic hornblende (Table 4.6, p. 200).

Morphology of Olivine

Olivine phenocrysts were examined in thin section and as grain mounts. Two olivine crystal habits were identified.

Type [I] olivines are euhedral to subhedral, equant to tabular crystals and are equivalent to the polyhedral and granular categories of Donaldson (1976). These olivines have characteristic high optical relief (Plate 4.2a) with compositions Fo82–88 (Figure 4.13, p. 201).

Type [II] olivines are euhedral elongate crystals (Plates 4.2b–f) and are classified as skeletal, after Drever and Johnston (1957) and Fleet (1975). Lofgren (1974) defines skeletal crystals as elongated, incomplete crystals with hollow interiors. Most of the phenocrysts observed in grain mounts and thin section show the primitive skeletal morphology of Drever and Johnston (1957) (Plates 4.2b,c), the porphyritic morphology of Donaldson (1974), and the hopper (hollow skeletal habit) and H-shaped chain morphologies of Donaldson (1976)

Table 4.6 Electron microprobe analyses (meaned) of clinopyroxene, orthopyroxene, and hornblende in members of Mangamate Tephra.*

Analysis	Poutu Lapilli Opx.†	Waihohonu Lapilli Opx.†	Oturere Lapilli Opx.†	Te Rato Lapilli Opx.†	Poutu Lapilli Cpx.†	Waihohonu Lapilli Cpx.†	Oturere Lapilli Cpx.†	Te Rato Lapilli Cpx.†	Te Rato Lapilli Hbe.†
SiO_2	52.72	53.10	52.59	52.91	52.38	52.24	50.87	51.53	42.87
Al_2O_3	0.84	2.01	2.59	1.06	2.23	1.67	3.65	2.24	11.23
TiO_2	nd	0.18	0.23	0.27	0.24§	0.22§	0.44	0.48	1.64
FeO‡	20.79	14.48	15.85	19.49	5.91	5.17	7.55	8.84	14.19
MnO	0.71	0.32	0.36	0.44	0.20§	0.19§	0.21§	0.26§	0.44§
MgO	22.98	26.98	25.81	23.68	16.95	17.19	15.66	15.13	12.79
CaO	1.13	1.54	1.67	1.61	21.33	21.76	21.20	20.83	10.92
Na_2O	nd	nd	nd	nd	0.22§	0.23§	0.28§	0.25§	1.63
K_2O	nd	nd	nd	nd	nd	nd	nd	nd	0.38
NiO	nd	nd	nd	nd	nd	nd	nd	nd	nd
Cr_2O_3	nd	nd	0.16§	nd	0.39§	0.62§	0.19§	0.89§	nd
Total	99.18	98.61	99.11	99.47	99.55	99.04	99.82	99.45	96.06
n	*n* = 1	*n* = 5	*n* = 9	*n* = 16	*n* = 28	*n* = 19	*n* = 14	*n* = 9	*n* = 28
Cations on the basis of 6 oxygens (Opx, Cpx) and 23 oxygens (Hbe)									
Si	1.969	1.938	1.924	1.962	1.930	1.935	1.886	1.924	6.448
Al	0.037	0.087	0.111	0.046	0.097	0.073	0.160	0.099	1.991
Ti	nd	0.005	0.006	0.008	0.007§	0.006	0.012	0.014	0.186
Fe‡	0.650	0.442	0.486	0.604	0.182	0.160	0.234	0.276	1.785
Mn	0.022	0.010	0.011	0.014	0.006§	0.006§	0.007§	0.008	0.056
Mg	1.279	1.468	1.407	1.308	0.931	0.949	0.866	0.842	2.868
Ca	0.045	0.060	0.066	0.064	0.842	0.863	0.842	0.833	1.760
Na	nd	nd	nd	nd	0.016§	0.016§	0.020§	0.018	0.476
K	nd	nd	nd	nd	nd	nd	nd	nd	0.073
Ni	nd	nd	nd	nd	nd	nd	nd	nd	nd
Cr	nd	nd	0.006§	nd	0.012§	0.018§	0.006§	0.027	nd
Total	4.004	4.010	4.011	4.006	4.009	4.017	4.024	4.002	15.638

* All values are for core values above detection limit only; nd = no values above detection limit.
† Opx. = orthopyroxene; Cpx. = clinopyroxene; Hbe. = hornblende.
‡ All Fe measured as FeO.
§ At least one analysis gave a result below detection limit; mean is for those above detection limit only.

(Plates 4.2c,e,f). Fewer examples of the lantern and chain habit of Fleet (1975) are seen only in thin section (Plate 4.2d), where various shapes can be seen depending on the phenocryst orientation. The skeletal olivine phenocrysts in the Mangamate tephras rarely show embayments, and hence have more complete outlines than the hopper olivines shown in Donaldson (1976).

These skeletal phenocrysts show straight extinction and display stepped terminations in grain mounts (Plate 4.2e,f). The phenocrysts show inclusions of pale orange to colourless glass (seen in crystal centres in Plate 4.2e,f) which are best observed in thin section. These inclusions may be discrete and joined. Centrally located inclusions in skeletal olivines are attributed to rapid elongation or edge growth principally along the *a*-axis. They are a persistent characteristic of forsteritic olivines, and possibly represent the original magma from which the olivines have crystallised (Drever and Johnston 1957).

Olivine phenocrysts within the Poutu Lapilli, Oturere Lapilli, and Te Rato Lapilli members comprise only skeletal olivines. In contrast, both skeletal (type [II]) and non-skeletal (type [I])

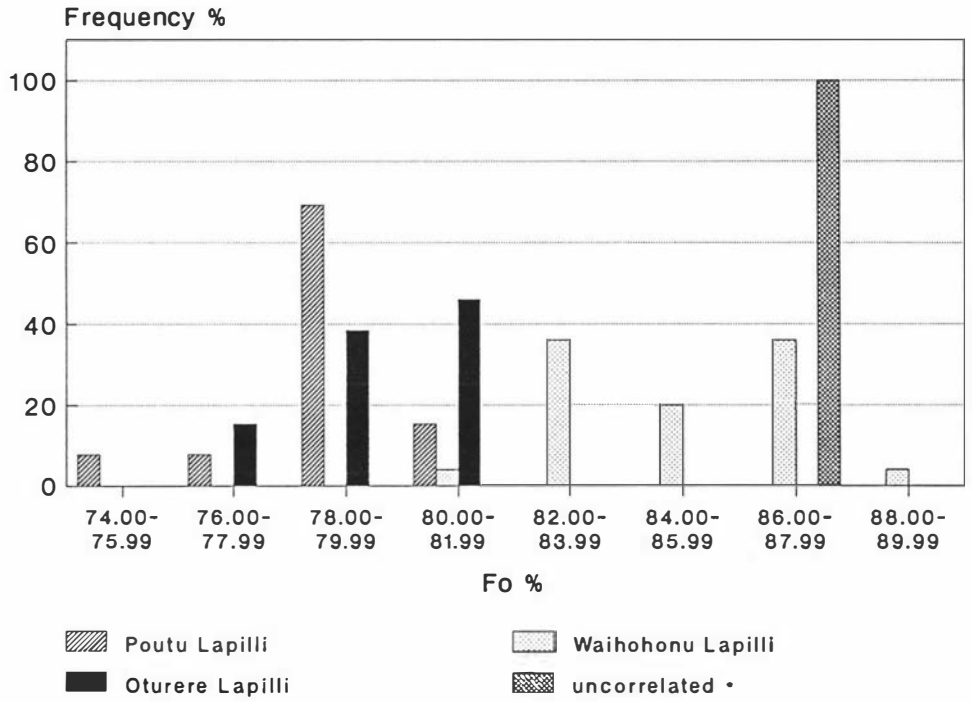

Figure 4.13 Olivine compositions in Mangamate tephras. (* Data from Lowe 1987, p. 118; member provisionally correlated with Waihohonu Lapilli *(see text)*; Fo% = Forsterite %).

olivines are found in Waihohonu Lapilli. Dominance of either type [II] or type [I] olivine is strongly dependent on grain size, with skeletal type [II] olivines dominant in the finer 0.125 – 0.250 mm fraction (Table 4.7, p. 202). The 'two-olivine' morphology of Waihohonu Lapilli readily distinguishes this tephra from the other members analysed.

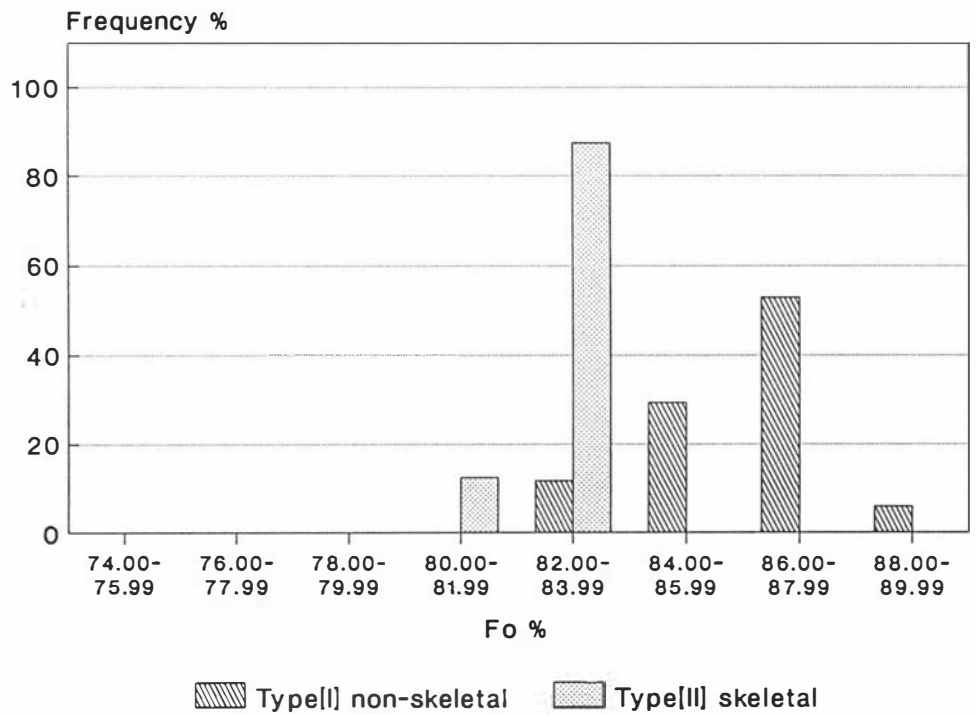

Figure 4.14 Compositions of type [I] non-skeletal and type [II] skeletal olivines in Waihohonu Lapilli Member, Mangamate Tephra. (Fo% = Forsterite %).

Table 4.7 Dominant olivine morphology of four members of Mangamate Tephra.

Tephra Member	Sieve Fraction	Eu-subhedral Type [I] Olivine %	Skeletal Type [II] Olivine %
Poutu Lapilli	0.125–0.250 mm	-	100
Waihohonu Lapilli	0.250–0.500 mm	98	2
Waihohonu Lapilli	0.125–0.250 mm	37	63
Oturere Lapilli	0.125–0.250 mm	-	100

Chemistry of Olivine

All olivine phenocrysts of the Poutu Lapilli, Waihohonu Lapilli, and Oturere Lapilli members are forsteritic (Fo75–88) (Figure 4.13, p. 201) as determined by electron microprobe analysis of olivine phenocrysts extracted from pumice lapilli (Table 4.8, p. 203). The chemistry of the olivines within Te Rato Lapilli has not been determined because of their rarity. The olivines are not zoned (as shown by both optical and back-scatter electron imagery and comparison of core and rim analyses).

Waihohonu Lapilli Member can be distinguished from the Poutu Lapilli and Oturere Lapilli members on the higher forsterite values of almost all olivine phenocrysts (Table 4.8, p. 203; Figure 4.13, p. 201). Within Waihohonu Lapilli, type [I] olivines with compositions of Fo82–88 differ from type [II] olivines which have compositions of Fo80–84 (Figure 4.14, p. 201; Table 4.8, p. 203). The Poutu Lapilli and Oturere Lapilli members cannot be distinguished by olivine chemistry (Figure 4.13, p. 201) or morphology.

Discussion

Variations in morphology of magnesium-rich olivines within basaltic igneous rocks and magmatic conditions giving rise to them have been investigated by Drever and Johnston (1957), Donaldson (1974, 1976), and Fleet (1975). Cooling rate and degree of melt supercooling, temperature at which nucleation takes place in the supercooled melt, melt viscosity, melt composition, and water content of the melt are the principal factors controlling the habit of crystallising olivine (Donaldson 1974, 1976; Fleet 1975). Several different habits are recognised: equant, tabular, skeletal, acicular, and dendritic (Fleet 1975). Ten morphological categories identified by Donaldson (1976) form a continuum in habit and show systematic change in morphology from complete (equant) to progressively less complete and elongated (skeletal, dendritic) crystals with increasing cooling rate and degree of supercooling. Equant morphologies result from crystallisation at near-equilibrium conditions (Fleet 1975). The 'skeletal' habit of magnesium-rich olivines results from structurally controlled preferential growth (elongation) in the direction of the *c* and *a* axes at lower cooling rates (Fleet 1975), with elongation more pronounced with greater degree of supercooling (Donaldson 1976).

Table 4.8 Electron microprobe analyses (means) of olivine in members of Mangamate Tephra.*

	Uncorrelated Member [#]			Poutu Lapilli		Waihohonu Lapilli						Oturere Lapilli	
	1	2a (core)	2b (rim)	Type [II]†		Types [I] + [II]†		Type [I]†		Type [II]†		Type [II]†	
SiO_2	39.39	39.25	39.31	38.46	(0.41)	38.91	(0.34)	39.04	(0.30)	38.63	(0.26)	38.43	(0.31)
Al_2O_3	0.02	0.01	0.02	nd	nd	0.07§	(0.00)§	0.07§	(0.00)§	nd	nd	0.07§	(0.00)§
TiO_2	0.04	0.05	0.04	nd	nd	nd	nd	nd	nd	nd	nd	nd	nd
FeO‡	13.14	12.98	13.03	19.45	(0.90)	14.23	(1.68)	13.43	(1.32)	15.92	(0.93)	19.09	(1.10)
MnO	0.18	0.20	0.22	0.30	(0.05)	0.25§	(0.07)§	0.24§	(0.08)§	0.26§	(0.04)§	0.32	(0.05)
MgO	47.36	46.88	46.85	41.47	(1.02)	44.99	(1.30)	45.63	(0.97)	43.64	(0.73)	41.36	(1.00)
CaO	0.15	0.16	0.15	0.17	(0.02)	0.17	(0.02)	0.16	(0.01)	0.19	(0.03)	0.16	(0.02)
Na_2O	-	0.05	0.01	nd	nd	nd	nd	nd	nd	nd	nd	nd	nd
K_2O	0.01	0.02	-	nd	nd	nd	nd	nd	nd	nd	nd	nd	nd
NiO	0.18	0.16	0.18	nd	nd	0.20§	(0.05)§	0.21§	(0.05)§	0.16§	(0.00)§	nd	nd
Cr_2O_3	0.06	0.04	0.05	nd	nd	0.17§	(0.02)§	nd	nd	0.17§	(0.02)§	nd	nd
Total	100.53	99.80	99.86	99.84	(0.76)	98.59	(0.47)	98.55	(0.54)	98.69	(0.26)	99.36	(0.72)
n				*n* = 13		*n* = 25		*n* = 17		*n* = 8		*n* = 13	
Cations on the basis of 4 oxygens													
Si	0.979	0.982	0.983	0.990	(0.005)	0.989	(0.003)	0.989	(0.002)	0.989	(0.003)	0.992	(0.004)
Al	0.001	-	0.001	nd	nd	0.002§	(0.000)§	0.002§	(0.000)§	nd	nd	0.002§	(0.000)§
Ti	0.001	0.001	0.001	nd	nd	nd	nd	nd	nd	nd	nd	nd	nd
Fe‡	0.273	0.272	0.272	0.419	(0.022)	0.303	(0.037)	0.286	(0.029)	0.341	(0.022)	0.412	(0.026)
Mn	0.004	0.004	0.005	0.006	(0.001)	0.005§	(0.002)§	0.005§	(0.002)§	0.006§	(0.001)§	0.007	(0.001)
Mg	1.754	1.748	1.746	1.590	(0.027)	1.704	(0.037)	1.723	(0.028)	1.665	(0.021)	1.591	(0.026)
Ca	0.004	0.004	0.004	0.004	(0.001)	0.005	(0.001)	0.004	(0.000)	0.005	(0.001)	0.005	(0.001)
Na	-	0.002	-	nd	nd	nd	nd	nd	nd	nd	nd	nd	nd
K	-	0.001	-	nd	nd	nd	nd	nd	nd	nd	nd	nd	nd
Ni	0.003	0.003	0.004	nd	nd	0.004§	(0.001)§	0.004§	(0.001)§	0.003§	(0.000)§	nd	nd
Cr	0.001	0.001	0.001	nd	nd	0.002§	(0.002)§	nd	nd	0.002§	(0.002)§	nd	nd
Total	3.020	3.018	3.017	3.010	(0.005)	3.008	(0.003)	3.008	(0.003)	3.007	(0.003)	3.006	(0.003)
Fo %	0.865	0.865	0.865	79.153	(1.149)	84.888	(1.838)	85.771	(1.413)	83.012	(1.068)	79.423	(1.302)

* Values presented are means for core values above detection limit, with standard deviations in parentheses; nd = no values above detection limit.

† Type [I] = non-skeletal olivine; type [II] = skeletal olivine.

‡ All Fe measured as FeO.

§ Some analyses gave results below detection limit; mean and standard deviation are for those above detection limit only.

Data from Lowe (1987, p. 118), not meaned; member provisionally correlated with Waihohonu Lapilli (see text).

Melt Conditions for Mangamate Tephras

Waihohonu Lapilli contains two populations of olivine (type [I] and type [II]), with different compositions. This suggests that the olivines were not crystallised from the same magma, but were probably derived by mixing of two magmas with different compositions. The presence of occasional grey and white colour-banded pumices in the tephras supports an origin by magma mixing.

The differing Fo values and crystal habits of type [I] and type [II] olivines indicate that they probably crystallised under differing conditions. The non-skeletal type [I] olivines are inferred to have crystallised from a less basic melt (lower Fo) than type [II] olivines, and at

equilibrium. In contrast, the skeletal type [II] olivines crystallised from a rapidly chilled, more basic melt.

One possible scenario accounting for these observations is as follows. The olivine textural and compositional relationships arose through the intrusion of a more basic magma into an existing zoned magma chamber. Zoning is evidenced by the occurrence of banded light and dark pumice in the Mangamate tephras. The type [I] olivine is thought to be associated with the basic end member of the zoned magma chamber. Subsequent intrusion into this zoned magma body by a hotter, more basic melt, induced supercooling in the intruding magma, and resulted in the crystallisation of skeletal olivine (Sparks *et al.* 1977; Nixon 1988). The habit of the skeletal olivine is consistent with 10 – 80°C of undercooling (Donaldson 1976). This rapid crystallisation occurred prior to physical mixing of the two magmas, the latter process giving rise to the mixed population of olivine present in Mangamate Tephra. The absence of compositional zoning and resorbtion textures in the olivines indicates that mixing was a rapid process and that it occurred immediately prior to eruption.

On the Mt Ruapehu ring plain, Mangamate Tephra overlies tephras principally erupted from Mt Ruapehu, which generally do not contain olivine in the ferromagnesian assemblages. One older lapilli unit from Mt Ruapehu, dated *c.* 11 000 years B.P. does, however, contain skeletal olivine. Thus, although skeletal olivine is characteristic of three members of Mt Tongariro-derived Mangamate Tephra, it is not unique to these tephras. The occurrence of abundant olivine principally within Mangamate Tephra, however, suggests an input of new magma coincident with, or just prior, to its eruption *c.* 10 000 years B.P.

Implications for Correlation of Distal Mangamate Tephras

Lowe (1987, 1988a) and Lowe *et al.* (1980), in determining the stratigraphy and chronology of tephras preserved within sediment cores taken from lakes in the central Waikato region, correlated an andesitic tephra layer to TgVC source using chemical composition of ferromagnesian minerals, titanomagnetites, andesitic glass, and stratigraphic position. The tephra is estimated to be *c.* 9950 years old based on three radiocarbon dates: 10 120 ± 100 [Wk213], 10 000 ± 120 [Wk232], and 9700 ± 140 [Wk231] years B.P. (Hogg *et al.* 1987; Lowe 1988a). The ferromagnesian assemblage comprises augite + olivine + hypersthene. The tephra layer was correlated with Mangamate Tephra. Its member status was regarded as uncertain, but it was provisionally correlated with Te Rato Lapilli Member based on its dark colour (Lowe *et al.* 1980). This member of Mangamate Tephra contains 26 – 34% forsteritic olivine by modal analysis of the ferromagnesian assemblage of three samples (Table 4.5, p. 199). Electron microprobe analyses of olivine from this tephra in Lake Rotomanuka are reproduced from Lowe (1987) in Table 4.8 (p. 203).

The analysis of Te Rato Lapilli Member from Poutu R.S. (Figure 4.10, p. 196; Figure 4.12, p. 198) shows the ferromagnesian assemblage to be hornblende dominant (Table 4.5, p. 199), with only traces of olivine in the 0.125 – 0.063 mm fraction. It is therefore suggested that the Mangamate Tephra member identified in the Waikato lakes is not a correlative of Te Rato Lapilli Member, but is more likely to be one of the three other members (Poutu Lapilli, Waihohonu Lapilli, Oturere Lapilli) analysed in this paper.

Comparison of the olivine phenocryst chemistry of the Mangamate Tephra correlative at Lake Rotomanuka (Lowe 1987; Table 4.8, p. 203) with Poutu Lapilli, Waihohonu Lapilli, and Oturere Lapilli (Table 4.8, p. 203) shows that it most closely resembles that of Waihohonu Lapilli Member. FeO, MgO, and NiO contents resemble those of type [I] non-skeletal olivines of Waihohonu Lapilli Member. In addition, fo values for olivine analyses from Mangamate Tephra in the Waikato lakes (Table 4.8, p. 203; Figure 4.13, p. 201) match the Waihohonu Lapilli type [I] olivines rather than the type [II] olivines of Poutu Lapilli and Oturere Lapilli. Ferromagnesian mineral assemblage, olivine morphology and olivine major element chemistry together suggest that the distal deposit in the Waikato lakes is a correlative of Waihohonu Lapilli Member of Mangamate Tephra.

Isopachs of Waihohonu Lapilli, especially in areas north of TgVC, are now required to help verify the correlation, but these have not been published.

Conclusions

(1) Four named members of Mangamate Tephra, derived from Mt Tongariro (Topping 1973) are mineralogically distinct from enclosing Mt Ruapehu derived tephras, allowing correlation and identification of a *c.* 10 000 years B.P. time plane within the TgVC tephra succession.

(2) Skeletal olivine (type [II]) morphology is characteristic of three members of Mangamate Tephra: Poutu Lapilli, Waihohonu Lapilli, and Oturere Lapilli members. Waihohonu Lapilli also contains euhedral – subhedral olivine (type [I]). Olivine morphology and major element chemistry can thus be used to distinguish between olivine bearing members of Mangamate Tephra.

(3) This paper documents the potential of phenocryst morphology for use as a valuable and confident means of correlating distal andesitic tephras to member level where field morphology of tephras is not diagnostic.

(4) Olivine morphology (as an indicator of melt conditions) and olivine chemistry, suggest changes in melt chemistry coincident with the *c.* 10 000 years B.P. eruption of Mangamate Tephra from Mt Tongariro.

Acknowledgements

The authors wish to thank Dr J. Gamble (Victoria University Research School of Earth Sciences) for a thoughtful and thorough review of an early version of this manuscript. We also thank colleagues Dr V.E. Neall and Dr R.C. Wallace (Massey University) for their helpful discussions. One of the authors (SLD) especially thanks Dr D.J. Lowe (University of Waikato) for providing his olivine analyses, and the time and effort generously given in reviewing this manuscript; and Mr K. Palmer, Dr J. Gamble and Dr P.C. Froggatt (Victoria University Research School of Earth Sciences) for providing access to the electron microprobe and assistance with analysis procedures.

Research funds for one of the authors (SLD) were provided in part by a Helen E. Akers Scholarship and the Ministry of Civil Defence.

Olivine

Olivine Morphology and Major Element Chemistry of Other Tongariro Volcanic Centre Tephras

Mt Tongariro Tephras

Skeletal olivine has been identified as a dominant ferromagnesian mineral in three Mangamate Tephra members (Poutu Lapilli, Waihohonu Lapilli, Oturere Lapilli) and is also identified in trace amounts within the <0.125 mm fractions of Wharepu Tephra and Ohinepango Tephra (also of Mangamate Tephra), and Pahoka Tephra. Non-skeletal olivine is identified in trace amounts in the older Rotoaira Lapilli, and has compositions of Fo86 – 82.

Major element analyses of olivines from all TgVC tephras are presented in Appendix IIId. Mean analyses are given in Table 4.9 (p. 208).

Mt Ruapehu Tephras

Olivine has been identified in Shawcroft Tephra, member L3, and Pourahu Member [tephra unit] of Bullot Formation, and Okupata Tephra. It occurs in significant quantities in both Shawcroft Tephra and member L3, and in trace amounts in Okupata Tephra and Pourahu Member. Olivine occurs as phenocrysts with both skeletal and non-skeletal habits.

All olivines in Shawcroft Tephra are skeletal in habit with compositions Fo81-74. All olivines in member L3 are non-skeletal in habit with compositions Fo84 – 81. A non-skeletal olivine phenocryst in Pourahu Member [tephra unit] of Bullot Formation has a composition of Fo82.

Hackett (1985) identified forsteritic olivine, Fo94 – 67 (Figure 4.2a, p. 176), in Mt Ruapehu lavas spanning the entire compositional range from basalt to dacite. Olivines in the acid andesites and dacites are xenocrysts (Hackett 1985; Graham and Hackett 1987).

Olivine Chemistry

In the olivines, the FeO and MgO contents of olivine cores are the most variable [7] with some of the tephras showing up to 6 wt.% variation in these elements between analyses. This variation is reflected in the higher than usual standard deviations on these elements. In Rotoaira Lapilli the large standard deviations are due in part to the small number of analyses obtained for this tephra.

NiO, Al_2O_3 and Cr_2O_3 occur in minor amounts in some olivines. Plots of the oxide contents MnO and CaO *vs* Fo% values of all phenocrysts show MnO contents in the olivines

---

[7] The minerals of the olivine group show complete diadochy between the atomic pairs Mg and Fe^{+2}, and Fe^{+2} and Mn, *i.e.* between forsterite, Mg_2SiO_4, and fayalite, Fe_2SiO_4, and between fayalite and tephroite, Mn_2SiO_4 (Deer *et al.* 1966).

Table 4.9 Electron microprobe analyses (meaned) of olivine in andesitic tephras of Tongariro Volcanic Centre.*

Formation	Poutu Lapilli		Waihohonu Lapilli		Oturere Lapilli		Pourahu Member [tephra unit] [OT]		Shawcroft Tephra		Rotoaira Lapilli		Member L3	
SiO_2	38.46	(0.41)	38.91	(0.34)	38.43	(0.31)	39.02	(0.00)	37.88	(0.37)	38.92	(0.55)	38.89	(0.29)
Al_2O_3	nd	nd	0.07 †	(0.00) †	0.07 †	(0.00) †	nd	nd	0.05 †	(0.02) †	nd	nd	0.07 †	(0.00) †
TiO_2	nd	nd	nd	nd	nd	nd	nd	nd	nd	nd	nd	nd	nd	nd
FeO	19.45	(0.90)	14.23	(1.68)	19.09	(1.10)	17.02	(0.00)	20.79	(1.83)	16.75	(3.51)	16.43	(0.39)
MnO	0.30	(0.05)	0.25 †	(0.07) †	0.32	(0.05)	0.22	(0.00)	0.33	(0.05)	0.27	(0.04)	0.26 †	(0.03) †
MgO	41.47	(1.02)	44.99	(1.30)	41.36	(1.00)	44.05	(0.00)	40.06	(1.48)	43.59	(2.87)	43.35	(0.24)
CaO	0.17	(0.02)	0.17	(0.02)	0.16	(0.02)	0.12	(0.00)	0.15	(0.02)	0.15	(0.01)	0.18 †	(0.01) †
Na_2O	nd	nd	nd	nd	nd	nd	nd	nd	nd	nd	nd	nd	nd	nd
K_2O	nd	nd	nd	nd	nd	nd	nd	nd	nd	nd	nd	nd	nd	nd
NiO	nd	nd	0.20 †	(0.05) †	nd	nd	0.14	(0.00)	nd	nd	0.19	(0.01)	0.27 †	(0.03) †
Cr_2O_3	nd	nd	0.17 †	(0.02) †	nd	nd	nd	nd	0.09 †	(0.00) †	nd	nd	nd	nd
Total	99.84	(0.76)	98.59	(0.47)	99.36	(0.72)	100.56	(0.00)	99.23	(0.54)	99.86	(0.18)	99.28	(0.41)
n	*n* = 13		*n* = 26		*n* = 13		*n* = 1		*n* = 13		*n* = 3		*n* = 14	

* All statistics are for core values above detection limit only; values in parentheses are standard deviations. nd = no values above detection limit.

† At least one analysis gave a result below detection limit (not included in these statistics).

increase with decreasing Fo% (Figure 4.15, p. 208), and CaO contents shows no trend, as in the clinopyroxenes and orthopyroxenes.

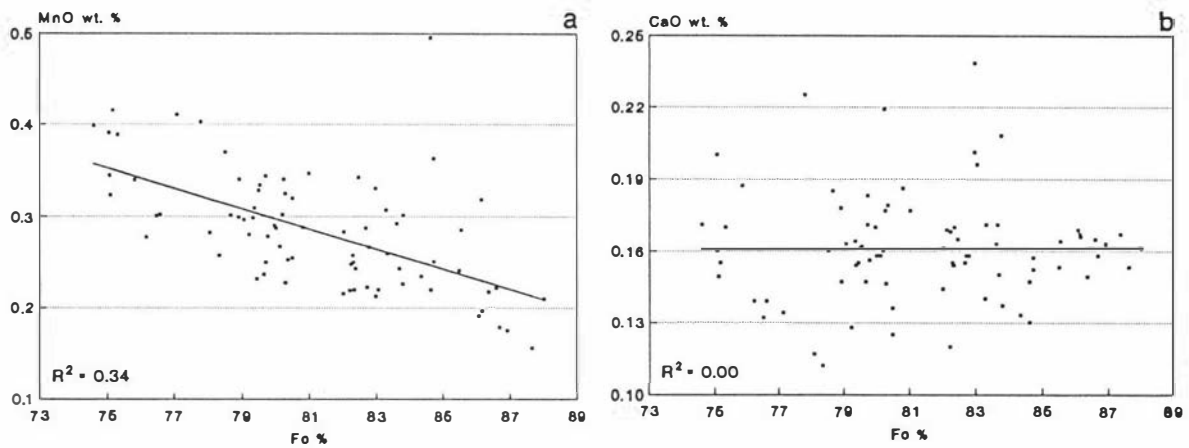

Figure 4.15 Plots of major oxide contents (MnO, CaO wt.%) *vs* Forsterite % (Fo%) in olivines of Tongariro Volcanic Centre tephras.

All olivines identified in tephras from TgVC have compositions between Fo74 – 88.

The compositions of the olivines and coexisting pyroxenes in each of the tephras (Poutu Lapilli, Waihohonu Lapilli, Oturere Lapilli, Shawcroft Tephra, member L3, Rotoaira Lapilli) are compared in Figure 4.16 (p. 209). In all but two of the tephras (Poutu Lapilli, Waihohonu Lapilli) the mean 100*Mg/(Mg + Fe) values of the olivines (Fo%) is higher than that of either the coexisting clinopyroxenes or orthopyroxenes (Mg Nº), and the clinopyroxene values are higher than those in the orthopyroxenes. This trend in mean Fo% and Mg Nº indicates that the olivines, clinopyroxenes and orthopyroxenes within each of the tephras probably crystallised from the same parent melt.

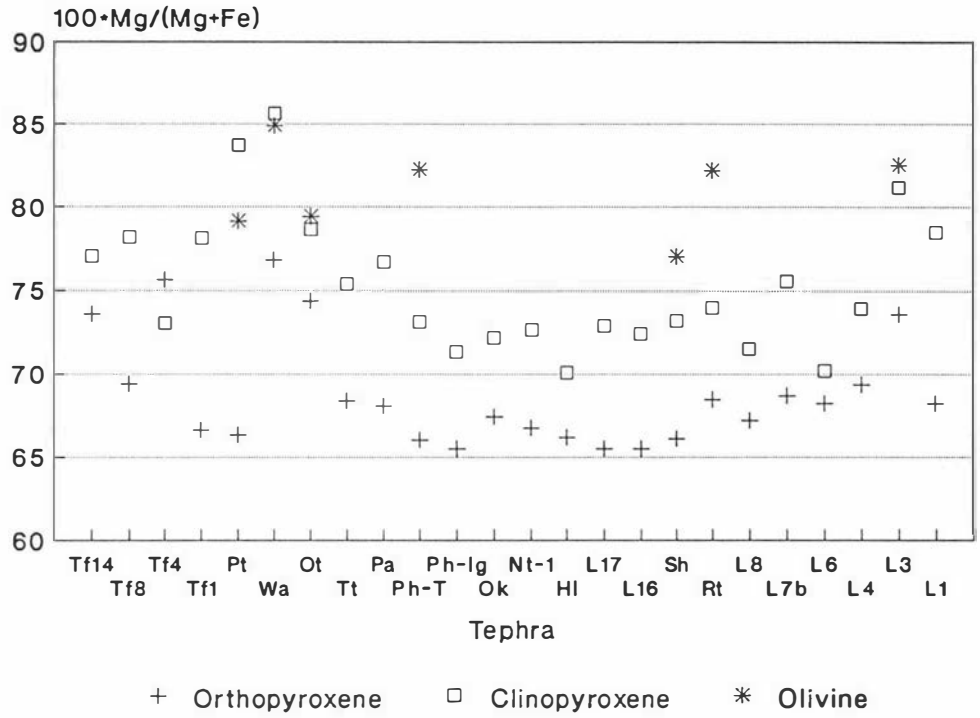

Figure 4.16 Mean compositions of olivine, and coexisting clinopyroxene and orthopyroxene in Tongariro Volcanic Centre tephras *(see text for tephra codes).*

The skeletal olivines in all tephras (Poutu Lapilli, Waihohonu Lapilli, Oturere Lapilli, Shawcroft Tephra) contain inclusions of pale orange to brown coloured glass (Plate 4.3). Non-skeletal olivines contain rare glass inclusions. Electron microprobe analyses of glass inclusions from skeletal olivines in Poutu Lapilli Member are presented in Appendix II. Glass compositions range between basaltic-andesite and andesite, using the classification of Le Maitre (1984), with a mean SiO_2 content of 56.5% (basaltic andesite).

Roeder and Emslie (1970) suggested that the olivine composition may be used to determine the Mg^{+2}:Fe^{+2} ratio of the coexisting liquid, or alternatively, the composition of the olivine in equlibrium with a liquid if the latter's Mg^{+2}:Fe^{+2} ratio is known. The partitioning of Mg^{+2} and Fe^{+2} between the olivine and liquid is expressed by the coefficient K_D, where:

$$K_D = \frac{\left(\frac{Fe^{+2}}{Mg^{+2}}\right)_{Ol.}}{\left(\frac{Fe^{+2}}{Mg^{+2}}\right)_{Liq.}} \quad [\,mol.\ \ ratios\,] \quad \simeq \quad 0.30$$

The Fe^{+2}/Mg^{+2} ratio (mean analysis) of the olivines is 0.26, and that of the liquid (*i.e.* the glass inclusions) is 1.31. These values (0.26/1.31 = 0.2) indicate that a non-equilibrium relationship exists between the skeletal olivines and liquid inclusions. Some of the inclusions may be residual liquid, which has infilled the hollow skeletal ('hopper') olivines following their crystallisation.

Source

The chemistry of olivine phenocrysts has been compared using an x-y scatter plot of MnO *vs* CaO (MNCA scatter plot; Figure 4.17, p. 210), mean oxide contents (FeO, MnO, MgO, CaO; Figure 4.18, p. 211) and mean Fo% values (Figure 4.19, p. 212). The olivine chemistry of tephras sourced from Mt Ruapehu and Mt Tongariro is similar, and cannot be used to distinguish between these two sources.

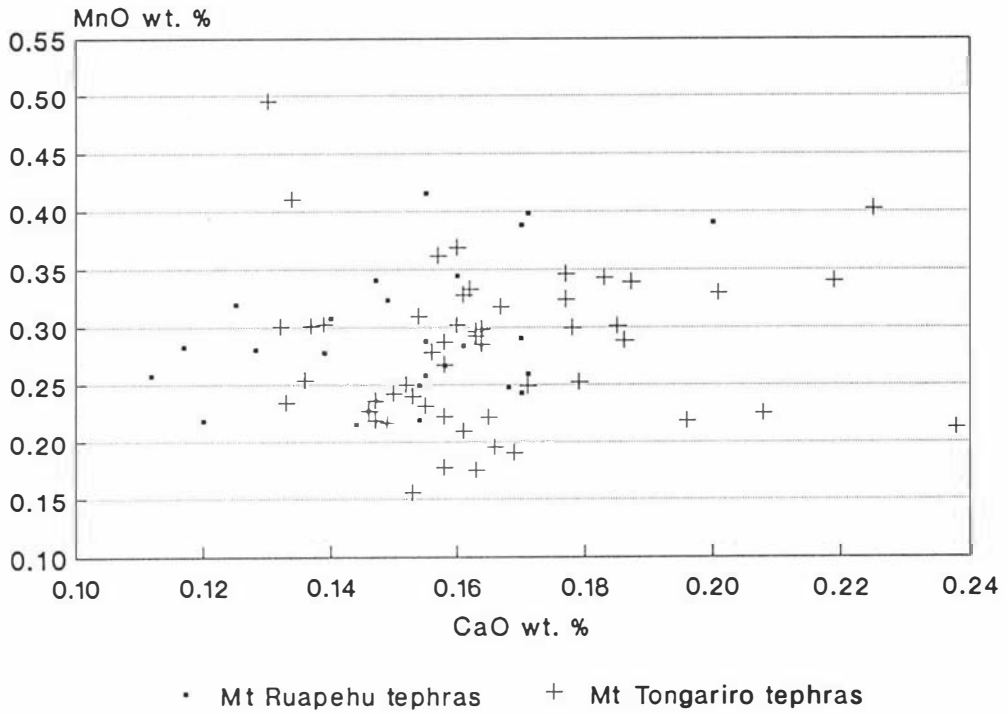

Figure 4.17 MNCA scatter plot showing compositions of olivines in Mt Ruapehu and Mt Tongariro tephras, Tongariro Volcanic Centre.

Comparison of Formation and Member Olivine Chemistries

While Mangamate Tephra, Rotoaira Lapilli, and Bullot Formation contain olivine-bearing andesitic tephras, they are not distinguished by their olivine chemistry.

Within Mangamate Tephra, only Waihohonu Lapilli Member is distinguished by the higher Fo contents of almost all its olivine phenocrysts (Figure 4.19, p. 212).

Within Bullot Formation, member L3 is distinguished from Shawcroft Tephra Member by the higher mean Fo% values (84 – 81 and 81 – 74 respectively) and NiO contents of its olivines (Table 4.9, p. 208; Figure 4.19, p. 212). Shawcroft Tephra is additionally distinguished from Waihohonu Lapilli on the lower mean Fo% value of its olivines, and member L3 is distinguished from Poutu Lapilli, Waihohonu Lapilli and Oturere Lapilli members of Mangamate Tephra on the higher mean NiO content of its olivines (Table 4.9, p. 208; Figure 4.19, p. 212).

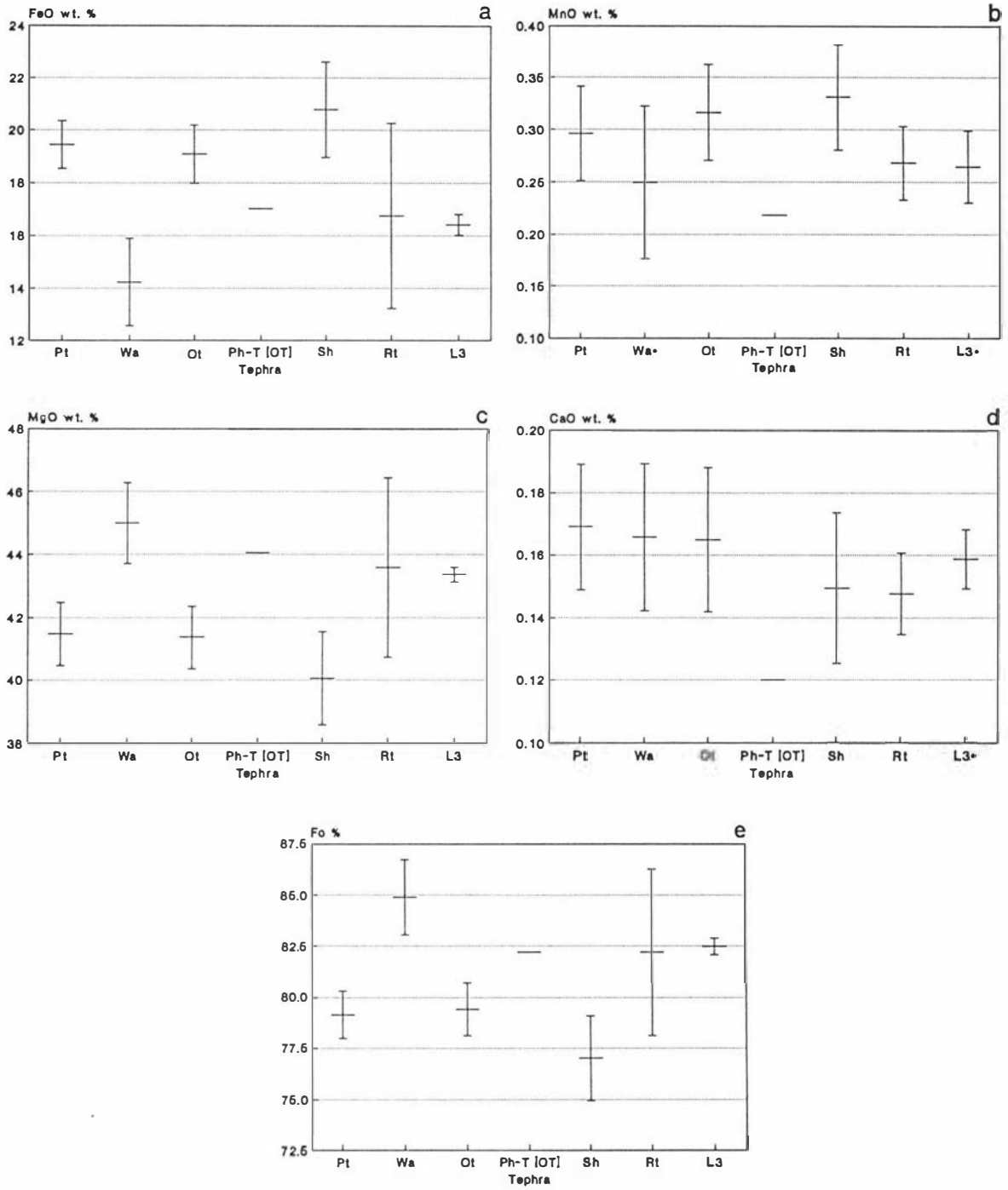

Figure 4.18 Mean oxide and Forsterite (Fo%) contents in olivines of Tongariro Volcanic Centre tephras. Bars show standard deviation from mean *(see text for tephra codes).*

Too few analyses were obtained on olivine from Rotoaira Lapilli (three analyses) and Pourahu Member (single analysis) to allow definition of compositional fields for these tephras. The fields shown in Figure 4.2 (p. 176) and Figure 4.19 (p. 212), although based on few analyses, suggest these tephras will not have distinctive chemistries.

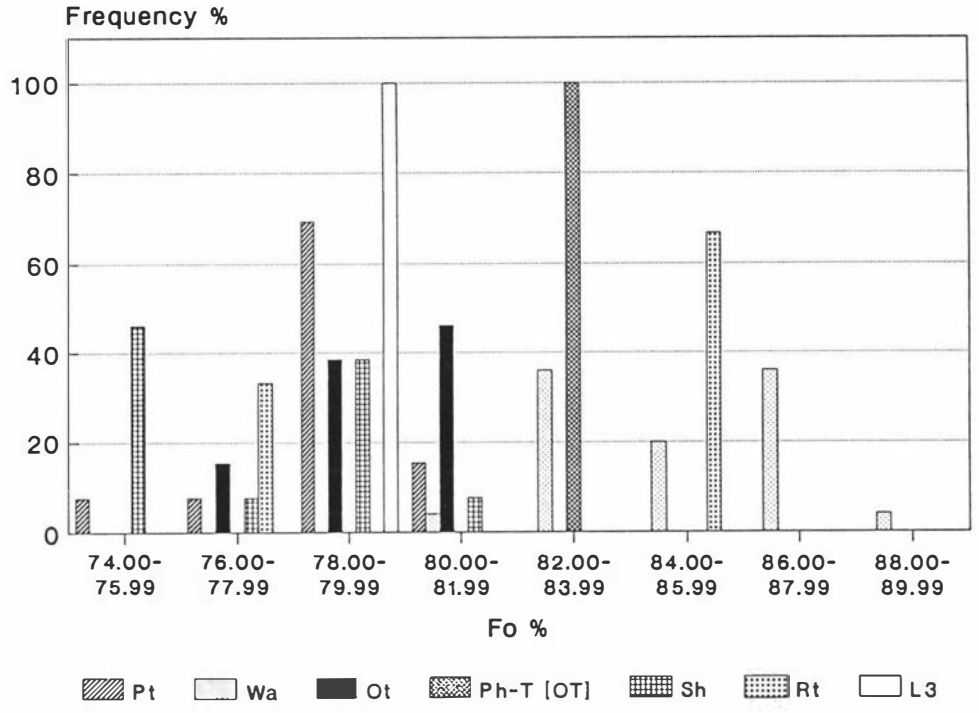

Figure 4.19 Olivine compositions in Tongariro Volcanic Centre tephras: Poutu Lapilli (Pt), Waihohonu Lapilli (Wa), Oturere Lapilli (Ot), Pourahu Member (Ph-T), Shawcroft Tephra (Sh), Rotoaira Lapilli (Rt), Bullot Formation member L3 (Fo% = Forsterite %).

Hornblende

Major element analyses of hornblende in TgVC tephras are presented in Appendix IIIe. Mean compositions are given in Table 4.10).

Calcic amphiboles are identified in the ferromagnesian mineral assemblage of tephras sourced from both Mt Tongariro and Mt Ruapehu. Amphibole has not previously been recognised as a major ferromagnesian mineral within tephras of TgVC. It has however been identified in trace amounts in some TgVC lavas (Ewart 1971; Hackett 1985; Cole *et al.* 1986).

Optical examination, back-scatter electron imagery, and comparison of core and rim analyses (Appendix IIIe) shows that most amphiboles are compositionally homogenous. Some grains show reverse zoning, indicated by higher MgO and lower FeO contents in rims compared with cores (Mg Nº 67 rim to Mg Nº 59 core). Hornblende cores range between Mg Nº 73 – 55 and in most tephras are lower than the Mg Nº of coexisting clinopyroxenes, and where present, coexisting olivines.

Table 4.10 Electron microprobe analyses (meaned) of hornblende in andesitic tephras of Tongariro Volcanic Centre.*

Formation	Oturere Lapilli		Te Rato Lapilli		Pahoka Tephra [8]		Ngamatea lapilli-1		Pourahu Member (tephra unit) (OT)		Pourahu Member (tephra unit) (DR16)		Member L17	
SiO_2	41.60	(0.04)	42.87	(0.51)	42.13	(0.86)	42.31	(0.13)	44.29	(1.23)	42.68	(0.87)	41.00	(0.00)
Al_2O_3	11.77	(0.05)	11.23	(0.38)	12.02	(0.57)	11.85	(0.38)	9.70	(1.77)	11.88	(1.24)	12.55	(0.00)
TiO_2	2.81	(0.17)	1.84	(0.15)	1.48	(0.34)	2.87	(0.54)	1.95	(0.31)	1.79	(0.26)	1.45	(0.00)
FeO	12.87	(0.03)	14.19	(0.64)	14.56	(0.94)	12.18	(0.27)	13.23	(1.78)	12.89	(1.71)	14.51	(0.00)
MnO	0.20	(0.04)	0.44'	(0.12)'	0.37'	(0.07)'	0.23'	(0.00)'	0.22	(0.05)	0.20	(0.05)	0.37	(0.00)
MgO	13.20	(0.21)	12.79	(0.49)	12.25	(0.68)	14.21	(0.26)	13.93	(0.93)	13.75	(1.18)	11.99	(0.00)
CaO	11.61	(0.09)	10.92	(0.30)	11.09	(0.35)	10.94	(0.08)	11.01	(0.25)	11.14	(0.11)	11.30	(0.00)
Na_2O	2.32	(0.02)	1.63	(0.50)	2.07	(0.13)	2.19	(0.01)	1.93	(0.20)	2.16	(0.08)	2.00	(0.00)
K_2O	0.47	(0.03)	0.38	(0.04)	0.37	(0.05)	0.46	(0.03)	0.40	(0.10)	0.36	(0.13)	0.45	(0.00)
Total	96.84	(0.28)	96.06	(0.63)	96.29	(0.57)	96.89	(0.37)	96.65	(0.75)	96.84	(0.47)	95.63	(0.00)
n	*n = 3*		*n = 28*		*n = 16*		*n = 2*		*n = 6*		*n = 3*		*n = 1*	

Formation	Member L6		Member L1	
SiO_2	41.98	(0.82)	42.40	(0.00)
Al_2O_3	12.93	(1.36)	11.04	(0.00)
TiO_2	1.71	(0.09)	2.95	(0.00)
FeO	11.87	(1.40)	14.04	(0.00)
MnO	0.18'	(0.03)'	0.18	(0.00)
MgO	14.41	(0.79)	12.36	(0.00)
CaO	11.46	(0.35)	11.00	(0.00)
Na_2O	2.25	(0.21)	2.30	(0.00)
K_2O	0.37	(0.15)	0.41	(0.00)
Total	97.12	(0.42)	96.68	(0.00)
n	*n = 4*		*n = 1*	

* All statistics are for core values above detection limit only; values in parentheses are standard deviations. nd = no values above detection limit.

† At least one analysis gave a result below detection limit (not included in these statistics).

[8] Statistics exclude an anomalous analysis for Pahoka Tephra with a MnO wt. % value of 2.75.

In the amphiboles the FeO and Al_2O_3 contents are the most variable [8] with some of the tephras showing up to 6% variation in these elements between analyses. Plots of mean oxide contents (cores only) *vs* mean Mg Nº (Figure 4.20, p. 214) shows that MnO content increases with decreasing Mg Nº. The same trend is observed in the pyroxenes. No trend is shown for Al_2O_3, TiO_2, CaO, Na_2O and K_2O contents.

Amphibole compositions in TgVC tephras project dominantly as pargasitic hornblende, and also as tschermakitic–hornblende, using the nomenclature of Deer *et al.* (1966) (Figure 4.21, p. 215). According to Leake (1978) all analyses are calcic amphiboles. Assuming all Fe as FeO, amphibole compositions fall within the ferroan pargasite, ferroan pargasitic hornblende, pargasite, pargasitic–hornblende, edenite, tschermakitic–hornblende and magnesio–hornblende fields.

[8] The general formula of the calcium-rich amphiboles can be expressed: $X_{2-3}Y_6Z_8O_{22}(OH)_2$ where X = Ca,Na,K,Mn; Y = Mg,Fe^{+2},Fe^{+3},Al,Ti,Mn,Cr,Li,Zn; Z = Si,Al. Important ionic substitutions in this structure include Mg⇌Fe, Al⇌Si, (Mg,Fe)⇌Al, and Na⇌Ca (Deer *et al.* 1966).

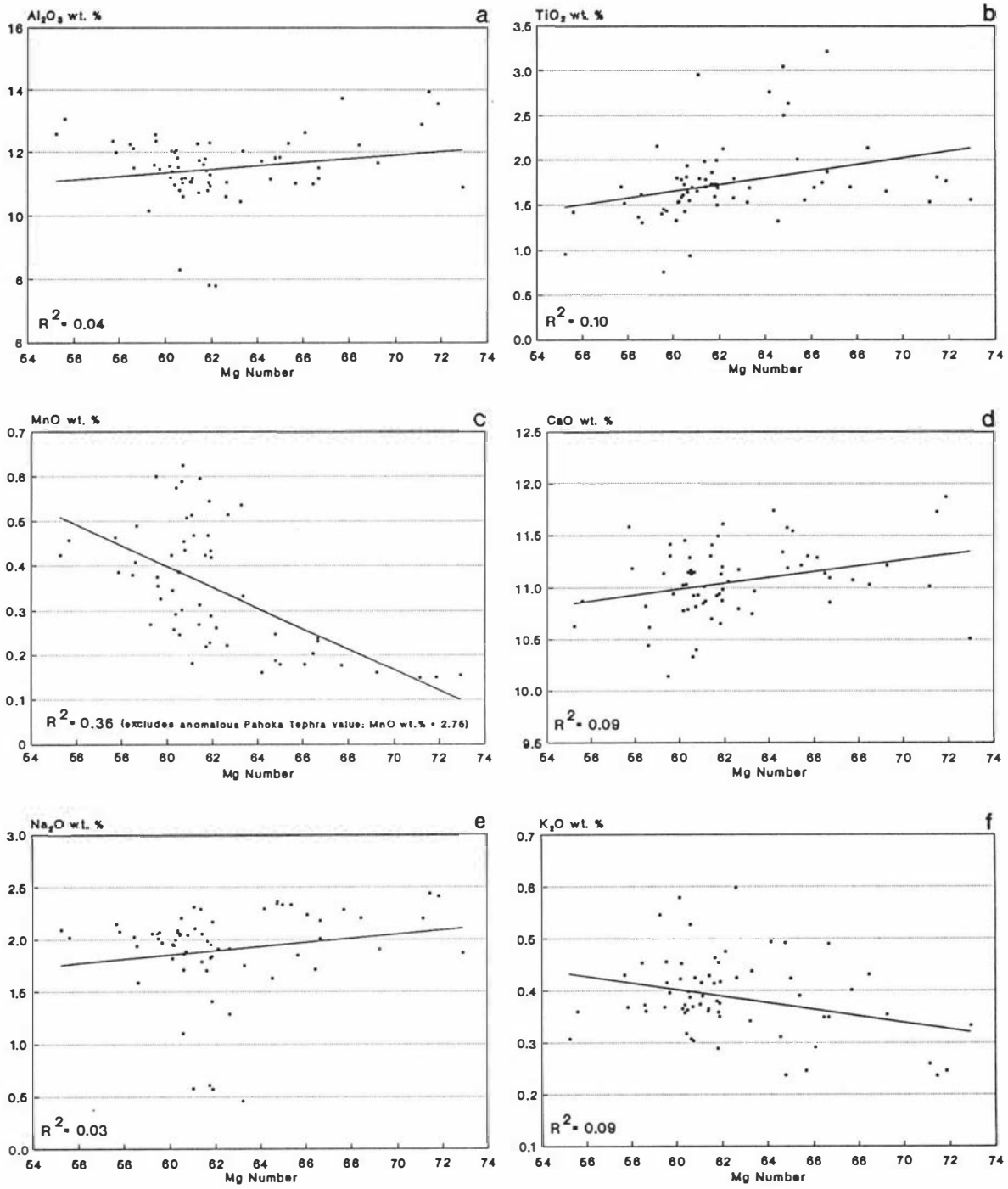

Figure 4.20 Plots of major oxide contents (wt.%) *vs* Mg number in hornblende phenocrysts of Tongariro Volcanic Centre tephras.

Only three amphibole analyses have been obtained from Mt Ruapehu lavas (Hackett 1985) and these project as ferroan pargasitic hornblende using the classification of Leake (1978). Using the classification of Deer *et al.* (1966) the compositions of these amphiboles project as pargasitic – hornblende (Figure 4.21, p. 215).

Recently Froggatt and Rodgers (1990) identified hornblende of more pargasitic composition than typical rhyolitic hornblende in distal tephras preserved in a montane – alpine

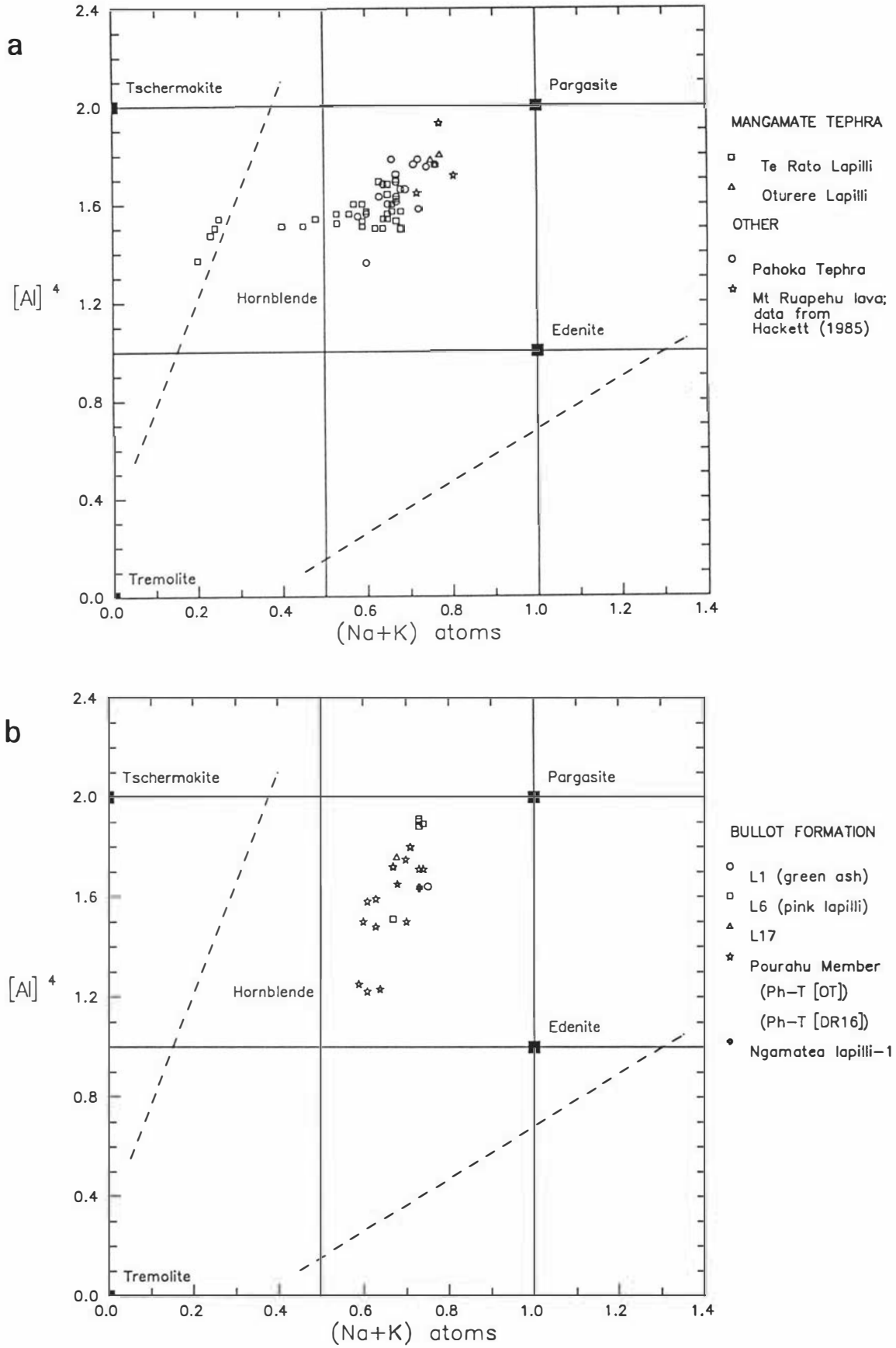

Figure 4.21 Compositions of calcic amphiboles in Mt Tongariro tephras and Mt Ruapehu lavas (Fig. 4.21a), and Mt Ruapehu tephras (Fig. 4.21b). Compositional fields are from Deer *et al.* (1966).

peat bog of the southern Kaimanawa Range, east of TgVC. An andesitic source for the hornblende is proposed because of the more pargasitic composition and the occurrence of the hornblende together with augite. Augite is not common in Holocene rhyolitic tephras but may be abundant in andesitic tephras (Froggatt and Rodgers 1990).

Hornblende compositions identified by Froggatt and Rodgers (1990) are of similar composition (pargasitic hornblende and hornblende compositions) to most hornblendes identified from near source TgVC tephras (this thesis), and EVC tephras (Wallace 1987), and would appear to support the authors' identification of an andesitic source for the hornblendes. It should be noted, however, that amphibole phenocryst chemistry does not clearly distinguish rhyolitic tephras sourced from TVC and andesitic tephras of TgVC (Figure 4.22, p. 220). Of the five analyses presented in Froggatt and Rodgers (1990), two plot within the EVC field, two fall between the EVC and TgVC fields, and one falls within the field defined by TgVC and TVC tephras, identifying both EVC and TgVC as probable sources for the amphiboles.

Hornblende Mineralogy and Chemistry of Te Rato Lapilli and Pahoka Tephra

Within the TgVC tephra record (spanning the period *c.* 22 500 years B.P. to the present) an abrupt change in the ferromagnesian mineralogy of TgVC tephras occurs at *c.* 10 000 years B.P., coincident with the eruption of Pahoka Tephra and Te Rato Lapilli Member of Mangamate Tephra. This change is identified by the presence of significant amounts of hornblende in the ferromagnesian mineral assemblages of these two tephras, and its virtual absence in older and younger tephras characterised by ferromagnesian mineral assemblages comprising orthopyroxene + clinopyroxene ± olivine ± hornblende (trace).

Both Te Rato Lapilli Member of Mangamate Tephra and the underlying Pahoka Tephra are prominent tephras sourced from Mt Tongariro. They are readily distinguished from other Mangamate Tephra members, and Mt Ruapehu-sourced tephras, by their field characteristics and ferromagnesian mineralogy; both contain dominant calcic amphibole in their ferromagnesian mineral assemblage (Table 4.2, p. 169).

Hornblendes in Pahoka Tephra are pargasitic – hornblendes with core Mg №'s ranging between 66 – 55. Pargasitic- to tschermakitic-hornblendes occur in Te Rato Lapilli. Mg №'s of hornblende cores in this tephra range between 67 – 58. Most hornblendes are either not zoned or are normally zoned with more Mg-rich cores (Mg № 72) and more Fe-rich rims (Mg № 62). Some hornblendes, however, show distinct reverse compositional zoning with more Fe-rich cores (Mg № 59) and Mg-rich rims (Mg № 67) (Appendix IIIe).

Magma Mixing in Pahoka Tephra and Te Rato Lapilli

A distinct change in the chemistry of titanomagnetites in TgVC tephras and comagmatic lavas occurred *c.* 10 000 years B.P. (Kohn 1973; Kohn and Topping 1978).

Titanomagnetites in tephras younger than Okupata Tephra show lower V, Cr, Ni, and Co contents compared with older andesites. Kohn (1973) and Kohn and Topping (1978) concluded that both Pahoka Tephra (previously Pahoka lapilli, Kohn and Topping 1974) and Te Rato Lapilli were erupted from a new, less basic andesitic magma. The bulk rock compositions of pumice lapilli within both tephras are dacitic (Topping 1974; Kohn and Topping 1978).

Petrographic and mineral data in this study supports the finding of these authors that both Pahoka Tephra and Te Rato Lapilli were erupted from a melt of new composition.

Pumiceous and scoriaceous lapilli in Pahoka Tephra, and in the slightly younger Te Rato Lapilli, are characterised by grey and white colour-banding. Most bands are continuous and the contacts between bands are both sharp and gradational. Both components are vesicular with the grey bands more phenocryst-rich. Acicular microphenocrysts of hornblende are flow aligned.

The occurrence of vesicles, flow structures and the glassy composition of lapilli indicate both components were molten at the time of eruption (Sparks and Sigurdsson 1977). Banded textures are evidence of magma mixing processes between at least two liquids of different composition (Eichelberger 1974; Cantagrel *et al.* 1984; Sakuyama 1984; Gourgaud *et al.* 1989). The white bands in the pumice represent the more acidic member and the grey bands the more basic member. Both components are vesiculated and were therefore mixed prior to their simultaneous eruption.

Some hornblende phenocrysts show distinct reverse zoning from more Fe-rich cores to more Mg-rich rims. The core-rim contacts are distinct. These reversely zoned hornblendes were most probably derived from the more acid member, with the zoning indicating attempts by the phenocrysts to re-equilibrate during mixing with a liquid of more basic composition (Eichelberger 1974; Nixon 1988; Gourgaud *et al.* 1989). Such disequilibrium textures (*i.e.* reversely zoned and resorbed phenocrysts) are considered to be evidence of magma mixing (Sakuyama 1984; Wörner and Wright 1984; Bourdier *et al.* 1985; Robin *et al.* 1990). The hornblendes may therefore be considered xenocrysts in this hybrid. Sharp contacts between the core and rim compositions in zoned hornblendes suggests the residence time of the hornblendes in the hybrid melt was short, because with longer residence times contacts become more diffuse (Wörner and Wright 1984; Gourgaud *et al.* 1989). The residence time determines whether crystals remain unreacted, change composition, or are completely resorbed (Eichelberger 1974). The sporadic occurrence of skeletal olivine in these tephras suggests supercooling of the more basaltic melt (as a result of magma mixing) and consequent forced crystallisation of olivine with skeletal (quenched) habits. Injection of a more basaltic magma into an acid magma causes superheating of the acid melt. As a consequence of superheating, crystals in the acid magma may be resorbed (Kuo and Kirkpatrick 1982; Nixon 1988). At the same time as the acid magma is superheated the more

basaltic melt is supercooled (quenched) and rapid crystallisation of skeletal phenocrysts may occur and be assimilated into the hybrid (Sparks and Sigurdsson 1977; Nixon 1988).

Textural banding in pumiceous lapilli, the coexistence of reversely zoned hornblendes and skeletal olivines, and resorbed textures and glass inclusions in some phenocrysts are evidence of magma mixing in these tephras.

Bimodal phenocryst compositions are also characteristic of mixed magmas where the phenocryst phases of compositionally different melts may be inherited by another during contamination and mixing (Eichelberger 1975; Federman and Scheidegger 1984; Flood et al. 1989). A comparison of the Mg Nºs of clinopyroxene and orthopyroxene phenocrysts in Pahoka Tephra and Te Rato Lapilli does not indicate bimodal phenocryst chemistries, suggesting they are derived from only one of the melts. The occurrence of two distinct hornblende compositions in Te Rato Lapilli is however consistent with mixing.

The banded hornblende-bearing pumiceous lapilli represent hybrid melts of new composition – most probably produced by the contamination of a small volume of rhyolitic liquid with a more basaltic liquid. Eruption of an acid end member identifies change in melt compositions beneath Mt Tongariro at this time, perhaps indicating longer magma residence times at high crustal level. Earlier eruptions presumably did not involve the more acid magma. This more acid end member may have evolved from fractional crystallisation of an andesite melt beneath Mt Tongariro. The process of magma mixing is believed to be an important mechanism in the triggering of explosive volcanic eruptions of acid magmas (Sparks and Sigurdsson 1977; Gerlach and Grove 1982; Cantagrel *et al.* 1984; Gourgaud *et al.* 1989), and was most probably an important process leading to the eruption of Pahoka Tephra and Te Rato Lapilli.

The eruption of Pahoka Tephra and Te Rato Lapilli is closely associated in time with the renewed onset of rhyolitic tephra eruptions at TVC (Karapiti and Poronui tephras of Taupo Subgroup) following about 10 000 years of quiescence. Kohn (1973) and Kohn and Topping (1978) propose that the rapid uprising of the andesitic magma at TgVC may have triggered eruptions in TVC.

Hornblende Mineralogy of Other Mt Tongariro and Mt Ruapehu Tephras

Calcic amphibole has been identified in minor to trace amounts within Poutu Lapilli and Oturere Lapilli members of Mangamate Tephra, Okupata Tephra, and five members of Bullot Formation (Pourahu Member [tephra unit], Ngamatea lapilli-1, Bullot S16, member L6, member L1) (Table 4.2, p. 169).

Major element analyses of hornblendes from some of these TgVC tephras are presented in Appendix IIIe. Mean analyses are given in Table 4.10 (p. 213). Using the nomenclature of

Deer *et al.* (1966) compositions project as hornblende and pargasitic hornblende (Figure 4.21, p. 215).

Source

Tephras sourced from Mt Tongariro (Oturere Lapilli, Te Rato Lapilli, Pahoka Tephra) cannot be distinguished from the Mt Ruapehu-sourced Bullot Formation tephras (Pourahu Member [tephra unit], Ngamatea lapilli-1, Bullot S16, member L6, member L1) from comparison of the major element chemistry of hornblendes. The variability in element concentrations within each tephra, the similarity in hornblende chemistry between tephras, and the small number of analyses obtained for the Mt Ruapehu tephras prevents clear distinction between these two sources.

Hornblende chemistry can, however, be used to clearly distinguish tephras erupted from EVC and TVC (Figure 4.22, p. 220). It does not, however, distinguish tephras sourced from TgVC and TVC.

Members

Valid comparisons cannot be made between members of the Bullot Formation because of the small number of hornblende analyses obtained for each of the tephras. Similarly, Oturere Lapilli (three analyses) cannot be distinguished from Te Rato Lapilli, although the latter does contain Tschermakitic hornblende.

Fe-Ti Oxides

Titanomagnetite and ilmenite are present in minor amounts in TgVC tephras. Both occur as microphenocrysts, and less commonly as inclusions in ferromagnesian phenocryst phases. Exolution lamellae have not been observed from electron-optical examination. Within the titanomagnetites, FeO and TiO_2 contents are the most variable. Cr_2O_3 occurs in measurable quantities in most analyses. CaO and NiO occur below accurate detection limits in all analyses of both ilmenites and titanomagnetites.

The major element chemistry of Fe-Ti oxides in six members of Bullot Formation was determined to assess the potential use of Fe-Ti oxide chemistry as a means of distinguishing and correlating Bullot Formation tephras. The members selected for comparison (Ngamatea lapilli-1, Pourahu Member [tephra and ignimbrite units], L17, L16, L8, L6) are not able to be distinguished using either pyroxene or hornblende chemistry.

Major element analyses of titanomagnetites (87 analyses) and coexisting ilmenite (23 analyses) are presented in Appendix IIIf. Mean analyses are given in Table 4.11, p. 221.

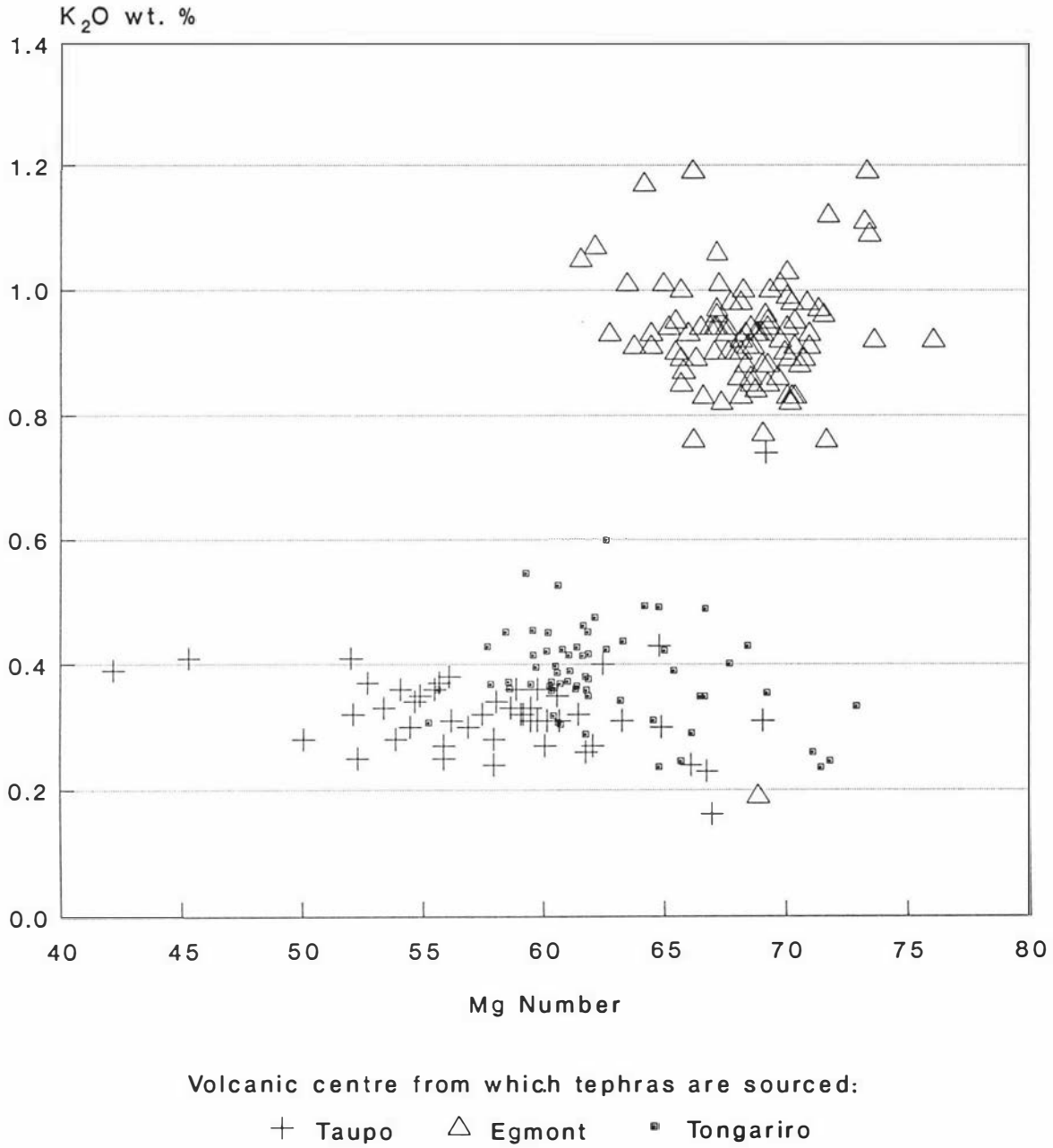

Figure 4.22 Plot of K_2O (wt.%) *vs* Mg number in amphiboles from tephras of Tongariro, Taupo and Egmont volcanic centres. Taupo and Egmont centre data are from Howorth (1976) and Wallace (1987).

Source

Titanomagnetite chemistry can be used to distinguish tephras from TgVC and EVC. The titanomagnetites from Mt Ruapehu-sourced tephras show higher Cr_2O_3 and lower MnO contents than EVC tephras (Figure 4.23, p. 222), consistent with the earlier findings of Kohn and Neall (1973), Lowe (1987, 1988a), and Alloway (1989).

Comparison of Formations and Members

Titanomagnetites analyses from the seven tephras have been compared using mean oxide contents (Al_2O_3, TiO_2, FeO, MnO, MgO, Cr_2O_3) (Figure 4.24, p. 223) and x-y scatter

Table 4.11 Electron microprobe analyses (meaned) of titanomagnetite (top of table) and ilmenite (bottom of table) in andesitic tephras of Tongariro Volcanic Centre.*

Formation	Ngamatea lapilli-1		Pourahu Member [tephra unit] (BT1)		Pourahu Member [ignimbrite unit] (CT)		Member L17		Member L16		Member L8		Member L6	
SiO_2	0.16	(0.05)	0.11	(0.03)	0.12	(0.03)	0.10	(0.01)	0.12	(0.06)	0.11	(0.01)	0.10	(0.02)
Al_2O_3	3.05	(0.37)	2.28	(0.11)	2.30	(0.04)	2.68	(0.22)	3.28	(0.30)	3.00	(0.10)	2.68	(0.10)
TiO_2	10.77	(0.81)	12.76	(0.23)	12.81	(0.22)	12.96	(1.00)	11.49	(0.94)	12.01	(0.42)	12.62	(0.39)
FeO	76.18	(1.10)	76.15	(0.67)	76.15	(0.56)	74.75	(0.82)	74.61	(1.49)	75.41	(0.65)	75.13	(0.73)
MnO	0.32	(0.06)	0.36	(0.05)	0.38	(0.04)	0.36	(0.03)	0.29†	(0.05)†	0.33	(0.03)	0.36	(0.04)
MgO	2.97	(0.30)	2.09	(0.14)	2.04	(0.06)	3.13	(0.16)	3.55	(0.37)	2.95	(0.13)	2.83	(0.15)
CaO	nd	nd	nd	nd	nd	nd	nd	nd	0.11	(0.00)	nd	nd	nd	nd
NiO	nd	nd	nd	nd	nd	nd	nd	nd	nd	nd	nd	nd	nd	nd
Cr_2O_3	0.47	(0.13)	0.29†	(0.09)†	0.30†	(0.09)†	0.28	(0.06)	0.29†	(0.06)†	0.24†	(0.05)†	0.47	(0.11)
Total	93.92	(0.92)	94.02	(0.60)	94.05	(0.68)	94.26	(0.66)	93.46	(0.81)	93.95	(0.53)	94.19	(0.72)
n	*n = 11*		*n = 14*		*n = 13*		*n = 11*		*n = 16*		*n = 12*		*n = 10*	
SiO_2	0.09†	(0.04)†	0.06†	(0.00)†	0.08†	(0.04)†	0.06†	(0.00)†	0.08†	(0.00)†	–	–	nd	nd
Al_2O_3	0.52	(0.04)	0.27	(0.01)	0.28	(0.01)	0.35	(0.03)	0.57	(0.01)	–	–	0.39	(0.02)
TiO_2	37.46	(1.05)	43.39	(0.36)	43.78	(0.49)	42.41	(0.42)	37.68	(0.14)	–	–	42.49	(0.11)
FeO	54.07	(1.23)	49.44	(0.20)	49.29	(0.76)	49.31	(1.49)	52.86	(0.10)	–	–	50.15	(0.42)
MnO	0.25	(0.04)	0.38	(0.03)	0.41	(0.04)	0.47	(0.10)	0.23†	(0.00)†	–	–	0.34	(0.07)
MgO	3.38	(0.20)	3.09	(0.02)	3.02	(0.10)	4.06	(0.78)	3.61	(0.02)	–	–	3.77	(0.02)
CaO	nd	nd	nd	nd	nd	nd	nd	nd	nd	nd	–	–	nd	nd
NiO	nd	nd	nd	nd	nd	nd	nd	nd	nd	nd	–	–	nd	nd
Cr_2O_3	0.21†	(0.00)†	nd	nd	nd	nd	nd	nd	nd	nd	–	–	nd	nd
Total	95.80	(0.85)	96.61	(0.34)	96.84	(0.96)	96.61	(0.39)	94.87	(0.06)	–	–	97.13	(0.49)
n	*n = 7*		*n = 3*		*n = 6*		*n = 3*		*n = 2*				*n = 3*	

* All statistics are for values above detection limit only; values in parentheses are standard deviations.
nd = no values above detection limit.
† At least one analysis gave a result below detection limit (not included in these statistics).

plots of MgO *vs* MnO contents, and MgO *vs* Al_2O_3 contents for all analyses (Figure 4.25, p. 224).

Within Bullot Formation, Pourahu Member [tephra and ignimbrite units] is distinguished from all other members on the lower Al_2O_3 and MgO contents of its titanomagnetites, and from members L16, L8 and Nt-1 on its higher mean TiO_2 contents (Figure 4.24a,b,e, p. 223; Figure 4.25, p. 224). The strong similarity in titanomagnetite chemistry of Pourahu Member [tephra unit] and Pourahu Member [ignimbrite unit] supports their correlation to the same eruptive event.

The other five members show similar titanomagnetite chemistries (Figure 4.24a-d, p. 223; Figure 4.25, p. 224). Some separation between members is shown by comparing mean oxide contents (Al_2O_3, TiO_2, MgO, and Cr_2O_3), but there is no consistent distinction using oxide abundances, and no systematic trend in titanomagnetite chemistry with time.

While there are some differences in the chemistry of the ilmenites (Appendix IIIf) using FeO, TiO_2, and Al_2O_3 contents, insufficient analyses have been obtained to permit distinction of tephras on this basis, primarily because of the low ilmenite contents of these tephras.

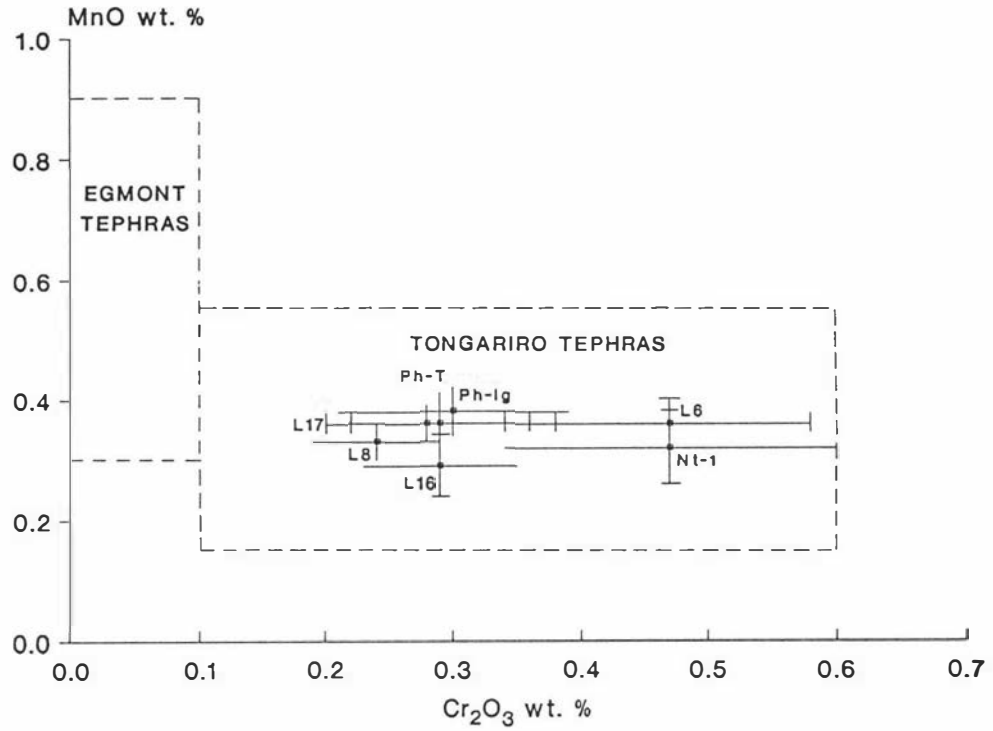

Figure 4.23 Plot of MnO *vs* Cr_2O_3 (wt.%) in titanomagnetites of some Mt Ruapehu (Bullot Formation) tephras. Bars show standard deviation from mean. Compositional fields for Tongariro Volcanic Centre and Egmont Centre tephras are based on data in Lowe (1988a) *(see text for tephra codes)*.

Glass

Within both Tufa Trig Formation and Bullot Formation the ability to readily identify and correlate members is limited by the lithologic similarity of most members and the lack of diagnostic field characteristics. The ferromagnesian mineralogy and chemistry of selected members in each formation were examined to determine if members could be distinguished on the basis of their ferromagnesian mineralogy and major element phenocryst chemistry (see earlier discussion).

Members of Tufa Trig Formation are not conclusively distinguished, and only a few members within Bullot Formation are uniquely identified by their ferromagnesian mineral assemblage, ferromagnesian phenocryst chemistry and titanomagnetite chemistry.

The chemistry of groundmass glass in pumice lapilli and vitric pyroclasts, glass shards and selvedges on ferromagnesian minerals was therefore determined to assess the potential of major element glass chemistry as a means of distinguishing and correlating Mt Ruapehu-sourced andesitic tephras.

The major element glass chemistry of seven Mt Ruapehu tephras (Tufa Trig Formation members Tf5, Tf8, Tf14; Bullot Formation members L3, L6, Pourahu Member [tephra and ignimbrite units]) was determined by EMP analysis. With the exception of Pourahu Member [ignimbrite unit], the low standard deviations on all measured elements indicate little

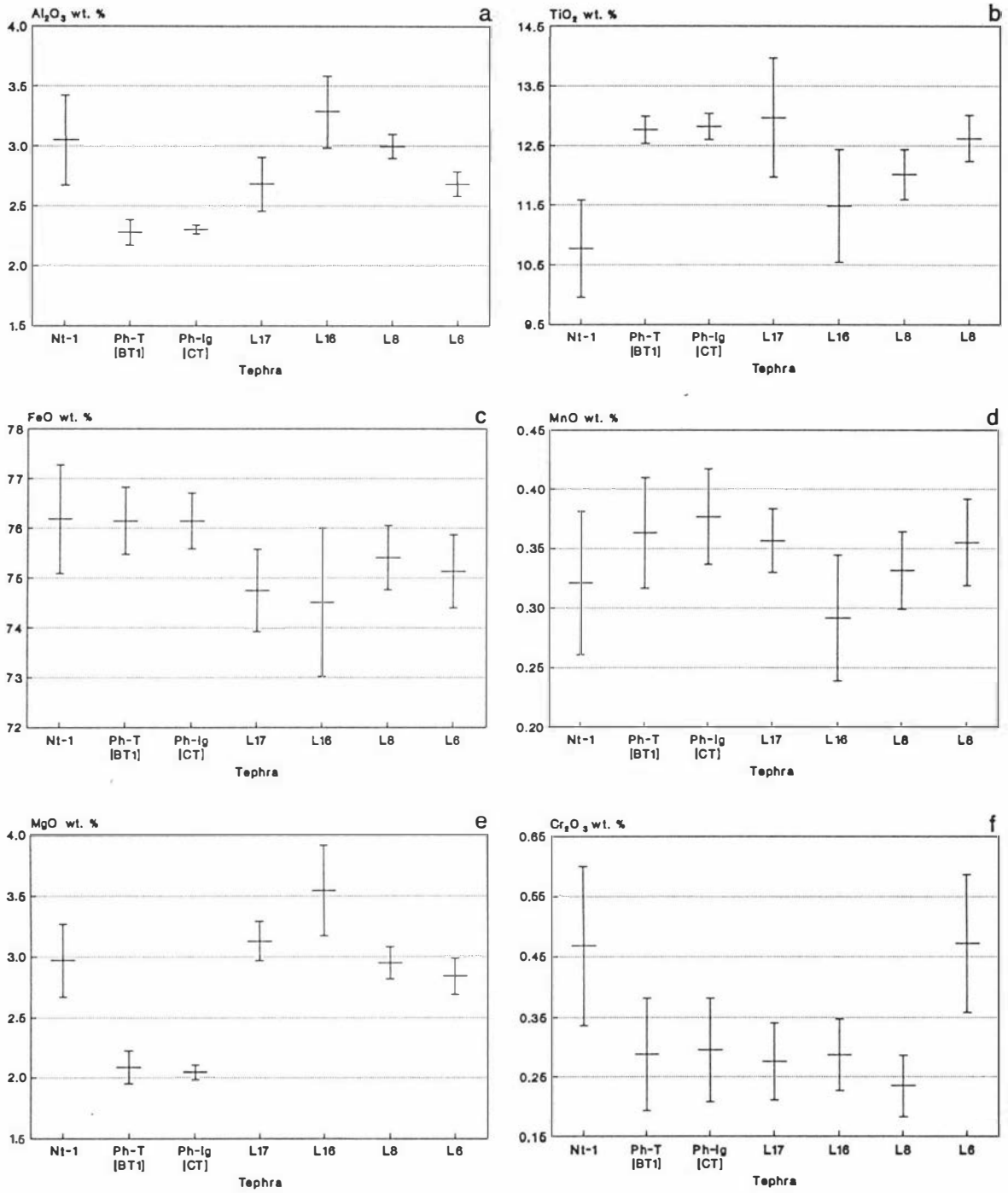

Figure 4.24 Mean oxide contents in titanomagnetites of some Mt Ruapehu tephras. Bars show standard deviation from mean *(see text for tephra codes).*

intra-sample variation in chemistry, and therefore, homogenous glass compositions (Appendix III_g). All analyses have been normalised to 100% loss free and are presented in Appendix III_g. Mean analyses are given in Table 4.12, p. 225. Using the classification of Le Maitre (1984), glass compositions project as andesite, dacite and rhyolite (Figure 4.26, p. 226).

Lowe (1988_a) attributed part of his observed variation in the CaO contents in andesitic glass to the effect of plagioclase microlites. However, little variation in the CaO contents of

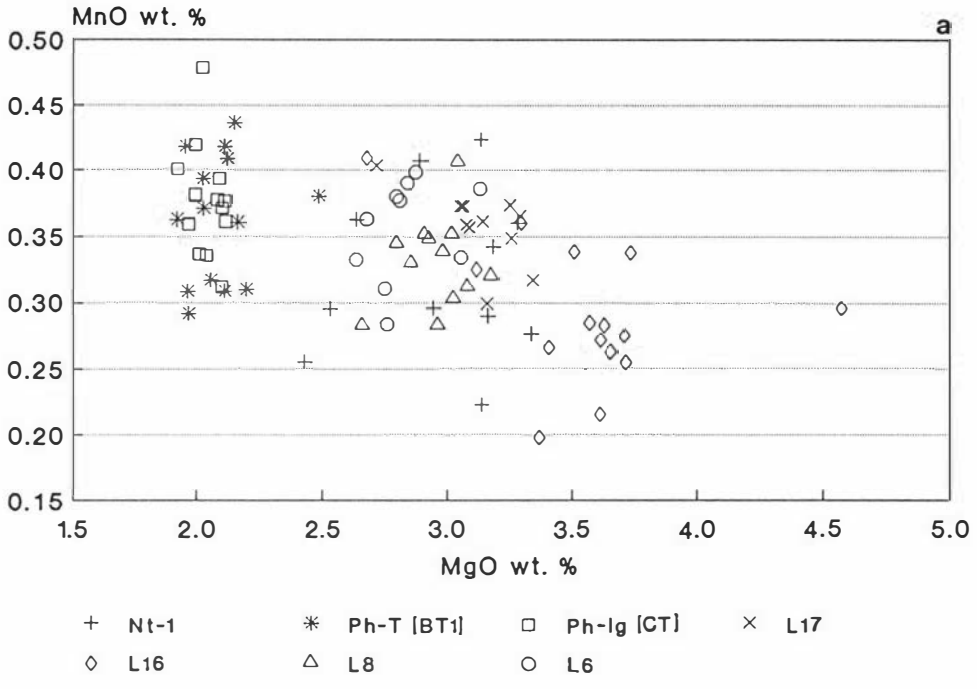

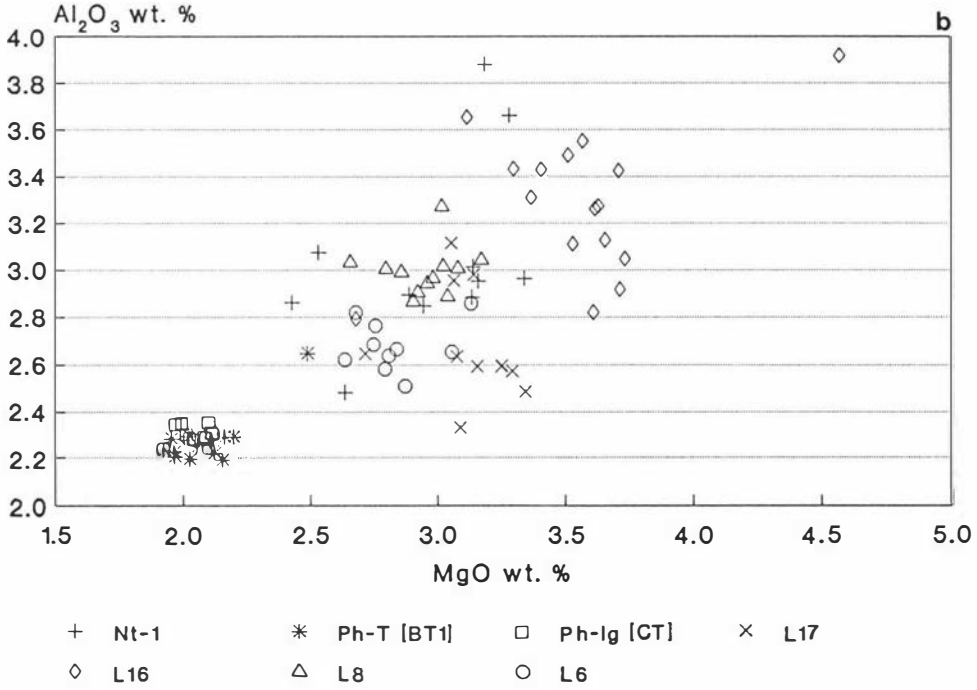

Figure 4.25 Plots of MnO *vs* MgO (wt.%) (Fig. 4.25a) and Al_2O_3 *vs* MgO (wt.%) (Fig. 4.25b) in titanomagnetites of some Mt Ruapehu tephras. (see text for tephra codes).

glasses is observed in the tephras analysed in this study, including those with microlite-rich groundmass glass.

Table 4.12 Electron microprobe analyses (normalised; meaned) of glass in andesitic tephras of Tongariro Volcanic Centre.*

Formation	Member Tf14		Member Tf8		Member Tf5				Poutu Lapilli		Pourahu Member [tephra unit] [BT1]			
	Groundmass		Groundmass		Groundmass		Incl. in Pyroxene		Incl. in Olivine		Groundmass		Incl. in Plagioclase	
SiO_2	63.63	(0.29)	63.74	(0.74)	64.49	(1.02)	66.94	(0.00)	56.50	(1.40)	73.11	(0.56)	72.04	(0.60)
Al_2O_3	14.87	(0.19)	14.87	(0.37)	15.20	(0.73)	14.67	(0.00)	17.23	(0.87)	13.54	(0.14)	13.84	(0.37)
TiO_2	1.08	(0.08)	1.08	(0.07)	1.03	(0.13)	1.05	(0.00)	0.75	(0.07)	0.55	(0.03)	0.68	(0.02)
FeO	6.59	(0.19)	6.33	(0.33)	5.85	(0.40)	4.86	(0.00)	8.09	(0.87)	2.73	(0.16)	2.91	(0.20)
MnO	0.28'	(0.00)'	0.19'	(0.00)'	0.14'	(0.03)'	nd	nd	0.23'	(0.08)'	nd	nd	nd	nd
MgO	2.21	(0.11)	2.30	(0.34)	1.82	(0.44)	1.09	(0.00)	4.02	(1.86)	0.48	(0.05)	0.48	(0.00)
CaO	5.04	(0.19)	5.08	(0.42)	4.98	(0.50)	3.74	(0.00)	8.86	(0.65)	2.01	(0.20)	2.48	(0.28)
Na_2O	3.81	(0.18)	3.85	(0.24)	3.79	(0.41)	3.83	(0.00)	3.08	(0.22)	3.51	(0.32)	3.65	(0.06)
K_2O	2.70	(0.22)	2.66	(0.38)	2.66	(0.38)	3.63	(0.00)	1.19	(0.17)	3.85	(0.24)	3.69	(0.30)
Cl	0.10'	(0.03)'	0.08'	(0.01)'	0.12	(0.03)	0.20	(0.00)	0.19'	(0.04)'	0.22	(0.03)	0.24	(0.01)
Total	1.11	(0.61)	0.74	(0.47)	1.00	(0.91)	0.23	(0.00)	4.17	(1.97)	1.42	(1.01)	2.65	(0.38)
n	*n = 14*		*n = 12*		*n = 12*		*n = 1*		*n = 8*		*n = 9*		*n = 2*	

Formation	Pourahu Member [tephra unit] [BT1]		Pourahu Member [tephra unit] [DR16]		Pourahu Member [ignimbrite unit] [CT] Unbanded				Pourahu Member [ignimbrite unit] [CT] Band 2		Pourahu Member [ignimbrite unit] [CT] Band 5			
	Incl. in Pyroxene		Groundmass		Groundmass		Incl. in Pyroxene		Groundmass		Groundmass		Incl. in Pyroxene	
SiO_2	71.44	(0.94)	72.40	(0.73)	72.55	(0.43)	69.86	(1.82)	68.36	(2.48)	66.70	(3.13)	71.01	(0.00)
Al_2O_3	14.24	(0.48)	14.08	(0.40)	14.14	(0.37)	12.94	(1.25)	14.12	(1.38)	14.81	(1.83)	14.29	(0.00)
TiO_2	0.69	(0.04)	0.59	(0.04)	0.53	(0.05)	0.53	(0.09)	0.65	(0.09)	0.71	(0.07)	0.57	(0.00)
FeO	3.01	(0.14)	2.71	(0.09)	2.61	(0.11)	3.63	(0.72)	4.48	(1.72)	5.11	(1.58)	2.94	(0.00)
MnO	nd	nd	0.13'	(0.02)'	nd	nd	0.11'	(0.00)'	0.16'	(0.01)'	0.20'	(0.00)'	nd	nd
MgO	0.56	(0.12)	0.54	(0.03)	0.50	(0.04)	1.87	(1.18)	2.25	(2.01)	2.21	(1.20)	0.68	(0.00)
CaO	2.47	(0.26)	2.13	(0.14)	2.01	(0.11)	3.48	(1.75)	3.53	(0.79)	3.96	(1.18)	2.30	(0.00)
Na_2O	3.68	(0.11)	3.48	(0.35)	3.49	(0.46)	3.89	(0.17)	3.29	(0.59)	3.68	(0.29)	4.19	(0.00)
K_2O	3.72	(0.13)	3.75	(0.18)	3.96	(0.10)	3.51	(0.43)	3.09	(0.54)	2.53	(0.59)	3.81	(0.00)
Cl	0.20	(0.03)	0.27	(0.08)	0.20	(0.04)	0.20'	(0.01)'	0.17	(0.03)	0.15	(0.04)	0.21	(0.00)
Total	3.11	(0.08)	3.12	(2.33)	3.10	(1.70)	2.52	(1.01)	3.78	(0.58)	4.06	(0.72)	1.63	(0.00)
n	*n = 4*		*n = 10*		*n = 12*		*n = 5*		*n = 6*		*n = 5*		*n = 1*	

Formation	Pourahu Member [ignimbrite unit] [CT] Band 6		Pourahu Member [ignimbrite unit] [CT] Band 7		Member L6		Member L3					
	Incl. in Pyroxene		Groundmass		Groundmass		Groundmass		Incl. in Plagioclase		Incl. in Pyroxene	
SiO_2	70.21	(0.68)	73.73	(1.52)	69.38	(0.91)	69.88	(0.23)	69.29	(0.00)	67.22	(0.47)
Al_2O_3	14.86	(0.12)	13.73	(0.79)	14.88	(0.45)	17.09	(0.20)	17.31	(0.00)	18.11	(0.18)
TiO_2	0.75	(0.04)	0.43	(0.07)	0.75	(0.07)	0.84	(0.08)	0.80	(0.00)	0.68	(0.09)
FeO	3.28	(0.21)	2.27	(0.25)	3.72	(0.22)	5.78	(0.20)	6.01	(0.00)	6.79	(0.11)
MnO	nd	nd	nd	nd	0.10'	(0.00)'	0.30'	(0.00)'	0.22	(0.00)	0.25'	(0.00)'
MgO	0.57	(0.07)	0.32	(0.08)	1.06	(0.23)	3.63	(0.16)	2.67	(0.00)	3.35	(0.28)
CaO	2.32	(0.31)	1.83	(0.57)	3.30	(0.42)	7.28	(0.13)	7.46	(0.00)	8.71	(0.34)
Na_2O	4.07	(0.05)	3.34	(0.22)	3.75	(0.37)	3.61	(0.16)	4.07	(0.00)	3.46	(0.23)
K_2O	3.73	(0.13)	4.15	(0.27)	2.95	(0.63)	1.78	(0.06)	2.01	(0.00)	1.43	(0.15)
Cl	0.20	(0.01)	0.19	(0.02)	0.21	(0.04)	0.09'	(0.03)'	0.16	(0.00)	0.14	(0.02)
Total	3.45	(0.14)	2.13	(1.26)	2.34	(1.34)	1.18	(0.35)	2.42	(0.00)	2.76	(0.51)
n	*n = 2*		*n = 6*		*n = 16*		*n = 11*		*n = 1*		*n = 3*	

* All statistics are for normalised values above detection limit only; values in parentheses are standard deviations. Incl. = inclusion; nd = no values above detection limit.

† At least one analysis gave a result below detection limit (not included in these statistics).

Source

Tephras from TgVC which show rhyolitic glass compositions (shards and groundmass glass in pumice lapilli) are distinguished from the Central North Island rhyolitic tephras of TVC

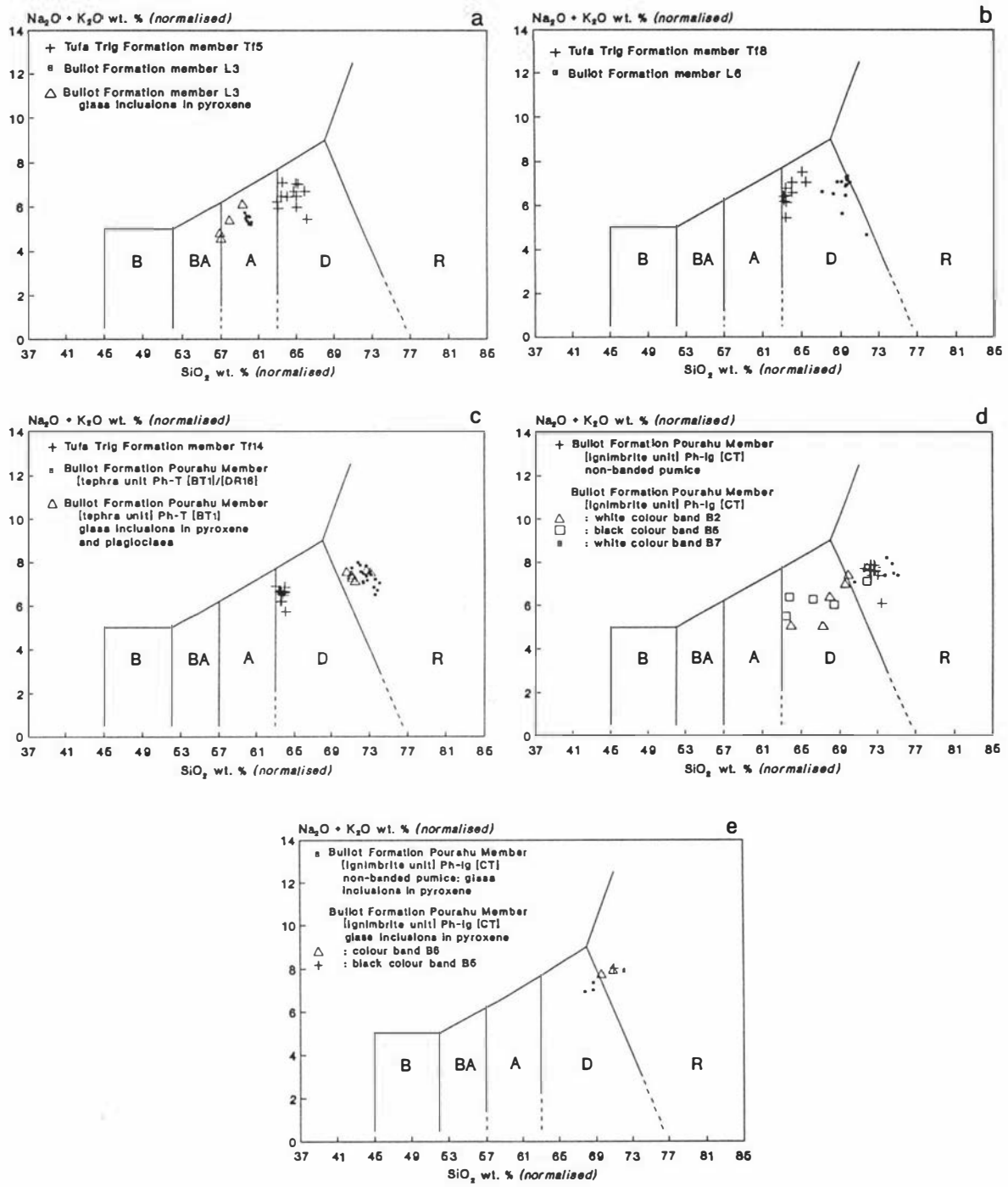

Figure 4.26 Total alkali silica (TAS) diagrams (after Le Maitre 1984) showing compositions of groundmass glass and glass inclusions in some Mt Ruapehu tephras (Fig. 4.26a – c) and Pourahu Member [ignimbrite unit] (Fig. 4.26d,e). Colour bands analysed in Pourahu Member [ignimbrite unit] are shown in Plate 4.5. Compositional fields are basalt (B), basaltic andesite (BA), andesite (A), dacite (D), and rhyolite (R).

and OVC by the major element chemistry of their glasses (Figure 4.27, p. 227). Rhyolitic glass (low silica-rhyolite) in Pourahu Member [tephra and ignimbrite units] sourced from Mt Ruapehu is more alkaline and less silicic in composition than the rhyolitic glass shards of TVC and OVC tephras. Further, mean FeO, CaO, TiO_2, Al_2O_3 and MgO contents are all higher in the Mt Ruapehu glasses.

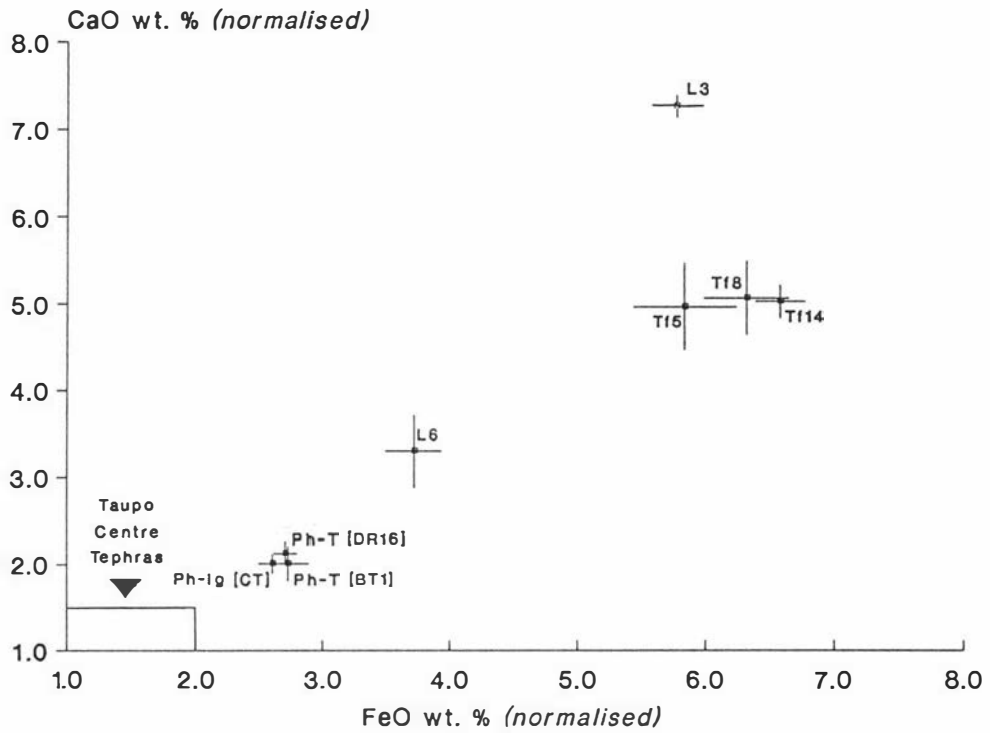

Figure 4.27 Plot of CaO *vs* FeO (wt.%) in glass of some Mt Ruapehu tephras and Pourahu Member [ignimbrite unit]. Glasses in Taupo Volcanic Centre rhyolitic tephras generally show CaO and FeO contents < 1.5% and < 2%, respectively (see also Figure 2.3, p.).

Southeast of TgVC, Froggatt and Rodgers (1990) identified glass with rhyolitic composition (> 70% SiO_2) preserved in Reporoa peat bog, located in the Ruahine Range. Based on the FeO and TiO_2 contents in the glasses Froggatt and Rodgers proposed that some of the shards were sourced from TgVC, and not TVC or OVC. Although the tephras are not correlated with known eruptives from Mt Ruapehu or Mt Tongariro, their glass chemistry (FeO and CaO contents) is consistent with analyses of TgVC glasses made in this study. Rhyolitic glass compositions have not been identified in previous mineralogical studies of TgVC andesitic tephras (*e.g.* Lowe 1987, 1988a; Stokes and Lowe 1988), but have been identified in tephras from EVC (*e.g.* Wallace 1987; R.B. Stewart, pers. comm. 1990).

Wallace (1987) and Lowe (1988a) showed that andesitic tephras from TgVC and EVC could be distinguished by a comparison of the major element chemistry (SiO_2, MgO, TiO_2 and alkali $Na_2O + K_2O$ contents) of their glasses. While results of this study support the findings of Wallace and Lowe, tephras from TgVC which show siliceous dacitic or rhyolitic glass compositions show very similar glass chemistry to the dacitic and rhyolitic glasses in EVC tephras and are therefore not distinguished from them.

Members

Tufa Trig Formation Tephras

The glass chemistry of three members (Tf5, Tf8, Tf14) has been determined. These tephras are of coarse ash to fine lapilli grade and comprise vitric pyroclasts, free ferromagnesian minerals (clinopyroxene and orthopyroxene) and minor vesicular pumice fragments. Some pyroxene phenocrysts show resorbed textures (embayed and rounded outlines). Some of the plagioclase phenocrysts show sieve textured cores with euhedral oscillatory zoned rims; others show anhedral resorbed outlines.

In thin section, the vitric pyroclasts comprise black or brown glass with many large included euhedral to subhedral, and embayed crystals of feldspar and pyroxene (Plate 4.4a,b). Abundant microlites of feldspar and pyroxene occur in the groundmass glass of most pyroclasts (Plate 4.4c). Others contain few microlites (Plate 4.4d). Pumice fragments occur in minor amounts. They are highly vesicular and pale yellow or white in colour. In thin section pumice fragments are distinctly more vesicular than the vitric pyroclasts and accessory rhyolitic glass shards of TVC source.

Rhyolitic glass shards (Plate 4.15a,b) are identified in all the tephras. These shards are derived from Taupo Pumice and have been incorporated into Tufa Trig Formation tephras during their deposition, and also in the interbedded Makahikatoa Sands by aeolian redeposition. Rhyolitic shards identified within member Tf8 and analysed by electron microprobe have major element concentrations (FeO and CaO) typical of Holocene tephras from TVC.

Most of the glass analyses from Tufa Trig Formation members were obtained from the groundmass glass of vitric pyroclasts, and others from glass shards and glass selvedges on pyroxene or plagioclase phenocrysts. All analyses show dacitic glass compositions (Figure 4.26, p. 226). Members show very similar glass chemistries and are not clearly distinguished on major element glass chemistry (Figure 4.27, p. 227; Figure 4.28, p. 229).

Members Tf5, Tf8 andTf14were selected for comparison because they are prominent units and collectively they span a large part of the depositional record of Tufa Trig Formation. The strong similarity in glass chemistry of these members suggests other members of the formation will show dacitic glass compositions and similarly would be unlikely to be distinguished by comparison of glass or ferromagnesian phenocryst chemistry.

Although members are not clearly distinguished from glass chemistry, comparison of the glass SiO_2, MgO, CaO and TiO_2 contents in Tufa Trig Formation tephras clearly distinguishes this formation from the other Mt Ruapehu tephras (Figure 4.27, p. 227; Figure 4.28, p. 229), all of which fall into discrete compositional groups.

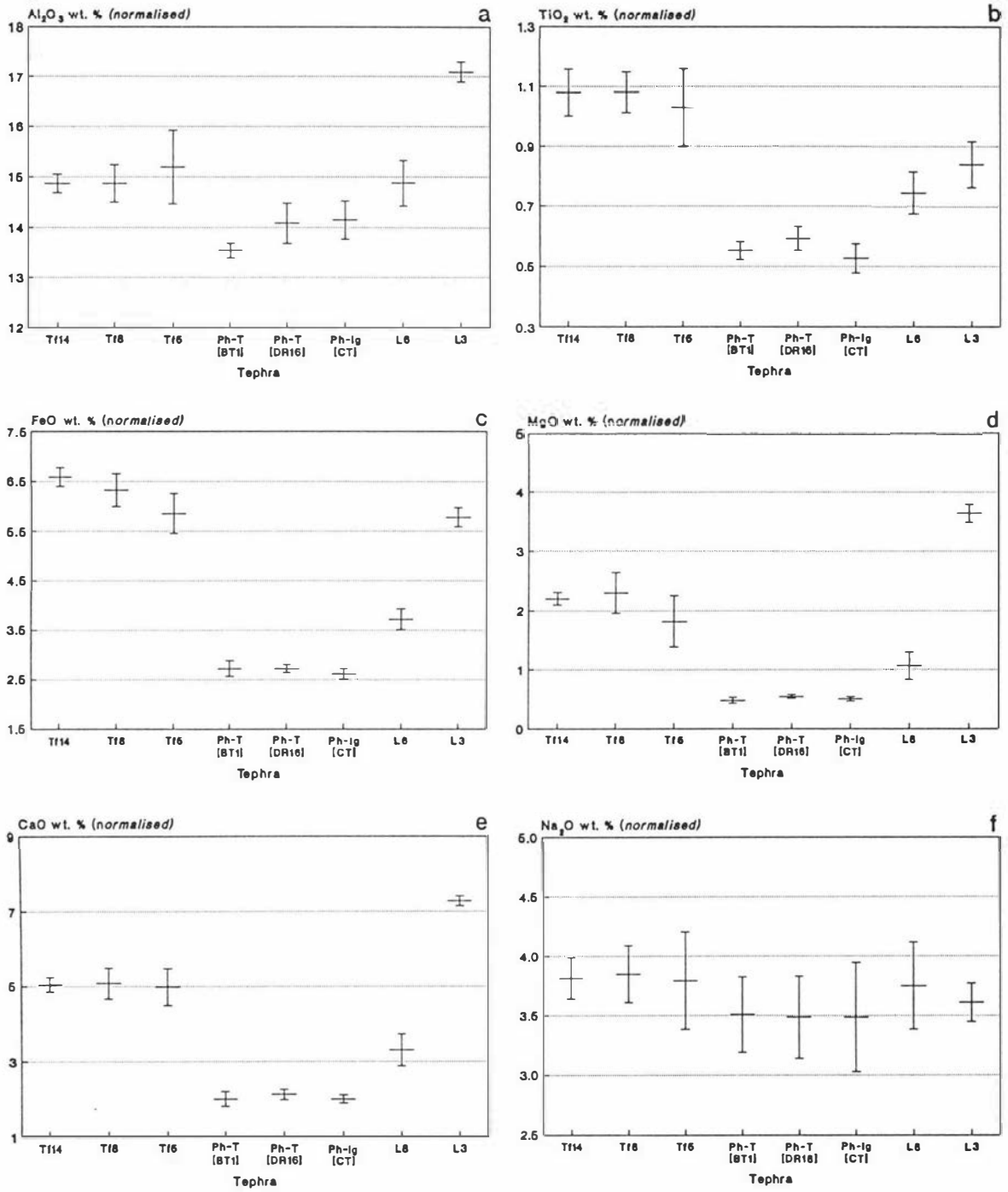

Figure 4.28 Mean oxide contents in glass of some Mt Ruapehu tephras and Pourahu Member [ignimbrite unit] bars show standard deviation. (see text for tephra codes).

Bullot Formation Pourahu Member

In thin section the groundmass glass of pumice lapilli from Pourahu Member [tep unit] is finely vesiculated, with numerous small, irregularly-shaped vesicles and stringy ve walls. There are no pyroxene or feldspar microlites within the groundmass glass.

The groundmass glass composition of Pourahu Member [tephra unit] sampled fr type section (Ph-T [DR16]) is rhyolitic (Figure 4.26, p. 226; Table 4.12, p. 22 groundmass glass of sample Ph-T [BT1], sampled Bullot Track S.1 and correla

Pourahu Member [tephra unit] on the basis of stratigraphic position, field characteristics and ferromagnesian mineral assemblage was also analysed by EMP and found to be of almost identical composition, thus supporting their correlation (Figure 4.27, p. 227; Figure 4.28, p. 229). The bulk rock composition of sample Ph-T [BT1] [9] is andesitic (60.6% SiO_2, Appendix IIIh). In contrast, these two tephras could not be correlated on either their clinopyroxene or orthopyroxene major element chemistries, which may suggest that clinopyroxene and orthopyroxene are early fractionating, possibly xenocrystic phases.

Within the ignimbrite unit of Pourahu Member there are two texturally different pumice lapilli and block types – dominant, white phenocryst-rich vesicular pumices, and less abundant white and black colour-banded vesicular pumices (Plate 4.5).

The non-banded pumice lapilli in Pourahu Member [ignimbrite unit] are moderately vesicular and contain phenocrysts of plagioclase, orthopyroxene, clinopyroxene and trace olivine. In thin section the groundmass glass, which is microlite free, shows numerous small, irregularly shaped vesicles with stringy vesicle walls.

Plagioclase phenocrysts show resorbed textures with sieve textured cores and embayed oscillatory zoned rims. Plagioclase also occurs as crystal aggregates or glomerocrysts. Pyroxene phenocrysts are not zoned and also occur in glomerocrysts. Many phenocrysts show resorbed textures (distinctly embayed and rounded crystal outlines) and inclusions of brown glass, indicative of magma mixing (Eichelberger 1975; Gerlach and Grove 1982; Kuo and Kirkpatrick 1982; Cantagrel *et al.* 1984; Sakuyama 1984; Gourgaud *et al.* 1989; Robin *et al.* 1990).

The groundmass glass composition in the non-banded lapilli is rhyolitic (Figure 4.26, p. 226), and analyses show homogenous glass compositions (Appendix IIIg). The bulk rock composition is, however, andesitic (60.9% SiO_2, Appendix IIIh). Glass inclusions within pyroxene phenocrysts show both dacitic to rhyolitic compositions (Table 4.12, p. 225) indicating the phenocrysts probably formed in equilibrium with an acid (dacitic) liquid. Glass inclusions in different crystals are assumed to have been trapped at the same point (Watson 1976).

These white non-banded pumices represent the more acidic end member involved in the magma mixing. Their glass chemistry may reflect the original liquid composition, representing either a residual fractionated liquid derived from an andesite melt, or alternatively, a hybrid formed from a previous mixing event, in which mixing occurred to completion, producing a hybrid with intermediate and homogenous groundmass glass compositions (Gourgaud *et al.*

[9] All bulk rock (XRF) analyses of Bullot Formation tephras are courtesy of Dr J. Gamble, Research School of Earth Sciences, Victoria University of Wellington. Analyst was K. Palmer.

1989). The presence of phenocrysts with disequilibrium resorbed textures lends support to the latter origin.

Colour-banded lapilli and blocks

The colour-banded lapilli provide textural evidence of magma mixing (Eichelberger 1974; Walker 1981a; Green 1982; Cantagrel *et al.* 1984; Sakuyama 1984; Gourgaud *et al.* 1989). The lapilli and blocks comprise bands of black, white, and black and white streaked pumice. Most bands are continuous and contacts between bands are sharp and distinct (Plate 4.5). In thin section the black bands are less vesicular and more phenocryst-rich.

Both pumice types and the colour-bands within banded lapilli have been analysed for their glass chemistries. Samples were collected from the type locality within Rangipo Desert [T20/437045]. Analyses are presented in Appendix IIIg, and mean analyses are given in Table 4.12 (p. 225). Glass analysed from within white pumice band 7 (Plate 4.5) is of rhyolitic composition and very similar chemistry to that of the white non-banded pumice. The glass composition in band 2, which is finely streaked with black and white glass, varies between dacitic and rhyolitic. Glass analysed from the black pumice band 5 also shows variable compositions ranging from andesitic to dacitic (Figure 4.26, p. 226). Some analyses approach the chemistry of TVC rhyolitic tephras.

Heterogenous groundmass glass compositions are evidence of magma mixing (De Rosa and Sheridan 1983; Sakuyama 1984). Presence of heterogenous glass compositions within the banded lapilli, ranging between dacite and rhyolite, indicates the lapilli are hybrids produced by the partial mixing of dacitic and dacitic-rhyolitic end members. The chemistry of glass inclusions within phenocrysts is also evidence of mixing. A single analysis of a glass inclusion within a plagioclase phenocryst in the dacitic band (B5) is of rhyolitic composition, and glass inclusions within plagioclase and pyroxene phenocrysts in the non-banded lapilli (with rhyolitic glass compositions) are dacitic to rhyolitic in composition.

The black pumice within these lapilli therefore represents the more basic end-member involved in the mixing (*e.g.* band 5) and the white bands (particularly band 7) and the non-banded white pumices the more acid end-member (Figure 4.29, p. 232). Bulk rock compositions determined for three mixed pumice lapilli are andesitic (60% SiO_2, Appendix IIh). Both the black and white components are vesiculated and were therefore mixed prior to eruption. Both banded pumices and pumice with homogenous compositions can be erupted together depending on the depth where vesiculation and following disruption of the magmas occurs (Kouchi and Sunagawa 1985, *in* Gourgaud *et al.* 1989).

Correlation

The tephra and ignimbrite units of Pourahu Member are believed to have been erupted during the same eruptive event based on their field characteristics, stratigraphic position and ferromagnesian mineral assemblage. Lapilli in the tephra unit comprise only white non-banded

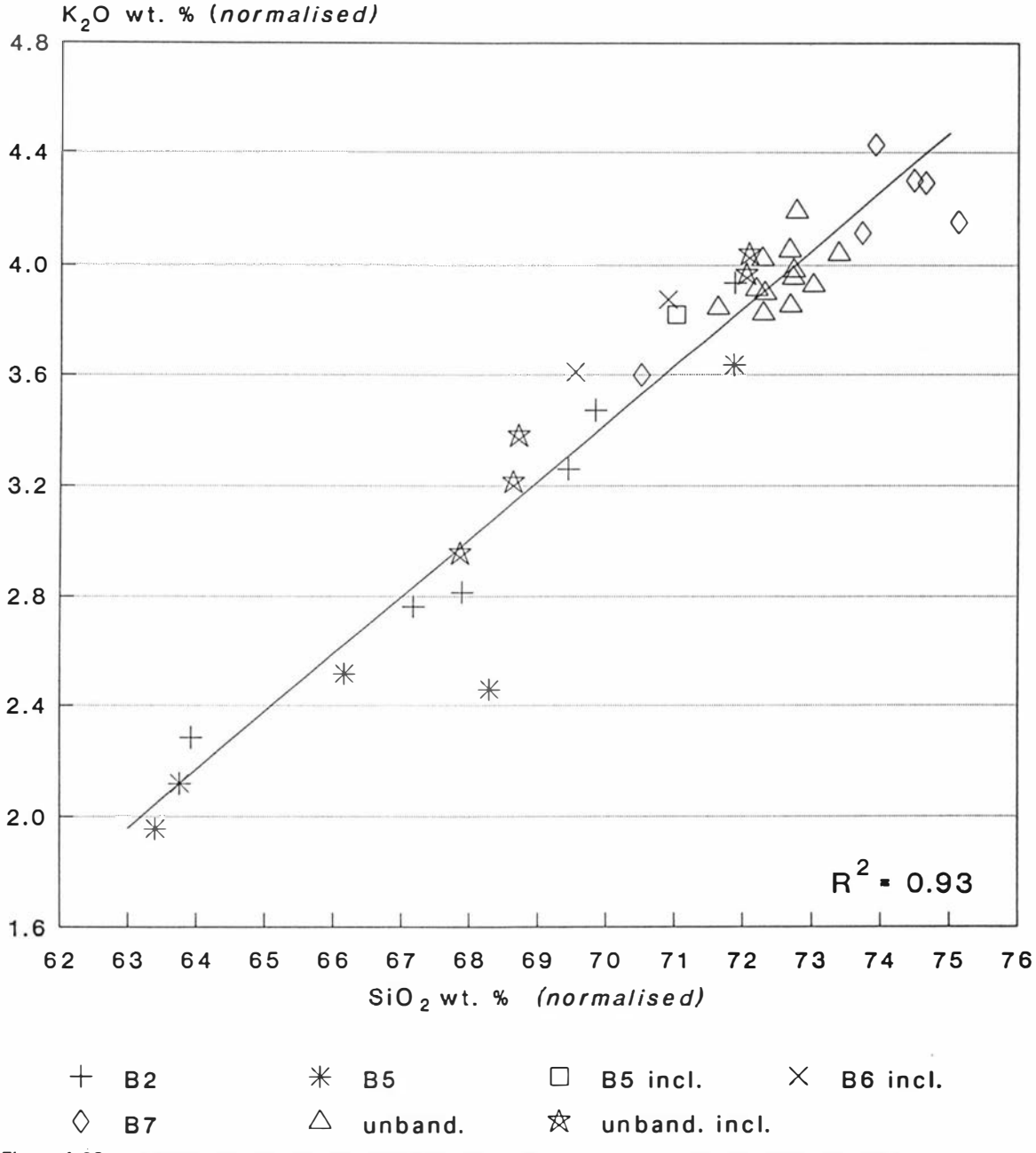

Figure 4.29 K_2O *vs* SiO_2 (wt.%) content in groundmass glass and glass inclusions from banded (B2, B5, B6, B7; see Plate 4.5), and non-banded (unbend.) pumice of Pourahu Member [ignimbrite unit]. Glass compositions range from rhyolite to dacite. The collinear relationship exhibited between the glasses suggests a derivation from mixed magma.

lapilli and cannot be chemically distinguished from the non-banded lapilli of the ignimbrite (Figure 4.27, p. 227). The almost identical glass chemistry supports the association of these two members with the same eruptive event.

Member L6 (Pink Lapilli)

The groundmass glass is of dacitic composition (Figure 4.26, p. 226) and is moderately vesicular with few microlites and phenocrysts of orthopyroxene and clinopyroxene and minor to trace amounts of hornblende. The bulk rock composition of the pumice lapilli is andesite

(56.9% SiO_2) (Appendix IIIh). Some clinopyroxene phenocrysts show distinctly rounded resorbed outlines. This tephra is clearly distinguished from the other Mt Ruapehu-sourced tephras on its glass chemistry (Figure 4.27, p. 227; Figure 4.28, p. 229).

Member L3 (Hokey Pokey Lapilli)

Pumice lapilli in member L3 are very vesicular, and in thin section appear coarsely cellular with thin vesicle walls. The groundmass glass contains few microlites with phenocrysts of orthopyroxene, clinopyroxene and skeletal forsteritic olivine.

Some pyroxene phenocrysts show resorbed textures and most orthopyroxene phenocrysts contain numerous inclusions of brown glass. Analyses of the groundmass glass in this tephra are presented in Appendix IIIg and the mean analysis is given in Table 4.12, p. 225. The composition of the groundmass glass is andesitic. The bulk rock composition of pumice lapilli is andesite (55.9% SiO_2) (Appendix IIIh). Glass inclusions in pyroxene phenocrysts show basaltic-andesite to andesite compositions.

Member L3 is clearly distinguished from the other Mt Ruapehu tephras examined on glass chemistry (Figure 4.27, p. 227; Figure 4.28, p. 229). The field appearance of this tephra (strong brown colouring and vesicularity) and its ferromagnesian mineralogy (opx + cpx + oliv) is consistent with its distinctly more mafic composition.

Tephra Fingerprinting – Summary and Conclusions

Results of this study show that in most cases both field and laboratory methods are needed to adequately characterise andesitic tephras so that they can be correlated locally and regionally. Diagnostic mineralogical characteristics provide a means of identifying and correlating tephras where correlation based on field appearances and stratigraphic position is equivocal.

Field Characteristics

Several of the tephra marker beds examined in this study are able to be correlated locally using field characteristics (colour, thickness, grain size) and their stratigraphic position relative to prominent andesitic and rhyolitic marker beds. The mineralogy and chemistry of these tephras has also been determined and provides an alternative means of correlation distally where field characteristics and stratigraphic position may be less reliable.

Most Mt Ruapehu-sourced tephras (Tufa Trig Formation and Bullot Formation tephras), however, lack diagnostic field characteristics useful to correlation and have therefore been 'fingerprinted' using laboratory methods as outlined in section 4.3.

It is possible to uniquely identify some of the andesitic tephras simply from the physical characteristics of their lapilli (*e.g.* colour-banded lapilli) and accessory constituents (*e.g.* xenoliths and accretionary lapilli).

Ferromagnesian Mineral Assemblage

The use of ferromagnesian mineral assemblage as a means of distinguishing TgVC tephras at both formation and member level is limited due to the similarity in assemblages exhibited by most of the tephras. However, seven andesitic marker beds are distinguished and can be correlated locally from their ferromagnesian mineral assemblages and stratigraphic positions. Distal hornblende- or olivine-bearing andesitic tephras potentially may be correlated with TgVC tephras from ferromagnesian mineral assemblage, olivine morphology, and proportions of olivine and hornblende. Presence of significant proportions of orthopyroxene suggest a TgVC source; however, the presence of hornblende can no longer be considered diagnostic of an EVC source.

Ferromagnesian Mineral Chemistry

Those tephras that cannot be distinguished by either field characteristics or ferromagnesian mineralogy are also generally not distinguished by the major element chemistry of ferromagnesian phenocrysts (clinopyroxene, orthopyroxene, olivine, hornblende and Fe-Ti oxides). Exceptions to this include some of olivine and hornblende-bearing tephras.

Results show that the 23 andesitic tephras examined show similar clinopyroxene and orthopyroxene chemistries. Tephra formations and members from both the same and different sources, are generally not distinguishable on the basis of major element cpx- and opx-chemistry. Only those members which show distinctive ferromagnesian mineral assemblages (*i.e.* contain significant levels of olivine or hornblende) have distinctive cpx- or opx-chemistries. Differences in the field appearances of tephras (*i.e.* pumice colour, vesicularity and phenocryst content) are generally not reflected in the chemistry of clinopyroxene or orthopyroxene phenocrysts.

The similarity in the chemistry of most tephras, and the variability in chemistry exhibited by each, limits the use of major element cpx- and opx-chemistry as a means of identifying and correlating andesitic tephras, and possibly reflects the early separation of both clinopyroxene and orthopyroxene from parental melts of rather similar composition in these andesites.

Olivine major element chemistry, when used in conjunction with olivine morphology and stratigraphic position, is a useful means of distinguishing between tephras from the same source, and a potentially useful means of distinguishing and correlating distal andesitic tephras from TgVC where a complete stratigraphy is not preserved.

The similarity in the major element chemistry of hornblende phenocrysts in most TgVC tephras, and the variability in chemistry exhibited by each limits the use of hornblende chemistry as a means of identifying and correlating TgVC andesitic tephras. Comparison of ferromagnesian mineral assemblages and the relative proportions of hornblende is a more useful means of distinguishing both source and members – hornblende has been found as a dominant ferromagnesian mineral in some Mt Tongariro tephras, and in minor to trace amounts in Mt Ruapehu tephras.

Near source each of the hornblende-bearing tephras can be identified and correlated from stratigraphic position and field appearances. The major element chemistry of hornblende phenocrysts in distal andesitic tephras is a useful indicator of source, but is not diagnostic of tephra formations or members.

Preliminary investigation shows that determination of the major element chemistry of titanomagnetites is of limited use as a means of uniquely identifying tephras from TgVC, and andesitic tephras in general; Kohn and Neall (1973) and Alloway (1989) also found titanomagnetite chemistry of limited use in distinguishing late Pleistocene and Holocene tephras sourced from EVC.

The similarity in major element chemistry of titanomagnetites within TgVC tephras prevents the distinction of most of the Bullot Formation members at source, and limits the use of titanomagnetite chemistry as a potential means of correlating distal TgVC tephras. The major element chemistry of titanomagnetites, however, appears to be a more useful means of distinguishing between tephras which exhibit similar ferromagnesian mineral assemblages than does clinopyroxene or orthopyroxene phenocryst chemistry, as shown by the discrete grouping of the tephra and ignimbrite units of Pourahu Member.

Glass Chemistry

Compared to the Central North Island rhyolitic tephras the glass chemistry of andesitic tephras has been little studied. The potential for use of glass chemistry as a means of distinguishing TgVC tephras has not previously been examined.

In comparison to rhyolitic glass, andesitic glass is more susceptible to weathering (Kirkman 1981; Friedman and Long 1984) and in many andesitic tephras the sparseness of fresh unweathered glass, the much greater vesicularity of the glass, and the high microlite contents makes analysis by microprobe methods difficult (Lowe 1988a).

Although the vesicularity of the pumice lapilli greatly restricts the surface area available for analysis, good results have been obtained from careful analysis of the thin microlite-free vesicle walls. Most analyses show totals between 97–99% (implying water contents of 1–3%) with low standard deviations on all elements. This investigation of the glass

chemistry of Mt Ruapehu tephras shows glass chemistry to be the most useful means of mineralogically distinguishing and correlating TgVC andesites. The discrete grouping of tephras achieved by comparing the major element chemistry of glass is not paralleled by comparing the major element chemistry of clinopyroxene, orthopyroxene, hornblende or titanomagnetite phenocrysts. With the exception of Bullot Formation member L3, tephras compared in Figure 4.27 (p. 227) and Figure 4.28 (p. 229) are not distinguished from their ferromagnesian mineral assemblages. These tephras are, however, clearly distinguished from their glass chemistry.

Differences in the field colour of pumice lapilli appear to be reflected in the glass chemistry, but tend not to be reflected in the phenocryst chemistry. Lapilli which are white in colour in the field situation are shown to have dacitic or rhyolitic glass compositions while strongly iron-stained lapilli, such as member L3 (hokey pokey lapilli), are more basic in composition. Tephras which can be clearly distinguished on colour and vesicularity are potentially able to be distinguished and correlated by the major element chemistry of their glasses.

From the few glass analyses obtained, it is clear that there is a wide range in the compositions of glasses (andesitic to rhyolitic), and less variation in the bulk chemistry. Potentially, therefore, glass chemistry offers the best opportunity for laboratory based identification (fingerprinting) and correlation of tephras. A multi-criterion approach to tephra identification and correlation, using stratigraphy, ferromagnesian mineralogy and glass chemistry should be employed. Results of both field and laboratory fingerprinting studies indicate, however, that there is no simple or single-parameter method for distinguishing TgVC andesitic tephras.

Changes in the Mineralogy and Chemistry of Tephras Over the Past *c.* 22 500 Years

Tephras erupted from Mt Ruapehu comprise two formations – Bullot Formation and Tufa Trig Formation.

The most active eruptive period at Mt Ruapehu was between *c.* 22 500 and *c.* 10 000 years B.P., during which the Bullot Formation tephras were erupted. The younger Tufa Trig tephras (dated *c.* 1800 – present) were erupted after a *c.* 8000 year period of intermittent activity at Mt Ruapehu following the eruption of the Bullot Formation tephras. During this relatively quiescent period, most of Mt Tongariro-sourced tephras were erupted.

There is little overall variation in the ferromagnesian mineralogy in of the Mt Ruapehu tephras. Olivine and minor to trace amounts of hornblende occur in some tephras but their occurrence is sporadic and does not exhibit any trend with time. Comparison of ferromagnesian mineral assemblages and both glass and bulk rock chemistries does, however, identify changes in the melt chemistry below Mt Ruapehu within the last *c.* 22 500 years.

Within the Bullot Formation, changes in melt chemistry are identified by successive eruptions of olivine-bearing andesitic melts (*e.g.* Shawcroft Tephra and member L3) and more acidic mixed melts (members L6 and Pourahu Member) containing traces of hornblende. The eruption of the Tufa Trig Formation tephras between *c.* 1800 years B.P. and the present, may also have been from a more acidic melt. Glass in three of the members is of dacitic composition.

Tephras erupted from Mt Tongariro comprise three formations – Rotoaira Lapilli, Pahoka Tephra, and Mangamate Tephra (in order from oldest to youngest). The ferromagnesian mineralogy and chemistry of Rotoaira Lapilli, Pahoka Tephra and four members of Mangamate Tephra (Poutu Lapilli, Waihohonu Lapilli, Oturere Lapilli, Te Rato Lapilli), and bulk rock SiO_2 contents of three of these are summarised in Table 7.1, p. 314.

Pahoka Tephra, dated *c.* 10 000 – 9800 years B.P., and Te Rato Lapilli Member, dated 9780 ± 170 years B.P. [NZ1372], were erupted after a *c.* 4000 year period of quiescence at Mt Tongariro following the eruption of Rotoaira Lapilli, dated 13 800 ± 300 years B.P. During this interval distinct changes in melt chemistry occurred below Mt Tongariro. The earlier eruption of Rotoaira lapilli was from an andesite melt (58.9% SiO_2), which contained forsteritic olivine. The later eruptions of Pahoka Tephra and Te Rato Lapilli were from more acidic, hornblende-bearing hybrid (mixed) melts of dacitic composition (63.1% and 63.4% SiO_2, respectively). Some of the younger members of Mangamate Tephra were also erupted from hybrid (mixed melts) as indicated by banded textures in pumice and scoriaceous lapilli, and olivine morphologies.

The most distinct change in the ferromagnesian mineralogy of the collective TgVC tephras, identified by the change from assemblages dominated by hornblende to assemblages dominated by olivine, occurs within the *c.* 9780 – 9700 years B.P. Mangamate Tephra. The change may indicate that several mixing episodes, each marked by differences in the mixing ratio of the acidic and more basaltic end members, were associated with their eruption.

The eruption of the andesitic Pourahu Member [tephra and ignimbrite units] from Mt Ruapehu occurred shortly before the eruption of the dacitic Pahoka Tephra and Te Rato Lapilli from Mt Tongariro. These latter two tephras and Pourahu Member [ignimbrite unit] were erupted from hybrid (mixed) magmas. Their eruption identifies closely timed changes in melt chemistry below both Mt Tongariro and Mt Ruapehu, and the existence of a body of more acidic magma.

The groundmass glass of Pourahu Member [tephra unit] and Pourahu Member [ignimbrite unit] and the hornblendes in both Pahoka Tephra and Te Rato Lapilli show very similar chemistries to both the glass and hornblendes in TVC rhyolitic tephras. This similarity suggests that the same processes acting to produce rhyolites in TVC are also acting at TgVC on occasions to produce components of the more acidic hornblende-bearing melts.

Eruption Styles at Mt Ruapehu

Two eruption styles, subplinian and phreatomagmatic, are identified at Mt Ruapehu from examination of the tephra deposits preserved on the southeastern Mt Ruapehu ring plain. Subplinian eruptions account for the greater part of the tephra record. Later volcanism was characterised by phreatomagmatic eruptions, the deposits of which are volumetrically quite small in comparison to those of the subplinian eruptions.

Tephras erupted from Mt Tongariro are also the products of subplinian eruptions (Cole *et al.* 1986). Tephra eruptions from TgVC historically show strombolian, subplinian, phreatomagmatic and phreatic eruption styles (Houghton and Hackett 1984; Cole *et al.* 1986).

Subplinian Eruptions

Subplinian eruptions are intermediate between strombolian and plinian activity. They are gas-charged eruptions which produce high eruption columns. The division between plinian and subplinian eruptions is arbitrarily placed at a dispersal area (D) of 500 km^2 (Walker 1981b). Plinian and subplinian eruptions are characterised by widespread, well sorted, and coarse-grained pumice deposits with low fragmentation indexes. Deposits commonly show reverse grading and comprise juvenile pumice, crystals, and both juvenile and accessory lithic lapilli (Walker 1973, 1981b, 1982; Traineau *et al.* 1989).

Eruptions at Mt Ruapehu

The Bullot Formation represents some of the most widespread tephras erupted from Mt Ruapehu. They are interpreted as the products of subplinian eruptions, based on field characteristics and distribution. Tephras of this formation were not dispersed over large areas, and with the exception of one member, eruptions were not accompanied by pyroclastic flows.

The Bullot Formation tephras comprise mantle bedded lapilli and ash layers, most of which are less than 0.3 m thick. Lapilli layers are poorly sorted and dominated by vesicular pumice lapilli, occurring together with juvenile and accessory lithic lapilli, and pumiceous bombs in some layers. Accretionary lapilli have been found in two tephras and were most probably formed in the eruption columns by accretion of moist ash.

Eruptions at Mt Tongariro

Four members of Mangamate Tephra (Poutu Lapilli, Waihohonu Lapilli, Oturere Lapilli, Te Rato Lapilli) and the slightly older Pahoka Tephra are characterised by angular, blocky, and poorly vesicular scoriaceous lapilli and minor amounts of pumice. These members form thick deposits of loose poorly sorted and poorly bedded fine lapilli. The Mangamate tephras are the products of subplinian to plinian eruptions (Cole *et al.* 1986) involving mixed magmas. The low vesicularity and dense nature of these lapilli compared to other TgVC tephras may indicate partial degassing of the mixed magma prior to their eruption. Degassing of ponded magma

produced dense blocky ejecta in strombolian deposits of the Ohakune craters (Houghton and Hackett 1984).

The older Rotoaira Lapilli is also the product of a subplinian eruption (Cole *et al.* 1986), but in contrast to other Mt Tongariro tephras, it comprises very vesicular pumice lapilli and subordinate lithic lapilli.

Ignimbrite Eruptions

Pyroclastic flows and surges are eruption phenomena commonly associated with plinian eruptions (Sheridan 1979; Fisher and Schmincke 1984). Ignimbrites are the deposits of pyroclastic flows, the latter being hot fluidised mixtures of gas and pyroclasts that move rapidly across the ground surface (Smith 1960). Theoretical models explain the generation of pyroclastic flows by gravitational collapse of an overloaded eruption column (Sparks *et al.* 1978; Sheridan 1979). Other models suggest possible generation by explosion of domes or lava flows (Sheridan 1979).

Pourahu Member

The ignimbrite unit of Pourahu Member (Bullot Formation) is a small volume, unwelded pumice flow comprising poorly sorted ash, juvenile scoriaceous lapilli, and vesicular lapilli, blocks and breadcrusted andesitic pumice bombs – features characteristic of pyroclastic flow deposits.

Change in the style of eruption at Mt Ruapehu *c.* 11 000 years B.P. is evidenced by the eruption of Pourahu Member. The eruption of mixed magmas and subsequent generation of a pyroclastic flow (Pourahu Member [ignimbrite unit]) identifies a brief period of more explosive volcanism, and a change in magma chemistry at TgVC. The eruption of Pourahu Member, and the younger *c.* 10 000 years B.P. dacitic hornblende-bearing Pahoka Tephra and Te Rato Lapilli (Mt Tongariro) is closely associated with a change in melt chemistry at TVC and the eruption of Karapiti Tephra (*c.* 9910 years B.P.).

Although few pyroclastic flow deposits are recognised in the Mt Ruapehu eruptive record, they are a common phenomenon associated with eruptions from andesitic strato-volcanoes (Smith and Roobol 1982). Dacitic pumice flows were generated at Mt St Helens during the May 1980 eruption (Rowley *et al.* 1985).

Hydrovolcanic (Phreatomagmatic and Phreatic) Eruptions

"Hydrovolcanism refers to volcanic phenomena produced by the interaction of magma or magmatic heat with an external source of water", Sheridan and Wohletz (1983) and principally includes surtseyan and vulcanian eruption types, but may also include strombolian (Wohletz 1983) and phreatoplinian eruption types (Sheridan and Wohletz 1983) which can

contain a small hydrovolcanic component. Associated deposits are minor ash or lapilli falls and tuff deposits from base surges (Waters and Fisher 1971; Lorenz 1974; Sheridan and Wohletz 1983). Base surges are a common feature developed during hydrovolcanic eruptions (Moore 1967; Fisher 1977).

Characteristics

Deposits from hydrovolcanic eruptions are characteristically fine grained (highly fragmented), well bedded and poorly sorted with polymodal grain size distributions in the coarse and fine ash fractions (Walker and Croasdale 1972; Wohletz 1983, 1986). Accretionary lapilli are common in phreatomagmatic deposits (Waters and Fisher 1971; Walker and Croasdale 1972; Self and Sparks 1978). Accretionary lapilli and mud coatings on pyroclasts are evidence of steam condensation, but neither feature is necessarily diagnostic of a hydrovolcanic origin (Barberi *et al.* 1989).

Vitric, crystal and lithic pyroclasts are identified in hydrovolcanic deposits. The glassy (vitric) pyroclasts show distinctive morphologies, each relating to differences in the mechanism of fragmentation of quenched magmas (Heiken 1972; De Rosa and Sheridan 1983; Sheridan and Wohletz 1983; Wohletz 1983, 1986; Heiken and Wohletz 1985). The five dominant shapes of the glassy pyroclasts are: type-1 blocky equant shapes; type-2 vesicular, irregular shapes with rounded, fluid-formed surfaces; type-3 moss-like convoluted shapes; type-4 spherical or drop-like shapes; type-5 platy shapes (shards). Crystalline pyroclasts most commonly occur as blocky grains with large cleavage faces. Also present are perfect crystals with an adhering layer of vesiculated glass and both perfect and broken crystals without glass coatings (De Rosa and Sheridan 1983; Sheridan and Wohletz 1983; Wohletz 1983).

The glassy pyroclasts are non-vesicular to poorly vesicular and show faces bound by fracture surfaces which commonly show curviplanar (conchoidal) fracture. Vesicles are characterised by adhering dust (Heiken and Wohletz 1985). Angular euhedral particles (dust), chipped surfaces, grooves, scratches and conchoidal fracture are features related to grain collisions during transport (Heiken 1972; Sheridan and Wohletz 1983).

Eruptions at Mt Ruapehu

In the last *c.* 1800 years there has been a dramatic change in eruption styles at Mt Ruapehu, from subplinian to hydrovolcanic eruptions. This change is attributed to the formation of a semi-permanent crater lake occupying the presently active vent of Mt Ruapehu volcano.

The youngest tephra deposits from Mt Ruapehu are the Tufa Trig Formation tephras, dated *c.* 1800 years B.P. to present. Most members are interpreted as the airfall products of hydrovolcanic, probably surtseyan eruptions based on their field characteristics (grain size and bedding features) and pyroclast characteristics. The absence of bed forms characteristically associated with base surge deposits of hydrovolcanic eruptions (Waters and Fisher 1971;

Crowe and Fisher 1973; Fisher and Schmincke 1984) suggests they are airfall deposits, although the thin very fine ash bases of some members may represent distal surge deposits (but these have not been examined close to source).

The two oldest members of this formation are much coarser grained comprising pumiceous, scoriaceous and lithic lapilli. They do not show features characteristic of hydrovolcanic eruptives, are probably the products of small plinian style eruptions sourced from a different vent.

The dominant grain size of the Tufa Trig Formation tephras at source is coarse ash. The tephras show restricted dispersals, with few found at distances greater than 20 km from source. The fine grain size and restricted distribution of these tephras suggests they are the products of surtseyan eruptions, using Walker's (1973) classification based on the fragmentation index and thickness – dispersal of tephras.

Vitric pyroclasts are the dominant component (~80%) in each of the Tufa Trig Formation members Tf3 – Tf18, and occur together with essential ferromagnesian minerals and feldspar (in approximately equal proportions) and minor pumice. Lithic lapilli are uncommon in these tephras. Approximately 60% of all vitric pyroclasts are black or steel grey, with the remainder brown.

Examples of four of the recognised glassy pyroclast morphologies (type-1,-2,-4 and -5 of Wohletz [1983] and Heiken and Wohletz [1985]) are identified in the Tufa Trig Formation tephras, providing strong evidence that these tephras are the products of hydrovolcanic eruptions.

Most vitric pyroclasts are type-1 non-vesicular pyroclasts with characteristic blocky morphology (Plate 4.6a,b). Some faces on these pyroclasts show conchoidal fracture (Plate 4.7). Other pyroclasts show varying degrees of vesicularity (Plate 4.8a,b). Some are classified as type-2 irregular-shaped glassy pyroclasts with rounded fluid-formed surfaces (Plate 4.9). Vesicles in these glassy pyroclasts contain 'adhering dust' (Plate 4.10a,b). The most vesicular pyroclasts are pumice fragments (Plate 4.11). Few of the pyroclasts show type-4 spherical or drop-like shapes (Plate 4.12). Shards (type-5) derived from these glassy pyroclasts are uncommon.

Pyroxene crystals occur both as broken and complete crystals with vesiculated glassy coatings (Plate 4.13) but most commonly occur as blocky crystals without glass coatings and with conchoidally fractured faces (Plate 4.14a – c). Rhyolitic glass shards (Plate 4.15a,b) identified in the Tufa Trig Formation tephras are derived from aeolian reworked Taupo Ignimbrite. The contrasting vesicularity between the pumice fragments, the vesicular glassy coatings on phenocrysts, and the non-vesicular blocky vitric pyroclasts indicates eruption of pyroclasts at quite different stages of magma vesiculation, and possibly degassed magma.

Glass analysed from all three pyroclast types, and glassy selvedges on pyroxenes, is dacitic (Appendix IIIg). Each of the eruptions may have been associated with growth of a dome in the crater. The very low lithic content in the tephras indicates the eruptions principally involved fresh magma rather than near-vent solidified lavas.

Future Tephra Eruptions

The style of future eruptions from Mt Ruapehu will be strongly influenced by the presence of Crater Lake which occupies the presently active vent, and any subsequent changes in vent geometry which may affect the interaction of rising magma with groundwater. Recent activity from this volcano has been dominated by phreatic to phreatomagmatic eruptions through Crater Lake (Cole *et al.* 1986). Deposits from these eruptions typically include ballistic blocks, surge deposits, juvenile andesitic magma and scoria bombs, lake sediments, minor amounts of ash, and lahar deposits (Wood 1977, 1978; Nairn *et al.* 1979; Cole *et al.* 1986). Recent activity at Mt Ruapehu (8 December, 1988-February 1989) was accompanied by several minor phreatic eruptions and the generation of a small lahar.

The past record, however, shows that the most explosive volcanism has been associated with the eruption of mixed magmas, producing the widespread Mangamate Tephra plinian deposits from Mt Tongariro, and a small volume pyroclastic flow (pumice flow) of Pourahu Member at Mt Ruapehu. Future eruptions of mixed magmas at TgVC could initiate subplinian to plinian tephra eruptions which may also generate pyroclastic flows.

CHAPTER FIVE
STRATIGRAPHY AND CHRONOLOGY OF LAHAR DEPOSITS OF THE SOUTHEASTERN MT RUAPEHU RING PLAIN

Introduction

Within the last *c.* 22 500 years, numerous lahar events and tephra eruptions from Mt Ruapehu have built much of the ring plain east and south of the volcano. A stratigraphy and chronology of the lahar (debris flow and hyperconcentrated flow) deposits preserved on the southeastern Mt Ruapehu ring plain over this time has been determined from the correlation of dated andesitic and rhyolitic tephras found interbedded with these deposits. The stratigraphy and chronology of both tephras and lahar deposits provides an integrated record of eruptive, constructional and erosional events that may be used as a basis for future volcanic hazard assessment at Mt Ruapehu.

The first part of this chapter reviews previously established stratigraphy and chronology of lahar deposits mapped at Mt Ruapehu. The second section details the stratigraphy, chronology and distribution of lahar deposits mapped in this study on the southeastern Mt Ruapehu ring plain, while the depositional and erosional environments are interpreted from the stratigraphic record in the last section.

5.1 Nomenclature

Many terms, including lahar, debris flow, mudflow, hyperconcentrated stream flow, lahar-runout and slurry flood, have been used within the literature to describe sediment–water flow processes and the resulting deposits of these processes or events in volcanic and alluvial terrains. A review of nomenclature is found in Smith (1986) and Pierson and Costa (1987). Much of the nomenclature has been erected from studies of ring plain deposits of the volcanoes of the Cascade Range (United States), in particular Mt St Helens and Mt Rainier. Recent publications by Smith (1986, 1987), Pierson and Costa (1987), and Smith and Fritz (1989) have addressed the problems of nomenclature in the interests of establishing common terminology. Their nomenclature is adopted for use in this study. Definitions and characteristics of processes and deposits are outlined below.

Use of the term 'lahar' to describe both the flow process and the resulting deposits (*e.g.* Crandell 1971) has led to recent clarification and redefinition of a lahar by Smith and Fritz (1989) as 'a general term for a rapidly flowing mixture of rock debris and water (other than stream flow) from a volcano'. Thus the term lahar is restricted to debris flows and hyperconcentrated flood flows of volcanic origin. It is not used to describe sediment-water

flows of alluvial environments (Pierson 1980; Schultz 1984; Schmitt and Olsen 1986; Hubert and Filipov 1989).

Types of Lahars

Lahar processes include debris flows and hyperconcentrated flood flows (or hyperconcentrated stream flow) (Smith 1986; Smith and Fritz 1989). The term mudflow is also used in the literature (Crandell 1957, 1969, 1971; Janda *et al.* 1981; Brantley and Waitt 1988; Alloway 1989) to describe events in which the resulting deposits have muddy appearances and cohesive matrices. Distinction between these events is made on the basis of their rheologic properties and the sedimentology of their deposits (Smith 1986; Pierson and Costa 1987; Maizels 1989), although a continuum of flow conditions and sediment concentrations occurs between the debris flow and stream flow end members (Costa 1988).

(a) Debris Flow [DF]

Debris flows are viscous, cohesive, high density, water saturated flows, which move and deposit sediments *en masse* (Smith 1986). They are non-Newtonian fluids and are characterised by non-turbulent laminar and plug flow (Schultz 1984; Pierson and Costa 1987). The high yield strength of many debris flows allows transportation of exceptionally large clasts within a rigid plug (Rodine and Johnson 1976; Schultz 1984). The yield strength is dependent upon the sediment/water concentration (sediment concentrations in debris flows are typically >70 wt.%; Costa 1988), and declines with increased water content. Debris flows characterised by high clay contents indicate origins in hydrothermally altered slope deposits (Schultz 1984).

Sedimentological Characteristics

The deposits of debris flows show sedimentological characteristics consistent with mass deposition. Features such as cross-bedding and horizontal stratification which characterise deposits of turbulent flow are not seen in debris flow deposits (Smith 1986).

The deposits of debris flows show reverse-to-normal grading, reverse, or normal grading throughout the depth of the deposit. Reverse grading is generally limited to the basal few centimetres of the deposit, representing the high-shear basal layer of the moving flow (Smith 1986; Hubert and Filipov 1989). The thickness of this reversely graded layer is, however, dependent on the temperature of the lahar, being generally only a few centimetres in cold lahars (Arguden and Rodolfo 1990). Debris flow deposits contain typically angular clasts supported in a finer grained matrix, and are poorly sorted and massive (*i.e.* they lack internal stratification). This lack of stratification is a diagnostic feature of debris flows (Mullineaux and Crandell 1962; Schmincke 1967; Crandell 1971; Smith 1986). The deposits are characterised by flat topography and digitate, steep fronted, boulder-rich flow margins (Crandell and

Waldron 1956; Crandell 1971; Pierson and Scott 1985; Costa 1988). They form tabular deposits with near planar boundaries (Walton and Palmer 1988).

(b) Hyperconcentrated Flood Flow [HFF]

Hyperconcentrated flood flows are high concentration, turbulent dispersions, in which the sediment/water ratios are intermediate between debris flow and normal stream flow. Sediment concentrations are typically between 40 – 70 wt.% (Costa 1988). They may be viewed as a form of flood, which is characterised by high sediment concentrations and rapid transport and deposition of sediment (Smith 1986, 1987). Although they exhibit turbulent flow, they are notably less turbulent than stream flow (Pierson and Costa 1987) and exhibit higher yield strengths.

Sedimentological Characteristics

Deposits of hyperconcentrated flood flows show characteristics that are atypical of both debris flow and normal stream flow deposits (Smith 1986, 1987; Costa 1988). They are clast-supported, and are characterised by poor sorting and generally show normal grading throughout most of the unit, but lack reversely graded bases (Smith 1986; Scott 1988).

Smith (1986) subdivides the deposits of hyperconcentrated flood flows into gravel-dominated, sand-dominated, and graded-stratified deposits. Gravel-dominated deposits are coarse (pebbles, cobbles and boulders), poorly sorted, clast-supported deposits. The sand-dominated deposits are horizontally stratified, comprising laterally continuous alternating coarse and fine beds, with scattered clasts of much larger size and lenses of gravel. Bed contacts are indistinct. Graded-stratified deposits comprise a normally graded base with a horizontally bedded upper portion.

Hyperconcentrated flood flows are transitional between stream flow and debris flow. Their deposits are more poorly sorted (wider clast size range) and stratified than stream flow deposits, but better sorted than debris flow deposits. They lack large matrix-supported clasts.

(c) Normal Stream Flow [SF]

Normal stream flow is characterised by fully turbulent Newtonian flow with virtually no yield strength and therefore much lower sediment concentrations than are present in either hyperconcentrated flood flows or debris flows (Pierson and Scott 1985; Smith 1986; Pierson and Costa 1987; Costa 1988). Sediment concentrations in stream flows are typically less than 40 wt.% (Costa 1988).

Sedimentological Characteristics

The deposits of stream flow are clast-supported, and characterised by their better sorting and overall finer grain size. They show well developed sedimentary structures, including horizontal stratification, cross-bedding, ripple laminae, cut-and-fill structures, and imbrication (Harrison and Fritz 1982; Smith 1986; Costa 1988).

Flow Transitions

A channelised debris flow may transform to a hyperconcentrated flood flow by progressive dilution with stream water, and the transition from hyperconcentrated flood flow to debris flow may occur if there is a rapid loss of water or entrainment (bulking) of sediment during flow (Schultz 1984; Pierson and Scott 1985; Scott 1985; Smith 1986). Stream flow can similarly transform to the less turbulent hyperconcentrated flood flow by entrainment of sediments.

The transition from debris flow in areas proximal to source, to hyperconcentrated flood flow in distal areas is commonly observed in volcanic terrains (Scott 1985; Smith 1986). The term lahar-runout was used by Pierson and Scott (1985) and Scott (1988) to describe hyperconcentrated stream flows derived from dilution of a distal lahar. However, use of the term hyperconcentrated flood flow is more appropriate in most instances, as direct facies relationships between distal and proximal deposits of these flows are often not established.

Erosivity of Lahars

Confined or channelised lahars are powerfully erosive, and can quickly erode new channels (Pierson 1980, 1985; Janda *et al.* 1981; Costa 1988; Scott 1988; Rodolfo 1989). A significant proportion of the sediment within a channelised lahar may be incorporated by erosion of pre-existing pyroclastic deposits or country rock over which the lahar flows. As unconfined flows (sheet-like flows) on low slopes, most lahars do not erode (Crandell 1957, 1971; Schmincke 1967; Pierson 1985; Arguden and Rodolfo 1990). Here, vegetation, soil, and pyroclastic materials beneath the lahar deposits are generally undisturbed.

Distinction Between Volcanic Debris Avalanche and Lahar Deposits

A volcanic debris avalanche is a rapidly moving incoherent and unsorted mass of rock and soil mobilised by gravity on the slopes of a volcano (Schuster and Crandell 1984). The term rockslide avalanche was used by Voight *et al.* (1981). Volcanic debris avalanches are formed by slope failure of a portion of a volcanic cone (Ui 1983; Siebert 1984) and may travel large distances from their source areas (Siebert 1984).

Volcanic debris avalanches are relatively dry, whilst lahars are water saturated flows. Water within debris avalanches is mostly meteoric, but may also be derived from incorporation of surface water, or ice and snow (Voight *et al.* 1981; Schuster and Crandell 1984).

Deposits of debris avalanches are characterised by megablocks (Ui 1983), also termed fragmental rock clasts (Alloway 1989) and debris avalanche blocks (Palmer and Neall 1989). These megablocks comprise fragments of the volcanic edifice and commonly preserve their original layering (Siebert 1984). Matrix between avalanche blocks is termed the interblock matrix, while that within the blocks is intrablock matrix (Palmer and Neall 1989). Interblock matrix comprises a wide variety of materials, including soil, tephra, wood, plant and rock fragments (Ui 1983; Alloway 1989).

Volcanic debris avalanche deposits commonly include altered rocks derived from hydrothermally altered areas of a volcano that are particularly susceptible to slope failure (Schuster and Crandell 1984).

The surface physiography of debris avalanche deposits is characterised by numerous hummocks, small mounds, or conical hills, cored by debris avalanche blocks (Ui 1983; Crandell, Miller *et al.* 1984; Schuster and Crandell 1984; Siebert 1984; Ui *et al.* 1986; Alloway 1989; Palmer and Neall 1989).

The textural distinction between lahars and debris avalanches may be difficult where the lahars have been derived from remobilised portions of an avalanche deposit (*e.g.* Osceola Mudflow, Crandell 1971). The deposits of lahars, however, can generally be distinguished from those of volcanic debris avalanches by comparison of their surface topography; low debris avalanche block contents; grading within matrix deposits; and arrangement of clasts. Clasts in avalanche deposits tend to show a jigsaw fit, and are contained within matrices dominated by fragmental materials (Siebert 1984).

5.2 Lahar Stratigraphy of the Southeastern Mt Ruapehu Ring Plain

Early descriptions of the lahar deposits of the Mt Ruapehu ring plain (Te Punga 1952; Grindley 1960, 1965; Hay 1967; Topping 1974) have established a framework stratigraphy and chronology of these deposits. In this study a more detailed stratigraphy and chronology of DF and HFF deposits is established on the southeastern Mt Ruapehu ring plain, in the

< *c.* 22 500 years B.P. period. Five formations are defined on the basis of lithology, and each of these has been dated using interbedded rhyolitic and andesitic tephras [1].

Onetapu Formation [On]

Definition and Age

Onetapu Formation is a new formation name for diamictons comprising dark grey sands and silts with andesitic pebbles, cobbles and boulders, and finer grained bedded pebbly sands, sourced from Mt Ruapehu which overlie Mangaio Formation. Where the Mangaio Formation is absent, Onetapu Formation deposits overlie Manutahi Formation.

Onetapu Formation takes its name from the former [Te] Onetapu Desert (O'Shea 1954), since renamed Rangipo Desert. The formation includes currently accumulating sands and gravels sourced principally from Whangaehu River, and other tributaries which drain the southeastern flanks of Mt Ruapehu. The formation also includes Grindley's (1960) lahars of Whangaehu River. At sites where the rhyolitic Taupo Pumice (dated *c.* 1819 B.P.) is preserved, Onetapu Formation deposits are found overlying it. Onetapu Formation deposits therefore date between *c.* 1819 years B.P. and the present.

Description and Identification

The type locality for Onetapu Formation is here defined at Tangiwai Swamp [TS], located approximately 300 m north of the Tangiwai railway bridge over Whangaehu River, in the southernmost part of Karioi State Forest (Figure 5.1, p. 250). Best localities in Rangipo Desert are exposures at Scorpion Gully S.1 [T20/442054] and S.2 [T20/432062], and Whangaehu River S.6 [T20/438033].

At the type locality Onetapu Formation deposits are exposed in a NW–SE trending drainage ditch located immediately west of Whangaehu River (Plate 5.1), and in cuttings along the river banks of Whangaehu River for short distances both upstream and downstream of the Tangiwai Rail bridge. The type locality, although 20 km from the headwaters of Whangaehu River, is a particularly important locality because it is one of few sites providing stratigraphic and chronologic control of these deposits. Here, flood events that were channelled down Whangaehu River have been preserved in a back-swamp environment where they are found interbedded with peats. Tangiwai type locality is the only presently recognised site in the study area where Onetapu Formation deposits and peats are found interbedded, and where members of the formation can be numerically dated.

---

[1] In previous publication by the author (Donoghue 1990) the five formations were referred to as Whangaehu Formation, Tahurangi Formation, Mangaio Formation, Tangatu Formation and Waiharakeke Formation. These are now named Onetapu Formation, Manutahi Formation, Mangaio Formation, Tangatu Formation, and Te Heuheu Formation, respectively, in order to prevent repetition of existing stratigraphic names.

Table 5.1 Stratigraphy of laharic deposits on the southeastern Mt Ruapehu ring plain, and the interbedded rhyolitic (italicised) and andesitic tephra marker beds used to date them.

^{14}C N°	Age * (years B.P.)	Member	Formation	Formation/Tephra	Age * (years B.P.)
NZ7728	<282 ± 35	Ong	Onetapu Formation [On]	Tufa Trig Formation	
NZ7728 NZ7388	*c.* 390 ± 55 – 282 ± 35	Onf			
NZ7388	*c.* 400 †	One1 One2			
NZ7465	450 ± 55	Ond			
		Onc			
NZ1684 NZ1363	?700 – 400 † [a]	Onb			
	<1819 ± 17	One			
				Taupo Pumice	*1819 ± 17* †
				Mangatawai Tephra	2500 ± 200
				Papakai Formation	*c.* 9700 – 2500 †
				Waimihia Tephra	*c. 3400*
	c. 4600 – 3400 †	Manutahi Formation [b] [Mi]		Papakai Formation : black ash-2	
NZ7729 NZ7532	*c.* 4600	Mangaio Formation [Mn]			
				Papakai Formation : black ash-1	
	c. 5370 – 4600 †	Manutahi Formation [Mi]		*Hinemaiaia Tephra*	*4650 ± 80*
				Whakatane Tephra	*4770 ± 170* †
				Motutere Tephra	*5370 ± 90*
				Papakai Formation	
	c. 14 700 – 5370	Tangatu Formation [Ta]		Bullot Formation : Ngamatea lapilli-1	*c.* 11 000 – 10 000 †
				Bullot Formation : Pourahu Member	*c.* 11 000 – 10 000 †
				Waiohau Tephra	*11 250 ± 200*
				Rerewhakaaitu Tephra	*14 700 ± 200*
	c. >22 590 – 14 700	Te Heuheu Formation [Hh]		*Kawakawa Tephra Fm.*	*22 590 ± 230* †

* All ^{14}C ages discussed are conventional ages in radiocarbon years B.P. based on the old (Libby) half life of 5568 years. Radiocarbon numbers and reference to age for tephras are presented in Table 2.1, p. 16 and Table 3.1, p. 90.

† Average or combined radiocarbon age.

‡ Estimated age.

[a] Member Onb is estimate-age dated by correlation with a lahar unit in central Whangaehu Valley radiocarbon dated [NZ1584, NZ1363] by Campbell 1973.

[b] Where Mangaio Formation is absent, upper Papakai Formation and Waimihia Tephra overly Manutahi Formation deposits.

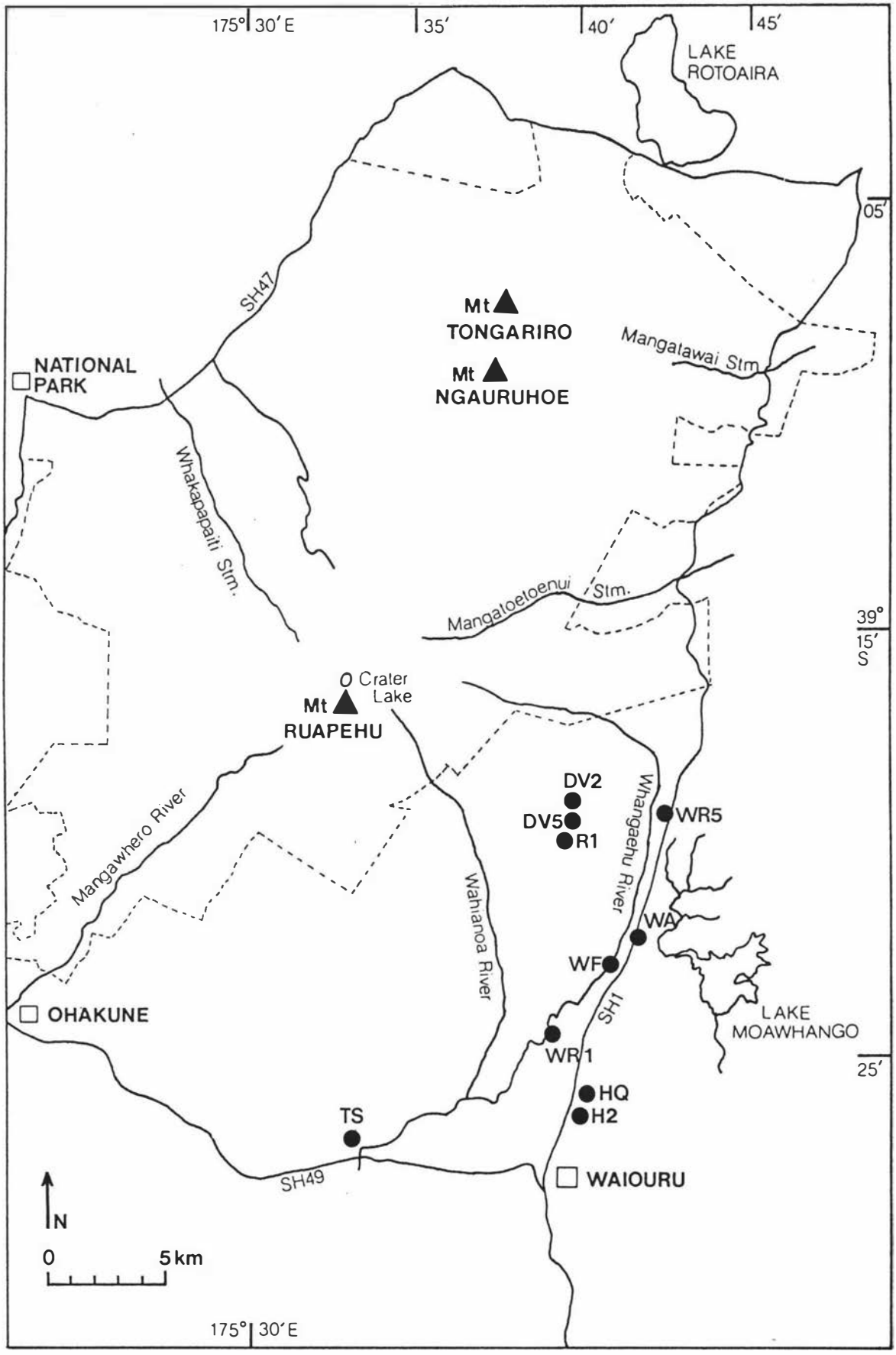

Figure 5.1 Location of type and reference sections designated for laharic formations identified in the study area (see text for section codes).

At the type locality Onetapu Formation comprises dominantly grey, poorly to weakly bedded sands with low concentrations of fine pebbles, and some coarser diamicts with sand and granule matrices and matrix-supported andesitic pebbles and cobbles. These deposits are interpreted as HFF and DF deposits. Most HFF and DF units show sharp smooth contacts, and are separated by paleosols or peat layers. Several units contain reworked Taupo Pumice and distinctive white hydrothermally altered lithic clasts. Two reference sections are defined at this locality.

The type section is located in the drainage ditch, 60 m west of the junction with Whangaehu Road [T20/319906] (Figure 5.2, p. 251; Chart 4). To the west side of the exposure, DF and HFF deposits of Onetapu Formation conformably overlie in turn, 0.08 m of Taupo Pumice (Plate 5.2) and distal deposits of Mangaio Formation. These units can be traced along the channel westwards away from Whangaehu River, but progressively fewer units are exposed as the channel shallows. To the east side of the exposure, the youngest deposits of Onetapu Formation (Ond – Ong) (Plate 5.3) have infilled a former channel cut into older Onetapu Formation deposits. The basal unit Ond, therefore unconformably overlies all older Onetapu Formation units (Ona – Onc). These younger deposits can be traced along the channel eastwards toward Whangaehu River.

The stratigraphy of the deposits identified within the drainage channel at the type section, and other sites, is shown in Chart 4. Seven major units, each representing a lahar event (Ona – Ong) are recorded above Taupo Pumice and are designated as informal members of Onetapu Formation.

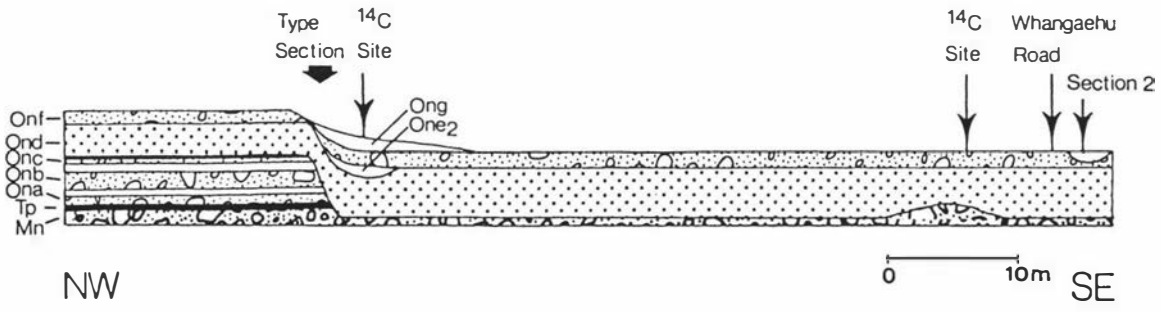

Figure 5.2 Sketch of type locality for Onetapu Formation (Tangiwai Swamp T.L.). The stratigraphy of Onetapu Formation deposits is discussed in the text. Sites where members have been radiocarbon dated are indicated.

Members

Members are given informal status so that units identified and possibly correlated in future studies may be formally defined.

Member Ong

At the type section, member Ong is 0.45 m thick and comprises non-stratified, ungraded dark grey sand, with distinctive yellowish brown mottling. It overlies an unnamed 0.07 m thick unit comprising bedded grey sands. Member Ong is described as a deposit of a hyperconcentrated flood flow, and is dated <*c.* 280 years B.P., based on the radiocarbon age [NZ7728] of an underlying peat layer.

Member Onf

Member Onf is 0.56 m thick and comprises non-stratified, ungraded dark greyish brown coarse sand with distinctive yellowish brown mottles. It is interpreted as the deposit of a hyperconcentrated flood flow.

At the type section, member Onf is enclosed by two thin fibrous peat layers (Plate 5.3). Both peat layers have been radiocarbon dated. The lowermost peat is dated [NZ7388] at 390 ± 55 years B.P., and the uppermost peat is dated [NZ7728] at 282 ± 35 years B.P. These dates provide maximum and minimum ages for member Onf. Based on these ages this member is dated at *c.* 350 years B.P.

Members One1 and One2

Member One1 is 0.15 m thick, and comprises a pale grey sand and granule matrix with matrix-supported pebbles and cobbles. This unit is discontinuous at the type locality and is only identified in exposures near the western end of the drainage channel. It is a reversely graded DF deposit which occupies a similar stratigraphic position to member One2, and is therefore of similar age (Chart 4).

At the type section, member One2 is 0.13 m thick and comprises non-stratified, ungraded very dark grey sand with distinctive yellowish brown mottles. The unit is lenticular and laterally discontinuous. It is described as a HFF deposit, and is dated at *c.* 400 years B.P., based on the radiocarbon age (390 ± 55 years B.P. [NZ7388]) of the overlying peat layer (Plate 5.3)

Member Ond

Member Ond is the most prominent member of Onetapu Formation at the type section. Here it is 0.83 m thick and comprises a grey coarse sand and granule matrix with andesitic pebbles, and a few cobbles and boulders. Black scoria pebbles are the dominant lithology. Clasts show slight reverse grading. Reworked rhyolitic Taupo Pumice is found scattered throughout the deposit.

The deposit is interpreted to be of DF origin, but grades laterally to a HFF deposit toward the western end of the drainage channel.

Wood found within the base of member Ond, at an exposure located on the south side of the channel and 7 m from the junction with Whangaehu Road, has been radiocarbon dated [NZ7465] at 450 ± 55 years B.P. A peat layer overlying this member is radiocarbon dated [NZ7388] at 390 ± 55 years B.P. The member therefore dates between *c.* 390 and 450 years B.P., but an age closer to *c.* 450 is likely. This member is the oldest of the units which have infilled the channel cut into older Onetapu Formation deposits, and thus dates this event.

A major event of similar age was mapped by Campbell (1973) in Whangaehu Valley. Campbell described the deposit as poorly sorted and poorly bedded volcanic gravel, probably originating from lahars. Wood within the underlying paleosol was dated [NZ1363] at 407 ± 70 years B.P. (Campbell 1973). Member Ond at Tangiwai Swamp is very probably a correlative of Campbell's *c.* 407 years B.P. lahar.

Member Onc

Member Onc is 0.28 m thick and is separated from the overlying member Ond by a 0.18 m thick paleosol developed in medial materials, and a thin lens of grey loamy sand. This member comprises non-stratified dark greyish brown coarse sand with distinctive yellowish red mottles and scattered reworked Taupo Pumice. It is described as a deposit of a hyperconcentrated flood flow.

Member Onb

Member Onb is a prominent 0.75 m unit, comprising a gleyed grey and purplish grey coarse sandy loam and granule matrix, with distinctive yellowish brown mottles, and matrix-supported pebbles, cobbles and occasional boulders. Many of the pebbles are hydrothermally altered. The matrix of this deposit is very similar to that of the older Mangaio Formation, and quite distinct from all other Onetapu Formation members at this site. Unlike Mangaio Formation however, reworked Taupo Pumice occurs throughout the unit, and in greater concentration than in member Ond. This member is interpreted as a deposit of a debris flow.

Campbell (1973) recorded only three major lahar events of post-Taupo Pumice age in the central Whangaehu Valley. The two youngest deposits (separated by a paleosol) are described as volcanic gravels probably originating from lahars. The oldest deposit is described as poorly bedded andesitic sand. Wood from within a paleosol developed on the sand is dated [NZ1584] at 756 ± 56 years B.P. giving a minimum age for the oldest deposit and a maximum age for the middle deposit. Wood from within a paleosol found overlying the middle

deposit is dated [NZ1363] at 407 ± 70 years B.P. giving a minimum age for the middle deposit.

At the type locality members Onb and Ond are the largest and coarsest units. Their thickness and grain size suggests they are likely to be of sufficient magnitude to be recorded in sequences downstream of Tangiwai. Member Onb is very probably a correlative of Campbell's middle post-Taupo Pumice lahar deposit, dated between *c.* 750-400 years B.P.

Member Ona

At the type locality member Ona is the oldest of the Onetapu Formation deposits, and is separated from member Onb by a greasy sandy clay loam textured paleosol developed in medial material. Member Ona has a gleyed purplish grey sand and granule matrix, with common matrix-supported fine and medium pebbles. It is interpreted as the deposit of a debris flow, but may be transitional between a debris flow and hyperconcentrated flood flow. This member directly overlies Taupo Pumice (Taupo Ignimbrite Member) and therefore has a maximum age of *c.* 1800 years B.P.

At Tangiwai Swamp S.2 [T20/320904] (Figure 5.2, p. 251; Map 1), the stratigraphy of Onetapu Formation deposits is complex (Plate 5.4). A DF deposit exposed at the western end of the section is correlated with member Ond, dated *c.* 450 years B.P. An overlying sandy textured HFF unit is correlated with member Onf. Above member Onf there are three HFF deposits (Plate 5.4). Each unit has infilled a former small lenticular channel scour cut into older deposits. Although each of these deposits is volumetrically small, they are important because they record the most recent lahar events that have travelled down Whangaehu River as far as Tangiwai, and which were big enough to overtop the river bank at this point.

Although these three units occupy a similar stratigraphic position to that of member Ong, they are much younger. Interbedded within the paleosols separating these units, and within two of the HFF deposits, are wood fragments and pine cones (Plate 5.4). A pine cone extracted from the paleosol, below the three HFF deposits, has been identified as *Pinus nigra* (Corsican Pine), and other cones have been identified as *Pinus radiata* and *Pseudotsuga menziessi* (Douglas Fir) [2]. *Pinus nigra* was first planted at Karioi in 1928. Here, this species takes between 12 and 15 years to produce cones, and therefore deposits containing *Pinus nigra* cones cannot be older than 1940 A.D. The deposits therefore record recent lahar events which travelled down Whangaehu River after 1940 A.D. and probably identify the three major post-1940 A.D. events (1953, 1969, 1975). The presence of weak paleosols between these units indicates that each was associated with a discrete event, and that they were not pulses of a single event.

---

[2] Species identified by Mr R. Guest, Ministry of Forestry, Palmerston North.

At Tangiwai Swamp S.3 [T20/319904], five discrete HFF deposits and three DF deposits are preserved above Taupo Pumice (Plate 5.5). At the southern end of the section the uppermost DF deposit (at ground surface) is correlated with member Ond. At the northern end of this section, however, the stratigraphy is complicated by a series of channel fills. Here member Ond is at river level, infilling a former channel cut into older Onetapu Formation deposits. This member therefore unconformably overlies older Onetapu Formation deposits. Here it is overlain by member Onf in the channel. Other units at this site are not correlated to members identified at the type section because matrix characteristics and lithology are not sufficiently distinct to permit correlation on field appearances. The complex arrangement of channel cut and fill structures in sections proximal to Whangaehu River, and the transition within single units between DF and HFF deposits complicates correlation between sections.

Stratigraphy of Onetapu Formation Deposits at Other Sites

Onetapu Formation DF deposits are exposed in sections proximal to Wahianoa River, at the northern end of Karioi Forest. At Wahianoa River S.1 [T20/369027], two DF deposits occur above Taupo Pumice (Taupo Ignimbrite Member). They are separated by a thick (0.13 m) peaty loam, and underlie Tufa Trig Formation member Tf4. This member has a minimum age of *c.* 830 years B.P., and provides a minimum age for the DF deposits. Neither DF deposit has been correlated with members at the type section. There are no records of major lahars down Wahianoa River (Paterson 1976). However, preservation of Onetapu Formation and older ?Tangatu Formation DF deposits at this site and at Wahianoa River S.2 [T20/371016] shows lahars have descended Wahianoa Valley in recent time.

Rangipo Desert

Within Rangipo Desert, Onetapu Formation is represented by DF, HFF, and minor SF deposits. The principle source of these deposits is Whangaehu River, which is the main river draining the southeastern Mt Ruapehu ring plain.

The Whangaehu Fan (Figure 1.5, p. 13) is an area of actively accumulating lahar and stream flow deposits in the northern Rangipo Desert, and represents the greatest accumulation of Onetapu Formation deposits on the southeastern ring plain. Above 1200 m a.s.l., the course of Whangaehu River is confined by lava flows. Below this point Whangaehu River is no longer constricted, and spills out in a network of braided channels over Rangipo Desert, depositing lahar and stream flow materials to form the Whangaehu Fan. This fan marks the transition between channelised and unconfined flow. Where Whangaehu River meets the Whangaehu escarpment braided channels converge to form one main course flowing to the southeast, and directing lahars downstream.

Within Rangipo Desert the stratigraphy of Onetapu Formation deposits is best exposed in tributary channels proximal to Whangaehu River and on the Whangaehu Fan. Active stream erosion and remobilisation of Onetapu Formation deposits by subsequent flood events and

ephemeral stream flow both on the fan and within the Whangaehu River channel has, however, masked much of the original stratigraphy of the units at these sites.

The Whangaehu Fan is characterised by very coarse DF deposits, HFF and SF deposits. The distinctive dark coloured sands, and loose sandy matrices of these deposits distinguishes the formation from older deposits. The loose sandy matrices indicate deposition from dilute, watery lahars.

In the northern Rangipo Desert the erosion of matrix materials in the younger DF deposits has produced distinctive boulder strewn surfaces (Plate 5.6). Areas proximal to Whangaehu River, and tributary channels on the Whangaehu Fan, are characterised by levee deposits and coarse boulder banks within and alongside channels (Plate 5.7; Plate 5.8).

Most of the southern Rangipo Desert is covered by a thin 'lag' deposit of coarse sand, pebbles and cobbles above Taupo Pumice (Plate 5.9). Much of the fine sand from within this lag deposit has been eroded and incorporated into actively accumulating sand dunes, leaving behind a fines-depleted veneer. Most of this veneer, or lag deposit, has been eroded from braided ephemeral stream channels. These channels lack the concentrations of coarser pebbles and cobbles, and are characterised by sandy pumice-rich channel floor wash deposits, and small levees comprising cross-bedded sands, silt, and reworked Bullot Formation tephras and Taupo Ignimbrite. The pumice-rich nature of these deposits distinguishes them from the pumice-poor SF deposits preserved on the Whangaehu Fan. This lithological difference indicates an additional source of sediment for Onetapu Formation deposits in the southern Rangipo Desert.

Description and Identification

At Whangaehu River S.6 [T20/438033] and other sites within the southern Rangipo Desert, *e.g.* Aqueduct S.1 [T20/418982] and S.3 [417984], Onetapu Formation DF deposits are found interbedded with Tufa Trig Formation tephras.

At Whangaehu River S.6, seven DF and HFF deposits overlie an erosional unconformity on Taupo Ignimbrite. Five of these overlie Tufa Trig Formation member Tf6, and are therefore younger than *c.* 650 years B.P. The lower two units underlie Tufa Trig Formation member Tf5, and are therefore relative-age dated between *c.* 1819 and 830 years B.P.

A 0.65 m thick DF deposit found overlying Tufa Trig Formation member Tf6, and separated from it by greasy sandy clay, is distinguished from the other units in the section by the dominance of black scoria clasts. This DF deposit is provisionally correlated with member Ond at the type section at Tangiwai, based on its distinctive lithology and relative stratigraphic position (Chart 4). At the type section member Ond is dated at *c.* 420 years B.P.

At Aqueduct S.1 [T20/418982], three DF deposits of Onetapu Formation are found above the 3.0 m thick Taupo Pumice (Taupo Ignimbrite Member). The younger unit, which is 0.68 m thick, overlies Tufa Trig Formation member Tf5. It is distinctive due to the dominance of black scoria clasts and is thus correlated with member Ond, based on lithological similarity and age (Chart 4).

At more southern sites within Rangipo Desert, Onetapu Formation deposits are most commonly found overlying Taupo Pumice. Over much of the northern Rangipo Desert, however, particularly on the Whangaehu Fan, Taupo Pumice and older tephras have been eroded. In these areas, Onetapu Formation deposits unconformably overlie the Mangaio Formation DF deposit (*e.g.* at Scorpion Gully T.L., Plate 5.10). Where Mangaio Formation does not occur, Onetapu Formation deposits unconformably overlie lower Papakai Formation (*e.g.* at The Chute).

The establishment of a detailed stratigraphy and chronology of Onetapu Formation deposits preserved within Rangipo Desert was conducted by Purves (1990). Thirteen DF deposits were recognised, including the recent 1975 lahar event. Onetapu Formation member Onb at Tangiwai Swamp is provisionally correlated with Lahar Deposit 6 (dated 800-500 years B.P.) of Purves (1990) based on relative stratigraphic position and age. Member Ond, dated at *c.* 450 years B.P. represents a major event which could be a correlative of lahar deposit 11, recognised by Purves (1990) as the last major lahar to inundate Rangipo Desert in post-Taupo Pumice time.

Distribution and Source

The distribution of Onetapu Formation deposits on the southeastern Mt Ruapehu ring plain is shown in Figure 5.3 (p. 258) and Map 2. The estimated total volume for the Onetapu Formation deposits preserved within Rangipo Desert and at Tangiwai is 36 x 10^6 m^3. Volume estimates for the lahar deposits are for existing deposit volumes preserved within the study area. No allowance is made for reduction in volume as a result of post-depositional erosion and water loss, or for volumes of associated deposits which may occur outside of the study area. The actual discharge volume of the lahars may be many times larger than that of the resulting deposits. [3]

Rangipo Desert

In the northern Rangipo Desert, Onetapu Formation lahar deposits sourced from Whangaehu River are bounded by tributaries of Whangaehu River, on the Whangaehu Fan. Lahar and stream flow deposits of Onetapu Formation age found north of the Whangaehu Fan in the vicinity of Bullot Track and Waikato Stream (Map 2) may have been sourced from other tributary rivers draining the southeastern flanks of Mt Ruapehu in addition to Whangaehu

[3] The volume of the 1975 lahar event down Whangaehu Valley was measured at 1.8 x10^6 m^3 (Page and Paterson 1976), while the resulting deposits have an estimated volume of only 0.09 x10^6 m^3; a factor of 20:1 (Purves 1990).

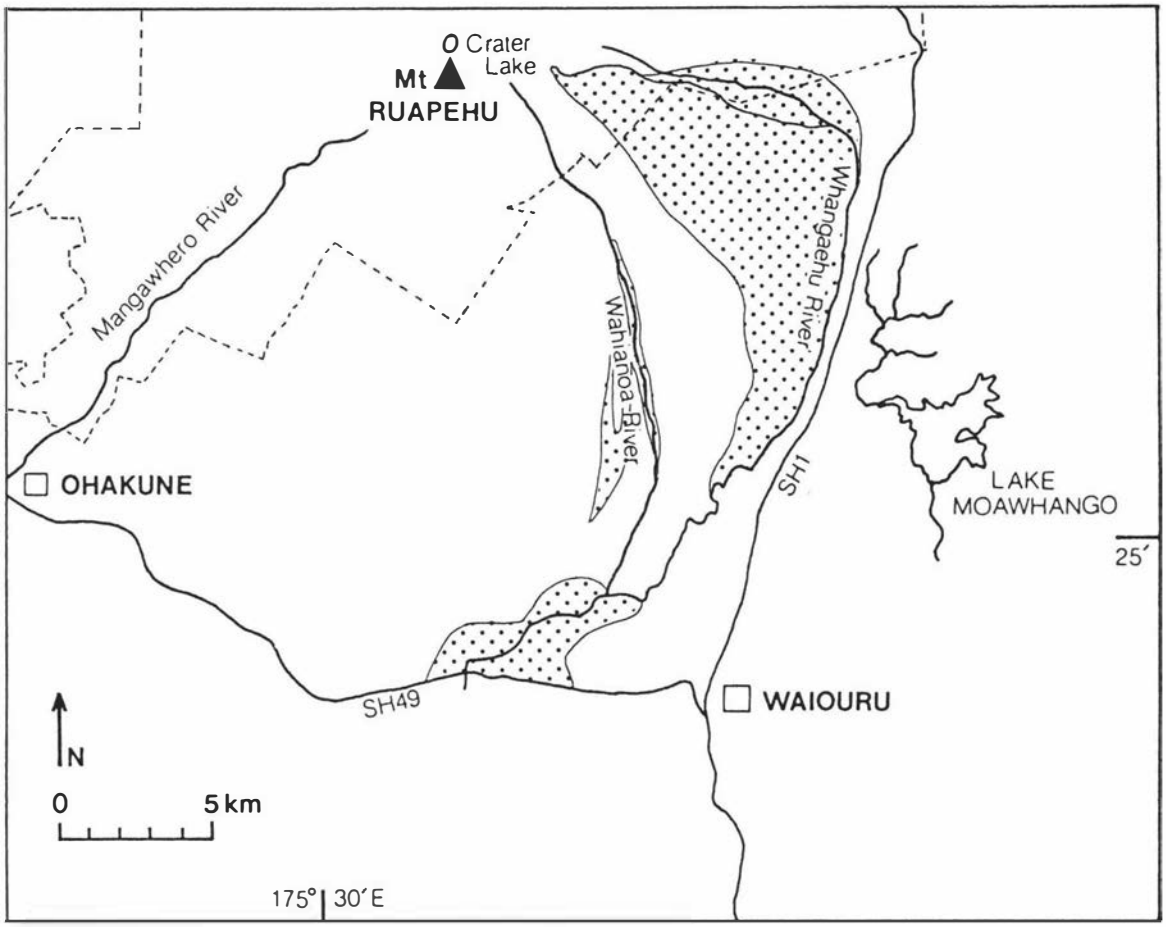

Figure 5.3 Generalised distribution of Onetapu Formation laharic deposits (shaded) on the southeastern Mt Ruapehu ring plain (see also Map 2).

River. In the east, the formation is confined by a prominent northeast trending escarpment, which has confined Onetapu Formation and older deposits to the west of the Desert Road – the scarp itself now forming the eastern boundary of Rangipo Desert. In the west, the formation is bounded by Seagull Gully and the western margin of Karioi Forest. In the south, Onetapu Formation deposits form a thin and incomplete cover over areas more distal to Whangaehu River, in the southern part of Rangipo Desert (Map 2).

Karioi Forest

Onetapu Formation deposits have been mapped south of Rangipo Desert to Tangiwai type locality. Between these two localities, Whangaehu River is confined, thus restricting deposition along this stretch of the river. Here, Onetapu Formation deposits are represented by low terraces and boulder beds built against much older deposits of the Te Heuheu Formation along channel margins. Only at the southern limit of the Karioi Forest does flow within Whangaehu River again become unconfined. In this area, Onetapu Formation lahar and hyperconcentrated flood flows have spilled over lowland areas both east and west of the Whangaehu River channel.

Deposits of Onetapu Formation age, not sourced from Whangaehu River, have also been mapped in the northern Karioi Forest at Wahianoa River and tributary rivers immediately to the west.

Mangaio Formation [Mn]

Definition and Age

Mangaio Formation is a new formation name for a distinctive orange coloured diamicton with a clay textured matrix and matrix-supported andesitic lithic pebbles and boulders, sourced from Mt Ruapehu. Mangaio Formation overlies Manutahi Formation, and is ^{14}C dated at *c.* 4600 years B.P.

Description and Identification

The type section for Mangaio Formation is designated at Death Valley S.2 [DV2] [T20/408047] (Figure 5.1, p. 250; Chart 4). This site was selected to show both the upper and lower contacts of the formation. The lithological characteristics of the formation are, however, best described at the reference localities, although at these sites the base of the formation is not exposed. Reference localities are here designated within Rangipo Desert at Scorpion Gully and Death Valley. Description of the deposit at the reference localities therefore precedes discussion of the type section.

At Scorpion Gully R.L. (Plate 5.11; Chart 4), Mangaio Formation shows a maximum exposed thickness of *c.* 3.10 m, and is directly overlain by upper Papakai Formation and the interbedded rhyolitic Waimihia Tephra. The contact with Papakai Formation is sharp and distinct.

At this site, Mangaio Formation comprises three poorly sorted clay-rich diamictons (Plate 5.12). Each of these is characterised by a strong brown and grey gleyed, sticky, sandy clay textured matrix, with matrix-supported, dominantly white hydrothermally altered andesitic pebbles, cobbles and boulders. The hydrothermally altered lithic clasts are very soft and crumbly, with clay-like textures. Each of the units probably represents pulses within a single event. Contacts are conformable with no evidence of erosion between the units.

The uppermost unit is 0.63 m thick and is distinguished from the lower units by its paler colour and finer clast sizes. The dominant clast size is coarse pebble. Clasts are matrix-supported, with many soft pale yellow and white hydrothermally altered lithic pebbles and minor grey, black and red lithic pebbles. The unit is ungraded. The upper contact with Papakai Formation is sharp and marked by strong iron-staining in the top of Mangaio Formation. The basal contact with the middle unit is indistinct. The middle flow unit is 0.62 m thick. It is distinguished from the lowermost unit by its finer grain size. The dominant clast size is very coarse pebble. The lowermost flow unit has a minimum thickness of 1.85 m. It is

distinguished from the two overlying units by its distinctive purplish grey, and strong brown coloured matrix and coarser clast size (dominantly cobbles with boulders).

At the type section (Plate 5.13), Mangaio Formation is 2.03 m thick. Here, the base of the formation is exposed. It overlies a 0.03 m thick peat layer which occurs 0.10 m above the andesitic black ash-1 member of Papakai Formation, and 0.12 m above Hinemaiaia Tephra. Mangaio Formation is overlain by upper Papakai Formation (with interbedded rhyolitic Waimihia Tephra) and andesitic black ash-2 member. Here, all three flow units are recognised and are characterised by grey and strong brown gleyed, clayey textured matrices. The lowermost unit, which is 0.90 m thick, is distinguished by its purplish grey coloured matrix. This unit also contains small uncarbonised branches. The peat layer found immediately below the formation has been radiocarbon dated [NZ7532] at 4850 ± 90 years B.P. Branches from within the DF deposit have also been dated [NZ7729] at 4600 ± 110 years B.P. The age of the overlying rhyolitic Waimihia Tephra is *c.* 3400 years B.P. The formation therefore dates between *c.* 4600 and 3400 years B.P., but an age close to *c.* 4600 years B.P. is likely. Wood is also found within the formation at Rangipo S.1 (T20/410035], but is absent in exposures at Scorpion Gully R.L.

Mangaio Formation is also identified in exposures along the Whangaehu escarpment at Whangaehu River S.5 [T20/443045] and further north at Whangaehu Junction [T20/445069] (Chart 4) and T20/445072. At these sites it is thought to have overtopped the fault scarp, and is preserved in thick (*c.* 2 m) discontinuous lenses.

In most exposures along Whangaehu River south of Scorpion Gully (Chart 4), Mangaio Formation differs in appearance, being characterised by a sequence of finer grained sandier textured HFF units. These deposits represent the more distal and dilute margins of the flow. At Whangaehu River S.6 [T20/438033] eight distinct units are present. Matrices are typically grey and iron-stained. The dominant clast size is fine pebble. All units contain distinctive and dominant white hydrothermally altered lithic pebbles.

Mangaio Formation is characterised and distinguished from all other formations by its gleyed grey, purplish grey and strong brown colour, clay textured matrix and presence of soft, white, hydrothermally altered lithic clasts. The lithological contrast between this formation and the younger and distinctly sandier Onetapu Formation deposits is clearly shown in Plate 5.10 and Plate 5.11.

Other Deposits Associated With the Formation

At sites within Scorpion Gully, a *c.* 0.30 m thick DF deposit is found interbedded with Mangatawai Tephra. It is characterised by a grey and strong brown sandy clay matrix, with matrix-supported iron-stained rounded pebbles and cobbles. It is more clast-rich, but otherwise is very similar in appearance and composition to Mangaio Formation. This unit has been recognised only within Scorpion Gully.

Distribution and Source

The distribution of Mangaio Formation is shown in Figure 5.4 (p. 261) and Map 2. It is mapped as a single lobe covering most of the northeastern Rangipo Desert, where it is found exposed in tributary channels. The formation is also recognised in exposures at the apex of the Whangaehu Fan, indicating that this DF deposit was sourced from an area close to Whangaehu Gorge.

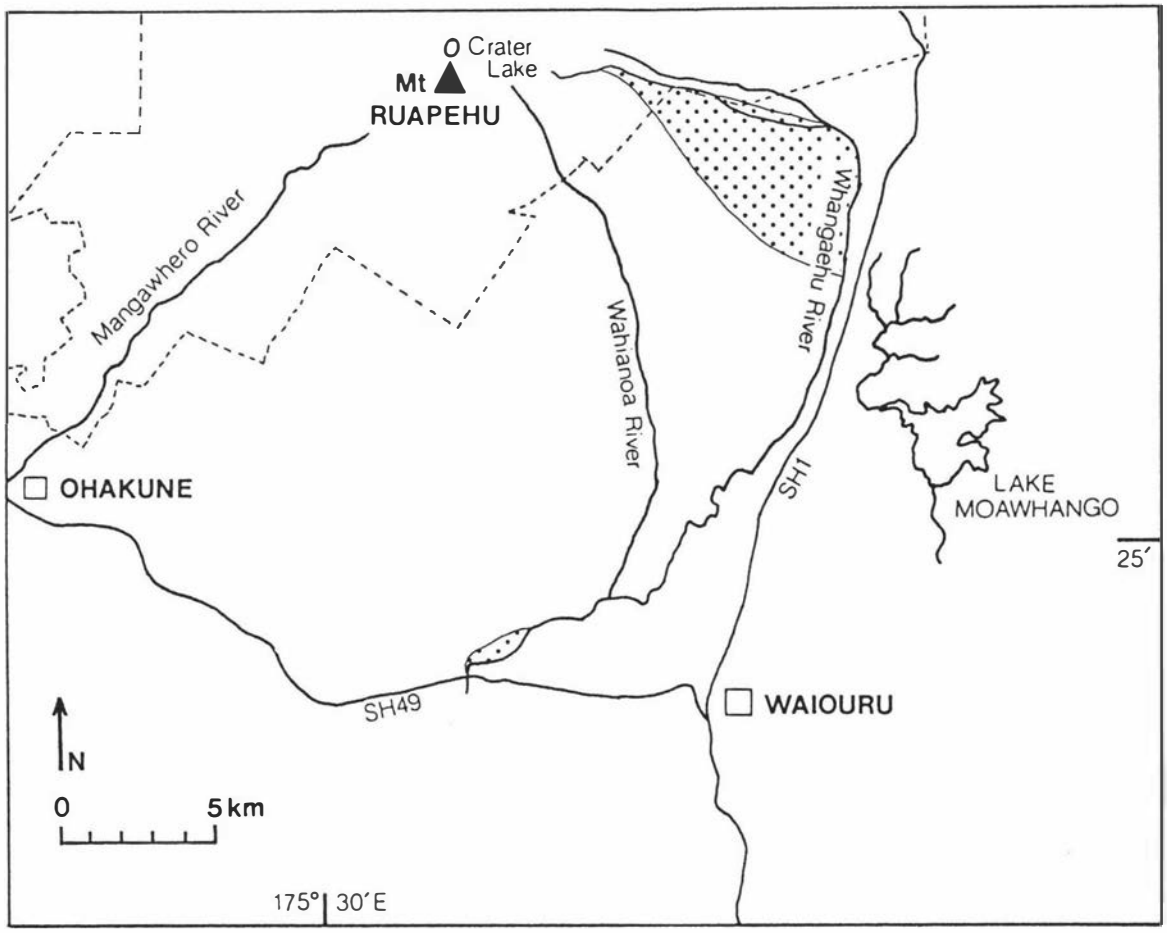

Figure 5.4 Generalised distribution of Mangaio Formation laharic deposit (shaded) on the southeastern Mt Ruapehu ring plain (see also Map 2).

The formation is bounded in the north by Whangaehu River and its tributary channels, and to the east by the Whangaehu escarpment. The western margin occurs just west of Death Valley. The southern boundary is placed in the vicinity of Whangaehu River S.6, where more dilute distal facies are identified. It is also identified at isolated localities further south along Whangaehu River (*e.g.* at Whangaehu Ford and Tangiwai T.L.).

The formation has an estimated volume of 34×10^6 m^3 based on the distribution of the deposit shown in Map 2.

Manutahi Formation [Mi]

Definition and Age

Manutahi Formation is a new formation name for weakly bedded sands, gravels and silts sourced from Mt Ruapehu which overlie Tangatu Formation, and underlie Mangaio Formation, or where this is absent, upper Papakai Formation (with interbedded Waimihia Tephra), younger tephras, and Onetapu Formation. Manutahi Formation deposits are of similar age to Mangaio Formation. They have not, however, been grouped into this formation because of their lithologic dissimilarity.

The lower boundary between Manutahi Formation and Tangatu Formation is approximately marked by the position of the rhyolitic Motutere Tephra. Motutere Tephra, dated at *c.* 5370 years B.P. provides a maximum age for Manutahi Formation deposits. Waimihia Tephra, which is found overlying both Manutahi Formation and Mangaio Formation deposits provides a minimum age of *c.* 3400 years B.P. (Table 5.1, p. 249).

Description and Identification

The type section for Manutahi Formation is here defined at Rangipo S.1 [R1] [T20/410035] (Plate 5.14). Reference sections are defined at Death Valley S.5 [DV5] [T20/409045] (Plate 5.16) and Whangaehu Ford [WF] [T20/425984] (Figure 5.1, p. 250; Chart 4). The reference locality is at Death Valley.

At the type section, Manutahi Formation overlies Tangatu Formation deposits and underlies the Mangaio Formation DF deposit which is 2 m thick.

Here, Manutahi Formation is 5.3 m thick and comprises thin (<0.10 m) laminar and low-angle cross bedded sands and pebbles. Pebble-rich beds contain minor amounts of sand, and dominantly clast-supported fine rounded pumice and subrounded to angular lithic pebbles. Sand-rich beds are moderately well sorted and contain only low concentrations of fine rounded pebbles. Also present are finer grained, sandy loam and silt textured beds and laminae with prominent relief. Small scale scour and fill structures are observed in some of the sand-rich beds. Beds are discontinuous, with indistinct boundaries (Plate 5.15). The rhyolitic Hinemaiaia Tephra dated [NZ4574] *c.* 4650 years B.P. is found interbedded within a 0.16 m thick coarse sandy loam textured bed 1.26 m below the upper contact with Mangaio Formation (Plate 5.14). The rhyolitic Motutere Tephra is found interbedded within medial sandy loam textured bed, at the base, and northern end of the exposure.

At this site the deposits are interpreted to be transitional between stream flow and hyperconcentrated flood flow (SF-HFF) because they are more poorly bedded and poorly sorted than is typical of stream flow (SF) deposits. The marked contrast in bedding characteristics of Manutahi Formation deposits and the overlying Mangaio DF deposit is shown in Plate 5.14.

At Death Valley R.S.5 (Plate 5.16), Manutahi Formation overlies Tangatu Formation, and underlies Onetapu Formation due to the absence of Mangaio Formation at this site. Here, Manutahi Formation is represented by deposits which are older than Hinemaiaia Tephra. The formation is *c.* 2.5 m thick and comprises weakly bedded, discontinuous fine pebble-rich and sand-rich beds, with clast-supported rounded lithic and pumice pebbles, and lenses and laminae of grey fine sand and sandy loam. These deposits are interpreted as transitional between stream flow and hyperconcentrated flood flow, *i.e.* SF–HFF units. The contrast in colour between the pale grey Manutahi Formation deposits and the dark grey Onetapu Formation gravels and sands is distinctive. Near the base of the formation, Whakatane Tephra (dated at *c.* 4770 years B.P.) is found interbedded within a 0.17 m thick bed comprising bedded silty clay and fine sand.

At some sites within Death Valley R.L., deposits of Manutahi Formation are distinctly sandier, and horizontally stratified, with low concentrations of clast-supported lithic and pumice pebbles and cobbles. Bed contacts are wavy and distinct. These are interpreted as the deposits of hyperconcentrated flood flows.

At Whangaehu Ford R.S., Manutahi Formation is *c.* 3.4 m thick. It overlies Tangatu Formation deposits, and underlies in turn the Mangaio (*c.* 3.4 m thick) and Onetapu (*c.* 1.8 m thick) formations. Here, Manutahi Formation deposits are older than Hinemaiaia Tephra and comprise weakly bedded coarse pebbly sands, interpreted as HFF deposits and coarser grained and more poorly sorted diamicts, with angular, matrix-supported coarse pebbles and cobbles, interpreted as DF deposits. At this site the approximate boundary between Manutahi and Tangatu formations is indicated from the position of Motutere Tephra.

At Bullot Track S.2 [T20/420110] Manutahi Formation deposits infill former channels cut into tephras older than Hinemaiaia Tephra (*e.g.* Mangamate Tephra and Bullot Formation tephras). Manutahi Formation deposits overlie Hinemaiaia Tephra and lower Papakai Formation which drape the channel cut and unconformably overlie older tephras. At the base of the exposure, lower Papakai Formation overlies a small peat deposit and bedded (beds < 100 mm) silty clays and very fine sands which fill the very base of the channel. Neither Mangaio Formation, nor Tangatu Formation deposits younger than *c.* 10 000 years B.P. were deposited at this site. Manutahi Formation is therefore overlain by upper Papakai Formation and the interbedded Waimihia Tephra. Here, and at a proximal exposure (Plate 5.17), the formation comprises horizontally bedded, dominantly well sorted dark grey sand-rich beds with subrounded lithic and rounded pumice pebbles. Fine pebble-rich beds, dominated by either lithic or pumice pebbles also occur together with silt, sandy loam and sandy clay textured beds. Beds are discontinuous with indistinct contacts, and are interpreted as the deposits of stream flow. Near the base of the exposure (Plate 5.17) are weakly bedded sands with scattered cobbles and pebbles which may represent a HFF component.

Within Rangipo Desert, Manutahi Formation comprises SF – HFF, HFF, DF, and minor SF deposits. At Death Valley R.L., the formation is dominated by SF-HFF deposits. The boundary between Manutahi and Tangatu formations is best identified at Death Valley R.S.5, where it is marked by a distinct lithological change in the deposits. The boundary is also approximated from the position of Motutere Tephra.

Distribution and Source

The distribution of Manutahi Formation is shown in Figure 5.5 (p. 265) and Map 2. Manutahi Formation deposits are principally exposed in the central Rangipo Desert, in the vicinity of Death Valley, and in areas south and west of there. To the south, streams have not incised to the same extent, and so the formation becomes progressively less exposed, being buried by deposits of the Mangaio and Onetapu formations, and recent dune sands. Where the tephra cover beds have been eroded, ephemeral channels have cut into Manutahi Formation deposits. Here the surface deposits are a composite of Manutahi SF – HFF sands and gravels, and recent Onetapu Formation HFF and DF lag deposits.

Isolated occurrences of Manutahi Formation occur at the western margin of the Badlands (Figure 1.5, p. 13). Over most of this area Manutahi Formation deposits and cover bed tephras (Taupo Pumice, Mangatawai Tephra, upper Papakai Formation) have been almost entirely eroded. Here, the eroded remnants of Manutahi Formation comprise a thin planar bed of lithified grey sands above the rhyolitic Motutere Tephra.

The eastern boundary of the formation is provisionally placed just east of Death Valley. Manutahi Formation deposits are not present in more eastern exposures at the southern end of The Chute. Deposits exposed in the northern end of The Chute, which are older than Mangaio Formation are lithologically dissimilar, being much coarser bouldery diamicts. The eastern boundary therefore probably occurs west of The Chute, although absence of exposures within this area that show the stratigraphy of deposits older than Mangaio Formation prevents accurate placement of this boundary.

Manutahi Formation deposits appear to have been sourced from numerous tributary rivers draining the southeastern flanks of Mt Ruapehu. The pumice content in the SF – HFF deposits indicates sediment sources from the older surfaces of the Mt Ruapehu ring plain which are mantled by thick, loose pumice-rich tephras.

The present-day volume of Manutahi Formation is estimated to be $\sim 50 \times 10^6$ m^3.

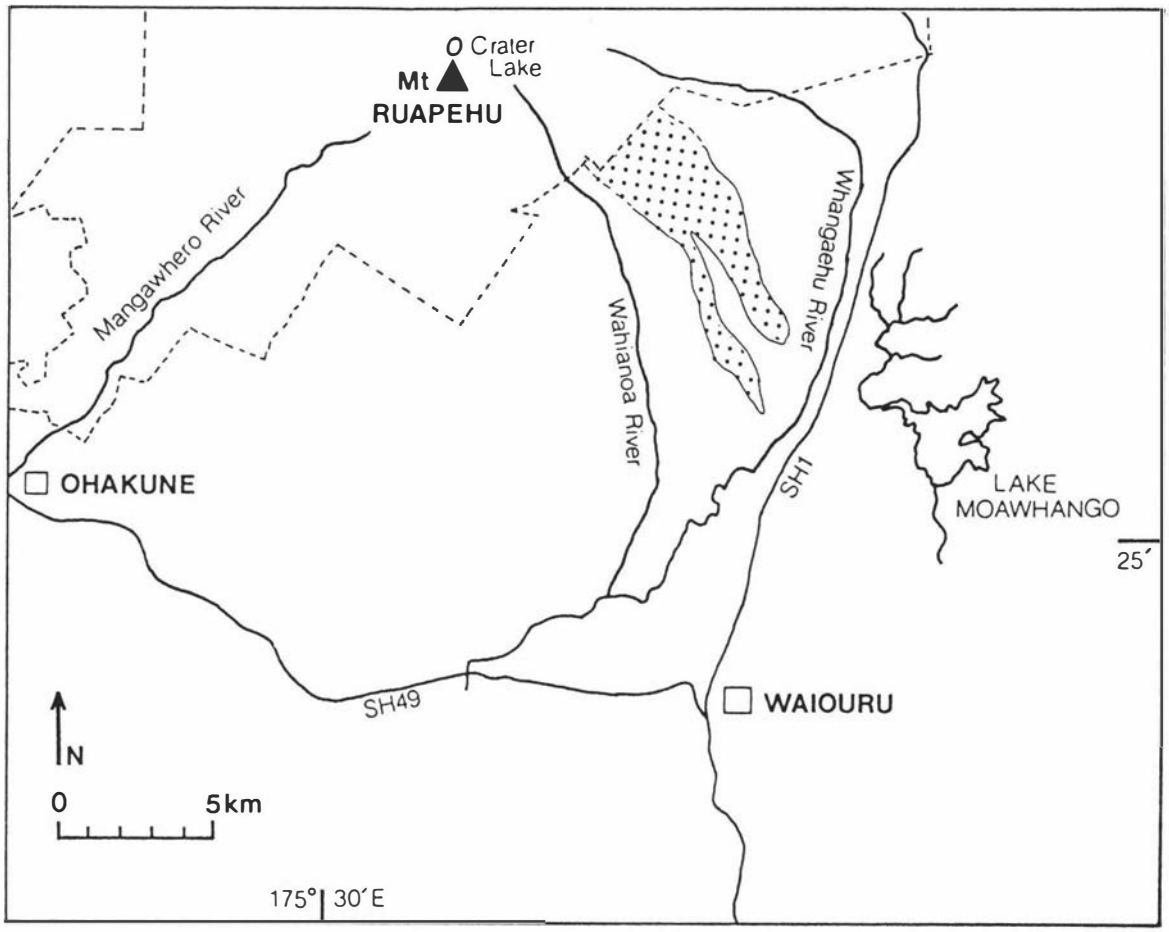

Figure 5.5 Generalised distribution of Manutahi Formation laharic deposits (shaded) on the southeastern Mt Ruapehu ring plain (see also Map 2).

Tangatu Formation [Ta]

Definition and Age

Tangatu Formation is a new formation name for pale grey weakly bedded sands with pockets of clast-supported clasts, and diamictons comprising poorly sorted sands and gravels, with matrix-supported andesitic pebbles and cobbles, sourced from Mt Ruapehu. Tangatu Formation deposits overlie the Te Heuheu Formation and underlie Motutere Tephra and Manutahi Formation deposits. The overlying rhyolitic Motutere Tephra, dated [NZ4846] at *c.* 5370 years B.P. provides a minimum age for the formation, and approximates to the boundary between the Tangatu Formation and Manutahi formations. The boundary between the Tangatu and Te Heuheu formations is marked by a regional unconformity, which identifies the transition from an unstable to stable paleo-environment over much of the region. At most sites, Rerewhakaaitu Tephra (dated at *c.* 14 700 years B.P.) is the basal rhyolitic tephra found overlying this unconformity, providing a maximum age for Tangatu Formation deposits.

Description and Identification

The type section for Tangatu Formation is here designated at Death Valley S.5 [DV5] [T20/409045] (Plate 5.16). Reference sections are here defined at Helwan S.2 [H2] and

Helwan Quarry [HQ] [T20/408921] (Figure 5.1, p. 250; Chart 4). Best localities within Rangipo Desert are at Lower Seagull Gully and The Chute.

At the type section, Tangatu Formation is *c.* 3.6 m thick. It is overlain by Motutere Tephra and Manutahi Formation deposits. The base of the formation is not exposed at this site. Here, the formation comprises weakly bedded ungraded, and reversely graded, grey sands with pockets of clast-supported fine andesitic lithic and pumice pebbles, and scattered cobbles. The finer grained, better sorted, and stratified sandier units, which typically show reverse grading (Plate 5.18) are interpreted as HFF deposits. The coarser grained more poorly sorted units are interpreted as deposits of debris flows. Twelve discrete units are recognised. Ten of these are described as HFF deposits, with some units pinching out laterally. The distinct lithological change seen here between the SF–HFF units of the overlying Manutahi Formation, and the HFF and DF deposits of Tangatu Formation is the basis for establishing the two formations. Tangatu Formation is dominated by HFF deposits, the younger Manutahi Formation by SF–HFF deposits.

At Lower Seagull Gully S.2 Tangatu Formation deposits are found above and beneath upper Bullot Formation tephras. The youngest units overlie two Bullot Formation marker beds correlated with members L16 and L17 (which identify the stratigraphic position of Waiohau Tephra, Chart 3), and underlie lower Papakai Formation with the interbedded Motutere Tephra, and thin Manutahi Formation deposits. Thus the youngest units are $<$*c.* 11 250 years old, and the oldest units which occur below member L16 are $>$*c.* 11 250 years old.

The upper part of Tangatu Formation (post-Waiohau Tephra) is represented by a 0.45 m thick grey, fine grained sandy HFF unit, which laterally thickens down-channel to *c.* 2 m. Below this is a sequence of bedded pebbly sands, with small scour and fill structures and cross bedded pumiceous sands, interpreted as SF deposits, which also thicken appreciably down-channel to *c.* 0.75 m.

At the base of the section, Bullot Formation member L16 overlies a coarse DF deposit which thickens up-channel to *c.* 1.10 m. It comprises a yellowish brown coarse sandy matrix with matrix-supported andesitic lithic clasts, and distinctive orange pumice pebbles. It overlies *c.* 10 m of dark grey weakly bedded sands and gravels with indistinct bed contacts and lenses of brown sandy loam. Cross-bedded sands occur near the base of the exposure. This sequence is interpreted as comprising SF deposits. Further up-channel, below these deposits, an additional three DF deposits are exposed, each $<$1.0 m thick.

Over most of the Badlands (Plate 5.19) the tephra cover has been eroded down to a thin hard pan comprising pale grey lithified sands of Manutahi Formation, on Motutere Tephra. Motutere Tephra occurs as distinct pink 'cream cakes' of fine and coarse ash above Tangatu Formation. Here, the upper part of Tangatu Formation comprises bedded brown fine sandy silts and grey laminated sands. In deeper channels HFF and DF deposits are exposed, being

interbedded with tephras of Bullot Formation. Near the western margin of the Badlands there are nine HFF units totalling 1.15 m in depth.

Within Rangipo Desert, Tangatu Formation is represented by HFF and DF deposits, and minor SF deposits. Twelve HFF and DF deposits exposed below Pourahu Member in The Chute S.2, ten HFF and DF deposits exposed at Whangaehu Ford below Motutere Tephra, and four DF deposits at Aqueduct S.2 found below Ngamatea lapilli-1 are correlated with Tangatu Formation based on their stratigraphic position to Motutere Tephra and Ngamatea lapilli-1 (Chart 4).

At Helwan S.2 (Plate 5.20), Tangatu Formation is >*c.* 1.8 m thick and underlies Ngamatea lapilli-1 member of Bullot Formation. The base of the formation is not exposed at this site. The deposit is correlated with unit C, at the nearby Helwan Quarry (Plate 5.23; Plate 5.24), which unconformably overlies older Bullot Formation tephras (including Shawcroft Tephra) and DF and HFF deposits older than Waiohau Tephra (dated at *c.* 11 250 years B.P.). At Helwan S.2, the deposit comprises alternating thin (generally <70 mm) coarse (pebble-rich) and fine (sand-rich) beds, becoming more massive toward the base. Pebble-rich beds are dominated by fine pumice, and typically show reverse grading. The maximum clast size is very coarse pebble (40 mm). The deposit is interpreted as the product of a hyperconcentrated flood flow, or possibly many flows, and is almost identical in character to a slightly older *c.* 3.5 – 6 m HFF deposit exposed below unit C at Helwan Quarry.

Thick HFF and DF deposits of similar age (directly overlain by Ngamatea lapilli-1) are seen in large exposures at Waiouru Tip [T20/417935, 419938], Helwan Dam [T20/398911] and cuttings along the Desert Road between Waiouru Tip and Helwan S.2 [T20/407917].

At Helwan Quarry (Plate 5.21), a thick *c.* 7.7 m sequence of grey bedded sands and pebbles, and diamictons is exposed below Waiohau Tephra (dated *c.* 11 250 years B.P., Table 2.1, p. 16). These deposits are correlated with Tangatu Formation based on the apparent absence of both an erosion break and Rerewhakaaitu Tephra above them, and the lithologic dissimilarity with older Te Heuheu Formation diamicts seen in exposures north of this site.

Here, the formation comprises nine pale grey DF and HFF deposits. The DF deposits are poorly sorted and poorly bedded with sandy matrices and matrix-supported andesitic lithic pebbles and cobbles. The finer grained and better sorted sandier units are interpreted as deposits of hyperconcentrated flood flows. At this site, DF deposits overlie between *c.* 3.5 and 6 m of horizontally bedded sands and gravels (Plate 5.22). Overall the deposit is reversely graded, with a more massive and finer grained sand-rich basal unit, and a thinner and coarser distinctly bedded top. It comprises alternating pebble-rich and sand-rich beds (generally <100 mm thick) with occasional scattered cobbles. Most of the pebble-rich beds show reverse grading, and comprise fine lithic and pumice pebbles and granules. The deposit is

interpreted as the product of a hyperconcentrated flood flow, or possibly many flows. Rapid deposition is indicated by the absence of scouring at the base of clasts, and the presence of laminar bed contacts both below and above clasts. Pillar-shaped water escape structures occur at the contact between the lower more massive, and the upper distinctly bedded parts of the deposit (Plate 5.22). Water escape structures are commonly seen in sands and coarse silts, which involved rapid sedimentation. They are soft-sediment deformation structures, formed during sediment dewatering and compaction (consolidation) in unlithified deposits, or alternatively they may form concurrently with or immediately following deposition, in which case the structures result largely from gravitational loading (Lowe 1975).

Volume

The volume of Tangatu Formation is estimated to be about 94 x 10^6 m^3, based on the distribution shown in Map 2.

Distribution and Source

The distribution of Tangatu Formation on the southeastern Mt Ruapehu ring plain is shown in Figure 5.6 (p. 269) and Map 2. The formation can only be mapped with certainty between the type section in the west and Whangaehu River in the east. In the north, it has not been found between The Chute and Bullot Track, *i.e.* over the bulk of the Whangaehu Fan. Here it may be buried, and probably occurs as a channelised deposit. Its distribution elsewhere, however, indicates it is widespread and very probably occurs over the entire southern Rangipo Desert. Provisional boundaries have been placed in the north and east, bordering Whangaehu River and the Whangaehu escarpment. The western margin is placed at the junction between Karioi Forest and Rangipo Desert, where these two areas are separated by a distinct topographic divide. Exposures at the northern end of Karioi Forest at Makahikatoa Stream, and south at Rangipo S.2 [T20/417981] indicate Tangatu Formation deposits may underlie the eastern margin of the forest. Tangatu Formation-aged deposits have not, however, been identified in more western exposures within Karioi Forest, with the exception of two sites, at Wahianoa River and at T20/347014. A local sediment source in Wahianoa Valley, rather than Whangaehu Valley is indicated.

HFF and DF deposits of Tangatu Formation-age, overlain by Waiohau and Shawcroft tephras, are found capping the Whangaehu escarpment at Whangaehu River S.9 [T20/410966], S.8 [T20/397951] and T20/396952. They are also exposed in a low river terrace on the east side of Whangaehu River at the base of the escarpment [T20/397957], indicating this formation was channelled south beyond Rangipo Desert. The occurrence of thick Tangatu Formation DF and HFF deposits preserved in the vicinity of Helwan Quarry suggests lahars were able to breach the southern margin of Rangipo Desert. The capture and channelling of these lahars by tributary rivers south of Rangipo Desert led to their deposition in areas just north of Waiouru.

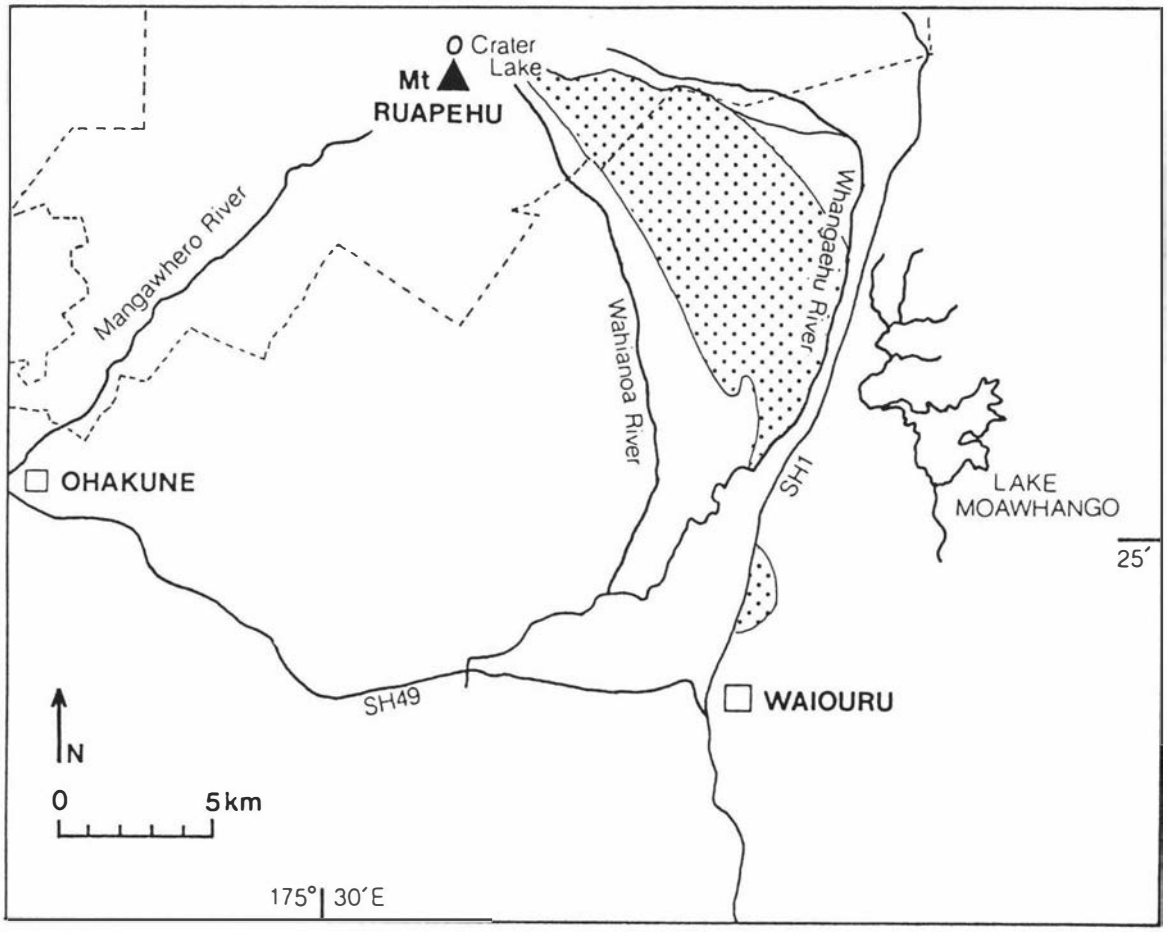

Figure 5.6 Generalised distribution of Tangatu Formation laharic deposits (shaded) on the southeastern Mt Ruapehu ring plain (see also Map 2).

Other Deposits of Tangatu-age

At Bullot Track S.2, and proximal exposures, a *c.* 0.75 m thick DF deposit is interbedded within the Bullot Formation. This deposit which may be a correlative of Tangatu Formation is closely overlain by Bullot marker ash sequence M_1, and is therefore older than Pourahu Member [ignimbrite unit], dated *c.* 11 000 – 10 000 years B.P. (estimated age) and younger than Waiohau Tephra, dated *c.* 11 250 years B.P. It comprises a poorly sorted fine loamy sand and granule matrix with many matrix-supported angular andesitic lithic, and pumice clasts (pebbles and cobbles ≤20 cm).

At Mangatoetoenui Quarry [T20/459153] (Plate 3.20), a *c.* 12 m thick sequence of DF deposits, comprising at least eight distinct units, is exposed below Pahoka Tephra. Pourahu Member of Bullot Formation is interbedded near the top of the sequence. These deposits are of Tangatu Formation age, and are dated at >*c.* 11 000 years B.P. Most were probably sourced from the northern slopes (Mangatoetoenui Valley) of Mt Ruapehu. A similarly aged sequence of laharic deposits is exposed north of the quarry at T20/470178, near Waihohonu Stream. Here, five units with sandy matrices and either matrix- or clast-supported multi coloured lithic pebbles, cobbles and boulders are exposed. They appear to have been sourced

from Mt Tongariro. These deposits are directly overlain by Pourahu Member and the younger Pahoka and Mangamate tephras.

Te Heuheu Formation [Hh]

Definition and Age

Te Heuheu Formation is a new name for diamictons comprising coarse sands with matrix-supported andesitic pebbles, cobbles, and pumice clasts, and finer grained weakly bedded pebbly sands, sourced from Mt Ruapehu. Te Heuheu Formation deposits underlie those of the Tangatu Formation, being separated from them by an erosional unconformity and the rhyolitic Rerewhakaaitu Tephra. Rerewhakaaitu Tephra provides a minimum age for the formation. The base of the formation is not defined. Deposits forming the major constructional surfaces of the southern Mt Ruapehu ring plain (dated between *c.* 22 500 – 14 700 years B.P.) are included in the formation.

The late Pleistocene-aged Murimotu, Hautapu and Waimarino lahars, mapped by Grindley (1960) mapped on the southeastern ring plain are included in this formation.

Description and Identification

Te Heuheu Formation deposits are best exposed along the Whangaehu escarpment, east of Rangipo Desert (Plate 5.25), where they underlie late Pleistocene and Holocene-aged andesitic and rhyolitic tephras. Within Rangipo Desert, these deposits are deeply buried by the younger Tangatu, Manutahi, Mangaio and Onetapu formations and Holocene-aged tephra cover beds. They have not been exposed by faulting.

Te Heuheu Formation deposits accumulated between *c.* > 22 500 – 14 700 years B.P., during the Last (Otira) Glaciation. During this time tills, glaciofluvial outwash deposits and lahar deposits accumulated on the ring plain. It is difficult to distinguish between glacial and laharic deposits on a sedimentological basis (Crandell 1971; Hackett 1985; M^{c}Arthur and Shepherd 1990). Both till and DF deposits are poorly sorted coarse diamictons. The distinction between these is most commonly based on the recognition of distinctive deposit morphology and presence of striated boulders and glacial irons within the deposit. Distinction between outwash deposits, comprising stratified sands and gravels, and stratified HFF deposits is also difficult. In the absence of diagnostic criteria, the coarse deposits, described from sites distal to areas where moraines have previously been mapped, are described as deposits of debris flows, and the finer grained and stratified deposits as deposits of hyperconcentrated flood flows. The near planar surfaces of Te Heuheu Formation deposits (Plate 5.25) suggests they are most probably laharic. There is one exception - at Tufa Trig S.2., the deposits below Rerewhakaaitu Tephra are probably of glaciofluvial origin sourced from the Wahianoa catchment, downstream of the glacial moraines of Wahianoa Valley.

The type section is here designated at Whangaehu River S.5 [WR5] [T20/443045]. Reference sections are at Whangaehu River S.1 [WR1] and Wahianoa Aqueduct [WA] [T20/435990] (Figure 5.1, p. 250; Chart 4).

At Whangaehu River R.S.5, Te Heuheu Formation comprises poorly sorted, coarse sandy diamictons with matrix-supported andesitic lithic and pumice pebbles, cobbles and boulders (DF deposits), and finer grained weakly bedded pebbly-sands with clast to matrix-supported dominantly fine andesitic pebbles (HFF deposits). Many of the HFF deposits have lithified sandy matrices. All units are bluff forming. Twenty discrete units are preserved in the upper *c.* 50 m of the exposure. These deposits are interbedded with minor fluvial units comprising clays and cross-bedded sands. Contacts between units are distinct and smooth. At this site Te Heuheu Formation DF and HFF deposits underlie 0.52 m of Bullot Formation tephras below Rerewhakaaitu Tephra. Kawakawa Tephra Formation is not interbedded within the formation, and was most probably eroded by the lahars.

At Whangaehu River S.1 (Plate 2.21), Te Heuheu Formation deposits underlie 0.11 m of loamy sand below Rerewhakaaitu Tephra. They are exposed in the cliff face, *c.* 50 m above Whangaehu River. Here, the coarse poorly sorted bouldery deposits and finer grained sandy units are interpreted as the products of debris flows and hyperconcentrated flood flows. Kawakawa Tephra Formation has not been identified within accessible parts of the exposure.

At Wahianoa Aqueduct (Plate 2.20), Te Heuheu Formation directly underlies Rerewhakaaitu Tephra. Five deposits interpreted to be of DF and HFF origin are exposed between Rerewhakaaitu Tephra and the base of the section. At both Whangaehu River S.1 and Wahianoa Aqueduct S., the late Pleistocene regional unconformity is identified by the abrupt change in lithology between thick sequences of andesitic diamicts, and the overlying primary tephra cover beds (Rerewhakaaitu Tephra and younger tephras). Kawakawa Tephra Formation has not been identified at these sites. It was either not deposited, or was eroded during the deposition of Te Heuheu Formation.

The most southern exposure of Te Heuheu Formation DF deposits in the study area, is at Ngamatea Swamp (Map 2). Here the formation is exposed at the base of a NE–SW trending drainage channel, and underlies ?Waiohau Tephra. Although Rerewhakaaitu Tephra and Kawakawa Tephra Formation are not recognised at this site, the basal lahar deposits can be correlated with Te Heuheu Formation by surface mapping. South of Waiouru at Hihitahi [T21/428779], *c.* 15 000 years B.P. lahar deposits are found overlying Kawakawa Tephra Formation.

Volume

It is difficult to accurately determine the volume of Te Heuheu Formation deposits within the study area due to the lack of exposure. A conservative estimate of volume is 6×10^9 m^3.

Distribution

The distribution of the Te Heuheu Formation is shown in Figure 5.7, p. 272 and Map 2. Te Heuheu Formation deposits are the most extensive, and form the major constructional surfaces of the southeastern Mt Ruapehu ring plain. The formation is mapped east and west of the Whangaehu escarpment, and south to Waiouru. It is bounded in the east by the Kaimanawa Ranges, and in the west it underlies the Rangataua Lava flow.

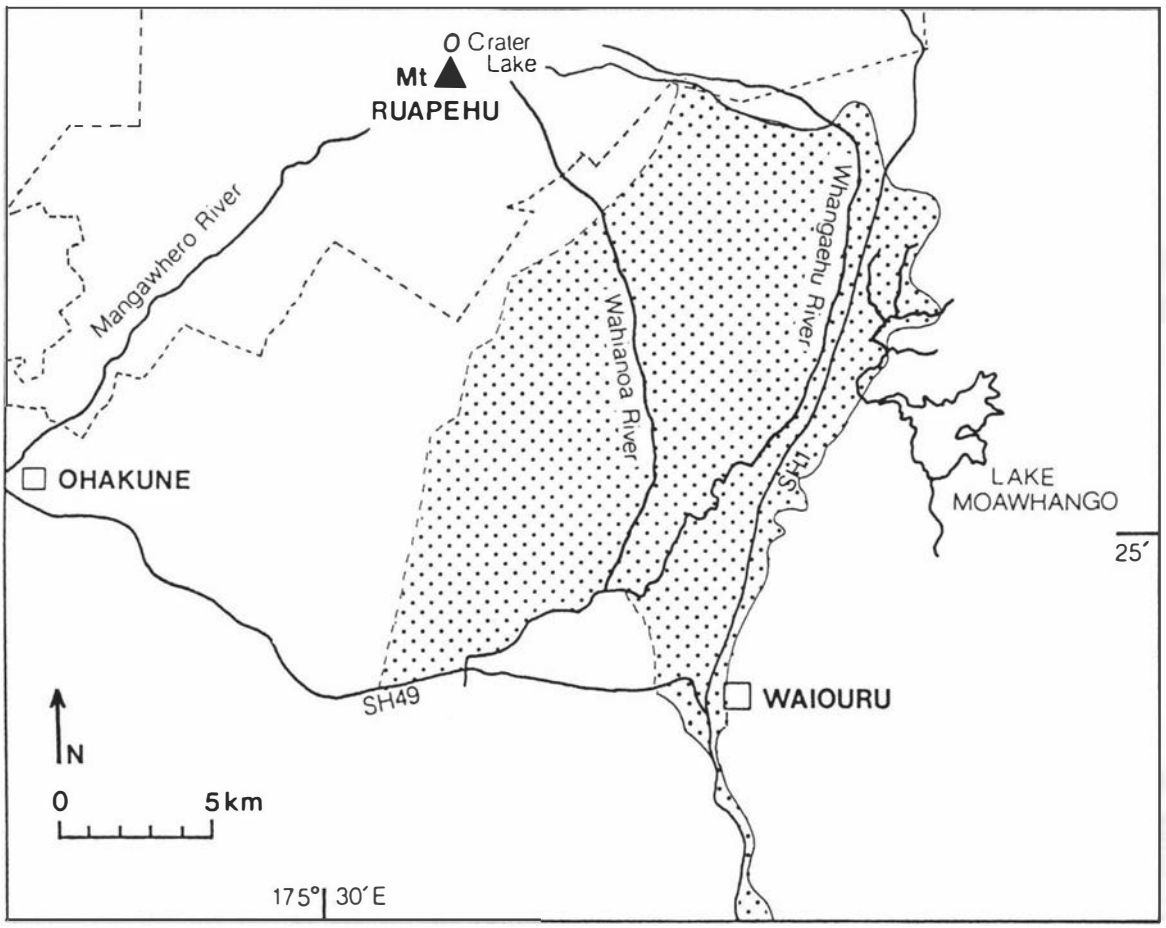

Figure 5.7 Generalised distribution of Te Heuheu Formation laharic deposits (shaded) on the southeastern Mt Ruapehu ring plain (see also Map 2).

In the study area the formation has an estimated volume of 6 $x10^9$ m^3.

Within the study area, Te Heuheu Formation deposits are distributed over four distinct topographical surfaces, labelled A – D in Map 2. The basal rhyolitic tephra identified in exposures on surface A, occurring east of the fault escarpment (*e.g.* at Wahianoa Aqueduct R.S. [T20/435990] and north of here at Whangaehu River S.5 and Whangaehu Junction [T20/445069]) is Rerewhakaaitu Tephra (Figure 5.8, p. 273). The basal rhyolitic tephra identified on surface B (*e.g.* at Helwan Quarry, where it is found overlying Tangatu Formation deposits) is Waiohau Tephra. Rerewhakaaitu Tephra is not identified because tephras and laharic deposits older than Tangatu Formation are not exposed on this surface.

The basal rhyolitic tephra found overlying surface C, east of Karioi Forest (*e.g.* in exposures at Whangaehu River S.1 is Rerewhakaaitu Tephra. In proximal exposures on this surface ([T20/410966] and [T20/397951]) where younger Tangatu Formation deposits occur, only Waiohau Tephra is preserved. Rerewhakaaitu Tephra and similarly aged Bullot Formation tephras were probably eroded during deposition of Tangatu Formation. On surface D (Karioi Forest) Waiohau Tephra is the basal rhyolitic tephra.

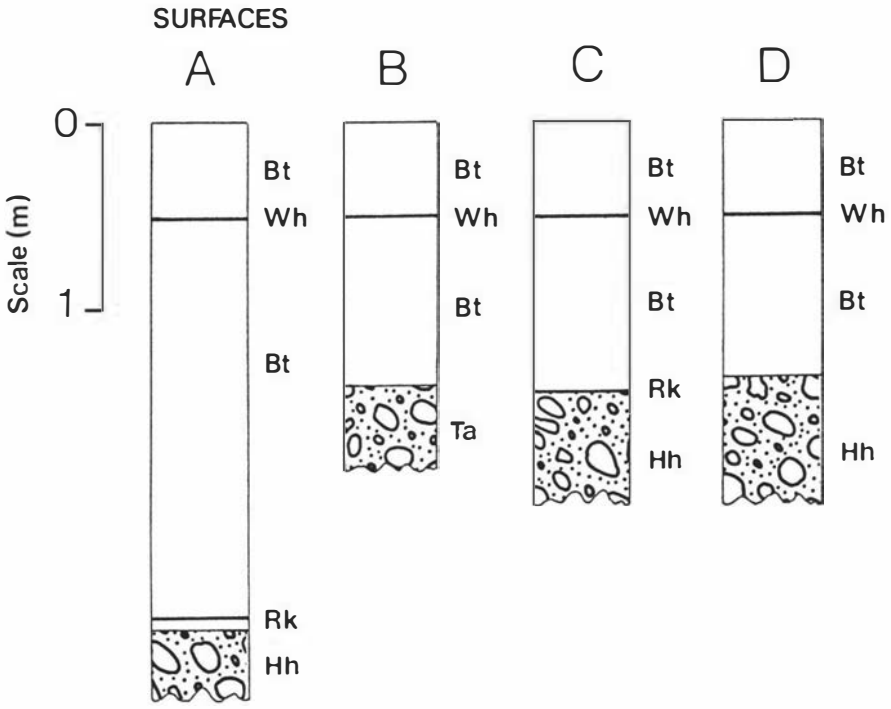

Figure 5.8 Generalised stratigraphy of tephras on Te Heuheu Formation surfaces A – D, showing basal rhyolitic tephras (Rerewhakaaitu Tephra [Rk], Waiohau Tephra [Wh]), Bullot Formation tephras [Bt], Tangatu Formation [Ta], and Te Heuheu Formation [Hh].

Two possible scenarios are presented below to account for the differences in the rhyolitic tephra cover bed stratigraphy, and physiography between Te Heuheu Formation surfaces.

Formation of the initial Te Heuheu surface

A prominent drainage divide between rivers flowing to the north and south of Mt Ruapehu occurs at Bullot Track just north of Whangaehu River. Lahars older than *c.* 22 500 years B.P. (pre-Kawakawa Tephra Formation) were directed both to the north and south of this divide (Figure 5.9a, p. 277). Younger lahars, *c.* 22 500-15 000 years B.P. (post-Kawakawa Tephra Formation), were directed principally to the south [4] (Figure 5.9b) where

[4] Lahar deposits of Te Heuheu Formation age are identified north of the drainage divide at Desert Road S.11, and possibly underlie Tangatu Formation-aged lahars at Mangatoetoenui Quarry [T20/459152].

they overlie older deposits and form the major constructional surfaces of the southeastern Mt Ruapehu ring plain.

Scenario 1: The four Te Heuheu Formation surfaces (A – D) are of the same age, dated at *c.* 15 000 years B.P., a little older than the overlying basal rhyolitic Rerewhakaaitu Tephra.

(1) Origin of surfaces **A** and **B**

Movement along the Whangaehu fault, and subsequent uplift (*c.* 40 – 50 m) east of the Whangaehu River led to the formation of surface A (Figure 5.9c). The tephra cover on surface A became vegetationally stabilised, facilitating preservation of the tephra cover beds.

Further movement along a splinter fault east of the Whangaehu fault offset the original surface A to form surface B, which is down-faulted and of equivalent age (*c.* 15 000 years B.P.) (Figure 5.9d).

Surface B subsequently was partially degraded, prior to formation of surfaces C and D.

(2) Origin of surfaces **C** and **D**

Following degradation of surface B, slightly younger lahars (also *c.* 15 000 years B.P.) were directed principally to the south, forming surfaces D and C. Surface C abuts the slightly older and partially eroded surface B. Surfaces D and C are topographically equivalent, and approximately the same age (Figure 5.9e).

Subsequently Rerewhakaaitu Tephra was deposited on all surfaces. Localised erosion within Karioi Forest by the widespread network of tributary rivers eroded Rerewhakaaitu Tephra and similarly aged Bullot Formation tephras on surface D so that the basal rhyolitic tephra seen on surface D is Waiohau Tephra. The stratigraphy at some sites (*e.g.* along Aqueduct Road) shows a number of Bullot Formation tephras below Waiohau Tephra, suggesting the age of the Karioi surface is close to *c.* 15 000 years B.P., but Rerewhakaaitu Tephra has not been found.

At exposures on surface B, tephras older than Waiohau Tephra (Rerewhakaaitu Tephra and Bullot Formation tephras) are not seen because of the localised deposition of Tangatu Formation-aged laharic deposits.

(3) Bracketing stratigraphy

Given that the four surfaces are *c.* 15 000 years old, they should overlie older (*c.* >15 000 years B.P.) Bullot Formation tephras. These tephras were therefore either eroded by the lahars, or occur below the exposed outcrop. At Whangaehu River S.5, three lapilli beds are found interbedded between debris flows within the upper 50 m of exposure. This suggests most of the older Bullot tephras have been eroded, rather than deeply buried.

Scenario 2: Surfaces A and B are older than *c.* 22 500 years B.P., and surfaces C and D are *c.* 15 000 years B.P.

(1) Origin of surfaces **A** and **B**

Movement along the Whangaehu fault, and subsequent uplift (*c.* 40 – 50 m) east of Whangaehu River led to the formation of surface A (Figure 5.9b′).

Further movement along a splinter fault east of the Whangaehu fault offset the original surface A to form surface B, which is down-faulted and of equivalent age (*c.* >22 500 years B.P.) (Figure 5.9c′). Widespread erosion in the southern Mt Ruapehu region removed Kawakawa Tephra Formation and Bullot Formation tephras deposited between *c.* 22 500 – 14 700 years B.P. on these two surfaces. In vegetationally stabilised areas, *e.g.* at sites north of the Whangaehu River and immediately south of Waiouru, Kawakawa Tephra Formation and younger Bullot Formation tephras were however preserved.

Surface B subsequently was partially degraded, prior to formation of surfaces C and D.

(2) Origin of surfaces **C** and **D**.

Following degradation of surface B, younger lahars dating *c.* 15 000 years B.P. were directed principally to the south, forming the younger surfaces D and C. Surface C abuts the partially eroded and much older surface B. Surfaces D and C which are topographically equivalent, are approximately the same age (Figure 5.9d′).

(3) Bracketing stratigraphy

Following the deposition of the *c.* 15 000 years B.P. C and D surfaces, and the return to stability, the late Pleistocene Rerewhakaaitu Tephra and similarly aged

Bullot Formation tephras were deposited over all surfaces, giving the appearance of equivalently aged surfaces. Incision of tributary rivers within Karioi Forest removed the older (post-*c.* 14 700 years B.P.) deposits from some areas so that at most sites Waiohau Tephra is the first rhyolitic tephra found overlying laharic deposits.

Younger Tangatu Formation deposits were channelled south along tributary river systems and a proto-Whangaehu River, and lapped onto surfaces C and B.

Overall, Scenario 2 seems the most probable portrayal. The absence of Tangatu Formation and younger deposits preserved east of the Whangaehu escarpment indicates faulting and subsequent inception of the Whangaehu escarpment occurred at some time prior to Tangatu Formation deposition. A minimum rate of uplift on the Whangaehu fault is estimated to be 3 mm $year^{-1}$, given a present-day offset of *c.* 50 m and assuming that the first uplift on this fault occurred *c.* 15 000 years B.P. during Te Heuheu Formation time.

5.3 Discussion

Summary of Stratigraphy

Lahar and stream flow deposits of the southeastern Mt Ruapehu ring plain have been grouped into five new formations, dating between > *c.* 22 500 years B.P. and the present (of late Pleistocene to Holocene age). They are defined on lithology, and are dated using interbedded rhyolitic and andesitic tephras (Table 5.1, p. Table 5.1; Table 7.1, p. 309). The stratigraphy of these formations is summarised in Table 5.1, p. 249. The stratigraphy at reference sites, and the correlations made between these is shown in Chart 4.

Lahar Distribution

The distribution of laharic deposits on the southeastern Mt Ruapehu ring plain is shown in Map 2. These laharic sediments form the major constructional surfaces of the southeastern ring plain, and are capped by late Pleistocene and Holocene tephras. The Holocene-aged Onetapu, Mangaio and Manutahi formations, and the late Pleistocene to Holocene-aged Tangatu Formation have been confined west of the Desert Road, within Rangipo Desert, by the formation of the prominent Whangaehu fault scarp. Holocene-aged deposits, preserved only at the lower northern end of this escarpment, most probably represent spill-over deposits. Absence of such deposits elsewhere along the escarpment indicates this feature formed at some time during or after the deposition of the Te Heuheu Formation, and prior to deposition of Tangatu Formation deposits (*c.* 22 500 – 14 700 years B.P.). Deposition of Tangatu, Mangaio and Onetapu formations south of Rangipo Desert indicates channelised

SCENARIO I

SCENARIO II

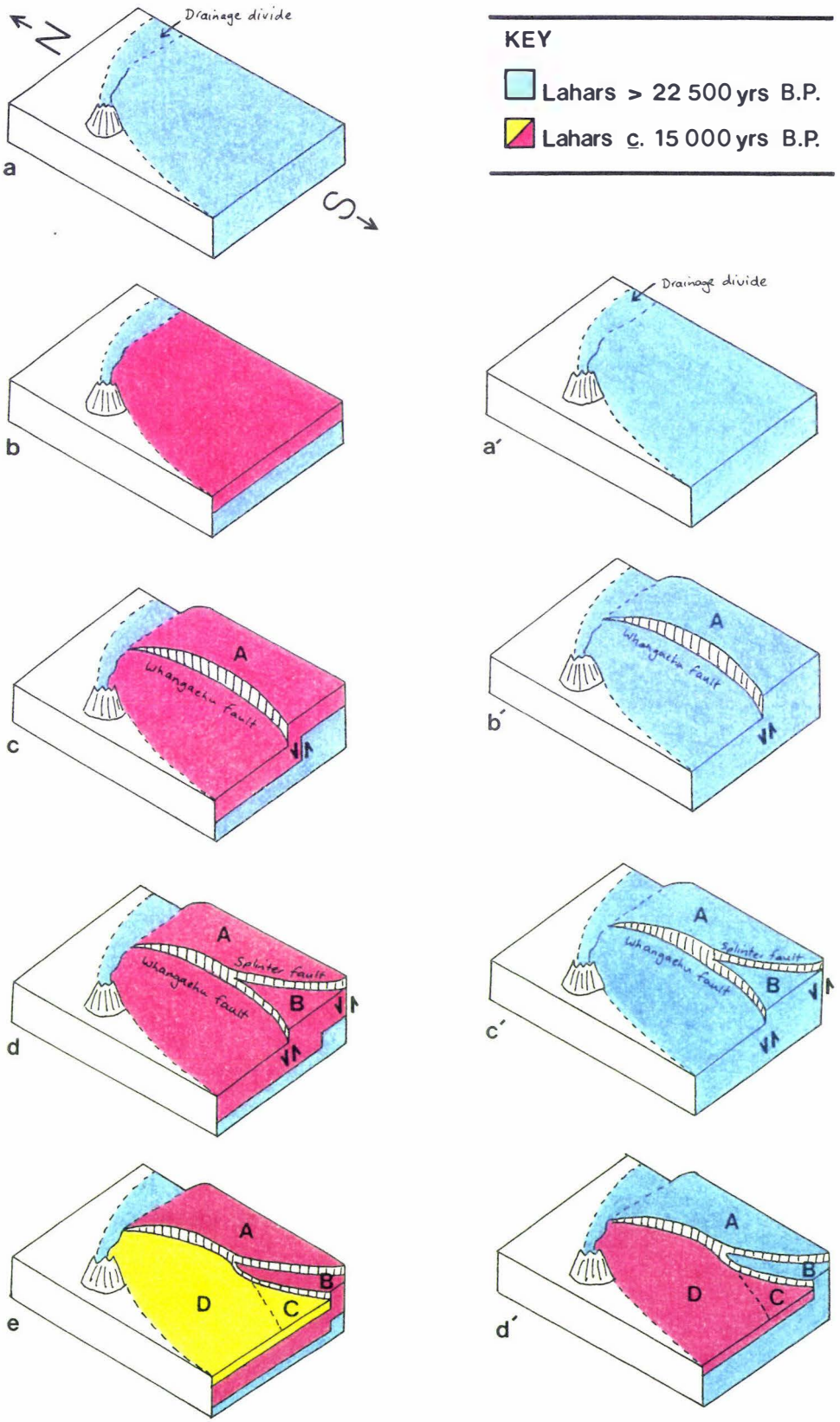

Figure 5.9 Illustrations of scenarios proposed to account for differences in the rhyolitic tephra coverbed stratigraphy and physiography between Te Heuheu Formation surfaces (A – D) *(see text)*.

flow down a proto-Whangaehu River and its tributaries. These distal deposits are characterised by more dilute HFF deposits. Onetapu Formation deposits are also recognised well south of the study area, within the lower Whangaehu Valley [5].

The age and distribution of lahar deposits of the southeastern Mt Ruapehu ring plain as mapped by Grindley (1960) (Figure 1.3, p. 9) is now revised. Originally three late Pleistocene-aged lahar formations (Waimarino, Hautapu, Murimotu) were mapped, together with Holocene-aged 'lahars of the Whangaehu River' (Grindley 1960). The areas mapped by Grindley (1960) as Waimarino, Murimotu and Hautapu lahars are here mapped as Te Heuheu and Tangatu formations. The stratigraphy of tephras preserved on the surface mapped by Grindley as Hautapu Lahars shows this surface immediately pre-dates Rerewhakaaitu Tephra and it is therefore of Te Heuheu Formation-age. Five formations (Te Heuheu, Tangatu, Manutahi, Mangaio, Onetapu) are now mapped throughout Rangipo Desert.

Mechanisms of Lahar Formation

Historically, lahars have been shown to be generated by several different mechanisms, which do not necessarily involve volcanic eruptions. Abundant loose sediment, steep slopes and sudden influxes of water are required to generate lahars (Arguden and Rodolfo 1990). Sources of water include crater lakes, rivers and streams, heavy rains, melting of ice and snow, and jökulhlaups (Neall 1976). Lahars associated with volcanic eruptions may be generated by eruption-induced sector collapses; eruptions through crater lakes; melting of debris-laden snow and ice by hot pyroclastic materials; mixing of pyroclastic flows or other large volumes of volcanic debris with water; and evolution by gravity segregation within pyroclastic surges (Neall 1976; Janda *et al.* 1981; Pierson 1985; Scott 1985; Major and Newhall 1989). Sector collapses or major slope failures associated with Bezymianny-type (magmatic) and Bandai-type (phreatic) eruptions and the subsequent generation of debris avalanches and associated debris flows are recognised at a number of andesitic volcanoes (Boudon *et al.* 1987; Siebert *et al.* 1987).

Lahars generated by the melting of glacial ice and snow by pyroclastic flows were recently recorded at Mt St Helens during the May 1980 eruptions (Janda *et al.* 1981; Waitt 1989), and the 1985 eruption at Nevado del Ruiz (Lowe *et al.* 1986). Pyroclastic flows and surges, and blasts of hot gases and pyroclastic debris are common volcanic events that generate lahars. These events cause rapid melting of glacial ice and snow and produce large volumes of water (Major and Newhall 1989; Waitt 1989).

The presence of tephras found immediately above or below DF deposits records the onset of eruptive activity (Smith *et al.* 1988) and indicates lahars generated as a result of

---

[5] Lahar deposits of Whangaehu Valley, south of Tangiwai are currently being studied by Miss K. Hodgson, Department of Soil Science, Massey University.

volcanic eruptions (*e.g.* the upper Muddy River lahar at Mt St Helens which is overlain by a tephra rich in accretionary lapilli, Janda *et al.* 1981). Pumice-rich DF deposits with well rounded pumice pebbles and clasts were thought to have been generated by melting of heavily debris- and tephra-laden glaciers due to accumulation of hot tephra or by a hot pyroclastic flow (Janda *et al.* 1981), or may form by transition of a pumice flow to a lahar by mixing with stream flow.

Lahars disassociated with volcanic eruptions can be generated by; heavy rains producing 'rain lahars' by mobilising loose sediment; slumping and flowing of water-saturated parts of debris avalanche deposits; collapse of a crater lake; and earthquake triggered collapses (Crandell 1971; Neall 1976; Janda *et al.* 1981; Rodolfo 1989; Arguden and Rodolfo 1990). Water required to generate lahars on the surfaces of debris avalanches is provided by pulverised glacial ice incorporated into the deposit (Janda *et al.* 1981). Large blocks of ice provide a water source for later dilution downstream.

Onetapu Formation

The Onetapu Formation represents the most recent and the most active period of lahar deposition within the Holocene at Mt Ruapehu. Documented records of historical eruptions at Mt Ruapehu show that most of the lahars were generated during phreatic or phreatomagmatic eruptions through Crater Lake, and subsequent channelling of flood waters down Whangaehu Glacier into the Whangaehu and other valleys. Phreatomagmatic eruptions through Crater Lake in 1969 and later in 1975 produced lahars in Whangaehu Valley as a result of the eruptive ejection of Crater Lake waters (Healy 1978; Nairn *et al.* 1979).

The earlier 1953 lahar was generated by the collapse of an ash barrier retaining Crater Lake, and the subsequent release of some of the Crater Lake waters down Whangaehu Glacier and into the Whangaehu Valley. This event was not directly associated with volcanic activity. The most recent lahar generated by phreatic eruptions within Crater Lake occurred in December 1988. This event was small, and the lahar was confined to the upper reaches of Whangaehu Glacier.

Many of the older lahars of Onetapu Formation (pre-1860 A.D.) do not appear to have been generated by contemporaneous phreatomagmatic eruptions of Tufa Trig Formation tephras, as these tephras are not seen directly above or below the lahar deposits (they are separated from the DF deposits by thin paleosols and aeolian sands). Either the associated tephras have been eroded by subsequent flood events, or the debris flows were generated by non-tephra producing eruptions, or heavy rains and slope failures within Whangaehu Valley.

Sources of sediment for Onetapu lahars include volcanic ejecta (ballistic blocks, surge deposits, and tephra) deposited in the summit area. Possibly the greatest sediment source is

derived from unstable channel deposits in the upper reaches of Whangaehu Valley. Much volcanic debris is also probably derived from erosion and entrainment of existing lahar deposits during flow over the Whangaehu Fan. Debris flows can derive a large proportion of their sediment load by eroding channels into pre-existing laharic deposits (Rodolfo 1989; Janda *et al.* 1981). Onetapu Formation lahars have eroded much of the recent tephra cover beds (Taupo Pumice, Mangatawai Tephra) and Papakai Formation.

The sandy matrices of the DF and HFF deposits indicates deposition from dilute, watery lahars. Sources of water for these lahars include Crater Lake waters ejected during volcanic eruptions, rains, and snow and ice melted by hot pyroclastic ejecta.

Mangaio Formation

The Mangaio Formation is characterised by abundant white hydrothermally altered lithic clasts, supported within a distinct grey, purplish grey and orange clayey matrix. Similar clay textured DF deposits which contain hydrothermally altered lithic clasts have been described as originating from sector collapses within unstable hydrothermally altered flank areas of a volcano (Crandell 1971; Boudon *et al.* 1987). Clay textured DF deposits of Holocene age, sourced from Mt Rainier were derived from avalanches of hydrothermally altered rocks (*e.g.* Osceola Mudflow, Crandell 1969, 1971). Possible source deposits for Mangaio Formation are the pervasive hydrothermally altered deposits of Hackett's (1985) central volcanic facies of Wahianoa Formation, exposed in the upper Whangaehu Valley.

The Mangaio debris flow may originally have been derived from a debris avalanche deposit produced by slope failure in hydrothermally altered rocks. Parts of this avalanche deposit may have been remobilised, generating the debris flow, although no associated avalanche deposit is recognised on the lower southeastern ring plain and the deposit does not contain debris avalanche blocks.

The absence of tephras either directly under- or overlying the lahar suggests the lahar event was not associated with eruptive activity. It was deposited during a period of relative quiescence at Mt Ruapehu and Mt Tongariro, during which time Papakai Formation gradually accumulated. An origin by slope failure (sector collapse) is therefore favoured.

Many small uncarbonised branches found within the deposit suggest the lahar was of sufficiently large volume to fell stands of *Nothofagus* forest [6]. The lahar was probably not hot, since neither the wood within the deposit, nor the peat found immediately beneath it, is charred.

---

[6] Pollens extracted from within the peat and analysed by Dr M. M^{c}Glone (Botany Division, DSIR, Christchurch) showed the vegetation existing in the area prior to deposition of the debris flow was dominantly *Nothofagus fusca* type forest (93.6% of pollen). Pollen analysis is presented in Appendix IVb.

Manutahi Formation

Manutahi Formation is characterised by thick accumulations of pebbly-sands, transitional in character between SF and HFF deposits. Deposition was coeval with that of the Papakai Formation largely erupted from Mt Tongariro. Manutahi Formation deposits are thus unlikely to be directly related to eruption events and were probably initiated by stream flow events transformed to hyperconcentrated flood flow events by entrainment of sediments ('bulking') on the lower flanks of the volcano. Pumice pebbles are a significant component in these deposits, and were probably derived from erosion of Bullot Formation tephras. During the more inactive depositional periods, the rhyolitic Whakatane and Hinemaiaia tephras were deposited and preserved throughout the study area.

Much of the water for these flood events was probably derived from ablation of the summit glaciers during the early-mid Holocene, as a result of climatic warming after the Last (Otira) Glaciation. Meltwater from these glaciers possibly fed a proto-Whangaehu River which deposited sediment on the southeastern ring plain.

The difference in lithology between these deposits and the similarly aged Mangaio Formation, shows the deposits of the two formations were derived from entirely different source areas, and were deposited under quite different rheological conditions.

Tangatu Formation

Tangatu Formation comprises deposits of hyperconcentrated flood flows and debris flows, which accumulated intermittently between *c.* 14 700 – 5800 years B.P. During this period, most of the Bullot Formation tephras were erupted.

Some of the lahars were directly associated with the eruption of Pourahu Member of Bullot Formation *c.* 11 000 years B.P. At the southern end of The Chute, deposits of Tangatu Formation and Pourahu Member [ignimbrite unit] interfinger. The stratigraphic association of these deposits, and the presence of perfectly preserved pumice bombs with jigsaw jointing (derived from Pourahu Member [ignimbrite unit]) found within Tangatu Formation DF deposits, indicates these flows were generated as a result of the eruption of the pyroclastic flow. Eruptions of hot pyroclastic flows onto snow and ice cause melting and subsequent lahar-forming floods (Crandell 1971). Preservation of these fragile bombs indicates they were transported, possibly in a hot plastic condition by laminar 'plug flow' within lahars, and the fracturing followed transportation and cooling (Enos 1977; Hackett 1985). Other Tangatu Formation lahars, closely overlain by Ngamatea lapilli-1 or the Waiohau and Shawcroft tephras, and found interbedded with Bullot Formation tephras, were probably generated shortly after magmatic volcanic eruptions.

The lahars associated with the eruption of Pourahu Member [ignimbrite unit] may have been hot lahars. At Mayon Volcano in the Philippines, hot lahars are found closely associated with pyroclastic flow deposits, while cold lahar deposits are more closely associated with debris avalanche sediments (Arguden and Rodolfo 1990). Deposits of 'hot lahars' can be distinguished from 'cold lahars' by determination of the thermoremnant magnetisation (TRM) of clasts, and by the prominent, thick, inversely graded bases. Other features of hot lahars include erosion resistant baked crusts, gas-escape structures, and higher concentrations of fines than in cold lahars. While some of the Tangatu Formation debris flows show distinct reversely graded bases, further sedimentological characterisation, including TRM, is needed before a hot origin can be proven.

Most of the deposits show sandy matrices with low sediment concentrations. Much of the water required to generate these was probably derived from ablation of the Whangaehu and summit glaciers during the early Holocene as a result of climatic warming following the Last Glaciation. Moraines preserved just above the lava flows at the head of the Whangaehu Fan *c.* 1200 m a.s.l. (Whangaehu end moraines, M^{c}Arthur and Shepherd 1990) show the former extent of the Whangaehu Glacier. A considerable volume of water would have been derived from the retreat of this glacier, and large volumes of sediment would have been available within rivers and channels. Floods within the Whangaehu Valley would quickly generate lahars.

The greater distribution of Tangatu Formation compared to that of the later Mangaio and Manutahi formations, and the more dilute nature of the flows considered to have deposited Tangatu Formation compared to the older Te Heuheu Formation, probably indicates the greater availability of water during the interval of Tangatu Formation deposition.

Te Heuheu Formation

Te Heuheu Formation comprises a thick sequence of cliff-forming diamictons which accumulated during the Last Glaciation. Compared to Holocene climates, there would have been greatly reduced amounts of water available during the Last Glaciation when Te Heuheu Formation debris flows were deposited. Additional sources of water for the lahars may have been derived from pulverised glacial ice incorporated into debris avalanches or by the melting of snow and ice by hot pyroclastic ejecta.

The lahars were probably initiated by large scale sector collapses of the southeastern flanks of Mt Ruapehu. Large scale collapses, possibly triggered by subplinian volcanic eruptions (which led to the contemporaneous deposition of the Bullot Formation tephras) would have been required to generate such widespread lahars. The coarser grained, bouldery appearance of the Te Heuheu Formation lahars may reflect origins of some lahars from debris avalanche deposits.

5.4 Holocene Geology of the Upper Whangaehu River

The Holocene geology of the upper Whangaehu River is dominated by the accumulation of laharic deposits and tephras from Mt Ruapehu. The most active period of lahar generation within the Holocene has been within the last *c.* 1800 years B.P., in which 36 $x10^6$ m^3 of DF and HFF deposits of the Onetapu Formation were deposited by the Whangaehu River.

Onetapu Formation laharic deposits are characteristically dark grey in colour, with loose sandy and gravelly matrices (Plate 5.11), indicating source from dilute, watery lahar events. They show a predominance of coarse clasts (boulders – cobbles). The lithology of Onetapu Formation deposits contrasts markedly with that of the older Holocene-aged Mangaio Formation (Plate 5.10), and also with deposits of the Manutahi and Tangatu formations.

The Mangaio Formation is characterised by a distinctive purplish grey and orange coloured clay-rich matrix, with higher sediment concentration. The Manutahi and Tangatu formations are dominated by pale grey sandy laharic deposits. Bedding characteristics and outcrop appearances of these formations are quite different to those of the Onetapu Formation deposits, with deposits lacking the concentration of large (boulders – cobbles) clasts seen in Onetapu Formation deposits.

The lithological dissimilarities, and changes in lahar distribution between the youngest Onetapu Formation laharic deposits, and older Holocene-aged deposits indicates both a shift in source areas and changes in lahar regimes over time. The greater frequency of lahar generation and the dominance of this activity during the deposition interval of the Onetapu Formation also indicates a change in lahar regime to more dilute, watery lahars. It is proposed that this change is related to the inception of the present-day Crater Lake *c.* 2000 years B.P. The melting of summit snow and glacial ice surrounding the vent and the periodic overflow of Crater Lake waters into the headwaters of the Whangaehu River led to an increase in lahar frequency within Whangaehu Valley, and the generation of more dilute, watery lahars.

Support for inception of a crater lake at *c.* 2000 years B.P. is also provided by the Holocene tephra record. The most recent tephras erupted from Mt Ruapehu comprise the Tufa Trig Formation. These tephras, like the lahars, differ lithologically from earlier events. The lithological characteristics of the Tufa Trig tephras are consistent with origin from hydrovolcanic (phreatomagmatic or phreatic) eruptions (Heiken 1972; Wohletz 1983). In contrast the older Bullot Formation tephras are distinctly pumiceous, and are interpreted as the products of sub-plinian eruptions.

A time constraint on the inception of this crater lake is also obtained by the dating of a lava flow situated at the apex of the Whangaehu Fan, within Whangaehu Gorge. The lava flow is correlated with the Whakapapa Formation of Hackett (1985) dated between *c.* 15 000 years B.P. and the present. Here, the lava flow directly overlies the *c.* 4600 years B.P. Mangaio

Formation DF deposit, and is further overlain by Taupo Pumice preserved within crevices of the lava surface (Figure 5.10, p. 284). The rhyolitic Waimihia Tephra (dated *c.* 3400 years B.P.) and andesitic tephras found overlying the Mangaio Formation in exposures beyond the lava flow front, are not present at the contact of the debris flow and lava flow, suggesting emplacement of the lava flow soon after the lahar event (post-4600 years B.P.). Mangaio Formation provides a maximum age for the lava flow, and Taupo Pumice a minimum age. The flow is thus dated between *c.* 4600 – 1800 years B.P.

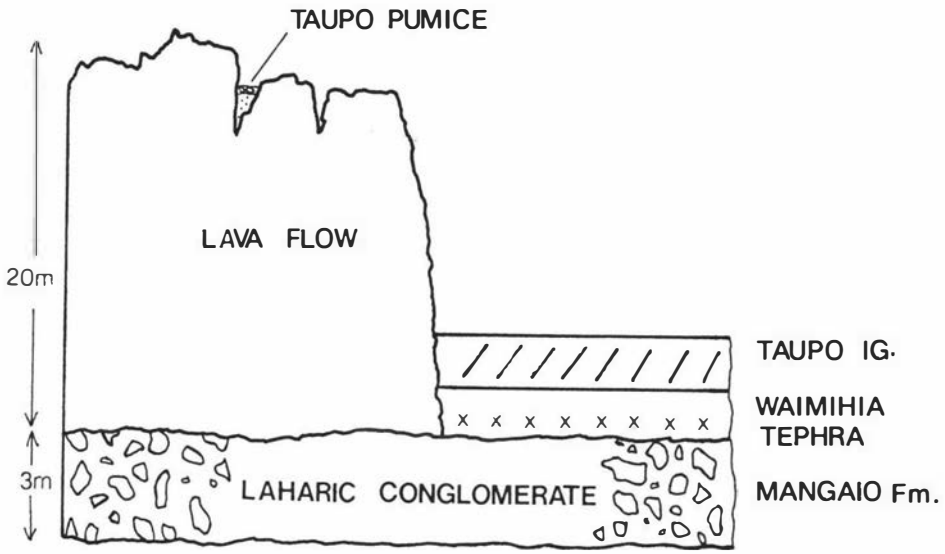

Figure 5.10 Generalised stratigraphy, upper Whangaehu River.

It is proposed that a sector collapse of the eastern flank of Mt Ruapehu led to the emplacement of the Mangaio Formation lahar deposit. It is probable that subsequent eruptions of Whakapapa Formation lavas, occurring soon after this collapse, and prior to deposition of Taupo Pumice, filled the breach created by the collapse, changing the summit configuration and vent physiography, allowing subsequent formation of Crater Lake. The inception of Crater Lake would therefore post-date the deposition of both the Mangaio Formation and the lava flow. The tephra and lahar stratigraphy of Rangipo Desert, however, shows that no lahar deposits with Onetapu Formation characteristics occur in the stratigraphic record prior to deposition of Taupo Pumice. Thus inception *c.* 1800 years B.P., rather than 4600 years B.P. is indicated.

5.5 Ring Plain Construction and Erosion

Deep gullies and valleys carved into Holocene and late Pleistocene ring plain deposits show a stratigraphy built principally from laharic deposits, capped by andesitic and rhyolitic tephras and aeolian sands.

Five laharic formations were deposited in the last *c.* 22 500 years, each of these identifying periods of ring plain construction. The Holocene-aged Onetapu, Mangaio and Manutahi formations, and the late Pleistocene to Holocene-aged Tangatu Formation, coincide with Hackett's (1985) Whakapapa Formation cone construction period. Deposition of the older Te Heuheu Formation coincides with a major period of erosion during late Mangawhero time (*c.* 25 000 – 20 000 years B.P.) (Hackett 1985).

Holocene-aged lahars have built much of the present-day southeastern Mt Ruapehu ring plain. Deposits of these lahars have in recent years been confined to the Whangaehu Fan, and areas proximal to Whangaehu River. The Whangaehu River and its tributaries continue to deposit and erode sediments across this active Fan, but over the rest of Rangipo Desert tributary channels are dry, being occupied only by ephemeral stream flow. Here, erosion and deposition is dominated by aeolian processes, with little present-day contribution of Onetapu Formation laharic sediments.

Isolated peat deposits and laminated silts of Holocene age preserved within Death Valley and the northern Rangipo Desert (in the vicinity of Bullot Track) identify areas where tributary channels had once existed but have been cut off, creating small ponds and allowing vegetation to establish. Much of this shift in the drainage network has been caused by damming or blocking of tributaries by lahars. The effect of lahars on the damming of drainage systems is best exemplified at Ngamatea Swamp where an extensive peat swamp has developed above *c.* 15 000 year old Te Heuheu Formation lahar deposits.

The Mangaio Formation debris flow which covers a large area of the southeastern Rangipo Desert was responsible for changes in the drainage network, and probable destruction of *Nothofagus* forest. Changes in drainage are indicated by the presence of a peat deposit found immediately beneath the lahar. Pollens within this peat are dominantly *Nothofagus* (99%), indicating former existence of stands of native *Nothofagus*. Branches found within the lahar deposit, together with the underlying pollen record, indicate probable destruction of *Nothofagus* forest at this time.

Bedded silts and clays of similar age found in the northern Rangipo Desert (which contain abundant *Nothofagus* leaves, and which are overlain by thick sequences of Manutahi Formation sands and gravels) record similar destruction of *Nothofagus* forest, and ponding of former drainage channels. The deposition of the Manutahi Formation, following a period of erosion, was most probably responsible for the local deforestation.

Today, *Nothofagus* forest occurs only in isolated stands within Rangipo Desert, in areas where the Holocene tephra cover has not been eroded by lahars or stream flow.

Susceptibility of Tephra and Lahar Deposits to Erosion

Tephras

The Holocene tephra cover beds within Rangipo Desert are particularly susceptible to erosion by lahars. Over much of Rangipo Desert, Taupo Ignimbrite, Mangatawai Tephra, and upper Papakai Formation have been eroded by Onetapu Formation lahars and the action of ephemeral streams. In some areas on the Whangaehu Fan, this erosion is marked by a prominent unconformity above the Mangaio Formation.

Within Rangipo Desert, poorly vegetated surfaces are also susceptible to erosion by aeolian processes. Aeolian reworked Taupo Ignimbrite and charcoal fragments derived from it are found interbedded within dune sands which cover large areas of the southern Rangipo Desert. Plate 5.26 shows an incipient dune field in the southern Rangipo Desert. Here, dune sands are accumulating on partially eroded Papakai Formation.

Within the Badlands of the western Rangipo Desert (Plate 5.19) all tephras overlying Motutere Tephra (dated *c.* 5800 years B.P.) have been eroded. Here, surfaces are devoid of vegetation and are dissected by numerous small ephemeral channels. A thin hard pan representing remnant Manutahi Formation laharic deposits covers much of the surface, inhibiting colonisation by plants, and possibly slowing the rate of erosion. Preservation of upper Papakai Formation, Mangatawai Tephra and Taupo Pumice in areas immediately west and east of here indicates the erosion of this area occurred at some time after the deposition of the Taupo Ignimbrite. Purves (1990) identified two periods of erosion within Rangipo Desert in post-Taupo Pumice time, between 1800-1500 years B.P. and a continued period since 665 years B.P.

At the margins of this area, where the stratigraphy of cover bed deposits is preserved, the Taupo Ignimbrite and older Holocene tephras are found overlain by dune sands.

The older coarse pumiceous tephras of the Bullot Formation are particularly susceptible to erosion because the physical characteristics of the lapilli inhibit colonisation by plants. The absence of paleosols or peat deposits interbedded between individual Bullot Formation tephras indicates that these surfaces have always been sparsely vegetated. Today, they remain essentially devoid of vegetation. The action of ephemeral streams, particularly in the northern Rangipo desert, has thus caused deep gullying in these tephra deposits.

Stream flow can quickly be transformed into a hyperconcentrated flood flow or debris flow event by 'bulking', *i.e.* the inclusion of bed material (Scott 1985, 1988). Eroded Bullot Formation pumice provides an ideal bulking material, and is identified as a significant component of some Manutahi Formation laharic deposits. Fine material is also eroded and transported during dust storms which frequent the region (Plate 5.27).

Lahar Deposits

The erosive nature of Onetapu Formation lahars has led to erosion of much of the pre-existing tephra cover beds, and recent lahar deposits. Many of the tributary channels of the Whangaehu Fan may have been eroded by lahars.

Over much of the Rangipo Desert, the surface is covered by lag deposits of Onetapu Formation. Much of the sandy matrix materials of these lahars have been eroded by subsequent flood events and by aeolian processes leaving a coarse bouldery remnant deposit. The greatest contribution of sand-sized material to the currently accumulating sand dunes (Makahikatoa Sands) appears to be from the loose sandy matrix materials of the Onetapu Formation lahar (DF and HFF) deposits.

The Chute

The Chute, located within Rangipo Desert is a large NW–SE trending channel, which has been cut into pre-existing Holocene and possibly late Pleistocene-aged lahars. It is approximately 5 km long, and at the northernmost end is *c.* 50 m wide and *c.* 20 m deep. The channel narrows and shallows toward its southernmost end, ranging in altitude from 1220 m a.s.l. (northern end) to 1040 m a.s.l. (southern end), and is separated from Whangaehu River by the Whangaehu Fan. It is a dry channel, occupied only by ephemeral stream flow and periodically by Onetapu Formation lahars, which have overtopped Whangaehu River at the head of the fan, and spilled into The Chute.

The Chute is a young geological feature, formed at some stage following deposition of the Mangaio Formation DF deposit, and possibly during Onetapu Formation time. Mangaio Formation is exposed along the length of the channel, where it is overlain by dark grey Onetapu Formation laharic sands. The Chute represents a lahar channel, which has been active in very recent time (Plate 5.28).

A channel of similar dimensions (Mabinit Channel) on the southeastern slopes of Mayon Volcano, in the Philippines, is described by Rodolfo (1989) as having been formed by rain lahars, associated with volcanic eruption. These lahars, both in confined and unconfined flow states (including hyperconcentrated flood flows) were able to erode the channel, generating over half of their sediment load during flow by eroding pre-existing DF and pyroclastic deposits. Avalanches in the ravine above the channel provide loose debris which can be mobilised into lahars (Rodolfo 1989).

There are distinct similarities between Mabinit Channel and The Chute. Both channels have acted as lahar routes, and have formed at the margins of pyroclastic fans. The upper reaches of the channels are straight, becoming sinuous and shallower in their lower reaches.

Avalanches within the upper Whangaehu Valley were very likely the principal source of debris for lahars of The Chute.

The most destructive lahars are those which are generated by crater collapses, or eruptions through crater lakes (Neall 1976; Arguden and Rodolfo 1990). It is therefore possible that catastrophic emptying of Crater Lake generated lahars which, while channelised, were highly erosive. These erosive lahars were able to erode a deep channel at the head of the present-day Whangaehu fan. Southward extension of this channel may have been achieved by the rigid plug-flow portions of unconfined flows (Rodolfo 1989).

Summary of Events

In Holocene time, the greatest period of erosion on the southeastern Mt Ruapehu ring plain has occurred within the last *c.* 1800 years B.P. Similar accelerated erosion within this time period was also observed by Topping (1974) on the Mt Tongariro ring plain. Much of the erosion has been attributed to the destruction of forest cover by the Taupo Ignimbrite (Topping 1973; Purves 1990), and deposition of the Onetapu Formation lahars. The lahars have been identified by Purves (1990) as the major contributing cause of the destruction of the pre-existing vegetation of Rangipo Desert within the last *c.* 1800 years B.P. The role of pre-European and early European fires, and climate, has had a lesser effect on erosion and vegetation patterns (Purves 1990). The deposition of the Mangaio and Manutahi formations also appear closely associated with destruction of pre-existing *Nothofagus* forest. Stream flow and aeolian processes have also contributed to the erosion during this time.

A summary of constructional and erosional events on the southeastern Mt Ruapehu ring plain is as follows:

Period 1: *c.* 22 500 – 14 700 years B.P.

- Widespread deposition of Te Heuheu Formation laharic sands and gravels, with sediments derived from erosion of the flanks of Mt Ruapehu volcano.
- Ring plain aggradation in response to the introduction of large volumes of pyroclastic material (Bullot Formation tephras) and glaciofluvial sediments.
- Subsequent erosion of some Bullot Formation tephras.
- Uplift east of the Whangaehu fault.

Period 2: *c.* 14 700 – 5800 years B.P.

- Major period of ring plain aggradation due to the deposition of the middle and upper Bullot Formation tephras.
- Widespread deposition of Tangatu Formation HFF and DF deposits, resulting from erosion of the flanks of Mt Ruapehu volcano.

Period 3: *c.* 5800 – 1800 years B.P.

- Deposition of the Mangaio Formation debris flow, and Manutahi Formation laharic sands and gravels, resulting from erosion of both the flanks of Mt Ruapehu volcano, and pre-existing ring plain deposits.
- Localised erosion of Bullot Formation tephras. Destruction of Nothofagus forest.

Period 4: *c.* 1800 years B.P. to present

- Deposition of Tufa Trig Formation tephras, and contemporaneous deposition of Onetapu Formation laharic sands and gravels. Aggradation by Onetapu Formation lahars and construction of the Whangaehu Fan.
- Accumulation of aeolian Makahikatoa Sands in relatively stable areas of the Rangipo Desert.
- Erosion of Holocene tephra cover beds over much of the Rangipo Desert and partial erosion of laharic deposits by subsequent lahars and stream flow events. Accelerated erosion in the western Rangipo Desert led to formation of the Badlands.

CHAPTER SIX
VOLCANIC HAZARD

Introduction

Volcanic activity can generate many phenomena potentially hazardous to life and property – including tephra, gas emissions, lava flows and domes, pyroclastic flows, pyroclastic surges, debris avalanches and lahars.

Most tephra eruptions at strato-volcanoes such as Mt Ruapehu, produce moderate amounts of ash, which may be dispersed over relatively large areas. In the immediate fall-out area, tephra may be extremely hazardous to life and property, but the affects decrease markedly downwind. The magnitude of destruction is generally less than that of rhyolitic eruptions.

Lava flows are usually restricted to summit and flank areas and generally pose little threat to life (Crandell and Mullineaux 1967, 1978).

Lahars (debris flows and hyperconcentrated flood flows) are particularly common phenomena at strato-volcanoes world wide (*e.g.* Mt Egmont [Neall 1972, 1976]; Mt Rainier [Crandell and Mullineaux 1967; Crandell 1971]; Mt St Helens [Crandell and Mullineaux 1978; Siebert *et al.* 1987]; Mt Shasta [Miller 1980]; Mt Kelut, Java [Zen 1965; Williams and M^{c}Birney 1979]; Nevado del Ruiz, Colombia [Lowe *et al.* 1986]; Mayon Volcano, Philippines [Rodolfo 1989]) [1]. The predisposition of strato-volcanoes to debris avalanches and lahars is largely attributable to their typically steep slopes, unconsolidated and weakened flank deposits, and the presence of summit crater lakes (Schuster and Crandell 1984). Lahars are destructive events, and represent the greatest hazard to life at many of these volcanoes because of their frequency and ability to travel large distances (Crandell and Mullineaux 1967; Crandell 1971). Historically, lahars have claimed many thousands of lives. A lahar generated during the 1985 eruption of Nevado del Ruiz, Colombia, killed 25 000 people (Clapperton 1986; Lowe *et al.* 1986; M^{c}Dowell 1986), and more than 5000 people were killed by hot lahars at Mt Kelut in 1919 (Zen 1965; Williams and M^{c}Birney 1979). In New Zealand 215 people have died as a result of lahars within the last 150 years (Houghton *et al.* 1988) – 151 in the 1953 Tangiwai railway disaster.

While the absence of any large population base in the immediate vicinity of Mt Ruapehu restricts the potential for loss of life of the proportions encountered at Nevado del Ruiz, the region is subject to a large transient ski population, which frequents areas at greatest risk from future lahars and tephra eruptions. At risk also are regional towns (Waiouru, Ohakune,

---

[1] A comprehensive account of the global occurrence of lahars is given in Neall (1976).

National Park, and possibly Turangi [2]), the principal North Island transport and communication routes (Desert Road, main trunk railway), and recent capital-intensive developments in forestry and hydroelectric power (Figure 6.1, p. 292; Figure 6.2, p. 293).

Hazard Assessment

Past records of eruptions provide the best basis for anticipating probable future eruptive behaviour and the associated volcanic hazard. Future eruptions are likely to be of similar frequency and magnitude as events which have occurred in the past (Crandell and Mullineaux 1978; Miller *et al.* 1981), although 'catastrophic eruptions can exceed any known precedent at the same volcano' (Miller *et al.* 1981), *e.g.* the directed blast of the 18 May, 1980 Mt St Helens eruption.

The historical record of eruptions at Mt Ruapehu dates back only to 1861 A.D. and provides limited information on the types of eruptions and hazards which have occurred at this volcano.

Previous Work

In recent years, the volcanic hazard at Mt Ruapehu has been addressed by many workers (Healy 1978; Cole and Nairn 1979; Latter 1985; Hackett and Houghton 1986; Houghton *et al.* 1987), with hazard assessment based on the historic eruption records (1861 A.D. to the present day).

In this study, an assessment of the types of volcanic hazard at Mt Ruapehu is based on the stratigraphy, chronology, and distribution of tephra and lahar events of the past *c.* 22 500 years; a much greater record of events than previously available.

6.1 Products of Eruptions and Associated Hazard

Eruptions at Mt Ruapehu during the last *c.* 22 500 years have produced lava flows, lava domes, tephras, pyroclastic flows, volcanic debris avalanches, debris flows and hyperconcentrated flood flows. Magmatic eruptions have involved basaltic, andesitic and dacitic magmas.

---

[2] 1986 N.Z. census gives population figures: Ohakune Borough (1496), Raetihi Borough (1323) [total Waimarino County (4252)], Waiouru Township (3318), and Turangi District Community (3913).

Figure 6.1 Major features at risk from future lahars and tephra eruptions at Ruapehu Volcano.

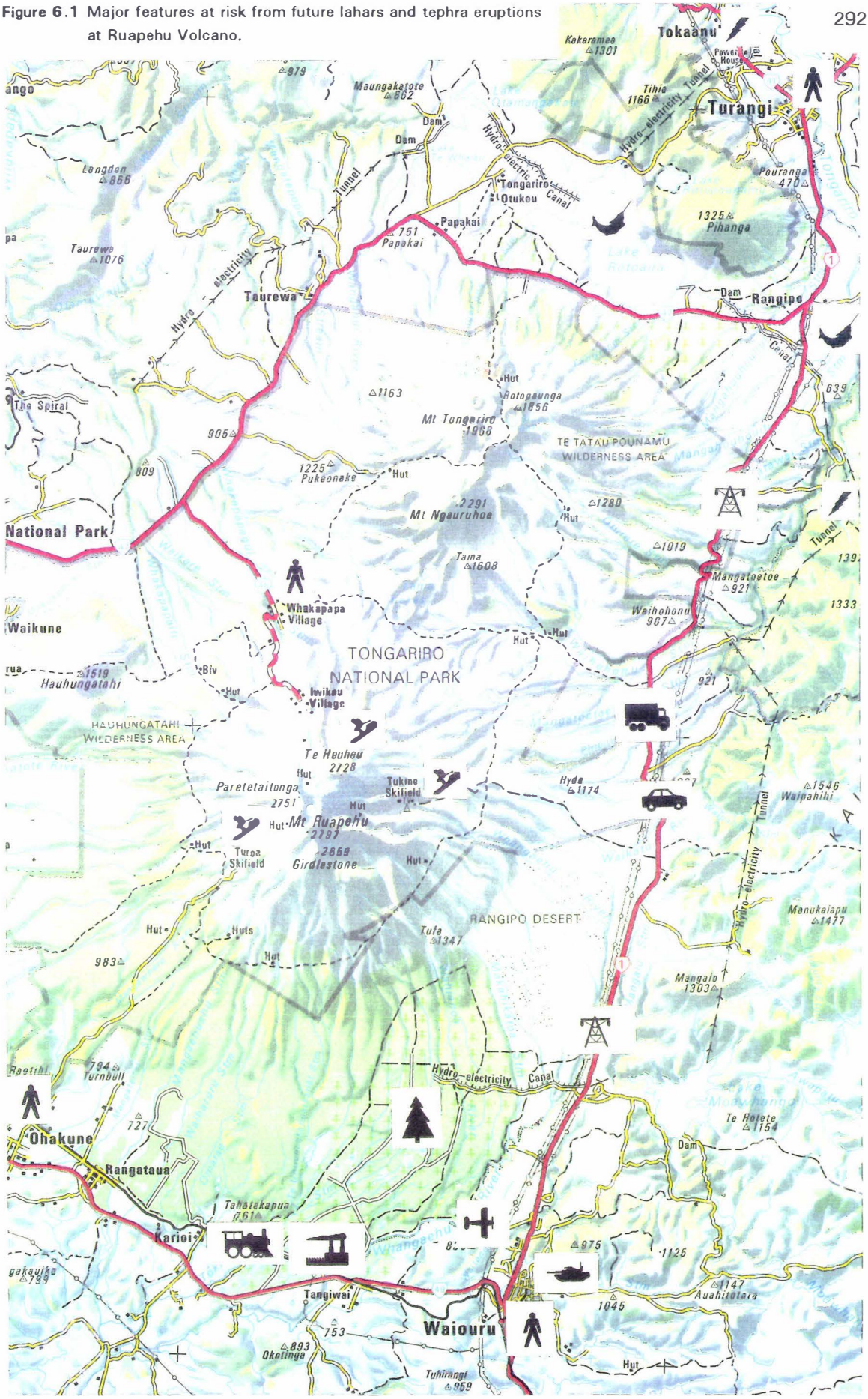

Figure 6.2
Tongariro Power Development showing the Western and Moawhango diversions and the Tokaanu and Rangipo projects. Installations of the Western and Moawhango diversions were damaged by lahars generated during the 1975 eruption at Mt Ruapehu *(see text)*.

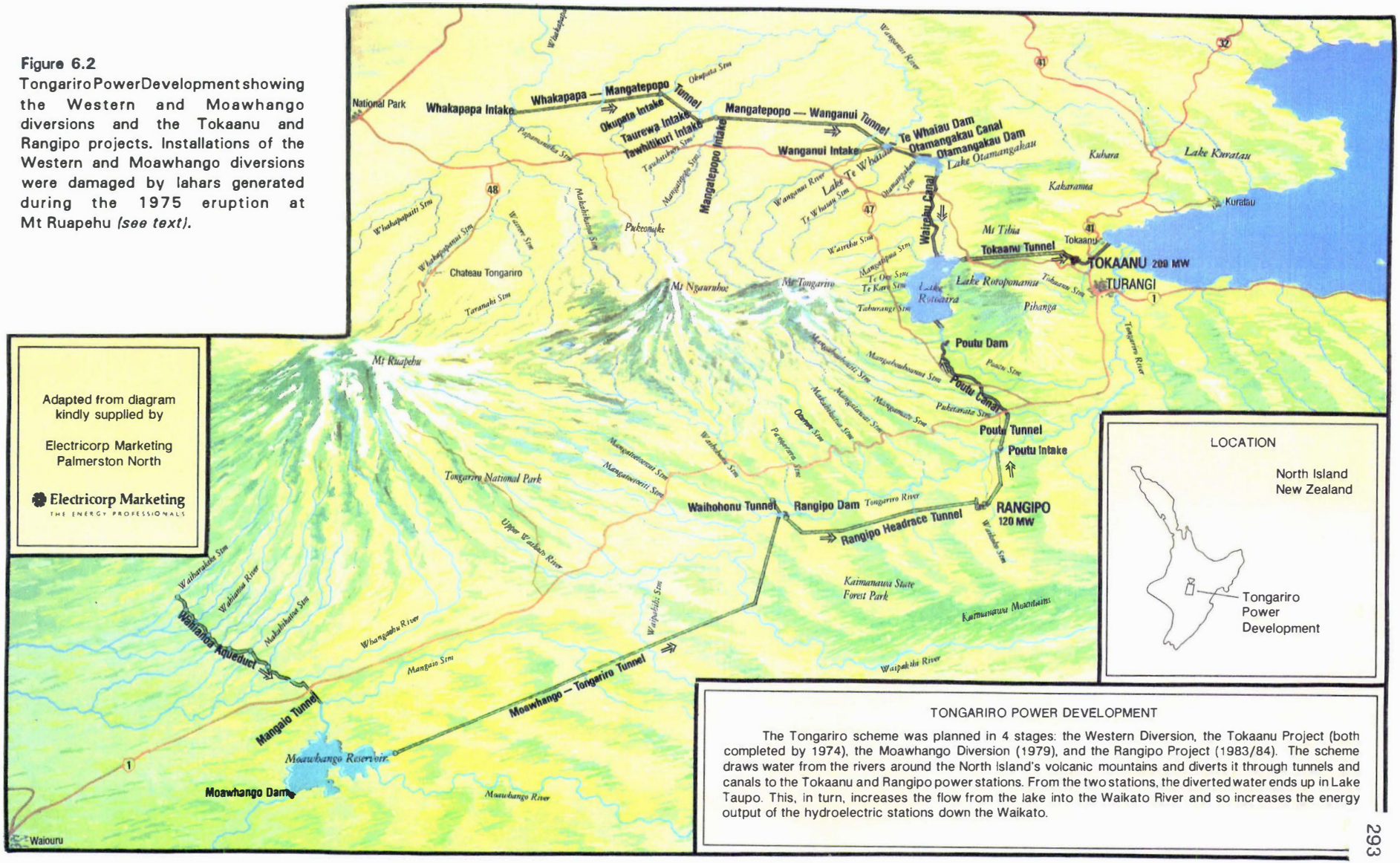

TONGARIRO POWER DEVELOPMENT

The Tongariro scheme was planned in 4 stages: the Western Diversion, the Tokaanu Project (both completed by 1974), the Moawhango Diversion (1979), and the Rangipo Project (1983/84). The scheme draws water from the rivers around the North Island's volcanic mountains and diverts it through tunnels and canals to the Tokaanu and Rangipo power stations. From the two stations, the diverted water ends up in Lake Taupo. This, in turn, increases the flow from the lake into the Waikato River and so increases the energy output of the hydroelectric stations down the Waikato.

Hazard Zones

Hazard zones depict areas that are at risk from future eruptions of a given type, frequency, and severity (Crandell and Mullineaux 1978). Hazard zones delineated for tephras (Figure 6.3, p. 297) and lahars (Figure 6.4, p. 303) on the southeastern Mt Ruapehu ring plain are defined following the principles of Crandell and Mullineaux (1978), and Miller (1980). Potential hazard is greatest in zone 1, and progressively less in consecutively numbered zones.

Hazard from Tephra Eruptions

Tephras have been erupted at Mt Ruapehu intermittently throughout the last *c.* 22 500 years. The most complete tephra record is found east of the volcano where tephras have been deposited by prevailing westerly and northwesterly winds. The tephrostratigraphy on the southeastern ring plain reveals no catastrophic tephra eruptions within this time period. Okupata Tephra (dated between *c.* 13 000 – 10 000 years B.P.) very probably represents the largest tephra eruption of this time. It is however dispersed to the north of Mt Ruapehu (Topping 1973) and therefore is not identified on the southeastern ring plain. The volume of the basal lapilli of Okupata Tephra is estimated at *c.* 0.2 km^3 (Topping 1973).

Frequent tephra eruptions occurred between *c.* 22 500 and 10 000 years B.P.). The deposits of these are mapped as the Bullot Formation. In the study area the formation comprises approximately 60 ash and lapilli layers, deposited over about 12 500 years, and representing an average periodicity of one eruption every *c.* 200 years. The maximum thickness of individual tephra layers is about 0.30 m, and the total formation thickness is *c.* 11 m. Few of these tephras were deposited to the south and north, where thicknesses are generally less than *c.* 0.10 m. The most explosive eruptions of this time were probably those associated with the eruption of the tephra and ignimbrite units of Pourahu Member. Most of the tephras appear to be the products of subplinian eruptions of andesitic magma, with less than 500 $x10^6$ m^3 of tephra produced in each eruption (Table 6.1, p. 295). By comparison with tephra eruptions at Mt Tongariro, those at Mt Ruapehu (excluding Okupata Tephra) have been small events. Volumes calculated for the Te Rato Lapilli and Poutu Lapilli members of Mangamate Tephra, and Rotoaira Lapilli, are ~ 100 $x10^6$ m^3, ~ 900 $x10^6$ m^3, and ≥ 200 $x10^6$ m^3 respectively (Topping 1973).

Few tephras were erupted from Mt Ruapehu between *c.* 10 000-1800 years B.P. They occur as thin lapilli and ash layers within Papakai Formation (dated *c.* 9780-2500 years B.P.).

The younger Tufa Trig Formation tephras, erupted between *c.* 1800 years B.P. and the present, are the products of relatively small hydrovolcanic (phreatomagmatic) eruptions which may have involved the explosive disruption of summit domes (tholoids). They show restricted dispersal, being confined mostly to within a few kilometres east of the vent, where most

Table 6.1 Estimates of volume for some Tongariro Volcanic Centre tephras (to nearest calculated 10 $x10^6$ m^3).

Formation : Member	(Source)	Volume Estimate (m^3) [circle *]	Volume Estimate (m^3) [ellipse *]	Volume Estimate (m^3) [Topping 1973]
Tufa Trig Formation				
: Member Tf8	(Ruapehu)	100 $x10^6$	50 $x10^6$	
: Member Tf6	(Ruapehu)	100 $x10^6$	30 $x10^6$	
: Member Tf5	(Ruapehu)	270 $x10^6$	90 $x10^6$	
: Member Tf4	(Ruapehu)	60 $x10^6$	20 $x10^6$	
Mangatawai Tephra	(Ngauruhoe)	1450 $x10^6$		
Mangamate Tephra				
: Poutu Lapilli	(Tongariro)	1070 $x10^6$		~900 $x10^6$ [a]
: Wharepu Tephra	(Tongariro)	1410 $x10^6$	360 $x10^6$	
: Waihohonu Lapilli	(Tongariro)	2000 $x10^6$	490 $x10^6$	
: Oturere Lapilli	(Tongariro)	1480 $x10^6$	370 $x10^6$	
: Te Rato Lapilli	(Tongariro)			~100 $x10^6$ [a]
Pahoka Tephra	(Tongariro)	970 $x10^6$	250 $x10^6$	
Okupata Tephra	(Ruapehu)			~200 $x10^6$ [a]
Bullot Formation				
: Pourahu Member	(Ruapehu)	700 $x10^6$	90 $x10^6$	
Rotoaira Lapilli	(Tongariro)			≥200 $x10^6$ [a,b]

* Volume $= 2\pi T_0 \sigma / (k_a)^2$ ($= 13.08 T_0 (a_{½})^2 \sigma$); where:
T_0 = extrapolated thickness of tephra at isopach centre (assumed point of maximum thickness and source);
$a_{½}$ = half thickness distance along major axis;
σ = isopach "ellipticity" (minor axis/major axis) [for a circle $\sigma = 1$];
k_a = thickness decay constant along major axis (slope on log(thickness) – distance plot).
In elliptical calculations the point of maximum tephra thickness (tephra source) is assumed to be at ellipse centre and not at a focus.
Discussion of tephra volume formulae can be found in Froggatt (1982b) and Pyle (1989).

[a] Volumes calculated by $13.08 T_0 (a_{½})^2$ (circular isopach assumption). For calculation purposes and to allow use of formula with circular isopach assumption, asymmetrical distribution patterns were approximated by circles giving same area as that enclosed by the true isopachs.
[b] Volume estimate of the basal lapilli.

tephra thicknesses are less than *c.* 0.10 m. The largest and thickest of these tephras is member Tf5, which is recognised 24 km northeast of the source area, and which has a volume of ~90 $x10^6$ m^3. The average periodicity of eruptions in this period is one every 100 years.

The most recent eruptions (within the last 130 years) have been dominated by phreatomagmatic activity and emplacement of lava domes. Many of these eruptions have been small and have left no visible deposits. The larger eruptions are characterised by ballistic clasts (blocks of old lava and lake sediments), pumice, ash, and surge deposits, with dispersal of these restricted mostly to the near vent areas (Nairn *et al.* 1979; Hackett and Houghton 1989). During this period, Mt Ruapehu has erupted, on average, at least once every 2.5 years (Latter 1985) [3].

[3] Detailed records of historical eruptions at Mt Ruapehu (from 1861 to 1986) are found in Gregg (1960a), Cole and Nairn (1975), Healy *et al.* (1978) and Houghton *et al.* (1987).

The style and magnitude of future tephra eruptions at Mt Ruapehu will be strongly controlled by the presence of Crater Lake, which occupies the only currently active vent. Eruptions will very probably be phreatomagmatic, with small tephra volumes ($< 100 \times 10^6$ m^3) and dispersal areas. The hazard presented by these tephra eruptions in areas beyond the immediate fall-out zone is small.

Tephra Hazard Zones

Based on the thickness – distribution of tephras erupted within the last *c.* 22 500 years, three hazard zones are defined. Risk does not change abruptly at the boundaries between zones but should be regarded as gradational. In defining these zones, the assumption is made that tephras will most often be dispersed east of the volcano under the influence of the prevailing winds.

Zone 1 Identifies the area at greatest risk from future subplinian, phreatomagmatic and strombolian eruptions. Future eruptions will affect this zone more frequently than any other area. Phreatomagmatic eruptions could be expected to occur every 2.5 years, with tephra thicknesses likely to be > *c.* 0.10 m. Subplinian eruptions could be expected every *c.* 200 years, with tephra thicknesses likely to be > 0.30 m.

Zone 2 Identifies areas at intermediate risk (affected less frequently) from future subplinian, phreatomagmatic and strombolian eruptions. Phreatomagmatic eruptions could occur every *c.* 100 years, with tephra thicknesses < 0.10 m. Damaging subplinian eruptions could be expected every *c.* 200 years, with tephra thicknesses likely to be between 0.30 and 0.15 m thick, and decreasing in thickness downwind. This area is also at risk from tephras erupted from Mt Tongariro and Mt Ngauruhoe.

Zone 3 Identifies areas of relatively low risk from subplinian, phreatomagmatic and strombolian eruptions. This area would be affected by infrequent eruptions of tephra (return period > *c.* 200 years) depositing thin layers (< *c.* 0.15 m) of ash and lapilli.

Indirect Effects of Ash Eruptions

In areas downwind of an erupting volcano, both the physical and chemical properties of volcanic ash present a hazard to: human health, resulting from injury to respiratory systems; water supplies and aquatic life, due to increased sediment loading and possible chemical contamination of lakes, rivers and streams, including also residential water supplies (Paterson 1972, 1976; Collins 1978); vegetation and livestock, resulting from both the physical injury to crops and pastures and burial by thick accumulations of ash;

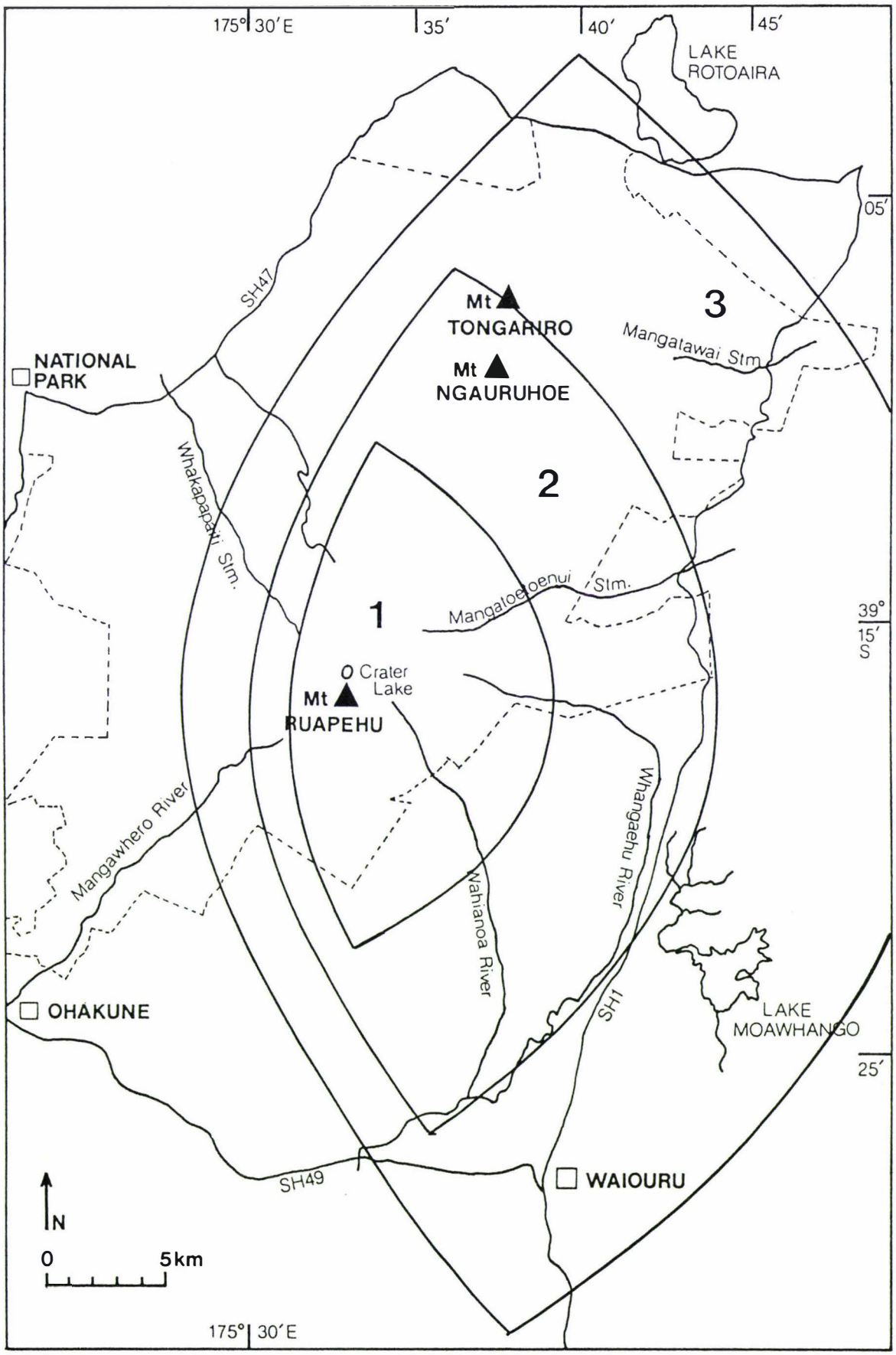

Figure 6.3 Tephra hazard zones. Risk from future tephra eruptions at Mt Ruapehu is greatest in zone 1, and progressively less in zones 2 and 3 (see text).

communications, resulting from the disruption to radio and telephone communication, and electrical services *e.g.* overhead power cables; transport services (including aircraft), due to wear and corrosion of vehicle machinery; and buildings which may collapse under the weight of accumulating ash (Miller 1980; Crandell and Nichols 1989).

Hazard from Lahars

Lahars at Mt Ruapehu have been generated principally by large scale slope failure of parts of the volcanic edifice, and ejection of crater lake waters.

Frequency and Magnitude

Lahars have been generated at Mt Ruapehu over at least the last *c.* 22 500 years. The oldest deposits mapped in this study (Te Heuheu Formation) are of late Pleistocene age. They are the most extensive and form the major constructional surfaces of the southeastern Mt Ruapehu region. They most probably represent major sector collapses of the eastern and southern flanks of the volcano.

Numerous lahar events are also recorded within the last 14 700 years, with distributions largely restricted to within Rangipo Desert and the Whangaehu River. The oldest of these deposited the Tangatu Formation which, within the study area, has an estimated volume of *c.* 94 $x10^6$ m^3. The Formation accumulated over a period of *c.* 9300 years, with at least 24 recorded events (14 of these are preserved at the type section and ten at Helwan Quarry R.S.; Chart 4) indicating a minimum average periodicity of one event every *c.* 388 years.

Less frequent events occurred between *c.* 5370 and 3400 years B.P., and are represented by the Manutahi and Mangaio formations. Laharic sands and gravels of the Manutahi Formation appear to have been deposited by numerous widespread flood events over a period of *c.* 1900 years. The Mangaio Formation, deposited *c.* 4600 years B.P. following a sector collapse in hydrothermally altered flank deposits, very probably represents the largest single event of Holocene age. This formation has an estimated volume of 34 $x10^6$ m^3.

The Onetapu Formation (dated at *c.* 1800 years B.P. to present) represents the most recent and active period of lahar deposition during the Holocene. Although an absolute stratigraphy and chronology of Onetapu Formation deposits is yet to be established, current work (this thesis; Purves 1990) indicates the formation is represented by numerous events which have spilled over the lower ring plain. The volume of Onetapu Formation lahar deposits preserved within the study area is estimated to be 36 $x10^6$ m^3.

Within Onetapu Formation, at least seven major lahar events within the Whangaehu Valley are recorded in the Holocene stratigraphy at Tangiwai Swamp. Four of these events

are radiocarbon dated at >*c.* 450, *c.* 450, *c.* 450-280, and <*c.* 282 years B.P. Two lahar events recorded by Campbell (1973) in the lower Whangaehu Valley are dated at 756 ± 56 and 407 ± 70 years B.P. The average periodicity of lahars within Whangaehu Valley during the last 1800 years, as indicated at Tangiwai Swamp is at least one every *c.* 250 years. The frequency of these events has increased markedly in historical times (last 130 years). Published records of eruptions at Mt Ruapehu date between 1861 and 1986, with lahars recorded in 1861, 1889, 1895, 1903, 1925, 1953, 1969, 1971, 1975 and 1977. The most recent lahar occurred on 8 December, 1988. Most of these have occurred within the Whangaehu Valley. The average periodicity of lahars in historical time is approximately one event every 11 years. Volume estimates of some of these events are given in Page and Paterson (1976), Houghton *et al.* (1987), Purves (1990), and Vignaux and Weir (1990).

Historically, lahars have presented the greatest hazard to life and property in the southeastern Mt Ruapehu region. Three events occurring in 1953, 1969 and 1975 are historically significant.

The 1953 Tangiwai Disaster

In March – July 1945, lava rose under Crater Lake, displacing the lake waters into the Whangaehu Valley. The crater was subsequently filled by a lava dome, originating from explosive eruptions. The dome was later destroyed by further eruptive activity, and a 100 m wide, 400 m deep crater formed. Ash from the eruptions built a barrier at the outlet of Crater Lake, allowing the new lake which formed in the vent to rise eight metres above its former level. On the 24th December 1953, crevassing movements in the ice of Whangaehu Glacier caused the collapse of the retaining ash barrier, and Crater Lake waters were subsequently released into the Whangaehu Valley. A large lahar (*c.* 1.9 $x10^6$ m^3, Houghton *et al.* 1987) formed, and swept down the Whangaehu River, damaging the piers of the Tangiwai rail bridge. The Wellington – Auckland express train was derailed as it crossed the damaged bridge and plunged into the Whangaehu River. As a result, 151 lives were lost (Healy 1954; O'Shea 1954; Gregg 1960a).

The 22 June 1969 Eruption

The phreatomagmatic eruption of June 1969 was the largest since the eruption in 1945. It was characterised by tephra and base surge eruptions from Crater Lake, and the generation of lahars down four major valleys - Whakapapanui, Whakapapaiti, Mangaturuturu and Whangaehu. Lahars within the Whakapapaiti and Whakapapanui valleys had a total volume of ~0.12 $x10^6$ m^3, and those in the Mangaturuturu and Whangaehu valleys were ~0.02 $x10^6$ m^3 and ~0.07 $x10^6$ m^3 respectively (Houghton *et al.* 1987). Southeasterly winds carried much of the tephra toward Whakapapa Village. Water erupted from Crater Lake, and snow and debris from the summit area were the sources of the lahars. The level of Crater Lake fell by *c.* 2 m (Nairn *et al.* 1979).

Dome Shelter on the Summit Plateau was destroyed by a strong lateral blast associated with the eruptions (Cole *et al.* 1986), but the resulting lahars presented the greatest hazard. The Whakapapanui lahar swept down the northern slopes of Mt Ruapehu, and damaged installations at Iwikau Village, terminating only 3.5 km above Whakapapa Village. Both villages support a large ski population during winter months, with up to 8000 people a day at Whakapapa Skifield. Had the eruption occurred during the day, or during the peak of the ski season (August – September) many lives could have been lost (Healy *et al.* 1978; Cole and Nairn 1975).

The 24 April 1975 Eruption

The April 1975 phreatomagmatic eruption was the largest of the historical eruptions recorded at Mt Ruapehu. The eruption was characterised by tephra and base surge eruptions from Crater Lake, generation of lahars down the Whakapapanui, Whakapapaiti, Mangaturuturu and Whangaehu Valleys, and mudflow deposits on summit glaciers. The Crater Lake level fell by 8 m (*cf.* 2 m in the 1969 eruption), with an estimated net 1.6 $x10^6$ m^3 of water ejected [4] (Nairn *et al.* 1979). Lahars within the Whakapapaiti and Whakapapanui valleys had a total volume of ~0.9 $x10^6$ m^3, and those in the Mangaturuturu and Whangaehu valleys ~0.6 $x10^6$ m^3 and ~1.8 $x10^6$ m^3 respectively (Nairn *et al.* 1979; Houghton *et al.* 1987). Tephra was dispersed 115 km to the southeast by prevailing winds (Houghton *et al.* 1987).

As in the 1969 eruption, the greatest hazard was from the lahars, which damaged bridges, installations at Iwikau Village (as had occurred in the 1969 eruption, Mazey [1978]; Traill [1978]) and hydroelectric power scheme constructions (associated with development of the Wahianoa aqueduct), and severely contaminated the Manganui-a-te-ao and Wanganui rivers killing fish life. Most of the ejected Crater Lake water was channelled down Whangaehu River. Large amounts of laharic debris from this event filled the Wahianoa Aqueduct and Mangaio Tunnel which were under construction as part of the Tongariro Power Development Scheme. Contaminated water and debris entered the Mangaio Stream and Moawhango River via the aqueduct. The lahar struck shortly after construction workers had vacated the tunnel. Debris and contaminated water also flowed into the western diversion of the power scheme, depositing silt in tunnels and canals, and contaminating lakes (Paterson 1976; Nairn *et al.* 1979).

Future eruptions at Mt Ruapehu will very probably produce lahars within the Whangaehu, Mangaturuturu, Whakapapaiti and Whakapapanui valleys. Most of the water ejected from Crater Lake, however, flows into the Whangaehu Valley because of the proximity of its headwaters to the Crater Lake outlet, thus establishing the Whangaehu River as the principal lahar route on Mt Ruapehu.

---

[4] This represents about 23% of the total lake volume (7 $x10^6$ m^3) as measured in 1970 (Nairn *et al.* 1979).

Lahars within the Whangaehu Valley produced by phreatomagmatic eruptions can be expected to be of similar magnitude to past events. Most deposition from these lahars will occur proximal to Whangaehu River in areas of relatively unconfined flow (*e.g.* on the Whangaehu Fan), and downstream at Tangiwai. Paterson (1976) and Nairn *et al.* (1979) suggest that future eruptions could eject considerably more lake water than was ejected in the 1975 eruption. It is possible that more than half of the total lake volume could be displaced, generating lahars with twice the volume of the 1975 lahars (Paterson 1976).

Lahars occurring within the Whangaehu and Whakapapanui valleys represent the greatest hazard to life and property. Three events, in 1895, 1969 and 1975 produced lahars on the northern slopes. The deposits of debris avalanches (*e.g.* Murimotu Formation, Palmer and Neall 1989) have also inundated areas northwest of the volcano. Murimotu Formation (dated *c.* 9540 years B.P.) covers *c.* 23 km^2, and has a volume of ~200 $x10^6$ m^3 (Palmer and Neall 1989).

The magnitude and dispersal of lahars generated by sector collapses induced either by volcanic eruptions, or failure not associated with eruption (*e.g.* sudden collapse of the southeast wall impounding Crater Lake), are difficult to predict. The lahars may be of small volume with localised distribution, or much larger catastrophic events. Areas of weakened hydrothermally altered flank materials represent areas most likely to collapse in future eruptions (Boudon *et al.* 1987).

On occasions, prior to uplift east of the Whangaehu River and formation of the Whangaehu escarpment, large magnitude lahars generated by collapse of the volcanic edifice reached Waiouru. Although the township is topographically isolated from present-day lahar routes, a breach of the southern margin of Rangipo Desert by lahars within Whangaehu River, immediately south of Wahianoa Aqueduct (breach B: Figure 6.4, p. 303; Figure 6.5, p. 304) would provide access toward Waiouru (*e.g.* as occurred with Tangatu Formation lahars). At this point future lahars could spill over the Desert Road and become channelled down Waitangi Stream. A breach of the Rangipo Desert at more northern sites by Whangaehu River, is prevented by the Whangaehu escarpment (Figure 6.5c,d).

Rapid aggradation of the Whangaehu Fan, following large scale sector collapse and deposition by debris avalanches and lahars, or future movements along the Whangaehu fault, could potentially alter the course of the Whangaehu River across the fan. Migration of Whangaehu River to the north could result in it being captured by Waikato Stream (breach A: Figure 6.4, p. 303). Such capture would have serious implications for lahar hazard downstream of the Waikato and Tongariro rivers. A lahar of any magnitude would pose a major threat the Tongariro Power Scheme, and in large events to Turangi township. Discharge of acidic Whangaehu water into the Tongariro River catchment would adversely affect its use for power generation (corrosion) and recreation (depleted fish stocks). The distribution of Onetapu Formation laharic deposits to the north of Whangaehu River is shown in Map 2,

indicating that small volumes of material possibly have been channelled into Waikato River in the past.

Lahar Hazard Zones

Based on the distribution of past lahar events, 4 hazard zones are defined. Risk does not change abruptly at the boundaries of zones 1, 2 and 3, but should be regarded as gradational.

Zone 1 Identifies the zone of immediate and high risk from lahars and debris avalanches. Lahars will occur most frequently within this zone. Here a return period of approximately one event every 11 years is estimated. This area has been repeatedly inundated by lahars of Whangaehu River over the last *c.* 1800 years. This zone includes most of Rangipo Desert, Whangaehu River, and low lying areas to the south at Tangiwai.

Zone 2 Identifies areas of intermediate risk from lahars of Whangaehu River. Lahars have spilled onto these areas less frequently within the last 1800 years. This zone includes the western margin of Rangipo Desert.

Zone 3 Identifies areas of low risk from infrequent, but high magnitude events, generated principally by sector collapses of the volcanic edifice. Lahars are likely to cover broad areas within this zone, at infrequent intervals, with probable return periods of >2000 years.

Zone 4 Identifies areas at very low risk from lahars, resulting from their elevation above frequently inundated laharic surfaces, *e.g.* the Whangaehu escarpment and Waiouru.

Hazard from Lavas

Lava flows (block flows and autoclastic breccias) are principally confined to flank and summit areas of the volcanic edifice (central and flank vent, and proximal cone-building associations), forming only a minor component of the distal ring plain deposits. Lavas of basaltic and dacitic compositions are identified (Hackett 1985).

The youngest lava flows belong to the Holocene-aged Whakapapa Formation of Hackett (1985), dated between *c.* 15 000 years B.P. and the present. They were erupted from at least six vents, including Crater Lake (Hackett 1985). The most extensive of these is the Rangataua Lava Flow which extends in a well defined lobe *c.* 4 km wide and 14 km from its vent, over the southern ring plain. No quantitative age estimate has been determined for this

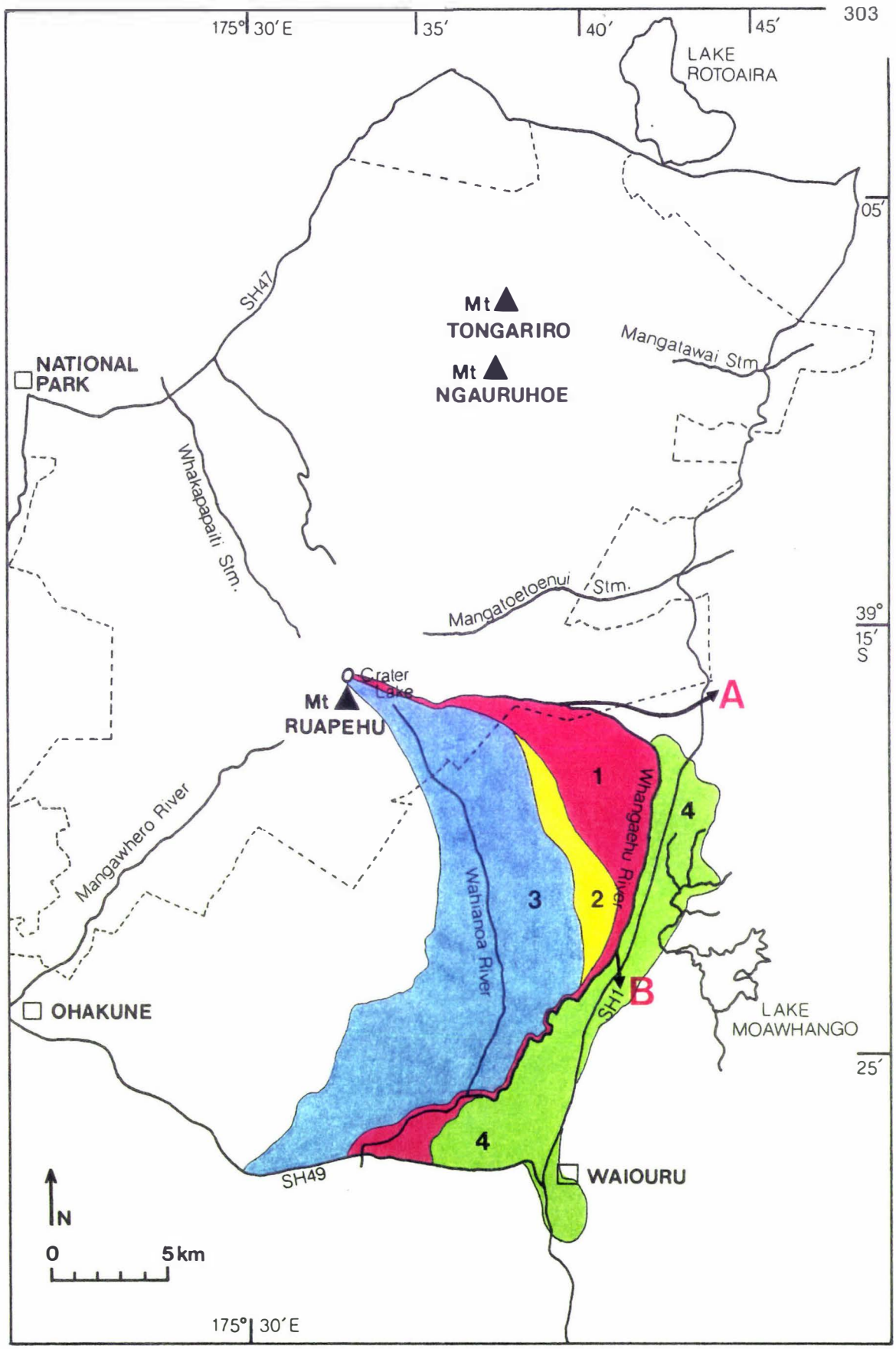

Figure 6.4 Lahar hazard zones defined for the southeastern Mt Ruapehu ring plain. Risk from future lahars at Ruapehu Volcano is greatest in zone 1, and progressively less in zones 2, 3 and 4. A and B indicate possible breach points of future lahars *(see text)*.

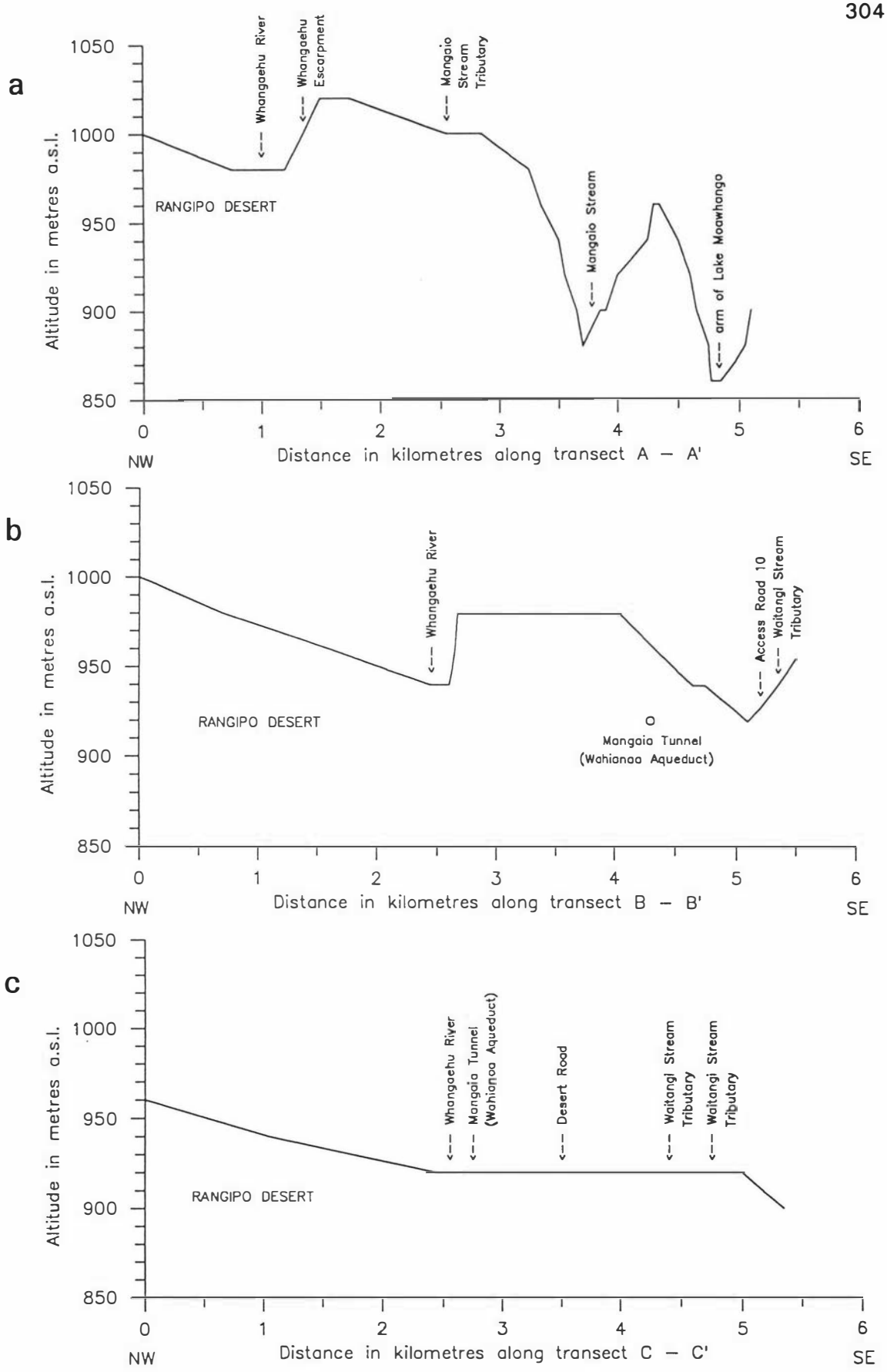

Figure 6.5 Profiles along transects across the southeastern margin of Rangipo Desert *(see Map 1)*. Possible breach point by future Whangaehu River lahars (Fig. 6.5c) occurs south of Wahianoa Aqueduct *(see text)*.

flow (Hackett 1985), although estimated ages, cited in the newsletter of the Geological Society of N.Z. [5] and Latter *et al.* (1981), range between 20 000 and 2000 years B.P. The stratigraphy of tephra deposits found overlying the margins of the flow immediately west of Karioi Forest indicate it is likely to be older than the Waiohau Tephra, dated at *c.* 11 250 years B.P., and younger than the Te Heuheu Formation surface (dated between *c.* 14 700 and >22 500 years B.P.) which underlies the southeastern Mt Ruapehu region.

The lava flows present little hazard to life since they are slow moving and their courses can often be predicted. Future flows will probably not extend far beyond the base of the volcano, however, renewed activity at the Whakapapa vent could threaten Iwikau and Whakapapa villages on the northern slopes. The autobreccias can be readily mobilised into hot pyroclastic avalanches, and therefore represent a greater hazard in this area (Houghton *et al.* 1987).

Small townships (*e.g.* Karioi, Tangiwai, Ohakune) are potentially at risk from flank eruptions producing lava flows of similar magnitude to the Rangataua Lava Flow.

Hazard from Pyroclastic Flows

Pyroclastic flows comprise a very small proportion of the deposits found on the southeastern Mt Ruapehu ring plain. Only a few pyroclastic flow deposits have been identified in the pre-historic record. Hackett (1985) identified small volume flows within the Iwikau and Rangataua members of Whakapapa Formation. In this study, Pourahu Member contains the only ignimbrite unit identified on the southeastern ring plain. This pyroclastic flow appears to have been directed down tributary channels south of Whangaehu River within Rangipo Desert, and Mangatoetoenui Valley.

Future eruptions involving mixed magmas may generate pyroclastic flows. Such eruptions would undoubtedly be accompanied by lahars.

6.2 Discussion

Examination of the types and ages of deposits preserved on the Mt Ruapehu ring plain provides a basis for the interpretation of eruption styles and magnitudes and therefore the potential hazard from future eruptions. On the southeastern Mt Ruapehu ring plain, lahar and tephra deposits dominate the stratigraphic record of the past 22 500 years. These events represent the greatest hazard to the southeastern Mt Ruapehu region in future eruptions.

At present there is no method for precisely determining when an eruption will next occur at Mt Ruapehu. Based on the present frequency of eruptions, however, small

---

[5] *Tongariro National Park Enlarged* anonymous article in October 1984 edition, p. 51.

magnitude phreatomagmatic events can be expected every few years and much larger events every *c.* 100 years. Most of these events will probably generate lahars, at least within Whangaehu Valley.

The Tangiwai disaster of 1953, and the eruptions of 1969 and 1975 heightened awareness of the lahar hazard and the need for adequate lahar and eruption surveillance at Mt Ruapehu. Presently, both geophysical and geochemical monitoring techniques are being used to detect precursory activity at this volcano. Seismograph recorders are permanently installed at Dome Shelter and at the Chateau Volcanological Observatory. Continuous seismic recording identifies earthquakes and tremors that may indicate the onset of eruptive activity. A tiltmeter has also been installed to detect swelling of the edifice. The temperature and water chemistry of Crater Lake are also regularly monitored (Cole and Nairn 1975).

A lahar warning scheme has been installed to provide advance warning of lahars at Whakapapa Skifield. Similar schemes, using automatic flood level detectors and conductivity probes installed at various points along the Whangaehu River (north of Tangiwai), Whakapapa River, Wahianoa River and Mangatoetoenui Stream have been established. Water levels along these rivers, particularly Whangaehu River, are closely monitored by Electricorp and New Zealand Railways (Paterson 1976; Williams 1986).

A partial solution to the lahar hazard resulting from phreatomagmatic eruptions at Mt Ruapehu requires partial or complete draining of Crater Lake. This method was used to reduce the lahar hazard from the summit lake at Mt Kelut in Indonesia (Zen 1965), however, the protected status of Mt Ruapehu, as part of Tongariro National Park, makes this an unlikely proposition.

CHAPTER SEVEN
SUMMARY

7.1 Summary of Findings

The findings of this study are summarised with reference to the objectives outlined in chapter one.

Objective 1: To elucidate the stratigraphic record of pre-historic lahars and tephras sourced from Mt Ruapehu within the last *c.* 22 500 years and directed to the east of the volcano.

Stratigraphy of rhyolitic tephras (Charts 1, 2 and 3)

A nearly complete late Pleistocene and Holocene stratigraphy of TVC rhyolitic tephras is recorded in sequences throughout the Mt Ruapehu region. Fourteen rhyolitic tephras belonging to the Taupo and Rotorua subgroups (Kaharoa Tephra, Mapara Tephra, Taupo Pumice, Waimihia Tephra, Hinemaiaia Tephra, Whakatane Tephra, Motutere Tephra, Poronui Tephra, Karapiti Tephra, Waiohau Tephra, ?Rotorua Tephra, Rerewhakaaitu Tephra, Okareka Tephra, and Kawakawa Tephra Formation) have been identified and correlated from their stratigraphic positions, field appearance, ferromagnesian mineral assemblages, and major element glass chemistries as determined by electron microprobe analysis.

The chronology of these tephras was determined from their stratigraphic positions relative to dated andesitic marker beds with which they are found interbedded, and two radiocarbon dates.

The rhyolitic tephras have been used to relative-age date andesitic tephras sourced from Mt Ruapehu, and the deposits of lahars (debris flows and hyperconcentrated flood flows) found preserved on the southeastern Mt Ruapehu ring plain.

Stratigraphy of andesitic tephras (Charts 1, 2 and 3)

The stratigraphy and chronology of andesitic tephras sourced from Mt Ruapehu has been established from their stratigraphic and age relationships to dated late Pleistocene and Holocene rhyolitic tephras and andesitic marker beds (Ngauruhoe Tephra, Mangatawai Tephra, Papakai Formation, Mangamate Tephra and Pahoka Tephra) of the Tongariro Subgroup, sourced from Mt Tongariro and Mt Ngauruhoe. Three new radiocarbon dates have provided additional chronological control.

Tephras erupted from Mt Ruapehu have been grouped into two newly defined formations of the Tukino and Tongariro subgroups. They are the Bullot Formation dated at *c.* 22 500 – 10 000 years B.P. and the Tufa Trig Formation, dated between *c.* 1800 years B.P. and the present. Other Mt Ruapehu tephras occurring stratigraphically between these two formations have been defined as members of the Papakai Formation, also of the Tongariro Subgroup.

Most of the tephras erupted from Mt Ruapehu comprise the Bullot Formation. They are pumiceous tephras, the coarsest of which are interpreted to be the products of subplinian magmatic eruptions. The presence of interbedded rhyolitic tephras allows a useful, informal division of the Bullot Formation into upper, middle and lower units. Twenty two members are defined within the formation. Some of these have been correlated locally.

The younger vitric-rich Tufa Trig Formation tephras are interpreted as the products of hydrovolcanic eruptions. Eighteen members are defined, with most correlated locally to sites in the western Rangipo Desert. A few (members Tf4, Tf5, Tf6) are useful marker beds in the eastern Rangipo Desert and along the Desert Road, where they are found interbedded with lahar deposits and dune sands.

A single small volume pyroclastic flow (Pourahu Member [ignimbrite unit]) erupted between *c.* 11 000 – 10 000 years B.P. has been identified on the southeastern ring plain. Although pyroclastic flows are common phenomena at many of the worlds andesitic volcanoes, these events are uncommon within the pre-historic eruption record at Mt Ruapehu, and represent a previously unrecognised hazard.

Volcanic activity within TgVC during the period *c.* 22 500 – 10 000 years B.P. was centred principally at Mt Ruapehu with the eruptions of the Bullot Formation tephras (Figure 7.1, p. 310). The Rotoaira Lapilli (Topping 1973) dated *c.* 13 800 years B.P. is the only presently recognised tephra erupted from Mt Tongariro during this time.

A short period of quiescence at Mt Ruapehu followed the deposition of the Bullot Formation tephras. During this time (*c.* 10 000-9800 years B.P.) the Pahoka and Mangamate tephras were erupted from Mt Tongariro. Later intermittent tephra eruptions from Mt Ruapehu between *c.* 9700 and 2500 years B.P. contributed ash and lapilli to the Papakai Formation (Figure 7.1, p. 310).

The Tufa Trig Formation tephras began to be erupted approximately 8000 years after the deposition of the Bullot Formation tephras. Their deposition also followed approximately 700 years of activity at Mt Ngauruhoe during which time Mangatawai Tephra was deposited. Historic and present-day eruptions contribute small amounts of ash to the Tufa Trig Formation.

Stratigraphy of lahars (Chart 4)

The stratigraphy and chronology of debris flow and hyperconcentrated flood flow deposits of the southeastern Mt Ruapehu ring plain has been determined by correlation of andesitic and rhyolitic tephra marker beds found over- and underlying the lahar deposits.

The deposits have been grouped into five formations on the basis of lithology (Table 7.1, p. 309). The formations (Onetapu, Manutahi, Mangaio, Tangatu, Te Heuheu) are of Holocene and late Pleistocene age.

Table 7.1 Lahar formation lithology and age.

Formation	Dominant Lithology	Age
Onetapu Formation	Debris flow	*c.* 1800 to present
Manutahi Formation	Hyperconcentrated flood flow	*c.* 5800 – 3400
Mangaio Formation	Debris flow	*c.* 4600
Tangatu Formation	Hyperconcentrated flood flow	*c.* 14 700 – 5800
Te Heuheu Formation	Debris flow	*c.* 22 500 – > 14 700

Lahars have been generated at Mt Ruapehu throughout the past *c.* 22 500 years, during periods of active tephra eruption and accumulation (*e.g.* Te Heuheu Formation lahars, early Holocene-aged Tangatu Formation lahars, and Onetapu Formation lahars), and relative quiescence and erosion (*e.g.* Tangatu Formation, Mangaio Formation and Manutahi Formation lahars). Most of the southeastern Mt Ruapehu ring plain has been built from the deposits of these lahars.

Objective 2: To map the distribution of the tephra and lahar deposits identified on the southeastern Mt Ruapehu ring plain.

Rhyolitic tephras

Distal rhyolitic tephras sourced from TVC and OVC are identified throughout the Mt Ruapehu and Mt Tongariro regions where they are preserved as thin discontinuous layers of fine or coarse ash. The most complete stratigraphy of rhyolitic tephras occurs in the northern part of the study area. At more southern localities most of the Holocene rhyolitic tephras are absent.

Identification of these tephras within the study area extends the previously recognised distributions of many of the tephras from source. The Kaharoa, Whakatane and Waiohau tephras have not previously been identified at TgVC.

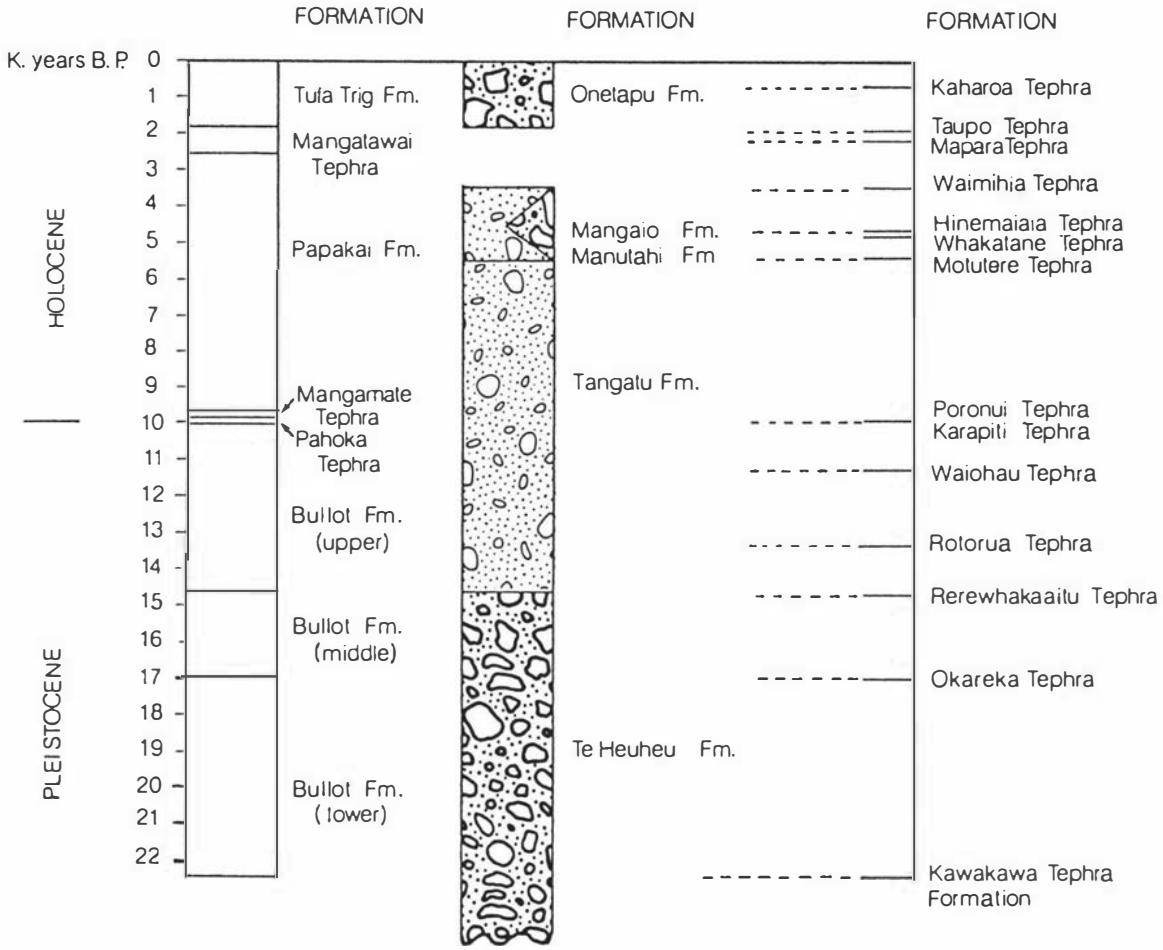

Figure 7.1 Summary stratigraphy and chronology (22 500 – 0 years B.P.) of Tongariro Volcanic Centre andesitic tephras, distal rhyolitic tephras from Taupo and Okataina volcanic centres, and laharic deposits preserved on the southeastern Mt Ruapehu ring plain.

Andesitic tephras

Most of the tephras erupted from Mt Ruapehu have been deposited east of the volcano where they form thick deposits comprising bedded lapilli and ash units. The stratigraphy at more distal localities is dominated by medial units and interspersed lapilli.

Tephras are excellent stratigraphic and chronologic marker beds useful for dating of geologic deposits and the surfaces that they form, and paleo-environmental interpretation. In this study both rhyolitic and andesitic tephra marker beds have been used to erect a stratigraphy of tephric and non-tephric sedimentary deposits of the southeastern Mt Ruapehu ring plain.

In the Mt Ruapehu region, rhyolitic tephras are found interbedded with andesitic tephras in most tephra sections. However andesitic tephras are considerably more numerous and are often found as the basal tephra cover beds overlying debris flow and fluvial constructional surfaces. In order to be able to correlate both tephras and sedimentary deposits, and hence geomorphic surfaces, the stratigraphy of local andesitic tephras has had to be established.

This in turn has required the identification of andesitic tephra marker beds within the 22 500 – 0 years B.P. tephra sequence.

By definition a marker bed must be widespread, be able to be mapped, be identifiable in isolated occurrences, be distinguishable from any tephra beds associated with it, and preferably be able to be dated (Wilcox 1965; Mullineaux 1974). Field attributes of tephra such as colour, degree of weathering, lithic content, granulometry, distribution, thickness and stratigraphic position may provide sufficient control for identification and correlation in regions close to source vents (Westgate and Gorton 1981). Tephra colour, composition, grain size, contact features, and stratigraphic position in relation to interbedded rhyolitic tephras have been used to correlate tephras sourced from Mt Ruapehu and Mt Tongariro.

Only a small number of the tephras erupted from Mt Ruapehu can be reliably correlated and mapped, due to the absence of diagnostic field characteristics of most of the tephras. Tephra colour varies with changes in site hydrology, and many of the tephras show rapid changes in thickness and grain size between sites moving away from the dispersal axis. In contrast, andesitic tephras sourced from Mt Tongariro are more readily correlated from field characteristics and stratigraphic positions. A number of tephras sourced from Mt Ruapehu and Mt Tongariro have therefore been fingerprinted using laboratory methods to identify distinguishing characteristics by which they can be correlated both locally, and regionally within TgVC.

Lahars

The distribution of each of the five laharic formations identified on the southeastern Mt Ruapehu ring plain is shown in Map 2.

Debris flow and hyperconcentrated flood flow deposits of the Te Heuheu Formation are the most extensive, and form the major constructional surfaces (dated >*c.* 22 500 – 14 700 years B.P.) of the southeastern Mt Ruapehu ring plain. Two stages of deposition at >*c.* 22 500 and *c.* 15 000 years B.P. are possibly indicated from the topographic offset between surfaces, and the cover bed tephra stratigraphy preserved on each.

The younger lahars show more restricted distributions, being principally confined within Rangipo Desert. Some of these lahars became channelised in tributary river systems.

Source areas for the lahars are the southeastern and southern flank and vent areas of Mt Ruapehu. The most recent lahars (Onetapu Formation), principally within Whangaehu Valley have been directed to the east and south by the Whangaehu River. Small recent lahars have also flowed down Wahianoa River.

Objective 3: To investigate the mineralogy and chemistry of tephras erupted from Mt Ruapehu and Mt Tongariro.

Andesitic tephras sourced from Mt Ruapehu and Mt Tongariro have been fingerprinted using both field and laboratory methods. Tephras have been examined for their physical characteristics, ferromagnesian phenocryst mineralogy and chemistry, Fe-Ti oxide and groundmass glass compositions. The major-element chemistry of the ferromagnesian phenocrysts (orthopyroxene, clinopyroxene, olivine, hornblende, Fe-Ti oxides) and glasses have been determined by electron microprobe analysis.

The field and mineralogical characteristics of 23 TgVC tephras (sampled from the Bullot, Rotoaira, Pahoka, Mangamate, and Tufa Trig formations) are summarised in Table 7.1, p. 314.

It is possible to characterise TgVC tephras as follows:

Ferromagnesian mineral assemblage

Assemblage
1: Orthopyroxene > Clinopyroxene
2: Orthopyroxene > Clinopyroxene > Olivine ± Hornblende
3: Olivine > Clinopyroxene >> Orthopyroxene ± Hornblende
4: Hornblende >> Orthopyroxene > Clinopyroxene ± Olivine

The total mineral assemblage also contains plagioclase feldspar and Fe-Ti oxides.

Clinopyroxene chemistry

Most clinopyroxenes within TgVC tephras are augite. Phenocryst core compositions range between Wo49 – 36, En54 – 37, Fs21 – 5 and Mg №91 – 64

Orthopyroxene Chemistry

Orthopyroxenes within TgVC tephras project as hypersthene and bronzite. Phenocryst core compositions range between En83 – 59, Fs38 – 14, Wo5 – 1, and Mg №88 – 61.

Olivine chemistry

Phenocryst core compositions ranging between Fo88 – 74. All are high-Mg forsteritic olivines.

Hornblende Chemistry

Phenocryst core compositions range between Mg №73 – 55 and project as hornblende, pargasitic – hornblende and tschermakitic – hornblende using the classification of Deer *et al.* (1966).

Glass chemistry

In the seven tephras analysed, glass compositions range from andesitic (53% SiO_2) to rhyolitic (75% SiO_2). Bulk rock compositions are andesite (54 – 61% SiO_2).

Distinguishing Tongariro Volcanic Centre Tephras

Ferromagnesian mineral assemblages, and the major element chemistry of ferromagnesian mineral phenocrysts have proven of limited use in distinguishing and correlating TgVC andesitic tephras, due to the similarity in assemblages and phenocryst chemistries exhibited by the tephras.

The presence of the diagnostic ferromagnesian minerals, olivine and hornblende is, however, useful in clearly distinguishing and correlating some tephras (Pahoka Tephra, Te Rato Lapilli, Oturere Lapilli, Waihohonu Lapilli, Poutu Lapilli [Mt Tongariro source], Shawcroft Tephra, member L3 [Mt Ruapehu source]). Hornblende has not previously been recognised as a major ferromagnesian mineral in TgVC lavas or tephras. Olivine which occurs with two distinct morphologies (non-skeletal and skeletal) is a particulary useful mineral in tephra correlations.

Results show that these tephras may best be distinguished by their groundmass glass compositions - some tephras not distinguished by ferromagnesian assemblage, ferromagnesian mineral and Fe-Ti oxide chemistries have been shown to be clearly distinguished by their glass compositions.

There are no clear trends exhibited by the ferromagnesian assemblages, ferromagnesian chemistry, Fe-Ti oxide or glass chemistries with time. Ferromagnesian assemblages and glass chemistry do, however, identify the introduction of new melt beneath the TgVC volcanoes at *c.* 10 000 years B.P., coincident with the eruption of hornblende-bearing dacitic mixed magmas of the Pahoka and Mangamate Tephra formations.

Table 7.2 Summary of characteristics of 23 Tongariro Volcanic Centre tephras fingerprinted using both field and laboratory based methods.

TEPHRA		FIELD		LABORATORY						
Formation	**Member**	**Properties, Colour and Dominant Grain Size (D.G.S.)**	**Diagnostic Stratigraphic Position**	**Tephra Composition** >2 mm fraction	**Ferromagnesian Assemblage** 0.125 – 0.250 mm	**Clinopyroxene Chemistry** phenocryst cores (mean)	**Orthopyroxene Chemistry** phenocryst cores (mean)	**Olivine Chemistry** phenocryst cores (mean)	**Hornblende Chemistry** phenocryst cores (mean)	**Glass & Bulk Rock (BR) Chemistry**
Tufa Trig Formation	Member Tf14	Dark greyish-brown and black coarse ash D.G.S. coarse ash	-	Vitric pyroclasts, crystals & lithics	Opx + Cpx	Augite + Endiopside Wo% 42.86 (0.72) En% 43.99 (2.71) Fs% 13.15 (3.11)	Bronzite + Hypersthene En% 73.59 (6.76) Fs% 26.45 (6.48) Wo% 3.65 (0.40)	-	-	SiO_2 63.63 (0.29) Na+K 6.51 (0.30)
	Member TfB	Black and grey coarse ash Some very fine brown pumice lapilli D.G.S. coarse ash	-	Vitric pyroclasts, crystals & lithics	Opx + Cpx	Augite + Endiopside + Salite Wo% 43.08 (1.76) En% 44.46 (3.08) Fs% 12.46 (3.35)	Hypersthene + Bronzite En% 67.01 (4.95) Fs% 29.52 (4.70) Wo% 3.47 (0.34)	-	-	SiO_2 63.74 (0.74) Na+K 8.51 (0.50)
	Member Tf6	Dark greyish-brown coarse ash D.G.S. coarse ash	-	Vitric pyroclasts, crystals & lithics	Opx + Cpx	Augite + Endiopside Wo% 42.30 (1.39) En% 42.06 (2.43) Fs% 15.64 (3.54)	Bronzite + Hypersthene En% 73.25 (5.29) Fs% 23.56 (5.11) Wo% 3.19 (0.30)	-	-	SiO_2 64.49 (1.02) Na+K 8.49 (0.47)
	Member Tf1	Vesicular, pale yellow pumice D.G.S. fine lapilli	Overlies Taupo Pumice	Pumice, lithic & scoria lapilli	Opx + Cpx	Augite + Endiopside Wo% 40.48 (1.87) En% 46.48 (4.27) Fs% 13.08 (4.36)	Hypersthene + Bronzite En% 64.40 (2.04) Fs% 32.25 (2.03) Wo% 3.35 (0.28)	-	-	-
Mangamate Tephra *(continued ...)*	Poutu Lapilli	Angular dark greyish-brown lithic and poorly vesicular strong brown pumice lapilli Some colour-banded pumice D.G.S. fine lapilli	Underlies Papakai Formation	Scoria, pumice & lithic lapilli Schist xenoliths	Cpx + Opx + Ol + Hb (tr)	Endiopside + Augite + Diopside Wo% 43.07 (1.61) En% 47.61 (1.32) Fs% 9.32 (1.31)	Hypersthene En% 64.79 (0.00) Fs% 32.93 (0.00) Wo% 2.28 (0.00)	Fo% 79.15 (1.15)	-	-
	Waihohonu Lapilli	Angular very dark grey lithic and poorly vesicular yellowish-brown pumice lapilli Weakly bedded D.G.S. medium lapilli	-	Scoria, lithic & pumice lapilli	Ol + Cpx + Opx	Endiopside + Diopside + Augite Wo% 43.75 (1.55) En% 48.10 (2.49) Fs% 8.15 (3.35)	Hypersthene En% 74.48 (3.59) Fs% 22.46 (3.70) Wo% 3.06 (0.32)	Fo% 84.89 (1.84)	-	-
	Oturere Lapilli	Angular very dark grey lithic and poorly vesicular yellowish-brown pumice lapilli Weakly bedded	-	Scoria, pumice & lithic lapilli	Opx + Cpx + Ol + Hb(m)	Augite + Salite Wo% 43.38 (1.65) En% 44.55 (2.49) Fs% 12.07 (1.46)	Bronzite + Hypersthene En% 71.86 (4.02) Fs% 24.78 (3.92) Wo% 3.36 (0.32)	Fo% 79.42 (1.30)	Mg № 64.64 (0.35)	-

continued ...

TEPHRA		FIELD		LABORATORY						
Formation	**Member**	**Properties. Colour and Dominant Grain Size (D.G.S.)**	**Diagnostic Stratigraphic Position**	**Tephra Composition** >2 mm fraction	**Ferromagnesian Assemblage** 0.125–0.250 mm	**Clinopyroxene Chemistry** phenocryst cores (mean)	**Orthopyroxene Chemistry** phenocryst cores (mean)	**Olivine Chemistry** phenocryst cores (mean)	**Hornblende Chemistry** phenocryst cores (mean)	**Glass & Bulk Rock (BR) Chemistry**
Mangamate Tephra *(... continued)*	Te Rato Lapilli	Angular poorly vesicular, dark grey lithic lapilli and vesicular white & grey colour-banded pumice D.G.S. fine lapilli	-	Scoria, pumice & lithic lapilli Schist xenoliths	Hb + Opx + Cpx + Ol(tr)	Augite + Endiopside Wo% 42.71 (0.72) En% 43.17 (2.22) Fs% 14.12 (2.55)	Hypersthene + Bronzite En% 66.18 (2.01) Fs% 30.59 (2.02) Wo% 3.23 (0.21)	-	Mg Nº 61.63 (1.82)	SiO_2 [BR] 63.47 Na+K [BR] 5.82 *(note 2)*
Pahoka Tephra	-	Vesicular, grey & white colour-banded pumice and scoriaceous lapilli D.G.S. fine lapilli	Underlies Karapiti Tephra	Pumice, scoria & lithic lapilli Schist xenoliths	Hb + Cpx + Opx + Ol(tr)	Augite + Diopside Wo% 43.02 (2.24) En% 43.65 (2.60) Fs% 13.33 (3.05)	Hypersthene + Bronzite En% 66.20 (4.79) Fs% 31.00 (4.50) Wo% 2.80 (0.31)	-	Mg Nº 59.98 (2.79)	SiO_2 [BR] 63.10 Na+K [BR] 5.50 *(note 2)*
Okupata Tephra	-	Vesicular, pale yellow pumice lapilli D.G.S. fine lapilli	-	Pumice and lithic lapilli	Opx + Cpx + Hb(tr) + Ol(tr)	Augite Wo% 42.22 (0.73) En% 41.69 (2.33) Fs% 16.09 (2.44)	Hypersthene + Bronzite En% 65.41 (3.61) Fs% 31.56 (3.36) Wo% 3.03 (0.30)	-	-	-
Bullot Formation	Ngamatea lapilli-1	Vesicular, strong brown pumice and grey lithic lapilli Weak reverse grading D.G.S. fine lapilli	-	Pumice, scoria & lithic lapilli	Opx + Cpx + Hb(m)	Augite Wo% 41.86 (0.93) En% 42.22 (0.79) Fs% 15.92 (0.58)	Hypersthene En% 64.84 (1.58) Fs% 32.25 (1.42) Wo% 2.91 (0.21)	-	Mg Nº 67.56 (0.89)	-
	Pourahu Member [tephra] *(note 1)*	Vesicular, white and pinkish-white pumice lapilli and coarse ash D.G.S. medium lapilli	-	Pumice, lithic & scoria lapilli	Opx + Cpx + Hb(m) + Ol(tr)	Augite Wo% 42.57 (1.15) En% 41.98 (1.67) Fs% 15.46 (2.31)	Hypersthene + Bronzite En% 64.05 (2.54) Fs% 32.92 (2.42) Wo% 3.03 (0.28)	Fo% 82.20 (0.00)	Mg Nº 65.33 (4.58)	SiO_2 [BR] 60.67 Na+K [BR] 5.11
	Pourahu Member [ignimbrite] *(note 1)*	Vesicular white, pinkish-white, and white & grey colour-banded lapilli D.G.S. coarse lapilli	-	Pumice, scoria & lithic lapilli	Opx + Cpx + Hb(m) + Ol(tr)	Augite Wo% 41.71 (0.84) En% 41.56 (0.80) Fs% 16.73 (1.12)	Hypersthene + Bronzite En% 63.50 (2.24) Fs% 33.45 (2.23) Wo% 3.05 (0.26)	-	-	SiO_2 72.55 (0.43) Na+K 7.45 (0.44) SiO_2 [BR] 61.00 Na+K [BR] 5.22
	Helwan lapilli	Vesicular, strong brown pumice and grey lithic lapilli D.G.S. fine lapilli	-	Pumice and lithic lapilli	Opx + Cpx	Augite Wo% 41.96 (0.66) En% 40.67 (0.75) Fs% 17.37 (0.80)	Hypersthene + Bronzite En% 64.18 (2.26) Fs% 32.76 (2.34) Wo% 3.07 (0.21)	-	-	-

... continued ...

TEPHRA		FIELD		LABORATORY						
Tephra	**Member**	**Properties, Colour and Dominant Grain Size (D.G.S.)**	**Diagnostic Stratigraphic Position**	**Tephra Composition** >2 mm fraction	**Ferromagnesian Assemblage** 0.125–0.250 mm	**Clinopyroxene Chemistry** phenocryst cores (mean)	**Orthopyroxene Chemistry** phenocryst cores (mean)	**Olivine Chemistry** phenocryst cores (mean)	**Hornblende Chemistry** phenocryst cores (mean)	**Glass & Bulk Rock (BR) Chemistry**
Bullot Formation *(continued ...)*	Member L17	Vesicular, dark brown pumice and black lithic lapilli D.G.S. fine lapilli		Pumice, lithic & scoria lapilli Accretionary lapilli	Opx + Cpx + Hb(tr)	Augite + Salite Wo% 43.55 (1.03) En% 41.09 (2.00) Fs% 15.36 (2.84)	Hypersthene + Bronzite En% 63.35 (2.55) Fs% 33.36 (2.33) Wo% 3.29 (0.26)	-	Mg № 66.95 (0.00)	-
	Member L16	Vesicular, strong brown pumice and dark grey lithic lapilli D.G.S. medium lapilli	-	Pumice, lithic & scoria lapilli Accretionary lapilli	Opx + Cpx	Augite Wo% 42.52 (0.72) En% 41.61 (1.29) Fs% 15.87 (1.23)	Hypersthene En% 63.36 (1.16) Fs% 33.36 (1.20) Wo% 3.29 (0.16)	-	-	-
	Shawcroft Tephra	Very dark grey lithic and strong brown pumice lapilli Distinct strong brown pumice base D.G.S. fine lapilli	Overlies Waiohau Tephra	Pumice, scoria & lithic lapilli	Opx + Cpx + Ol	Augite Wo% 41.94 (1.05) En% 42.46 (2.55) Fs% 15.60 (3.11)	Hypersthene + Bronzite En% 64.10 (2.15) Fs% 32.84 (2.08) Wo% 3.06 (0.24)	Fo% 77.02 (2.08)	-	-
	Member L8	Vesicular, olive-brown pumice and black lithic lapilli D.G.S. fine lapilli	-	Pumice, lithic & scoria lapilli	Opx + Cpx	Augite Wo% 42.48 (1.09) En% 41.12 (1.70) Fs% 16.39 (1.06)	Hypersthene + Bronzite En% 65.03 (2.07) Fs% 31.71 (2.27) Wo% 3.25 (0.67)	-	-	SiO_2 (BR) 64.16 Na+K (BR) 3.33
Rotoaira Lapilli	-	Vesicular, yellowish-brown pumice and dark grey lithic lapilli Bedded D.G.S. fine lapilli		Pumice, lithic & scoria lapilli	Opx + Cpx + Ol(tr)	Augite + Endiopside Wo% 41.18 (0.18) En% 43.47 (4.23) Fs% 15.35 (4.22)	Hypersthene + Bronzite En% 66.16 (1.42) Fs% 30.41 (1.51) Wo% 3.43 (0.13)	Fo% 82.20 (4.07)	-	SiO_2 68.99 Na+K 5.23 *(note 2)*
Bullot Formation *(continued...)*	Member L7b	Strong brown pumice and grey lithic lapilli D.G.S. fine lapilli	-	Pumice and lithic lapilli	Opx + Cpx	Augite + Endiopside Wo% 42.50 (0.79) En% 43.42 (1.83) Fs% 14.08 (2.48)	Hypersthene + Bronzite En% 66.64 (1.85) Fs% 30.33 (1.85) Wo% 3.03 (0.24)	-	-	-
	Member L6 (pink lapilli)	Vesicular, pinkish-grey and pale brown pumice lapilli and black lithic lapilli D.G.S. fine lapilli	-	Pumice, lithic & scoria lapilli	Opx + Cpx + Hb(rn)	Augite Wo% 42.57 (1.24) En% 40.28 (1.43) Fs% 17.15 (2.02)	Hypersthene + Bronzite En% 66.08 (2.18) Fs% 30.70 (2.02) Wo% 3.21 (0.27)	-	Mg № 68.71 (3.38)	SiO_2 69.38 (0.91) Na+K 6.71 (0.67) SiO_2 (BR) 67.00 Na+K (BR) 4.09

... continued ...

TEPHRA		FIELD		LABORATORY						
Tephra	**Member**	**Properties, Colour and Dominant Grain Size (D.G.S.)**	**Diagnostic Stratigraphic Position**	**Tephra Composition** >2 mm fraction	**Ferromagnesian Assemblage** 0.125–0.250 mm	**Clinopyroxene Chemistry** phenocryst cores (mean)	**Orthopyroxene Chemistry** phenocryst cores (mean)	**Olivine Chemistry** phenocryst cores (mean)	**Hornblende Chemistry** phenocryst cores (mean)	**Glass & Bulk Rock [BR] Chemistry**
Bullot Formation *(... continued)*	Member L4	Vesicular, pale brown and yellowish-brown pumice lapilli and bombs	Overlies Okareka Tephra	Pumice, lithic & scoria lapilli	Opx + Cpx	Augite Wo% 42.49 (1.63) En% 42.52 (3.06) Fs% 14.98 (1.82)	Hypersthene + Bronzite En% 67.24 (2.42) Fs% 29.67 (2.19) Wo% 3.09 (0.30)	-	-	-
	Member L3 (hokey pokey lapilli)	Very vesicular, yellowish-brown pumice lapilli and blocks Black scoria lapilli D.G.S. medium lapilli	Underlies Okareka Tephra	Pumice, lithic & scoria lapilli	Opx + Cpx + Ol(m) + Hb(tr)	Augite + Endiopside Wo% 41.89 (2.01) En% 47.20 (3.72) Fs% 10.91 (2.63)	Bronzite + Hypersthene En% 71.14 (6.63) Fs% 25.58 (6.82) Wo% 3.28 (0.71)	Fo% 82.47 (0.39)	-	SiO_2 59.88 (0.23) Na+K 5.19 (0.60) SiO_2 [BR] 65.92 Na+K [BR] 3.20
	Member L1 (green ash)	Olive-grey to greenish-grey coarse ash and lapilli D.G.S. coarse ash	Overlies Kawakawa Tephra Formation	Pumice, crystal & lithic ash	Opx + Cpx + Hb(tr)	Augite + Endiopside Wo% 42.23 (1.20) En% 45.40 (3.89) Fs% 12.37 (3.09)	Hypersthene + Bronzite En% 66.40 (3.33) Fs% 30.93 (3.54) Wo% 2.67 (0.70)	-	Mg № 61.07 (0.00)	-

[note 1] Means from data from several sampling sites.
[note 2] Data from Topping (1974).

... continued

Determining Tephra Source

(a) Andesitic tephras from TgVC can be distinguished from EVC tephras by (i) ferromagnesian mineral assemblages and (ii) clinopyroxene, orthopyroxene, hornblende and titanomagnetite major element chemistry. TgVC tephras show ferromagnesian mineral assemblages dominated by orthopyroxene and clinopyroxene. Tephras from Egmont Centre rarely contain orthopyroxene. TgVC tephras are distinguished by the higher Mg-numbers of clinopyroxene phenocrysts; the lower Mg-numbers and MnO contents of orthopyroxenes; the lower Mg-numbers of hornblendes; and the higher Cr_2O_3 and lower MnO contents of titanomagnetites. Most TgVC and EVC andesitic tephras are additionally distinguished by the major element chemistry (SiO_2 and alkali contents) of their glasses.

(b) TgVC tephras are also able to be distinguished from Central North Island rhyolitic tephras on clinopyroxene abundance in the ferromagnesian mineral assemblage, and glass major element chemistry. Augite rarely occurs in the ferromagnesian mineral assemblage of Central North Island rhyolitic tephras, and its presence in large amounts is attributed to contamination from andesitic tephras.

Comparison of the major element glass chemistry in TgVC andesites with TVC and OVC rhyolites also distinguishes TgVC tephras. Glasses in tephras from TgVC show lower SiO_2 and higher FeO, MgO, CaO and TiO_2 contents.

Used in combination, glass chemistry and ferromagnesian mineral assemblages appears the most useful means of distinguishing source.

Objective 4: To produce integrated lahar and tephra hazard maps based on the distribution and frequency of the late Quaternary and Holocene tephra and lahar deposits recognised and mapped in this study.

Tephras erupted from Mt Ruapehu form a thick tephra mantle on the ring plain directly east of the volcano. Most of the tephras belong to the Bullot Formation. The younger Tufa Trig tephras, and members of the Papakai Formation have contributed comparatively little tephra to the ring plain, with distributions of most members confined to within a few kilometres of source.

Three tephra hazard zones have been depicted based on the known distribution of tephras erupted from Mt Ruapehu within the last *c.* 22 500 years, and the frequency of eruptions. Eruptions from Mt Tongariro present additional hazard to the Mt Ruapehu region,

as many of the Mt Tongariro tephras form thick deposits on the southeastern Mt Ruapehu ring plain.

Debris flows and hyperconcentrated flood flows are common phenomena at Mt Ruapehu, with at least 35 events recorded on the southeastern ring plain within the past *c.* 22 500 years. Four hazard zones have been depicted based on the distribution and frequency of debris flows and hyperconcentrated flood flows within this time period. The present-day lahar risk is greatest on the slopes of Mt Ruapehu and within Whangaehu Valley. Debris flows generated by sector collapses of the volcanic edifice, induced by volcanic eruptions or possibly earthquakes present the greatest long term hazard at Mt Ruapehu. In the past these events have inundated extensive areas of the southeastern ring plain.

7.2 Future Work

Tephrostratigraphy

The stratigraphy and chronology of tephra and lahar deposits presented in this study represents the first detailed stratigraphic record of past eruptive events at Mt Ruapehu. The record is not regarded as being complete, and work remains to be done on the following aspects:

1. Elucidating the stratigraphy of medial materials found interbedded with Holocene and late Pleistocene Mt Ruapehu tephras.

2. Detailed examination of the stratigraphy and composition of the Papakai Formation. Presently this formation comprises andesitic tephras and tephric loess deposited over a period of *c.* 9000 years. Interbedded within the formation are four rhyolitic tephras (Waimihia Tephra, Hinemaiaia Tephra, Whakatane Tephra, Motutere Tephra). It is possible that the Whakaipo, Rotoma, and Opepe rhyolitic tephras might also be preserved as microscopic tephras.

3. Continued correlation of Bullot Formation tephras both locally and regionally – particularly the distal deposits found on the northern Mt Tongariro ring plain for which the stratigraphy and mineralogy have not yet been detailed.

Future attempts at correlating andesitic tephras would benefit from use of both field and laboratory fingerprinting methods. Where possible, laboratory methods should include determination of tephra glass chemistry.

Tephra Mineralogy

The tephra and mineral studies undertaken in this thesis provide a natural basis for further petrographic studies of TgVC tephras. The purpose of the present work has been to document the mineralogy of marker beds identified on the Mt Ruapehu ring plain for purposes of aiding their correlation. Further mineralogical study of these and other tephras would provide a comprehensive data base useful to regional correlation and the interpretation of magmatic processes operating at TgVC.

Areas of study which would complement the existing work include:

1. Determination of bulk rock chemistries of pumice from Mt Ruapehu and Mt Tongariro tephras.

   Tephras with dacitic and rhyolitic glass compositions, andesite bulk compositions, and tephras with ferromagnesian mineral assemblages dominated by olivine and hornblende indicate wide chemical diversity in the TgVC tephras. To date there are very few bulk rock analyses on Mt Ruapehu tephras. Determination of bulk chemistries would further characterise this diversity.

2. Further analyses of groundmass glass compositions of Mt Ruapehu tephras to fully evaluate the use of glass chemistry as a means of correlating both near source and distal andesitic tephras.

Lahar Studies

Interesting avenues for future study include:

1. Determination of the thermoremnant magnetisation of clasts within lahars to determine if they are 'hot' or 'cold' lahars, and thereby allowing possible alternative interpretations of the mechanisms of generation of these lahars throughout the eruptive record at Mt Ruapehu.

2. Study of the deposits within the Whangaehu and Hautapu valleys to determine the age, extent and volumes of Mt Ruapehu lahar deposits preserved south of the study area.

3. A study of the sedimentology of debris flow and hyperconcentrated flood flow deposits, and deposits transitional between these, presently found preserved within Rangipo Desert. Rangipo Desert is an ideal environment for such a study, with a lahar expected every *c.* 11 years depositing fresh material over much of the area.

BIBLIOGRAPHY

ALLOWAY, B.V. 1989: *The late Quaternary cover bed stratigraphy and tephrochronology of north-eastern and central Taranaki, New Zealand.* Unpublished Ph.D. Thesis, Massey University.

AOMINE, S.; WADA, K. 1962: Differential weathering of volcanic ash and pumice, resulting in formation of hydrated halloysite. *American Mineralogist* 47: 1024-1048.

ARGUDEN, A.T.; RODOLFO, K.S. 1990: Sedimentologic and dynamic differences between hot and cold laharic debris flows of Mayon Volcano, Philippines. *Geological Society of America Bulletin* 102: 865-876.

BARBERI, F.; CIONI, R.; ROSI, M.; SANTACROCE, R.; SBRANA, A.; VECCI, R. 1989: Magmatic and phreatomagmatic phases in explosive eruptions of Vesuvius as deduced by grain-size and component analysis of the pyroclastic deposits. *Journal of Volcanology and Geothermal Research* 38: 287-307.

BAUMGART, I.L. 1954: Some ash showers of the Central North Island. *N.Z. Journal of Science and Technology* B35: 456-467.

BAUMGART, I.L.; HEALY, J. 1956: Recent Volcanicity at Taupo, New Zealand. *Proceedings of the 8th Pacific Science Congress* 2: 113-127.

BLAKEMORE, L.C.; SEARLE, P.L.; DALY, B.K. 1987: Methods for chemical analysis of soils. *N.Z. Soil Bureau Scientific Report* 80.

BOGAARD, V.D.P.; SCHMINCKE, H-U. 1985: Laacher See Tephra: A widespread isochronous late Quaternary tephra layer in central and northern Europe. *Geological Society of America Bulletin* 96: 1554-1571.

BORCHARDT, G.A.; HARWARD, M.E.; SCHMITT, R.A. 1971: Correlation of volcanic ash deposits by activation analysis of glass separates. *Quaternary Research* 1(2): 247-260.

BOUDON, G.; SEMET, M.P.; VINCENT, P.M. 1987: Magma and hydrothermally driven sector collapses: The 3100 and 11 500 year B.P. eruptions of la grande Decouverte (La Soufrière) Volcano, Guadeloupe, French West Indies. *Journal of Volcanology and Geothermal Research* 33: 317-323.

BOURDIER, J.L.; GOURGAUD, A.; VINCENT, P.M. 1985: Magma mixing in a main stage of formation of Montagne Pelée: The Saint Vincent-type scoria flow sequence (Martinique, French West Indes). *Journal of Volcanology and Geothermal Research* 25: 309-332.

BRANTLEY, S.R.; WAITT, R.B. 1988: Interrelations among pyroclastic surge, pyroclastic flow, and lahars in Smith Creek valley during first minutes of 18 May 1980 eruption of Mount St Helens, U.S.A. *Bulletin of Volcanology* 50: 304-326.

CALLAHAN, J. 1987: A non-toxic heavy liquid and inexpensive filters for separation of mineral grains. *Journal of Sedimentary Petrology* 57(4): 765-766.

CAMPBELL, I.B. 1973: Recent aggradation in Whangaehu Valley, Central North Island, New Zealand. *N.Z. Journal of Geology and Geophysics* 16(3): 643-649.

CANTAGREL, J.M.; GOURGAUD, A.; ROBIN, C. 1984: Repetitive mixing events and Holocene pyroclastic activity at Pico de Orizaba and Popocatepetl (Mexico). *Bulletin of Volcanology* 47-4(1): 735-748.

CASHMAN, K.V. 1979: *Evolution of Kakaramea and Maungakatote volcanoes, Tongariro Volcanic Centre, New Zealand.* Unpublished M.Sc. Thesis, Victoria University of Wellington.

CLAPPERTON, C.C. 1986: Fire and water in the Andes. *Geographical Magazine* February 1986: 74–79

CLARK, R.H. 1960: Petrology of the volcanic rocks of Tongariro subdivision. *Appendix in N.Z. Geological Survey Bulletin,* n.s. 40: 107-123.

COLE, J.W. 1970a: Description and correlation of Holocene volcanic formations in the Tarawera-Rerewhakaaitu Region. *Transactions of the Royal Society of New Zealand*, Earth Sciences 8(7): 93-108.

——— 1970b: Structure and Eruptive history of the Tarawera Volcanic Complex. *N.Z. Journal of Geology and Geophysics* 13(4): 879-902.

——— 1970c: Petrography of the rhyolite lavas of Tarawera Volcanic Complex. *N.Z. Journal of Geology and Geophysics* 13(4): 903-24.

——— 1978: Andesites of the Tongariro Volcanic Centre, North Island, New Zealand. *Journal of Volcanology and Geothermal Research* 3: 121-153.

——— 1981: Genesis of lavas of the Taupo Volcanic Zone, North Island, New Zealand. *Journal of Volcanology and Geothermal Research* 10: 317-337.

——— 1982: Tonga-Kermedec-New Zealand. *In* R.S. Thorpe (Ed.): *Andesites: Orogenic Andesites and Related Rocks*, pp. 245-258. John Wiley & Sons Ltd.

COLE, J.W.; GRAHAM, I.J.; HACKETT, W.R.; HOUGHTON, B.F. 1986: Volcanology and petrology of Quaternary composite volcanoes of Tongariro Volcanic Centre, Taupo Volcanic Zone. *In* I.E. Smith (Ed.): *The Royal Society of New Zealand Bulletin* 23, pp. 224-250.

COLE, J.W.; NAIRN, I.A. 1975: *Catalogue of the active volcanoes of the world including solfatara fields, Part XXII New Zealand.* International Association of Volcanology and Chemistry of the Earth's Interior, Rome.

COLLINS, C.M. 1978: Contamination of water supplies and water courses. *Appendix in* J. Healy, E.F. Lloyd, D.E.H. Rishworth, C.P. Wood, R.B. Glover, R.R. Dibble: The Eruption of Ruapehu, New Zealand, on 22nd June 1969, pp. 72–74. *N.Z. DSIR Bulletin* 224.

COLMAN, S.M.; PIERCE, K.L.; BIRKELAND, P.W. 1987: Suggested terminology for Quaternary dating methods. *Quaternary Research 28: 314-319.*

COSTA, J.E. 1988: Rheologic, geomorphic, and sedimentologic differentiation of water floods, hyperconcentrated flows, and debris flows. *In* V.R. Baker, R.C. Kochel, P.C. Patton: *Flood Geomorphology*, pp. 113-122. John Wiley & Sons.

COWIE, J.D. 1964: Aokautere Ash in the Manawatu District, New Zealand. *N.Z. Journal of Geology and Geophysics* 7: 67-77.

CRANDELL, D.R. 1957: Some features of mudflow deposits. *Geological Society of America Bulletin* 68(2): 1821.

——— 1969: Surficial Geology of Mt Rainier National Park Washington. *U.S. Geological Survey Bulletin* 1288.

——— 1971: Postglacial lahars from Mount Rainier Volcano, Washington *U.S. Geological Survey Professional Paper* 677.

CRANDELL, D.R.; BOOTH, B.; KAZUMADINATA, K.; SHIMOZURU, D.; WALKER, G.P.L.; WESTERCAMP, D. 1984: *Source-book for Volcanic Hazards Zonation.* Paris, UNESCO.

CRANDELL, D.R.; MILLER, C.D.; GLICKEN, H.X.; CHRISTIANSEN, R.L.; NEWHALL, C.G. 1984: Catastrophic debris avalanche from ancestral Mount Shasta volcano, California. *Geology* 12: 143-146

CRANDELL, D.R.; MULLINEAUX, D.R. 1967: Volcanic hazards at Mt Rainier, Washington. *Geological Survey Bulletin* 1238.

——— 1973: Pine Creek volcanic assemblage at Mount St Helens, Washington. *U.S. Geological Survey Bulletin* 1383-A.

——— 1978: Potential hazards from future eruptions of Mount St Helens Volcano, Washington. *U.S. Geological Survey Bulletin* 1383-C.

CRANDELL, D.R.; NICHOLS, D.R. 1989: Volcanic Hazards at Mount Shasta, California. U.S. Geological Survey pamphlet based on C.D. Miller 1980: Potential Hazards from Future Eruptions in the Vicinity of Mt Shasta Volcano, Northern California. *U.S. Geological Survey Bulletin* 1503.

CRANDELL, D.R.; WALDRON, H.H. 1956: A recent volcanic mudflow of exceptional dimensions from Mt Rainier, Washington. *American Journal of Science* 254: 349-362.

CROWE, B.M.; FISHER, R.V. 1973: Sedimentary structures in base-surge deposits with special reference to cross-bedding, Ubehebe Craters, Death Valley, California. *Geological Society of America Bulletin* 84: 663-682.

DE ROSA, R.; SHERIDAN, M.F. 1983: Evidence for magma mixing in the surge deposits of the Monte Guardia Sequence, Lipari. *Journal of Volcanology and Geothermal Research* 17: 313-328.

DEER, W.A.; HOWIE, R.A.; ZUSSMAN, J. 1966: *An Introduction to the Rock-Forming Minerals.* Longman Group Limited, England.

DONALDSON, C.H. 1974: Olivine crystal types in harrisitic rocks of the Rhum Pluton and in Archean spinifex rocks. *Geological Society of America Bulletin* 85: 1721-1726.

——— 1976: An experimental investigation of olivine morphology. *Contributions to Mineralogy and Petrology* 57: 187-213.

DONALDSON, C.H.; HENDERSON, C.M.B. 1988: A new interpretation of round embayments in quartz crystals. *Mineralogical Magazine* 52: 27-33.

DONOGHUE, S.L. 1990: Lahar stratigraphy of the southeastern Mt Ruapehu ring plain. *In* New Zealand Geology and Geophysics Conference, 1990, Programme and Abstracts. *Geological Society of New Zealand Miscellaneous Publication* 50A.

DREVER, H.I.; JOHNSTON, R. 1957: Crystal growth of forsteritic olivine in magmas and melts. *Transactions of the Royal Society Edinburgh* LXIII (II) (13): 289-315.

DUDAS, M.J.; HARWARD, M.E.; SCHMITT, R.A. 1973: Identification of dacitic tephra by activation analysis of their primary mineral phenocrysts. *Journal of Quaternary Research* 3(2): 307-315.

EDEN, D.N.; WHITTON, J.S. 1988: Sodium Polytungstate - A new non-toxic liquid for density separations. *N.Z. Soil News* 36(2): 71.

EICHELBERGER, J.C. 1974: Magma contamination within the volcanic pile: Origin of andesite and dacite. *Geology* 2: 29-33.

——— 1975: Origin of andesite and dacite: Evidence of mixing at Glass Mountain in California and at other circum-Pacific volcanoes. *Geological Society of America Bulletin* 86: 1381-1391.

ENOS, P. 1977: Flow regimes in debris flow. *Sedimentology* 24: 133-142.

EWART, A. 1963: Petrology and petrography of Quaternary pumice ash in the Taupo area. *Journal of Petrology* 4: 392-431.

——— 1966: Review of mineralogy and chemistry of the acidic volcanic rocks of Taupo Volcanic Zone, New Zealand. *Bulletin Volcanologique* 29: 147-169.

——— 1967a: Pyroxene and magnetite phenocrysts from the Taupo Quaternary rhyolitic pumice deposits, New Zealand. *Mineralogical Magazine* 36: 180-194.

——— 1967b: The Petrography of the central North Island rhyolitic lavas. Part 1 - correlations between the phenocryst assemblages. *N.Z. Journal of Geology and Geophysics* 10: 182-197.

——— 1968: The Petrography of the central North Island rhyolitic lavas. Part 2 - regional petrography including notes on associated ash-flow pumice deposits. *N.Z. Journal of Geology and Geophysics* 11: 478-545.

——— 1969: Petrochemistry and feldspar crystallisation in the silicic volcanic rocks, central North Island, New Zealand. *Lithos* 2: 371-388.

——— 1971: Notes on the chemistry of ferromagnesian phenocrysts from selected volcanic rocks, central volcanic region. *N.Z. Journal of Geology and Geophysics* 14: 323-340.

EWART, A.; GREEN, D.C.; CARMICHAEL, I.S.E.; BROWN, F.H. 1971: Voluminous low temperature rhyolitic magmas in New Zealand. *Contributions to Mineralogy and Petrology* 33: 128-144.

EWART, A.; HILDRETH, W.; CARMICHAEL, I.S.E. 1975: Quaternary acid magma in New Zealand. *Contributions to Mineralogy and Petrology* 51: 1-27.

EWART, A.; TAYLOR, S.R. 1969: Trace element geochemistry of the rhyolitic volcanic rocks, Central North Island, New Zealand. Phenocryst data. *Contributions to Mineralogy and Petrology* 22: 127-146.

FEDERMAN, A.N.; SCHEIDEGGER, K.F. 1984: Compositional heterogeneity of distal tephra deposits from the 1912 eruption of Novarupta, Alaska. *Journal of Volcanology and Geothermal Research* 21: 233-254.

FERGUSSON, G.J.; RAFTER, T.A. 1959: New Zealand C^{14} Age measurements - 4. *N.Z. Journal of Geology and Geophysics* 2: 208-241.

FISHER, R.V. 1961: Proposed classification of volcaniclastic sediments and rocks. *Geological Society of America Bulletin* 72: 1409-1414.

——— 1977: Erosion by volcanic base-surge density currents: U-shaped channels. *Geological Society of America Bulletin* 88: 1287-1297.

FISHER, R.V.; SCHMINCKE, H-U. 1984: *Pyroclastic Rocks.* Springer-Verlag, Berlin.

FLEET, M.E. 1975: The growth habits of olivine - A structural interpretation. *Canadian Mineralogist* 13(3): 293-297.

FLEMING, C.A.; STEINER, A. 1951: Sediments beneath Ruapehu Volcano. *N.Z. Journal of Science and Technology* B32(6): 31-32

FLOOD, T.P.; SCHURAYTZ, B.C.; VOGEL, T.A. 1989: Magma mixing due to disruption of a layered magma body. *Journal of Volcanology and Geothermal Research* 36: 241-255.

FRIEDMAN, I.; LONG, W. 1984: Volcanic glasses, their origins and alteration processes. *Journal of Non-crystalline Solids* 67: 127-133.

FROGGATT, P.C. 1981a: Karapiti Tephra Formation: a 10 000 years B.P. rhyolitic tephra from Taupo. *N.Z. Journal Geology and Geophysics* 24: 95-98.

——— 1981b: Motutere Tephra Formation and redefinition of Hinemaiaia Tephra Formation, Taupo Volcanic Centre, New Zealand. *N.Z. Journal of Geology and Geophysics* 24: 99-105.

——— 1981c: Review of the Holocene eruptions from Taupo. *In* R. Howorth, P.C. Froggatt, C.G. Vucetich, J.D. Collen (Eds): *Proceedings of tephra workshop, June 30th – July 1st 1981,* pp. 21-28. Publication № 20 of Geology Department, Victoria University of Wellington.

——— 1981d: Stratigraphy and nature of Taupo Pumice Formation. *N.Z. Journal of Geology and Geophysics* 24: 231-248.

——— 1982a: *A study of some aspects of the volcanic history of the Lake Taupo Area, North Island, New Zealand.* Unpublished Ph.D. Thesis, Victoria University of Wellington.

——— 1982b: Review of methods of estimating rhyolitic tephra volumes; applications to the Taupo Volcanic Zone, New Zealand. *Journal of Volcanology and Geothermal Research* 14: 301-318.

——— 1983: Toward a comprehensive upper Quaternary tephra and ignimbrite stratigraphy in New Zealand using electron microprobe analysis of glass shards. *Quaternary Research* 19: 188-200.

FROGGATT, P.C.; GOSSON, G.J. 1982: *Techniques for the preparation of tephra samples for mineral and chemical analysis and radiometric dating.* Publication № 23 of Geology Department, Victoria University of Wellington.

FROGGATT, P.C.; HOWORTH, R.; VUCETICH, C.G. 1988: Wairakei Formation, New Zealand: stratigraphy and correlation. *N.Z. Journal of Geology and Geophysics* 31: 391-392.

FROGGATT, P.C.; LOWE, D.J. 1990: A review of late Quaternary silicic and some other tephra formations from New Zealand: their stratigraphy, nomenclature, distribution, volume, and age. *N.Z. Journal of Geology and Geophysics* 33(1): 89-109.

FROGGATT, P.C.; RODGERS, G.M. 1990: Tephrostratigraphy of high-altitude peat bogs along the axial ranges, North Island, New Zealand. *N.Z. Journal of Geology and Geophysics* 33(1): 111-124.

FROGGATT, P.C.; SOLLOWAY, G.J. 1986: Correlation of Papanetu Tephra to Karapiti Tephra, central North Island, New Zealand. *N.Z. Journal of Geology and Geophysics* 29: 303-313.

GALEHOUSE, J.S. 1969: Counting grain mounts: number percentage *vs* number frequency. *Journal of Sedimentary Petrology* 39(2): 812-815.

GARCIA, M.O.; JACOBSON, S.S. 1979: Crystal clots, amphibole fractionation and the evolution of calc-alkaline magmas. *Contributions to Mineralogy and Petrology* 69: 319-327.

GERLACH, D.C.; GROVE, T.L. 1982: Petrology of Medicine Lake Highland volcanics: characterization of end members of magma mixing. *Contributions to Mineralogy and Petrology* 80: 147-159.

GIGGENBACH, W. 1974: The chemistry of Crater Lake, Mt Ruapehu (New Zealand) during and after the 1971 active period. *N.Z. Journal of Science* 17: 33-45.

GORTON, M.P. 1966: *A description of a group of explosion craters at Ohakune.* Unpublished B.Sc.(Hons) Thesis, Victoria University of Wellington.

GOURGAUD, A.; FICHAUT, M.; JORON, J-L. 1989: Magmatology of Mt Pelée (Martinique, French West Indes). I: Magma mixing and triggering of the 1902 and 1929 Pelean nuées ardentes. *Journal of Volcanology and Geothermal Research* 38: 143-169.

GOW, A.J. 1966: Petrographic and petrochemical studies of Mt Egmont andesites. *N.Z. Journal of Geology and Geophysics* 11: 166-90.

GRAHAM, I.J. 1985: *Petrochemical and Sr isotopic studies of lavas and xenoliths from Tongariro Volcanic Centre - implications for crustal contamination of calc-alkaline magmas.* Unpublished Ph.D. Thesis, Victoria University of Wellington.

——— 1987: Petrography and origin of metasedimentary xenoliths in lavas from Tongariro Volcanic Centre. *N.Z. Journal of Geology and Geophysics* 30: 139-157.

GRAHAM, I.J.; HACKETT, W.R. 1986: Petrogenesis of lavas from Ruapehu Volcano and nearby vents, Taupo Volcanic Zone, New Zealand. *In Abstracts of the International Volcanological Congress, Auckland-Hamilton-Rotorua, 1-9 February,* p. 11.

——— 1987: Petrology of calc-alkaline lavas from Ruapehu Volcano and related vents, Taupo Volcanic Zone, New Zealand. *Journal of Petrology* 28(3): 531-567.

GRANGE, L.I. 1929: A classification of soils of Rotorua County. *N.Z. Journal of Science and Technology* 11: 219-228.

——— 1931: Volcanic ash showers: a geological reconnnaisance of volcanic ash showers of the central part of the North Island. *N.Z. Journal of Science* 12: 228-240.

GRANGE, L.I.; HURST, J.A. 1929: Tongariro Subdivision. *N.Z. Geological Survey 23rd Annual Report*, n.s., pp. 5-8.

GRANGE, L.I.; TAYLOR, N.H. 1931: Reconnaissance soil survey of the central part of the North Island. *N.Z. Geological Survey 25th Annual Report*, n.s., pp. 7-8.

GRANGE, L.I.; WILLIAMSON, J.H. 1930: Tongariro Subdivision. *N.Z. Geological Survey 24th Annual Report*, n.s., pp. 10-13.

GREEN, J.D.; LOWE, D.J. 1985: Stratigraphy and development of *c.* 17 000 year old Lake Maratoto, North Island, New Zealand, with some inferences about postglacial climatic change. *N.Z. Journal of Geology and Geophysics* 28: 675-699.

GREEN, N.L. 1982: Co-existing calcic amphiboles in calc-alkaline andesites: possible evidence of a zoned magma chamber. *Journal of Volcanology and Geothermal Research* 12: 57-76.

GREGG, D.R. 1960a: The Geology of Tongariro Subdivision. *N.Z. Geological Survey Bulletin* 40, n.s., pp. 107-123.

——— 1960b: Volcanoes of Tongariro National Park. *N.Z. DSIR Information Series* 28.

GREGORY, M.R.; JOHNSTON, K.A. 1987: A non-toxic substitute for hazardous heavy liquids - aqueous sodium polytungstate ($3Na_2WO_4.9WO_3.H_2O$) solution (Note). *N.Z. Journal of Geology and Geophysics* 30: 317-320.

GRINDLEY, G.W. 1960: *Geological Map of New Zealand*, Sheet 8 Taupo, 1:250 000. N.Z. DSIR, Wellington.

——— 1965: Tongariro National Park: Stratigraphy and structure. *In* B.N. Thompson, L.O. Kermode, A. Ewart (Eds): New Zealand Volcanology Central Volcanic Region. *N.Z. DSIR Information Series* 50.

HACKETT, W.R. 1985: *Geology and petrology of Ruapehu Volcano and related vents.* Unpublished Ph.D. Thesis, Victoria University of Wellington.

HACKETT, W.R.; HOUGHTON, B.F. 1986: Active composite volcanoes of Taupo Volcanic Zone. *In* B.F. Houghton, S.D. Weaver (Eds): Taupo Volcanic Zone Tour Guides C1, C4, C5 and A2. *N.Z. Geological Survey Record* 11.

——— 1989: A facies model for a Quaternary andesitic composite volcano: Ruapehu, New Zealand. *Bulletin of Volcanology* 51: 51-68.

HARRISON, S.; FRITZ, W.J. 1982: Depositional features of March 1982 Mount St Helens sediment flows. *Nature* 299: 720-722.

HAY, R.F. 1967: *Geological Map of New Zealand*, Sheet 7 Taranaki 1:250 000. N.Z. DSIR, Wellington.

HEALY, J. 1954: Origin of flood and Ruapehu lahars in Tangiwai railway disaster. *Report of Board of Inquiry into the Tangiwai Railway Disaster*, pp. 5-8. Government Printer, Wellington.

——— 1964a: Dating of the younger volcanic eruptions of the Taupo region. Part 1. *In* J. Healy, C.G. Vucetich, W.A. Pullar: Stratigraphy and chronology of late Quaternary volcanic ash in Taupo, Rotorua, and Gisborne districts, pp. 7-42. *N.Z. Geological Survey Bulletin* 73.

——— 1964b: Volcanic mechanisms in the Taupo Volcanic Zone, New Zealand. *N.Z. Journal of Geology and Geophysics* 7: 6-23.

——— 1965: *In* B.N. Thompson, L.O. Kermode, A. Ewart (Eds): New Zealand Volcanology Central Volcanic Region. *N.Z. DSIR Information Series* 50.

——— 1978: The nature of the eruption. *And* The eruption and volcanic risk. *In* J. Healy, E.F. Lloyd, D.E.H. Rishworth, C.P. Wood, R.B. Glover, R.R. Dibble 1978: The eruption of Ruapehu, New Zealand, on 22nd June 1969, pp. 59–67. *N.Z. DSIR Bulletin* 224.

HEALY, J.; LLOYD, E.F.; RISHWORTH, D.E.H.; WOOD, C.P.; GLOVER, R.B.; DIBBLE, R.R. 1978: The eruption of Ruapehu, New Zealand, on 22nd June 1969. *N.Z. DSIR Bulletin* 224.

HEIKEN, G.H. 1972: Morphology and petrography of volcanic ashes. *Geological Society of America Bulletin* 83: 1961-1988.

HEIKEN, G.H.; WOHLETZ, K. 1985: *Volcanic Ash.* University of California Press, Berkeley.

HODDER, A.P.W.; WILSON, A.T. 1976: Identification and correlation of thinnly bedded tephra: the Tirau and Mairoa ashes. *N.Z. Journal of Geology and Geophysics* 19: 663-682.

HOGG, A.G.; LOWE, D.J.; HENDY, C.H. 1987: University of Waikato Radiocarbon dates I. *Radiocarbon* 29(2): 263–301.

HOGG, A.G.; M^{c}CRAW, J.D. 1983: Late Quaternary tephras of Coromandel Peninsula, North Island, New Zealand: a mixed peralkaline and calcalkaline tephra sequence. *N.Z. Journal of Geology and Geophysics* 26: 163-187.

HOUGHTON, B.F.; HACKETT, W.R. 1984: Strombolian and phreatomagmatic deposits of Ohakune Craters, Ruapehu, New Zealand: A complex interaction between external water and rising basaltic magma. *Journal of Volcanology and Geothermal Research* 21: 207-231.

HOUGHTON, B.F.; LATTER, J.H.; FROGGATT, P.C. 1988: Volcanic hazard in New Zealand: identifying the problem and practical measures to mitigate the risk. *Geological Society of New Zealand Miscellaneous Publication* 41d.

HOUGHTON, B.F.; LATTER, J.H.; HACKETT, W.R. 1987: Volcanic hazard assessment for Ruapehu composite volcano, Taupo Volcanic Zone, New Zealand. *Bulletin of Volcanology* 49: 737-751.

HOWORTH, R. 1975: New formations of late Pleistocene tephras from the Okataina Volcanic Centre, New Zealand. *N.Z. Journal of Geology and Geophysics* 18(5): 683-712.

HOWORTH, R.; FROGGATT, P.C.; ROBERTSON, S.M. 1980: Late Quaternary volcanic ash stratigraphy of the Poukawa area, central Hawke's Bay, New Zealand. *N.Z. Journal of Geology and Geophysics* 23: 487-491.

HOWORTH, R.; FROGGATT, P.C; VUCETICH, C.G.; COLLEN, J.D. (Eds) 1981: *Proceedings of tephra workshop, June 30th-July 1st 1980.* Publication Nº 20 of Geology Department, Victoria University of Wellington.

HOWORTH, R.; RANKIN, P.C. 1975: Multi-element characterisation of glass shards from stratigraphically correlated rhyolitic tephra units. *Chemical Geology* 15(4): 239-250.

HOWORTH, R.; ROSS, A. 1981: Holocene tephrostratigraphy and chronology at Tiniroto, Cook County. *In* R. Howorth, P.C. Froggatt, C.G. Vucetich, J.D. Collen (Eds): *Proceedings of Tephra Workshop, June 30th – July 1st 1980,* pp. 41-50. Publication Nº 20 of Geology Department, Victoria University of Wellington.

HUBERT, J.F.; FILIPOV, A.J. 1989: Debris-flow deposits in alluvial fans on the west flank of the White Mountains, Owens Valley, California, U.S.A. *Sedimentary Geology* 61: 177-205.

HYDE, J.H. 1975: Upper Pleistocene pyroclastic-flow deposits and lahars south of Mount St Helens Volcano, Washington. *U.S. Geological Survey Bulletin* 1383-B.

JANDA, R.J.; SCOTT, K.M.; NOLAN, K.M.; MARTINSON, H.A. 1981: Lahar movement, effects and deposits. *In* P.W. Lipman, D.R. Mullineaux (Eds): The 1980 Eruption of Mount St Helens, Washington, pp. 461-478. *U.S. Geological Survey Professional Paper* 1250.

KIRKMAN, J.H. 1981: Some primary mineral to clay transformations in New Zealand tephras and tephra-derived soils. *In Soils with variable charge conference program and abstracts, Massey University, Palmerston North, 11 – 18 February 1981*, pp. 169-170.

KITTLEMAN, L.R. 1973: Mineralogy, correlation, and grain-size distributions of Mazama Tephra and other post-glacial pyroclastic layers, Pacific Northwest. *Geological Society of America Bulletin* 84: 2957-2980.

KOHN, B.P. 1970: Identification of New Zealand tephra-layers by emission spectrographic analysis of their titanomagnetites. *Lithos* 3: 361-368.

——— 1973: *Some studies of New Zealand Quaternary pyroclastic rocks.* Unpublished Ph.D. Thesis, Victoria University of Wellington.

——— 1979: Identification and significance of a late Pleistocene tephra in Canterbury District, South Island, New Zealand. *Quaternary Research* 11: 78-92.

KOHN, B.P.; GLASBY, G.P. 1978: Tephra distribution and sedimentation rates in the Bay of Plenty, New Zealand. *N.Z. Journal of Geology and Geophysics* 21(1): 49-70.

KOHN, B.P.; NEALL, V.E. 1973: Identification of late Quaternary tephras for dating Taranaki Lahar deposits. *N.Z. Journal of Geology and Geophysics* 16(3): 781-92.

KOHN, B.P.; NEALL, V.E.; STEWART, R.B. 1981: Holocene tephrostratigraphy revisited at Tiniroto, North Island, New Zealand. *In* R. Howorth, P.C. Froggatt, C.G. Vucetich, J.D. Collen (Eds): *Proceedings of tephra workshop, June 30th – July 1st 1980,* pp. 60-66. Publication Nº 20 of Geology Department, Victoria University of Wellington.

KOHN, B.P.; TOPPING, W.W. 1978: Time-space relationships between late Quaternary rhyolitic and andesitic volcanism in the southern Taupo volcanic zone, New Zealand. *Geological Society of America Bulletin* 89: 1265-1271.

KUO, L-C.; KIRKPATRICK, R.J. 1982: Pre-eruption history of phyric basalts from DSDP Legs 45 and 46: Evidence from morphology and zoning patterns in plagioclase. *Contributions to Mineralogy and Petrology* 79: 13-27.

LATTER, J.H. 1981a: Volcanic earthquakes, and their relationship to eruptions at Ruapehu and Ngauruhoe volcanoes. *Journal of Volcanology and Geothermal Research* 9: 293-309.

——— 1981b: Location of zones of anomalously high S-wave attenuation in the upper crust near Ruapehu and Ngauruhoe volcanoes, New Zealand. *Journal of Volcanology and Geothermal Research* 10: 125-156.

——— 1985: Frequency of eruptions at New Zealand volcanoes. *Bulletin of the N.Z. National Society for Earthquake Engineering* 18(1) March 1985: 55-68.

LATTER, J.H.; HOUGHTON, B.F.; HACKETT, W.R. 1981: Volcanic risk assessment at Ruapehu Volcano. *In* B.F. Houghton, I.E.M. Smith (Eds): *Handbook and Proceedings of N.Z. Volcanological Workshop, Turangi, 27–29 November 1981.*

LAWLOR, I. 1980: Radiocarbon dates from Kohika Swamp Pa (N68/104), Bay of Plenty. *N.Z. Archaeological Association Newsletter* 23(4): 265-267.

LE MAITRE, R.W. 1984: A proposal by the IUGS Subcommission on the Systematics of Igneous Rocks for a chemical classification of volcanic rocks based on the total alkali silica (TAS) diagram. *Australian Journal of Earth Sciences* 31: 243-255.

LEAKE, B.E. 1978: Nomenclature of amphiboles. *American Mineralogist* 63: 1023-1052.

LEWIS, K.B.; KOHN, B.P. 1973: Ashes, turbidites and rates of sedimentation on the continental slope off Hawke's Bay. *N.Z. Journal of Geology and Geophysics* 16: 439-454.

LLOYD, E.F. 1972: Geology and Hot Springs of Orakeikorako. *N.Z. Geological Survey Bulletin* 85.

LOFGREN, G. 1974: An experimental study of plagioclase crystal morphology: isothermal crystallization. *American Journal of Science* 274: 243-273.

LORENZ, V. 1974: Vesiculated tuffs and associated features. *Sedimentology* 21: 273-291.

LOWE, D.J. 1980: *Origin and composite nature of late Quaternary air-fall deposits, Hamilton Basin, New Zealand.* Unpublished M.Sc. Thesis, University of Waikato.

——— 1986: Revision of the age and stratigraphic relationships of Hinemaiaia Tephra and Whakatane Ash, North Island, New Zealand, using distal occurrences in organic deposits. *N.Z. Journal of Geology and Geophysics* 29: 61-73.

——— 1987: *Studies on late Quaternary tephras in the Waikato and other regions in northern North Island, New Zealand, based on distal deposits in lake sediments and peats.* Unpublished D.Phil. Thesis, University of Waikato.

——— 1988a: Stratigraphy, age, composition, and correlation of late Quaternary tephras interbedded with organic sediments in Waikato lakes, North Island, New Zealand. *N.Z. Journal of Geology and Geophysics* 31: 125-165.

——— 1988b: Late Quaternary volcanism in New Zealand: towards an integrated record using distal airfall tephras in lakes and bogs. *Journal of Quaternary Science* 3: 111-120.

——— 1989: Distinguishing rhyolitic and andesitic tephra as soil parent materials for series definition. *N.Z. Soil News* 37(4): 90-93.

LOWE, D.J.; HOGG, A.G. 1986: Tephrostratigraphy and chronology of the Kaipo Lagoon, an 11 500 year-old montane peat bog in Urewera National Park, New Zealand. *Journal of the Royal Society of New Zealand* 16(1): 25-41.

LOWE, D.J.; HOGG, A.G.; GREEN, J.D.; BOUBEE, J.A.T. 1980: Stratigraphy and chronology of late Quaternary tephras in Lake Maratoto, Hamilton, New Zealand. *N.Z. Journal of Geology and Geophysics* 23: 481-485.

LOWE, D.R. 1975: Water escape structures in coarse-grained sediments. *Sedimentology* 22: 157-204.

LOWE, D.R.; WILLIAMS, S.N.; LEIGH, H.; CONNOR, C.B.; GEMMELL, J.B.; STOIBER, R.E. 1986: Lahars initiated by the 13 November 1985 eruption of Nevado del Ruiz, Colombia. *Nature* 324: 51-53.

MAIZELS, J. 1989: Sedimentology, paleoflow dynamics and flood history of jökulhlaup deposits: paleohydrology of Holocene sediment sequences in southern Iceland sandur deposits. *Journal of Sedimentary Petrology* 59(2): 204-223.

MAJOR, J.J.; NEWHALL, C.G. 1989: Snow and ice perturbation during historical volcanic eruptions and the formation of lahars and floods. *Bulletin of Volcanology* 52: 1-27.

MATHEWS, W.H. 1965: A contribution to the geology of the Mount Tongariro Massif, North Island, New Zealand. *N.Z. Journal of Geology and Geophysics* 10: 1027-38.

MAZEY, J.W. 1978: Damage to the Dome Shelter and Iwikau and Whakapapa villages. *Appendix in* J. Healy, E.F. Lloyd, D.E.H. Rishworth, C.P. Wood, R.B. Glover, R.R. Dibble: The Eruption of Ruapehu, New Zealand, on 22nd June 1969, pp. 69-71. *N.Z. DSIR Bulletin* 224.

M^{c}ARTHUR, J.L.; SHEPHERD, M.J. 1990: Late Quaternary glaciation of Mt Ruapehu, North Island, New Zealand. *Journal of the Royal Society of New Zealand* 20(3): 287-296.

M^{c}DOWELL, B. 1986: Eruption in Colombia. *National Geographic* 169(5): 640-653.

MEW, G.; HUNT, J.L.; FROGGATT, P.C.; EDEN, D.N.; JACKSON, R.J. 1986: An occurrence of Kawakawa Tephra from the Grey River valley, South Island, New Zealand. *N.Z. Journal of Geology and Geophysics* 29: 315-322.

MILLER, C.D. 1980: Potential hazards from future eruptions in the vicinity of Mount Shasta Volcano, Northern California. *U.S. Geological Survey Bulletin* 1503.

MILLER, C.D.; MULLINEAUX, D.R.; CRANDELL, D.R. 1981: Hazards assessment at Mount St Helens. *In* P.W. Lipman and D.R. Mullineaux (Eds): The 1980 Eruptions of Mount St Helens, Washington. *U.S. Geological Survey Professional Paper* 1250.

MILNE, J.D.G. 1973: Mount Curl Tephra, a 230 000-year-old marker bed in New Zealand, and its implications for Quaternary chronology. *N.Z. Journal of Geology and Geophysics 16: 519–32.*

MOORE, J.G. 1967: Base surge in recent volcanic eruptions. *Bulletin Volcanologique* 30: 337-363.

MOORE, J.G.; PECK, D.L 1961: Accretionary lapilli in volcanic rocks of the western continental United States. *Journal of Geology* 70: 182-193.

MULLINEAUX, D.R. 1974: Pumice and other pyroclastic deposits in Mount Rainier National Park, Washington. *U.S. Geological Survey Bulletin* 1326.

——— 1986: Summary of pre-1980 tephra-fall deposits erupted from Mount St Helens, Washington State, U.S.A. *Bulletin of Volcanology* 48: 17-26.

MULLINEAUX, D.R.; CRANDELL, D.R. 1962: Recent lahars from Mount St Helens, Washington. *Geological Society of America Bulletin* 73: 855-870.

MULLINEAUX, D.R.; HYDE, J.H.; RUBIN, M. 1972: Preliminary assessment of upper Pleistocene and Holocene pumiceous tephra from Mount St Helens, Southern Washington. *Geological Society of America*. Abstracts with programs. 4(3): 204-205.

——— 1975: Widespread late Glacial and post-glacial tephra deposits from Mount St Helens Volcano, Washington. *U.S. Geological Survey Journal of Research* 3(3): 329-335.

NAIRN, I.A. 1971: *Studies of Earthquake Flat Breccia Formation and other unwelded pyroclastic flow deposits of the Central Volcanic Region, New Zealand.* Unpublished M.Sc. Thesis, Victoria University of Wellington.

——— 1980: Source, age, and eruptive mechanisms of Rotorua Ash. *N.Z. Journal of Geology and Geophysics* 23: 193-207.

NAIRN, I.A.1981: *Some studies of the geology, volcanic history, and geothermal resources of the Okataina Volcanic Centre, Taupo Volcanic Zone, New Zealand.* Unpublished Ph.D. Thesis, Victoria University of Wellington.

NAIRN, I.A.; KOHN, B.P. 1973: Relation of the Earthquake Flat Breccia to the Rotoiti Breccia, central North Island, New Zealand. *N.Z. Journal of Geology and Geophysics* 16: 269-279.

NAIRN, I.A.; SELF, S. 1978: Explosive eruptions and pyroclastic avalanches from Ngauruhoe in February 1975. *Journal of Volcanology and Geothermal Research* 3: 39-60.

NAIRN, I.A.; WOOD, C.P.; HEWSON, C.A.Y. 1979: Phreatic eruptions of Ruapehu: April 1975. *N.Z. Journal of Geology and Geophysics* 22(2): 155-73.

NEALL, V.E. 1972: Tephrochronology and tephrostratigraphy of Western Taranaki (N108 - 109), New Zealand. *N.Z. Journal of Geology and Geophysics* 15: 507-557.

——— 1976: *Lahars - Global occurence and annotated bibliography.* Publication Nº 5 of Geology Department, Victoria University of Wellington.

NEALL, V.E.; STEWART, R.B.; SMITH, I.E.M. 1986: History and petrology of the Taranaki Volcanoes. *In* I.E.M. Smith (Ed.): Late Cenozoic Volcanism in New Zealand, pp. 251-263. *The Royal Society of New Zealand Bulletin* 23.

NIELSEN, C.H.; SIGURDSSON, H. 1981: Quantative methods for electron microprobe analysis of sodium in natural and synthetic glasses. *American Mineralogist* 66: 547-552.

NINKOVICH, D. 1968: Pleistocene volcanic eruptions in New Zealand recorded in deep-sea sediments. *Earth and Planetary Science Letters* 4: 89-102.

NIXON, G.T. 1988: Petrology of the younger andesites and dacites of Iztaccíhuatl Volcano, Mexico: I. Disequlibrium phenocryst assemblages as indicators of magma chamber processes. *Journal of Petrology* 29(2): 213-264.

NOBLE, S. (Ed.) 1988: Disappearing Ice. *Tongariro, the Journal of Tongariro National Park* 34: 12-16.

O'SHEA, B.E. 1954: Ruapehu and the Tangiwai disaster. *N.Z. Journal of Science and Technology* B36(2): 174-189.

——— 1959: Petrography of the Whakapapanui Gorge andesites, Mount Ruapehu. *N.Z. Journal of Geology and Geophysics* 2: 412-420.

PAGE, C.E.; PATERSON, B.R. 1976: Lahars from the 1975 Mt Ruapehu Eruption. *Appendix in* B.R. Paterson: The effects of lahars from the 1975 April Mt Ruapehu Eruption and the threat of future eruptions on Tongariro power development. *N.Z. Geological Survey Unpublished Engineering Geology Report* EG 230.

PALMER, B.A.; NEALL, V.E. 1989: The Murimotu Formation - 9500 year-old deposits of a debris avalanche and associated lahars, Mount Ruapehu, North Island, New Zealand. *N.Z. Journal of Geology and Geophysics* 32: 477-486.

PATERSON, B.R. 1972: The threat of volcanic pollutants to the fish of Lake Rotoaira. *N.Z. Geological Survey Unpublished Engineering Geology Report* EG 137.

——— 1976: The effects of lahars from the 1975 April Mt Ruapehu eruption and the threat of future eruptions on Tongariro power development. *N.Z. Geological Survey Unpublished Engineering Geology Report* EG 230.

PATTERSON, D.B.; GRAHAM, I.J. 1988: Petrogenesis of andesitic lavas from Mangatepopo Valley and Upper Tama Lake, Tongariro Volcanic Centre, New Zealand. *Journal of Volcanology and Geothermal Research* 35: 17-29.

PETERSON, D.W. 1970: Ash-flow deposits - their character, origin, and significance. *Journal of Geological Education* XVIII(2): 66-76.

PIERSON, T.C. 1980: Erosion and deposition by debris flows at Mt Thomas, North Canterbury, New Zealand. *Earth Surface Processes* 5: 227-247.

——— 1985: Initiation and flow behaviour of the 1980 Pine Creek and Muddy River lahars, Mount St Helens, Washington. *Geological Society of America Bulletin* 96: 1056-1069.

PIERSON, T.C.; COSTA, J.E. 1987: A rheologic classification of subaerial sediment-water flows. Geological Society of America: *Reviews in Engineering Geology* VII: 1-12.

PIERSON, T.C.; SCOTT, K.M. 1985: Downstream dilution of a lahar: transition from debris flow to hyperconcentrated streamflow. *Water Resources Research* 21(10): 1511-1524.

PILLANS, B.J. 1988: Loess Chronology in Wanganui Basin, New Zealand. *In* D.N. Eden, R.J. Furkert (Eds): *Loess: Its Distribution, Geology and Soils*, pp. 175 – 191. A.A. Balkema, Rotterdam, Netherlands.

PLAS, V.D.L.; TOBI, A.C. 1965: A chart for judging the reliability of point counting results. *American Journal of Science* 263: 87-90.

POWERS, H.A.; WILCOX, R.E. 1964: Volcanic Ash from Mount Mazama (Crater Lake) and from Glacier Peak. *Science* 144: 1334-1336.

PULLAR, W.A.; BIRRELL, K.S. 1973: Age and distribution of late Quaternary pyroclastic and associated cover deposits of the Rotorua and Taupo area, North Island, New Zealand. *N.Z. Soil Survey Report 1.*

PULLAR, W.A.; BIRRELL, K.S.; HEINE, J.C. 1973: Named tephras and tephra formations occurring in the Central North Island, with some notes on derived soils and buried paleosols. *N.Z. Journal of Geology and Geophysics* 16(3): 497-518.

PULLAR, W.A.; KOHN, B.P.; COX, J.E. 1977: Air-fall Kaharoa Ash and Taupo Pumice, and sea rafted Loisels Pumice, Taupo Pumice, and Leigh Pumice in northern and eastern parts of the North Island, New Zealand. *N.Z. Journal of Geology and Geophysics* 20(4): 697-717.

PURVES, A.M. 1990: *Landscape ecology of the Rangipo Desert.* Unpublished M.Sc. Thesis, Massey University.

PYLE, D.M. 1989: The thickness, volume and grain-size of tephra fall deposits. *Bulletin of Volcanology* 51: 1-15.

RANDLE, K.; GOLES, G.G.; KITTLEMAN, L.R. 1971: Geochemical and petrological characterization of ash samples from Cascade Range volcanoes. *Quaternary Research* 1: 261-282.

RANKIN, P.C.; HOWORTH, R.; WHITTON, J.S.; BURKE, A.S. 1975: Comparison of two extraction techniques for volcanic glass. *N.Z. Journal of Science* 18: 103-107.

RIEHLE, J.R.; BOWERS, P.M.; AGER, T.A. 1990: The Hayes Tephra Deposits, an upper Holocene marker horizon in South-Central Alaska. *Quaternary Research* 33: 276-290.

ROBIN, C,; KOMOROWSKI, J.C.; BOUDAL, C.; MOSSAND, P. 1990: Mixed-magma pyroclastic surge deposits associated with debris avalanche deposits at Colima Volcanoes, Mexico. *Bulletin of Volcanology* 52: 391-403.

RODINE, J.D.; JOHNSON, A.M. 1976: The ability of debris, heavily freighted with coarse clastic materials, to flow on gentle slopes. *Sedimentology* 23: 213-234.

RODOLFO, K.S. 1989: Origin and early evolution of lahar channel at Mabinit, Mayon Volcano, Phillipines. *Geological Society of America Bulletin* 101: 414-426.

ROEDER, P.L.; EMSLIE, R.F. 1970: Olivine-liquid equlibrium. *Contributions to Mineralogy and Petrology* 29: 275 – 289.

ROSS, C.S. 1928: Altered paleozoic volcanic materials and their recognition. *American Association of Petroleum Geologists Bulletin* 12: 143-164

ROWLEY, P.D.; M^cLEOD, N.S.; KUNTZ, M.A.; KAPLAN, A.M. 1985: Proximal bedded deposits related to pyroclastic flows of May 18, 1980, Mount St Helens, Washington. *Geological Society of America Bulletin* 96: 1373-1383.

SAKUYAMA, M. 1984: Magma mixing and magma plumbing systems in Island Arcs. *Bulletin Volcanologique* 47-4(1): 685-703.

SARNA-WOJCICKI, A.M.; MEYER, C.E.; WOODWARD, M.J.; LAMOTHE, P.J. 1981: Composition of air-fall ash erupted on May 18, May 25, June 12, July 22 and August 7. *In* P.W. Lipman, D.R. Mullineaux (Eds): The 1980 eruptions of Mount St. Helens, Washington, pp.667-681. *U.S. Geological Survey Professional Paper* 1250.

SCARFE, C.M.; FUJII, T. 1987: Petrology of crystal clots in the pumice of Mount St Helens' March 19, 1982 eruption; significant role of Fe-Ti oxide crystallization. *Journal of Volcanology and Geothermal Research* 34: 1-14.

SCHMID, R. 1981: Descriptive nomenclature and classification of pyroclastic deposits and fragments: recommendations of the IUGS Subcommission on the Systematics of Igneous Rocks. *Geology* 9: 41-43.

SCHMINCKE, H-U. 1967: Graded lahars in the type sections of the Ellensburg Formation, South-Central Washington. *Journal of Sedimentary Petrology* 37(2): 438-448.

SCHMITT, J.G.; OLSON, T.J. 1986: Hyperconcentrated flood-flow deposition of coarse-grained sediment on temperate, semi-arid to humid alluvial fans. *Geological Society of America Abstracts with Programs* 18: 741.

SCHULTZ, A.W. 1984: Subaerial debris-flow deposition in the upper Paleozoic Cutler Formation, Western Colorado. *Journal of Sedimentary Petrology* 54(3): 759-772.

SCHUSTER, R.L.; CRANDELL, D.R. 1984: Catastrophic debris avalanches from volcanoes. *Proceedings of the IV International symposium on landslides, Toronto.* 1: 567-572.

SCOTT, K.M. 1985: Lahars and flow transformations at Mount St Helens, Washington, U.S.A. *International Symposium on Erosion, Debris Flow and Disaster Prevention, Tsukuba, Japan, September 3rd-5th, 1985.* pp 209-214.

——— 1988: Coal Bank Bridge Section - lahar magnitude and frequency. *Guidebook for field excursions, Geological Society of America Penrose Confrence, August 28-September 2. pp6-11.*

SELF, S.; HEALY, J. 1987: Wairakei Formation, New Zealand: stratigraphy and correlation. *N.Z. Journal of Geology and Geophysics* 30: 73-86.

SELF, S.; SPARKS, R.S.J. 1978: Characteristics of widespread pyroclastic deposits formed by the interaction of silicic magma and water. *Bulletin Volcanologique* 41: 196-212.

SHERIDAN, M.F. 1979: Emplacement of pyroclastic flows: A review. *In* C.E. Chapin, W.E. Elston (Eds): Ash-flow tuffs. *The Geological Society of America Special Paper* 180: 125-134.

SHERIDAN, M.F.; WOHLETZ, K.H. 1983: Hydrovolcanism: basic considerations and review. *Journal of Volcanology and Geothermal Research* 17: 1-29.

SIEBERT, L. 1984: Large volcanic debris avalanches: characteristics of source areas, deposits, and associated eruptions. *Journal of Volcanology and Geothermal Research* 22: 163-197.

SIEBERT, L.; GLICKEN, H.; UI, T. 1987: Volcanic hazards from Bezymianny- and Bandai-type eruptions. *Bulletin of Volcanology* 49: 435-459.

SMITH, A.L.; ROOBOL, M.J. 1982: Andesitic pyroclastic flows. *In* R.S. Thorpe (Ed.): *Andesites: Orogenic Andesites and Related Rocks,* pp. 415-433. John Wiley & Sons Ltd.

SMITH, D.G.W.; WESTGATE, J.A. 1969: Electron probe technique for characterising pyroclastic deposits. *Earth and Planetary Science Letters* 5: 313-319.

SMITH, D.R.; LEEMAN, W.P. 1982: Mineralogy and phase chemistry of Mount St Helens Tephra sets W and Y as keys to their identification. *Quaternary Research* 17: 211-227.

SMITH, G.A. 1986: Coarse-grained non-marine volcaniclastic sediment: terminology and depositional process. *Geological Society of America Bulletin* 97: 1-10.

——— 1987: Sedimentology of volcanism-induced aggradation in fluvial basins: examples from the Pacific Northwest, U.S.A. *In* F.G. Ethridge, R.M. Flores, M.A. Harvey (Eds): Recent developments in fluvial sedimentology. *The Society of Economic Paleontologists and Mineralogists Special Publication* 39: 217-229.

SMITH, G.A.; CAMPBELL, N.P.; DEACON, M.W.; SHAFIQULLAH, M. 1988: Eruptive style and location of volcanic centers in the Miocene Washington Cascade Range: reconstruction from the sedimentary record. *Geology* 16: 337-340.

SMITH, G.A.; FRITZ, W.J. 1989: Volcanic influences on terrestrial sedimentation. *Geology* 17(4): 375-376.

SMITH, H.W.; OKAZAKI, R. 1977: Electron microprobe data for tephra attributed to Glacier Peak, Washington. *Quaternary Research* 7: 197-206.

SMITH, R.L. 1960: Ash flows. *Geological Society of America Bulletin* 71(6): 795-841.

SPARKS, R.S.J.; SELF, S.; WALKER, G.P.L. 1973: Products of ignimbrite eruptions. *Geology* 1(3): 116-123.

SPARKS, R.S.J.; SIGURDSSON, H.; WILSON, L. 1977: Magma mixing: a mechanism for triggering acid explosive eruptions. *Nature* 267: 315-318.

SPARKS, R.S.J.; WILSON, L.; HULME, G. 1978: Theoretical modeling of the generation, movement, and emplacement of pyroclastic flows by column collapse. *Journal of Geophysical Research* 83(B4): 1727-1739.

STEEL, M. 1989: *Mountain beech forest of Mount Ruapehu.* Unpublished Ph.D. Thesis, Auckland University.

STEEN-M^{c}INTYRE, V. 1977: *A Manual for Tephrochronology*. Idaho Springs, Colorado.

STERN, T.A. 1986: Geophysical Studies of the Upper Crust within the Central Volcanic Region. *In* I.E.M. Smith (Ed.): *The Royal Society of New Zealand Bulletin* 23: 92-112.

STEWART, R.B. 1982: *Origin of selected soil parent materials and sediments in North Island, New Zealand.* Unpublished Ph.D. Thesis, Massey University.

STIPP, J.J. 1968: *The geochronology and petrogenesis of the Cenozoic volcanoes of the North Island, New Zealand.* Unpublished Ph.D. thesis, Australian National University, Canberra.

STOKES, S.; LOWE, D.J. 1988: Discriminant function analysis of late Quaternary tephras from five volcanoes in New Zealand using glass shard major element chemistry. *Quaternary Research* 30: 270-283.

SWANSON, D.A.; CHRISTIANSEN, R.L. 1973: Tragic base surge in 1790 at Kilauea Volcano. *Geology* 1: 83-86.

TE PUNGA, M.T. 1952: The Geology of Rangitikei Valley. *N.Z. Geological Survey Memoir* 8.

TERRY, R.D.; CHILINGAR, G.V. 1955: Summary of "Concerning some additional aids in studying sedimentary formations" by M.S. Shvetsov. *Journal of Sedimentary Petrology* 25(3): 229-234

THOMAS, A.P.W. 1889: Notes on the geology of Tongariro and the Taupo District. *Transactions of the N.Z. Institute* 21: 338-53.

THORARINSSON, S. 1974: The terms Tephra and Tephrochronology. *In* J.A. Westgate and C.M. Gold (Eds): The World Bibliography and Index of Quaternary Tephrochronology. University of Alberta.

TOPPING, W.W. 1973: Tephrostratigraphy and chronology of late Quaternary eruptives from the Tongariro Volcanic Centre. *N.Z. Journal of Geology and Geophysics* 16(3): 397-423.

——— 1974: *Some aspects of Quaternary history of Tongariro Volcanic Centre.* Unpublished Ph.D. Thesis, Victoria University of Wellington.

TOPPING, W.W.; KOHN, B.P. 1973: Rhyolitic tephra marker beds in the Tongariro area, North Island, New Zealand. *N.Z. Journal of Geology and Geophysics* 16(3): 375-395.

TRAILL, W.E. 1978: Damage to buildings and equipment. Appendix. *In* J. Healy, E.F. Lloyd, D.E.H. Rishworth, C.P. Wood, R.B. Clover, R.R. Dibble: The eruption of Ruapehu, New Zealand, on 22nd June 1969, pp.68. *N.Z. DSIR Bulletin 224.*

TRAINEAU, H.; WESTERCAMP, D.; BARDINTZEFF, J-M.; MISKOVSKY, J-C. 1989: The recent pumice eruptions of Mt Pelée volcano, Martinique. Part I: Depositional sequences, description of pumiceous deposits. *Journal of Volcanology and Geothermal Research* 38: 17-33.

UI, T. 1983: Volcanic dry avalanche deposits - identification and comparison with non-volcanic debris stream deposits. *Journal of Volcanology and Geothermal Research* 18: 135-150.

UI, T.; KAWACHI, S.; NEALL, V.E. 1986. Fragmentation of debris avalanche material during flowage - evidence from the Pungarehu Formation, Mount Egmont, New Zealand. *Journal of Volcanology and Geothermal Research* 27: 255-264.

VIGNAUX, M.; WEIR, G.J. 1990: A general model for Mt Ruapehu lahars. *Bulletin of Volcanology* 52: 381 – 390

VOIGHT, B.; GLICKEN, H.; JANDA, R.J.; DOUGLASS, P.M. 1981: Catastrophic rockslide avalanche of May 18. *In* P.W. Lipman, D.R. Mulineaux (Eds): The 1980 eruptions of Mount St. Helens, Washington, pp347-377. *U.S. Geological Survey Professional Paper* 1250.

VUCETICH, C.G.; HOWORTH, R. 1976a: Proposed definition of the Kawakawa Tephra, the *c.* 20 000 years B.P. marker horizon in the New Zealand region. *N.Z. Journal of Geology and Geophysics* 19(1): 43-50.

——— 1976b: Late Pleistocene tephrostratigraphy in the Taupo District, New Zealand. *N.Z. Journal of Geology and Geophysics* 19(1): 51-69.

VUCETICH, C.G.; PULLAR, W.A. 1964: Stratigraphy of Holocene ash in the Rotorua and Gisborne districts. Part 2. *In* J. Healy, C.G. Vucetich, W.A. Pullar: Stratigraphy and chronology of late Quaternary volcanic ash in Taupo, Rotorua, and Gisborne districts, pp. 43-63. *N.Z. Geological Survey Bulletin* 73.

——— 1969: Stratigraphy and chronology of late Pleistocene volcanic ash beds in central North Island, New Zealand. *N.Z. Journal of Geology and Geophysics* 12: 784-837.

——— 1973: Holocene tephra formations erupted in the Taupo area, and interbedded tephras from other volcanic sources. *N.Z. Journal of Geology and Geophysics* 16(3): 745-80.

WAITT, R.B. 1989: Swift snow-melt and floods (lahars) caused by great pyroclastic surge at Mount St Helens volcano, Washington, 18 May 1980. *Bulletin of Volcanology* 52: 138-157.

WALKER, G.P.L. 1973: Explosive volcanic eruptions - a new classification scheme. *Geologische Rundschau* 62(2): 431-46

——— 1981a: The Waimihia and Hatepe plinian deposits from the rhyolitic Taupo Volcanic Centre. *N.Z. Journal of Geology and Geophysics* 24: 305-324.

——— 1981b: Plinian eruptions and their products. *Bulletin Volcanologique* 44(2): 223-240.

——— 1982: Eruptions of andesitic volcanoes. *In* R.S. Thorpe (Ed): *Andesites: Orogenic Andesites and Related Rocks,* pp. 403-413. John Wiley and & Sons Ltd.

WALKER, G.P.L.; CROASDALE, R. 1972: Characteristics of some basaltic pyroclastics. *Bulletin Volcanologique* 35: 303-317.

WALKER, G.P.L.; SELF, S.; FROGGATT, P.C. 1981: The ground layer of the Taupo Ignimbrite: A striking example of sedimentation from a pyroclastic flow. *Journal of Volcanology and Geothermal Research* 10: 1-11.

WALLACE, R.C. 1987: *The mineralogy of Tokomaru Silt Loam and the occurrence of cristobalite and tridymite in selected North Island soils.* Unpublished Ph.D. Thesis, Massey University.

WALLACE, R.C.; STEWART, R.B.; NEALL, V.E. 1985: Volcanic glass field laboratory test and procedure to prepare thin sections of the sand fraction of soils. *Department Soil Science Massey University Occasional Report* 7.

WALTON, A.W.; PALMER, B.A. 1988: Lahar facies of the Mount Dutton Formation (Oligocene-Miocene) in the Marysvale Volcanic Field, southwestern Utah. *Geological Society of America Bulletin* 100: 1078-1091.

WATERS, A.C.; FISHER, R.V. 1971: Base surges and their deposits: Capelinhos and Taal volcanoes. *Journal of Geophysical Research* 76: 5596-5614.

WESTGATE, J.A. 1977: Identification and significance of late Holocene tephra from Otter Creek, southern British Columbia, and localities in west-central Alberta. *Canadian Journal of Earth Science* 14: 2593-2600.

WATSON, E.B. 1976: Glass inclusions as samples of early magmatic liquid: determinative method and application to a south Atlantic basalt. *Journal of Volcanology and Geothermal Research* 1: 73-84.

WESTGATE, J.A.; FULTON, R.J. 1975: Tephrostratigraphy of Olympia inter-glacial sediments in south-central British Columbia, Canada. *Canadian Journal of Earth Science* 12: 489-502.

WESTGATE, J.A.; GORTON, M.P. 1981: Correlation techniques in tephra studies. *In* S. Self and R.S.J. Sparks (Eds): *Tephra Studies,* pp. 73-94. D. Reidel. Publishing Company, Dordrecht, Holland.

WILCOX, R.E. 1965: Volcanic-Ash Chronology. *In The Quaternary of the United States,* pp. 807-816. Princeton University Press.

WILCOX, R.E.; IZETT, G.A. 1973: Criteria for the use of volcanic ash beds as time-stratigraphic markers. *Abstracts with Programs. Geological Society of America 5(7): 863.*

WILLIAMS, H.; M^{c}BIRNEY, A.R. 1979: *Volcanology.* Freeman, Cooper & Co., San Francisco.

WILLIAMS, K. 1986: *Volcanoes of the South Wind: A field guide to the volcanoes and landscape of Tongariro National Park.* Tongariro Natural History Society, Wellington.

WILSON, C.J.N. 1988: Letters to the Editor: Wairakei Formation, New Zealand: stratigraphy and correlation. Comment. *N.Z. Journal of Geology and Geophysics* 31: 392-394.

WILSON, C.J.N.; ROGAN, A.M.; SMITH, I.E.M.; NORTHEY, D.J.; NAIRN, I.A.; HOUGHTON, B.F. (Eds) 1984: Caldera volcanoes of the Taupo Volcanic Zone, New Zealand. *Journal of Geophysical Research* 89: 8463-8484.

WILSON, C.J.N.; SWITSUR, V.R.; WARD, A.P. 1988: A new ^{14}C age for the Oruanui (Wairakei) eruption, New Zealand. *Geological Magazine* 125 (3): 297-300.

WOHLETZ, K.H. 1983: Mechanisms of hydrovolcanic pyroclast formation: Grain-size, scanning electron microscopy, and experimental studies. *Journal of Volcanology and Geothermal Research* 17: 31-63.

——— 1986: Explosive magma-water interactions: Thermodynamics, explosion mechanisms, and field studies. *Bulletin of Volcanology* 48: 245-264.

WOOD, C.P. 1977: Petrology of ejected lake sediment and the geochemical cycle of Ruapehu Crater Lake, New Zealand. *In* Geochemistry 1977. *N.Z. DSIR Bulletin* 218: 103-108.

——— 1978: Petrology of the tephras. *In* J. Healy, E.F. Lloyd, D.E.H. Rishworth, C.P. Wood, R.B. Glover, R.R. Dibble. The eruption of Ruapehu, New Zealand, on 22nd June 1969. *N.Z. DSIR Bulletin* 224: 35-39.

WÖRNER, G.; WRIGHT, T.L. 1984: Evidence for magma mixing within the Laacher See magma chamber (east Eifel, Germany). *Journal of Volcanology and Geothermal Research* 22: 301-327.

WRIGHT, J.V.; SMITH, A.L.; SELF, S. 1980: A working terminology of pyroclastic deposits. *Journal of Volcanology and Geothermal Research* 8: 315-336.

ZEN, M.T.; HADIKUSUMO, D. 1965: The future danger of Mt Kelut (Eastern Java - Indonesia). *Bulletin Volcanologique* 28: 275-282.

ZOLTAI, S.C. 1989: Late Quaternary volcanic ash in the peatlands of central Alberta. *Canadian Journal of Earth Science* 26: 207-214.